LAHAINA GROUNDWATER TRACER STUDY – LAHAINA, MAUI, HAWAII

Final Interim Report

Craig R. Glenn, Robert B. Whittier, Meghan L. Dailer, Henrieta Dulaiova, Aly I. El-Kadi, Joseph Fackrell, Jacque L. Kelly and Christine A. Waters

November 2012

This page is intentionally left blank.

LAHAINA GROUNDWATER TRACER STUDY – LAHAINA, MAUI, HAWAII

Final Interim Report

Craig R. Glenn, Robert B. Whittier, Meghan L. Dailer, Henrieta Dulaiova, Aly I. El-Kadi, Joseph Fackrell, Jacque L. Kelly and Christine A. Waters

November 2012

PREPARED FOR

State of Hawaii Department of Health
U.S. Environmental Protection Agency
U.S. Army Engineer Research and Development Center

Principal Investigator: Craig R. Glenn

School of Ocean and Earth Science and Technology
Department of Geology and Geophysics
University of Hawaii at Manoa
Honolulu, Hawaii 96822

This page is intentionally left blank.

Acknowledgements

This page is intentionally left blank.

EXECUTIVE SUMMARY

Overview

This report was prepared by the University of Hawaii for the U. S. Army Engineer Research and Development Center at Vicksburg, Mississippi, the State of Hawaii Department of Health and the U.S. Environmental Protection Agency to provide critical data about the possible existence of a hydrological connection between the injected effluent from the Maui County, Hawaii, Lahaina Wastewater Reclamation Facility (LWRF) and the nearby coastal waters, confirm the locations of emerging injected effluent discharge in these coastal waters, and determine a travel time from the LWRF injection wells to the coastal waters. The studies presented in this report provide the positive establishment of hydrologic connections between the municipal wastewater injection from the LWRF and the nearshore region of the Kaanapali coast on the Island of Maui, Hawaii, and provide the results from the study's principal objectives, which have been to: (1) implement a tracer dye study from the LWRF (Section 3), (2) conduct continuous monitoring for the emergence of the injected tracer dyes at the most probable points of emergence at nearshore sites within the coastal reaches of the LWRF (Section 2), (3) conduct an airborne infrared sea surface temperature mapping survey of coastal zone fronting the LWRF in an effort to detect cool and/or warm temperature anomalies that may be indicative of cool submarine groundwater discharge and warm wastewater effluent (Section 4), (4) complete radon and radium radiochemical surveys to detect the emergence points and flow rates of the naturally occurring submarine groundwater along the coastal zone (Section 5), (5) complete geochemical and stable isotopic analyses of LWRF effluent, upland well waters, terrestrial surface waters, marine waters, and submarine groundwater discharge in an effort to help partition the relative contribution of effluent waters to the ocean (Section 6), and (6) combine complete dye emergence breakthrough curves with which to develop groundwater models to determine the LWRFs effluent flow paths and rates of emergence to the coastal zone (Section 7). Our principal findings include the following key results:

(1) Fluorescein tracer dye added to LWRF injection Wells 3 and 4 arrived at coastal submarine spring sites with a minimal travel time of 84 days; a second dye, Sulpho-Rhodamine-B added to LWRF injection Well 2, has yet to be confirmed.

(2) Submarine springs releasing the fluorescein dye to the coastal ocean are located at North Kaanapali Beach, approximately 0.85 km (0.5 miles) to the southwest of the LWRF, and within 3 to 25 meters of shore.

(3) Waters discharging the fluorescein dye from the submarine springs are warm and brackish, and have an average salinity of 4.5 and a pH of 7.5.

(4) Geochemical mixing analyses indicate that the submarine spring waters are predominately LWRF treated wastewater which while in transit to the submarine springs undergo oxic, suboxic and likely anoxic microbial degradation reactions that consume dissolved oxygen, dissolved nitrate, and organic matter.

(5) The N concentration of the submarine springs is reduced compared to LWRF treated wastewater, while the P concentration is enriched. Averaged N and P concentrations collected from the submarine springs were ca. 1,100 µg/L and 425 µg/L, respectively.

(6) As based on radon mass balance measurements, average total (fresh + marine) discharge from the submarine springs and the surrounding diffuse flow was about 2.76 million gallons per day (mgd) (10,450 m^3/d). The freshwater component of that flow was about 2.25 mgd (8,500 m^3/d), or about 75% of the LWRF total average daily injection rate (~3.0 mgd; 11,350 m^3/d).

(7) High-resolution airborne thermographic infrared mapping identified a large sea surface thermal anomaly associated with the warm water submarine springs. The nearshore surface area of this thermal anomaly is ~ 674,000 m^2, or about 167 acres in size.

Introduction

The study area is located in the Kaanapali District of West Maui, Hawaii. Current West Maui land use can be subdivided into (1) an urban center in the Lahaina area, (2) various diversified agriculture and pasture land on former pineapple and sugarcane fields on the lower slopes of the West Maui Mountains, (3) residential and resort development (including golf courses) along the shoreline, and (4) natural evergreen forest in the interior of the West Maui Mountains (Figure ES-1). Historical changes in agricultural land use within the western half of West Maui were estimated by Engott and Vana (2007) in order to estimate the effects of rainfall and agricultural land use changes on West and Central Maui groundwater recharge. During the early 1900s until about 1979, land use was mostly unchanged except for some minor urbanization along the coasts, but as large-scale plantation agriculture declined after 1979 land-use changes became more significant. From 1979 to 2004, agricultural land use declined about 21 percent, mainly from the complete cessation of sugarcane agriculture. The Pioneer Mill Co. was the major sugarcane cultivator on the west side of the West Maui Mountains, operating during the late 1800s until 1999, when it ceased sugarcane production on approximately 6,000 acres and some of the land was subsequently converted to pineapple cultivation including the area north of Honokowai Stream. The extent of pineapple agriculture in West Maui decreased extensively since the late 1990s, and stopped entirely in 2009 (Gingerich and Engott, 2012). Today, large portions of the former sugarcane and pineapple fields remain fallow while other parcels have been converted to low-density housing and diversified agriculture.

The LWRF is about 3 mi north of the town of Lahaina and serves the municipal wastewater needs for that community including the major resorts along the coast. The LWRF receives approximately 4 million gallons per day (mgd) of sewage from a collection system serving approximately 40,000 people. The facility produces treated wastewater (tertiary treated with filtration and since October 2011 has been disinfected with chlorine to an R-2 standard), which is disposed of via four on-site injections wells, and tertiary treated wastewater that is disinfected with UV radiation to meet R-1 reuse water standards. Approximately 0.7 – 1.5 mgd of the facility's R-1 water is sold to customers such as the Kaanapali Resort to be used for landscape and golf course irrigation. R-1 water that is not sold is discharged into the subsurface via the four on-site injection wells along with the tertiary treated effluent.

Multiple studies have investigated the nutrient flux to the West Maui waters and the role of the LWRF in the nutrient flux. A nutrient balance study of West Maui (Tetra Tech, 1993) identified the LWRF as one of the three primary nutrient release sources to Lahaina District coastal waters, with sugarcane and pineapple cultivation being the other two. That study ranked the LWRF second in annual nitrogen contribution and first in phosphorous contribution to these waters. Since that study was completed, the cultivation of both sugarcane and pineapple has been sharply curtailed. This implies that the LWRF may now be the primary contributor of nutrients to water in the study area. The West Maui Watershed Owner's Manual (West Maui Watershed Management Advisory Committee, 1997) reevaluated nitrogen (N) and phosphorus (P) loadings in the watershed and concluded that in terms of relative nutrient loadings, the LWRF wastewater injection wells likely contributed about three times the amount of nitrogen, and at least an order of magnitude more phosphorus to the ocean than did that any other source. As our report discusses in Section 6, however, treatment process improvements and the institution of wastewater reclamation since the release of the Tetra Tech (1993) study appears to have facilitated an overall reduction of contributions of N and P to the LWRF injected effluent.

Hunt and Rosa (2009) investigated the use of multiple in situ tracers to identify where and how municipal wastewater effluent discharges to the nearshore marine environment. These researchers sampled the LWRF effluent, submarine springs, nearshore marine waters, groundwater, and terrestrial surface water in vicinity of effluent injection sites in Lahaina and Kihei, Maui. They concluded that the most conclusive tracers in the nearshore marine environment were the presence of pharmaceuticals, organic waste indicator compounds, and highly enriched $\delta^{15}N$ values (due to a higher proportion of the heavy ^{15}N isotope compared to the more abundant ^{14}N isotope in dissolved NO_3^-) in water samples and in coastal benthic macroalgal tissue. These researchers identified the submarine springs as the coastal locus of the LWRF injection plume, although they also cited nearshore marine samples collected further south towards Kaanapali Golf Course as showing geochemical evidence of effluent or effluent-derived irrigation water influence. Based on this evidence, Hunt and Rosa delineated the probable extent of the LWRF effluent plume (Figure ES-2). The minimum extent of the plume is shown in Figure ES-2 as a red arc. Hunt and Rosa were less certain of their interpretation for the yellow arc shown Figure ES-2 that reaches further south because the elevated $\delta^{15}N$ values in water

samples (from dissolved NO_3^-) could have been from irrigation recharge water that uses reclaimed water from the LWRF.

Submarine Springs and Marine Control Locations of Sampling, Water Quality, and Fluorescence

This segment of this report (Section 2) provides: (1) details of how the warm submarine springs at Kahekili were sampled for injected tracer dye, radioisotope tracers, and geochemical and stable isotope tracers, (2) information on in situ water quality parameters of the submarine springs and control locations, (3) additional assessments of the submarine springs, and (4) the field determined fluorescence of samples collected from submarine springs and from control locations.

To support the tracer and chemistry portions of the study an aggressive field effort was undertaken. This included the installation of the sampling infrastructure, collecting samples for the geochemical survey, collecting nearly 1,200 samples for field and tracer dye analysis, and deployment and collection of data from instruments for monitoring temperature and salinity.

Warm water submarine springs (seeps) occur at North Kaanapali Beach, and we grouped the general clustering of these submarine springs into two groups termed the North Seep Group (NSG) and the South Seep Group (SSG) (Figure ES-3). Samples were collected from both groups and at three control locations. The submarine springs were sampled directly by drawing on SCUBA diver emplaced piezometers driven into springs, with the fluids extracted by peristaltic pump. Samples at other sites were collected as "grab samples." The SSG is located approximately 25 m offshore and had three initial monitoring points (Seeps 3, 4, and 5). A fourth monitoring point, Seep 11, was added on November 24, 2011 due to high salinities being measured at Seeps 4 and 5. The Seep 4 piezometer was relocated in the North Seep Group (NSG) on April 24, 2012 to replace piezometers in that area that were covered by migrating sand. The NSG is located approximately 3 to 5 m offshore with three initial monitoring points (Seep 1, 2, and 6). This location has proven extremely problematic to maintain throughout the duration of the project. The NSG's close proximity to the shoreline subjects these piezometers to the persistent littoral migration of sand from the beach onto the seep group as a result of large north swells. As each piezometer was buried, however, it was replaced with a new one. All replacement piezometers were and are currently located within 2 m of the original deployments.

Marine control locations for the dye tracer portion of the study were Honokowai Beach Park, Wahikuli Wayside Park, and Olowalu. Honokowai Beach Park, located ~1.8 km north of the study site, served as a site of possible dye emergence should the LWRF effluent flow path proved to move to the north (Figure ES-3). Wahikuli Wayside Park, located ~4.3 km south of the main study, was targeted because of its proximity to the submarine spring locations. Olowalu is located ~13 km south of the main study area and was chosen to represent water with minimal anthropogenic impact due to lack of development and the termination of sugarcane operations in the late 1990's.

Water quality parameters of temperature, pH, specific conductivity, and salinity were measured on each seep sample (Table ES-1), the readings taken at the discharge point of a peristaltic pump on the beach. In most locations, the salinity of the samples was < 5, indicating that the captured seep waters were representative of submarine groundwater with little seawater influence. Since the sampling pump was located on the beach away from the surf zone, the temperature of the seep water was affected by the ocean and sand temperatures between the seep and the pump. Therefore, the temperatures recorded in this manner for a particular seep sample are not a good indicator of the actual seep water temperature at the point of discharge into the marine environment. The pH of seeps in the NSG varied between 7.2 and 7.9 with an average of about 7.5. The pH of seeps in the SSG varied between 6.8 and 7.9 also with an average of about 7.5. The salinity of seeps in the NSG varied between 2.5 and 23 with an average of about 4.8. Seeps in the SSG had salinities that were slightly lower, varying between 3.8 and 22, with an average of about 4.1.

The seep water samples were also screened in the field for the presence of the project's two tracer dyes, Fluorescein (FLT), and Sulpho-Rhodamine-B (SRB). A pre-dye tracer injection monitoring period was conducted from July 5th through July 28th, 2011, which was designed to measure the magnitude and variability of in situ fluorescence of the submarine spring water at the selected monitoring sites. Upon the addition of the dye, the sampling frequency was increased to two to three times per day. As the study progressed, the sampling frequency was decreased and currently occurs one to two times per week. The SRB and FLT fluorescence measured in the field remained indistinguishable from background levels until late October, 2011. Subtle increases in field fluorometry measurements of FLT started to occur in samples from the NSG in late October, 2011, which provided the first indication that dye was emerging from the submarine springs. This was followed in mid-November by increasing FLT fluorescence of samples from the SSG. As of May 2, 2012, there has been no confirmed detection of SRB.

Fluorescent Dye Groundwater Tracer Study

Two tracer dye tests were conducted at the LWRF (Section 3). These tests were aimed at providing critical data about any hydrological connection between the wastewater effluent injected and the coastal waters, confirming the locations where injected effluent discharges into the coastal waters, and determining a travel time from the injection wells to the coastal waters. In the first tracer test, Fluorescein (FLT) was added to LWRF Injection Wells 3 and 4 on July 28th, 2011. This was followed two weeks later by an addition of Sulpho-Rhodamine-B (SRB) into Injection Well 2 on August 11th, 2011, which has a significantly higher injection capacity than the other three wells. The second tracer test was conducted to investigate whether the effluent from this well discharges into the marine environment at the same location as Wells 3 and 4.

Samples collected at the submarines springs were pre-screened for FLT and SRB fluorescence in the field and then delivered to Honolulu for the laboratory fluorometry

analysis. The submarine spring sampling began three weeks prior to dye addition to assess the natural background fluorescence. Pre-dye addition average fluorescence of the seep waters was 0.11 parts per billion (ppb) for FLT wavelengths and 0.03 ppb for SRB wavelengths. The presence of the FLT dye from the first tracer test began discharging at the NSG submarine springs in late October, 2011, about 84 days after the addition of dye into Injection Wells 3 and 4. The FLT concentration increased from pre-dye background values to about 21 ppb, then plateaued in late February, 2012 at the NSG (Figure ES-4a). The presence of FLT tracer was first detected at the SSG in early November, 2011, and increased in concentration to about 33 ppb, then plateaued in early April, 2012 (Figure ES-4b). Maximum dye concentrations to date have been higher at the SSG than at the NSG (Figure ES-4). This could be due to spatial variability or that the SSG may be closer to the center of the plume than the NSG. If it is the latter case, then there is a probability of effluent discharging points existing to the south of the SSG.

The second dye tracer test was conducted using SRB dye to evaluate whether the effluent from Injection Well 2 discharges at the same locations as that from Injection Wells 3 and 4. Well 2 has a significantly higher injection capacity than the other wells, indicating that it may have a hydraulic connection to a preferential flow path. For this second test, SRB was added to the LWRF effluent on August 11th, 2011. To date, there has been no confirmed detection of the SRB dye in the nearshore marine waters. There were three samples collected in late February that more detailed analysis indicated may contain very low concentrations of SRB, but since no subsequent samples have been analyzed with similar fluorescent characteristics, these are only evaluated as possible detections.

Our dye tracer test results clearly demonstrate that a definite hydraulic connection does exist between Injection Wells 3 and 4 and the nearshore waters at North Kaanapali Beach near Kahekili Beach Park, although this work does not preclude the possibility of other discharge points also occurring elsewhere, including farther from shore and in deeper water. In addition to our having determined that the minimum transit time between the LWRF injection wells and the submarine springs in the NSG is 84 days, another important parameter that can be gained from this work is the average time of travel for the groundwater from point of injection to point of discharge. The peak of a breakthrough curve (BTC) can be used to estimate this parameter, and the apparent plateauing of the FLT BTC (Figure ES-4) suggests that the average time of travel from the injection wells to the submarine springs is in excess of seven months. At this point in the study, however, it is still too early to tell whether the peak of the BTC has actually been reached.

Aerial Infrared Sea Surface Temperature Mapping

The objective of thermal infrared mapping portion of this investigation (Section 4) has been to determine the locations of both warm and cool emerging fluids to the coastal waters near the LWRF. For this work, we used high-resolution (2.3 m) aerial infrared remote sensing techniques to produce sea-surface temperature (SST) maps which revealed the existence of anomalously warm (~26.5°C), buoyant, emerging fluids relative to ambient coastal waters (25.5°C), as well as the presence of cooler, natural submarine

groundwater discharge (20-22°C). These data were collected at night to eliminate the effects of solar surface water heating.

Our aerial thermal infrared methodology successfully identified a 673,900 m^2 (166.5 acre) thermal anomaly extending from the shoreline to at least 575 m (1886 ft) offshore (Figure ES-5). The thermal plumes from the springs themselves varied from 140 to 315 m^2 (1507 to 3391 ft^2). Aside from the large thermal anomaly and the known warm submarine springs it resides over, no new warm water submarine spring locations were identifiable by the infrared thermography.

The co-variance of the thermal anomaly and the warm effluent discharge from the submarine springs appears quite apparent (compare Figures ES-2, ES-5 and ES-6). The thermal anomaly is located southwest of the LWRF and occurs in association with the submarine springs (seeps) shown by our tracer tests to be hydraulically connected to the injected effluent from the LWRF. In addition, the anomaly lies well centered within the projected LWRF effluent plume trajectory predicted by Hunt and Rosa (2009). Furthermore, the spatial covariance between the TIR thermal anomaly and the δ^{15}N in macroalgae appears excellent. Approaching the locus of the submarine springs from the north, the thermal anomaly's surface water warming incrementally increases (~24.5 to 26.8°C) in agreement with the progressive increases in the δ^{15}N values of benthic macroalgae (+4.8 to +48.8 ‰) that reach a maxima centered at the submarine springs (Dailer et al., 2010). Dailer et al. (2012) found that the discharge from the submarine spring locations rises to the surface due to its positive buoyancy relative to the seawater column. Once on the surface, the anomalously warm waters flow toward the south, along with the most predominant current in the area (Storlazzi and Field, 2008).

Despite the collection of these findings, we feel that there is possibly one, or some combination of three potential heat sources that could contribute to the noticeably warm submarine spring water emerging from the ocean floor and would also support heat transfer to the thermal anomaly. These sources include the heat retained in warm LWRF wastewater effluent from the time it was injected, exothermic reactions related to microbial degradation of the organic matter of the subterranean effluent flow, and/or geothermal heating of groundwater and possibly heating of the water column from below the surface expression of the thermal anomaly. Further assessments of the source(s) of heat generating the thermal anomaly would be required to determine the relative contributions from each.

Submarine Groundwater Discharge

Submarine groundwater discharge (SGD) to the nearshore waters in the study (Section 5) was measured using two technologies. In the first, the predictable release of radon from the aquifer matrix to the groundwater, its radioactive decay rate, and the near absence of radon in seawater were used in a coastal radon mass balance to measure SGD over the expanse of the study area. In the second, to measure point discharges of SGD, an Acoustic Doppler Current Profiler (ADCP) was used. This instrument measures water

velocity profiles in 3 dimensions by transmitting short pulse pairs into the water, and calculating the phase shift between the two acoustic return signals.

Both the radon mass balance method and ADCP measurements provide total submarine groundwater discharge [freshwater + recirculated marine water], but cannot identify if and what fraction of the groundwater is wastewater effluent. It is, however, possible to calculate the fraction of fresh groundwater and, in combination with other geochemical information, also the fraction of the injected LWRF effluent (see Section 6). The relevance of these methods to the overall objectives of the project is to provide groundwater flux from the submarine springs to help determine the degree of dye recovery and the discharge of effluent through the submarine springs as the project progresses.

Radon and radium isotopes are highly enriched in groundwater and depleted in ocean water, and in the absence of other sources, their detection in coastal waters is an indication of SGD. A mass balance of these tracers can be used to estimate the amount of groundwater discharge required to supply the observed inventory of these tracers in the coastal zone. Radon is a naturally occurring radiogenic isotope that enters subterranean groundwater aquifers as a dissolved and chemically inert noble gas after being released in predictable quantities from all igneous rocks, including basalt. Thus, groundwater is accordingly enriched in ^{222}Rn, with activities often 3 to 4 orders of magnitude higher in groundwater than in coastal seawater, making it a superior tracer of coastal SGD (Burnett et al., 2006). Owing to its short half-life (3.8 days) and the fact that ocean water has very low levels of radon, this gas has now almost universally become the routinely measured tracer for SGD flow rates, as the decay rate of ^{222}Rn is comparable to the time scales of many coastal circulation processes (Burnett et al., 2006). Thus, the dynamics of groundwater inputs as well as estimates of groundwater discharges may be examined via radon monitoring of coastal waters (Burnett and Dulaiova, 2003).

A radon mass balance model was constructed to estimate discharge from time series radon measurements in the surface water. It was found that groundwater discharge from the submarine springs is tidally modulated with minimal discharge at high tide and increased fluxes at low tide. Due to this variability, we expressed discharge as a 24-hour average. Figure ES-7 shows the area where the radon survey identified significant fluxes of groundwater discharge. The total (fresh + saline) groundwater discharge from the submarine spring groups including the direct discharge from the submarine springs and the surrounding diffuse flow was 8,300 and 12,600 m^3/d in June and September, respectively. Out of this, fresh groundwater discharge amounted to 6,100 and 10,900 m^3/d in June and September, respectively. Coastal radon surveys showed that there is significant groundwater discharge along the coastline north and south of the submarine springs. We found several sites with a total groundwater discharge ranging from 2,000 to 28,000 m^3/d, the highest flux at 28,000 m^3/d was at Hanakao`o Beach Park, the second largest at 15,000 m^3/d was at Honokowai Beach Park. We also used the nearshore-marine radon survey to estimate the coastal SGD from North Honokowai to south of Hanakao'o Beach (Figure ES-7). This calculation did not represent the entire shoreline, but rather the areas of the highest discharge rates shown by the boxes in Figure ES-7.

The summed total SGD for the areas of highest SGD was 54,000 m^3/d (14.3 mgd). This represents a total (freshwater + recirculated marine water) SGD of 7.45 m^3/m/d (3.17 mgd/mi), as integrated over the 11.8 km of shoreline for this portion of the coast. As this value only represents the areas contained in the boxes in Figure ES-7, it represents a minimum estimate to total SGD. The large uncertainties in these estimates are discussed in Section 5.

The Acoustic Doppler Current Profiler (ADCP) was deployed at a major submarine spring (seep) at each seep group. Despite the intense swell that produced noise in the data, the net vertical flux was positive indicating that the instrument recorded the upward flux from the seep. The ADCP record showed that the discharge from the seeps was tidally influenced, with lows at high tide and larger fluxes at low tide. At Seep 4 in the south seep group, the average vertical velocity during the 6-hour deployment was 0.02 m/s. At Seep 6 in the north seep group, the upward vertical velocity averaged at 0.0036 m/s. These water velocities translate to a discharge of approximately 70 and 12 m^3/d water from Seep 4 and Seep 6, respectively. Our ADCP measurements at the submarine spring sites remain ongoing.

Aqueous Geochemistry and Stable Isotopes

This portion of the study (Section 6) utilized a multi-tracer approach similar to, but broader in scope than that applied to this study area by Hunt and Rosa (2009). The purpose of our approach was to (1) determine the origins of nutrients in the area's groundwater, (2) evaluate the down-gradient geochemical evolution of the area's groundwater prior to its discharge to the ocean, and (3) identify the impact of land-derived nutrient fluxes on the geochemistry of coastal marine waters. Special emphasis was placed on determining the geochemical evolution and ultimate fate of the LWRF effluent after its injection. Data collection for this section was accomplished over two separate sampling intervals in 2011 (June 19-30 and September 19-25). Temperature, conductivity, salinity, pH, chloride (Cl^-) concentrations, nutrient concentrations, and stable isotope ratios of hydrogen (H) and oxygen (O) in water, and nitrogen (N) and O in dissolved nitrate (NO_3^-) were measured in order to characterize the geochemistry of the study area's groundwater, surface waters, treated wastewater, and coastal waters. Samples of gas bubbles emanating from the submarine springs and black precipitates that coat the rocks and coral rubble around submarine spring sites were also geochemically analyzed. Generally conservative tracers such as the isotopic ratios of H and O in water and Cl^- concentrations were used to evaluate mixing between potential end-members, while N loading was considered together with the isotopic ratios of N and O in dissolved NO_3^- to evaluate origin, evolution, and mixing of N species. Figure ES-6 shows the distribution of $\delta^{15}N$ values in the samples collected from this study and compares this data with the intertidal macroalgal $\delta^{15}N$ values from Dailer et al. (2010), and the aerial TIR measured sea-surface temperatures obtained at night. Very highly enriched $\delta^{15}N$ values of dissolved nitrate from the submarine spring samples spatially correlates with the most highly enriched $\delta^{15}N$ values from the intertidal benthic macroalgae samples presented in Dailer (2010). Tables ES-2 and ES-3 summarize the nutrient chemistry for the samples collected in June and September, 2011, respectively.

Though a thorough quantitative evaluation of nutrient sources was not accomplished in this portion of the study, this work identifies several potential nutrient sources to the coastal zone based on the spatial distribution of nutrient species with respect to current and former land-use practices. These potential sources are:

(1) Fertilizer applied in support of former agriculture appears to still be contributing to N and P loading of basal groundwater (though to a lesser extent than in the past, when these agricultural practices were ongoing). The production wells upgradient of the past and present agricultural influence had N and P concentrations of about 30 and 60 µg/L, respectively. The production wells most impacted by agriculture had N and P concentrations of about 2,500 and 180 – 300 µg/L, respectively.

(2) Injected LWRF effluent appears to contribute significant amounts of N and P to groundwater (although the concentrations are much less than prior to wastewater treatment upgrades in 1995), but the temporally variable and non-conservative behavior of these species complicates the overall assessment of the magnitude of the source. The N and P concentrations in the LWRF effluent were ca. 7,200 and 700 µg/L, respectively for June, 2011, and ca. 6,200 and 170 µg/L, respectively for September, 2011. The N concentration of the submarine springs appears to be reduced compared to the LWRF wastewater effluent, while the P concentration appears to be enriched. The average N and P concentrations in samples collected from the submarine springs were ca. 600 and 400 µg/L, respectively, for June, 2011, and ca. 1,600 and 450 µg/L, respectively, for September, 2011.

(3) R1 irrigation water and possibly fertilizer appear to contribute to N and P loading in groundwater supplying Black Rock lagoon. During the June, 2011 sampling event the N and P concentrations in the Black Rock Lagoon were 3,400 and 190 µg/L, respectively.

All biological compounds can undergo various forms of alteration and decomposition. As a result of this decomposition, organic matter is degraded into simpler molecules and inorganic species, including nutrients. Whether it be in soils, fresh water or marine conditions, the most important and fundamental of these processes is the microbial decomposition of organic matter, which generally follows a succession of steps that depend largely on the nature and availability of the oxidizing agent, as shown in Table ES-4 (e.g. Froelich et al, 1979; Berner, 1980; Appelo, and Potsma, 1993; Berner and Berner, 1996; Stumm and Morgan, 1996). Thus, as shown in Table ES-4, when provided with an ample supply of labile organic matter (shown for simplicity as CH_2O), such as the injected wastewater effluent at the LWRF, O_2 is first used as the oxidizing agent until it becomes sufficiently to completely depleted by aerobes. After aerobic O_2 depletion, further decomposition occurs in steps as nitrate reduction, manganese oxide reduction, iron reduction, and so on. Within this framework, we have found evidence for significant down-gradient oxygen depletion and geochemical evolution of the groundwaters within the study area including:

(1) Mixing analysis using conservative tracers suggests that the submarine spring water is primarily injected LWRF wastewater effluent.

(2) Although likely subject to temporal variation, the majority of the NO_3^- present in the LWRF wastewater effluent has been acutely attenuated via suboxic denitrification (nitrate reduction) prior to its emergence at the submarine springs at the time of this study (cf. Table ES-4). A bi-product of these reactions is the ubiquitous presence of highly N_2-enriched gas bubbles that conspicuously vent from both the submarine springs and nearby unconsolidated sands into the ocean in this area.

(3) As manganese must be in the reduced state ($Mn^{2+)}$ in order to be aqueous and mobile, the presence of solid phase Mn-oxide and/or Mn-oxyhydroxide impregnations and coating rocks and coral rubble surrounding the submarine springs indicates that the exiting waters have additionally undergone anoxic manganese reduction.

(4) The injected LWRF wastewater effluent is augmented in PO_4^{3-} in the subsurface prior to its emergence at the submarine spring sites. We believe this is likely due to aquifer conditions promoting the release or dissolution of previously particle-adsorbed and/or mineral-bound PO_4^{3-}.

(5) Groundwater at, and down gradient of locations subjected to significant artificial recharge is augmented in SiO_4^{4-} mobilized via accelerated rock weathering.

By analyzing the spatial distribution of various water parameters in the marine environment, including nutrient concentrations and stable isotope values Tables ES-5 and ES-6; Figure ES-6), we have located several coastal ocean areas with terrestrial nutrient contribution. These are:

(1) The marine environment immediately surrounding the submarine springs, which shows a dissolved NO_3^- isotopic signature consistent with the heavily ^{15}N-enriched (very positive $\delta^{15}N$) values characteristic of nitrate reduction measured in the submarine spring water.

(2) The area near the mouth of Black Rock lagoon, which shows generally elevated nutrient concentrations relative to nearby waters and a dissolved NO_3^- isotopic signature consistent with values measured in Black Rock lagoon itself.

(3) The area near Wahikuli Wayside Park, which also shows generally elevated nutrient concentrations relative to nearby waters, and shows a dissolved NO_3^- isotopic signature suggestive of denitrification from fertilizer or natural sources and/or sewage/manure content. Sugarcane was grown in the Wahikuli area until 1999, and the current community is unsewered with many cesspools and septic systems.

Preliminary Groundwater Model

Groundwater modeling (Section 7) is being used in this study to interpret the BTC, assess processes that affect the fate and transport of the injected effluent, and evaluate the potential for other deep submarine emergence points. Two modeling approaches have been used to date: 1) a more geologically complex groundwater flow and transport model that does not consider the interaction between saline and non-saline water; and 2) a geologically simplified model that does consider this interaction.

The first model was used in the design plan of the tracer field experiment to estimate the mass of dye needed for a successful tracer test. With minimal calibration it successfully estimated a reasonable first arrival and peak time. However, the model's peak concentration of 7 ppb was significantly less than the measured FLT peak of about 21 ppb for the NSG and 33 ppb for the SSG. A simulated barrier along the track of the ancestral Honokowai Stream (cf. Hunt and Rosa, 2009) was added to the model to see if the simulated FLT flow direction would be more consistent with the physical evidence. With the barrier in place, the simulated FLT arrival time to the NSG was about a month earlier than the actual first detection. However, the peak concentration of 28 ppb compared more favorably with the measured concentration than that of model runs used to plan the tracer test experiment. The model result of a near absence of FLT at the SSG, however, is problematic. The good agreement between this model and NSG BTC, but the poor agreement with SSG BTC may indicate that the cause of the observed oblique tracer path is a combination of a subterranean barrier and a preferential flow path. The BTC interpretation model predicted an SRB arrival at the NSG in March, 2012. To date, there has been no confirmed detection of this dye at either seep group. The second model considered the interaction between the fresh groundwater, the non-saline effluent, and the saline groundwater. This model supported the notion that buoyancy forces the non-saline effluent into the shallow groundwater zone, to ultimately exit in the nearshore environment, despite the low vertical conductivity of the volcanic formation.

Future modeling for this project will investigate the processes that affect the transport of the injected LWRF treated wastewater effluent and its eventual discharge into the marine environment. The processes may include: 1) the role that the high horizontal to vertical ratio of hydraulic conductivity in any vertical migration of the LWRF treated wastewater effluent; 2) the likely amount of heat loss that would occur from the LWRF treated wastewater effluent as it travels from the point of injection to the point of discharge; and 3) evaluating whether or not any significant mass of the fluorescent tracer dye has lost to sorption or degradation. The results of the modeling will be detailed in the final supplemental report.

Table ES-1: North and South Seep Group water quality parameters.
Data (means ± SD and range) were collected from 7/19/2011 through 5/2/2012 with a handheld YSI Model 63.

South Seeps	Temp. (°C)	pH	Spec. Cond. (mS/cm)	Salinity
Seep 3	28.7 ± 2.0	7.52 ± 0.12	6.43 ± 2.57	3.25 ± 1.5
	24.9 to 34.9	7.22 to 7.94	5.20 to 28.18	2.50 to 16.1
Seep 4	28.6 ± 2.0	7.50 ± 0.12	8.98 ± 6.57	4.77 ± 4.0
	24.5 to 34.6	7.20 to 7.90	5.63 to 37.70	2.80 to 22.5
Seep 5	28.4 ± 2.0	7.53 ± 0.20	9.24 ± 6.59	4.94 ± 4.0
	24.9 to 34.9	7.32 to 7.90	5.29 to 34.75	2.90 to 21.8
Seep 11	26.8 ± 2.5	7.61 ± 0.20	6.48 ± 0.62	3.39 ± 0.3
	25.2 to 29.0	7.37 to 7.68	5.00 to 8.32	3.10 to 4.5
North Seeps				
Seep 1	29.1 ± 2.0	7.45 ± 0.09	8.33 ± 1.04	4.25 ± 0.5
	24.8 to 34.4	7.18 to 7.76	7.32 to 14.80	3.90 to 7.3
Seep 2	28.9 ± 2.3	7.46 ± 0.11	8.47 ± 1.41	4.35 ± 0.7
	24.0 to 34.9	7.13 to 7.75	7.04 to 17.36	3.80 to 9.9
Seep 6	29.3 ± 2.2	7.41 ± 0.14	8.33 ± 0.90	4.25 ± 0.4
	23.8 to 35.9	6.90 to 7.94	7.00 to 13.54	3.80 to 7.0
Seep 7	27.5 ± 1.7	7.51 ± 0.19	8.19 ± 1.32	4.31± 0.8
	22.4 to 30.3	7.26 to 7.81	7.24 to 15.08	3.90 to 8.2
Seep 8	27.4 ± 1.7	7.35 ± 0.18	9.36 ± 5.98	5.01± 3.6
	24.7 to 31.0	7.09 to 7.90	7.47 to 37.88	4.00 to 22.0
Seep 9	27.4 ± 1.7	7.43 ± 0.21	13.65 ± 11.35	7.58 ± 6.7
	23.3 to 30.5	6.75 to 7.80	7.21 to 42.91	3.90 to 25.3
Seep 10	28.2 ± 1.0	7.60 ± 0.15	9.02 ± 1.17	4.70 ± 0.6
	26.5 to 29.5	7.26 to 7.76	7.99 to 11.85	4.10 to 6.2
Seep 12	28.2 ± 1.1	7.60 ± 0.11	8.37 ± 0.50	4.35 ± 0.2
	26.6 to 29.6	7.36 to 7.78	7.88 to 9.55	4.10 to 4.9
Seep 13	28.0 ± 1.9	7.69 ± 0.02	8.18 ± 0.53	4.27 ± 0.1
	26.0 to 29.7	7.67 to 7.71	7.69 to 8.74	4.20 to 4.4
Seep 14	27.1 ± 2.1	7.67 ± 0.05	7.91 ± 0.21	4.17 ± 0.1
	24.7 to 28.7	7.66 to 7.72	7.67 to 8.02	4.10 to 4.2
Seep 15	28.4 ± 2.4	7.58 ± 0.10	9.99 ± 3.28	5.31 ± 2.1
	24.6 to 30.6	7.45 to 7.72	7.86 to 16.54	4.20 to 9.3
Seep 16	30.1 ± 0.6	7.63 ± 0.12	8.85 ± 0.09	4.47 ± 0.1
	29.4 to 30.6	7.50 to 7.71	8.79 to 8.95	4.40 to 4.5

Table ES-2: Summary of the June, 2011 Nutrient Data

Sample Type	No. of Samples		TP	TN	PO$_4^{3-}$	SiO$_4^{4-}$	NO$_3^-$	NO$_2^-$	NH$_4^+$
			(µg/L as P)	(µg/L as N)	(µg/L as P)	(µg/L as Si)	(µg/L as N)	(µg/L as N)	(µg/L as N)
Terrestrial Surface	6	Min.	21	88	18	4,852	1	0.8	0.6
		Avg.	161	2,121	75	17,427	1,189	9.0	51
		Max.	255	4,043	159	25,679	3,166	31	129
		Std. Dev.	91	1,566	50	8,431	1,540	11	49
Production Wells	7	Min.	60	292	48	17,944	205	0.7	0.8
		Avg.	100	1,330	72	19,283	968	1.1	1.4
		Max.	184	2,429	105	21,958	1,916	2.0	2.9
		Std. Dev.	52	778	25	1,611	731	0.5	0.8
Monitoring Well	1		91	2,342	52	16,206	1,608	6.2	0.0
Treated Wastewater	1		206	7,245	102	17,231	2,641	530	1,307
Submarine Springs	4	Min.	350	326	279	11,984	142	14	4
		Avg.	396	486	340	16,948	278	23	6
		Max.	421	651	365	20,624	366	31	7
		Std. Dev.	32	146	41	4,069	108	9	1
Marine Surface	25	Min.	11	64	3	134	3	0.3	0.0
		Avg.	14	100	6	356	22	0.3	1
		Max.	34	306	26	1,249	146	1	10
		Std. Dev.	5	57	5	303	34	0.1	2

PW = Production Well
MW = Monitor Well
TS = Terrestrial Surface
TW = Treated Wastewater
SS = Submarine Spring
MS = Marine Surface

Table ES-3: Summary of the September, 2011 Nutrient Data

Sample Type	No. of Samples		TP (µg/L as P)	TN (µg/L as N)	PO$_4^{3-}$ (µg/L as P)	SiO$_4^{4-}$ (µg/L as Si)	NO$_3^-$ (µg/L as N)	NO$_2^-$ (µg/L as N)	NH$_4^+$ (µg/L as N)
Terrestrial Surface (TS)	3	Min.	123	2,146	42	8,237	1,083	6	24
		Avg.	201	4,551	86	16,373	2,923	86	59
		Max.	261	6,751	155	24,160	4,239	237	103
		Std. Dev.	70	2,309	60	7,967	1,642	131	40
Production Wells (PW)	7	Min.	66	277	50	17,948	226	0.7	2.2
		Avg.	136	1,463	112	20,115	1,142	1.0	5.9
		Max.	309	2,559	254	23,792	2,487	1.5	7.1
		Std. Dev.	88	874	76	2,400	817	0.2	1.7
Monitoring Well (MW)	1		73	2,759	55	18,085	1,210	2.8	17
Treated Wastewater (TW)	2	Min.	164	6,061	70	16,462	3,172	423	156
		Avg.	177	6,238	88	16,678	3,313	466	211
		Max.	191	6,415	106	16,893	3,454	509	267
		Std. Dev.	19	250	25	304	199	61	79
Submarine Springs (SS)	2	Min.	451	1,573	393	19,693	96	10	6.4
		Avg.	459	1,598	404	20,426	121	18	6.8
		Max.	468	1,624	415	21,159	145	27	7.1
		Std. Dev.	12	36	16	1,037	35	12	0.5
Marine Surface (MS)	23	Min.	11	127	2.8	98	0.0	0.3	0.1
		Avg.	13	173	4.5	202	5.7	0.5	1.4
		Max.	20	225	14	607	41	1.1	2.9
		Std. Dev.	1.9	19.8	2.3	136	8.6	0.2	0.9

PW = Production Well
MW = Monitor Well
TS = Terrestrial Surface
TW = Treated Wastewater
SS = Submarine Spring
MS = Marine Surface

Table ES-4: The progressive microbial decomposition of organic matter.
Reactions succeed each one another in the order written as each oxidant is completely consumed. From Berner and Berner, 1996.

Oxygenation (oxic)
$$CH_2O + O_2 \rightarrow CO_2 + H_2O$$
Nitrate reduction (mainly anoxic)
$$5CH_2O + 4NO_3^- \rightarrow 2N_2 + CO_2 + 4HCO_3^- + 3H_2O$$
Manganese oxide reduction (mainly anoxic)
$$CH_2O + 2MnO_2 + 3CO_2 + H_2O \rightarrow 2Mn^{++} + 4HCO_3^-$$
Ferric oxide (hydroxide) reduction (anoxic)
$$CH_2O + 4Fe(OH)_s + 7CO_2 \rightarrow 4Fe^{++} + 8HCO_3^- + 3H_2O$$
Sulfate reduction (anoxic
$$2CH_2O + SO_4^{--} \rightarrow H_2S + 2HCO_3^-$$
Methane formation (anoxic)
$$2CH_2O \rightarrow CH_4 + CO_2$$
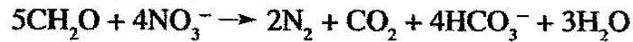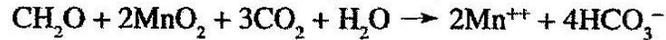
Note: Organic matter schematically represented as CH_2O.

Table ES-5: June, 2011 stable isotope data
(- denotes measurement not performed)

Sample Name (Type)	$\delta^{18}O$ of H_2O (‰)[1]	δ^2H of H_2O (‰)[1]	$\delta^{15}N$ of NO_3^- (‰)[2]	$\delta^{15}N$ σ (‰)[3]	$\delta^{18}O$ of NO_3^- (‰)[1]	$\delta^{18}O$ σ (‰)[3]
Kaanapali 1 (TS)	-	-	12.63	2.26	2.84	4.3
Kaanapali 2 (TS)	-	-	14.99	2.26	-1.82	4.3
Kaanapali GC-1 (TS)	-	-	4.96	1.67	-1.62	1.45
Hahakea 2 (PW)	-3.77	-15.33	0.65	1.15	0.7	1.17
Honokowai B (PW)	-3.79	-15.05	3.15	1.67	-3.5	1.45
Kaanapali P-1 (PW)	-3.8	-14.94	1.31	1.67	-1.74	1.45
Kaanapali P-2 (PW)	-3.75	-15.3	1.07	1.67	-0.16	1.45
Kaanapali P-4 (PW)	-3.57	-14.51	0.92	0.52	4.3	1.78
Kaanapali P-5 (PW)	-3.45	-14.46	4.19	1.67	3	1.45
Kaanapali P-6 (PW)	-3.39	-13.85	3.29	1.67	3.3	1.45
Lahaina Deep Monitor (MW)	-3.55	-13.75	1.8	1.67	-0.22	1.45
LWRF Treated Effluent (TW)	-	-	29.25	0.52	19.82	1.78
Seep 1 Piez-1 (SS)	-3.21	-11.01	86.47	1.15	21.56	1.17
Seep 1 Piez-2 (SS)	-	-	77.82	0.56	22.86	0.19
Seep 2 Piez-1 (SS)	-1.52	-5.19	-	-	-	-
Seep 3 Piez-1 (SS)	-3.03	-10.91	83.89	0.56	22.07	0.19
Seep 4 Piez-1 (SS)	-2.26	-7.64	-	-	-	-
Maui 10 (MS)	-	-	52.46	1	16.35	0.82
Maui 12 (MS)	-	-	57.73	1	21.55	0.82
Maui 14 (MS)	-	-	55.5	1	15.52	0.82
Maui 15 (MS)	-	-	54.43	1	15.67	0.82
Maui 2 (MS)	-	-	12.71	2.26	6.55	4.3
Maui 5 (MS)	-	-	19.71	1	9.24	0.82
Maui 6 (MS)	-	-	18.04	0.56	9.69	0.19
Wahikuli (MS)	-	-	11.86	0.56	3.53	0.19

[1]Measured relative to VSMOW
[2]Measured relative to AIR
3Average standard deviation of standards and duplicate samples
PW = Production Well
MW = Monitor Well
TS = Terrestrial Surface
TW = Treated Wastewater
SS = Submarine Spring
MS = Marine Surface

Table ES-6: September, 2011 stable isotope data
(- denotes measurement not performed)

Sample Name (Type)	$\delta^{18}O$ of H_2O (‰)[1]	$\delta^{2}H$ of H_2O (‰)[1]	$\delta^{15}N$ of NO_3^- (‰)[2]	$\delta^{15}N$ σ (‰)[3]	$\delta^{18}O$ of NO_3^- (‰)[1]	$\delta^{18}O$ σ (‰)[3]
Black Rock 1 (TS)	-	-	10.12	0.23	2.29	0.49
Black Rock 2 (TS)	-	-	8.84	1	2.41	0.82
Kaanapali GC-R1 Pond (TS)	-3.09	-11.34	30.78	0.23	11.72	0.49
Hahakea 2 (PW)	-3.63	-14.69	0.91	0.23	-0.91	0.49
Kaanapali P-1 (PW)	-3.67	-14.64	2.32	0.23	-1.87	0.49
Kaanapali P-2 (PW)	-3.73	-15.11	2.21	0.23	-2.16	0.49
Kaanapali P-4 (PW)	-3.59	-14.65	2	0.39	-0.27	1.54
Kaanapali P-5 (PW)	-3.46	-14.03	2.41	0.39	0.5	1.54
Kaanapali P-6 (PW)	-3.42	-13.93	3.49	0.39	0.33	1.54
Honokowai B (PW)	-3.68	-14.69	2.03	0.39	-1.18	1.54
Lahaina Deep Monitor (MW)	-3.65	-15.7	1.98	0.39	0.79	1.54
LWRF Treated Effluent (TW)	-3.06	-11.37	30.85	0.23	15.92	0.49
LWRF-R1 (TW)	-3.12	-11.39	31.54	0.23	15.03	0.49
Seep 1-2 Piez (SS)	-3.1	-11.45	83.03	0.23	24.46	0.49
Seep 3-2 Piez (SS)	-2.85	-10.54	93.14	0.23	22.45	0.49
Maui 19 (MS)	-	-	22.8	1	1.76	0.82
Maui 22 (MS)	-	-	29.22	1	8.77	0.82
Maui 23 (MS)	0.37	2.32	17.72	1	4.87	0.82
Maui 25 (MS)	0.44	2.82	-	-	-	-
Maui 28 (MS)	0.39	2.24	-	-	-	-
Maui 32 (MS)	0.47	2.64	-	-	-	-

[1]Measured relative to VSMOW
[2]Measured relative to AIR
3Average standard deviation of standards and duplicate samples
 PW = Production Well
MW = Monitor Well
TS = Terrestrial Surface
TW = Treated Wastewater
SS = Submarine Spring
MS = Marine Surface
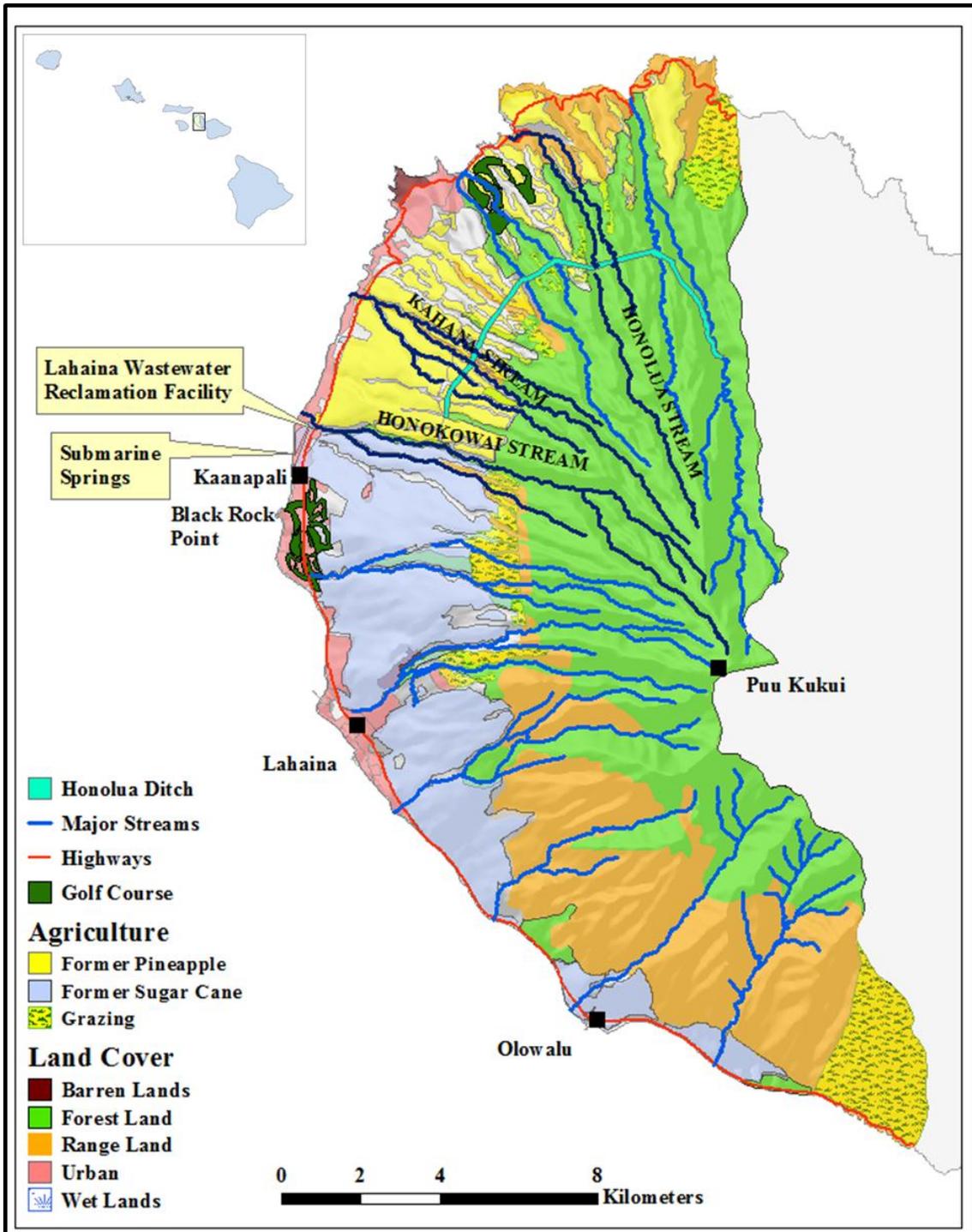
Figure ES-1. Western Maui land-use map.
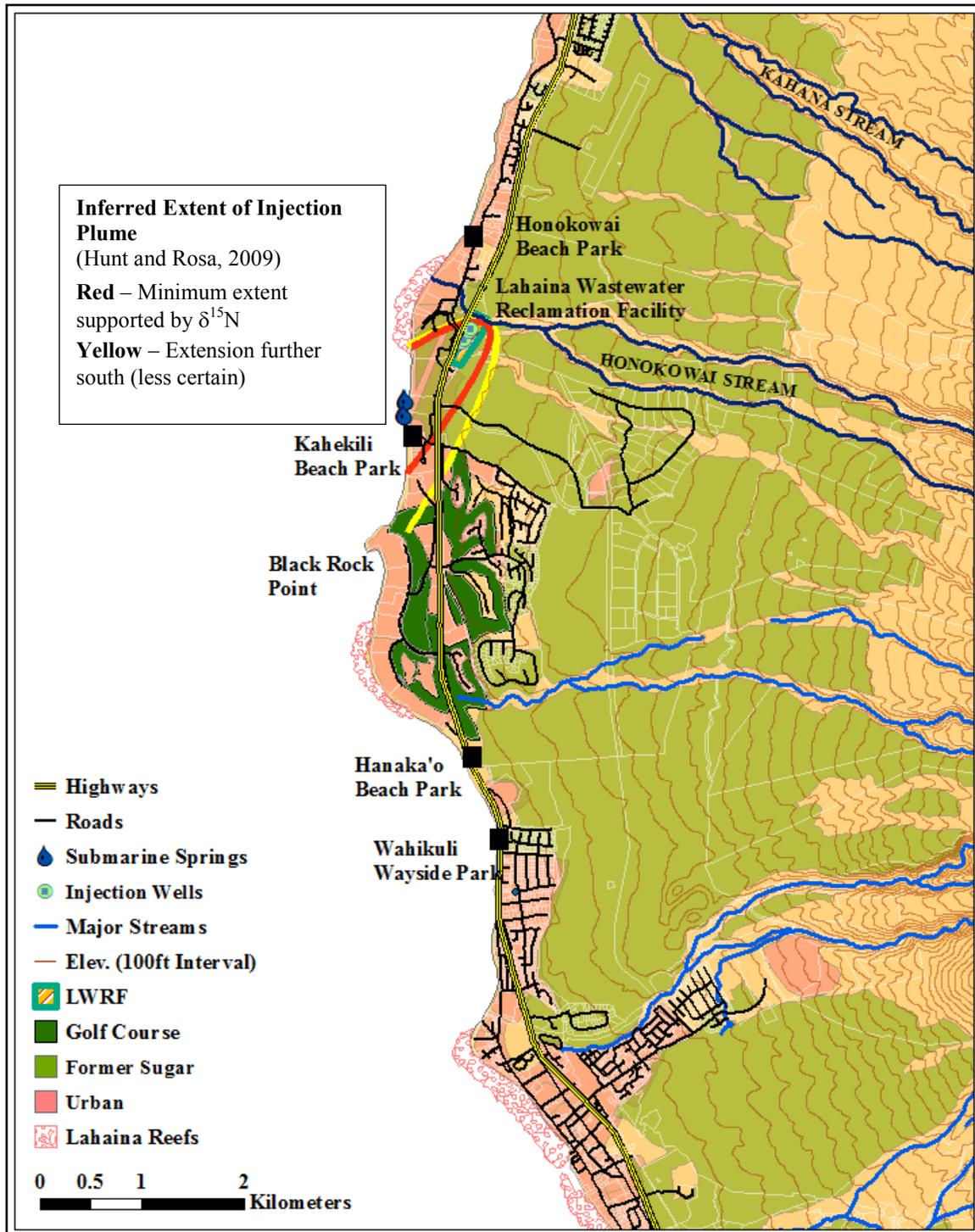
Figure ES-2. Detail of study area showing key locals along the coast.
LWRF injection wells and inferred subsurface minimum and maximum spatial extent of LWRF injection plume from Hunt and Rosa (2009) is also shown.
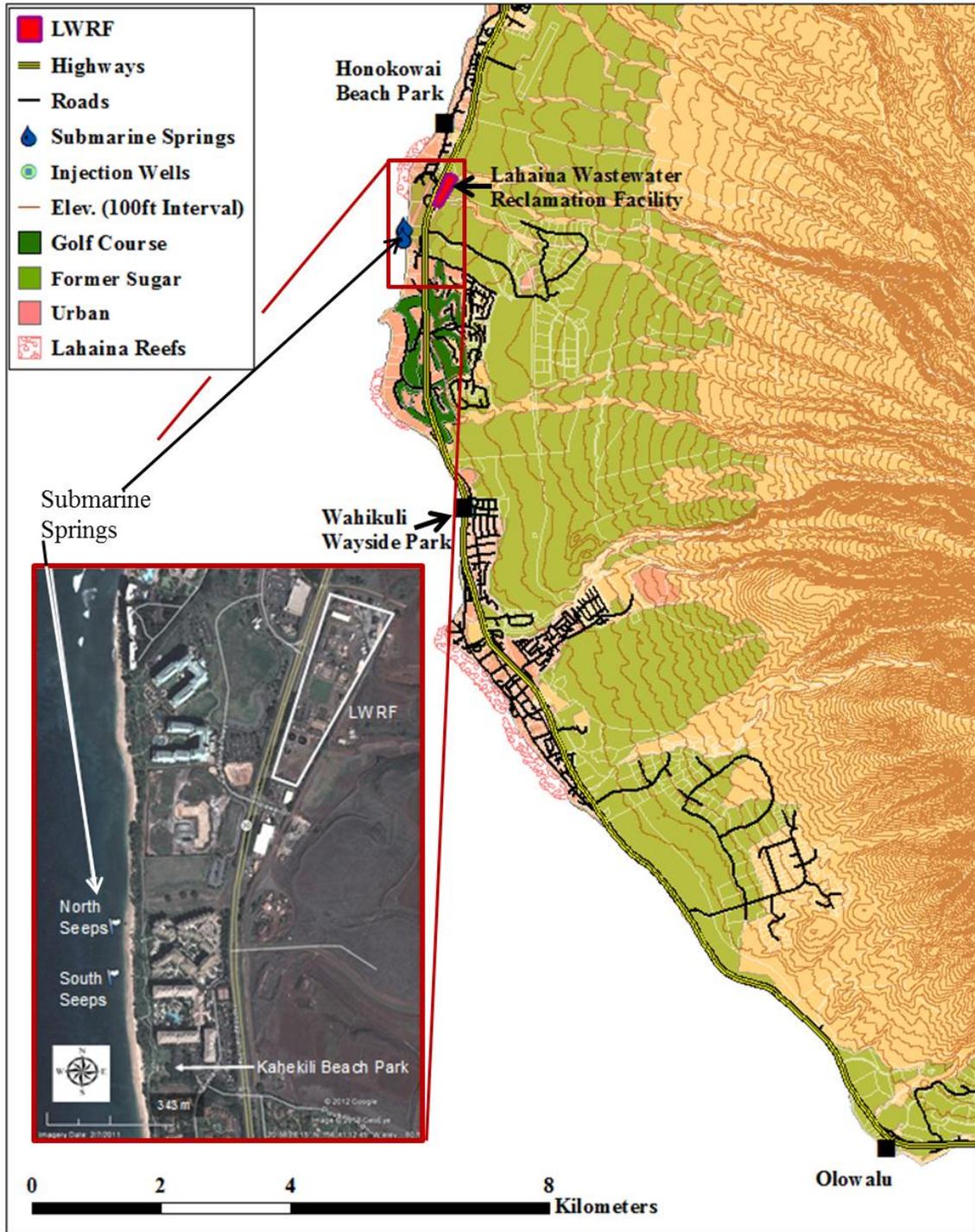
Figure ES-3: Control and submarine spring sampling locations.
Control locations include: Honokowai Beach Park, Wahikuli Wayside Park, and Olowalu. Also shown are the North and South Seep Groups.
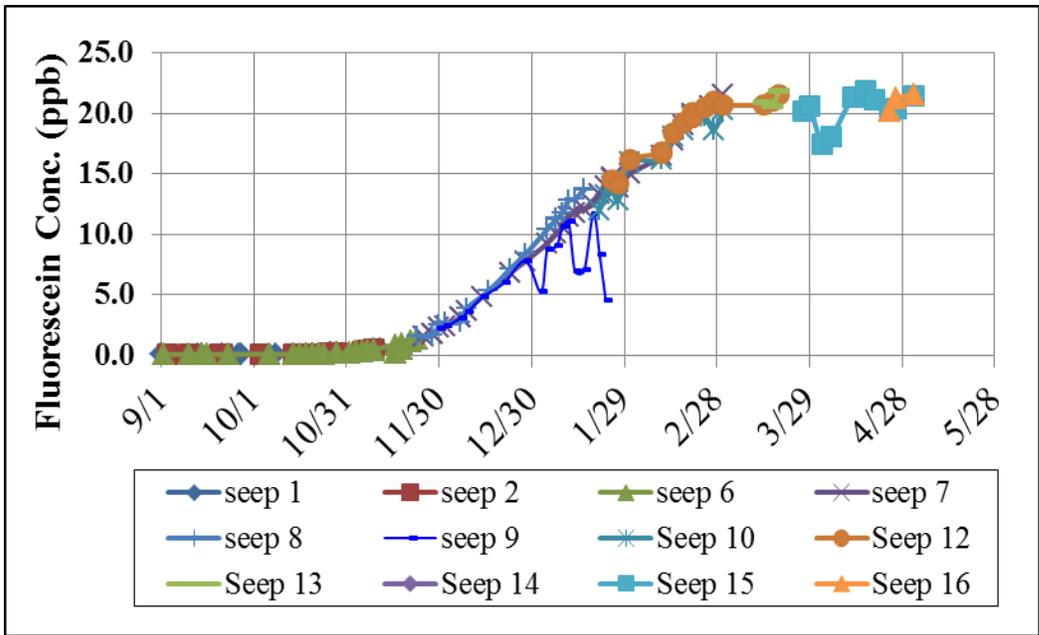
(a) North Spring Group
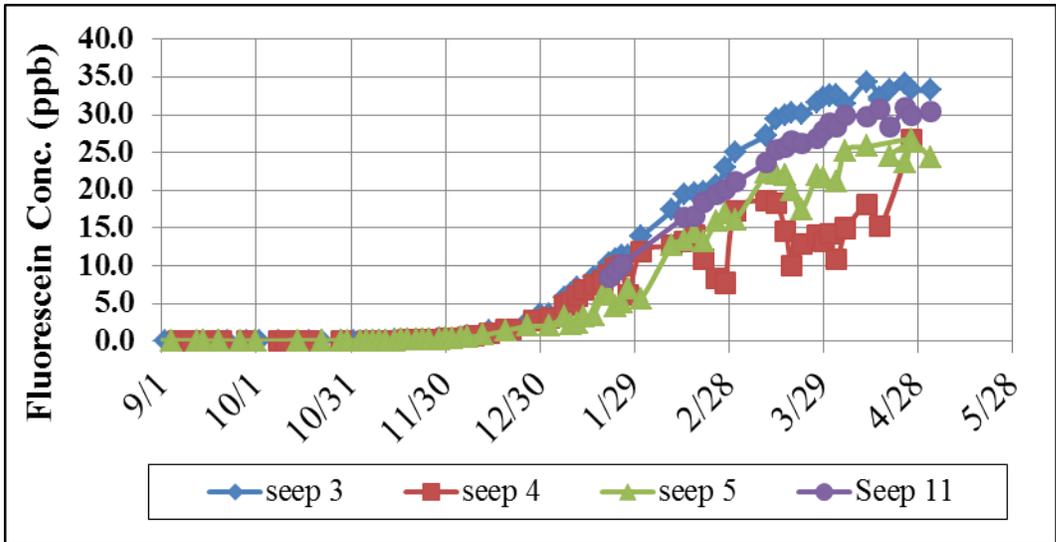
(b) South Spring Group

Figure ES-4: Submarine spring water FLT breakthrough curves for (a) the NSG and (b) the SSG.

The first arrival of dye occurred in late October, 2011 at the NSG and early November, 2011 at the SSG. Both BTCs appear have reached maximum concentrations by early spring with the FLT concentration at the SSG being about 1.5 times that at the NSG.
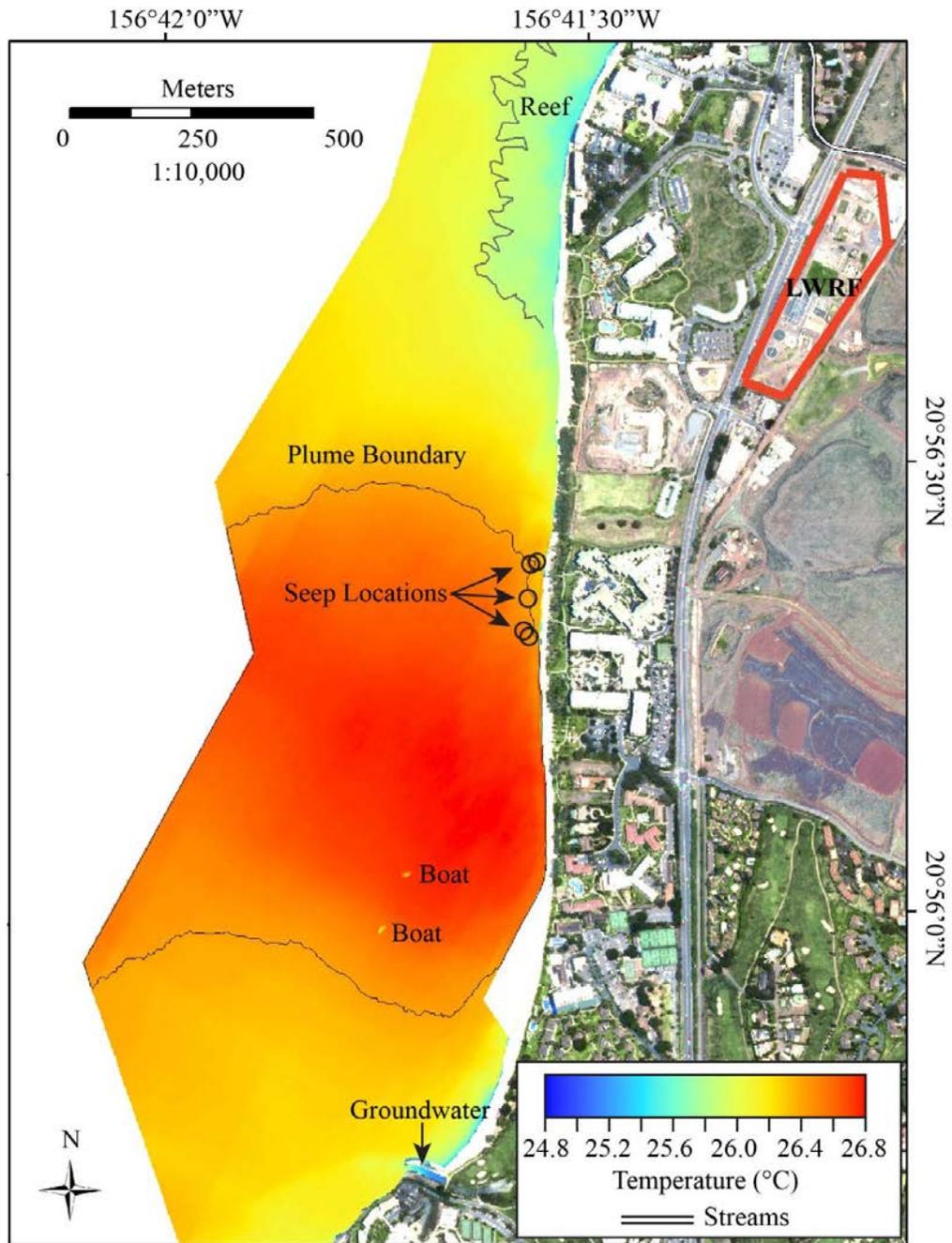
Figure ES-5: Aerial TIR sea surface temperature map thermal anomaly at North Kaanapali Beach.

The plume is greater than 575 m (1886 ft) in width (from the shoreline to the edge of the flight line). There is less than 0.6°C temperature variation within the plume area. The lagoon emptying into the ocean at the southern end of the figure is fed by cold groundwater. Submarine spring (seep) locations are shown on the map correspond to small-scale and semi-isolated thermal anomalies.
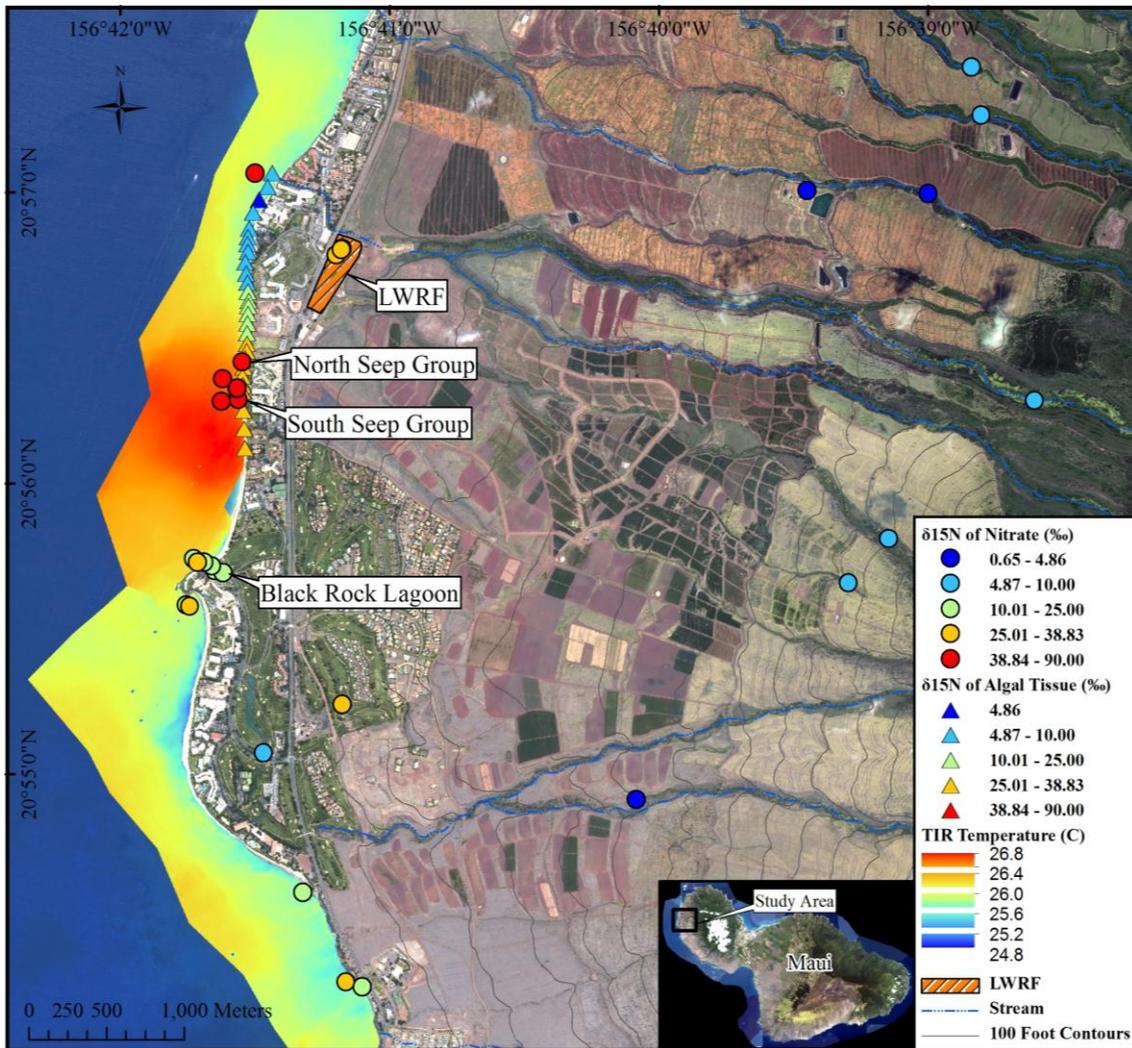
Figure ES-6: Infrared SST pictured with δ^{15}N values of terrestrial and marine waters, and the intertidal macroalgae.

Shown are the δ^{15}N values of intertidal macroalgae (triangles) reported by Dailer et al. (2010) and δ^{15}N values of NO_3^- dissolved in water (circles) reported in this study. The region of elevated SST offshore of Kahekili Beach Park corresponds with elevated δ^{15}N values of macroalgal tissue and dissolved NO_3^-. Note that the majority of marine samples collected had dissolved NO_3^- concentrations below 0.9 μM, the minimum concentration required to perform the dissolved NO_3^- δ^{15}N analysis used in this study. The marine samples pictured here are the few that were above this analytical threshold and thus provide a good spatial representation of above-background dissolved NO_3^-.
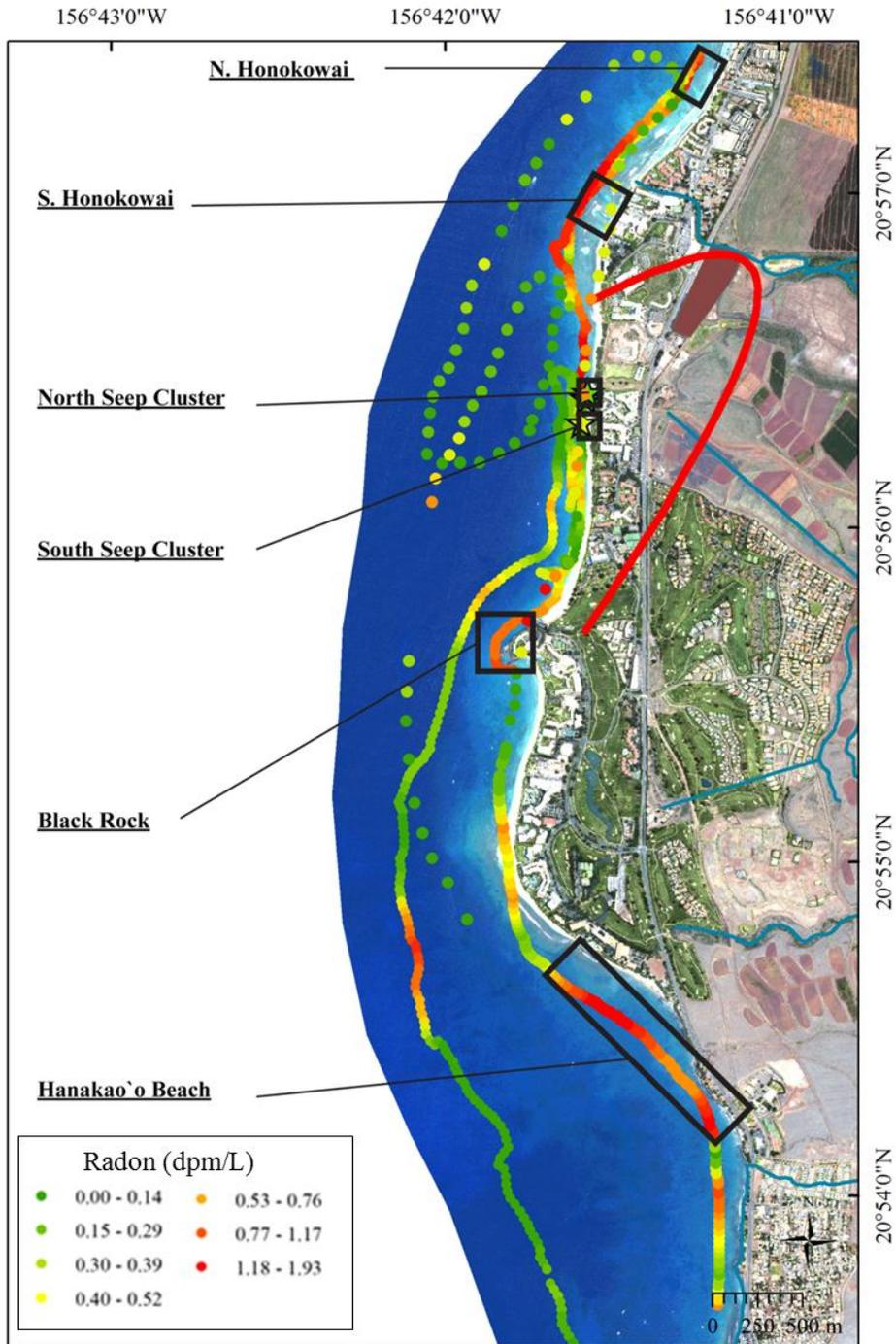
Figure ES-7: Radon activities measured during coastal surveys in June and September, 2011.

Sites with elevated surface radon activities are outlined with a black box. The lengths of the boxes are the approximate lengths of coastline that was within 100 dpm/m^3 of the mean radon concentration for each site and the widths are the distance of the radon survey from the coastline. The latter assumes that groundwater emanates at the coastline. Coastal groundwater fluxes were estimated from these areas.

This page is intentionally left blank.

TABLE OF CONTENTS

LIST OF TABLES

LIST OF FIGURES

.

ACRONYMS

[Cl⁻]	chloride ion concentration
[Mg²⁺]	magnesium ion concentration
°C	degrees Celsius
°F	degrees Fahrenheit
α	Ostwald's solubility coefficient (Section 5), Fractionation factor (Section 6)
ε	Enrichment factor
μm	micrometer
μM	micro-moles
τ	Residence time
ϖ	Advection Rate
A	Activity
ADCP	Acoustic Doppler Current Profiler
AIR	air (stable isotope primary standard for N)
asl	Above sea level
BTC	breakthrough curve
C	Concentration
CFR	Code of Federal Regulations
Cl:Mg	chloride to magnesium ratio
cm	centimeter
CTD	Conductivity, temperature, depth sensor
d	day
dpm	decays per minute (units of radioactivity)
dpm/m³	decays per minute per cubic meter
dpm/m²/hour	decays per minute per square meter per hour
Ex²²²Rn	excess radon isotope with atomic mass 222
F	Flux
FLT	Fluorescein
ft	feet
ft²	square feet
gal.	gallon
HCl	hydrochloric acid
HDOH	State of Hawaii Department of Health
HDPE	high density polyethylene
HR ADCP	high resolution Acoustic Doppler Current Profiler
HST	Hawaii Standard Time
Hz	hertz
I	inventory
IAEA	International Atomic Energy Agency
in	inch
INS/GPS	inertial navigational system and global positioning system
km	kilometer
k	Gas transfer coefficient

L	liter
LxDxW	Length multiplied by depth multiplied by width
L/min	liters per minute
lbs	pounds
LDPE	low density polyethylene
LWRF	Lahaina Wastewater Reclamation Facility
m	meter
m msl	meter reference to mean sea level
m/d	meter/day
m/s	meters per second
m^2	square meter
m^3	cubic meter
m^3/d	cubic meter/day
$m^3/m^2/d$	volume of cubic meter per area of square meter per day
MDL	Method Detection Limit
mg	milligram
mg/L	milligrams per liter
mgd	million gallons per day
ml	milliliter
ML & P	Maui Land and Pineapple
MODFLOW	Modular three-dimensional finite-difference ground-water flow model
MODPATH	A particle-tracking postprocessor model for MODFLOW
mph	miles per hour
mrad	milliradian
MT3DMS	A modular 3-D multi-species transport model for simulation of advection, dispersion, and chemical reactions of contaminants in groundwater systems
MW	monitor well
n	number of samples in a statistical analysis
N	normality
na	not available
NAD-83	North American Datum of 1983
nm	Nano-meters
NOAA	National Oceanic and Atmospheric Administration
NSG	North Seep Group
ppb	parts per billion
ppm	parts per million
PSU	practical salinity units
PW	production well
Q	Discharge
QTracer2	Program for tracer-breakthrough curve analysis for tracer tests in Karstic aquifers and other hydrologic systems
REV	Representative elementary volume
RWT	Rhodamine WT

SEAWAT	A computer program for simulation of three-dimensional variable-density ground-water flow and transport
SGD	submarine groundwater discharge
SOEST	University of Hawaii School of Ocean and Earth Science and Technology
SRB	Sulpho-Rhodamine-B
SS	submarine spring
SSG	South Seep Group
SST	sea-surface temperature
TIR	thermal infrared
TN	Total nitrogen
TP	Total phosphorous
TS	terrestrial surface
TW	treated wastewater
UNESCO	United Nations Educational, Scientific, and Cultural Organization
USACE	United States Army Corps of Engineers
USEPA	United States Environmental Protection Agency
USGS	United States Geological Survey
V	volume
VSMOW	Vienna Standard Mean Ocean Water (stable isotope standard for water)
WGS-84	World Geodetic Survey of 1984

This page is intentionally left blank.

SECTION 1: INTRODUCTION, BACKGROUND, AND PURPOSE

1.1 INTRODUCTION

This report was prepared by the University of Hawaii (UH) under the United States (U.S.) Army Corp of Engineers Cooperative Agreement Number W912HZ-11-2-0020 for the U. S. Army Engineer Research and Development Center at Vicksburg, Mississippi; and State of Hawaii, Department of Health Agreement Number 11-047 with funding provided by a grant from the U.S. Environmental Protection Agency. The purpose of this study has been to provide critical data about the hydrological connection between the injected effluent from the Maui County, Hawaii, Lahaina Wastewater Reclamation Facility (LWRF) and the nearby coastal waters, confirm the locations of emerging injected effluent discharge in these coastal waters, and determine a travel time from the LWRF injection wells to the coastal waters. This report provides the initial results of those findings and provides the results from the study's principal objectives, which have been to: (1) to implement a tracer dye study from the LWRF, (2) conduct continuous monitoring for the emergence of the injected tracer dyes at the most probable points of emergence at nearshore sites within the coastal reaches of the LWRF, (3) conduct an airborne infrared sea surface temperature mapping survey of coastal zone fronting the LWRF in an effort to detect warm and/or cool temperature anomalies that may be indicative of submarine groundwater discharge and possibly warm wastewater effluent, (4) complete radon and radium radiochemical surveys to detect the emergence points and flow rates of the naturally occurring submarine groundwater along the coastal zone, (5) complete geochemical and stable isotopic analyses of LWRF effluent, fresh groundwaters and submarine groundwater discharge in an effort to help partition the relative contribution of effluent waters to the ocean, and (6) combine complete dye emergence breakthrough curves with which to develop groundwater models for the flow paths and rates of effluent to the coastal zone. Each of these six primary objectives are addressed Sections 2 – 7 of this report. Each section contains its own set of methodologies, results, and conclusions, and each has its own appendices, grouped together at the end of the report. Appendices A-F provide ancillary data, maps, and field and laboratory protocols. Appendix G provides comments and replies to the June 2012 draft of this report.

A very important step in this study has been the conductance of a fluorescent dye tracer test to investigate any linkage that may exist between the underground injection of treated municipal wastewater effluent into the sub-surface waters north of the town of Lahaina, Maui, Hawaii, and the discharge of that effluent to the nearshore waters close to the treatment facility. As detailed in Section 3 (Fluorescent Dye Groundwater Tracer Study), we completed two tracer dye injections at the LWRF. In the first tracer test, Fluorescein (FLT) was added to two wells (Injection Wells 3 and 4), and this was followed two weeks later by an addition of Sulpho-Rhodamine-B (SRB) into Injection Well 2, which

1

has a significantly higher injection capacity than Wells 3 and 4. The second tracer injection was completed to investigate whether the effluent from this well discharges into the marine environment at the same location as Wells 3 and 4. At the time of this writing, the FLT tracer dye injected at the LWRF has been well detected in the coastal waters, but the establishment of the full FLT breakthrough curve needed to adequately calculate travel times is still in progress. When established, travel times will be estimated and this part of the study will be combined with continued coastal water flux measurements to estimate the total flux of effluent and nutrient load being discharged into the nearshore waters. Groundwater and transport modeling will be used to interpret the tracer breakthrough curve. Also at the time of this writing, SRB has yet to be conclusively detected in the nearby coastal waters. As such, this portion of the project is still underway, the results of which will be provided in a Final Report that, based on our current best estimates of the degree of tracer dye recovery, is estimated to be completed by April, 2013.

1.2 GEOGRAPHIC SETTING

Located between 155° 57' and 156° 42' west longitude, and 20° 34' and 20° 59' north latitude, the Island of Maui lies near the middle of the Pacific Ocean, far from any continental land mass. Maui is part of an island chain that is formed as the Pacific Tectonic Plate passes over a mid-ocean hotspot. The primary shield volcanoes forming this island chain generally occur in parallel trending pairs (Langenheim and Clague, 1987). Maui is no exception to this trend, consisting of the East Maui Volcano, Haleakala, and the West Maui Volcano. The older volcano – the West Maui Volcano, also referred to as the West Maui Mountains - rises to an altitude of 5,788 ft above sea level (asl) and the younger volcano, the East Maui Volcano (commonly referred to as Haleakala), rises to an altitude of 10,023 ft asl (Figure 1-1). The two volcanoes are separated by an isthmus, generally at an altitude less than 300 ft asl, which is covered with terrestrial and marine sedimentary deposits (Stearns and MacDonald, 1942). The site of this study is located on the northwestern extent of the West Maui Volcano, near the towns of Lahaina and Kaanapali. Steep mountain slopes and narrow stream channels in the uplands and gently dipping plains towards the coast characterize the area. According to the United States Census Bureau (USCB, 2000), there were 1,375 people, 537 households, and 380 families residing in the Kaanapali district with a population density of 282.8 people per square mile. The LWRF is located about 3 mi north of the town of Lahaina.

1.3 OVERVIEW OF THE LAHAINA WASTEWATER RECLAMATION FACILITY

The study area (Figure 1-2) is located in the Kaanapali District of West Maui, Hawaii. The LWRF is about 3 mi north of the town of Lahaina and serves the municipal wastewater needs for that community including the major resorts along the coast. The LWRF receives approximately 4 million gallons per day (mgd) of sewage from a collection system serving approximately 40,000 people. The facility produces tertiary

treated wastewater, which is disposed of via four on-site injections wells, and tertiary treated wastewater that is disinfected with UV radiation to meet R-1 reuse water standards. This R-1 water is sold to customers such as Kaanapali Resort to be used for landscape and golf course irrigation. R-1 water that is not sold is also discharged into the subsurface via the injection wells.

The LWRF consists of two separate plants capable of operating in parallel. The first plant, constructed in 1976 (and currently not in operation), has an average flow capacity of 3.2 mgd, while the other, constructed in 1985 (and modified in 1995) has an average flow capacity of 6.7 mgd. After primary settling to remove a majority of the suspended solids, the LWRF effluent undergoes secondary treatment. This treatment reduces the biodegradable dissolved solids by microbial action that metabolizes the organic matter. The LWRF also incorporates biological nutrient removal to promote nitrogen removal. The effluent is sand filtered to remove solids before injection or further treatment. The effluent that is subjected disinfection using ultraviolet radiation is sold as R-1 grade reuse water for irrigation. This grade of reuse water can be used for irrigation with very little restrictions. The treatment for the water not sold as irrigation water is stopped at the secondary level (Limtiaco Consulting Group, 2005). Prior to October 28, 2011, the effluent discharged into the LWRF injection wells was only partially disinfected with chlorine. Starting from that date to the present time, the injected effluent has undergone full chlorine disinfection.

Limtiaco Consulting Group (2005) summarized the history of the reuse water production at the LWRF. Up to the late 1980s, the LWRF provided R-2 water (reclaimed wastewater with restrictions placed on its use) to the Pioneer Mill for sugarcane irrigation. However, with the phase-out of sugarcane this disposal option disappeared. In the mid-1990s Maui County upgraded the plant to produce R-1 water to address concerns about seasonal benthic algal blooms that were proliferating along the coast. This water is sold to customers such as the Honua Kai Timeshare Resort and the Kaanapali Resort to be used for landscape and golf course irrigation (Scott Rollins, Maui County Department of Environmental Management, Wastewater Reclamation Division, personal communication). The distribution system was extended to make R-1 water available to the Maui Land and Pineapple Company for pineapple irrigation in 2003. This water was to be blended with non-potable water from the Honolua Ditch. However, due to ample rain and the phase-out of pineapple, little use has been made of this option. This infrastructure may be beneficial to the emerging diversified agriculture in West Maui.

The LWRF injects the secondary treated effluent into four injection wells (Figures 1-3 and 1-4). Under the Safe Drinking Water Act an Underground Injection Control (UIC) permit is required from the U.S. Environmental Protection Agency (USEPA) for the injection of subsurface wastewater effluents that might affect potential sources of drinking water. The LWRF's UIC permit expired on June 6, 2005 but per the USEPA's approval the facility is operating under the expired permit until a renewal is approved. Sections 1421 through 1445 and Section 1450 of the Safe Drinking Water Act require that each state establish an UIC program to protect drinking water sources from contamination due to sub-surface fluid injection. Title 40 of the Code of Federal

Regulations, Parts 144 through 148 details the UIC permit regulations. Part 144 lays out the minimum permitting and program requirements. Part 145 details the elements and permitting procedures for a state program, while Part 146 spells out the technical requirements. Part 147 sets forth the UIC program for each state including Hawaii. Much of the oversight of UIC activities is delegated to the states. However, the UIC program for the State of Hawaii is administered by the EPA. The Hawaii UIC program requirements are codified in the Hawaii Revised Statutes (HAR) Title 11, Chapters 23 and 23a

The State of Hawaii UIC restrictions are less stringent if an aquifer is not a potential source of drinking water due to high concentrations of total dissolved solids (TDS). The area of an aquifer that is seaward of an UIC Line is classified as an exempted aquifer. Class V injection wells are allowed in exempted aquifers and this class includes the injection of sewage derived wastewater. The LWRF is located seaward of the UIC line (Figure 1-3) and injects treated effluent to depths of between -55 and -229 feet above mean sea level (ft msl). The screen length or open interval of the wells varies from 95 to 150 feet (ft). Table 1-1 gives the construction details for the injection wells. The average flow rate into the plant is currently about 4.0 mgd (Table 1-2). After reuse, the injection volume averaged 3.1 mdg in May and 3.0 mgd in June. With warmer, dryer months no more than 3.0 mgd is expected to be injected underground. The permitted daily maximum rate is 19.8 mgd and the maximum weekly average injection was 9.0 mgd (County of Maui, 2010). Flows have exceeded 5.0 mgd only 34 days in the last 18 months. As mentioned above, Maui County is in the process of renewing the UIC permit for these wells. However, concerns about the impact of injection well operations have on the coastal environment has prompted research into the amount, distribution, and discharge points of nutrients and other chemicals into the marine environment.

Scientific evidence (e.g. Hunt and Rosa, 2009; Dailer et al., 2010, 2012) supports the hypothesis that effluent injectate from the LWRF is discharging into the nearshore waters southwest of the plant. However, at the time that the present study was started, the extent of that link had not been irrefutably established. One of the goals of this project has therefore been to tag the effluent with a fluorescent dyes prior to injection and monitor the nearshore for emergence of the dye at nearby coastal submarine springs, particularly those identified by Hunt and Rosa (2009) and Dailer et al. (2010, 2012). Figure ES-2 and Figure 1-4 shows the location of the submarine springs relative to the LWRF.

1.4 HISTORY OF RELATED INVESTIGATIONS

Examples of relevant previous studies include nutrient characterizations and loading estimates for this area (Souza, 1981, Tetra Tech, 1993; Soicher and Peterson, 1997), a dye tracer test (e.g. Tetra Tech, 1994), and those concerning the potential linkages land-derived nutrients and algae blooms (e.g. Dollar and Andrews, 1997; Borke, 1996; Smith et al., 2005; Smith and Smith, 2007). More recent scientific investigations on Maui include Hunt and Rosa's (2009) multi-tracer approach to detect effluent discharges in Lahaina and Kihei, Dailer et al.'s (2010, 2012) extensive work using stable isotope data

from intertidal and nearshore cultivated algae, and recent groundwater investigations for West Maui modeling by the USGS (Gingerich, 2008, Gingerich and Engott, 2012).

In response to concerns prompted by seasonal algae blooms in West Maui, the USEPA sponsored a nutrient balance study of West Maui (Tetra Tech, 1993). That report identified the LWRF as one of the three primary nutrient release sources to Lahaina District coastal waters, with sugarcane and pineapple cultivation being the other two. This study ranked the LWRF second in annual nitrogen contribution and first in phosphorous contribution to these waters. Since that study was completed, the cultivation of both sugarcane and pineapple has been sharply curtailed. This implies that the LWRF may now be the primary contributor of nutrients to water in the study area. The West Maui Watershed Owner's Manual (West Maui Watershed Management Advisory Committee, 1997) reevaluated N and P loadings in the watershed and concluded that as of 1996, wastewater injection wells contributed ca. 94% of land-derived phosphorus-loading and ca. 57% of land-derived nitrogen-loading to the ocean, relative to the other sources evaluated (cesspools and inputs from pineapple-, sugarcane- and golf course-developed lands). However, as discussed in Section 6, it must be noted that since the release of the Tetra Tech (1993) report, all nutrient species concentrations in the LWRF effluent appear to have been significantly reduced, likely in association with the inception of treatment process improvements such as biological nutrient removal in 1995.

Tetra Tech (1994) also estimated the travel time of effluent from the point of injection to the coast using a two-dimensional numerical flow model. Based on that model, the travel time could be as short as 10 days. In absence of any injection, the travel time would be increased to 50 days based on the average groundwater-flow velocity. The model assumed an aquifer thickness of 20 ft. Using the Ghyben-Hertzberg principle, the freshwater lens thickness is 41 times the groundwater elevation above sea level (Fetter, 1988), which yields a more accurate aquifer thickness of 80 to 100 ft near the LWRF. This is based on a water table elevation of 2 to 2.5 ft msl (Gingerich, 2008). The thinner modeled aquifer thickness would result in a shorter travel time. Also, the distance between the LWRF injection wells and the nearest identified submarine spring is approximately 0.49 mi, which is greater than the direct path distance to the shoreline. The eastern boundary of the Tetra Tech model was the interface between the high level water at the interior of the island and the basal groundwater. This was assigned as a no-flow boundary condition. In actuality, however, there is significant groundwater flow from the high-level water body to the basal groundwater (Gingerich, 2008; Gingerich and Engott, 2012).

Since the LWRF was identified as a major contributor of nutrients to the marine environment in the 1993 study, an effluent fate and transport study was commissioned by the USEPA. Tetra Tech (1994) conducted a tracer test to identify the submarine locations where the effluent was discharging into the marine environment. They added Rhodamine WT (RWT), a fluorescent tracer dye, into the effluent stream prior to underground injection at a concentration of approximately 100 parts per billion (ppb). This injection lasted for 58 days. To monitor for the emergence of the effluent tagged

with RWT, they completed a series of monitoring transects offshore north-northeast transects. Every 200 yards, a pump suction was let drift to the ocean bottom. The suction line was connected to a pump on the survey boat with the discharge from the pump ported through a constant monitoring fluorometer. In that study, only two occurrences of elevated fluorescence were detected at adjacent sampling locations, in the southeast corner of their sampling grid (Figure 1-4). The fluorescence value was low, about three times that of background. The first detection occurred 55 days after the start of injection and the second detection occurred 61 days after the start of injection. The location of the Tetra Tech elevated fluorescence detections was very near the submarine springs identified by Hunt and Rosa (2009) and Dailer et al. (2010, 2012) as probable discharge points for the LWRF effluent. Due to the fluorescence values being only slightly above background, it is uncertain whether the source was the RWT dye, or another fluorophore such as dissolved organic matter. Figure 1-4 illustrates the location where Tetra Tech detected RWT fluorescence, the submarine springs suspected of discharging effluent, and the plume area proposed by Hunt and Rosa (2009).

Hunt and Rosa (2009) investigated the use of multiple in-situ tracers to identify where and how municipal wastewater effluent discharges to the nearshore marine environment. These researchers sampled the LWRF effluent, submarine springs, nearshore marine waters, groundwater, and terrestrial surface water in vicinity of effluent injection sites in Lahaina and Kihei, Maui. They concluded that the most conclusive tracers were the presence of pharmaceuticals, organic waste indicator compounds, and a highly elevated $\delta^{15}N$ values (due to a higher proportion of the heavy ^{15}N isotope compared to the more abundant ^{14}N isotope in dissolved NO_3^-) in water samples and coastal benthic macroalgal tissue. These researchers identified the submarine springs as the coastal locus of the LWRF injection plume, though they also cited nearshore marine samples collected further south towards the Kaanapali Golf Course as showing geochemical evidence of effluent or effluent-derived irrigation water influence. They also noted elevated nutrient concentrations and potential effluent or effluent-derived irrigation water influence in Black Rock lagoon, an apparently groundwater fed, ocean-connected drainage feature located on the Kaanapali Golf Course at the southern end of North Kaanapali beach. Particularly pertinent to the current study, they investigated background fluorescence along the shoreline near the LWRF, where they measured fluorescence with a handheld fluorometer with an optical brightener and a Rhodamine WT channel. They detected optical brightener fluorescence in samples collected at the submarine springs that was 15 times that in the water column near the submarine springs. There was no difference in Rhodamine WT fluorescence between the submarine spring and the water column samples. This indicates that non-dye fluorophores in LWRF effluent were probably not responsible for the elevated RWT fluorescence detected by Tetra Tech (1994). This further indicates that the elevated fluorescence in the RWT wavelength detected by Tetra Tech (1994) was likely from the dye they added to the effluent.

Dailer et al. (2010, 2012) used the stable isotopic composition of macroalgae ($\delta^{15}N$) to map the anthropogenic input of nitrogen to the nearshore waters of Maui. Atmospheric and fertilizer $\delta^{15}N$ values generally fall in the range of -4‰ to +4‰. Input from sewage can generally be identified by its higher $\delta^{15}N$ values that range from 7‰ to 38‰ (e.g.

Kendall, 1998; Gartner et al., 2002), although isotope effects associated with various biogeochemical N transformations must be carefully considered when attempting to identify original N sources using this methodology. The two highest $\delta^{15}N$ values (33.2 and 43.3‰) measured by Dailer et al. (2010) were found at sites near the submarine springs. These researchers also observed that the submarine spring discharge was warmer than ambient seawater and that the discharge points were surrounded by rocks coated with a distinctive black precipitate thought to consist of iron oxides.

Significant work has been done on the wastewater injection and the fate of this injectate in Hawaii. Oberdorfer and Peterson (Oberdorfer and Peterson, 1982; Oberdorfer, 1983) studied the processes that lead to injection well clogging and the fate of nutrients in the injected effluent. They found that a significant amount of denitrification (nitrate reduction) occurs in the subsurface after injection. Petty and Peterson (1979) investigated sewage injection practices in West Maui including resorts and condominiums. The fate of wastewater injection plumes was modeled by Hunt (2007), Burnham et al. (1977), Wheatcraft et al. (1976), Tetra Tech (1993) and Hunt and Rosa (2009) and all studies showed that once the wastewater effluent is injected, the plume tends to rise due to its positive buoyancy relative to the surrounding saline groundwater.

There have been several chemistry surveys and studies of anthropogenic inputs into the coastal waters of West Maui in addition to those already cited. Laws et al., (2004) showed that coastal nutrient concentrations exceeded State water-quality standards for marine waters. Street et al. (2008) investigated submarine groundwater discharge (SGD) using multiple tracers such as the radon/radium pair, silica, and salinity. They estimated that the SGD near the study site was 0.07 to 0.12 meters cubed (m^3) per meters squared (m^2) per day (d), delivering a dissolved inorganic nitrogen load of 13.3 to 36.8 mM per m^2/d. Dollar et al. (1999) and Atkinson et al. (2003) monitored for estrogen as indicator of discharge of cesspool effluent to the waters of west and south-central Maui. Soicher and Peterson (1997) studied the nutrient input to West Maui coastal waters and concluded that stream discharges were an acute nitrogen source, but chronic SGD was the major contributor.

1.5 STUDY AREA DESCRIPTIONS AND BACKGROUND

1.5.1 Climate

Maui's climate is characterized by mild and uniform temperatures, seasonal variation in rainfall, and great geographic variation in rainfall (Lau and Mink, 2006). The average temperature in Lahaina, on the leeward coast of the West Maui Volcano, is 75.7º F, whereas the average at Haleakala summit is 47º F (WRCC, 2011). During the warmer dry season (May-September), the stability of the north Pacific anticyclone produces persistent northeasterly trade winds, which blow 80-95 % of the time (Gingerich, 2008). During the cooler rainy season (October–April), migratory weather systems often travel past the Hawaiian Islands, resulting in less persistent trade winds that blow 50-80 % of the time (Gingerich, 2008). Low-pressure systems and associated southerly (Kona) winds

can bring heavy rains to the island, and the dry coastal areas can receive most of their rainfall from these systems.

The variation in mean annual rainfall with altitude is extreme on Maui, with differences of more than 130 inches within one mile of the summit of West Maui Volcano where average annual rainfall exceeds 340 inches per year (in/yr) (Giambelluca et al., 2011). Mean annual rainfall at the Kaanapali coast in the dry leeward areas south of Lahaina is less than 15 in/yr (Giambelluca et al., 2011). At higher altitudes, precipitation is a combination of rainfall and fog drip where the montane forest canopy intercepts cloud water. Engott and Vana (2007) and Scholl et al. (2004) estimated that fog drip contributes to an additional 20% of rainfall along the windward flanks of West Maui above an elevation of 2000 ft asl.

Annual pan evaporation of West Maui has been reported by Ekern and Chang (1985) and Engott and Vana (2007) to range between 90 and 100 in/yr near the Kaanapali coast and from 50 to 60 in/yr near the summit of the West Maui Volcano. The streams in the Lahaina area are typically perennial above 1,000 ft asl, but diversions and loss to groundwater at lower altitudes result in intermittent flow as the streams approach the ocean. Honokohau Stream (Figure ES-1 and ES-2) is the only true perennial stream in the immediate study area, however stream flow is flashy due to intense rainfall and the steep topography (Tetra Tech, 1993).

1.5.2 Land Use

Current West Maui land use can be subdivided into (1) an urban center in the Lahaina area, (2) various diversified agriculture and pasture land on former pineapple and sugarcane fields on the lower slopes of the West Maui Mountain, (3) residential and resort development (including golf courses) along the shoreline, and (4) natural evergreen forest in the interior of the West Maui Mountain (Figure ES-1). Historical changes in agricultural land use within the western half of West Maui were estimated by Engott and Vana (2007) in order to estimate the effects of rainfall and agricultural land use changes on West and Central Maui groundwater recharge, and the following sections on land use are summarized from their work, and as summarized by Gingerich (2008) and Gingerich and Engott (2012). During the early 1900s until about 1979, land use was mostly unchanged except for some minor urbanization along the coasts. However, as large-scale plantation agriculture declined after 1979, land-use changes were more significant. From 1979 to 2004, agricultural land use declined about 21 percent, mainly from the complete cessation of sugarcane agriculture.

The Pioneer Mill Co. was the major sugarcane cultivator on the west side of the West Maui Mountain, operating during the late 1800s until 1999, when it ceased sugarcane production and the land was subsequently bought by Maui Land and Pineapple (ML & P) and other private investors. ML&P had a long history of cultivating pineapple on the northwest slope of West Maui Mountain generally on land located to the north of the former sugarcane fields. More recently, they grew pineapple on former Pioneer Mill Co. sugarcane lands located north of Honokowai Stream. The extent of pineapple agriculture

in West Maui decreased extensively since the late 1990s and was stopped entirely in 2009 (Gingerich and Engott, 2012). Large portions of the former sugarcane and pineapple fields remain fallow while other parcels have been converted to low-density housing and diversified agriculture.

1.5.3 Geology

The study site is located on the northwestern extent of the West Maui Volcano. This is the older of the two Maui shield volcanoes. Figure 1-5 shows the geology of West Maui, which consists of a central caldera and two main rift zones that trend north-northwest and south-southeast from the caldera (Stearns and MacDonald, 1942; Sherrod et al., 2007). Numerous dikes occur as thin, near-vertical sheets of massive, low-permeability rock that are present within the rift zones and increase in abundance toward the caldera and with depth. Other dikes also exist outside the two major rift zone trend (Figure 1-5), creating a radial pattern of dikes emanating from the caldera (MacDonald et al., 1983). The volcanic rocks that originated from vents in and near the caldera and rift zones comprise (1) the mostly shield-stage Wailuku Basalt, (2) the postshield-stage Honolua Volcanics, and (3) the rejuvenated-stage Lahaina Volcanics, a minor unit of the West Maui Volcano. All these rocks are Pleistocene in age and are mainly comprised of tholeiitic/picritic basalt, trachyte and basanite layers ranging in thickness from 1 to 500 ft (Stearns and MacDonald, 1942; Langenheim and Clague, 1987; Sherrod et al., 2007). These layers in the Wailuku Basalt show numerous interflow structures within a series of lava flows and associated pyroclastic and sedimentary formations. The volcanic rocks in the area are characterized by high permeability and storage capacity and comprise the main aquifers for groundwater withdrawal (Gingerich, 2008). The Honolua Volcanics were produced by late eruptions, and overlie the Wailuku basalts. They are more massive and tend toward andesitic compositions. Due to their increased thickness and denser nature, their permeability is much lower than those of the Wailuku Basalts. They are more prevalent in the northeast and northwest slopes of the West Maui Volcano (Gingerich, 2008: Sherrod et al., 2007) and do not intersect the groundwater in the study area. The Lahaina Volcanics resulted from rejuvenation stage eruptions that took place 610,000 - 385,000 years ago. As with the Honolua Volcanics, they are more massive in nature. However, their small areal extent and proximity to the coast makes this unit less important when assessing groundwater flow than the other volcanic units. An outcrop of the Lahaina Volcanic series known as Puu Kekaa, or Black Rock, is located in the southwest portion of the study area (Figure 1-5).

Gingerich and Engott's (2012) work projected the top of the West Maui Wailuku Basalts to reach depths of about 600 meters below sea level (mbsl) at a distance of about 10 km from the shore. Wedge-shaped consolidated Quaternary alluvium forms a sedimentary surface veneer that drapes and overlies the Wailuku Basalt along the coast, infills the deep canyons in the West Maui Volcano, and very likely into the offshore (Stearns and MacDonald, 1942; see Figure 1-6). These alluvial deposits formed as a result of the extensive erosion that has carved the deep valleys into the eastern flanks of the West Maui Volcano, and form West Maui's low-permeability caprock. It is probable that some of these sediments also contain relict marine carbonates deposited in relation to former

stands of the sea. This formation, like elsewhere in Hawaii, is of great hydraulic importance as it overlies high-permeability dike-free volcanic rocks below and, due to its relatively low conductivity, generally impedes fresh groundwater discharge towards the coast (cf. Lau and Mink, 2006; Rotzoll et al., 2007; Gingerich and Engott, 2012, and discussion and references therein).

1.5.4 Regional Groundwater Hydrology

The precipitation that falls on West Maui is partitioned between surface runoff, evapotranspiration, soil moisture storage, and groundwater recharge. Recharge, (the fraction of groundwater that reaches the water table), flows radially out from the central highlands to discharge areas along the coast. Figure 1-7 shows the groundwater recharge distribution for West Maui and the extent of the high-level water body (Engott and Vana, 2007; Gingerich, 2008). Recharge rates range from 350 inches per year (in/yr) at the high elevations to less than 10 in/yr along the coast. The high recharge and low hydraulic conductivity of the dike zones in the interior regions of the West Maui Volcano result in a water table with elevations up to 3,000 feet above mean sea level (ft msl) (Gingerich, 2008; Figures 1-5 - 1-7). Figure 1-5 shows the approximate interface between the high level and basal aquifers (Mink and Lau, 1990). The dike impoundment of the groundwater is breached in areas where erosion has cut deep valleys and subterranean water provides baseflow for the streams.

In the subsurface, once the groundwater flows out of the high-level water body, it becomes a lens of freshwater floating the underlying saltwater with a water table elevation of less than a few tens of feet above sea level. This Ghyben-Herzberg principal states the thickness of the freshwater lens is 41 times the elevation of the water table above sea level. This is only an estimation based on simplifying assumptions, however, and the actual thickness of the freshwater lens can deviate from this value due to factors such as non-horizontal flow and heterogeneous geology (Izuka and Gingerich, 1998). The mixing of the two waters in the basal lens along the groundwater flow path results in a sloping transition rather than a sharp interface between fresh and saltwater.

As the groundwater approaches the shoreline, it may encounter the sedimentary caprock described above, which retards the groundwater's seaward flow (Figure 1-6). The effective hydraulic conductivity of the caprock is significantly lower than that of thin-bedded lavas, causing a thicker freshwater lens due to the higher potentiometric (or hydraulic head) surface and a barrier that reduces saltwater intrusion into the aquifer. As shown in the highly generalized Figure 1-6, the condition in the basalt aquifer changes from unconfined condition to a confined condition where the water table meets the bottom of the caprock, which can be considered itself as an unconfined aquifer. The height of the water table within this aquifer should be lower than the potentiometric surface. Drilling logs from the injection wells at the LWRF indicate that sedimentary deposits extend below the potentiometric surface caused by that overlying confining layer for a portion of the aquifer between the facility and the coast (County of Maui, 2004). Preferential flow paths in the aquifer can result in well-defined submarine springs, as is

the case in this study area. In addition to preferential-flow point discharges, a more diffuse discharge may also be present over a larger area.

1.5.5 Aquifer Properties

Total porosity estimates for basaltic rocks on Hawaii and elsewhere ranges from less than 0.05 to more than 0.5 (Hunt, 1996; Kwon et al., 1993; Nichols et al., 1996). Low porosity values may be associated with massive features, including dense flows, a'a cores, dikes, and thick lava flows, and high values may be associated with fractures and a'a clinker zones. Estimates of effective porosity (which includes only the hydraulically interconnected pore spaces) derived from modeling studies range between 0.04 and 0.10 for volcanic-rock aquifers (Gingerich and Voss, 2005; Oki, 2005). Souza and Voss (1987) and Gingerich (2008) estimated an average effective porosity of the volcanic rocks on Hawaii of 0.15. Rotzoll and El-Kadi (2007) analyzed aquifer-test data from wells in central Maui and estimated specific storage and specific yield from one test to be 2.0×10^{-6} ft^{-1} and 0.07, respectively. Hydraulic conductivities (K) of the igneous and sedimentary rocks on West Maui are highly variable and are distributed heterogeneously around the area. Regional K values have been estimated from specific capacity values of aquifers to range between 250 ft/d to 4,100 ft/d (Rotzoll and El-Kadi, 2007).

Though high and low conductivity volcanic aquifers may alternate over several feet depth (Stearns and MacDonald, 1942), the volcanic aquifers on Maui are generally regarded as one unconfined system (Gingerich, 2008). This is because highly permeable structures, such as clinkers and vertical fractures have been commonly observed in all lava flows both in outcrops and rock cores (Langenheim and Clague, 1987). Additionally, numerical groundwater flow models yielded a relatively good agreement between modeled and measured water levels on Maui when uniform conductivity, porosity and specific yield values had been assigned (Gingerich, 2008).

The water transport characteristics of the various aquifer materials vary greatly along the flow path. The hydraulic conductivity of the dike-intruded lavas in Hawaii is estimated to range from 1 to 500 ft/d (Hunt, 1996). The low end of this estimate would be more representative of the West Maui Volcano due to the high density of dikes in the high water body. In a groundwater model of West Maui, Gingerich (2008) assigned a horizontal hydraulic conductivity of 2,097 ft/d and a vertical hydraulic conductivity of 10.5 ft/d for the Wailuku Basalts in the Lahaina area. These estimates equate to a horizontal to vertical anisotropy of 200. For the sedimentary deposits he used values of 17 and 0.38 ft/d for the horizontal and vertical hydraulic conductivity, respectively.

1.5.6 Submarine Groundwater Discharge

The ultimate natural and final release of most groundwater in the Hawaiian Islands is to the ocean as submarine groundwater discharge (SGD). Nearly all groundwaters undergo chemical modifications and additions due to natural leaching of nutrients along their flow paths. Infiltration from agricultural, urban and metropolitan lands, and wastewater injections near the coast can also additionally contribute to the dissolved load of the SGD

subterranean flow. These waters thus exit as chemically-modified mixtures of freshwater and recirculated seawater which flow seaward throughout each island's peripheral aquifers. Geohydrological budgets (Shade, 1996, 1997, 1999) indicate that the majority of groundwater which enters and recharges Maui's uplands is eventually discharged as SGD (Figure 1-8). In most settings in Hawaii, SGD exits along the coast as relatively cool, brackish waters.   The most strikingly anomalous expression of SGD within the present study area, however, is the seepage of localized and anomalously warm and brackish SGD, particularly in the area described as submarine springs (or "seeps") along the Kaanapali coast near Kahekili Beach Park, about 0.5 miles southwest of the LWRF. The warm and brackish SGD issuing from these warm water submarine springs entrain gas bubbles and discharge from cracks and small vents in the semi-consolidated hard bottoms, as well as from unconsolidated patches of surficial sands on the seafloor. During this study, we have grouped clustering of these warm water submarine springs into two groups, and termed these the North Seep Group (NSG), which occur within 3 to 5 m of shore, and the South Seep Group (SSG), which occur within 25 m of shore (Figures ES-3 and 1-4). Over 10 months of study, the salinity of seeps in the NSG varied between 2.5 and 23 with an average of about 4.8. Seeps in the SSG had salinities that were slightly lower, varying between 3.8 to 22, with an average of about 4.1.   The detection, mapping and investigation of the warm SGD issuing from these submarine springs, as well the occurrences of SGD elsewhere in this region, is a major focal point addressed throughout this report.

Table 1-1. Construction Details of the LWRF Injection Wells

Injection Well No.	1	2	3	4
Construction Date	1979	1979	1985	1985
Elevation (ft msl)	33	33	28	29
Total Depth of Well (ft bgs)	200	180	225	255
Solid Casing Length (ft)	88	88	108	108
Bottom of Well (ft msl)	-168	-150	-200	-229
Screen/open hole length (ft)	115	95	120	150
Top of Screen/Open Hole elevation (ft msl)	-55	-55	-80	-79
Bottom of Screen/Open Hole Elevation (ft msl)	-170	-150	-200	-229

Data from Maui County Department of Environmental Management

Table 1-2. Effluent injections rates for April 2011 through June 2012

	Well 1 (mgd)	Well 2 (mgd)	Well 3 (mgd)	Well 4 (mgd)	Total Injection (mgd)
April, 2011					
Minimum	0.17	0.99	0.66	0.58	2.86
Average	0.22	1.63	0.88	0.82	3.55
Maximum	0.27	2.75	1.05	1.06	4.86
May, 2011					
Minimum	0.15	0.31	0.74	0.67	2.41
Average	0.21	1.04	1.05	0.83	3.14
Maximum	0.29	2.1	1.36	0.94	4.23
June, 2011					
Minimum	0.1	0.14	0.31	0.86	2
Average	0.2	0.7	1.18	1.03	3.11
Maximum	0.28	1.52	1.62	1.27	4.03
July, 2011					
Minimum	0.07	0.02	1.19	1.03	2.56
Average	0.19	0.41	1.36	1.15	3.11
Maximum	0.27	1.14	1.74	1.32	3.8
August,2011					
Minimum	0	0.21	1.1	1.04	2.57
Average	0.2	0.62	1.22	1.13	3.17
Maximum	0.27	2.12	1.47	1.46	5.05
September, 2011					
Minimum	0.02	0.01	1.02	0.93	2.36
Average	0.13	0.25	1.23	1.07	2.69
Maximum	0.23	0.72	1.56	1.41	3.73
October, 2011					
Minimum	0.12	0.07	1.11	1	2.61
Average	0.17	0.5	1.25	1.12	3.04
Maximum	0.29	0.97	1.43	1.36	3.75
November, 2011					
Minimum	0.06	0.07	1.16	1.14	2.59
Average	0.16	0.63	1.32	1.37	3.48
Maximum	0.22	1.06	1.48	1.67	4.30
December, 2011					
Minimum	0.00	0.00	0.00	0.00	0.00
Average	0.13	0.67	1.13	1.30	3.24
Maximum	0.19	2.19	1.41	1.67	4.89

Table 1-2. Effluent injections rates for April of 2011 through June of 2012 (Continued)

	Well 1 (mgd)	Well 2 (mgd)	Well 3 (mgd)	Well 4 (mgd)
January, 2012				
Minimum	0.04	0.18	1.04	1.18	3.17
Average	0.13	0.75	1.25	1.51	3.64
Maximum	0.19	1.65	1.54	2.08	4.76
February, 2012				
Minimum	0.01	0.00	0.58	1.21	2.06
Average	0.08	0.18	1.59	1.53	3.38
Maximum	0.13	0.56	2.53	1.81	4.03
March, 2012				
Minimum	0.00	0.00	1.57	1.07	2.72
Average	0.07	0.06	1.90	1.39	3.42
Maximum	0.19	0.20	2.41	1.87	4.65
April, 2012				
Minimum	0.00	0.00	1.56	0.84	2.40
Average	0.04	0.01	1.81	1.16	3.03
Maximum	0.16	0.15	2.14	1.49	3.79
May, 2012				
Minimum	0.00	0.00	1.46	0.79	2.32
Average	0.03	0.01	1.80	1.19	3.03
Maximum	0.16	0.06	2.25	1.74	4.07
June, 2012				
Minimum	0.00	0.00	1.53	0.96	2.52
Average	0.08	0.02	1.94	1.33	3.36
Maximum	0.22	0.12	2.35	1.84	4.48

Data from Maui County Department of Environmental Management
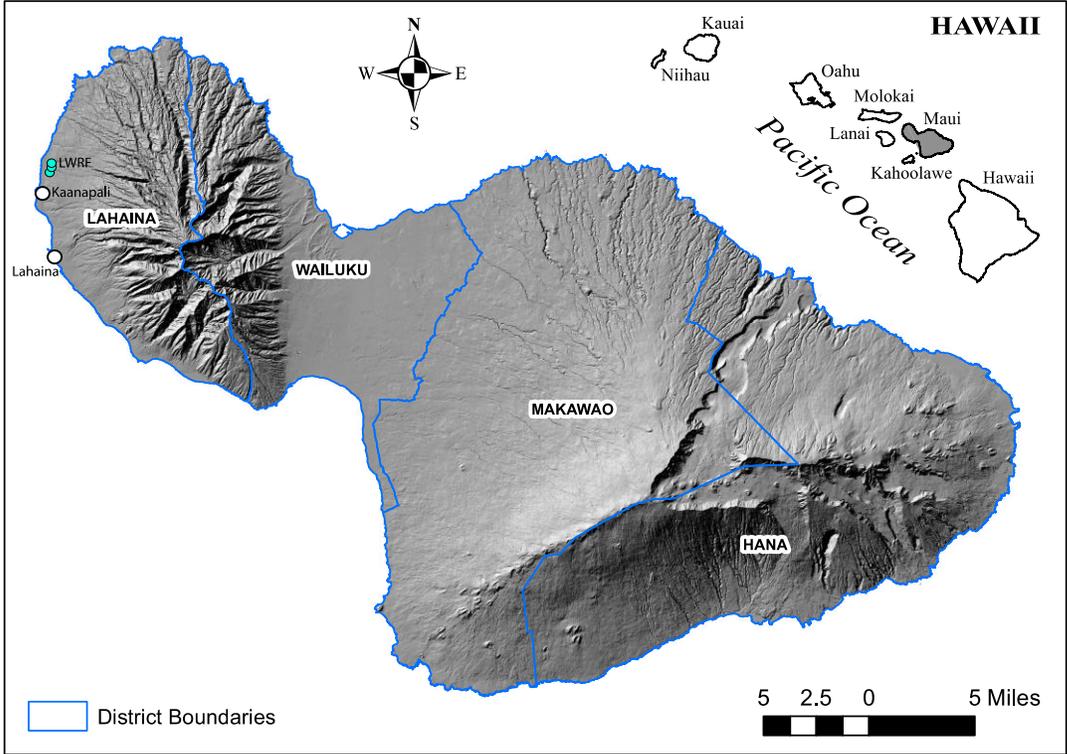
Figure 1-1: Location and topography of the Island of Maui
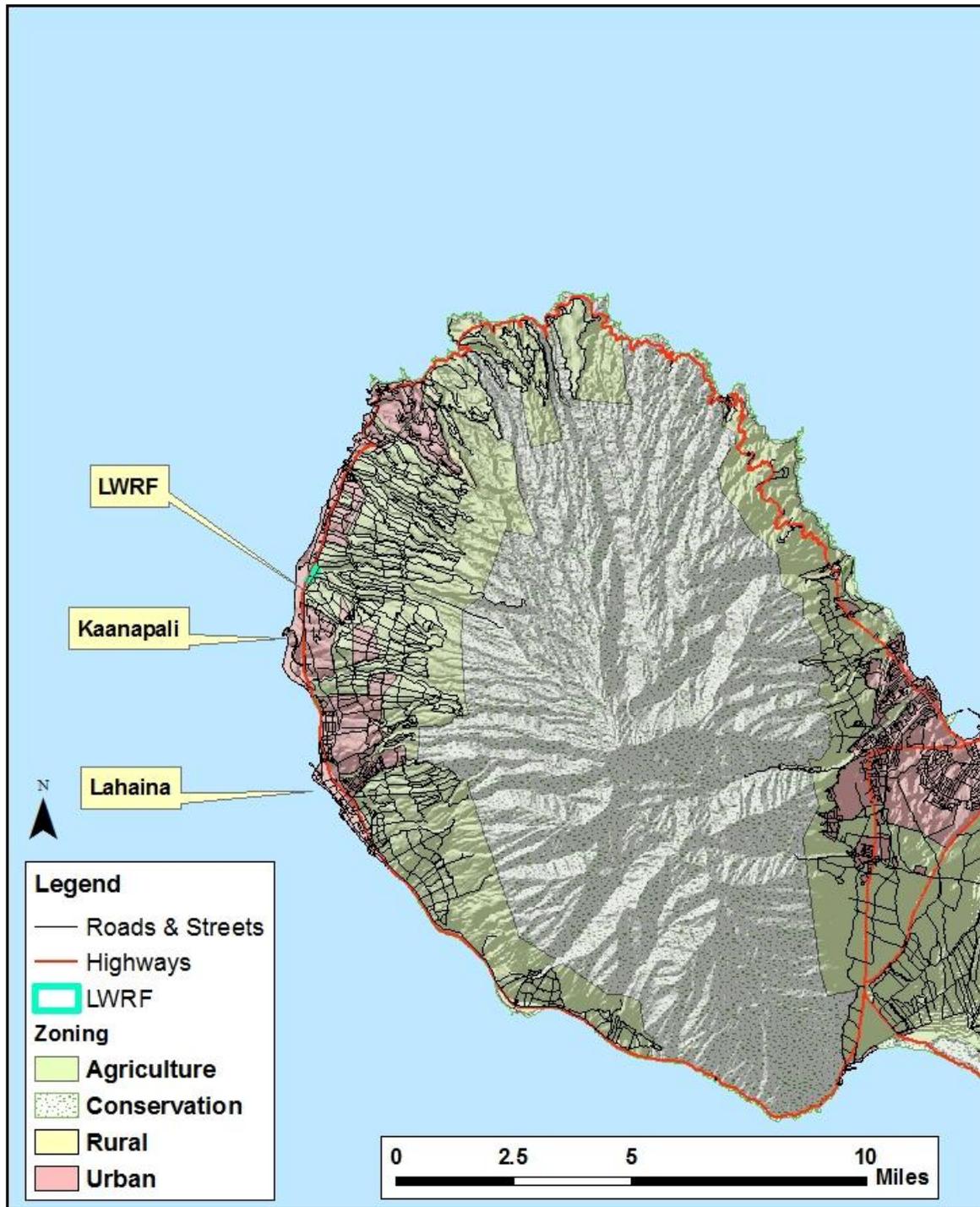
Figure 1-2: Map showing the location of the LWRF in West Maui.
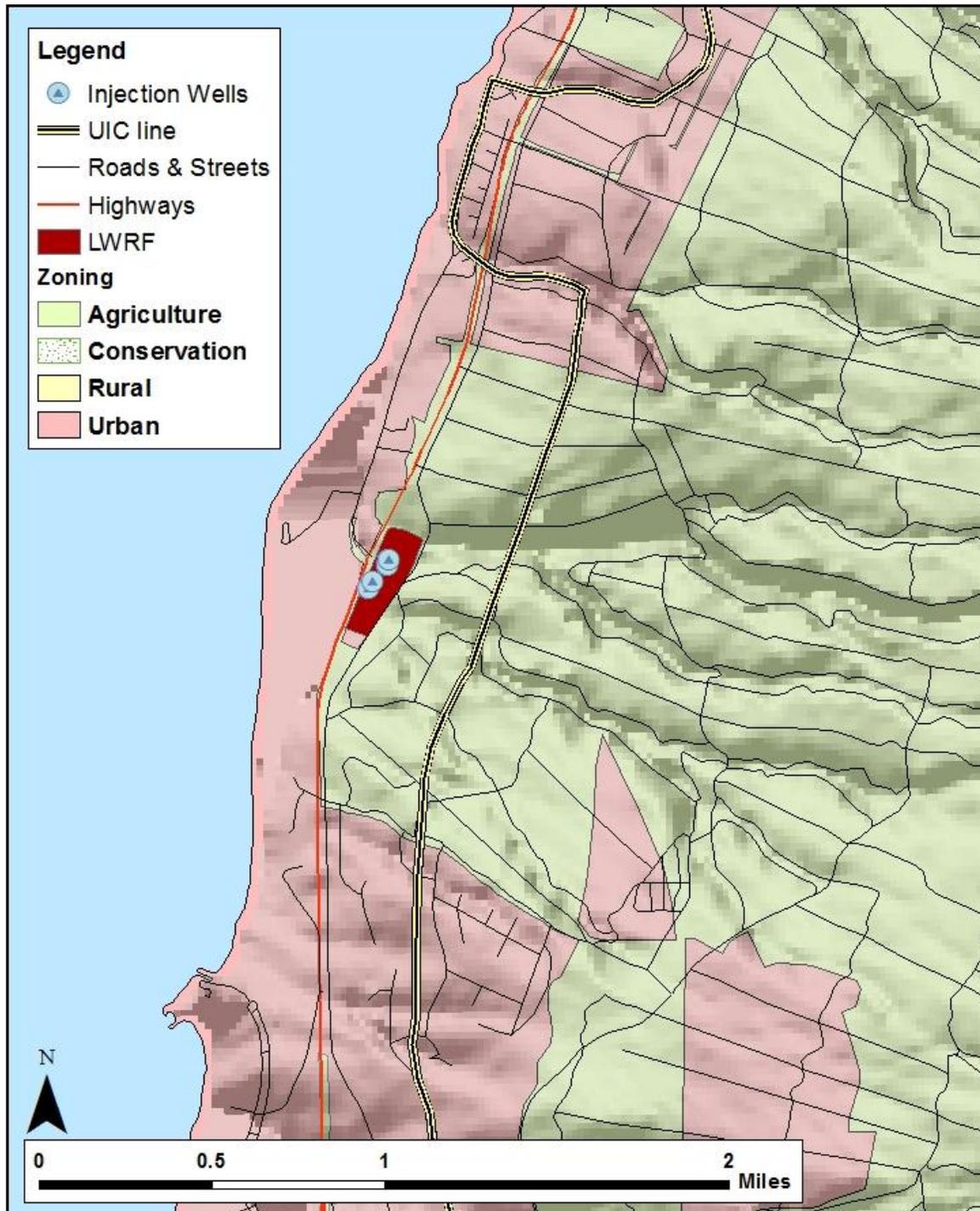
Figure 1-3: Location of the LWRF in relation to the coast and the UIC line.
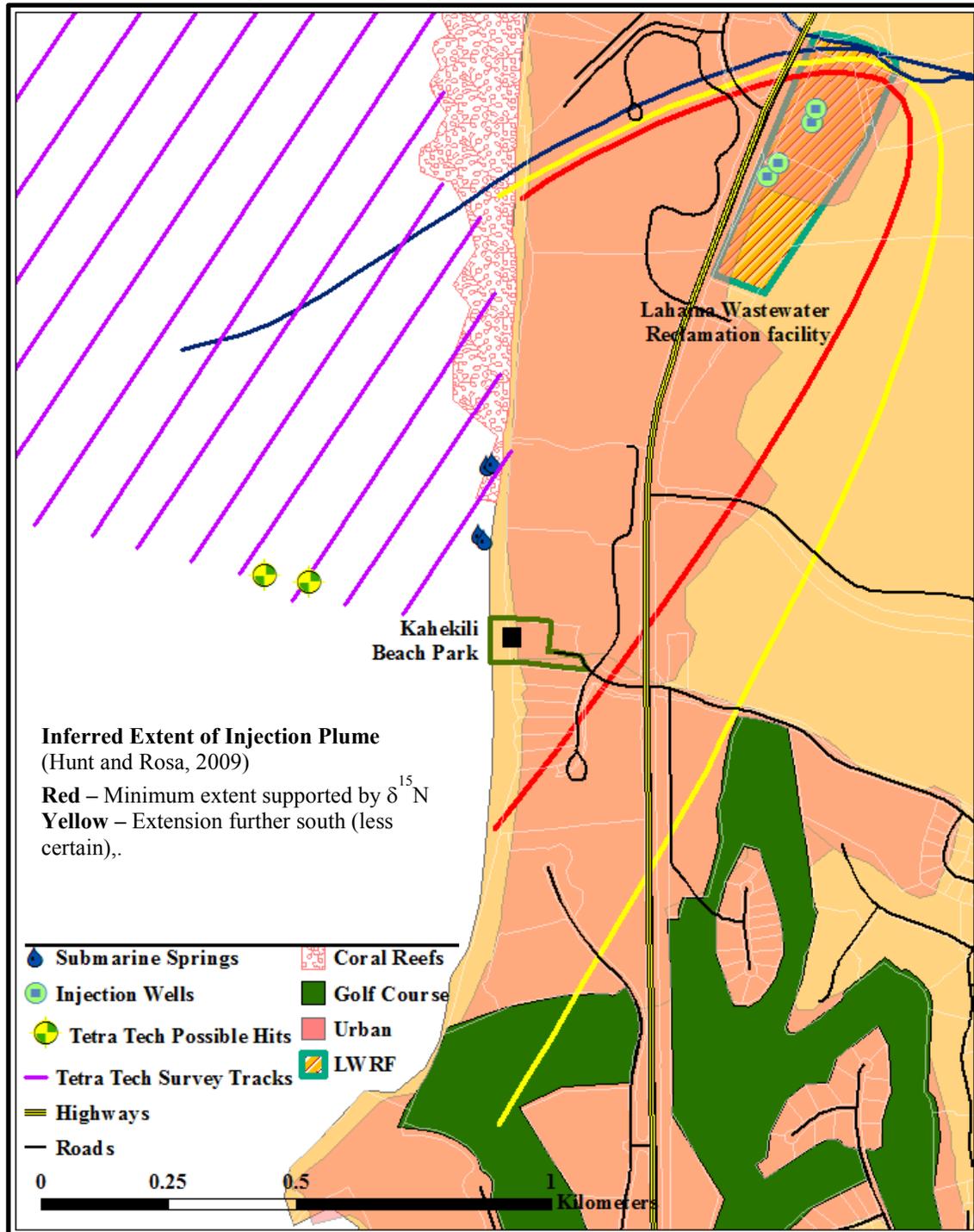
Figure 1-4: Map of the LWRF, submarine springs, and Tetra Tech (1994) ocean sampling tracts.
The location of the two occurrences of elevated fluorescence ("Hits") measured by Tetra Tech (1994) are shown. Also shown (Hunt and Rosa, 2009) are the likely minimum (red) and less certain maximum (yellow) spatial extents of the LWRF injectate plume, and inferred subsurface paleo-stream alluvium hydraulic barrier (blue).
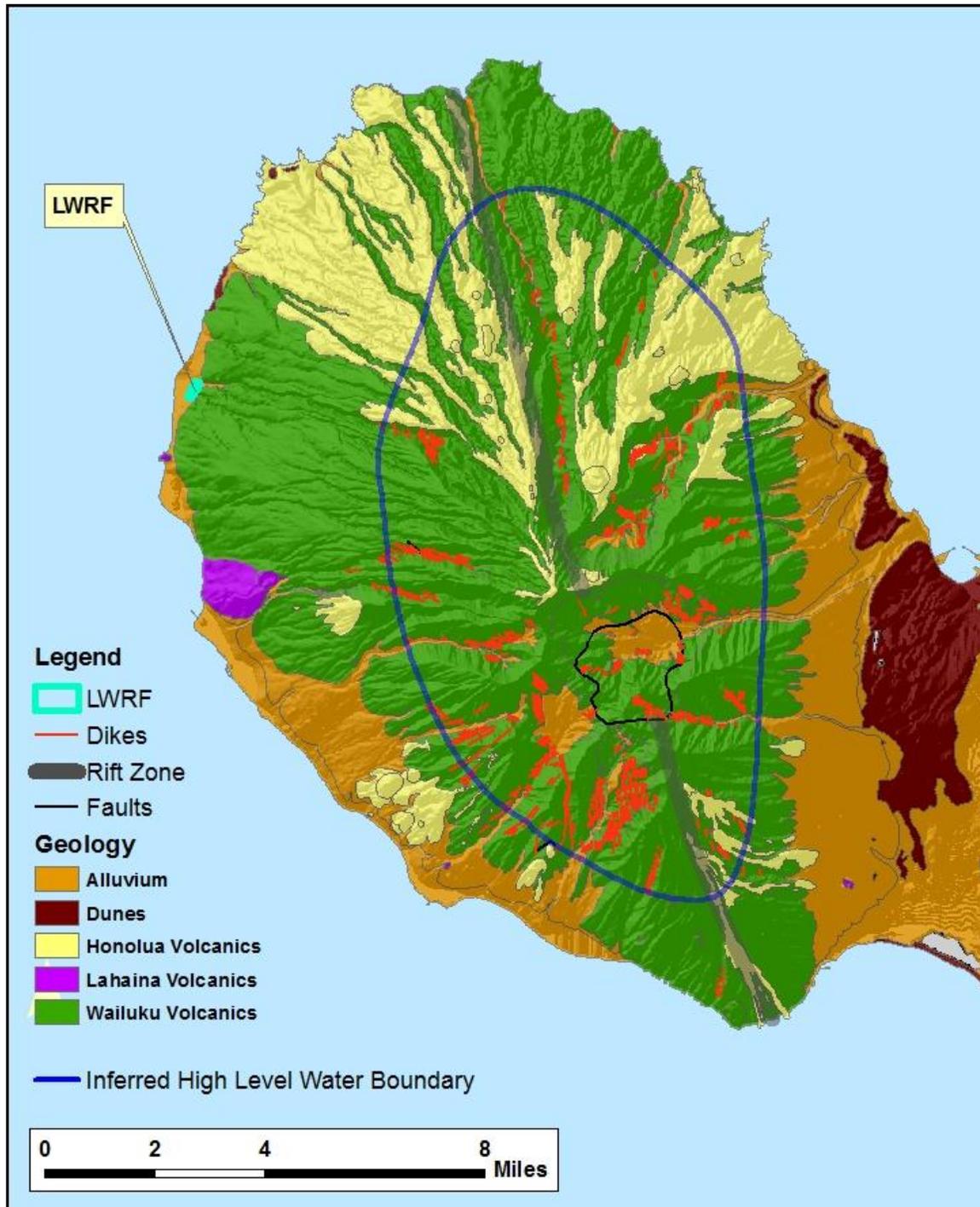
Figure 1-5: West Maui geology and inferred high level/peripheral basal lens boundary. Geology from Sherrod et al. (2007).
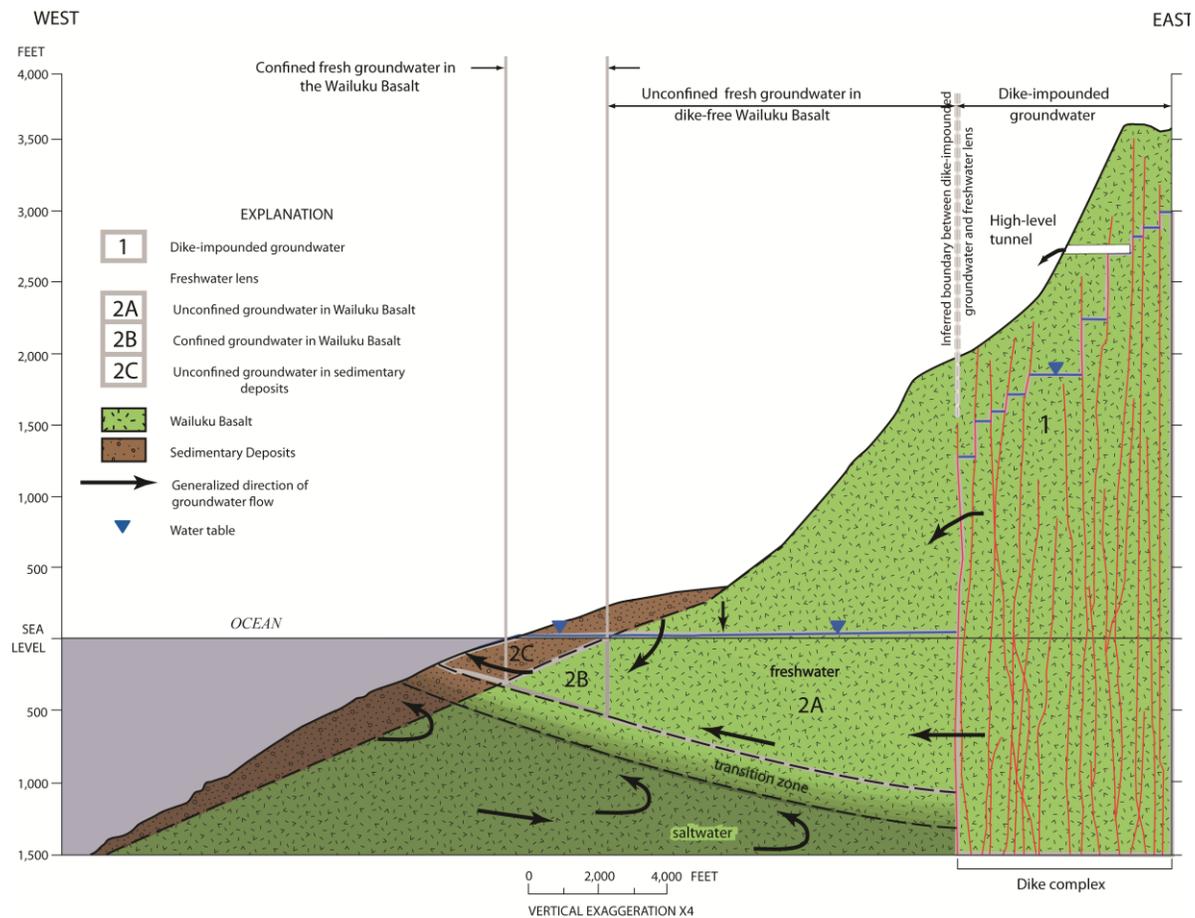
Figure 1-6: Geologic section of West Maui showing SGD and groundwater occurrence and movement.
The figure (from Gingerich and Engott, 2012) is diagrammatic and generalized. Within the study area the actual lateral distribution and thickness of caprock and subterranean freshwater-marine mixing (transition zone) is not well known, but the upper boundary of the transition zone (freshwater-seawater mixing zone) in the present study area at North Kaanapali Beach is assuredly higher than that shown here and resides at or slightly above present sea level.

21
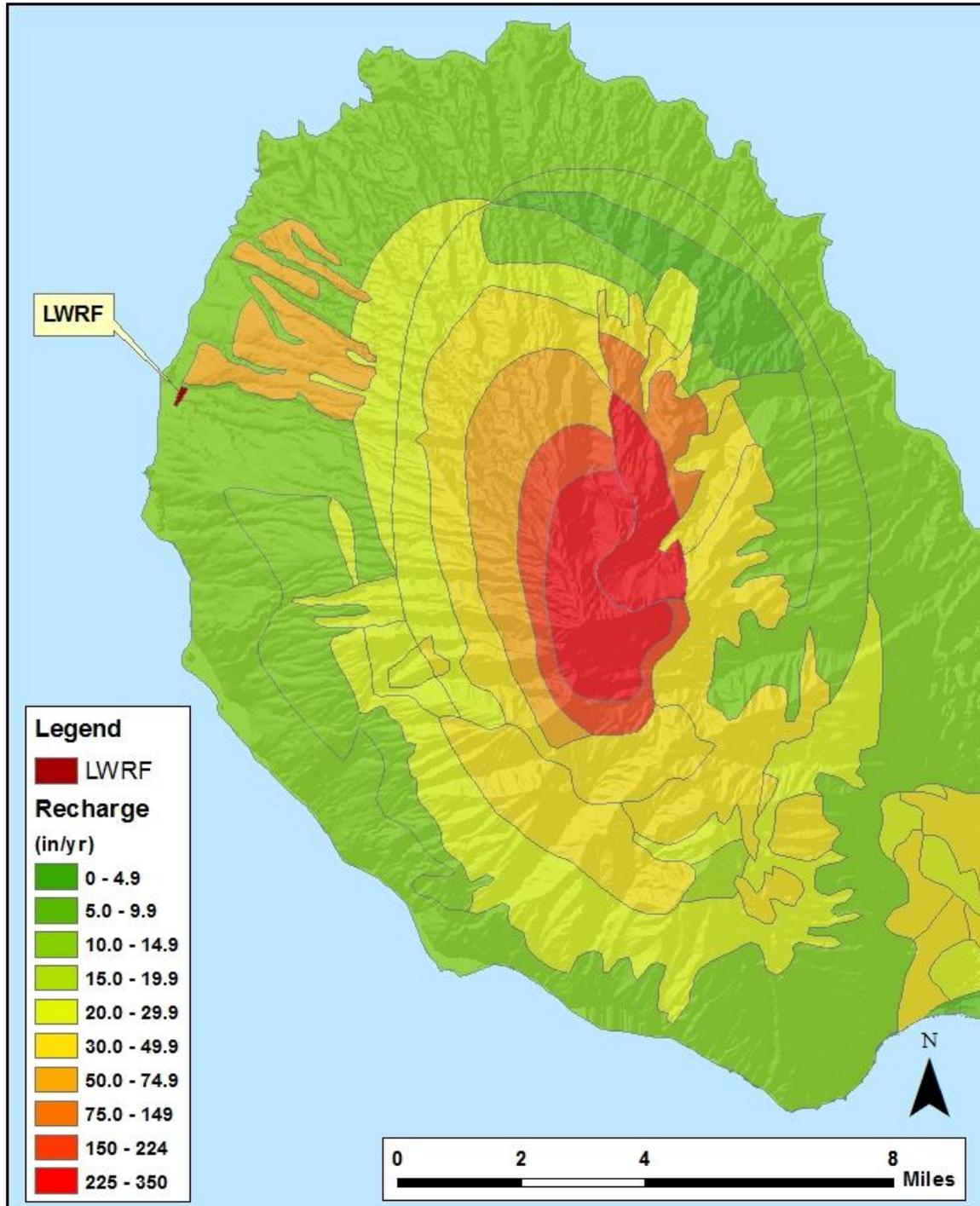
Figure 1-7: Groundwater recharge distribution in West Maui.
From Engott and Vana (2007) and Gingerich, (2008).
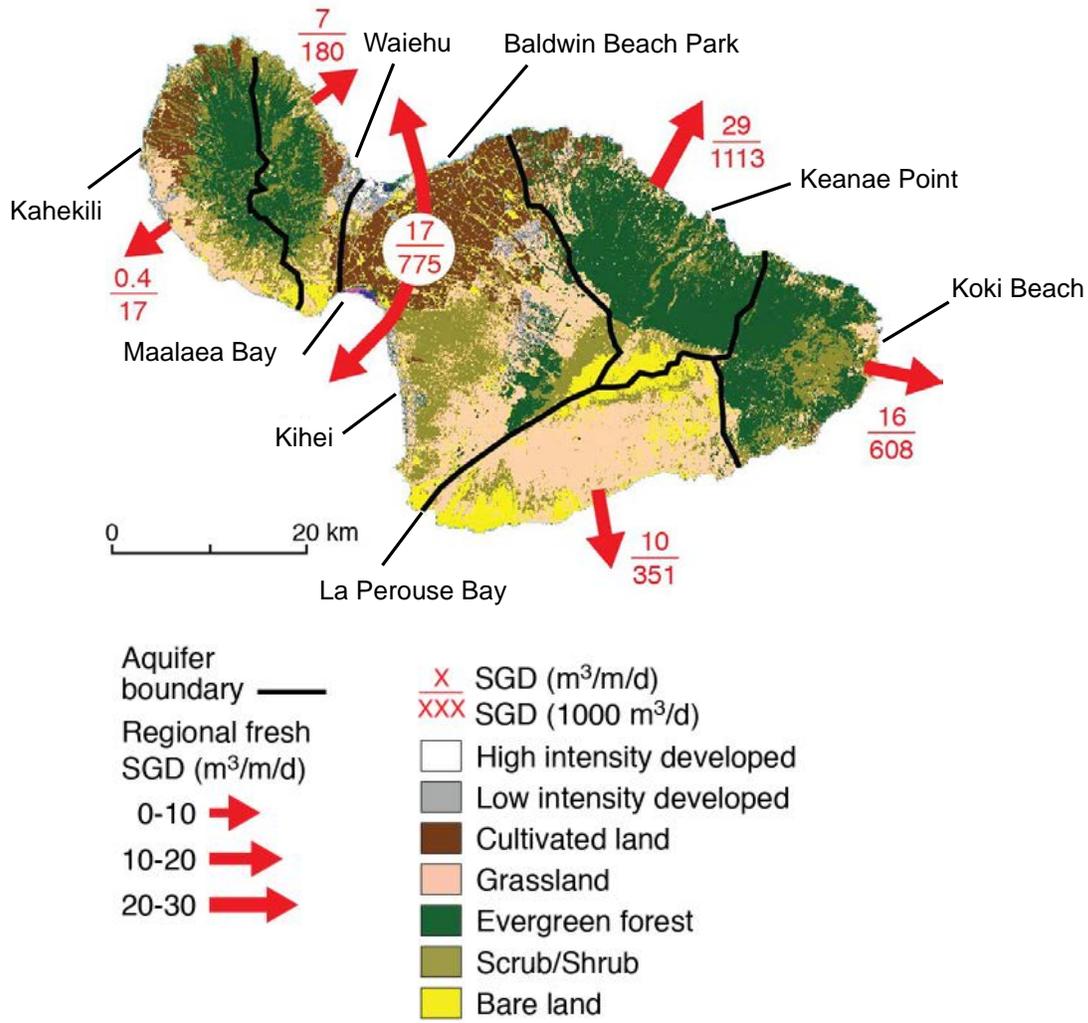
Figure 1-8: Calculated fresh submarine groundwater discharge to the ocean for the Island of Maui.

Satellite derived land-use of Maui is shown. Fresh groundwater discharge to ocean of Maui's principal aquifer divides are shown in black lines. Fresh groundwater discharges are based on large, regional-scale hydrologic budgets calculated for each aquifer as based on data of Shade (1996, 1997, and 1999), and are indicated by the red arrows. The magnitude of discharge per aquifer sector (regional fresh SGD) is shown in 1000 cubic meters per day and fresh SGD per meter of coastline within the aquifers is indicated in cubic meters per day. Satellite base from NOAA's Coastal Change Analysis Program.

This page is intentionally left blank.

SECTION 2: SUBMARINE SPRING AND MARINE CONTROL LOCATION SAMPLING, WATER QUALITY, AND FLUORESCENCE

2.1 INTRODUCTION

Over the past five years, researchers have repeatedly observed brackish, warmer-than-ambient-oceanic water emerging from the seafloor in the nearshore region (< 3 m depth) of Kahekili Beach Park (Hunt and Rosa, 2009; Dailer et al., 2010; Dailer et al., 2012). These submarine springs (termed freshwater seeps in other studies) were first found by scuba diving researchers in 2007. The interesting observation that these submarine springs were noticeably warm, combined with the 2008 discovery of extremely elevated $\delta^{15}N$ values of macroalgae in the area (as high as 43.3 ‰; Dailer et al., 2010) increased the thought that this area might be affected by effluent from the Lahaina Wastewater Reclamation Facility (LWRF). Since then, multiple research efforts focused in the nearshore region and on the submarine spring water have occurred. Hunt and Rosa (2009) sampled the entire nearshore region including the submarine springs in 2008 for a suite of parameters including: (1) $\delta^{15}N$ values of macroalgae and water column samples, (2) temperature, (3) salinity, (4) turbidity, (5) dissolved oxygen, (6) pH, (7) chlorophyll a, (8) fluorescence, (9) conductivity, (10) nutrient concentrations of water column samples, (11) waste indicator compounds of water column samples, and (12) pharmaceuticals. Their results concluded that the $\delta^{15}N$ values of macroalgae and water samples, and pharmaceuticals and fluorescence levels of the submarine spring water were among the best indicators of the presence of wastewater. In 2009, transplantation deployments of macroalgae were conducted to map the extent of the wastewater plume across the coral reef at Kahekili (Dailer et al., 2010). In consideration of the fact that the wastewater is freshwater and more buoyant than the ambient oceanic water, these deployments were extended to the surface in 2010 to determine if the wastewater was more prevalent in the offshore surface waters and to attempt to produce a three-dimensional model of the effluent plume (Dailer et al., 2012). Every effort that has looked for signs of the LWRF effluent in this area, including this study, has determined that the effluent is indeed present, and that the signal is highest in the submarine spring water (Hunt and Rosa, 2009; Dailer et al., 2010; Dailer et al., 2012).

This section of the project provides: (1) the details of how the submarine springs at Kahekili were sampled for the injected tracer dye (Section 3), radioisotope tracers (Section 5), and geochemical and stable isotope tracers (Section 4 and 6), (2) the water quality parameters of the submarine springs and control locations, (3) additional assessments of the submarine springs, and (4) the field determined fluorescence of samples collected from submarine springs and control locations.

2.2 METHODS

2.2.1 Submarine Spring Sampling

Hunt and Rosa (2009) employed an inverted funnel to sample the submarine springs which undesirably allowed for oceanic water to mix with the submarine spring water. To provide the best submarine spring samples for this study the submarine springs were sampled through steel-shaft piezometers (Model 615 6" Drive-point piezometers, Solinst Canada Limited, Georgetown, Ontario, Canada, part number 103160) that were installed while scuba diving. In the nearshore region of the study area, the seafloor consists of limestone, dead coral and basalt. Therefore, the piezometers were driven into fissures at submarine spring discharge points with a mallet and a 0.5 m connective pipe temporarily attached to the top of the piezometer. A short (15 to 20 cm) piece of polyethylene tubing equipped with a quick-connect fitting was permanently attached to each piezometer with a steel compression fitting (see Figure 2-3). Submarine spring sample collection was accomplished using a variable speed DC-battery-powered peristaltic pump (Geotech Environmental Inc., Series II, Denver, Colorado) fitted to a 50 m section of polyethylene tubing that was temporarily attached to the piezometer with a quick-connect fitting. During the June and September 2011 radiochemical and geochemical tracer sampling, the peristaltic pump was stationed on an inflatable dinghy that was moored directly above each piezometer sampling point with two 20 kg cement blocks to the north and south. During the collection of all other samples, the peristaltic pump was stationed on shore. The peristaltic pump flow rate ranged from 0.33 to 0.5 L/min. The tubing used for sample collection was purged for four minutes prior to acquiring each sample to ensure adequate and complete flushing of the piezometer-to-pump-station tubing. This same installation and configuration was used to sample the submarine springs for the injected dye tracers (Section 3), radiochemical tracers (Section 5), and geochemical and stable isotope tracers (Sections 4 and 6).

Submarine spring samples for the injected dye tracer portion of this study were collected in 125 mL HDPE (high density polyethylene) amber plastic bottles to prevent photo-degradation of any dye tracer present in the submarine spring water. Prior to sample collection, the sample bottles were thoroughly cleaned with Fisher Brand Sparkleen laboratory detergent (5 mL to 1.0 L). Sample bottles were rinsed twice with the submarine spring water, filled and labeled with the submarine spring (seep) number, date and time of collection. Additional 250 or 500 mL submarine spring water samples were collected approximately every 20 samples for quality assurance and quality control purposes. Submarine spring samples were immediately placed in a dry and light-proof cooler in the field, transported in that cooler from the field to the location of analytical procedures, and stored at room temperature in a larger dry cooler until field fluorescence measurements of Fluorescein (FLT) and S-Rhodamine-B (SRB) (see Section 2.2.5 below) were performed. The calibration solutions were also stored at room temperature in a dry, light-proof cooler. After analyses were performed, the samples were stored at room temperature in a large dry light-proof cooler until shipment to Oahu for further analyses of FLT using a Turner Designs 10AU Fluorometer (Turner Designs, 1999)

26

(Section 3) and for SRB measurements using a Hitachi F-4500 Fluorescence Spectrophotometer (Hitachi High-Technologies Corporation) (Section 3).

Our sample handling and storage methods changed since the EPA expressed concerns of sample stability in non-chilled environments. To ensure sample stability, the adapted procedure used on Maui Island since early September 2012 has been: Submarine spring samples were collected into 125 mL HDPE amber plastic bottles and immediately placed into the cooler with blue ice, then transported to the location of analytical procedures, then transferred to and stored in a refrigerator until analytical procedures occurred. The calibration standards were also stored in the same refrigerator as the submarine spring samples. When the analytical procedures were performed on Maui, the calibration standards and the samples to be analyzed were removed from the refrigerator and placed in a plastic bin with a lid over night to keep the samples in a dark space and allow for room temperature equilibration prior to analyses for the tracer dye. After analyses were performed, the samples were stored in the same refrigerator until shipment to Oahu Island for further analyses. The samples were shipped in light-proof coolers with blue ice to maintain a chilled environment during the transfer.

Immediately following every submarine spring sample collection, another clear 750 mL container was rinsed two times with the submarine spring water and then filled for water quality measurement of temperature, pH, specific conductivity, and salinity. These parameters were measured with a YSI Model 63 (YSI Inc., Yellow Springs, OH), recorded, and the submarine spring water was discarded. The YSI was calibrated with YSI standards of pH 7.00 and 10.00 and Equipco specific conductivity standards of 1,000 and 58,700 µS; calibrations are provided in Appendix Table A-1. Once all submarine spring water sampling was completed, the long tubing was disconnected from the piezometer and returned to the beach or the dinghy.

2.2.2 Submarine Spring Sampling Frequency and Placement

In July, 2011, three piezometers installed in the North and South Seep Groups (six total) were selected for the most intense monitoring for the dye tracer emergence (Figure 2-1). It is important to note that the submarine spring sampling locations (seeps) were renamed at this time to simplify sampling efforts as clarified in Table 2-1. A pre-dye tracer injection monitoring period that occurred from 7/5/2011 to 7/28/2011 was designed to measure the magnitude and variability of in situ fluorescence of the submarine spring water at the selected monitoring sites. Following the dye tracer injection of Fluorescein (FLT) on 7/28/2011 into injection wells 3 and 4, the submarine spring water sampling occurred two times per day from 7/28/2011 to 9/6/2011. From 7/30/2011 to 8/18/2011 one of the submarine springs in the North Seep Group was sampled at midnight in order not to miss the dye tracers if the arrival time of the effluent was faster than expected. As the time increased after the injection of the dye tracers, the frequency of submarine spring sampling decreased. Submarine spring sampling occurred thereafter once per day from 9/7/2011 to 10/6/2011, every two days from 10/8/2011 to 1/31/2012, and two to three times per week from 2/5/2012 to 5/2/2012. Currently the submarine spring water is sampled two to three times per week.

The South Seep Group is located approximately 25 m offshore. The submarine spring piezometer locations (Seeps 3, 4, and 5) remained unchanged through the duration of the high frequency sampling portion of the project and have been sampled from 7/5/2011 to the present time. Seep 11 was installed in the South Seep Group on 1/19/2012 (Figure 2-1) because Seeps 4 and 5 began to have high salinity values (> 5), although the piezometers and associated tubing appeared structurally intact. Seep 4 consistently displayed salinity values > 15, so the piezometer was removed and installed in the North Seep Group on 4/24/2012. A total of 573 submarine spring samples were collected from the South Seep Group from 7/5/2011 through 5/2/2012.

The North Seep Group is located approximately 3 to 5 m offshore and has been extremely problematic to maintain sampling locations throughout the duration of the project. The North Seep Groups' close proximity to the shoreline subjects these piezometers to the persistent littoral migration of sand from the beach onto the seep group as a result of large north swells. In every instance that a piezometer was re-installed, it was given a new seep number designation. The history of the submarine springs in the North Seep Group is as follows: initially Seeps 1, 2, and 6 were installed; Seeps 1 and 2 were lost on 11/14/2011 and were replaced with Seeps 7 and 8; Seep 6 was lost on 11/24/2011 and replaced with Seep 9; Seep 8 was lost on 1/19/2012 and replaced with Seep 10; Seep 9 was lost on 1/24/2012 and replaced with Seep 12; Seeps 7 and 10 were lost on 3/10/2012 and replaced with Seeps 13 and 14; Seeps 12, 13, and 14 were lost on 3/24/2012 and replaced with Submarine spring 15, leaving only one sampling point in the north (due to the amount of lost piezometers) until Submarine spring 16 was installed on 4/24/2012. Currently submarine spring monitoring occurs at two points in the north, Submarine springs 15 and 16. It is important to note that despite this apparent "hop-scotch" of submarine spring sampling locations, the re-installation of piezometers in the North Submarine spring Group has always occurred within 2 m of the original piezometer locations (Submarine springs 1, 2, and 6) and generally occurred within 0.25 m of each other (Figure 2-1). A total of 557 submarine spring samples were collected from the North Submarine spring Group from 7/5/2011 through 5/2/2012.

2.2.3 Sampling Control Locations

Control locations for the dye tracer portion of this study were Honokowai Beach Park (20°57'16.80"N, 156°41'13.60"W), Wahikuli Wayside Park (20°54'9.64"N, 156°41'7.50"W), and Olowalu (20°48'26.24"N, 156°36'9.06"W; Figure 2-2). Honokowai Beach Park, located ~2 km to the north of the main study area, served as a site of possible dye emergence if the LWRF effluent flow path was to the north. Wahikuli Wayside Park is ~4 km south of the main study area and therefore served as a southern control site with the possibility to detect the dye tracers. It is important to note that the Wahikuli area has many unconnected cesspools. Olowalu is located ~13 km south of the main study area and currently has no major land-based pollution impacts due to the lack of major development and the termination of sugarcane operations in the late 1990's. At the three locations, samples were taken from the nearshore surface water (2.0 m offshore and 1.0 m depth). The water quality parameters (temperature, pH, salinity, and specific

conductivity) were also recorded with a handheld YSI Model 63. The locations were sampled weekly from the following dates: Honokowai and Wahikuli Wayside Parks, 8/5/2011 to present and Olowalu, 12/2/2011 to present. Samples from these sites were collected in cleaned 125 mL HDPE amber plastic bottles (as described above), which were rinsed twice prior to nearshore sample collection.

2.2.4 Additional Submarine Spring Parameters

To record a time series of the submarine spring water parameters, we deployed two Schlumberger "CTD Diver" loggers (Schlumberger Water Services, Houston, Texas) that measured conductivity, depth and temperature. One was deployed directly next to Seep 4 in the South Seep Group and the second next to Seep 6 in the North Seep Group from 8/12/2011 to 9/3/2011. We also deployed temperature loggers (HOBO pendant UA-001-08; Onset, Cape Cod, Massachusetts) in the following locations in both seep groups: in the seep, above the seep, 1 m south of the seep group, and 5 m offshore of the seep group (Figure 2-3). It is important to note that the "in the north seep" temperature logger was completely buried by sand and the "in the south seep" temperature logger was not buried by the substrata, but flush with the limestone/basalt seafloor.

2.2.5 Field Measurements of Fluorescein and S-Rhodamine-B Fluorescence

All samples collected for the tracer dye monitoring portion of this project were analyzed in the field for fluorescence using a handheld Aquafluor fluorometer model 8000-010 (Turner Designs, Sunnyvale, California). Sample cuvettes were cleaned with FisherBrand Sparkleen laboratory detergent (5 mL to 1.0 L) and thoroughly rinsed with steamed distilled water prior to use. Prior to analyzing samples, the fluorometer was calibrated with 100 ppb standards of Fluorescein and S-Rhodamine-B prepared as described in Section 3 (calibrations are provided in Appendix Table A-2). Samples from the submarine springs and control locations were analyzed in the following way: cleaned cuvettes were rinsed three times with the sample water then completely filled and placed in the fluorometer. Once the sample was analyzed, the fluorescence values were recorded and the bottle cap was electrical taped on the bottle to ensure that it wouldn't open during shipment to Oahu for additional fluorescence measurements (see Section 3).

2.3 RESULTS

2.3.1 Water Quality of Submarine Springs

The submarine spring water sampled through piezometers generally had lower pH, lower salinity, and lower specific conductivity compared to oceanic values throughout the project. Water quality parameters for samples taken from 7/19/2011 through 5/2/2012 are provided in Appendix Table A-3 for the South Seep Group and Appendix Table A-4 for the North Seep Group. Measured analytical means, standard deviations and ranges

for each of the submarine springs are provided in Table 2-2. Seep 3 consistently had the lowest salinity averaging at 3.25 ± 1.5 and ranging from 2.50 to 16.1 (Table 2-2).

2.3.2 Water Quality of Control Locations

All control locations generally show little to no freshwater influence with salinities, specific conductivity and pH values close to those of oceanic levels. All water quality parameters for the control locations are provided in Appendix Table A-5. Measured analytical means, standard deviations and ranges for each control location is provided in Table 2-3.

2.3.3 Additional Submarine Spring Parameters

The data from the CTD divers deployed from 8/12/2011 to 9/14/2011 in the north (Seep 6) and the south (Seep 4) are provided in Figures 2-4 and 2-5, respectively. The CTD divers were located slightly above the seafloor and were carefully positioned to sample submarine spring water. They were purposely not buried in the substrata to avoid damage; however, sand movement in the North Seep Group buried the CTD diver four times during the deployment. This is evident by the four large decreases in specific conductivity from ~50 mS/cm to ~5 mS/cm and accompanied increases in temperature to 28.0°C (Figure 2-4). Other than these burials, the data show parameters close to oceanic levels of 50 to 55 mS/cm for specific conductivity, and diurnal temperature ranges from ~27.1°C during the day to ~25.5°C at night (Figures 2-4 and 2-5).

The data from the temperature loggers, placed in and around the seep groups in the south and north is provided in Figures 2-6 and 2-7, respectively. The temperature loggers deployed in the South Seep Group show temperatures that were all fairly consistent regardless of placement ranging from 77.5°F to 82.0°F (25.3°C to 27.8°C) (Figure 2-6). The temperature logger deployed in the North Seep Group in Seep 6, which was completely covered with sand, however, reported temperatures vastly different than those around it. The temperature logger deployed in Seep 6 had a nearly continuous temperature reading of ~82.1°F (~27.8°C) (Figure 2-7a). Assuming that the temperature logger was working properly, these data demonstrate that the submarine spring water is warmer than the surrounding oceanic water and that the temperature is not affected by the time of day or tidal activity. A second temperature logger deployment was performed (with a different logger) to determine if the same results would be obtained, but unfortunately the logger was lost in a large north swell and accompanied sand migration event. We will re-deploy additional temperature loggers in the near future to confirm or refute these findings. However, if the submarine springs are in fact consistently warmer than the oceanic water then, the submarine spring water is a potential source of the warm sea surface temperature anomalies measured by the aerial TIR remote sensing portion of this study (Section 4).

2.3.4 Field Measurements of Fluorescein and S-Rhodamine-B Fluorescence

The fluorescence of Fluorescein (FLT) and S-Rhodamine-B (SRB) measured in the field of samples collected from 7/19/2011 through 5/2/2012 are provided in Appendix Table A-3 for the South Seep Group (545 samples total) and Appendix Table A-4 for the North Seep Group (529 samples total). The fluorescence of FLT and SRB measured in the field of the control locations for samples collected from 8/5/2011 to 5/2/2012 (61 samples total) is provided in Appendix Table A-5.

Although there is a difference between the field and laboratory fluorescence measurements, a notable increasing trend in FLT fluorescence was found in all submarine spring water samples beginning on January 4th 2012 (Figures 2-8 to 2-11; Appendix Tables A-3 and A-4), while no change in fluorescence was observed in the samples obtained from the control locations. Although the obvious increase if FLT fluorescence occurred on January 4th 2012, subtle increases in field fluorometry started at the North Seep Group in late October 2011 and provided the first indication that the FLT dye was emerging from the submarine springs. The follow-up laboratory analysis that confirmed the presence of dye was prompted by a review of the field data. The field fluorescence of FLT and SRB and salinity of submarine spring water samples is graphed in Figure 2-8, for Seeps 3, 4, 5, and 11; Figure 2-9 for Seeps 1, 2, 6, and 7; Figure 2-10 for Seeps 8, 9, 10, and 12; and Figure 2-11 for Seeps 13 to 16. The fluorescence of FLT and SRB and salinity values of samples from control locations are provided in Figure 2-12. The effect of salinity on the fluorescence values of FLT in the submarine spring water is quite substantial, as seen in Seep 4, where increased salinity coincides with decreases in the dye concentration (Figure 2-8). Increased salinity of the submarine spring water is indicative of ocean water mixing with the submarine spring water, which therefore dilutes the concentration of the dye tracer. The fluorescence data collected in the field has not been corrected for the salinity. Additional details on the relationship between the variations in dye concentration and salinity can be found in Section 3.

The FLT fluorescence values from the field fluorometer are higher than those measured using the laboratory fluorometer. This is due to a problem with the calibration standards. Early laboratory calibration standards and those sent to the field were mixed using deionized (DI) water. During the Method of Detection Limit study (Section 3), however, it was found that the fluorescence intensity of the standards mixed with submarine spring water was significantly greater that those mixed with DI water. The original calibration standards were left in the field so continuity could be maintained with earlier measurements made with the handheld fluorometer. The field fluorometry was used to screen the submarine spring water samples for changes in fluorescence that would indicate the arrival a dye or, in the case of FLT, a peaking of the breakthrough curve. When the problem with the DI based calibration solution was discovered, the research team was awaiting the arrival of SRB. Thus, an uninterrupted analytical history for the handheld fluorometer was desired. To correct the readings of the handheld fluorometer, the field and laboratory FLT results were compared. This comparison indicated that the

field values could be corrected to the approximate laboratory values by multiplying the field FLT concentration by 0.33 (Figure 2-13).

A second potential complication arose with the discovery that the strong fluorescence of FLT produced a false indication of SRB dye detection as read by the field fluorometer. Figures 2-8 and 2-10 show an apparent increase of fluorescence in the SRB wavelength. Although we initially believed that SRB was being detected when this was first observed, subsequent laboratory analysis found no SRB in the samples. It was noted that a good correlation existed between the FLT and SRB concentrations (Figure 2-14). This correlation and the disagreement between the field and laboratory fluorometry was investigated when the field fluorometer was returned to UH for maintenance. The response of the SRB channel to the FLT calibration solutions was measured with the handheld fluorometer. These solutions were prepared using submarine spring water collected prior to the FLT and SRB dye addition into the effluent stream. Therefore, FLT that was added in the laboratory was the only dye in these solutions. This test showed that the strong FLT fluorescence carried over into the wavelength monitored by the Rhodamine channel, giving a false positive indication of SRB. Figure 2-15 shows the results of this test and the linear response ($r^2 = 1.000$) of the SRB channel to solutions containing only FLT. In the absence of the high FLT dye concentration, however, our laboratory calibrations do indicate that when SRB calibration solutions are used the field fluorometer responds faithfully to the detection of SRB, and is thus suitable for tracer studies using Rhodamine dyes.

2.4 SUMMARY

The field portion of this study installed the sampling infrastructure, collected samples for the geochemical survey, collected nearly 1,200 samples for field and tracer dye analysis, and deployed and collected data from instruments for monitoring temperature and salinity.

Submarine springs were sampled with a variable speed DC-battery-powered peristaltic pump (Geotech Environmental Inc., Series II, Denver, Colorado) fitted to a 50 m section of polyethylene tubing that was temporarily attached to the piezometer with a quick-connect fitting. The peristaltic pump flow rate ranged from 0.33 to 0.5 L/min. This method of sampling the submarine springs was found to be a very effective method of sampling the submarine springs. In most locations the salinity of the samples collected was less than 5, indicating the water captured was representative of submarine groundwater with little seawater influence. Water quality parameters of temperature, pH, specific conductivity, and salinity were measured with a YSI Model 63. The sample water was screened for the presence of the two tracer dyes (Fluorescein [FLT] and Sulpho-Rhodamine-B [SRB]) using a Turner Designs 10AU Fluorometer.

Samples were collected at submarine springs in the North and South Seep Groups, and at three control locations. The South Seep Group is located approximately 25 m offshore and had three initial monitoring points (Seeps 3, 4, and 5). A fourth, Seep 11 was added

on November 24th, 2011 due to high salinities being measured at Seeps 4 and 5. The Seep 4 piezometer was relocated in the North Seep Group on April 24th, 2012 to replace piezometers in that area that were covered by migrating sand. To date a total of 573 submarine spring samples were collected from the South Seep Group. The North Seep Group is located approximately 3 to 5 m offshore with three initial monitoring points (Seep 1, 2, and 6). This location has been extremely problematic to maintain throughout the duration of the project. The North Seep Groups' close proximity to the shoreline subjects these piezometers to the persistent littoral migration of sand from the beach onto the seep group as a result of large north swells. By 11/24/2011 all of the original piezometers had been buried by migrating sand. As a piezometer was buried it was replace with a new one. All replacement piezometers were and are currently located within 2 m of the original ones. To date a total of 557 submarine spring samples were collected from the North Seep Group.

Control locations for the dye tracer portion of this study were Honokowai Beach Park, Wahikuli Wayside Park, and Olowalu. Honokowai Beach Park served as a site of possible dye emergence if the LWRF effluent flow path was to the north. Wahikuli Wayside Park is south of the main study, but specifically targeted because of its proximity to the submarine spring locations, and therefore served as a southern control site with the possibility to detect the dye tracers. Olowalu is located ~13 km south of the main study area and currently has no known major land-based pollution impacts due to the minimal development and the termination of sugarcane operations in the late 1990's.

A pre-dye tracer injection monitoring period that occurred from July 5th through July 28th, 2011 was designed to measure the magnitude and variability of in situ fluorescence of the submarine spring water at the selected monitoring sites. Following the dye tracer injection of Fluorescein (FLT) into injection wells 3 and 4, the submarine spring water sampling occurred two times per day, with one spring being sampled three times per day, for ~40 days following the FLT addition to ensure that the dye transported by preferential flow paths would not be missed. As time progressed, the sampling frequency was decreased to the current tempo of two to three times per week.

Migrating sand in the North Seep Group buried the CTD diver four times during the deployment. This is evident by the four large decreases in specific conductivity from ~50 mS/cm to ~5 mS/cm and accompanied increases in temperature to 28.0°C (Figure 2-4). Other than these burials, the data show parameters close to oceanic levels of 50 to 55 mS/cm for specific conductivity, and diurnal temperature ranges from ~27.1°C during the day to ~25.5°C at night (Figures 2-4 and 2-5).

The SRB and FLT fluorescence measured in the field remained indistinguishable from background levels until late October, 2011. Subtle increases in field fluorometry measurements of FLT started to occur in samples from the North Seep Group in late October 2011 and provided the first indication that dye was emerging from the submarine springs. This was followed in mid-November by increasing FLT fluorescence of samples from the South Seep Group. However, no pronounced FLT fluorescence increase was noted in the field data until January, 2012. An inverse correlation was noted between the

FLT fluorescence and the salinity measured at the monitoring points. Increased salinity of the submarine spring water is indicative of ocean water mixing with the submarine spring water, which therefore dilutes the concentration of the dye tracer.

Field data indicated an apparent increase in SRB fluorescence. Subsequent testing showed this was actually a response of the SRB channel the strong FLT fluorescence in the samples being analyzed. As of May 2, 2012 there has been no confirmed detection of SRB.

Table 2-1: Submarine spring names and locations.
Locations were recorded with a handheld 76CS Plus Garmin GPS. It is important to note that Seeps 4, 5, and 11 in the south and 1, 2, 6, 7, 9, 10, 12, 13, 14, 15, and 16 in the north are all within 1 m of each other and therefore can only be represented by a single point within the spatial resolution obtainable with a GPS.

	Seep Number	Latitude	Longitude	Geochemistry Sample Numbers
South Seep Group	Seep 3	20°56'19.61"N	156°41'35.19"W	June 2011: Seep 4 Piez-1
	Seep 4	20°56'19.36"N	156°41'35.14"W	June 2011:Seep 1 Piez-1, Seep 1 Piez 2 September 2011: Seep 1-2 Piez
	Seep 5	20°56'19.36"N	156°41'35.14"W	
	Seep 11	20°56'19.36"N	156°41'35.14"W	
North Seep Group	Not used	20°56'23.28"N	156°41'34.08"W	June 2011: Seep 2 Piez-1
	Seep 1	20°56'24.69"N	156°41'34.08"W	
	Seep 2	20°56'24.69"N	156°41'34.08"W	
	Seep 6	20°56'24.69"N	156°41'34.08"W	June 2011: Seep 3 Piez-1 September 2011: Seep 3-2 Piez
	Seep 7	20°56'24.69"N	156°41'34.08"W	
	Seep 9	20°56'24.69"N	156°41'34.08"W	
	Seep 10	20°56'24.69"N	156°41'34.08"W	
	Seep 12	20°56'24.69"N	156°41'34.08"W	
	Seep 13	20°56'24.69"N	156°41'34.08"W	
	Seep 14	20°56'24.69"N	156°41'34.08"W	
	Seep 15	20°56'24.69"N	156°41'34.08"W	
	Seep 16	20°56'24.69"N	156°41'34.08"W	
	Seep 8	20°56'24.69"N	156°41'34.18"W	

Table 2-2: North and South Seep Group water quality parameters.
Data (means ± SD and range) were collected from 7/19/2011 through 5/2/2012 with a handheld YSI Model 63.

South	Temp. (°C)	pH	Spec. Cond. (mS/cm)	Salinity
Seep 3	28.7 ± 2.0	7.52 ± 0.12	6.43 ± 2.57	3.25 ± 1.5
	24.9 to 34.9	7.22 to 7.94	5.20 to 28.18	2.50 to 16.1
Seep 4	28.6 ± 2.0	7.50 ± 0.12	8.98 ± 6.57	4.77 ± 4.0
	24.5 to 34.6	7.20 to 7.90	5.63 to 37.70	2.80 to 22.5
Seep 5	28.4 ± 2.0	7.53 ± 0.20	9.24 ± 6.59	4.94 ± 4.0
	24.9 to 34.9	7.32 to 7.90	5.29 to 34.75	2.90 to 21.8
Seep 11	26.8 ± 2.5	7.61 ± 0.20	6.48 ± 0.62	3.39 ± 0.3
	25.2 to 29.0	7.37 to 7.68	5.00 to 8.32	3.10 to 4.5
North				
Seep 1	29.1 ± 2.0	7.45 ± 0.09	8.33 ± 1.04	4.25 ± 0.5
	24.8 to 34.4	7.18 to 7.76	7.32 to 14.80	3.90 to 7.3
Seep 2	28.9 ± 2.3	7.46 ± 0.11	8.47 ± 1.41	4.35 ± 0.7
	24.0 to 34.9	7.13 to 7.75	7.04 to 17.36	3.80 to 9.9
Seep 6	29.3 ± 2.2	7.41 ± 0.14	8.33 ± 0.90	4.25 ± 0.4
	23.8 to 35.9	6.90 to 7.94	7.00 to 13.54	3.80 to 7.0
Seep 7	27.5 ± 1.7	7.51 ± 0.19	8.19 ± 1.32	4.31± 0.8
	22.4 to 30.3	7.26 to 7.81	7.24 to 15.08	3.90 to 8.2
Seep 8	27.4 ± 1.7	7.35 ± 0.18	9.36 ± 5.98	5.01± 3.6
	24.7 to 31.0	7.09 to 7.90	7.47 to 37.88	4.00 to 22.0
Seep 9	27.4 ± 1.7	7.43 ± 0.21	13.65 ± 11.35	7.58 ± 6.7
	23.3 to 30.5	6.75 to 7.80	7.21 to 42.91	3.90 to 25.3
Seep 10	28.2 ± 1.0	7.60 ± 0.15	9.02 ± 1.17	4.70 ± 0.6
	26.5 to 29.5	7.26 to 7.76	7.99 to 11.85	4.10 to 6.2
Seep 12	28.2 ± 1.1	7.60 ± 0.11	8.37 ± 0.50	4.35 ± 0.2
	26.6 to 29.6	7.36 to 7.78	7.88 to 9.55	4.10 to 4.9
Seep 13	28.0 ± 1.9	7.69 ± 0.02	8.18 ± 0.53	4.27 ± 0.1
	26.0 to 29.7	7.67 to 7.71	7.69 to 8.74	4.20 to 4.4
Seep 14	27.1 ± 2.1	7.67 ± 0.05	7.91 ± 0.21	4.17 ± 0.1
	24.7 to 28.7	7.66 to 7.72	7.67 to 8.02	4.10 to 4.2
Seep 15	28.4 ± 2.4	7.58 ± 0.10	9.99 ± 3.28	5.31 ± 2.1
	24.6 to 30.6	7.45 to 7.72	7.86 to 16.54	4.20 to 9.3
Seep 16	30.1 ± 0.6	7.63 ± 0.12	8.85 ± 0.09	4.47 ± 0.1
	29.4 to 30.6	7.50 to 7.71	8.79 to 8.95	4.40 to 4.5

Table 2-3: Control location water quality parameters.
Data (means ± SD and range) were collected from 8/5/2011 to 5/2/2012 with a handheld
YSI Model 63 from Honokowai Beach Park, Wahikuli Wayside Park, and Olowalu.

Location	Temp. (°C)	pH	Spec. Cond. (mS/cm)	Salinity
Honokowai	27.5 ± 1.3	8.06 ± 0.09	54.2 ± 2.6	34.0 ± 1.7
Beach Park	25.1 to 30.3	7.90 to 8.27	47.3 to 58.0	29.9 to 35.7
Wahikuli	26.5 ± 1.2	8.06 ± 0.07	54.6 ± 1.9	34.9 ± 0.9
Wayside Park	24.9 to 29.7	7.89 to 8.16	50.4 to 57.7	32.7 to 36.4
Olowalu	28.1 ± 2.0	8.03 ± 0.07	55.5 ± 2.5	34.3 ± 1.7
	24.8 to 31.5	7.92 to 8.13	48.1 to 58.3	29.5 to 36.3
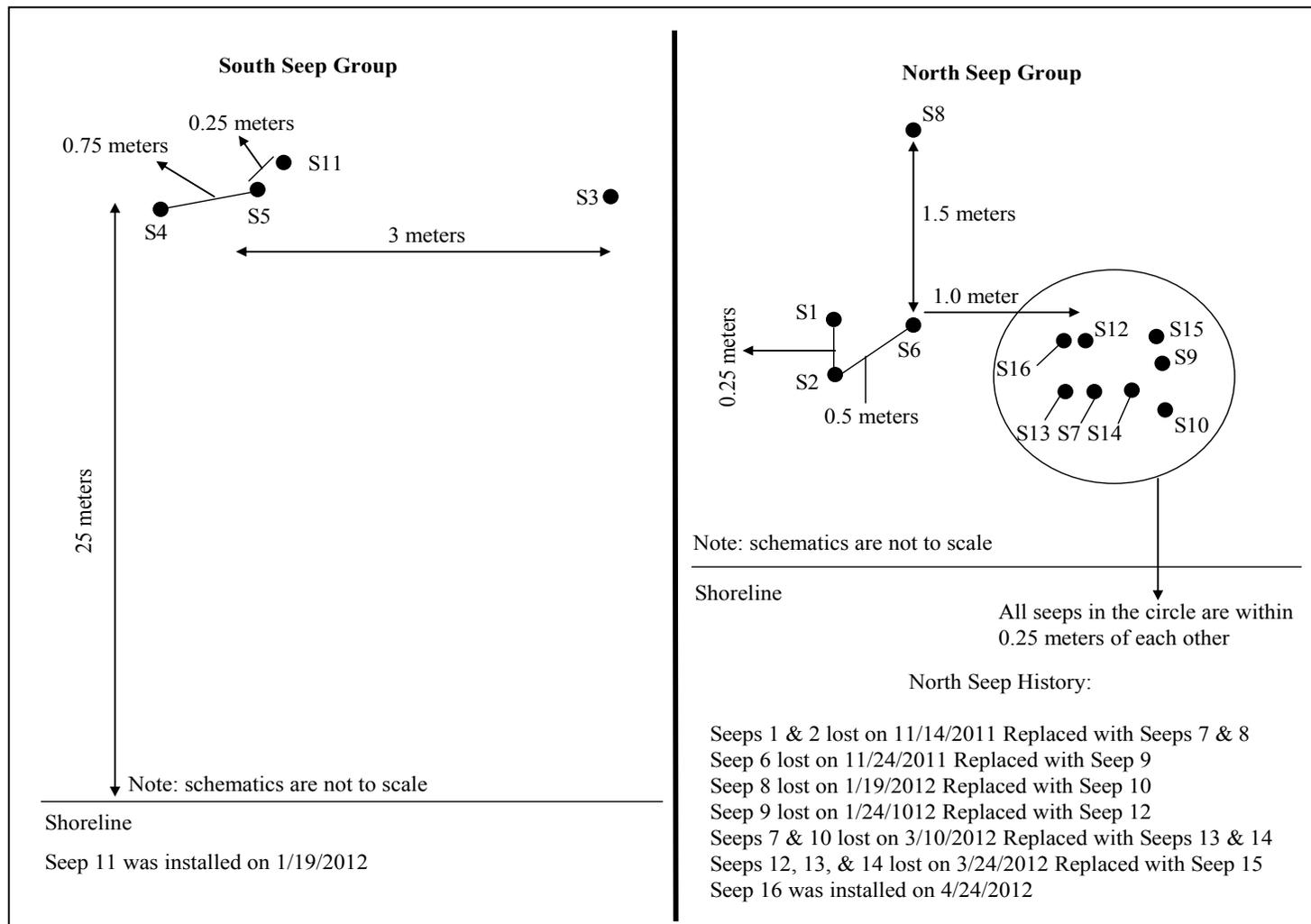
Figure 2-1: Schematics of submarine spring water sampling locations.
As specified in the North and South Seep Groups.
● = Seep location.
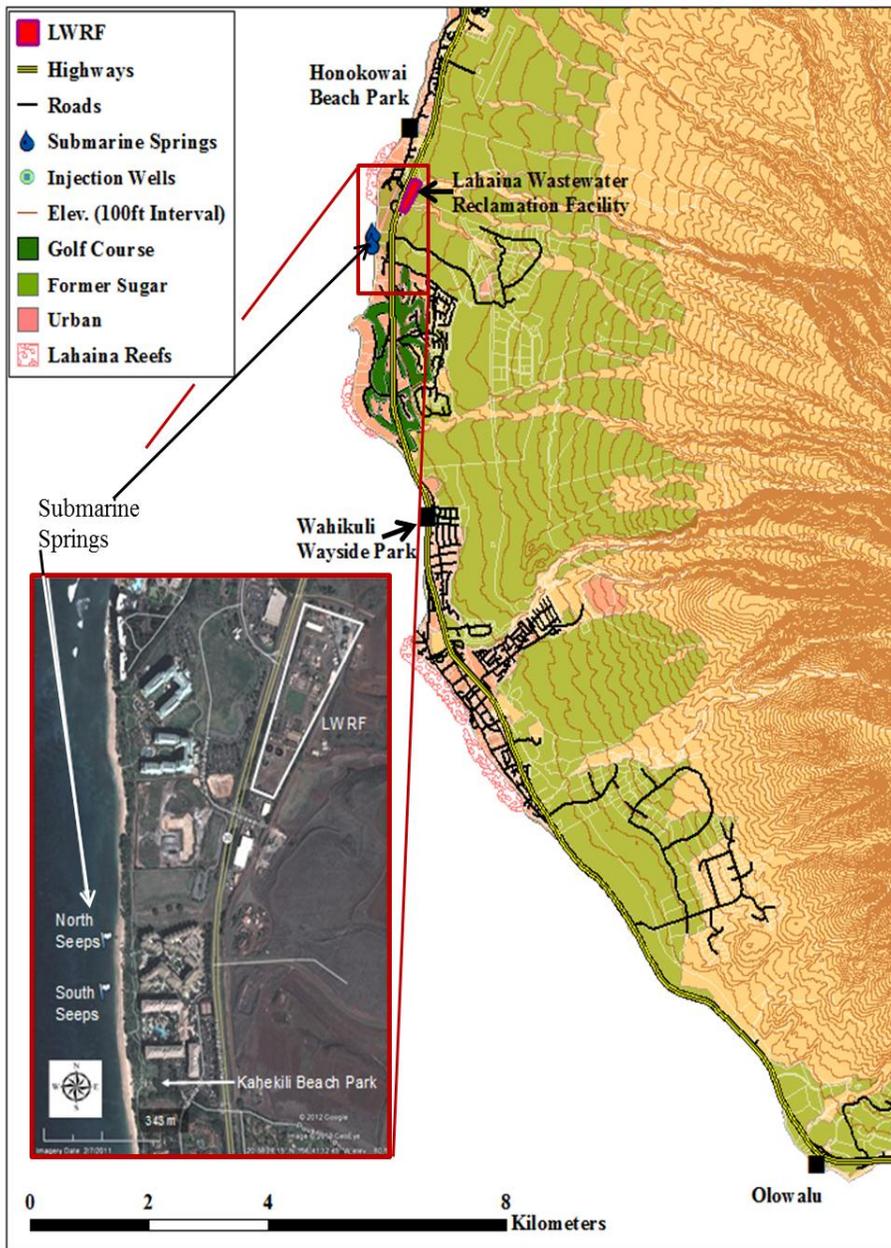
Figure 2-2: Control and submarine spring sampling locations.
Control locations include: Honokowai Beach Park, Wahikuli Wayside Park, and
Olowalu. Also shown are the North and South Seep Groups.
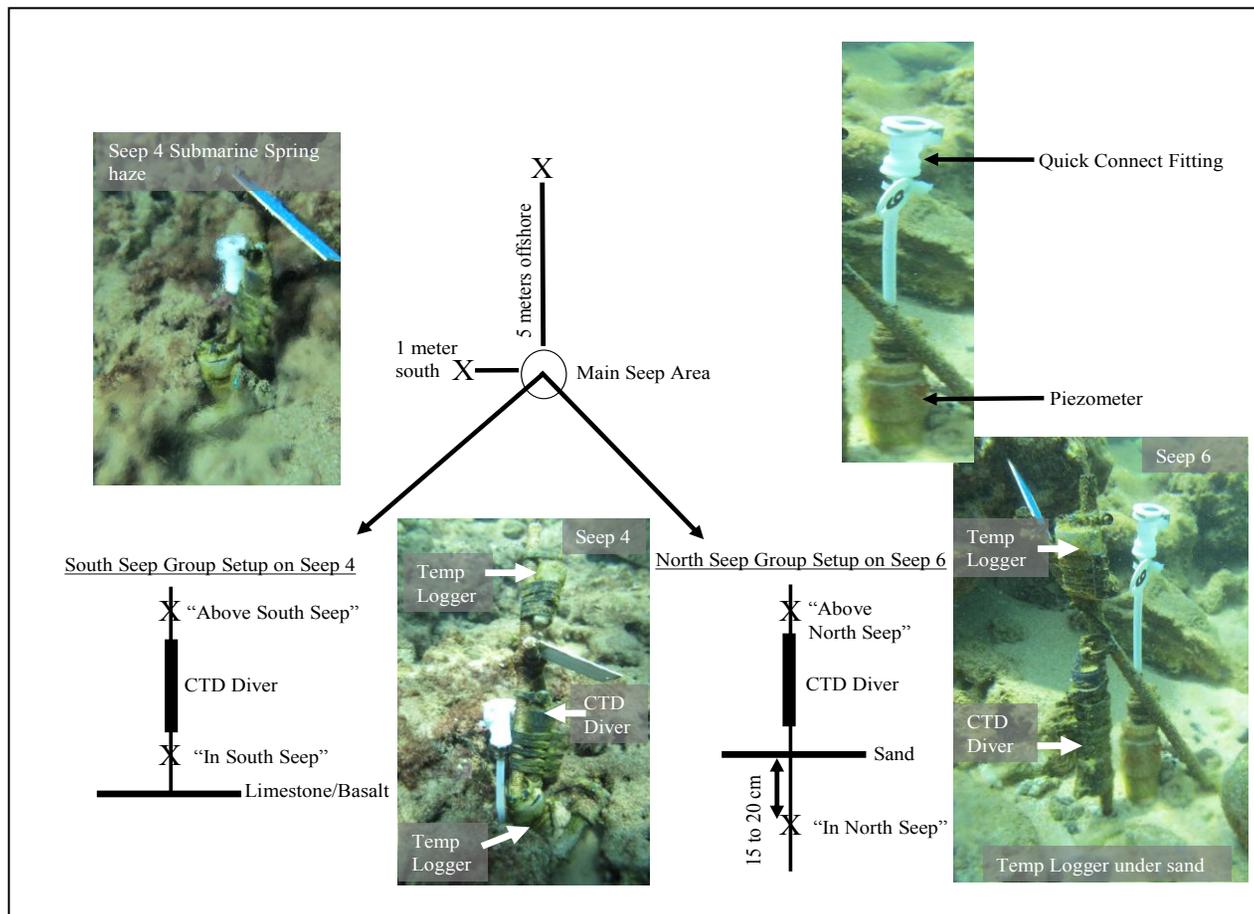
Figure 2-3: Schematic of CTD Diver and temperature logger deployment.
Deployment locations of temperature loggers and the CTD Divers in the North and South Seep Groups, also showing the quick connect fitting and piezometer installation.   X = Temperature logger
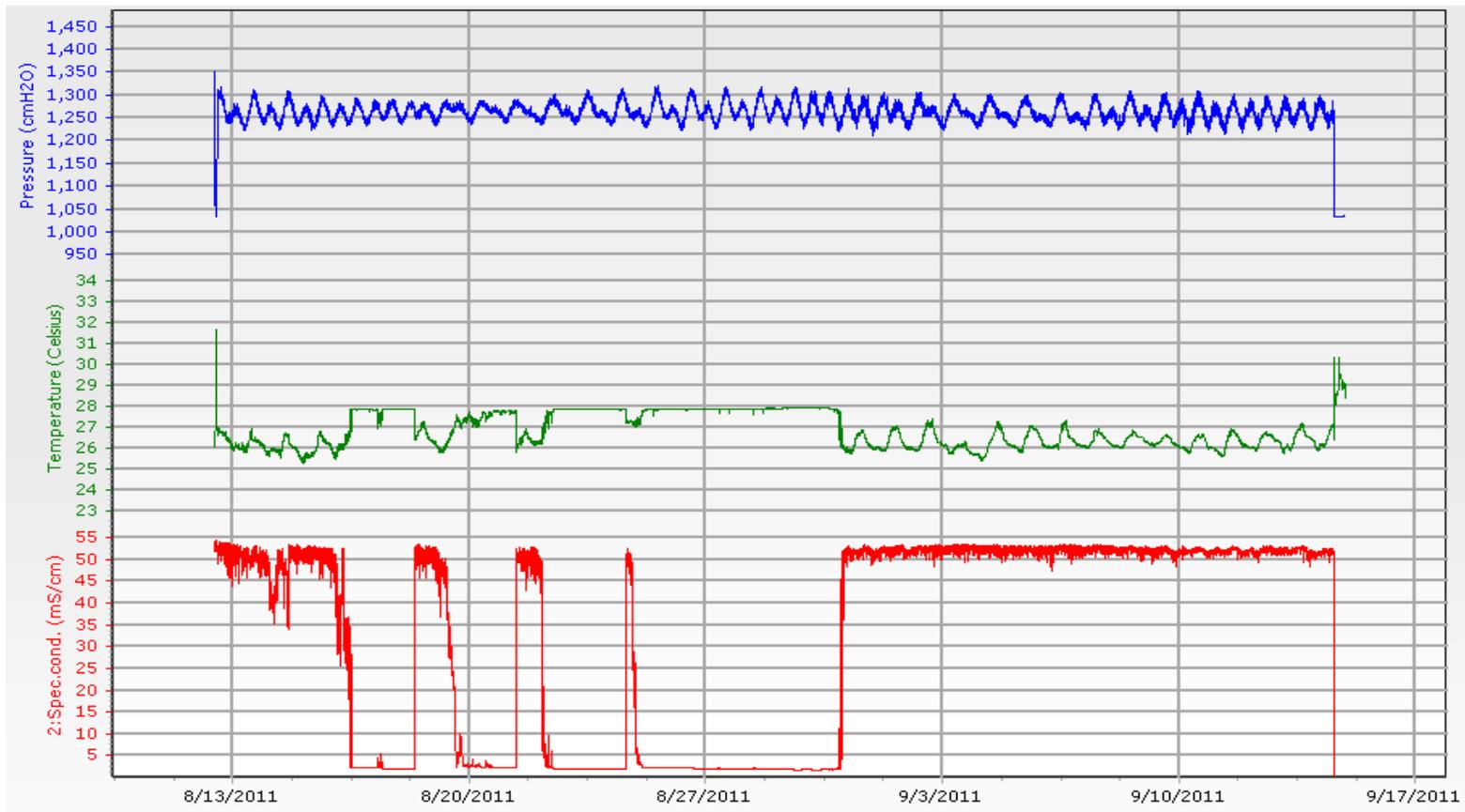
Figure 2-4: North Seep 6 CTD Diver data.
Depth is represented as pressure, temperature in °C, and specific conductivity in mS/cm. The CTD Diver was deployed from 8/12/2011 to 9/14/2011. The flat portions of the temperature and specific conductivity readings represent times during the deployment when the CTD Diver was completely buried by sand.

41
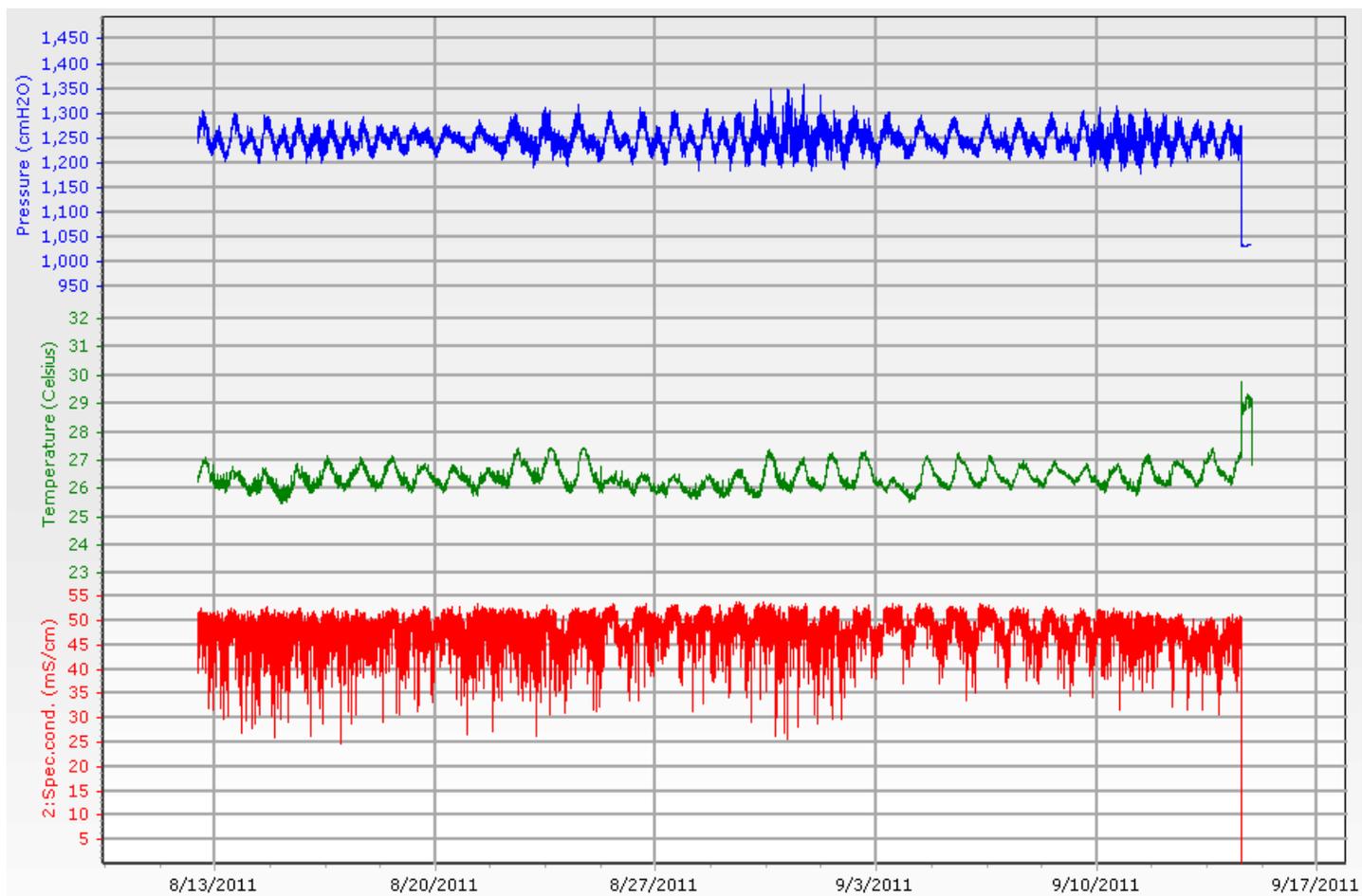
Figure 2-5: South Seep 4 CTD Diver data.
Depth is represented as pressure, temperature in °C, and specific conductivity in mS/cm. The CTD Diver was deployed from 8/12/2011 to 9/14/2011.
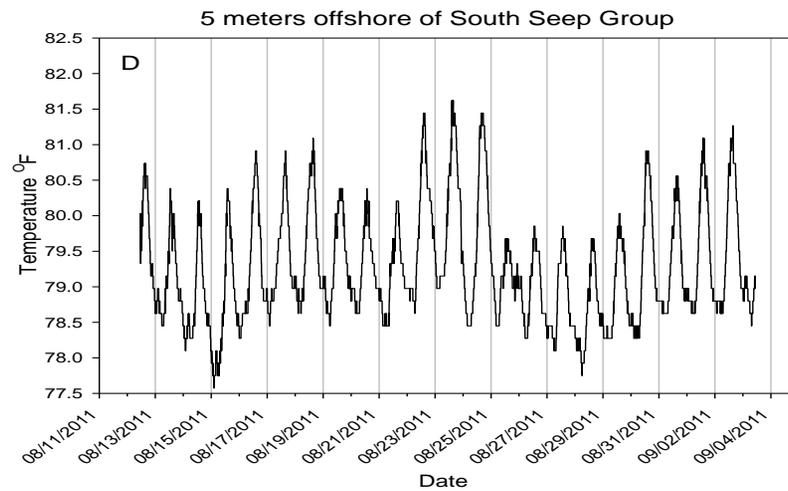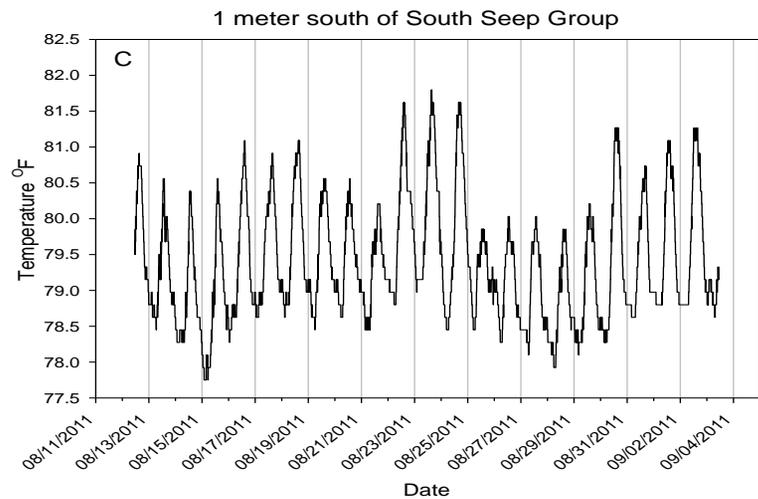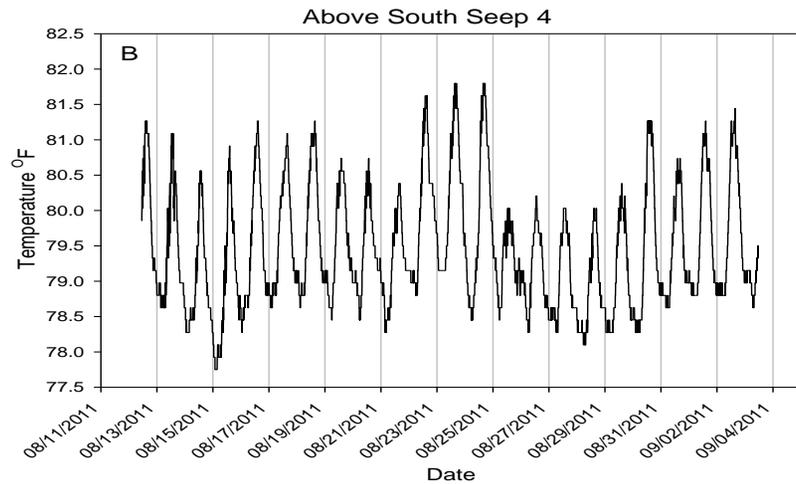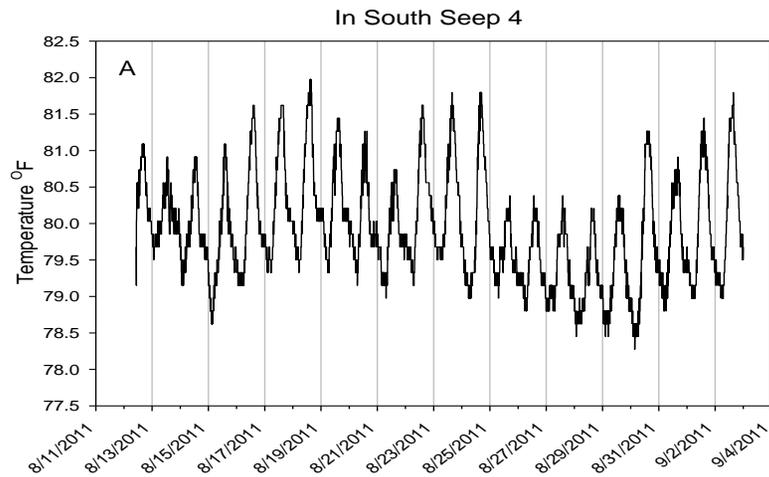
Figure 2-6: South Seep Group temperature data.
Loggers were deployed from 8/14/2011 to 9/4/2011 at the following locations: (a) in south Seep 4, (b) above south Seep 4, (c) 1 meter south of the South Seep Group, and (d) 5 meters offshore of the South Seep Group.
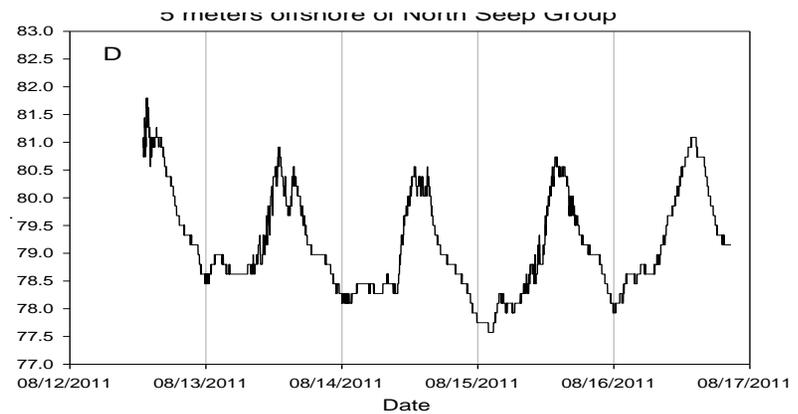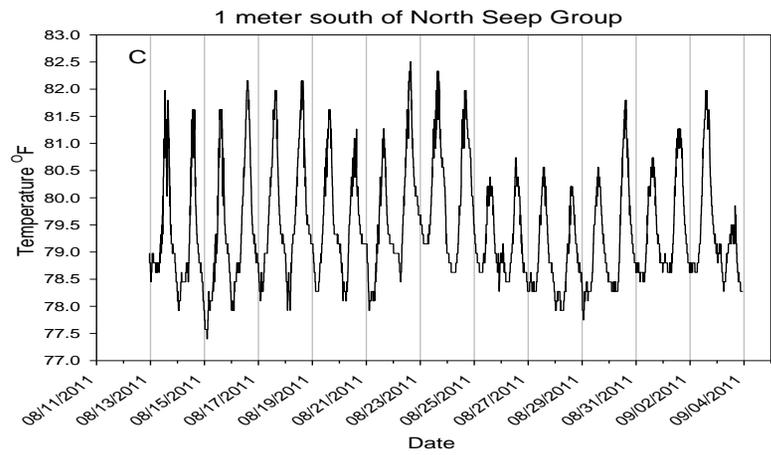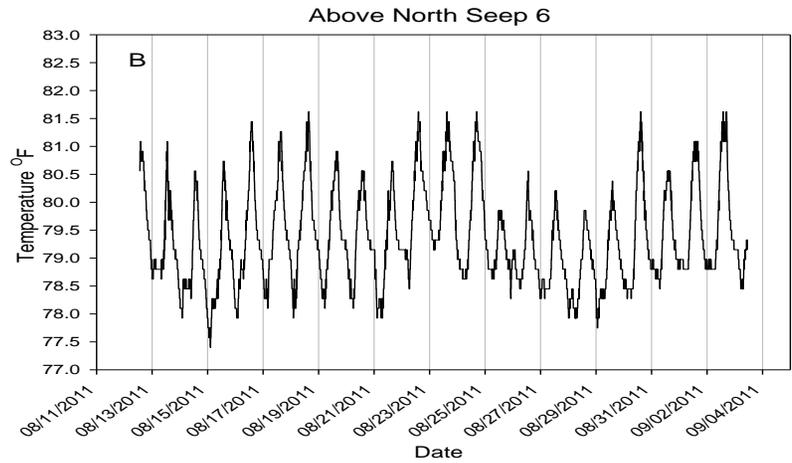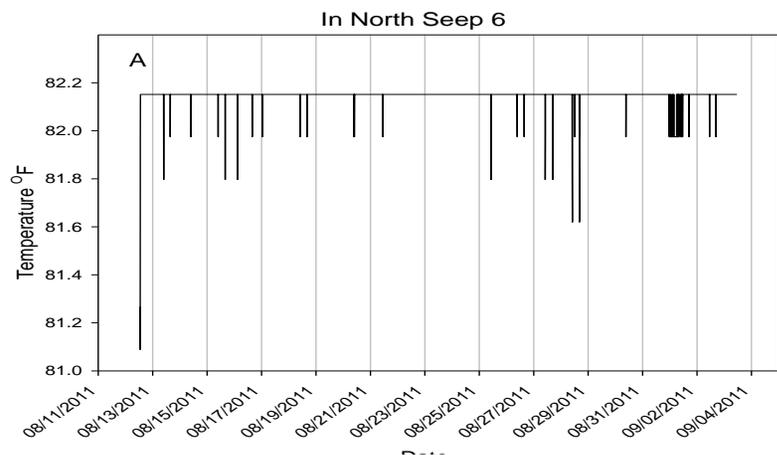
Figure 2-7: North Seep Group temperature data.
Loggers were deployed from 8/14/2011 to 9/4/2011 at the following locations: (a) in north Seep 6, (b) above north Seep 6, (c) 1 meter south of the North Seep Group, and (d) 5 meters offshore of the North Seep Group (note that due to an error in launching this logger the data only goes to 8/17/2011).

44
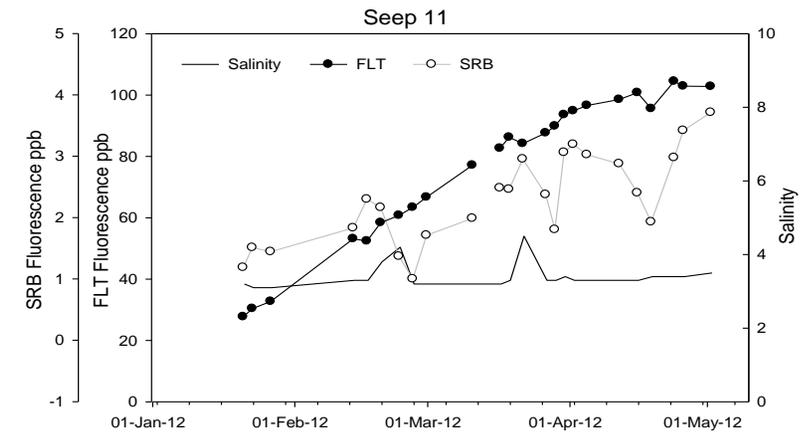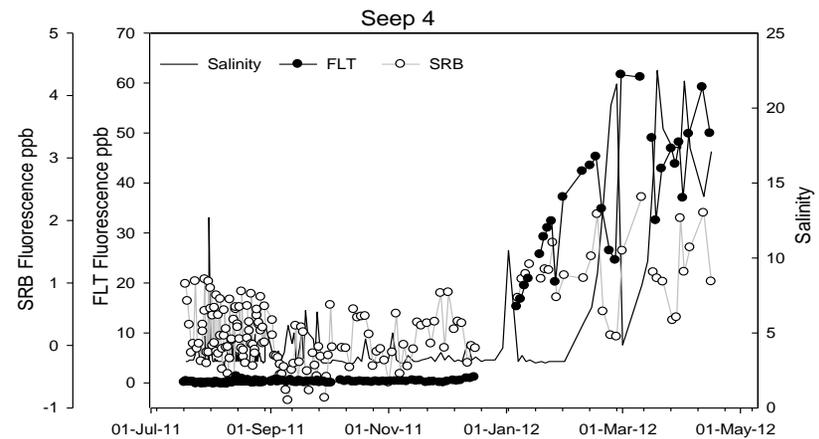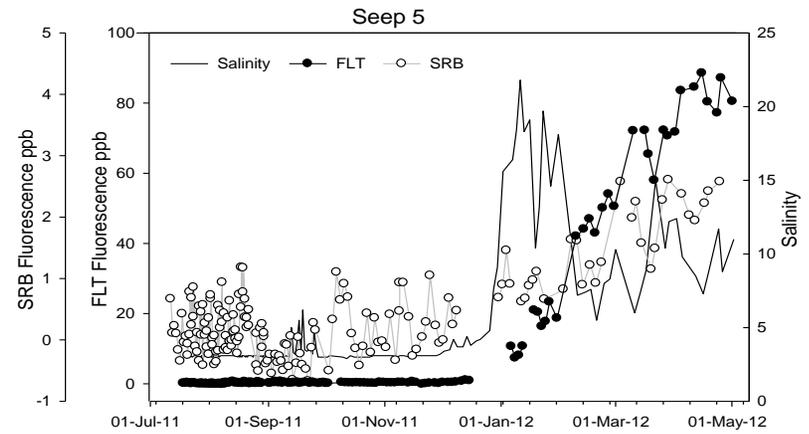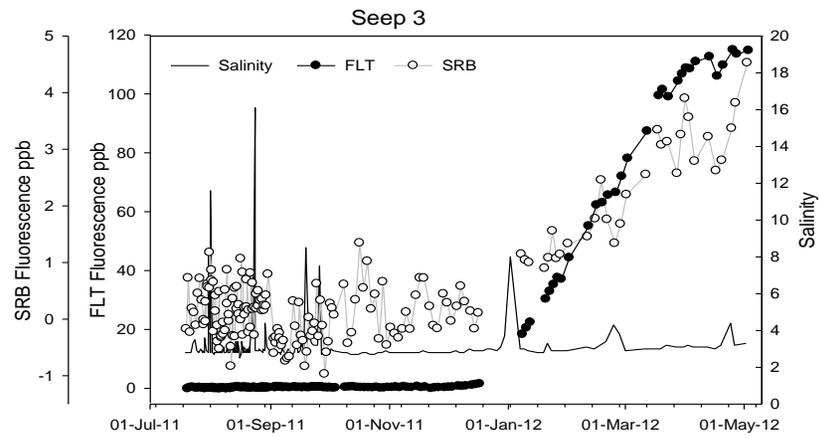
Figure 2-8: South Seep Group salinity and fluorescence.
Field salinity (solid line) and fluorescence of S-Rhodamine-B (SRB; in open circles) and Fluorescein (FLT; in closed circles) of samples collected from Seeps 3, 4, 5, and 11 over time. Note the change in scale of the FLT fluorescence and salinity per seep.
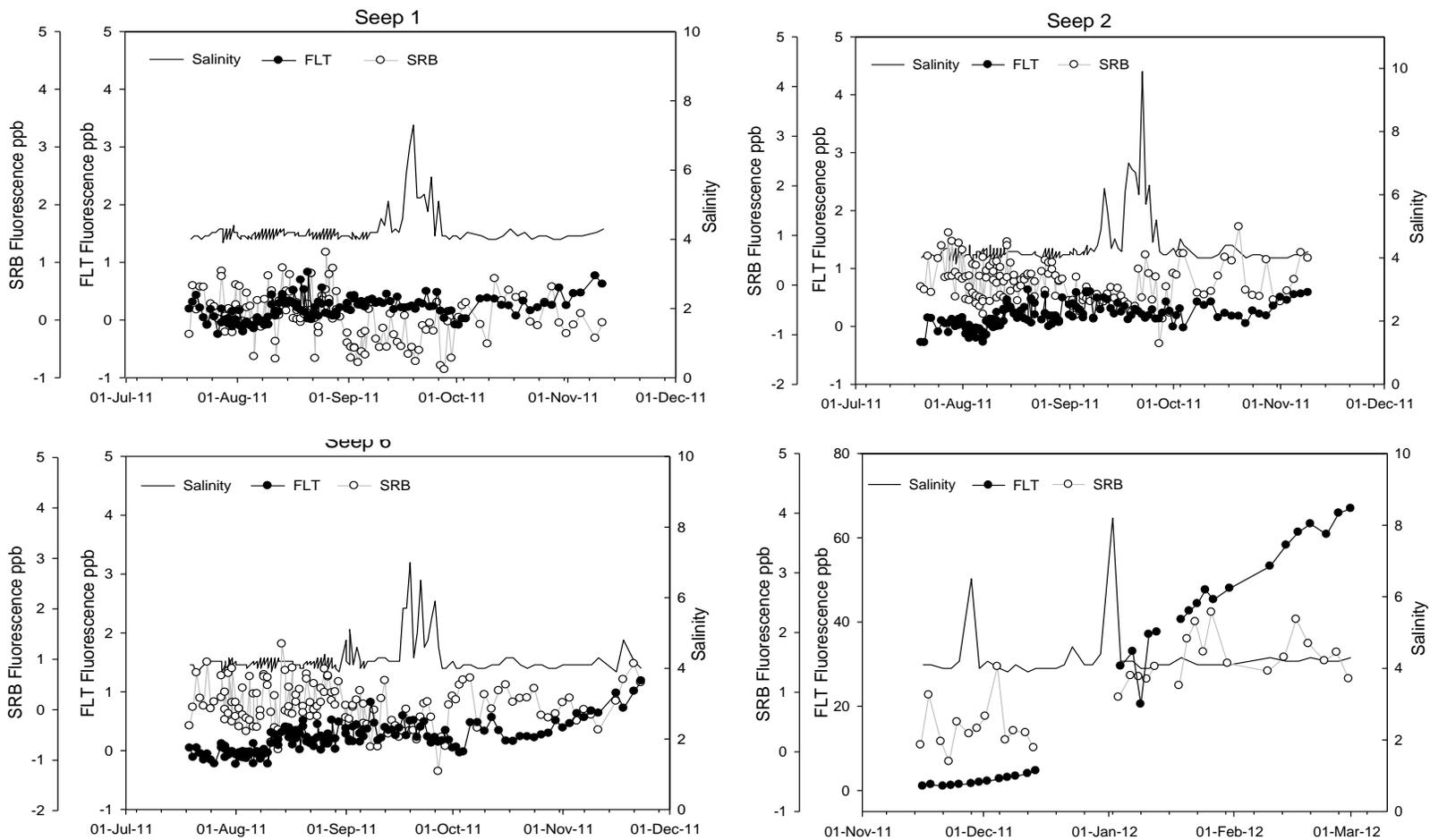
Figure 2-9: North Seep Group salinity and fluorescence (Seeps 1, 2, 6, 7).
Field salinity (solid line) and fluorescence of S-Rhodamine-B (SRB; in open circles) and Fluorescein (FLT; in closed circles) of samples collected from Seeps 1, 2, 6, and 7 over time. Note the change in scale of the FLT fluorescence axis for Seep 7.
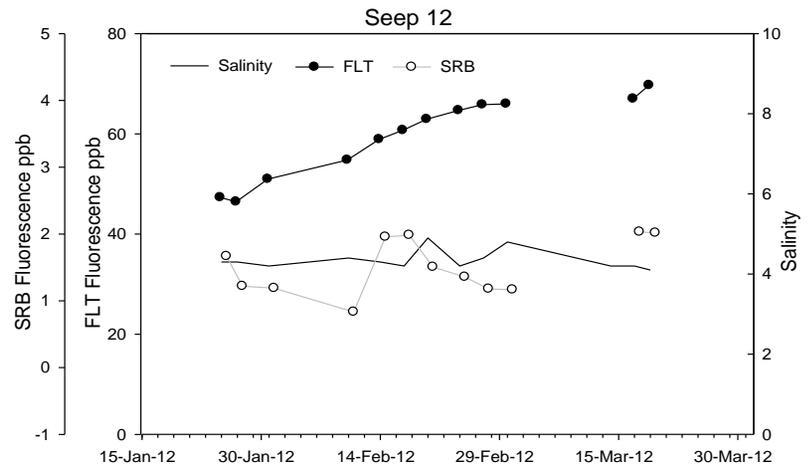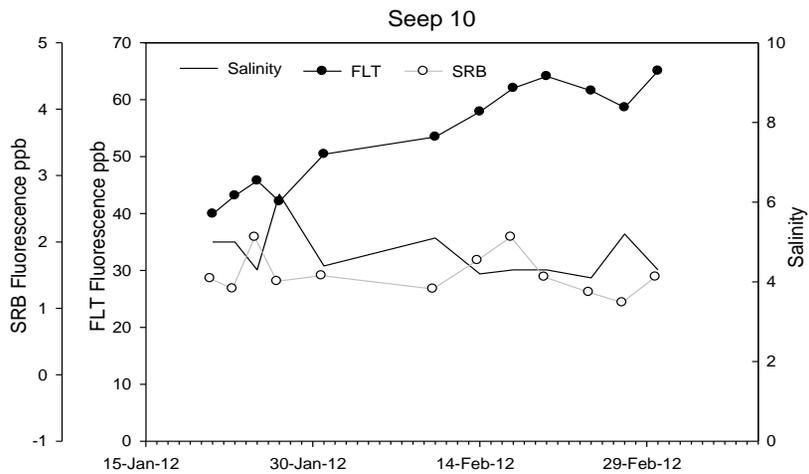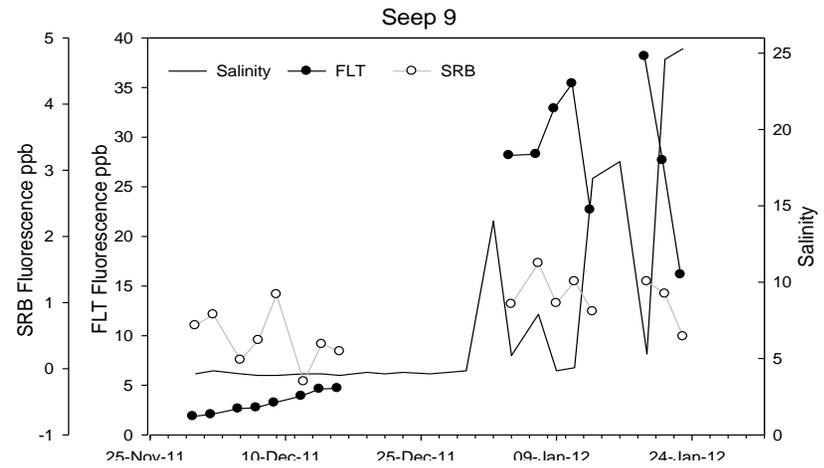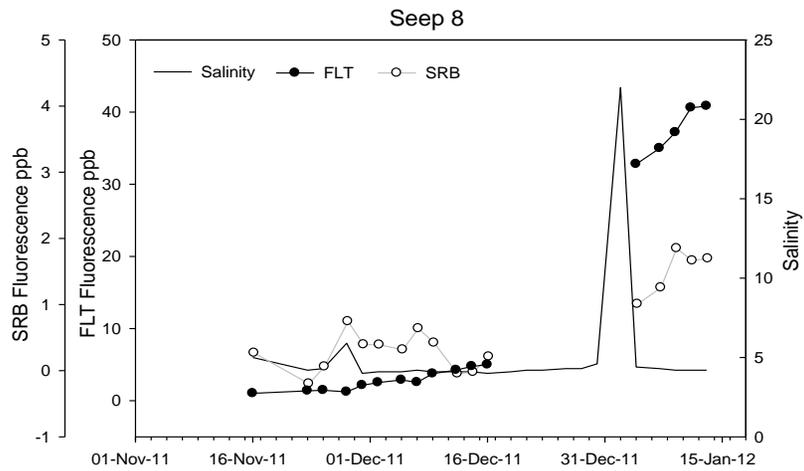
Figure 2-10: North Seep Group salinity and fluorescence (Seeps 8, 9, 10, 12).
Field salinity (solid line) and fluorescence of S-Rhodamine-B (SRB; in open circles) and Fluorescein (FLT; in closed circles) of samples collected from Seeps 8, 9, 10, and 12 over time. Note the change in scale of the FLT fluorescence and salinity axis per seep.

47
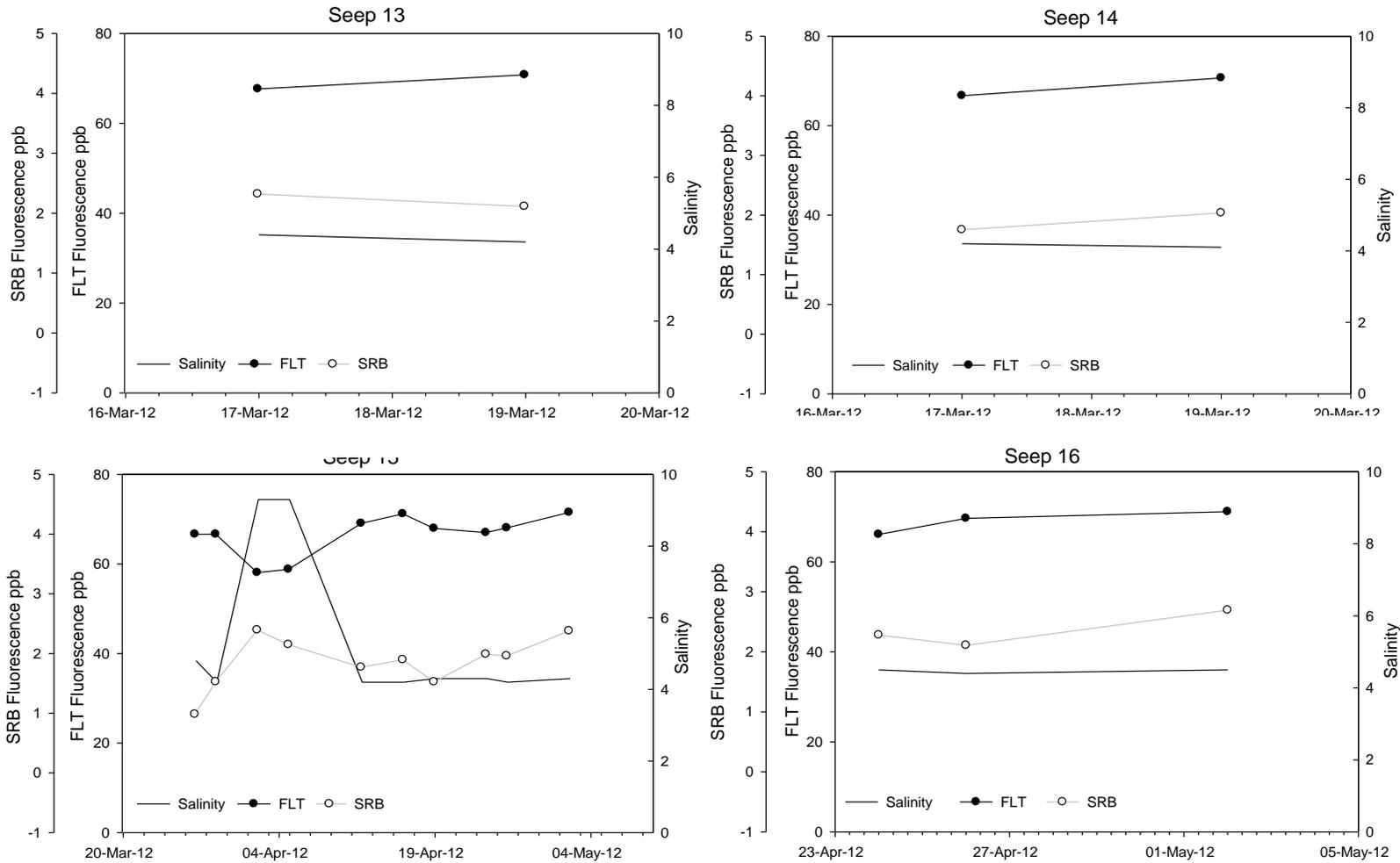
Figure

Figure 2-11: North Seep Group salinity and fluorescence (Seeps 13, 14, 15, 16).
Field salinity (solid line) and fluorescence of S-Rhodamine-B (SRB; in open circles) and Fluorescein (FLT; in closed circles) of samples collected from Seeps 13, 14, 15, and 16 over time.
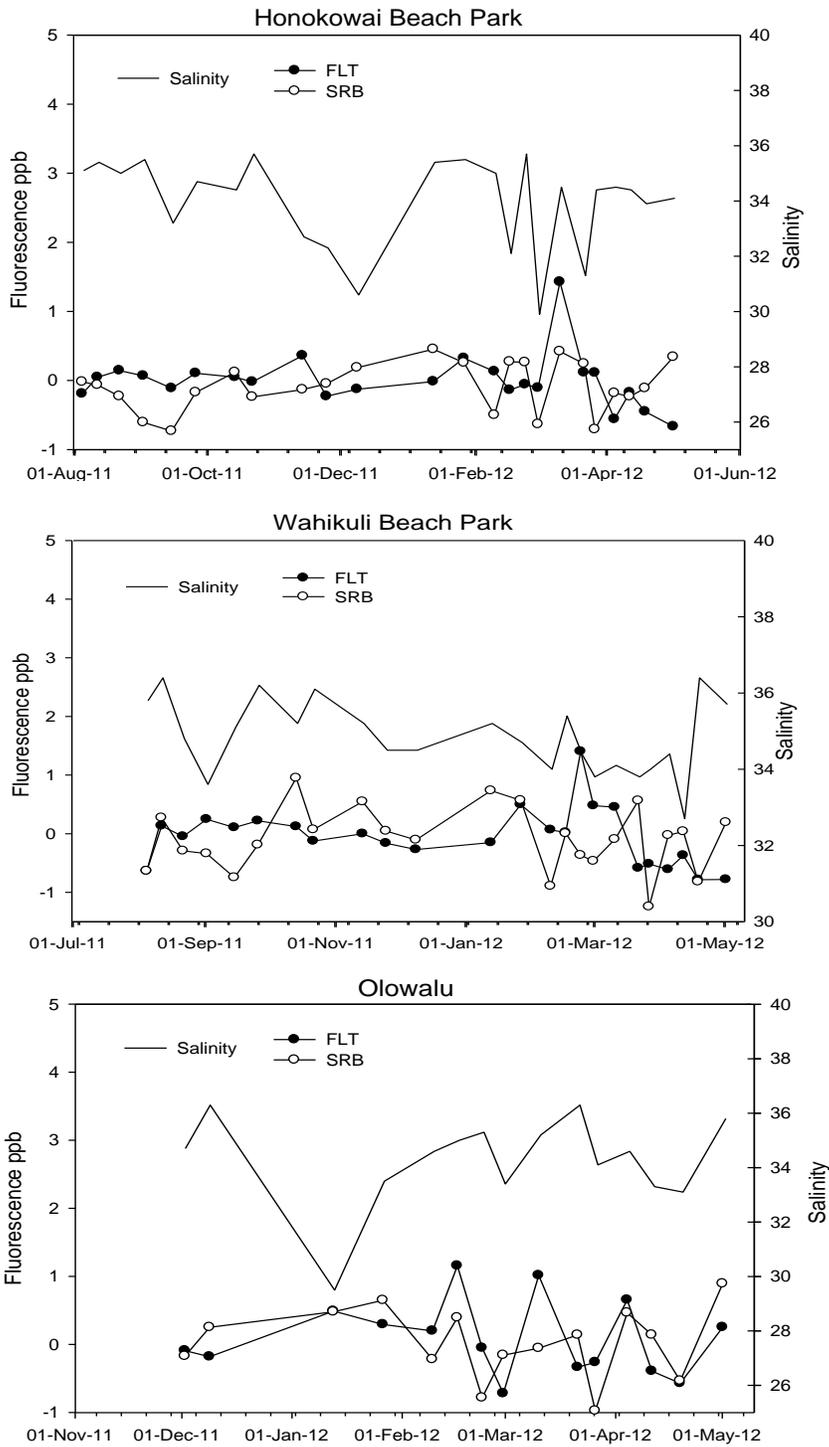
Figure 2-12: Control location salinity and fluorescence.
Field salinity (solid line) and fluorescence of S-Rhodamine-B (SRB; open circles) and Fluorescein (FLT; closed circles) of samples collected at the control locations Honokowai Beach Park, Wahikuli Wayside Park and Olowalu over time.
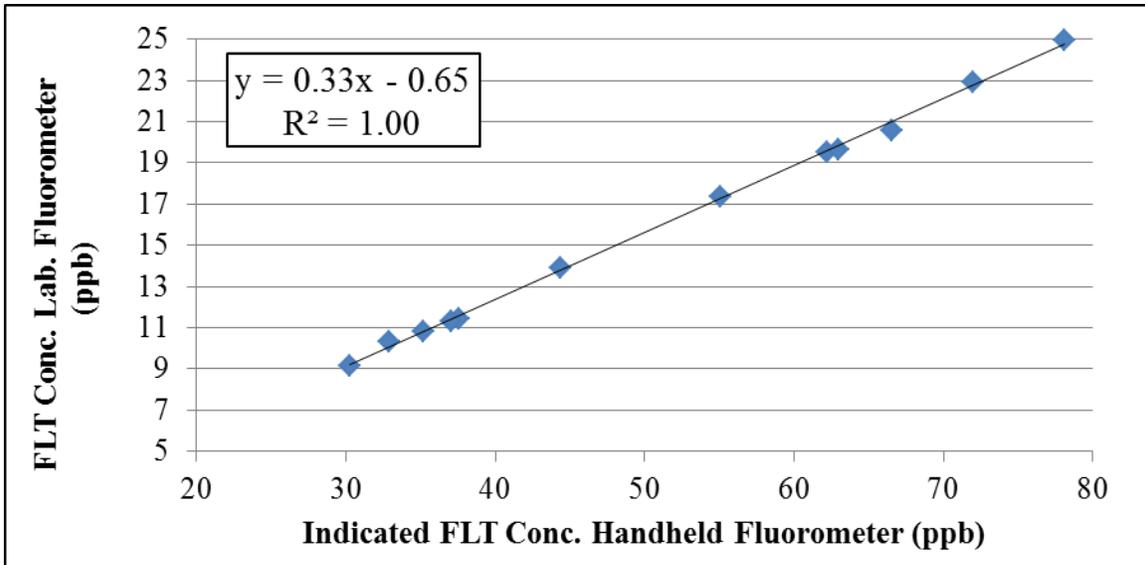
Figure 2-13. Correlation Between the Field and the Lab. Measured FLT.
A best-fit trend line shows that the actual FLT concentration is 0.33 times that of the field measured FLT concentration.
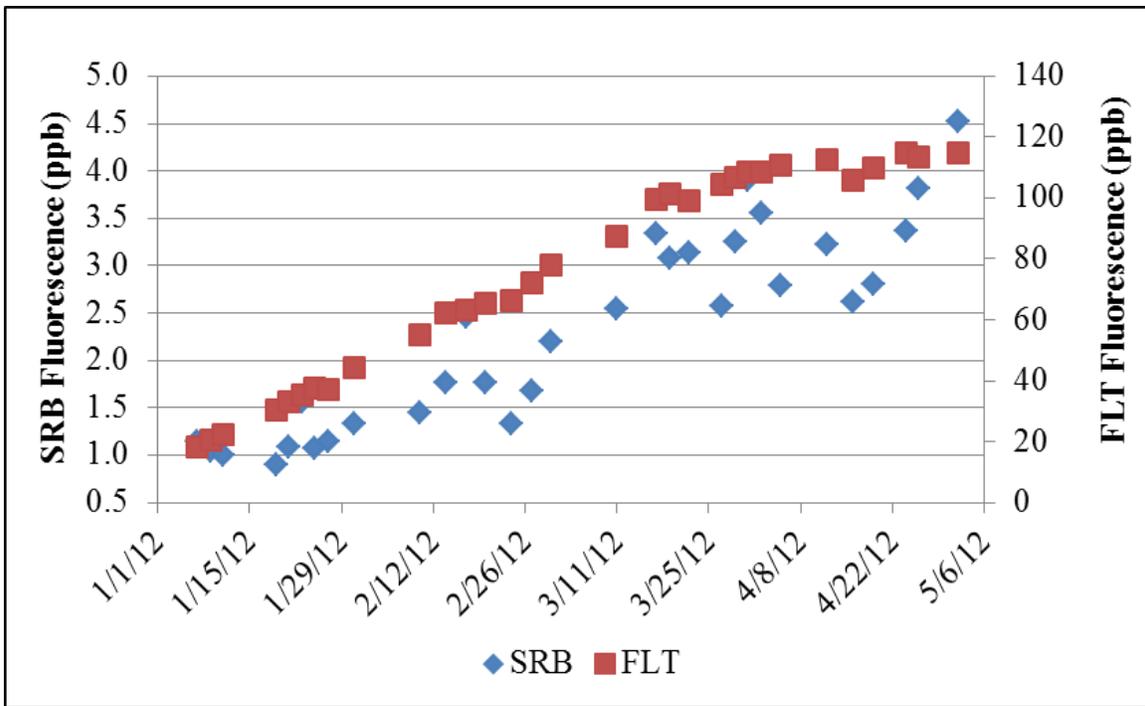
Figure 2-14. A time series showing the close correspondence between the field measured FLT concentration and the apparent SRB fluorescence.
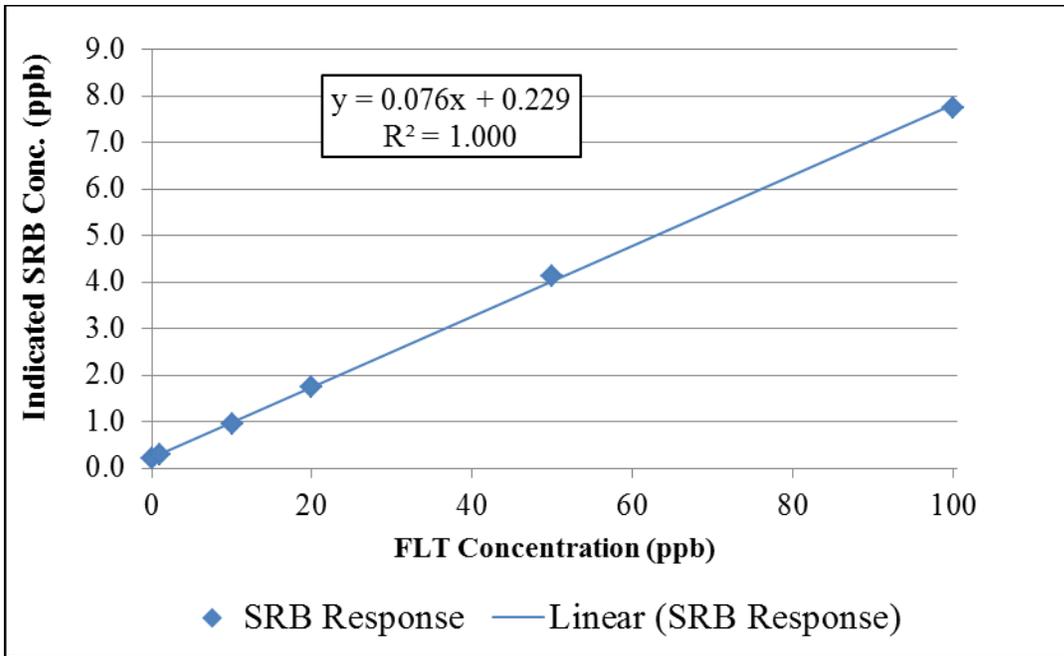
Figure 2-15. The handheld fluorometer SRB channel response to FLT (only) calibration solutions

This page is intentionally left blank.

SECTION 3: FLUORESCENT DYE GROUNDWATER TRACER STUDY

3.1 Introduction

This section provides a status report of the ongoing fluorescent dye tracer test at the site of the underground injection of treated municipal wastewater effluent at the Lahaina Wastewater Reclamation Facility (LWRF), north of the town of Lahaina, Maui, Hawaii (Figure 3-1). At the LWRF, treated wastewater effluent is injected into four wells, designated Injection Wells 1 through 4. The fluorescent dye tracer test is aimed at providing critical data about any hydrological connection between the wastewater effluent injected and the coastal waters, confirming the locations where the injected effluent discharges into the coastal waters, and determining a travel time from the injection wells to the coastal waters. Fluorescent dye was added to the effluent prior to injection followed by a robust surveillance program to monitor the dye arrival to the nearshore marine environment. Figure 3-1 shows the location of the LWRF, the injection wells, and the submarine springs where the dye is monitored. The map also displays details of the monitoring point arrangement including the relative spacing between the sampling points. Two tracer tests were conducted using fluorescent dyes. In the first tracer test, Fluorescein (FLT) was added to Injection Wells 3 and 4. This was followed two weeks later by an addition of Sulpho-Rhodamine-B (SRB) into Injection Well 2, which has a significantly higher injection capacity than the other three wells. The second tracer test was done to investigate whether the effluent from this well discharges into the marine environment at the same location as Wells 3 and 4.

To date, the only confirmed detection by the tracer dye-monitoring program has been FLT. This dye's first arrival occurred about three months following its addition to the LWRF's effluent stream. The concentration of this dye at the submarine springs may have peaked after 7 to 8 months following the initiation of the tracer test. There has been no confirmed detection of SRB, although low-level elevated fluorescence in the SRB wavelength range was observed in three samples collected in February, 2012. These samples showed SRB fluorescence slightly above the method detection limit (MDL) of 0.05 ppb and a wavelength spectra consistent with SRB. The reason for the lack of definitive detection of SRB at the submarine springs remains inconclusive. Factors such as dye degradation, sorption onto the aquifer matrix, or plume displacement by the discharge from Well 3 and Well 4 could account for the failure of this dye to reach the monitored submarine springs. One process of SRB degradation is deaminoalkylation (Käss, 1988) that causes the original SRB fluorescence to shift to a shorter wavelength. Evaluating samples for deaminoalylated SRB (DA-SRB) has not yet been done by this study. However, as described in Section 3.3.2.2 spectrophotometry can be used to detect the presence of this altered SRB.

3.1.1 Tracer Dye Selection

Many techniques exist for tracking the movement of groundwater using introduced or natural tracers. As specified by Stanley et al. (1980), an ideal tracer should be non-toxic, chemically stable over the duration of the tracer test, and detectable at very low concentrations. In addition, the tracer should move with the flow of groundwater and not be removed by natural filtration. Finally, and most importantly, it should not be naturally present in concentrations that would make it difficult to discriminate the added dye from the natural occurrence of the tracer.

There is no ideal tracer, but suitable candidates include ionic salts (Wood and Dykes, 2002; Levy and Chamber, 1987; Olsen and Tenbus, 2004), fluorescent dyes (Smart and Laidlaw, 1977; Chua et al., 2007; Flury and Wai, 2004; Sabatini, 2000), dissolved gases (Malcolm et al., 1980; Wilson and McKay, 1993), radionuclides, and spores and bacteria (Davis et al., 1980; Harvey, 1997). Ionic salts are attractive because they can be detected in low concentrations with ion specific probes. The most widely used are chloride and bromide salts. In this study, interference from marine salts is a problem due to the existence of seawater chloride. The bromide ion is present in Hawaii groundwaters at concentrations of 0.06 milligrams per liter (mg/L) to 0.8 mg/L (Hunt, 2004) making this an attractive secondary tracer. However, in this study, the tracer is monitored in submarine springs where a mixture of freshwater and re-circulated seawater is discharging. The seawater dissolved bromide-concentration measured by this study in September, 2011 varied from 9.1 to 14 mg/L and that measured at the submarine springs varied from 0.83 to 1.4 mg/L. The high tracer concentration required to overcome the interference from seawater bromide made this option too expensive. The presences of dissolved gas tracers can be monitored for on-site and in low concentrations (Davis et al., 1980), but the equipment is bulky and expensive. Radionuclides have safety and regulatory issues, while the special techniques needed to analyze for spores and bacteria are not field friendly.

The tracer of choice for many studies is fluorescent dyes. They are non-toxic (Field et al., 1995), detectable at parts per trillion concentrations with a fluorometer, many are stable, and tend to remain in solution rather than sorbing to the aquifer matrix or suspended particulate matter. Due to possessing the aforementioned desirable qualities, the yellow-green dye FLT and the orange-red dye Rhodamine WT (RWT) are the most widely used of this class of tracers. The tracer dyes considered for this study were FLT, RWT, and SRB. SRB has an absorption/emission couple nearly identical to RWT, and can be analyzed with existing equipment at UH or at the Hawaii Department of Health laboratory. It has the advantage over RWT in that it occurs in a single isomer.

FLT is a yellow-green dye that has been used in tracer studies since the end of the 19th century (Smart and Laidlaw, 1977). FLT is non-toxic to humans and the environment at concentration ranges used in tracer tests (1 to 2 mg/L) (Field et al., 1995). This dye has the advantage of being relatively economical and widely available. A disadvantage for this study is that some constituents in wastewater have fluorescence characteristics that may be similar to that of the tracer.

During fluorescence analysis, a dye is bombarded with light energy of a specific wavelength (the excitation wavelength - "ex"), and the energy state of the dye molecule is elevated. The dye then emits light of another wavelength (the emission wavelength - "em") (Brown, 2009; Guilbault, 1990). Literature reviews showed that the most common values for ex/em couples for Fluorescein were 490/520 nm (Smart and Laidlaw, 1977, Kasnavia et al., 1999, and Sabatini, 2000, for examples). In water, Käss (1998) lists the excitation/emission (ex/em) wavelength couple for FLT as 491/512. Other constituents in water, and particularly wastewater, emit light energy at similar wavelengths. Galapate et al. (1998) found fluorescence peaks at 524 nm for gray water and 531 nm for sewage effluent close to that of FLT. These findings necessitated a thorough background fluorescence investigation and resulted in our using tracer dyes at concentrations high enough to overcome such interference problems. In addition, FLT is unstable when exposed to artificial or natural light, which alleviates problems with dye coloring the nearshore waters, but necessitates the collection of samples in dark colored or opaque bottles. Since the travel path for the tracer test is underground, no photodegradation will occur prior to sample collection. Fluorescence of FLT also decreases at pH values less than 6.5 (Smart and Laidlaw, 1977). The pH of the effluent sampled in this study varied from 6.5 to 7.1, while the pH of the samples collected at the submarine springs varied from 7.2 to 7.9 (See Section 2). Hence, for this study, the pH of the water sampled does not adversely affect the fluorescence of FLT.

SRB is a red dye that is commonly used in wastewater investigations. Literature lists various ex/em couples for SRB. For example, Smart and Laidlaw (1977) list values 565/590, Nikon (http://www.microscopyu.com/articles/fluorescence/filtercubes/green/greenhome.html) lists values of 565/586 nm, while Käss (1998) lists values as 560/584. This is significantly longer than that of wastewater effluent reducing interference. It is stable in waters with a pH higher than 5 (Smart and Laidlaw, 1977). SRB was selected over RWT because RWT occurs in two isomers with differing sorption characteristics (Sutton et al., 2001). As the travel time of the tracer dye increases, there would be a separation of the two isomers resulting in double-peaked breakthrough curves with added difficulties for interpretation.

3.2 Injection Wells 3 and 4 Tracer Test

The first dye addition was into the south well group (Injection Wells 3 and 4) using FLT (see Figure 3-2 for a line diagram of the LWRF system) on July 28, 2011. The target dye concentration in the effluent was approximately 12,500 ppb based on an assumed injection rate of 2.5 million gallons per day (mgd) into this well group. The dye was received from the vendor in a powder form that was 77 percent active ingredient by weight. The dye was mixed on site in a utility shed by using ten pounds (lbs) of powder (one-half of a 20 lb bucket) and a sufficient amount of water to make 50 gallons (gal.) of dye solution. The strength of this concentrate was 1.8 percent active ingredient by weight. The powder was dissolved into the water using a heavy-duty paint/mortar mixer with a helical mixing paddle (Figure 3-3). The shaft length was extended from 15 inches

to 36 inches for use in the 55-gallon plastic drum. The mixing was done into two drums at a time so the entire contents of one powder bucket could be used during a single mixing iteration. Once mixed, the concentrate was transferred to 5 gal. pails using a small utility pump (Figure 3-4). The pails had screw-on lids with a sealing gasket to prevent spillage. The pails were then delivered from the mixing site to the injection wells via pickup truck. The dye was added to the injection wells through a port on the top flange of the well casing using a small submersible fountain pump (Figure 3-5). When the level in the bucket got below the suction of the fountain pump, the remaining dye concentrate was directly poured into the well port (Figure 3-6). A dose of dye was added every 15 minutes at an appropriate rate to sustain the target concentration of 12,500 ppb. Dye addition started at 07:00 on July 28th 2011 and continued uninterrupted until 02:00 on July 29th 2011 (Figures 3-7 and 3-8).

A total 262 lbs of active ingredient, or 340 lbs of total FLT powder weight, was purchased for this event. The weight of dye added would be slightly less than this amount due to minor spillage. At the planned mixing rate, this weight of powder should produce 1,700 gal. of concentrate. A volume of 1,700 gal. of concentrate represents 34 drums and 340 buckets of liquid with expected measurement error. Based on records kept at the wells, a total of 1,670 gal. of concentrate was added to the wells. The dye addition was terminated one hour early because the dye was expended. It was determined upon review of the mixing volumes and the rate at which the dye powder buckets used that one drum was mixed to a concentration twice as much as the target value. When this mixing error is taken into account, the planned volume added would be 1,650 gal. This leads to a difference of a little over 1 percent, well within the certainty of measurement methods.

Figure 3-9 compares actual FLT concentration in the effluent to the rate of effluent injection. The tracer injection started at the onset of the morning increase in effluent discharge. The initial pulse addition of FLT was small giving a starting dye concentration of about 4,400 ppb. However, by 08:00, the dye addition rate had been increased to match the rise in effluent injection resulting in a dye concentration of about 12,500 ppb. There was slight variation in both the injection rate into these wells and dye concentration during the hours from 09:00 on July 28th 2011 through hour 00:00 on July 29th 2011. The injection rate was 3.2 +/- 0.25 mgd. The average dye concentration was 13,700, varying between 12,500 and 14,300 ppb. Just after midnight, the effluent injection rate started to decrease resulting in a dye concentration of 17,400 ppb during the final hour of dye addition.

3.2.1 Fluorescein Analysis

In fluorescence analysis, the sample is subjected to a beam of light with a wavelength (excitation wavelength) specific to the species being analyzed. This excites the atoms of the analyte which emits light at another wavelength (the emission wavelength). The FLT concentration was measured using a Turner designs 10-AU Fluorometer (Turner Designs, 1999), which is capable of detecting FLT concentrations as low as 0.01 ppb. This instrument is equipped with a 10-086R optical kit that includes a blue mercury vapor

lamp, a 486 nm excitation filter, a 510-700 nm emission filter, and 485 nm and higher reference filter. All samples, including the submarine spring water used for preparing the calibration solutions for FLT and SRB, were filtered using a 0.45 micron paper pre-filter prior to analysis. To hold the samples and calibration solutions during analysis, 13-mm glass cuvettes were used. Following a half-hour warm-up period, the system baseline was set with a distilled water blank. The fluorometer span was then set using a 10 ppb FLT calibration solution. Linearity of the instrument response was verified with 0, 1, 10, 20, 50, and 100 ppb FLT solutions.

3.2.1.1 Sample Handling

Once received at UH, the samples are stored in an air-conditioned room until they are filtered and analyzed. The Fluorescein analysis is done at UH in an air-conditioned room separate from the building where the filtering is done. When filtering, a sample aliquot is discharged into an opaque brown Nalgene bottle to prevent photo-degradation. After filtering, the samples are taken to another building for analysis. Since the temperature of analysis room is much colder (16 – 19 ^{o}C) than the filtering room, the samples were stored in the analysis room overnight to allow the samples and calibration solutions to become temperature equilibrated prior to analysis.

Upon completion of all analyses the samples were refrigerated. The time between sample collection and completion of analysis can be up to 1.5 months. Delay in sample refrigeration could result in faster biological degradation of the dye in the samples and in the calibration solutions. To evaluate the stability of the dyes, we store the calibration solutions on the shelf, and not in the refrigerator. As part of the calibration process, we read the raw fluorescence of the standards (10 ppb only for Fluorescein and all solutions for SRB) to document any change in fluorescence intensity with time. Thus, if degradation during storage is a factor it would be detected by a decrease in the raw fluorescence intensity of the unrefrigerated calibration solutions. We also routinely do synchronous scans of selected solutions to document any change in the wavelength spectrum of the solutions. To date, no sign of degradation has been found.

After consultation with the EPA, we have revised our sampling handling procedures to minimize the time that samples are not refrigerated. Upon receipt of the samples at the UH, they are immediately filtered or place in a refrigerator until they can be filtered. Once the samples are filtered, they are delivered to the laboratory room where the analysis is done. They are again stored overnight in this room where the temperature varies between 16 to 19 ^{o}C, and are then analyzed the next day. The samples are also stored in this laboratory room until taken to the HDOH laboratory for SRB analyses. This typically occurs within a few days following the FLT analyses.

3.2.1.2 Laboratory Analysis

3.2.1.2.1 Preparation of Calibration Solutions

FLT calibration solutions were mixed to establish a basis from which to convert the measured fluorescence to a concentration of FLT. These calibration solutions were prepared by diluting a 100,000 ppb stock solution with water. Initially, deionized (DI) water was used, but this produced unstable solutions, possibly due to a low pH in the DI water. Subsequent solutions were prepared using pre-collected submarine spring water filtered with a 0.45-micron paper pre-filter.

An initial FLT stock solution with a concentration of 100,000 ppb was made by adding 133 milligrams (mg) of 75 percent active-ingredient FLT powder to a small glass beaker. The dye powder was weighed using a precision scale. One liter (L) of distilled water was measured in a volumetric flask that was filled to the 1 L mark. The majority of the water in the volumetric flask was decanted into a 1 L amber bottle. The dye powder was then added to the bottle. The water remaining in the volumetric flask was then used to rinse remaining powder from the small beaker into the solution added to the amber bottle. This stock solution was then used to prepare the calibration solutions. This was accomplished by completing a series of dilutions of the 100,000 ppb stock solution. These serial dilutions were limited to two to minimize the propagation error. A 100 ppb calibration solution was made by diluting 1 milliliter (ml) the stock solution with 999 ml of water using a precision pipette and volumetric flask. The remaining dye calibration solutions were mixed using the 100 ppb calibration solution as shown in Table 3-1.

3.2.1.2.2 Calibration Solutions – Deionized (DI) Water vs. Submarine Spring Water

When mixing solutions for the Method Detection Limit (MDL) study (described below) it was found that the indicated fluorescence was four times than expected. This increased fluorescence was confirmed by mixing two FLT solutions using the same mass of dye in each. One solution was mixed using DI water and the other solution was mixed using dye-free submarine spring water (collected prior the addition of FLT to effluent stream). The fluorescence of the submarine spring water was read with the fluorometer prior to adding dye to ensure that its natural fluorescence was consistent with background values measured by this study. FLT was added to DI water and submarine spring water solutions to produce concentrations of 1, 10, 20, 50, and 100 ppb. The fluorometer span was set using the 10 ppb submarine spring water based solution and the linearity was verified with the remaining submarine spring water based solutions. The fluorescence of both sets of solutions was then read with the fluorometer. Figure 3-10 shows that the fluorescence of the submarine spring water solutions was indeed about four times greater than that of the DI water based solutions. All subsequent calibration solutions have been mixed using submarine spring water collected prior to the FLT addition. New SRB calibration solutions were also mixed using submarine spring water to maintain consistency between the methods used to analyze the two dyes. However, comparison of the DI and submarine spring water based SRB solutions showed no difference.

58

After recognizing the problem with the use of DI water to mix the calibration solutions, a literature search that found this problem was not unique to this study. Brown (2009), for example, found that the indicated fluorescence of an FLT solution mixed using distilled water was about one-third of the indicated FLT fluorescence when natural spring water was used. This quenching of the FLT fluorescence by DI may be due to the lower pH of water with negligible dissolved ion content (i.e. the DI water used in the original calibration solutions). Smart and Laidlaw (1977) show a nearly complete quenching of FLT fluorescence at a pH of 3.0. Dever (1997) calculates the pH of pure water in equilibrium the atmosphere to be 3.1. Taken together, these references strongly indicate the problem encountered with the DI-based calibration solutions ion in the present study was due to the low pH of pure water. This problem was resolved by using submarine spring water to mix the calibration solutions, instead of DI water.

3.2.1.2.3 FLT Method Detection Limit (MDL)

The Method Detection Limit (MDL) is defined as: "the minimum concentration of a substance that can be measured and reported with 99% confidence that the analyte concentration is greater than zero, and is determined from analysis of a sample in a given matrix containing the analyte." (Wisconsin Dept. of Natural Resources, 1996). For this study, two methods were used to assess the MDL. The first is that used by the U.S. EPA and is codified in the U.S. Code of Federal Regulations (CFR), 40 CFR Appendix B to Part 136 (USEPA, 2011). This approach is based on a single concentration design, which assumes that variability at a certain concentration is equal to the variability at the true MDL. With this method:

- It is recommended that the candidate MDL sample have an analyte concentration one to five times that of the estimated MDL
- The analyte concentration in the MDL sample should not exceed 10 times the actual MDL
- At least seven aliquots at the candidate MDL concentration need to be analyzed to document the analytical variance
- The concentration of the MDL candidate should be at least three times solution deviation of the replicate analyses
- The signal to noise ratio should fall in the range between 2.5 to 5.

Details of this method are provided in Appendix B-1.

The second MDL assessment method was developed by Hubaux and Vos (1970) who were the first to apply the theory of statistical prediction to estimating the MDL. They defined the limit of detection as the point at which we can have 99% confidence that the response signal is not the critical level, which was defined as the value of the prediction limit for zero concentration (i.e. that no analyte is present in the sample). This method involves the use of a calibration design and assumes that the variability is constant throughout the range of concentrations used in the calibration design. Hubaux and Vos (1970) suggest that the limit of detection can be obtained graphically by locating the abscissa corresponding to critical level on the lower prediction limit. In order to

59

determine the MDL, a series of samples is spiked at known concentrations in the range of the hypothesized MDL. From these samples, the variability is determined by examining the deviations of the actual response signal on known concentrations. In this case, it is assumed that the distribution of these deviations from the fitted regression line is normal with a constant variance across the range of concentrations used in the study. The details of this method are elucidated in Appendix B-1.

To accommodate both MDL analysis methods, four sets of solutions were mixed. For FLT, these included concentrations of 0.0, 0.1, 0.2, and 0.5 ppb. The dye, in the appropriate volume, was added to 1 L of unfiltered submarine spring water. Each MDL solution batch was processed in the same way the tracer samples were, including filtering the sample with a 0.45-micron paper pre-filter into a 125 ml brown plastic bottle. This resulted in eight aliquots at each concentration for the MDL analysis. The individual aliquots were then analyzed in the same manner as the tracer samples and the results entered into an MDL calculator spreadsheet that was downloaded from http://www.chemiasoft.com/mdl_calc.html. The fluorescence values entered into the spreadsheet were the total fluorescence as read on the fluorometer minus the average no-dye fluorescence. Tables 3-2 and 3-3 summarize the results of the MDL calculations using the methods by EPA and by Hubaux and Vos (1970), respectively. The MDL calculated by the EPA method for the lowest concentration solution (0.1 ppb) was 0.011 ppb. However, this concentration is about one-tenth of the concentration of the lowest solution tested. This resulted in a signal to noise of ratio of 28.6, which is greater than the recommended range of 2.5 to 10.

The MDL calculated by the Hubaux and Vos (1970) method depends on the linearity of multiple concentrations rather than on that of a single concentration and resulted in a slightly higher MDL. For this method, the MDL calculator only allowed three samples per concentration so the lowest, the highest, and the average concentrations for MDL solution set was entered into the MDL calculator. The resulting MDL was 0.02 ppb above background, slightly higher than that of the EPA method and was used as the Fluorescein MDL for this study. The critical response concentration is the instrument response (Fluorescein plus background) at which the analyte (Fluorescein) can be distinguished from background and is considered detected. As described in the next section, the background concentration of FLT was 0.11 ppb making the MDL 0.13 ppb as read on the fluorometer. The critical concentration is the actual analyte concentration when it is first detected. The MDL differs from the critical concentration in that the former provides concentration values of the analyte detected with 95 percent certainty.

3.2.2 Background Fluorescence Assessment and First Detection

The fluorometer used in this study has a manufacturer specified detection limit of 0.01 ppb for FLT. But fluorescence variability in tracer samples collected in the field may mask very low concentrations of dye. Quantifying the natural fluorescence of the study area and the concentration at which the fluorometer can reliably discriminate between natural and tracer fluorescence is critical in establishing the first arrival time of the dye.

60

Natural and anthropogenic compounds in the water mixture emerging from the submarine springs have fluorescence characteristics that may mimic that of the dyes selected for this study (Meus et al., 2006; and Smart and Karunaratne, 2002). For example, these interferences can be caused by fabric brightener agents that fluoresce in the blue wavelengths (Poiger et al., 1998). Although these agents are expected in the LWRF wastewater effluent, the blue wavelengths are well below that of the dyes used in this study. Other in situ sources of fluorescence, such as fluvic acids, also fall in wavelengths significantly shorter than that of FLT (Baker et al., 2003). More problematic are fluorescent peaks at about 520 nm that have been identified in a number of studies. Smart and Karunaratne (2002) attributed this peak to antifreeze containing FLT. In a study of the fluorescence of domestic wastes in the Kurose River in Japan, Galapate et al. (1998) showed there was a 531 nm peak in sewage effluent; when effluent was mixed with river water, this peak shifted to a wavelength of 524 nm, which is very close to that of FLT.

Since organic matter may fluoresce in a manner similar to the tracer dyes (Mues et al., 2006; and Smart and Karunaratne, 2002), this interference needed to be evaluated. This process consisted of directly measuring the fluorescence of submarine spring water tagged with tracer at various concentrations (see Method Detection Limit sub-section for details) and measuring the fluorescence of the submarine spring samples collected for a period before the dye arrival.

Our background assessment served two purposes. First, it characterized the background or natural fluorescence in the FLT wavelength. This natural fluorescence can be subtracted from the measured fluorescence to quantify that attributable to the dye only. This is also important in estimating the percent of dye recovery where only low concentrations of dye are detected. The second purpose is that knowing the background fluorescence is important in estimating the time for dye's first arrival. Collection of samples from the submarine springs began on July 5th, 2011, more than three weeks prior to the first dye release to the LWRF injection wells. Since dye was not detected in the marine submarine springs (seeps) until mid-October 2011, the samples collected prior to October 1, 2011 were included in the background fluorescence assessment.

Table 3-4 and 3-5 provides a summary of the fluorescence in the FLT wavelength measured during the background evaluation period. The average background fluorescence for both the North Seep Group (NSG) and the South Seep Group (SSG) was equivalent to that 0.11 ppb FLT. There was minor variability except for Seep 4, where the lowest background concentration measured was equivalent to 0.01 ppb of FLT. The small number of samples included in the background analysis was due to problems with the calibration solutions prepared using DI water (previously described). After the fluorometer was calibrated with the submarine spring water calibration solutions, a minimum of twelve background samples from each of the original submarine spring locations were chosen at random and re-analyzed.

The background fluorescence in the FLT wavelength was much less than expected and very small compared to the FLT concentrations measured except those at the very

beginning of the tracer breakthrough curve. No adjustments were made to the measured FLT concentrations, but the background fluorescence combined with the computed MDL was used to establish the time of first dye detection. For this study, the time of first dye arrival is defined as when the first measured concentration that equaled or exceeded 0.13 ppb (the computed MDL of 0.02 ppb plus a background fluorescence of 0.11 ppb) and marked the start of an increasing trend in dye concentration. Using this definition, the first detection of FLT occurred at the NSG on October 20, 2011. This date was the same for all sampling points in this group. This gives an elapsed time between the dye addition and the first detection at this location of about 84 days. The first detection of FLT at the SSG occurred at Seep 3 on November 5, 2011. The last submarine spring in this group to reveal a detectable concentration was Seep 4 on November 11, 2011. With an average first detection date of November 8, 2011 at the SSG, the elapsed time between the dye addition and this seep group was about 103 days. FLT was detected at the SSG 19 days after it was detected at the NSG.

Grab samples were also collected to assess the marine water fluorescence just above each seep group and from "control" locations not expected to be affected by the discharged LWRF effluent (Section 2). These locations included Honokowai Beach Park, Wahikuli Wayside Park, and the beach fronting Olowalu (Figure 3-11). Table 3-6 summarizes the fluorescence of the marine samples collected prior to October 1, 2011. The average fluorescence in the FLT wavelength at these locations was negligible and equivalent to about 0.01 ppb of FLT.

3.2.3 The Breakthrough Curve - Fluorescein

A breakthrough curve (BTC) is a graph illustrating tracer concentration versus time. It is used to evaluate the time of first dye arrival, dispersion characteristics of the aquifer, average time of travel, and when combined with water flux, the mass of the tracer that can be accounted for. Relative to the total mass injected, this mass can be used to estimate the percent of tracer recovery.

3.2.3.1 North Seep Group

As described in the Section 2, sand moving off-shore (and likely along-shore) covered some of the sampling piezometers installed in the submarine springs (seeps) during the monitoring period. Heavy surf in early to mid-November buried all of the original piezometers (Seeps 1, 2, and 6) in the NSG. This problem continued to plague the project. As a piezometer was buried, a replacement was installed to maintain three sampling points in this group. However, with the burying of Seep 12 on March 19th, 2012 only Seep 15 was available until April 24th, 2012. On that date, the Seep 4 piezometer in the SSG was moved to the NSG to provide a second sampling point. Figure 3-12 shows the time intervals during which samples were collected from each submarine spring. Figure 3-13 shows the BTC for the NSG. In spite of losing multiple piezometers to the migrating sand, the data shows good fluorescence continuity between sampling points. The exception is the FLT concentration at Seep 9, and one data point at Seep 15. The low dye concentrations from these submarine springs correspond with high

salinities when compared to the salinities other sampling locations. In any event, the collective data set is sufficient, and once the leading edge of the BTC was established, the dye concentration increased at a rate of about 0.2 ppb/d until February 27th, 2012. On this date, there was an abrupt flattening of the BTC. Following this inflection point in the BTC, the dye concentration remained steady at about 21 ppb. Seep 15 showed a significant decrease in dye concentration in the sample that was collected on April 2nd, 2012. The salinity in this sample was 9.3, significantly greater than the average salinity of 4.4 at this group.

3.2.3.2 South Seep Group

All of the piezometers installed at this site at the beginning of the project are still in service except Seep 4 which, as mentioned earlier, was relocated April 24th, 2012 to provide a second sampling point for the NSG. Seep 11 was installed on January 21st, 2012 to augment the data collected at this site since the dye concentrations at Seep 4 and Seep 5 had significant variability. Figure 3-14 illustrates the BTC for this seep group, which displays much greater variability among the sampling points at this site than there is at the NSG. Seep 3 consistently has the highest concentration and shows a near linear increase of about 0.5 ppb/d during the majority of the rising limb of the BTC. Seep 4 has the lowest and most variable dye concentration. As is discussed below, this sampling point also has the greatest variability in salinity. Seep 5 also has significant variability in the salinity and in the dye concentration. However, the dye concentration of Seep 5 usually falls between that of Seep 3 and of Seep 4. Seep 11, although installed after the arrival of the dye, produces a good BTC very close to that of Seep 3. The FLT concentration at the SSG has appeared to plateau at about 33 ppb starting in early April. The delay between the plateau at the NSG and the SSG is about a month, which is slightly longer than the delay between first detections noted above.

3.2.3.3 The Relationship Between Dye Concentrations and Salinity

As described previously, the sampling locations that showed the greatest variability in FLT dye concentration also had the greatest variability in the salinity measured at the time of sampling. Table 3-7 is a summary of the salinities measured at each submarine spring from January 13th through May 2nd, 2012. The points with the greatest variability in salinity and the respective FLT concentration are Seeps 9, 4, and 5. The NSG had little variability in salinity except for Seep 9 and a single data point for Seep 15. With the exception of Seep 9, the FLT concentrations at the submarine springs in NSG were nearly identical across sampling points (Figure 3-13). In the SSG (Figure 3-14), the FLT concentrations at Seep 4 and Seep 5 showed a significant variability when compared to Seep 3. These submarine springs also had high solution deviations in their salinity.

The relationship between the FLT concentration variability and salinity variability was tested graphically and statistically. Figure 3-15 shows the relationship between salinity and dye concentration at Seep 4. Since the dye concentration varies with time, the data presented actually compares ratios. The ratio on the x-axis is that for the salinity measured at Seep 4 to that measured at Seep 3, while the ratio on the y-axis is that for the

respective dye concentration measured at the two submarine springs. The low variability in salinity at Seep 3 and the near linear increase in the dye concentration at this sampling location made this data set a good reference. The r-squared linear regression for these data was 0.85, indicating that variations in the salinity ratio can account for about 85 percent of the variability in the dye concentration ratio. There was one data point that could be an outlier. When this data point was removed, the r-squared value increased to 0.94.

The inverse relationship between the dye concentration and the salinity is caused by mixing of dye-tagged non-saline injected LWRF wastewater effluent with seawater that is nearly void of dye. This is a volumetric dilution effect. The pre-mixing dye concentration in the submarine spring water can be estimated by correcting the measured dye concentration for the fraction of seawater in the submarine spring water sample. This was done using the following formula.

$$FLT_{adj} = FLT_{meas}/[1-(Sal_{seep\ 4}- Sal_{seep\ 3-avg})/(Sal_{SW} – Sal_{seep3-avg})] \qquad (3\text{-}1)$$

Where:

FLT_{adj} = the dye concentration at Seep 4 adjusted for salinity (ppb)

FLT_{meas} = the dye concentration measured at Seep 4

$Sal_{seep\ 4}$ = the salinity measured at Seep 4

$Sal_{seep\ 3-avg}$ = the average salinity measured at Seep 3 (salinity is 3.1)

Sal_{SW} = the average salinity of seawater (salinity assumed to be 35)

Figure 3-16 provides a graph of the FLT concentrations at Seeps 3 and 4 versus time. Also shown on this graph are the FLT concentrations from Seeps 4, 5, and 11 that would be expected at the sampling locations if the salinities were the same as those of Seep 3. Even when the dye concentration in Seep 4 is adjusted to remove the effect of the higher salinity, the dye concentration at this location is still lower than that measured at Seep 3. The relative difference increases as the magnitude of the dye concentration increases. This indicates significant concentration differences over a small area, considering that the distance between Seep 3 and Seep 4 is about 4 m. Hence, it seems that the spatial variability of submarine spring concentration is significant and should not be overlooked.

In addition to collecting samples by drawing water from piezometers driven into the seafloor, grab samples were collected. At each seep group, a grab sample was collected by uncapping a submerged bottle just above a submarine spring discharge. Background grab samples were also collected north of the submarine springs (Honokowai Beach Park) and south of the submarine springs (Wahikuli Wayside Park and the beach fronting Olowalu). Figure 3-17 shows that, with the expectation of one grab sample collected at the SSG, the dye discharging from the submarine spring was diluted by a factor of one order of magnitude or greater, signifying strong mixing between the submarine spring and ocean water immediately adjacent to the submarine springs.

3.2.3.4 NSG and SSG Breakthrough Curves

To compare the BTCs of the NSG and SSG, a single representative sample for each group was graphed (provided in Figure 3-18). For the NSG the dye results from successive sampling locations were plotted. Except in cases where there was no overlap (i.e. between samples from Seep 12 and Seep 15), a two sample overlap was plotted to show that there was no significant difference in concentration. In addition, the dye concentration for Seep 15 was adjusted to correct for the higher salinity measured on April 2nd, 2012. Figure 3-18 shows the dye arriving first at the NSG, but the concentration at the SSG overtaking and exceeding that at the NSG in late February 2011. It also shows the abrupt change in the slope of the NSG BTC in late February 2011. Since Seep 12 was sampled from January 25th through March 19th, 2012, this shift in slope cannot be attributed to a change in sampling location. The history of the FLT fluorescence measured at the NSG and SSG is provided in Appendix B-2, Table B-2.1 and Table B-2.2.

3.2.4 Green Coloration of the South Seep Group Discharge

Starting in late February, 2012, a green coloration was noted in the waters discharging from the submarine springs in the SSG. This phenomenon was not observed prior to this, and to date it has not been observed at the NSG. To date, the source of the green coloration has not been conclusively resolved. While it might be assumed that this coloration is due to the FLT itself, the measured FLT concentration from the SSG of 23 ppb in late February and the maximum of 34 ppb in mid-April are below the generally accepted visual threshold for FLT, which is 100 ppb (Kingscote Chemical, 2010; and Stuart et al., 2008). Possible sources being investigated include: (1) FLT is present in visible concentrations, (2) iron containing minerals such as iron (II) hydroxides, (3) other green minerals, and (4) reactions between chlorine and other dissolved constituents.

Efforts to identify the source of this coloration are on-going, but include:
- Performing a broad spectrum fluorescence scan to determine if any fluorophores other than FLT are present;
- Analyzing these samples for dissolved iron and other metal content;
- Performing a light adsorption analysis on these samples to determine if the intensity of the green coloration correlates to the FLT fluorescence intensity;
- Collecting samples from deeper in the crevices to evaluate if the piezometers are capturing the highest FLT concentration in the submarine spring discharge.

A laboratory solution prepared by mixing optically clear submarine spring water with a 35 ppb FLT concentration showed a distinct green coloration when placed in a 2 liter beaker. This demonstrates that FLT is visible at concentrations less than 100 ppb. This observation is consistent with those of Aley (2002), and Stokes and Griffiths (2000). Also, the FLT concentration at the NSG has not reached 23 ppb, which was the FLT concentration at the SSG when the green coloration started to appear. Thus, the absence of the green coloration at the NSG where FLT is also discharging does not preclude this

dye from being the source of the green coloration at the SSG. The samples that the UH collects at the submarine springs are representative of the non-saline SGD. When UH samples the submarine springs, pH, specific conductivity, and salinity are measured. The salinity in the vast majority of the samples is less the 5, indicating that the samples are capturing non-saline groundwater. This shows that the piezometer screens are not clogged and are properly installed in the openings where groundwater is discharging, and are thus truly capturing the submarine groundwater prior to its emergence and mixing with marine bottom waters.

It is important to affirmatively state at this time that although the cause of the green coloration is as yet to be fully determined and understood, it's presence does not weaken our finding that FLT injected at the LWRF is being discharged from the submarine springs into the nearshore waters near Kahekili Beach Park. To illustrate this, Figure 3-19 shows the results of synchronous scans completed for two samples. A synchronous scan is a sequential series of fluorescence measurements performed on a sample. This is done by defining a starting and ending excitation wavelength, and designating an increment by which to increase the excitation wavelength for each step. Also defined when programming a synchronous scan is the emission wavelength monitored as a function of the excitation wavelength. For the results shown in Figure 3-19, the instrument was programmed to scan from 250 to 600 nm in increments of 0.2 nm. The fluorescence intensity of the emission wavelength monitored was the excitation wavelength plus 20 nm. The first sample was prepared in the laboratory, and contains 35 ppb of FLT and 0.1 ppb SRB. The second sample was collected from Seep 3 on June 7, 2012, and contains 33 ppb of FLT. The synchronous scans were thus completed to confirm or negate that the fluorescence being measured at the submarine springs is indeed FLT. The traces are identical, expect for a small peak at 580 nm, which is the fluorescence of the SRB in the laboratory prepared solution. This test strongly indicates that the FLT is the fluorophore in the samples collected at the submarine springs. Our other efforts to identify the source of the green coloration are continuing.

3.3 Injection Well 2 Tracer Test

A second tracer test was performed at the LWRF Injection Well 2 to investigate whether effluent from Well 2 discharges into the ocean at the same locations as that from Wells 3 and 4. The injection capacity of Well 2 is significantly greater than that of the other wells, implying it may have a hydraulic connection with a preferential flow path. In the second dye addition, Sulpho-Rhodamine-B (SRB) was added on August 11, 2011, two weeks after the first FLT dye additions at Wells 3 and 4.

Despite its higher injection capacity, the effluent flow into Well 2 is significantly less than that into Wells 3 and 4 because the wellhead elevation is higher, resulting in less gravity flow to this well. The average injection rate into the Well 2 during the period of August 3rd through August 10th, 2011 was 0.76 mgd, in contrast to that into Well 3 and Well 4 of 1.3 and 1.1 mgd, respectively. The flow into Well 2 generally occurred between the hours of 10:00 to 20:00. Our assessment indicated that the flow rate and duration into Well 2 was not sufficient to adequately assess the hydraulic connectivity

between the well and the nearshore waters. Therefore, the plant operations were modified to sustain an injection rate greater than 1 mgd. This was accomplished by diverting all R1 water to injection and throttling down on the well-head valves for Well 3 and Well 4 at the start of dye injection.

The dye mixing process for this test was the same as described above for FLT, with a mixing rate of 10 lbs per 50 gal. The active ingredient fraction of the SRB powder is approximately 25 percent, which resulted in a solution that is 0.60 percent active ingredient by weight. A total of 180 lbs of dye powder was used to provide a total of 900 gal. of SRB dye solution. The planned concentration of SRB mixed with the effluent in Well 2 was 2,600 ppb. The dye was added at the Effluent Splitter Box (Figure 3-20) at 15-minute intervals starting at 07:00 and continuing through 00:45.

Figure 3-21 shows the well injection rates and the resulting dye concentration in Well 2 for this test. When the dye addition started at 07:15 on August 11th, 2011, the flow into Well 2 had not reached the desired magnitude, which produced a very high concentration for the first hour at about 38,000 ppb. Throttling down of the valves at the wellhead of Wells 3 and 4 resulted in increased flow to Well 2, which decreased the injection concentration to about 1,500 ppb. For the period from 09:00 until 22:00, the flow into Well 2 was less variable and the dye injection concentration varied from about 2,100 ppb to about 3,500 ppb. At about 22:15, the flow into Well 2 started to decrease and less amount of dye was added to keep the dye concentration range in the range between 2,000 to 2,500 ppb until about midnight. At that point, due to the falling effluent injection into Well 2, the remaining dye concentrate (about 22.5 gal.) was added to the splitter box between 00:00 and 00:45. This increased the dye injection concentration for the final hour of dye addition to about 12,000 ppb. Dye addition was terminated at 00:45 on August 12th. For the 24-hour period from 07:00 August 11th until 07:00 on August 12th, 21022011, the flow into Well 2 was 2.1 million gal. and total flow to all wells was 5.1 million gal. The average SRB concentration in the Well 2 and all injected effluent was 2,500 and 1,000 ppb, respectively.

3.3.1 Sample Handling

All SRB analyses have been completed at the HDOH laboratories. Temperature can affect the dye fluorescence, so for these analyses the samples and calibration solutions are stored overnight at ambient temperature. Hawaii nighttime temperatures are similar to that of an air-conditioned room. Early the next morning (prior to 7:30 am) the samples are delivered to the HDOH laboratory for each analysis set. The warm-up time for the spectrophotometer is about 30 minutes, so calibration solutions, samples, and instrument are all located in same room for approximately one hour while we are setting up for analyses and starting the equipment. An hour does not ensure complete temperature equilibration with the instrument, but since the calibration solutions and the samples are stored and transported together, they are temperature equilibrated.

The temperature effect on a dye's fluorescence varies depending on the dye analyzed. The variation in the fluorescence intensity of a dye with a change in temperature is an

exponential coefficient. The coefficient for SRB is -0.029, so that for every 1 ^{o}C increase in the temperature, the fluorescence of this dye decreases the equivalent of approximately 0.7 ppb (Smart and Laidlaw, 1977). <u>This deviation in fluorescence would not, however, be reflected in the reported concentrations, since both instruments are calibrated with solutions that are at the same temperature as the samples</u>. Following SRB analysis, the samples are place in a refrigerator for long term storage.

3.3.2 SRB Results

SRB analyses were completed using a Hitachi F4500 Fluorescence Spectrophotometer, which is used to measure the fluorescence, phosphorescence, and luminescence in the ultraviolet and in the visible regions of the spectrum. This instrument is programmable, so that the fluorescence intensity of the wavelengths from 200 to 730 nm can be measured. When analyzing a specific dye, an excitation/emission couple is programmed into the instrument. For SRB, an excitation wavelength of 565 nm and an emission wavelength of 586 nm were used based on spectrophotometry guidance from Nikon Instruments
(http://www.microscopyu.com/articles/fluorescence/filtercubes/green/greenhome.html).
The bandwidth slit, which sets the bandwidth of the wavelengths, was set to 5 nm for both excitation and emission.

This instrument is also used for performing synchronous scans, where a sequential series of fluorescence measurements are performed on a sample. Synchronous scans were thus also completed to verify that any elevated fluorescence in the SRB wavelength couple was consistent with that of SRB and, further, to investigate any change in fluorescence characteristics of the low concentration SRB solutions with time. The synchronous scans were completed by defining a starting and ending excitation wavelength, and designating an increment by which to increase the excitation wavelength for each step. Also defined when programming a synchronous scan is the emission wavelength monitored as a function of the excitation wavelength. For the synchronous scan, the instrument was programmed to scan from 500 to 600 nm when evaluating the SRB spectrum and 400 to 600 nm when evaluating samples for FLT and DA-SRB. The spectrophotometer produces a spectra graph and printout (the printout is excitation wavelength versus fluorescence intensity in user defined increments, usually 2 nm) and an electronic file of fluorescent intensity at 0.2 nm increments of excitation or emission wavelengths. The fluorescence intensity of the emission wavelength monitored was measured at the excitation wavelength plus 20 nm.

The fluorescence spectrophotometer was calibrated using 0.0, 1.0, 10, 20, 50, and 100 ppb calibration solutions. These were mixed in the same manner as the FLT calibration solutions except for the 100,000 ppb stock solution. For formulating the SRB dye concentrate, 400 mg of 25 percent active ingredient powder were added to a small glass beaker. The dye powder was weighed using an analytical balance. The resultant calibration consisted of a linear best curve fit between the indicated fluorescence intensity and the actual dye concentration.

3.3.2.1 SRB Method Detection Limit (MDL) Assessment

As with FLT, the EPA and Hubaux and Vos (1970) method were used to assess the MDL for this dye. Solutions were prepared using submarine spring water and spiked to concentrations of 0.01, 0.02, and 0.05 ppb. In addition, a solution with no SRB was analyzed in the same manner as the MDL samples to establish background fluorescence for this assessment. The MDL samples were prepared in 1 L volumes that were then filtered and otherwise processed in the same manner as the field samples. Tables 3-8 and 3-9 list the results of the two MDL assessment methods.

For the EPA method, the average no-dye fluorescence of 0.046 ppb was subtracted from the fluorescence measured in the MDL samples. This was done so the percent recovery could be computed correctly. The sampled spiked to a concentration of 0.02 ppb was the only sample that met all of the requirements for MDL analysis. The associated computations gave a MDL of 0.013 ppb and a limit of quantification of 0.044 ppb. For sample analysis, the instrument response is the sum of the dye and background fluorescence. The average background fluorescence of samples collected in August and September was 0.03 ppb. This gives a MDL and limit of quantification of 0.043 and 0.071 ppb, respectively, as read directly from the spectrophotometer.

The Hubaux and Vos (1970) method gave a much lower MDL of 0.005 ppb. The aliquot spiked to 0.01 ppb was excluded because the percent error was greater than the recommended value of 20 percent. To more definitively evaluate the MDL, a synchronous scan was run on a dye free and MDL aliquot and aliquots spiked to 0.01 and 0.02 ppb. Figure 3-22 shows the results of the synchronous scan, which indicate that the sample spiked to a SRB concentration of 0.01 was not discernible from a sample with no dye. However, the sample spiked to a SRB concentration of 0.02 ppb had a marked increase in fluorescence at about 580 nm. Based on this analysis, the MDL for SRB is estimated to be 0.02 ppb. This is consistent with that estimated by the EPA method. Rounding the background fluorescence to the nearest tenth of a ppb, the MDL as read directly from the spectrophotometer is 0.05 ppb and the limit of quantification is 0.08 ppb.

3.3.2.2 Measured Fluorescence in the SRB Wavelength

To date, there has been no confirmed detection of SRB from the submarine springs. Figure 3-23 is a time series of the NSG analysis for SRB. The fluorescence measured by the spectrophotometer is that of background plus that of any dye that may be present. The average concentration for all submarine springs for the period from August 1st, 2011 through September 30th, 2011 was 0.03 ppb. The July, 2011 samples were excluded from background analysis due to the large number of outliers in the SSG, attributed to factors such as not having the sample properly seated in the spectrophotometer carousel. As proficiency developed in the use of this instrument, errors such as these decreased. Also plotted on this graph is the MDL of 0.05 ppb. Only nine samples collected at the NSG after the SRB addition on August 11th, 2011 had fluorescence greater the MDL of 0.05 ppb. Due to the isolated occurrence of this elevated fluorescence, it seems that these rises

were in most cases due to factors other than the presence of SRB. A sample collected at Seep 12 on February 20th, 2012 did show slightly elevated fluorescence at 580 nm consistent with SRB, but samples collected after that date showed no elevated fluorescence. Figure 3-24 illustrates a time series of the SRB analysis for samples collected at the SSG. At this site, twelve samples collected following the LWRF SRB addition had fluorescence greater than the MDL. Again, these points were isolated, indicating causes other than the presence of SRB. However, two samples collected at Seep 3, one on February 12th, 2012 and the other on February 20th, 2012 did show elevated fluorescence at 580 nm when evaluated by a synchronous scan. Figure 3-25 compares the synchronous scan of the sample collected from Seep 3 on February 20th with various solutions prepared for this study. The first two traces are samples that contained no FLT. One was also free of SRB, while the other was spiked to a SRB concentration of 0.05 ppb. The other two solutions were spiked to a FLT concentration of 35 ppb. Of these solutions, one contained no SRB, and the other was spiked to a SRB concentration of 0.1 ppb. This graph shows that the sample collected at Seep 3 had fluorescence characteristics very similar to sample spiked with 35 ppb FLT and 0.1 ppb SRB. However, this is only considered as a "possible" SRB detection, since there have been no subsequent samples collected with similar fluorescence characteristics. Figure 3-25 further shows that the trailing edge of the FLT trace slightly elevates the fluorescence in the SRB wavelength, and that this trailing edge needs to be considered when evaluating very low concentrations of SRB. The history of the SRB fluorescence measured at the NSG and SSG is provided in Appendix B-2, Table B-2.3.

The sub-ppb detection limit for the SRB dye, the significant amount of time that has elapsed since the dye addition, and the large amount of SRB added suggest the effluent from Well 2 may not be discharging into the nearshore waters monitored by this study. In addition, still to be evaluated are the role that dye degradation, sorption onto the aquifer matrix, and alternate flow paths might play in the failure to detect this dye. For example, Injection Wells 3 and 4 inject the majority of the effluent and are located between Injection Well 2 and the submarine springs where the FLT emergence is being monitored. The dominant flow from Wells 3 and 4 may thus likely displace the injected wastewater effluent from Well 2 around the Well 3 and 4 flow fields. If so, the probable result is that the flow from Well 2 takes a different path other than that directed towards the known submarine spring discharge points. This does not, however, preclude the possibility that the injected effluent into Well 2 would assume the same underground flow path as that of Wells 3 and 4 if it were Well 2 were to become the primary injection well.

The lack of detection of SRB may additionally be related to matrix sorption within the aquifer. Sorption of SRB onto the solid media of the aquifer would slow the transport velocity and decrease the concentration of SGD at points of emergence. Sorption could decrease the concentration to values less than the MDL, resulting in a non-detection even though the fluids injected into Well 2 are discharging at the monitored locations. The role of sorption will be evaluated in our future modeling efforts, as described in Section 7. To investigate SRB emergent locations other than the primary sample points, periodic

samples will be taken from accessible areas north and south of currently monitored locations.

The degradation of SRB through the process known as deaminoalkylation could result the failure of the primary SRB analysis methods (described above) to detect this dye. Deaminoalkylated SRB (DA-SRB) should fluoresce at wavelengths of 535 to 540 nm that is at wavelengths shorter than that of unaltered SRB (Käss, 1988). If the fluorescence intensity of DA-SRB relative to the concentration is similar to that of SRB, the fluorescence of either SRB or DA-SRB as indicated by the Rhodamine channel of the AquaFluor Handheld Fluorometer would show up clearly in synchronous scans. Figure 3-26, for example, compares synchronous scans done on a laboratory-prepared aliquot containing 35 ppb of Fluorescein and 0.1 ppb of SRB (shown as a red line) with a sample collected at Seep 3 on June 7, 2012 (shown as a green line). Both Fluorescein traces show symmetrical curves that extend from about 470 to 560 nm. The 0.1 ppb SRB in the laboratory prepared sample is clearly visible by the elevated fluorescence from about 562 to 605 nm. The Seep 3 apparent SRB concentration as read in the field on the AquaFluor Handheld Fluorometer was 3.3 ppb. Fluorescence from fluorophores tends to be additive (Meus et al., 2006). Since the fluorescence of Fluorescein extends beyond the 535 to 540 nm wavelengths identified by the (Käss (1998) as the zone of peak fluorescence for DA-SRB, then DA-SRB should be manifest as an asymmetrical Fluorescein trace with the descending limb showing a bulge. The third trace on Figure 3-26 (shown as a blue line) is a hypothetical computer-generated sample containing both Fluorescein and DA-SRB. This trace was generated by multiplying fluorescence of the portion of the 0.1 ppb SRB trace that extends above background by 33 to upscale it to 3.3 ppb. This trace was then shifted to the shorter wavelengths so the peak was centered over 538 nm, the approximate peak fluorescence of DA-SRB. Finally, the fluorescence of this hypothetical DA-SRB trace was added to the fluorescence of the Seep 3 sample to superimpose the DA-SRB fluorescence on the Fluorescein curve. The result is an easily observable bulge on the descending limb of the Fluorescein curve. All 25 of the synchronous scans completed to date were reviewed, and all show symmetrical Fluorescein curves. We will continue to complete analytical synchronous scans of selected samples to screen for DA-SRB.

3.4 Summary and Conclusions

Two tracer tests were conducted during this study to assess the hydraulic connectivity between the effluent injection wells at the LWRF and the coastal nearshore waters. During the first tracer test, FLT was added to Wells 3 and 4. The dye from this tracer test started discharging at the nearshore submarine springs in late October, 2011, after about 84 days. The FLT concentration increased to about 21 ppb then plateaued in late February, 2012 at the North Seep Group (NSG). At the South Seep Group (SSG), the FLT concentration increased to about 33 parts per billion (ppb) then plateaued in early April, 2012. The natural background fluorescence at the monitoring sites was assessed by analyzing the samples taken prior to the arrival of the dye. It was found that background fluorescence was very small, about 0.11 ppb, when compared to the magnitude of the FLT fluorescence detected. The background and Method Detection Limit (MDL) assessments were important in establishing the first arrival time of this dye.

The maximum dye concentrations to date have been higher at the SSG than at the NSG. This could be due to spatial variability, or that the SSG may be closer to the center of the groundwater plume than the NSG. If it is the latter case, then there is a probability of effluent discharging points existing to the south of the SSG. However, the elevated nitrogen-15 ratios in algal bioassay deployments indicate that the effluent discharge in the shallow waters assessable by this study are at locations already being monitored (Dailer et al., 2012), which would support the case for spatial variability. This issue will be investigated in the next phase of the study.

The second tracer test was conducted to evaluate whether the effluent from Injection Well 2 discharges at the same locations as that from Injection Wells 3 and 4. Well 2 has a significantly higher injection capacity than the other wells indicating that it may have a hydraulic connection to a preferential flow path. For this tracer test, Sulpho-Rhodamine-B (SRB) was added to the effluent on August 11th, 2011. To date there has been no confirmed detection of this dye. There were three samples that synchronous scans indicated may contain very low concentrations of SRB, but since no subsequent samples have been analyzed with similar fluorescent characteristics, these are only evaluated as possible detections.

Tracer test data collected to date do show a definite hydraulic connection between Injection Wells 3 and 4 and the nearshore waters near Kahekili Beach Park. The peak of a breakthrough curve can be used to estimate average tracer time of travel from the point of injection to the point of sample collection. The apparent plateauing of the BTC indicates the average time of travel from the injection wells to the submarine springs may be roughly seven months. At this point in the study, it is not yet known if the peak of the BTC has been reached. This proven hydraulic connection does not preclude other discharge points, including at deeper water depths In addition, the data collected to date are not yet sufficient to estimate percent of dye mass injected that can be accounted for by the discharge at the submarine springs monitored by this study. It is expected that the FLT concentration will start decreasing in the near future. When the declining limb of the BTC is confirmed, analysis of this tracer test can be completed. This will include a better estimate of the average time of travel between Wells 3 and 4 and the submarine springs, and an estimation of the mass of FLT that has been discharged at these springs.

The fate of the effluent injected into Well 2 remains unresolved. However, it may be instructive to re-evaluate a past tracer study done at the LWRF in light of the new findings of the current study. In 1993, the dye Rhodamine WT was added to Injection Well 2 at a concentration of approximately 100 parts per billion for 58 days (Tetra Tech, 1994). A marine survey was done from a boat in an attempt to identify areas where the LWRF wastewater effluent might be discharging into the marine environment. They used a pump with a hose attached that was lowered to seafloor for each sample collection. The discharge of the pump was connected to a fluorometer with a flow cell. The background fluorescence in the Tetra Tech study varied between 0.04 and 0.06 similar to that of this study. Elevated levels of fluorescence of about 0.18 ppb were detected 55 and 61 days after the start of injection at survey points adjacent to each other. Although scant, the location of the elevated fluorescence detections was very close to the area monitored

by this study, but deeper (about 30 m) and farther offshore (about 300 m) than the submarines springs monitored by this study. According to that report (Tetra Tech, 1994), the dye emergence was not expected at this location and the elevated fluorescence was evaluated as being from another fluorophore such as dissolved organic matter. It is not possible to confirm whether or not the Tetra Tech study did actually detect the dye, but our study indicates the effluent from Well 2 may not be discharging into the nearshore waters and a discharge point deeper and further from shore needs to be considered. In addition, the present and past nitrogen isotope data (see Section 6) and the thermal imaging data (see Section 4) suggest that significant submarine discharge of effluent to north is not occurring.

The lack of SRB detection by this study and the possible detection by the 1993 Tetra Tech (1994) tracer test indicate that the effluent from Well 2 may be discharging deeper and further out to sea than that from Wells 3 and 4. A study similar to that done by Tetra Tech would be needed to confirm this. However, since not all relevant processes have been evaluated, the nearshore discharge of effluent from Injection Well 2 cannot be ruled out.

Table 3-1. Mixing Schedule for the FLT Calibration Solutions

Desired Concentration (ppb)	Volume of 100 ppb Calibration Solution (ml)	Volume of Submarine spring Water (ml)	Comments
1	2.5	247.5	
10	50	450	Note 1
20	50	200	
50	125	125	

Note 1. An extra volume of the 10 ppb solution was mixed since it was used to calibrate the instrument and verify accuracy at the end of each analysis session

Table 3-2. The MDL Results for FLT Using the EPA Method

Spiked Conc. (ppb)	Mean (ppb)	Solution Deviation (ppb)	MDL (ppb)	Average Recovery (%)	Signal to Noise Ratio	Limit of Quantification (ppb)	Remarks
0	0.111	0.004	NA	NA	NA	NA	Note 1
0.1	0.101	0.004	0.011	101.25	28.6	0.035	
0.2	0.192	0.005	0.014	96.24	41.6	0.046	
0.5	0.479	0.006	0.019	95.7	74.7	0.064	Note 2

Red indicates a value outside of acceptable limits

Table 3-3. The MDL Results for FLT Using the Hubaux and Vos Method

Conc. (ppb)	Mean (ppb)	Calculated Concentration (ppb)	Percent Error	Included in Analysis
0.00	0.12	-0.006	NA	Yes
0.10	0.22	0.10	4.5	Yes
0.20	0.31	0.20	2.1	Yes
0.50	0.57	0.50	0.5	Yes
MDL (ppb)				0.02
Critical Response (ppb)				0.13
Critical Concentration (ppb)				0.008
r^2				0.9994

Table 3-4. Summary of Background Fluorescence for the NSG

	Seep 1	Seep 2	Seep 6	Average
Number of Samples	15	15	13	14
Minimum	0.09	0.08	0.11	0.09
Average	0.11	0.11	0.11	0.11
Maximum Solution	0.13	0.12	0.12	0.12
Deviation	0.01	0.01	0.00	0.01
First Detection	10/20/11	10/20/11	10/20/11	10/20/11

Table 3-5. Summary of Background Fluorescence for the SSG

	Seep 3	Seep 4	Seep 5	Average
Number of Samples	13	18	13	15
Minimum	0.09	0.01	0.08	0.06
Average	0.12	0.10	0.11	0.11
Maximum Solution	0.13	0.14	0.12	0.13
Deviation	0.01	0.03	0.01	0.02
First Detection	11/05/11	11/11/11	11/07/11	11/08/11

Table 3-6. Background Fluorescence for the Marine Waters

	North Seep Grab	South Seep Grab	Other Locations
Number of Samples	27	27	26
Minimum	-0.01	-0.01	0.001
Average	0.01	0.01	0.01
Maximum Solution	0.04	0.06	0.05
Deviation	0.02	0.02	0.02

Table 3-7. Summary of Salinity Measured at the Monitoring Points

Sampling Point	Group	No. of Samples	Minimum	Average	Maximum	Standard Deviation
Seep 7	NSG	13	4.1	4.2	4.3	0.08
Seep 8	NSG	3	4.1	4.2	4.2	0.07
Seep 9	NSG	5	5.3	18.0	25.3	8.06
Seep 10	NSG	12	4.1	4.7	6.2	0.62
Seep 12	NSG	13	4.1	4.3	4.9	0.24
Seep 13	NSG	6	4.2	4.3	4.4	0.12
Seep 14	NSG	3	4.1	4.2	4.2	0.06
Seep 15	NSG	3	4.2	6.1	9.3	2.79
Seep 3	SSG	23	2.8	3.1	4.3	0.34
Seep 4	SSG	24	3.0	10.6	22.5	7.39
Seep 5	SSG	23	5.5	11.7	19.7	4.47
Seep 11	SSG	21	3.1	3.4	4.5	0.39

Table 3-8. The MDL Results for SRB Using the EPA Method

Spiked Conc.	Mean	Standard Deviation	MDL	Average Recovery	Signal to Noise Ratio	Limit of Quantification	Remarks
(ppb)	(ppb)	(ppb)	(ppb)	(%)		(ppb)	
0.00	0.005	0.006	NA	NA	NA	NA	Note 1
0.01	0.004	0.003	0.01	45	1.4	0.03	Average recovery and SNR not acceptable
0.02	0.017	0.004	0.013	85	3.9	0.044	Met all requirements
0.05	0.054	0.018	0.058	108	2.4	0.18	SNR not acceptable

Note 1. The mean dye-free aliquot concentration 0.03ppb was subtracted from the fluorescence for the MDL samples

Red indicates a value outside of acceptable limits

Table 3-9. The MDL Results for SRB Using the Hubaux and Vos Method

Spiked Conc. (ppb)	Mean Conc.Note 1 (ppb)	Calculated Concentration Note 2 (ppb)	Percent Error	Included in Analysis
0.00	0.043	0.0015	NA	Yes
0.01	0.050	0.007	26.8	No Note 3
0.02	0.062	0.017	12.8	Yes
0.05	0.10	0.051	2.0	Yes
MDL (ppb)				0.005
Critical Response (ppb)				0.044
Critical Concentration (ppb)				0.0025
r^2				0.9922

Note 1: Mean concentration is the background (about 0.03 ppb) plus the dye fluorescence.
Note 2: Calculated concentration is based on best fit line through the MDL data.
Note 3: The 0.01 ppb aliquot excluded from the analysis due to the high percent error. Allowable error is 20 percent or less
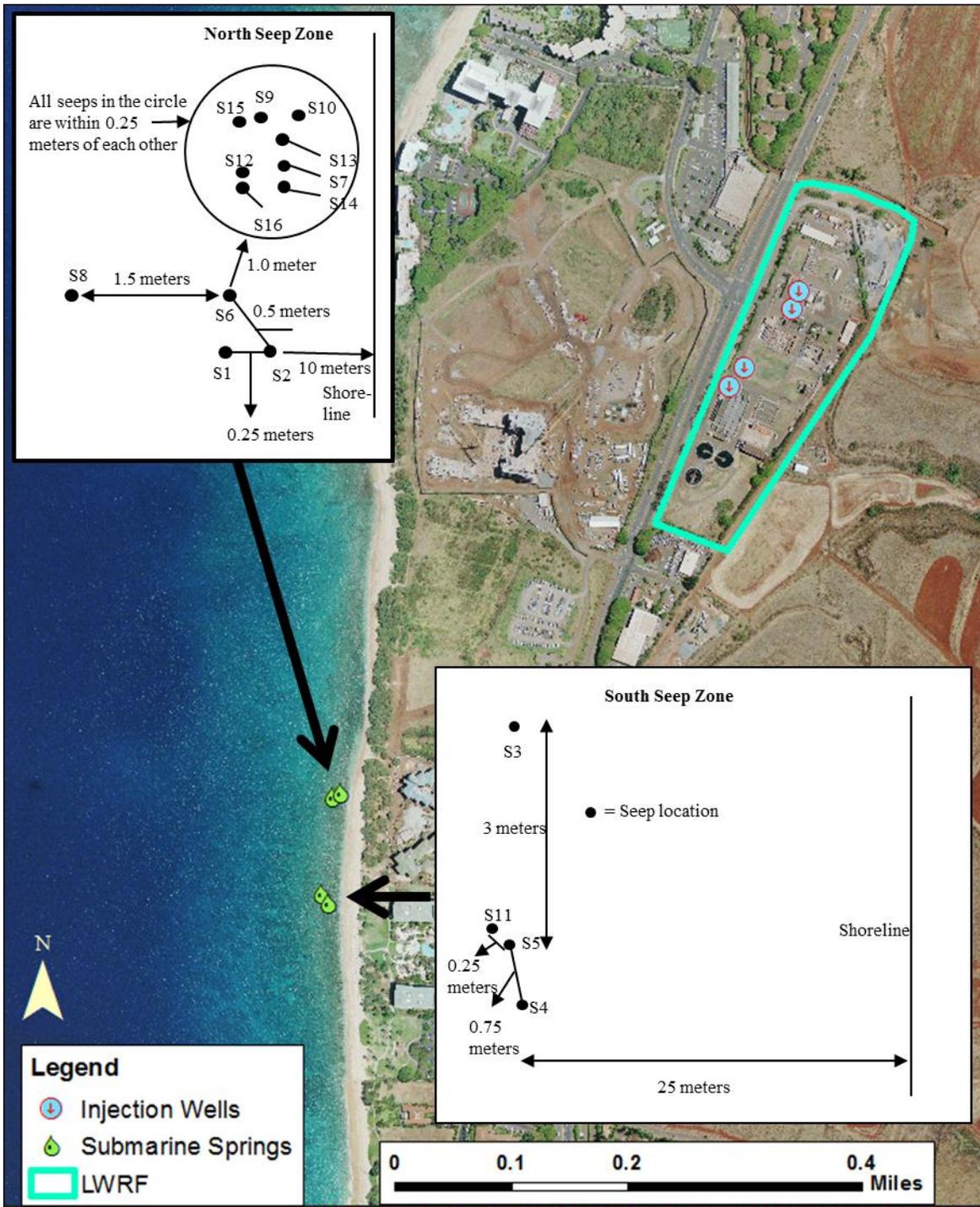
Figure 3-1: Location and arrangement of monitoring points
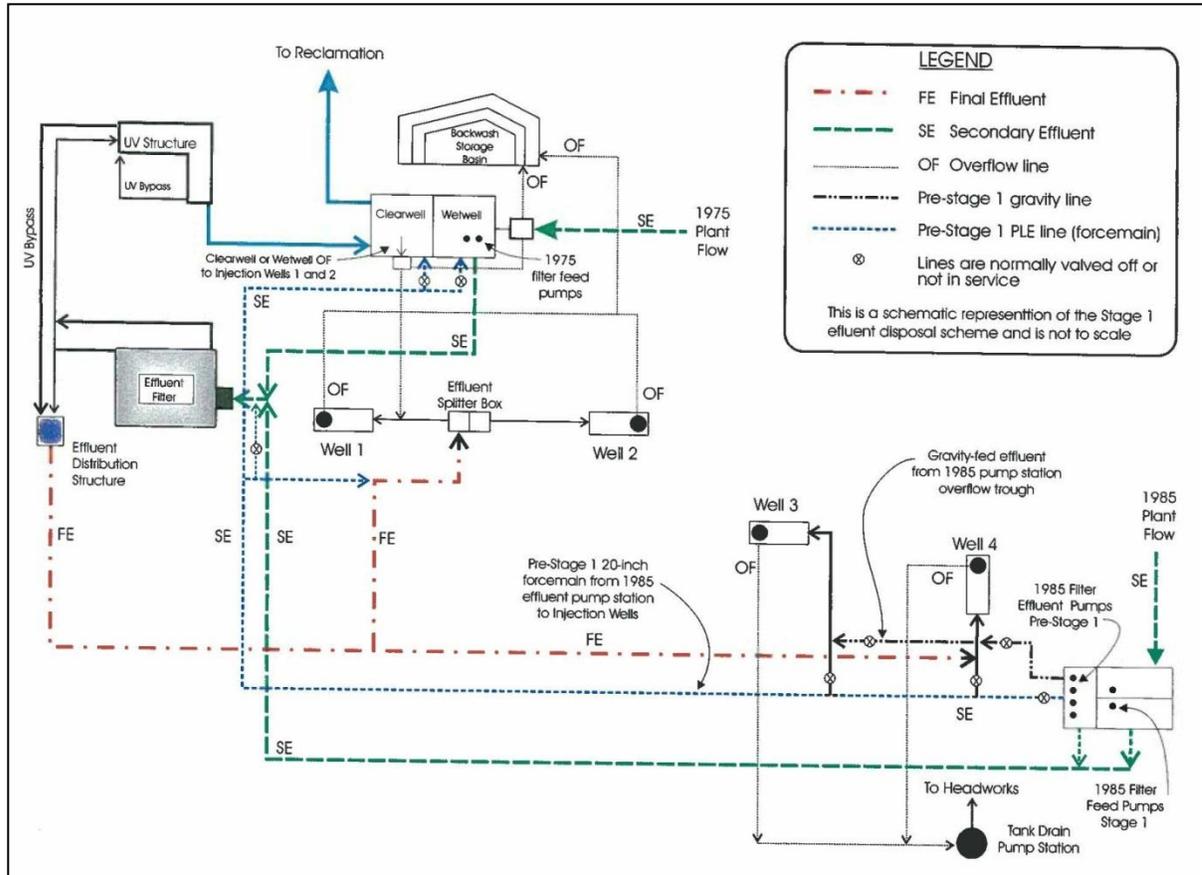
Figure 3-2: Line diagram of the LWRF showing the FLT dye addition points.
(Diagram from County of Maui, 2010)

Figure 3-3: Mixing fluorescein in 55 gal. drums

Figure 3-4: Transferring fluorescein concentrate to 5 gal. buckets for delivery to wells.

Figure 3-5: Transfer of dye concentrate into injection well 3.

Figure 3-6: Residual dye was poured directly into the well.

Figure 3-7: Fluorescein concentrate mixing continued until midnight.

Figure 3-8: Fluorescein addition continued until about 02:00.
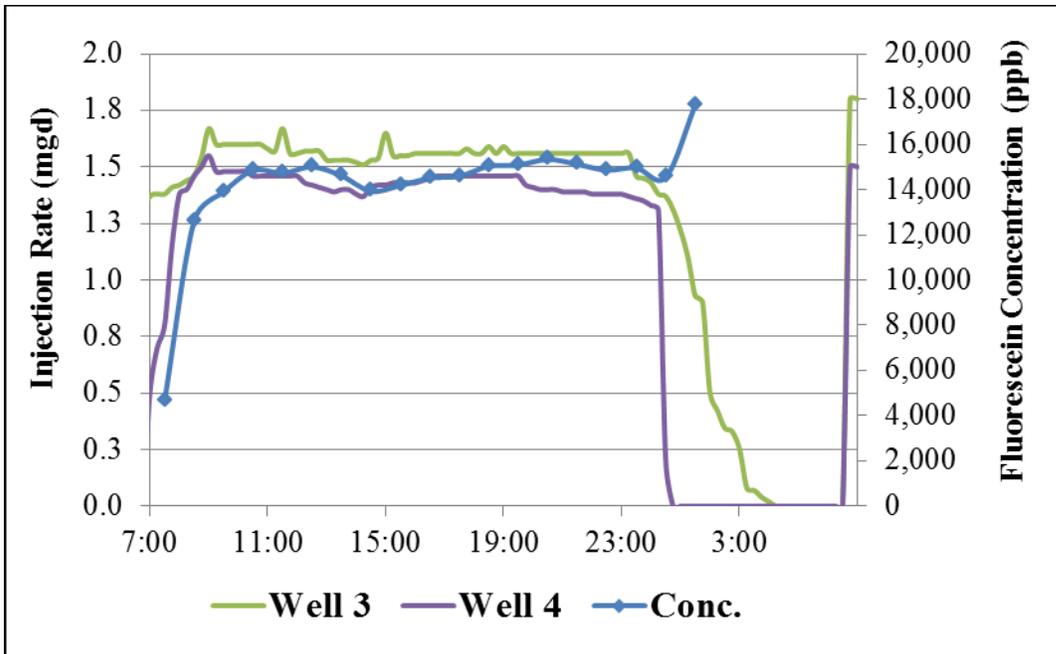
Figure 3-9: Effluent injection rates and resulting FLT concentrations for the first tracer test.
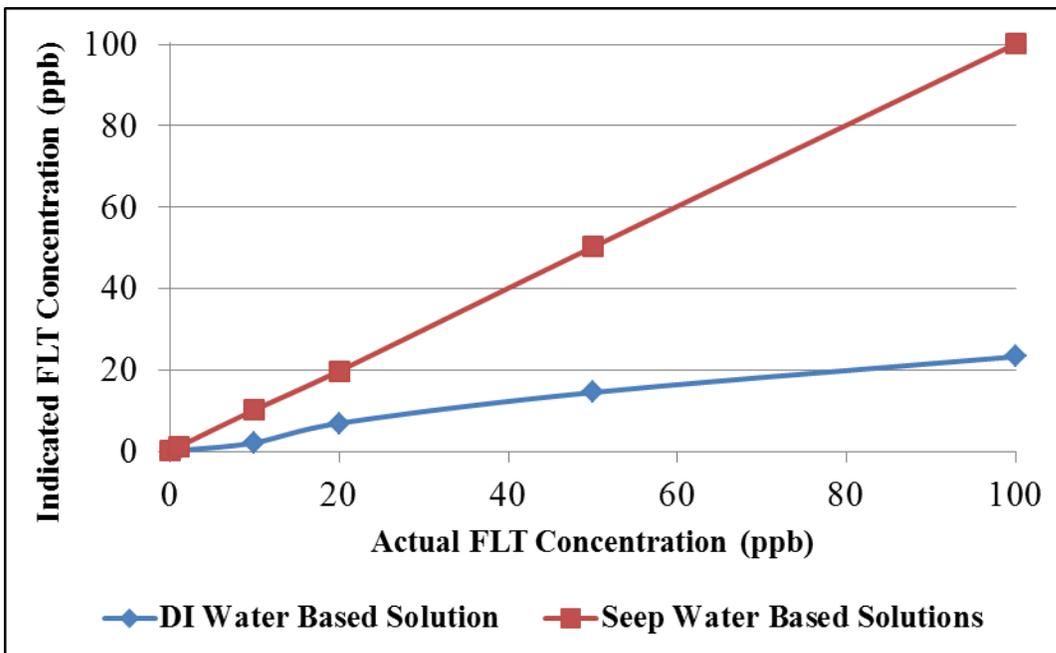
Figure 3-10: Turner 10AU response to DI water based and submarine spring water based FLT solutions.
The fluorometer was calibrated using the submarine spring water based FLT solutions.
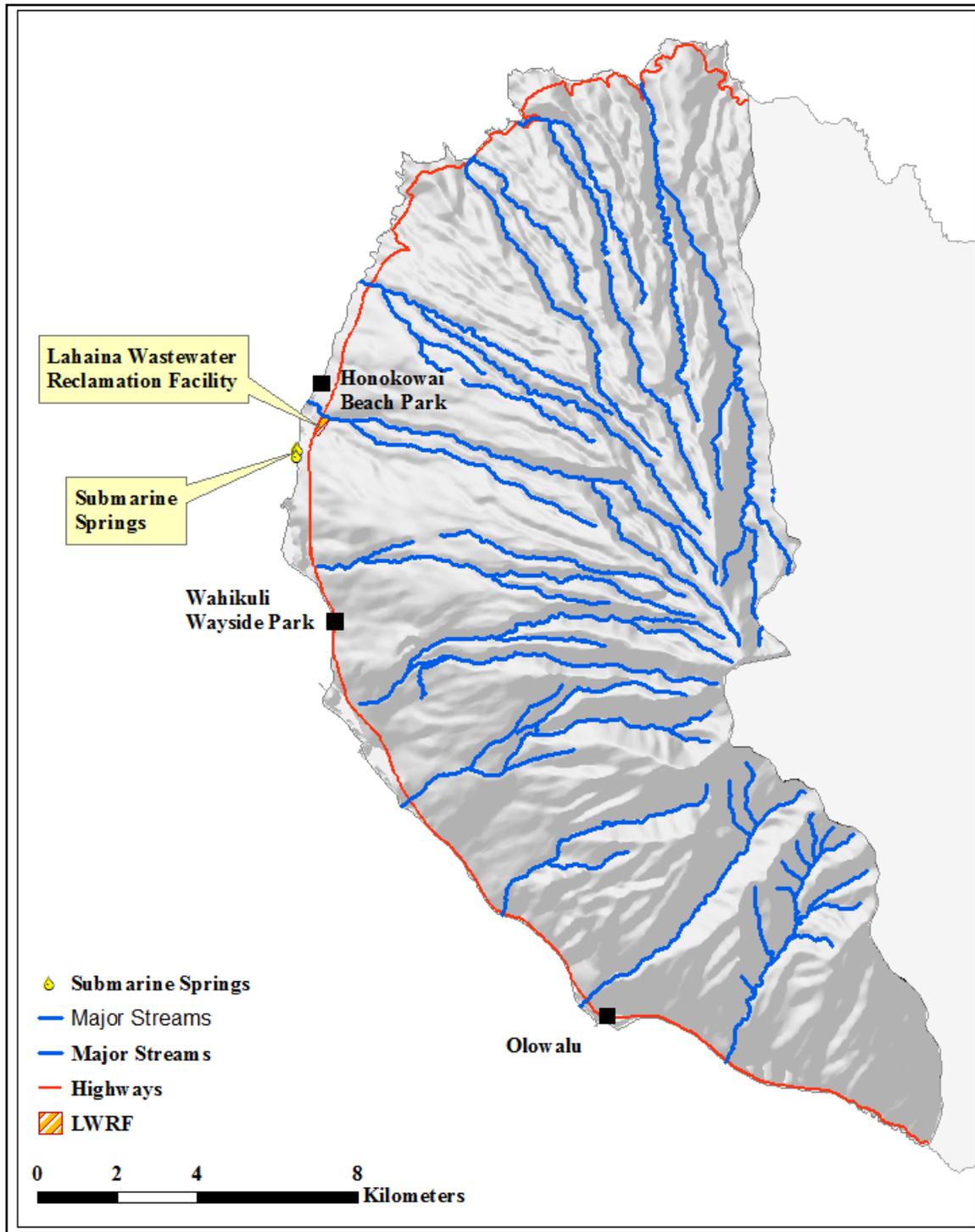
Figure 3-11: Location of the background sampling points.
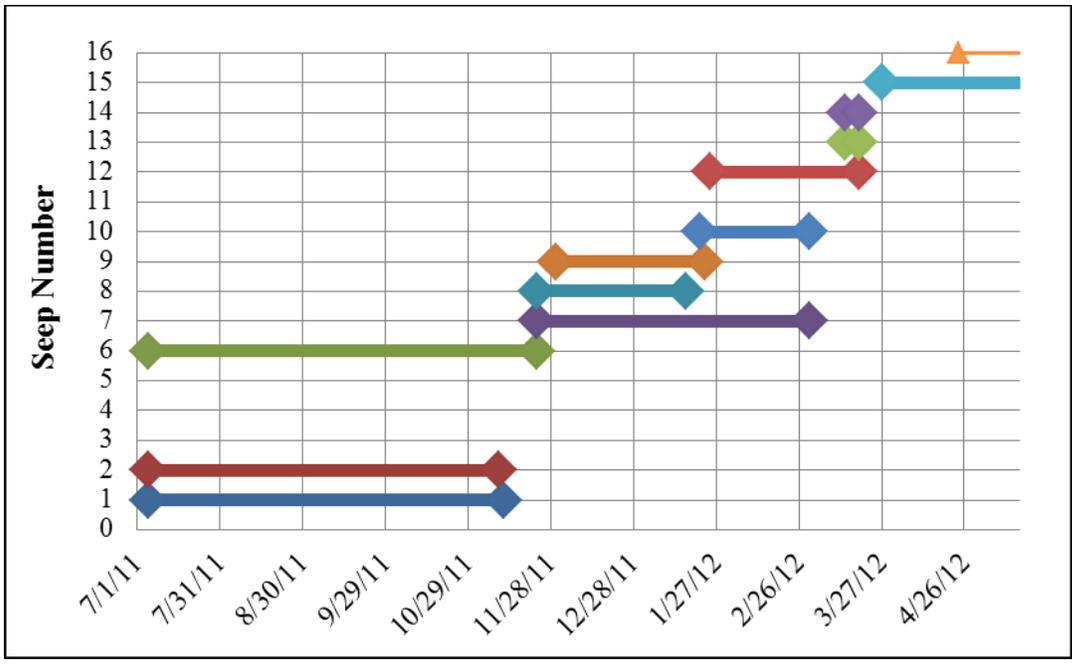
Figure 3-12: Periods of sample collection from each monitoring point at the NSG.
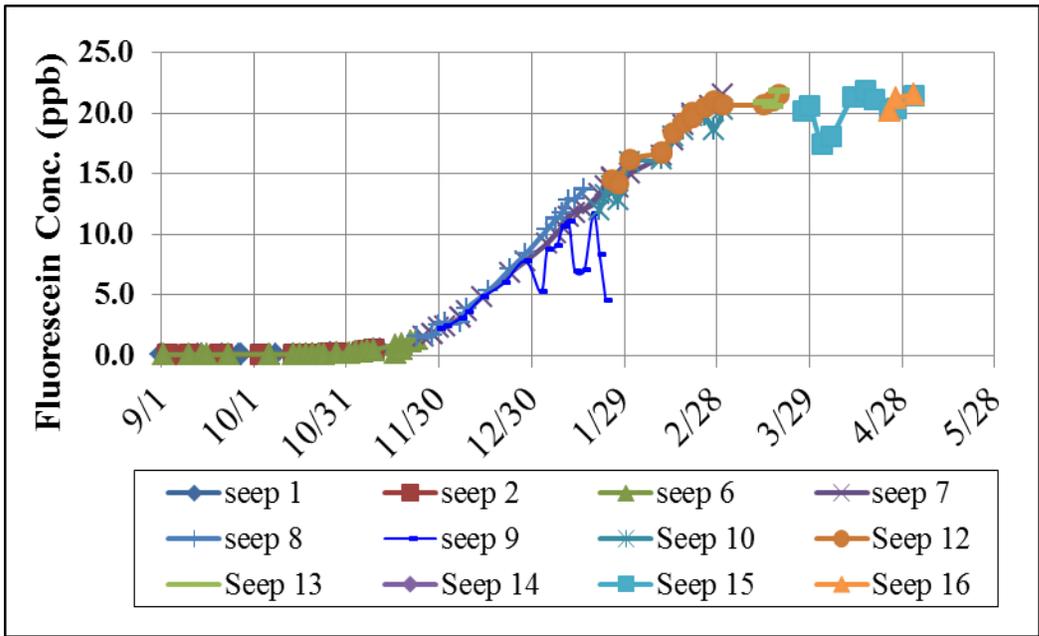
Figure 3-13: Fluorescein breakthrough curve at the NSG.
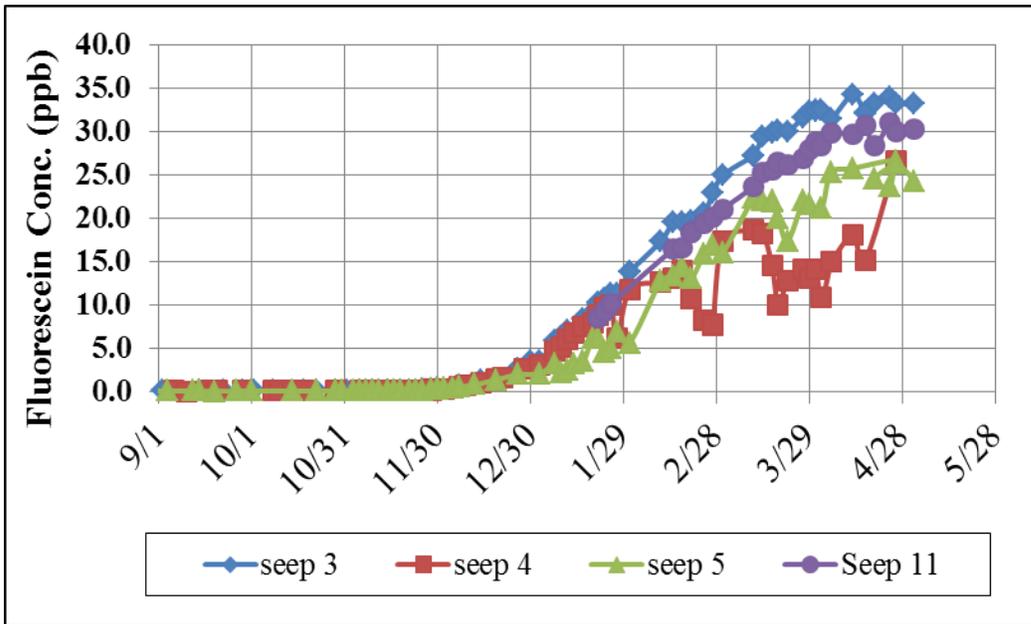
Figure 3-14: Fluorescein breakthrough curve for the SSG.
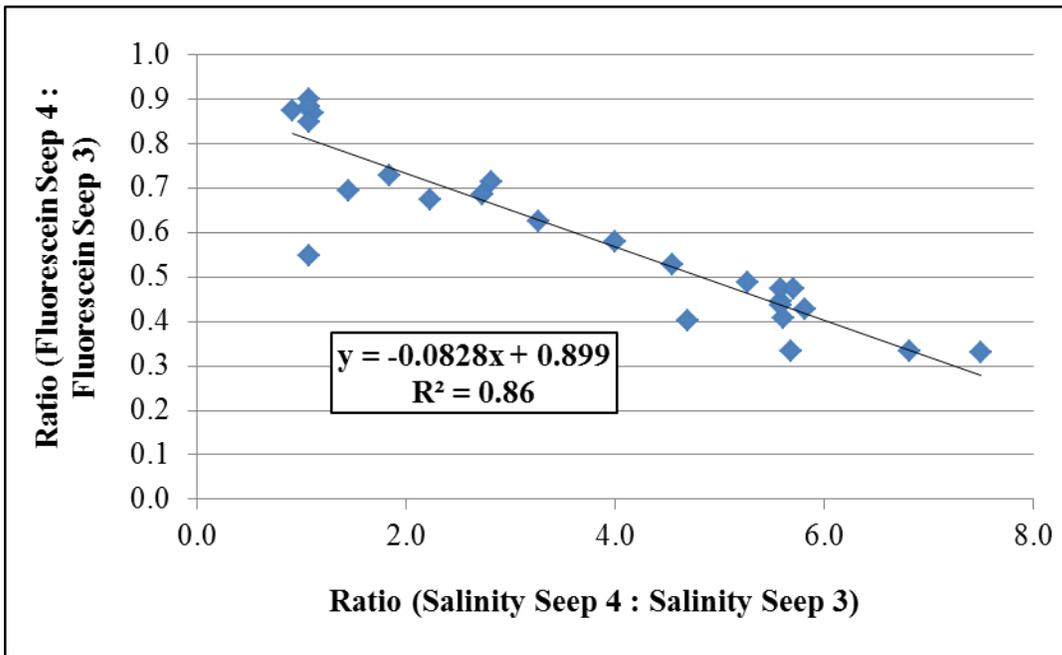
Figure 3-15: Relationship between salinity and the FLT concentration.
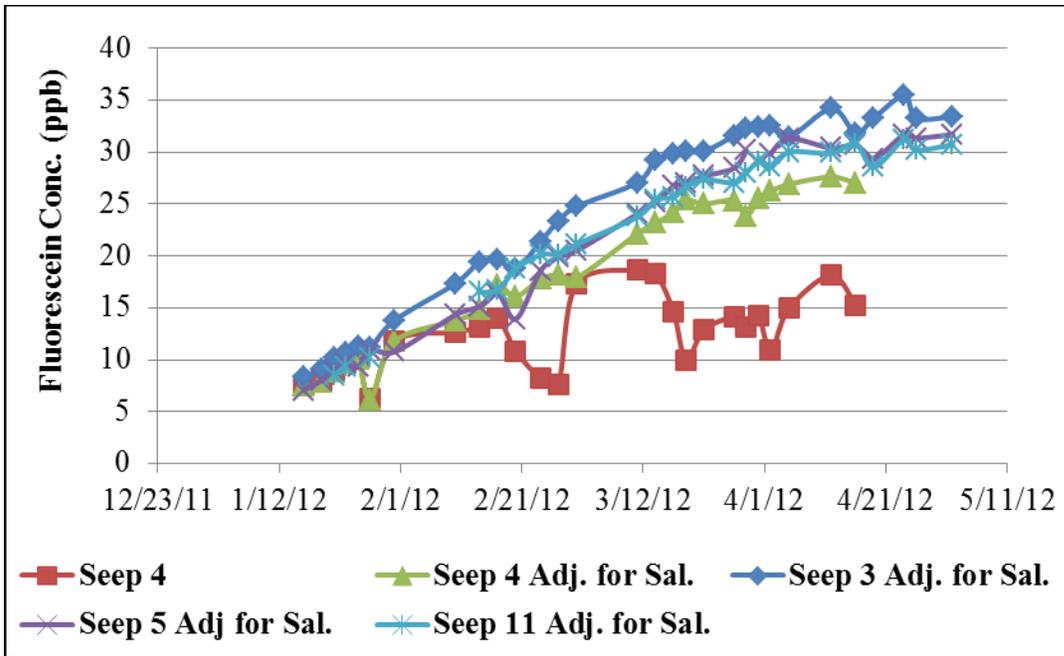
Figure 3-16: FLT concentration as measured and corrected for salinity at the SSG.
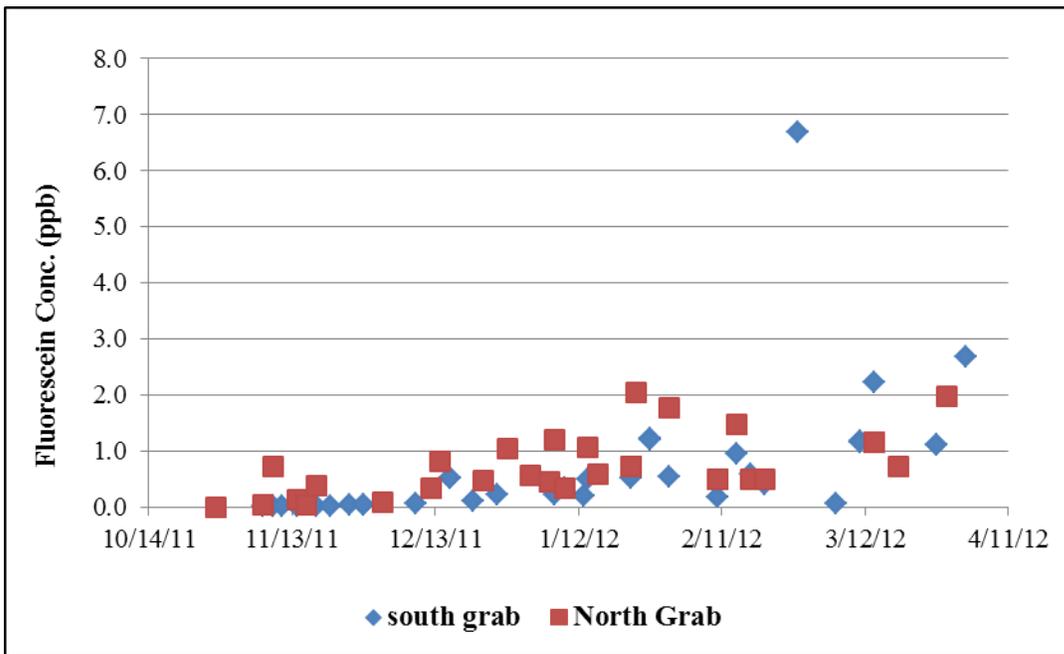
Figure 3-17: FLT concentrations in the grab samples collected at submarine springs.
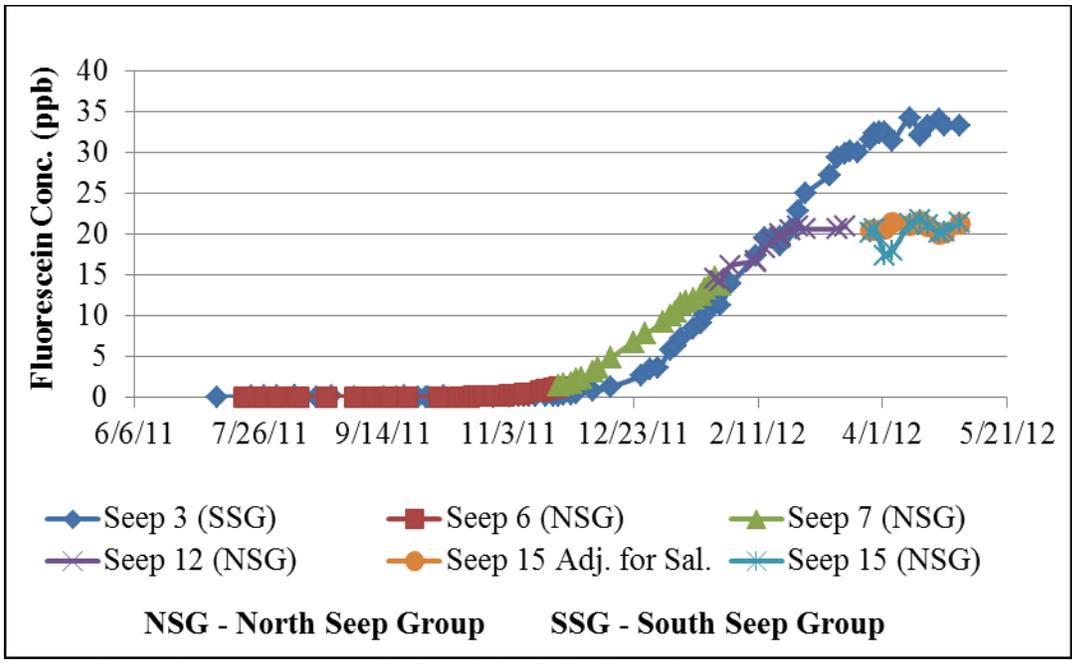
Figure 3-18: Comparison of NSG and SSG FLT breakthrough curves.
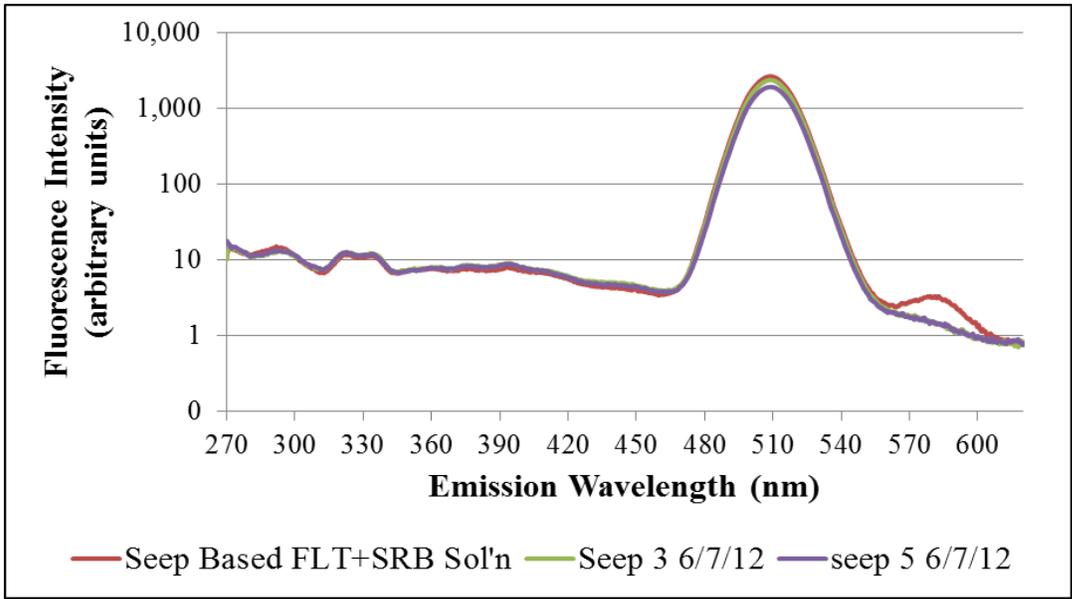
Figure 3-19: Two-dimension synchronous scans of a submarine spring sample and a laboratory sample.

The laboratory sample prepared with submarine spring water (Lab. FLT + SRB Sol'n) contains 35 ppb of FLT and 0.1 ppb of SRB. The submarine spring sample (Seep 3 6/7/12) has a fluorescence intensity spectrum nearly identical to that of the laboratory sample with the exception of the SRB peak at 580 nm.
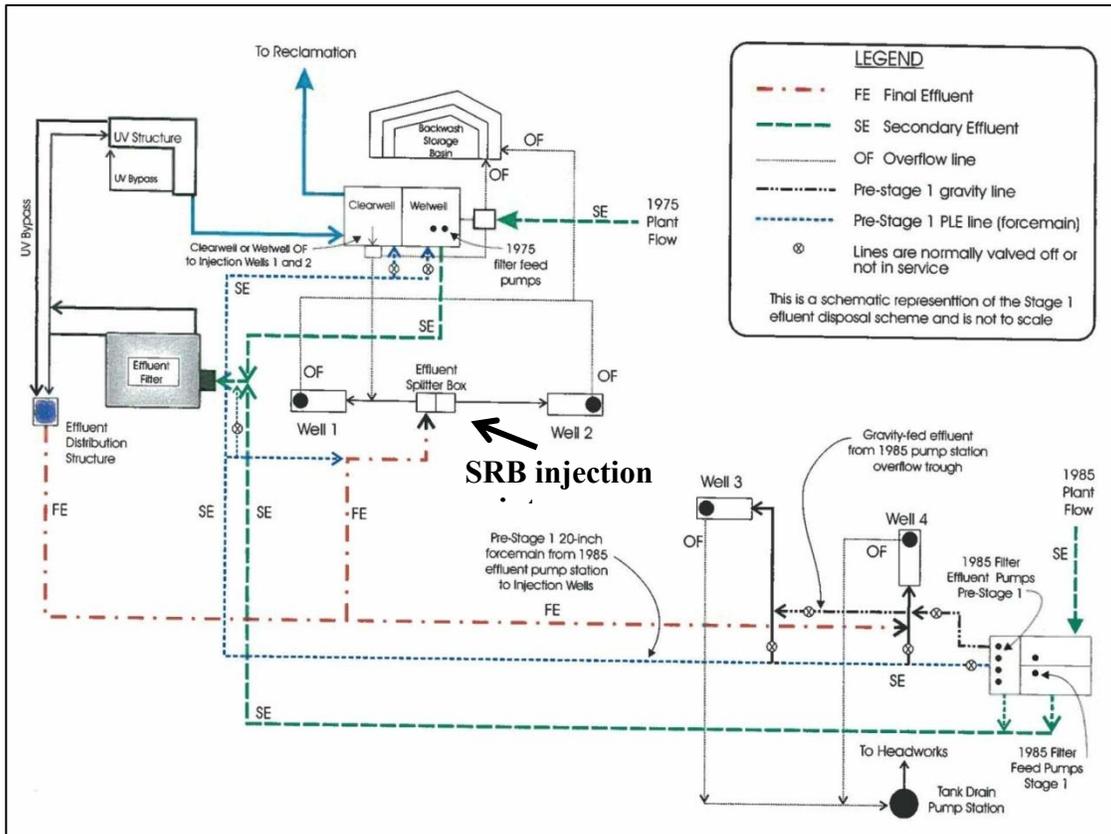
Figure 3-20: Line diagram of LWRF showing dye addition points for SRB.
(Diagram courtesy County of Maui, 2010).
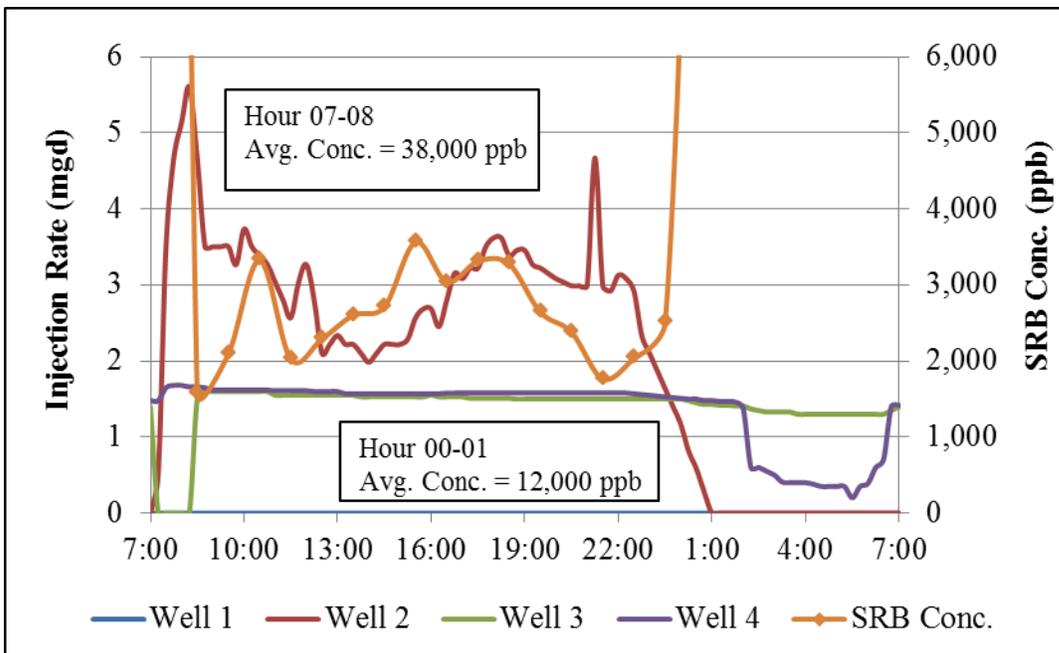
Figure 3-21: Effluent injection rates and resulting SRB concentration for SRB.
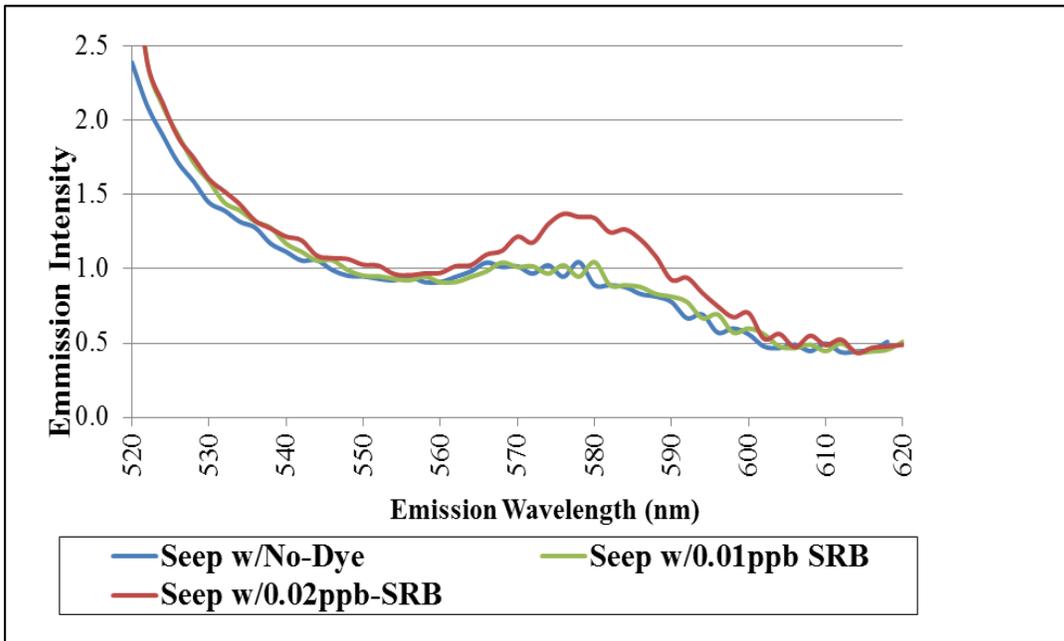
Figure 3-22: Synchronous Scans of SRB calibration solutions.
Solutions were mixed using submarine spring water containing no dye, and spiked to 0.01 and 0.02 ppb with SRB.
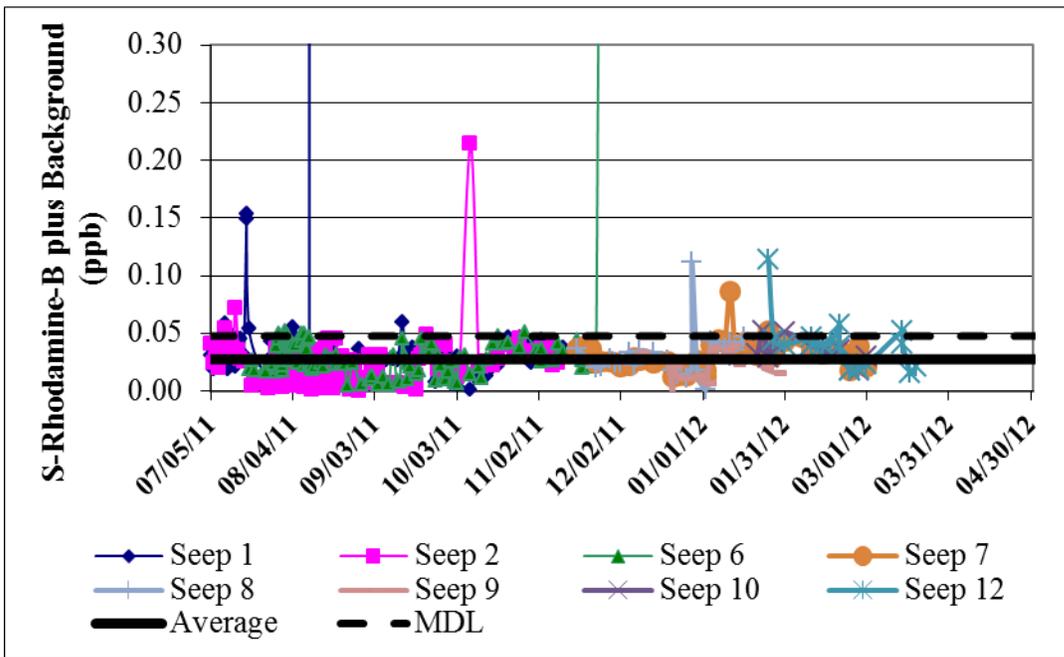
Figure 3-23: Fluorescence in the SRB Wavelength Measured at the NSG.
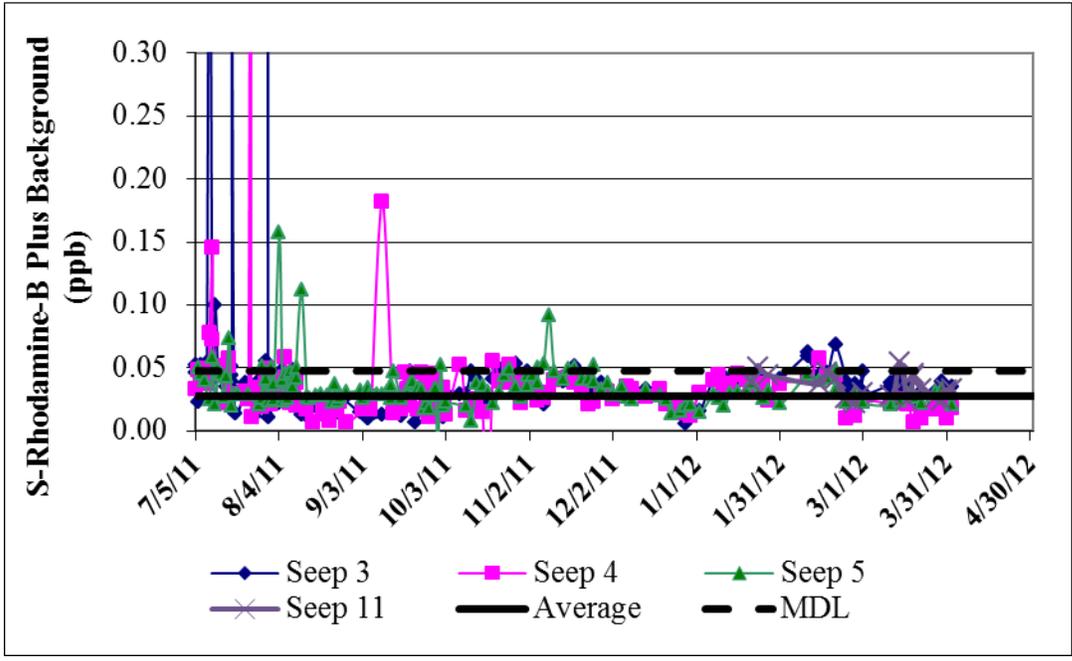
Figure 3-24: Fluorescence in the SRB wavelength for the SSG.
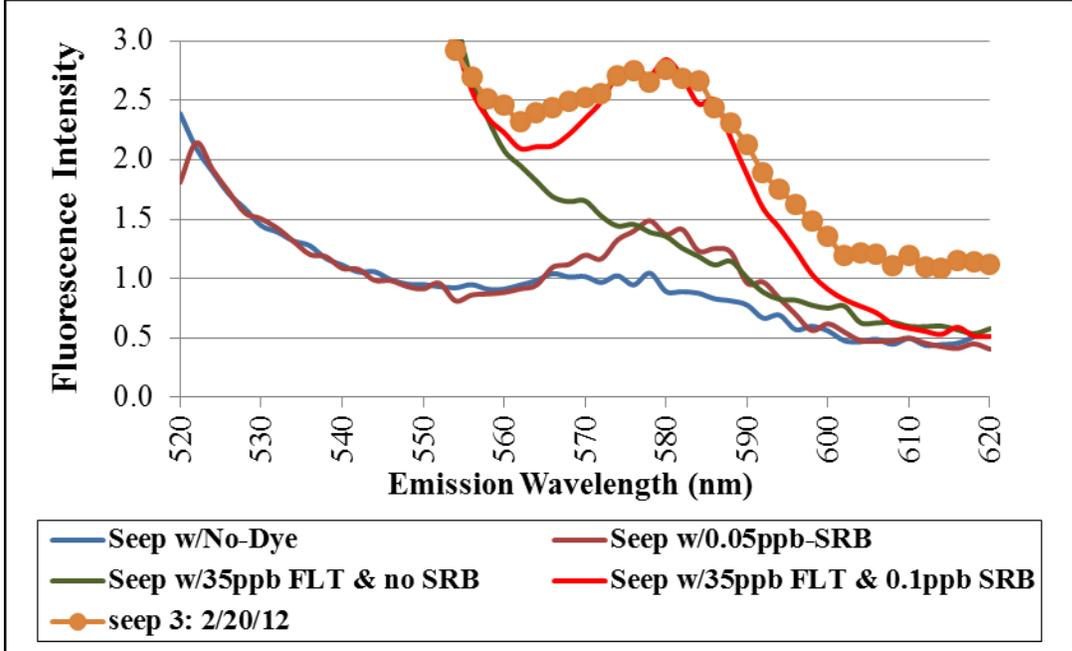
Figure 3-25: Synchronous scans of submarine spring water and solutions spiked with SRB.
Samples spiked with FLT and SRB are Compared to the fluorescence of the sample collected at Seep 3 on February 20th, 2012.

91
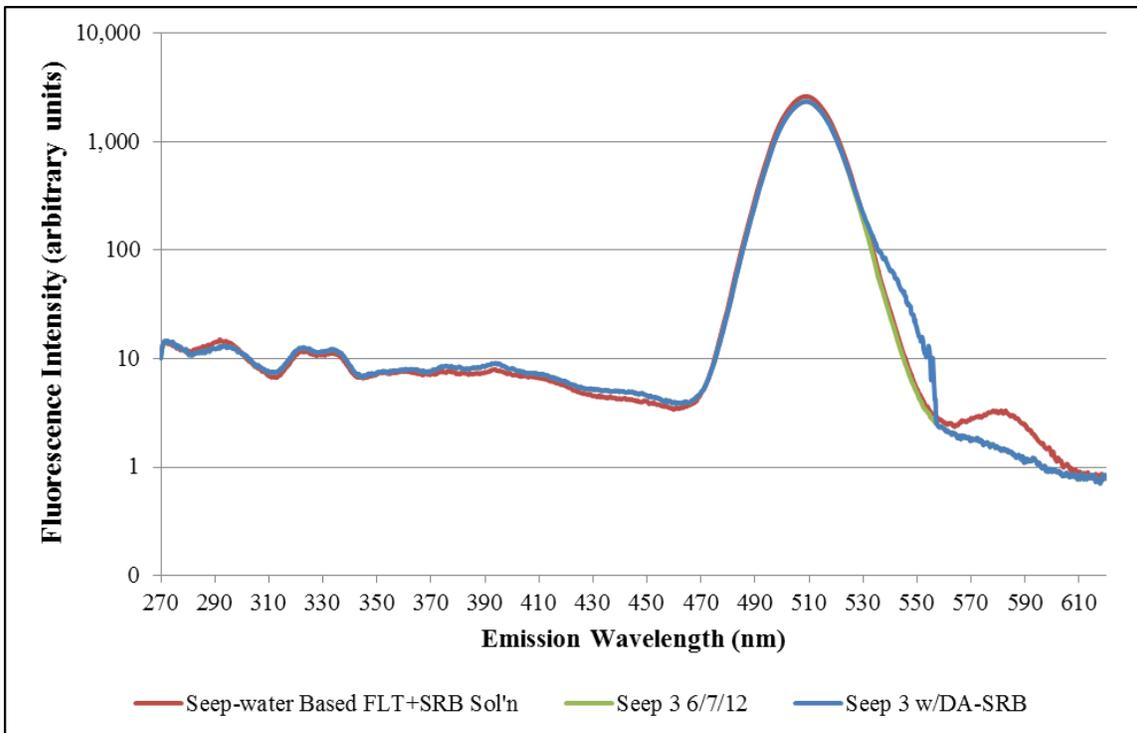
Figure 3-26. Graphed are three synchronous scans to show the spectra of Fluorescein, SRB, and Fluorescein, plus a hypothetical DA-SRB trace.

The first trace (red) is a laboratory-prepared sample containing about 35 ppb of Fluorescein and about 0.1 ppb of SRB. The second trace (green) is a scan of a sample collected at Seep 3 on June 7, 2012. The Fluorescein concentration in this sample was 32 ppb, but there is no indication this sample contains SRB. The AFHF indicated this sample contained 3.3 ppb of SRB. The third trace (blue) is the emission spectra of the Seep 3 sample might look like if it contained 3.3 ppb of DA-SRB. This degraded SRB results in an asymmetrical Fluorescein fluorescence trace with a "bulge" on the descending limb.

SECTION 4: AERIAL INFRARED SEA SURFACE TEMPERATURE MAPPING AND POTENTIAL HEAT SOURCES

4.1 INTRODUCTION

Recent scientific investigations (Tetra Tech Inc., 1994; Brown, 1995; Bourke, 1996; Hunt, 2006; Hunt and Rosa, 2009; Dailer et al., 2010, 2012; this report) near the Kahekili Beach Park area of Lahaina, Maui (Figure 4-1), conclude that effluent injectate from the nearby, and upslope Lahaina Wastewater Reclamation Facility (LWRF) flows toward the coast and discharges into the nearshore waters southwest of the facility via submarine springs. The LWRF produces treated wastewater and R1 effluent. Solar heating of the effluent during sludge pond settling and exothermic reactions during wastewater decomposition make the effluent warm (26 to 31°C; 78.8 to 87.8°F). Treated wastewater effluent is injected to depths between 70 and 45 m (229 to 150 ft) below mean sea level, approximately 600 m (0.37 mi) upslope of Kahekili Beach Park. Although the effluent is injected deep, Wheatcraft (1976), Burnham (1977), Tetra Tech Inc. (1993), and Hunt (2006) have all demonstrated through modeling that injectate plumes generally ascend within more saline coastal aquifers because effluent has positive buoyancy relative to the saline water in the aquifer. Once injectate waters are near the surface of the basal groundwater lens, the water likely disperses laterally as it flows toward the coast, whereupon it may discharge through submarine springs that are "noticeably" warm (Hunt and Rosa, 2009; Dailer et al., 2010, 2012).

The objective of this portion of the present study was to determine the locations of warm emerging fluids to the coastal waters near the LWRF. For this work, a high-resolution (2.3 m) aerial infrared remote sensing technique was used to produce sea surface temperature (SST) maps of the warm (~26.5°C), buoyant, emerging fluids relative to coastal waters (25.5°C) and natural submarine groundwater discharge (20-22°C). This work also discuss potential heat sources that may have caused the thermal anomaly observed in the coastal waters, including warm effluent, geothermal activity, and/or organic matter decomposition.

4.2 METHODS

4.2.1 Aerial Infrared Thermography

We used a FLIR Systems Inc. (Portland, Oregon) Photon 320 uncooled microbolometer array camera to collect thermal infrared (TIR) data. This camera has a 320 X 240 pixel detector array and operates in the 8.5-13.5 µm region of the electromagnetic spectrum, a range that reduces sensitivity to atmospheric water and carbon dioxide. The measured

sensitivity of this camera is 20 mK, well below environmental variables. This camera is not sensitive near the water absorption or emission area of the electromagnetic spectrum.

A temperature-adjustable blackbody with a flat-panel design, accurate to within 0.1°C, was used to calibrate the infrared data to 15 and 30°C during the flight. These calibration temperatures were chosen to bracket the temperatures of the waters of interest (cold SGD, ambient ocean, and warm discharge).

A combined inertial navigational system and global positioning system (INS/GPS) monitored aircraft velocity, roll, pitch, heading, and the three-dimensional position of the aircraft during the flight. This system (C-MIGITS; BEI Systron Donner Inertial Division, Concord, California; operated in standard positioning service mode) has rated performances of 78 m three-dimensional position accuracy, 45 m circular error probable horizontal position accuracy, and 52 m vertical error probable vertical position accuracy. Horizontal velocity accuracy is 0.5 m/s, vertical velocity accuracy is 1.0 m/s, roll and pitch accuracy is 2.5 mrad, and heading accuracy is 3 mrad.

The infrared system (camera, blackbody, INS/GPS, and data collection computer) was operated in a twin engine Piper Navajo aircraft. We designed and custom built a camera mount that fit into the aircraft's hull. The camera was affixed to the top of the mount with a nadir (looking directly down) view. The top and bottom of the mount were separated by vibration isolators that dampened aircraft vibrations and resonant frequencies. Except for vibration isolation, the camera was not otherwise stabilized. The blackbody calibration plate was incorporated into the camera mount directly below the camera. The plate was affixed on roller bars allowing manual movement out of the camera's field of view during data acquisition and movement into the camera's field of view for calibration. This integrated arrangement allowed blackbody calibration before and after the flight track.

Since water is almost opaque in the thermal infrared region of the electromagnetic spectrum (8-14 μm), the camera cannot view objects through clouds. We therefore collected all data during clear-sky conditions. We also collected data during calm water conditions, because rough water surfaces experience diffusing effects that direct high atmospheric radiance from the horizon toward the sensor. Furthermore, turbulent water and large waves can also mask SGD by mixing the water column. We collected all data at night to avoid temperature anomalies created from solar insolation that unevenly heats water or suspended matter in shallow water columns.

The Hawaiian Islands experience semi-diurnal tidal conditions. The tide during the flight mission was down-going to the lowest-low tide of the day. This tidal stage was specifically targeted because groundwater flow from the land to the ocean is greatest when the head difference between the ocean and aquifer is largest (see Section 5 for more discussion of this effect within the study area).

Thermal infrared data were collected on May 26th, 2011 between 00:45 and 01:21 a.m., Hawaii Standard Time (HST) at a frame rate of 30 Hz. All infrared data were collected at a flight altitude of 2134 m (7000 ft).

Post-flight data processing was accomplished following the exact protocol in Kelly et al. (submitted, and available upon request). Briefly, data were inspected for quality control, calibrated to in flight blackbody measurements, mosaicked, georeferenced, annotated (digitized) to retain only water, corrected to in situ temperatures measured by thermistors, false colored, and draped over 0.5 m-resolution georectified visible-light images available from DigitalGlobe Inc. (Longmont, Colorado).

Three thermistors (HOBO pendant UA-001-08; Onset, Cape Cod, Massachusetts) were deployed in the coastal area within the flight track prior to the flight and retrieved from the coastal area after the flight. Thermistors (accurate to 0.5°C) were deployed near Honokowai (20.95467 °N, 156.68715 °W), Kahekili Beach Park (20.93863 °N, 156.69321 °W), and Black Rock (20.92374 °N, 156.69568 °W). These thermistors recorded data every 7 minutes and were deployed to float at the water's surface. SSTs from the thermistors were used to calibrate all infrared maps, thereby correcting the data for atmospheric interferences (signal absorption by aerosols, water vapor, and carbon dioxide) between the camera detector and the water's surface.

4.2.2. Chloride and Magnesium Ions

Chlorine and magnesium dissolved anions were collected from water supply wells, a monitoring well, submarine springs, marine surface water, terrestrial surface water, and effluent in June and September, 2011. Samples were collected in 500 mL high-density polyethylene (HDPE) bottles that were pre-cleaned with 10% v/v hydrochloric acid (HCl; 1.2 N) and triple-rinsed with distilled, deionized (DI) water. During sample collection, HDPE bottles were triple-rinsed with sample water, filled, stored in a chilled cooler while in the field, and chilled in a refrigerator upon returning from the field. Dissolved anions were sub-sampled from the 500 mL bottles the evening of collection by filtering through 45 µm surfactant-free cellulose acetate filters (Nalgene, Thermo Scientific part number 190-9945) into 60 mL HDPE bottles that were triple-rinsed with filtered water. Prior to use, the 60 mL HDPE bottles were pre-cleaned with 10‰ v/v HCl (1.2 N) and triple-rinsed with distilled, DI water. Table 4-1 lists the locations of the submarine springs that the samples were collected from as well as the sample names.

Groundwater from seven water supply wells was collected in both June and September using in situ pumps and sample connections. A reducing adapter with a Tygon tube was affixed to existing connections to facilitate sampling. All pre-existing pump infrastructure was purged for a minimum of ten minutes prior to sample collection. Sample connections were purged for a minimum of two minutes to ensure adequate flushing of the water delivery line. At least three volumes of water were flushed through the delivery line.

Lahaina Deep Monitor Well (a monitor well with no in situ pumping apparatus) was sampled by lowering bailer bags down the borehole to immediately below the water table. Once immersed, bailer bags were opened, filled with water, and then returned to the surface, where the sample water was transferred directly to the sample bottle.

Four 15.24 cm (6 in) stainless steel drive point piezometers with 0.64 cm (0.25 in) compression fittings (Solinst Canada Limited, Georgetown, Ontario, Canada, part number 103160) were installed in the ocean floor at spring locations. Piezometers were attached to 20-30 m of plastic tubing with a quick-connect fitting. Spring water from the piezometers was collected at flow rates ranging from 0.33 to 0.50 L/min using a peristaltic geopump (geotech, Denver, Colorado). Prior to sampling, the entire tube and all fittings were purged for a minimum of two minutes to ensure that at least three volumes of water flushed through the water delivery line.

Eight marine samples of surface waters were collected in September, 2011 by directly filling sample bottles with water while stationed on a small boat. Four terrestrial water samples were collected in June and an additional three were collected in September. All terrestrial water samples were collected at the water's edge by directly filling sample bottles with surface water.

LWRF effluent was collected via dipping cup from the effluent stream just prior to injection and transferred to sample bottles using a 20 L collapsible, low density polyethylene (LDPE) container. R1 water was sampled directly from an on-site spigot using a reducing adapter with Tygon tubing to transfer water to sample bottles.

Concentrations of dissolved anions were measured at the University of Hawaii Water Resources Research Center Lab using a DX-120 ion chromatograph (Dionex Corporation, Sunnyvale, California). Check standards for each dissolved species were analyzed prior to and after sample analysis. Standard deviations (expressed as a percentage of the accepted values) for the check standard analyses (n = 2) were 28.9% for Mg^{2+} and 1.0 % for Cl^-.

4.3 RESULTS

4.3.1 Aerial Infrared Thermography

At the flight altitude of 2134 m (7000 ft), the camera configuration gave a swath width of 1038 m (3405 ft) and 2.3 m (7.5 ft) spatial resolution. The average aircraft ground speed was 58.76±9.59 m/s (131.44±21.45 mph), making consecutive images advance by 1.96 m (6.4 ft) on the ground.

SSTs from the three thermistors varied from ~23.0 to 26.3°C (Figure 4-2). Water cooled after sunset and stabilized in temperature between midnight and sunrise to within 0.4°C at both Kahekili and Black Rock and to within 0.9°C at Honokowai.

Figure 4-3 shows the location of the LWRF, the deeply incised topography of the field site, the relative proximity of the mountainous terrain to the coast, and the coastal SST map of the area. SSTs on the left (roughly north) and right (roughly south) sides of Figure 4-3 are similar to the average coastal SST for the month of May 2011 (25.5±0.5°C) determined at the Kahului tide station (1615680; Center for Operational Oceanographic Products and Services). The warmest area of Figure 4-3 occurs near the center of the mapped coastal zone.

The surface expressions of five marine spring locations are shown on the infrared image in Figure 4-4. These surface expressions are also visible in the gray-scale SST map in Figure 4-5. These springs exist in addition to the larger thermal anomaly (outlined in Figure 4-4) located to the southwest of the spring locations. Figure 4-4 also shows that the Black Rock Lagoon (near the Kaanapali Golf Course) was a source of cold groundwater to the area (also see Sections 5 and 6).

The plume boundary in Figure 4-4 was determined by the plume-boundary temperature inflection-point technique (Johnson, 2008), whereby the outer edge of the plume was established by averaging the maximum change in temperature, or inflection point, from five transects (ten inflection points) drawn laterally across the plume. The average plume boundary temperature was 26.50°C (79.69°F). The plume extends beyond the edge of the flight track, which is greater than 575 m (1886 ft) from the shoreline. The plume area estimate of 673,900 m^2 (166.5 acres; Table 4-2) is, therefore, a minimum estimate of the surface expression of the plume. The average plume boundary temperatures and surface areas for the five spring locations shown in Figures 4-4 and 4-5 are given in Table 4-2.

Temperatures inside the thermal anomaly were uniformly warm (0.6°C variation inside the plume) and were ~1°C warmer than the average coastal water temperature of 25.5±0.5°C (77.7±0.5°F). These temperatures contrast from natural submarine groundwater discharge (SGD), which ranges from 20 to 22°C (68 to 72 °F; Mink, 1964).

4.3.2 Chloride and Magnesium Ions

In June, chloride ion concentrations ([Cl$^-$]) from water supply wells varied from 121.0 to 277.4 mg/L (Table 4-3) and averaged 203.1±59.9 mg/L (n=7) while magnesium ion concentrations ([Mg^{2+}]) varied from 11.7 to 21.3 mg/L (Table 4-3) and averaged 17.3±3.8 mg/L (n=7). The exact same wells were sampled in September and yielded similar results. Measured chloride concentrations in September varied from 91.0 to 365.0 mg/L (Table 4-3) and averaged 208.6±102.0 mg/L (n=7) while [Mg^{2+}] varied from 7.0 to 23.6 mg/L (Table 4-3) and averaged 15.0±5.4 mg/L (n=7). Ratios of Cl:Mg for these supply wells varied from 9.6 to 13.4 in June and 9.6 to 15.9 in September (Figure 4-6).

The Lahaina Deep Monitor Well had fairly similar chloride ion concentrations for the two sampling events (327.4 and 452.0 mg/L; Table 4-3). Likewise, magnesium ion concentrations were similar for June and September (27.4 and 26.1 mg/L; Table 4-3). The Cl:Mg ratio of the monitoring well was 12.0 in June and 17.3 in September (Figure 4-6).

The four submarine springs sampled in June had [Cl⁻] that varied from 1,468.9 to 8,584.9 mg/L with an average value of 4,565.8±338.26 mg/L. The concentrations of magnesium varied from 69.2 to 164.2 mg/L (Table 4-3) and averaged 115.2±39.5 mg/L. Two submarine springs were sampled in September and had [Cl⁻] that varied from 1711.0 to 2,792.0 mg/L (Table 4-3) and averaged 114.5±40.6 mg/L, while [Mg^{2+}] varied from 85.8 to 143.2 mg/L (Table 4-3) and averaged 114.5±40.6 mg/L. The Cl:Mg ratios in June were variable (19.9 to 52.3) while the September data shows more consistent ratios (19.5 to 19.9; Figure 4-6).

No marine samples were collected in June. Eight samples from September had [Cl⁻] that varied from 20,450.0 to 35,745.0 mg/L (Table 4-3) and averaged 24,671.1±5,964.0 mg/L. Magnesium ion concentrations varied from 1,259.0 to 2,033.0 mg/L (Table 4-3) and averaged 1,493.6±309.2 mg/L. Cl:Mg ratios were consistent, varying from 16.0 to 17.6 (Figure 4-6) with an average value of 16.4±0.5 mg/L. These values are slightly larger than average seawater Cl:Mg ratios of 15:1 (Cox and Thomas, 1979b).

Terrestrial samples of surface water were variable, ranging from 5.8 to 5,970.1 mg/L for chloride and 2.8 to 192.5 mg/L for magnesium in June (Table 4-3). Although from different sampling locations, samples from September were also variable, ranging from 94.0 to 13,275.0 mg/L for chloride and 34.0 to 853.0 mg/L for magnesium (Table 4-3). Cl:Mg ratios of samples collected in June ranged from 2.1 to 31.0, while ratios ranged from 15.6 to 18.7 in September (Figure 4-6).

Treated effluent was sampled in both June and September. Chloride ion concentrations were similar (567.8 and 582.0 mg/L) for both samples (Table 4-3). Magnesium concentrations were also similar (39.3 and 32.8 mg/L; Table 4-3). R1 effluent was sampled in September and had similar chloride and magnesium concentrations as treated effluent, 571.0 and 32.2 mg/L, respectively (Table 4-3). The Cl:Mg ratio of treated effluent in June was 14.4 (Table 4-3). Both September samples had a Cl:Mg ratio of 17.7 (Figure 4-6).

4.4 DISCUSSION

4.4.1 Aerial Infrared Thermography

Since the camera perceived an opaque nature for water, emission sensed by the detector was derived from a thin skin (submillimeter) at the water's surface. This is called the "sea surface effect" (Schluessel et al., 1990; Banks et al., 1996; Fisher and Mustard, 2004). Bulk water temperatures are, therefore, not strictly determined by TIR remote sensing (Brown et al., 2005) since temperature micro-gradients between surface and bulk water exist (Fisher and Mustard, 2004). Skin temperatures at the water's surface are colder than bulk water because of evaporative cooling (Handcock et al., 2006); however, temperature differences between skin and bulk water are usually between 0.3 and 0.5°C (Schluessel et al., 1990; Emery et al., 1994; Donlon et al., 1998; Emery et al., 2001). Evaporative cooling did not obscure the underlying signal as thermal anomalies were

apparent in our data. Furthermore, relative temperature differences in the scene are more important than absolute temperatures assigned to each pixel for locating thermal anomalies.

Thermal infrared images represent a snapshot of the coastal SST distribution at the exact moment the airplane flew over the area. In our experience, the SST map will look different under varied seasonal, tidal, wind, and wave conditions.

Since the image was collected approximately five hours after sunset, the warming effects of the previous day's solar insolation were minimally or no longer present in the data as indicated by relatively stabilized SSTs (Figure 4-2). Thus, the thermal anomaly was a real feature of the coastal zone, not artificial warming by solar insolation.

The streams in the region are ephemeral and only flow after precipitation events. No precipitation was recorded in Lahaina in the days prior to the flight (National Oceanic and Atmospheric Administration (NOAA) climatological data station 22552 available at: http://cdo.ncdc.noaa.gov/qclcd/QCLCD?prior=N), so stream beds should not have contributed any water discharge signal to the coastal ocean during data collection.

Diurnal variations in wind speed occur rapidly in the field area and result in a thin (<1 m, 3.3 ft) wind-driven oceanic surface layer that is trade-wind controlled (Storlazzi and Field, 2008). The rate and direction of this surface layer can be significantly different than the rest of the water column (Storlazzi and Field, 2008). Known spring locations correspond to the locations of the springs in the SST map (Figures 4-4 and 4-5). Since the springs in the imagery correspond to the known and persistent locations of warm water discharge, currents, winds, and waves were likely not influencing or pushing the thermal signature of the plume in any predominant direction along the coastline during data collection.

The warmest area of the entire coastline mapped (Figures 4-3 and 4-4) corresponds to the geographic location where effluent enters the ocean through submarine springs, (see Sections 3 and 6; Hunt and Rosa, 2009; Dailer et al., 2010, 2012). The spatial boundaries of this plume, as suggested by Hunt and Rosa (2009) and which are based primarily on $\delta^{15}N$ values of macroalgae (Dailer et al., 2010), bracket the southern perimeter of the thermal anomaly and extend at least 400 m (1,312 ft) north of the northern boundary of the thermal anomaly. The thermal anomaly is, therefore, located in an area consistent with groundwater flow emanating from the LWRF.

The northern portion of the SST map is colder than the area near the thermal anomaly (Figure 4-3), consistent with depth-integrated temperatures from conductivity-temperature-depth (CTD) casts collected in February and June 2003 by Storlazzi et al. (2003). This temperature distribution is, therefore, likely a consistent occurrence for the field area. Offshore CTD casts collected near the Kahekili Park area (Storlazzi et al., 2003) show warm water, also consistent with the TIR data.

Storlazzi et al. (2003) attribute the area's cooler to warmer temperature gradient from north to south to higher precipitation and likelihood for greater cold temperature SGD contributions from the coastal zone in the northern portion of the area. This is a plausible explanation for the colder water observed to the north, but does not adequately describe the localized nature of the warm thermal anomaly southwest of the wastewater reclamation facility.

4.4.2 Nature of the Thermal Anomaly

Both Dailer et al. (2010) and (2012) found the highest δ^{15}N values of macroalgae near the submarine springs. To detail this comparison, the δ^{15}N (macroalgae) data from Dailer et al. (2010) are overlain on the SST map as shown in Figure 4-7. The match is excellent: as approaching the locus of submarine springs from the north, surface-water warming increases (~24.5 to 26.8°C) with increasing δ^{15}N(macroalgae) values (+4.8 to +48.8 ‰). Dailer et al. (2012) found that discharge from the spring locations rises to the surface due to its positive buoyancy relative to the seawater column. Once on the surface, the buoyant waters flow toward the south with the most predominant current in the area (Storlazzi and Field, 2008; Dailer et al., 2012). During calm conditions, Dailer et al. (2012), have determined that the water column is stratified with respect to macroalgal δ^{15}N values. Macroalgal bioassays deployed at four depths in the water column along ~500 m (1,640 ft) of shoreline and extending ~100 m (328 ft) offshore show that macroalgae deployed in the surface waters had higher δ^{15}N values than those at the benthos (Dailer et al., 2012). Dailer et al. (2012) attribute this pattern to greater effluent in the surface waters than near the benthos. This finding is consistent with positive buoyancy of the submarine spring discharge. The water column is also stratified with respect to radon (Section 5). In contrast, the water column has been found to be well-mixed with respect to temperature and salinity (Figure 4-8; Tetra Tech Inc., 1993; Storlazzi et al., 2003). At the most-seaward boundary of the plume (575 m, 1886 ft from shore), the water depth is ~15 m (50 ft). Since the water column is well-mixed with respect to temperature, and our infrared camera detected the warm signal from the top skin of the water, potential sources of heat necessary to generate the large thermal anomaly must be considered.

4.4.3 Potential Heat Sources

We have evidence to support three potential heat sources to the area including warm effluent, geothermal activity, and exothermic reactions from organic matter decomposition. We can neither implicate or exclude any one particular heat source to the area and therefore consider all three possibilities with equal discretion.

4.4.3.1 Warm Effluent

The injection waters are a potential source of heat to the coastal zone. The effluent is naturally warm with injection waters ranging from 26-31°C (79-88°F), the lower end of which is consistent with water temperatures observed in the thermal anomaly. The constant supply of warm effluent through concentrated subsurface pathways may create

the conditions conducive the fairly conservative heat transport through the aquifer's subsurface, despite the ca. 3 month minimum travel time (Section 3) of the warm effluent water from its input to its discharge in the coastal zone. Warm effluent cannot be ruled-out as a heat source, given the connection found between the warm waters emanating from the springs shown in Figure 4-4, the dye-tracer study (Section 3), the isotopic groundwater study (Section 6), and many other studies that have demonstrated that LWRF effluent emerges from the springs (Hunt and Rosa, 2009; Dailer et al., 2010, 2012).

4.4.3.2 Geothermal Activity

Cox and Thomas (1979a) found SiO_2 anomalies and temperature anomalies in excess of 30°C (86°F) in the Lahaina area (current Kaanapali Golf Courses to south of Lahaina proper) and noted that the area displayed definite indications of anomalous subsurface thermal conditions. The fact that no thermal springs exist on the land's surface does not preclude the existence of subsurface thermal activity (Cox and Thomas, 1979a). Furthermore, the most recent volcanism on West Maui occurred near Lahaina (Cox and Thomas, 1979b). We therefore consider geothermal activity as a possible contributing heat source.

The ratio of chloride to magnesium is a qualitative geothermometer that utilizes differences in reactivity between chloride and magnesium ions in thermally-impacted and non-thermally-impacted groundwater. Chloride in Hawaiian groundwater is essentially all of marine origin with minimal inputs from basaltic-rock weathering (only at temperatures in excess of 300°C; Ellis and Mahon, 1964; MacDonald et al., 1973). Chloride is virtually stable in groundwater. It does not undergo chemical reactions or anionic exchange with sediments (Schofield, 1956; Mink, 1961; Swain, 1973), ion exchange reactions when seawater infiltrates the aquifers, or during subsurface groundwater migration (Cox and Thomas, 1979a). Magnesium, on the other hand, is subjected to a wide variety of reactions at both low- and high-temperatures in aquifers. At low temperatures, magnesium primarily undergoes ion exchange reactions within sediments, during typical chemical weathering of basalts, and during seawater intrusion/mixing (Cox and Thomas, 1979b). Magnesium ion concentrations during low-temperature processes are significantly increased relative to chloride ion concentrations giving Cl:Mg ratios of between 1 and 6 for most non-thermally-impacted groundwater in Hawaii (Cox and Thomas, 1979b). During high-temperature reactions, magnesium can be effectively removed from solution by formation of high-temperature rock-alteration products such as chlorite and illite (Ellis and Mahon, 1964), minerals that have both been found in extinct hydrothermal systems in the Hawaiian Islands (Fujishima and Fan, 1977). Significant subsurface heat therefore lowers magnesium ion concentrations in relatively shallow groundwaters in the Hawaiian Islands (Cox and Thomas, 1979b).

Cox and Thomas (1979a, b) proposed that Cl:Mg values > 15 are significantly anomalous and are indicative of geothermally-altered groundwater, while Cl:Mg values between 12.0 and 14.9 are marginally anomalous. Cox and Thomas (1979a, b) measured significantly anomalous Cl:Mg values from well-water samples that were in excess of 15

from the Lahaina area. As Figures 4-9A and 4-9B show, the Cl:Mg values of spring water (19.93 to 52.88 in June and 19.50 to 19.94 in September, Table 4-3) measured during this study are larger than effluent (14.44 to 14.74), water supply wells (9.6 to 15.9), and average seawater for the area (16.42±0.51, n=8). Since the Cl:Mg values of waters extracted from the submarine springs are larger than all other end members in the area, magnesium must have been removed from these waters prior to their discharging from the springs.

4.4.3.3 Exothermic Reactions Related to Organic Decomposition by Bacteria

A third conceivable source of heat contribution to the area is exothermic reactions related to the bacterial consumption of organic matter (Hellström, 1997, 1999; Gallert and Winter, 2005, also see Section 6). The $\delta^{15}N$ of nitrate dissolved in the spring waters and other geochemical considerations discussed in Section 6 are consistent with extensive microbial nitrate reduction during organic matter degradation in these waters. Nitrogen bubbles were commonly seen emanating between the shoreline and the north spring group (Section 6). The nitrogen bubbles were enriched in nitrogen (91-98% nitrogen) relative to the atmosphere (79%; see Section 6). These results are consistent with nitrate reduction. Furthermore, manganese oxide crusts (indicative of suboxic conditions) have been found coating coral cobbles at the south spring group (Section 6).

4.5 SUMMARY

The aerial thermal infrared technique successfully identified a 673,900 m^2 (166.5 acre) thermal anomaly extending from the shoreline to at least 575 m (1,886 ft) offshore. The thermal anomaly is located southwest of the LWRF. Previously identified submarine spring locations were confirmed by the infrared technique, and reside at the northeast corner of the large thermal anomaly directly over the spring locations. These thermal plumes varied from 140 to 315 m^2 (1,507 to 3,391 ft^2). The plume discharge, therefore, buoyantly rose to the water's surface where it was detected by the TIR camera. Aside from the large thermal anomaly, no new spring locations were identifiable by infrared thermography. This study does not preclude the possibility that other submarine springs, in deeper offshore water, contributed to this anomaly.

The thermal anomaly may result from one or a combination of three heat sources. These sources include warm wastewater effluent, geothermal heating of groundwater and possibly heating of the water column from below the surface expression of the thermal anomaly, and exothermic reactions related to organic matter decomposition. Further assessments of the source(s) of heat generating the thermal anomaly are required to determine the relative contributions from each.

Table 4-1: Submarine spring locations and the names of samples

Location	Seep Group	Latitude	Longitude	Sample No.	Date	Time
Seep 3	South	20.93864	-156.69312	Seep 4 Piez-1	6/23/2011	17:00
Seep 4	South	20.93860	-156.69321	Seep 1 Piez-1	6/19/2011	15:00
				Seep 1 Piez 2	6/20/2011	15:33
				Seep 1-2 Piez	9/24/2011	16:40
NSG-a	North	20.93980	-156.69298	Seep 2 Piez-1	6/20/2011	16:15
Seep 6	North	20.94011	-156.69287	Seep 3 Piez-1	6/22/2011	12:58
				Seep 3-2 Piez	9/23/2011	16:40

Table 4-2: Plume boundary temperatures and plume areas of submarine springs. Boundary temperatures and plume areas were calculated from this Project's sea-surface temperature map. Springs and anomalies are described in a north to south direction and are identified in Figures 4-4 and 4-5. The plume boundary of the thermal anomaly includes the plume areas from Seeps 1-4 and 6. See Table 2-1 for more information about the specific submarine springs.

Description	Plume Boundary Temperature (°C)	Plume Boundary Temperature (°F)	Plume Area (m^2)	Plume Area (ft^2)
Seep 5	26.32±0.02	79.38±0.02	315	3390
Seeps 2 and 3	26.41±0.03	79.54±0.03	175	1880
Seep 6	26.44±0.03	79.59±0.03	210	2260
Seeps 1 and 4	26.65±0.02	79.97±0.02	140	1505
Thermal Anomaly	26.50±0.22	79.70±0.22	673,900	7,253,800

Table 4-3: Chloride and magnesium ion data.

Sample Names	Latitude[a]	Longitude[a]	Type[b]	Cl (mg/L)	Mg (mg/L)	Cl:Mg
Jun-11						
Lahaina Deep Monitor	20.94944	-156.65778	Monitor Well	327.4	27.4	12
Kaanapali P4	20.94917	-156.65028	Water Well	258.3	21.2	12.2
Kaanapali P5	20.95361	-156.64694	Water Well	132.4	11.7	11.3
Kaanapali P6	20.95639	-156.64750	Water Well	277.4	21.3	13
Honokowai B	20.93722	-156.64389	Water Well	221.3	18.9	11.7
Kaanapali P1	20.92694	-156.65556	Water Well	121	12.6	9.6
Kaanapali P2	20.92944	-156.65306	Water Well	226.9	16.9	13.4
Hahakea 2	20.91472	-156.66889	Water Well	184.6	18.2	10.2
Seep1Piez-1	20.93860	-156.69321	Spring	2085	104.6	19.9
Seep2Piez-1	20.93980	-156.69298	Spring	8584.9	164.2	52.3
Seep3Piez-1	20.94011	-156.69287	Spring	6124.2	122.7	49.9
Seep4Piez-1	20.93864	-156.69312	Spring	1468.9	69.2	21.2
Honolua Ditch	20.94957	-156.65773	Terrestrial	5.8	2.8	2.1
Kaanapali GC 1	20.91771	-156.69188	Terrestrial	1922.2	140.2	13.7
Kaanapali GC 2	20.91712	-156.69200	Terrestrial	196.5	15.9	12.4
LWRF Treated Effluent	20.94652	-156.68660	Treated Effluent	567.8	39.3	14.4
Kahana Stream	20.97703	-156.67772	Terrestrial	5970.1	192.5	31
Sep-11						
Lahaina Deep Monitor	20.94944	-156.65778	Monitor Well	452	26.1	17.3
Kaanapali P4	20.94917	-156.65028	Water Well	265	18.1	14.6
Kaanapali P5	20.95361	-156.64694	Water Well	201	13.9	14.5
Kaanapali P6	20.95639	-156.64750	Water Well	91	7	13
Honokowai B	20.93722	-156.64389	Water Well	365	23.6	15.5
Kaanapali P1	20.92694	-156.65556	Water Well	107	11.1	9.6
Kaanapali P2	20.92944	-156.65306	Water Well	288	18.1	15.9
Hahakea 2	20.91472	-156.66889	Water Well	143	13.2	10.8
Seep 3-2 Piez	20.94011	-156.69286	Spring	2792	143.2	19.5
Seep 1-2 Piez	20.93862	-156.69318	Spring	1711	85.8	19.9
LWRF-R1	20.94580	-156.68756	Treated Effluent	571	32.2	17.7
LWRF Treated Effluent	20.94652	-156.68660	Treated Effluent	582	32.8	17.7
Kaanapali GC-R1	20.92041	-156.68698	Terrestrial	594	34	17.5
Black Rock 1	20.92854	-156.69490	Terrestrial	1732	92.8	18.7
Black Rock 2	20.92882	-156.69543	Terrestrial	13275	853	15.6
Maui DP 3	20.94025	-156.69370	Marine	23290	1438	16.2

Table 4-3 (Continued)

Sample Names	Latitude[a]	Longitude[a]	Type[b]	Cl (mg/L)	Mg (mg/L)	Cl:Mg
Maui DP12	20.93237	-156.69478	Marine	32466	1936	16.8
Maui DP 14	20.92957	-156.69492	Marine	35745	2033	17.6
Maui 19	20.90451	-156.68701	Marine	20450	1259	16.2
Maui 23	20.92867	-156.69582	Marine	21017	1296	16.2
Maui 25	20.93715	-156.69345	Marine	22482	1381	16.3
Maui 28	20.95494	-156.68814	Marine	20669	1292	16
Maui 32	20.93907	-156.70074	Marine	21250	1314	16.2

[a]Latitude and longitude coordinates are relative to WGS 84 (World Geodetic Survey 1984).

[b]All water wells except for the Lahaina Deep Monitor were water supply wells. All springs were submarine springs. All terrestrial and marine samples were collected from surface water.
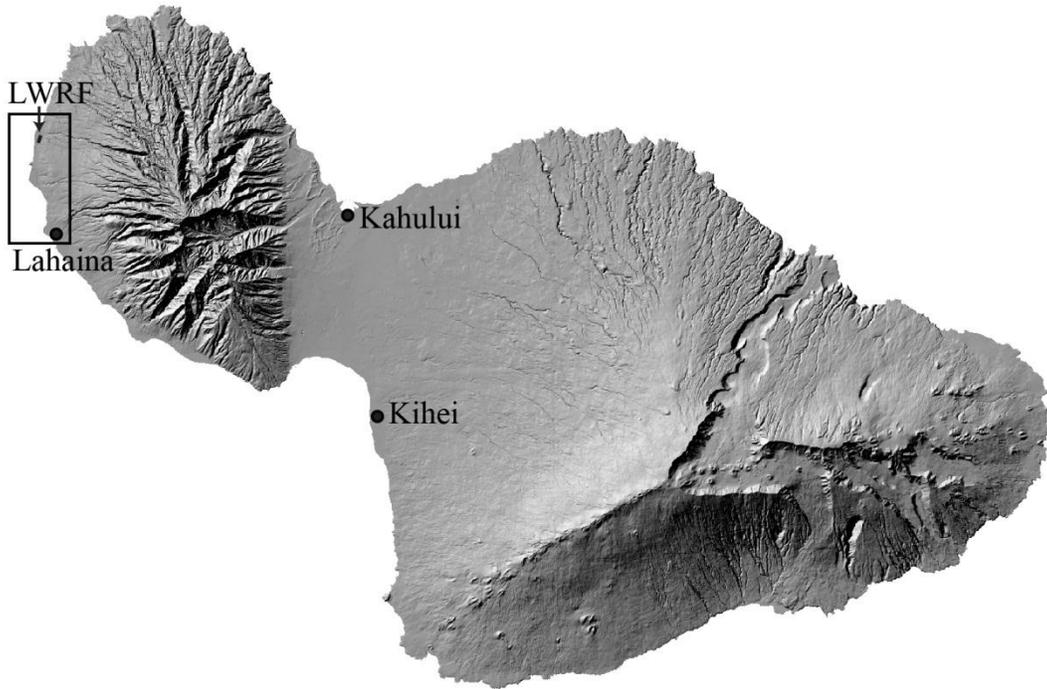
Figure 4-1: Study area.
The wastewater reclamation facility (LWRF) is shown relative to the island of Maui. The boxed area encompasses the study area.
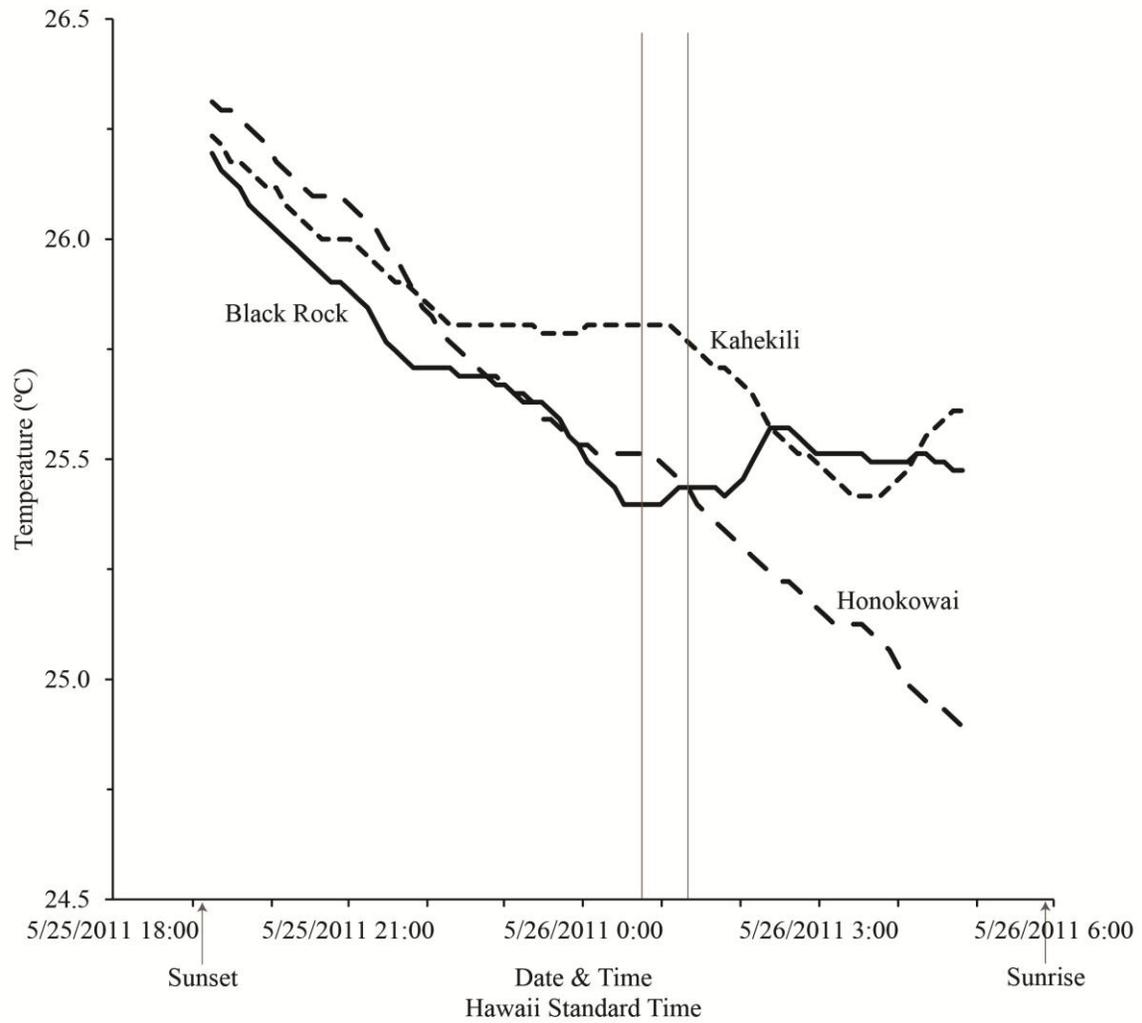
Figure 4-2: In situ sea-surface temperatures.
Data are from three thermistors deployed within the flight track and are displayed as five-point moving averages. The area inside the double vertical bars represents when the TIR data were collected. Sunset and sunrise are noted on the x-axis.
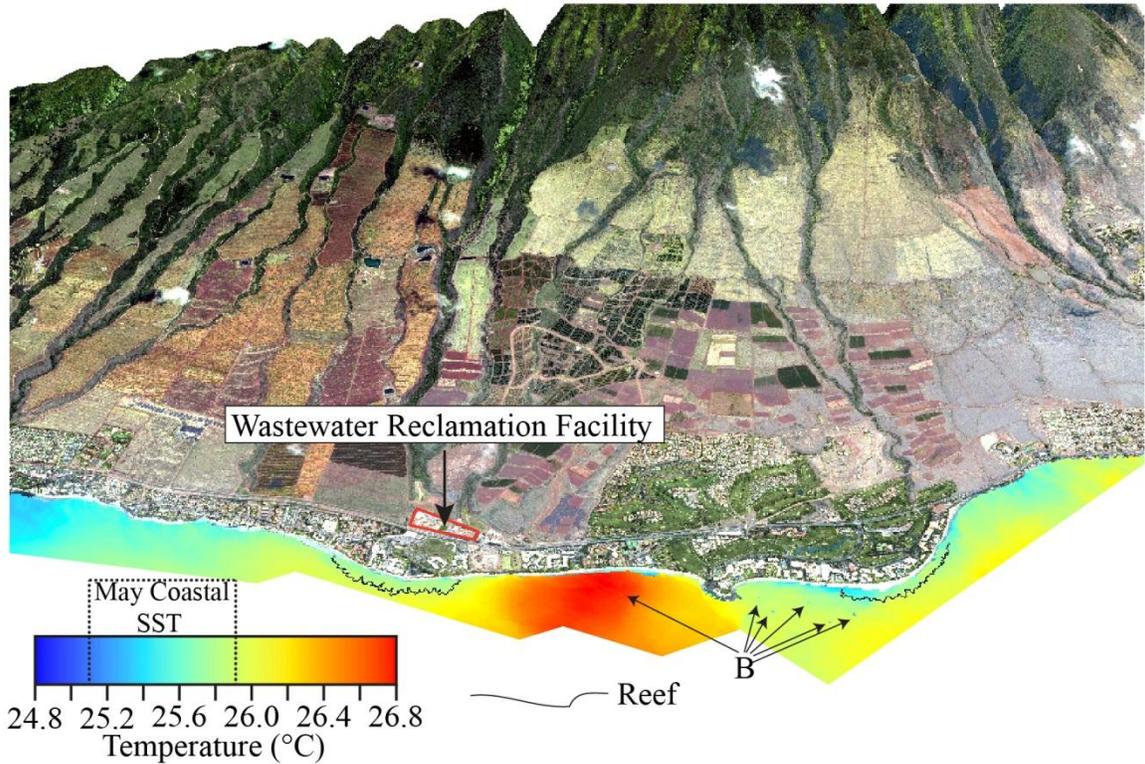
Figure 4-3: Sea-surface temperature map of Lahaina.
The map is in perspective view, so the left side of the figure is looking roughly to the north while the right side of the figure is looking roughly to the south. The tidal stage was down-going to the lowest-low tide of the day (+0.241 to +0.252 m; +0.791 to +0.827 ft, relative to mean lowerlow water; NOAA tide station 22552). Shallow reef is outlined in black. Boats are labeled with (B). Elevation data for the perspective view were obtained online from the national elevation data set (http://seamless.usgs.gov/).
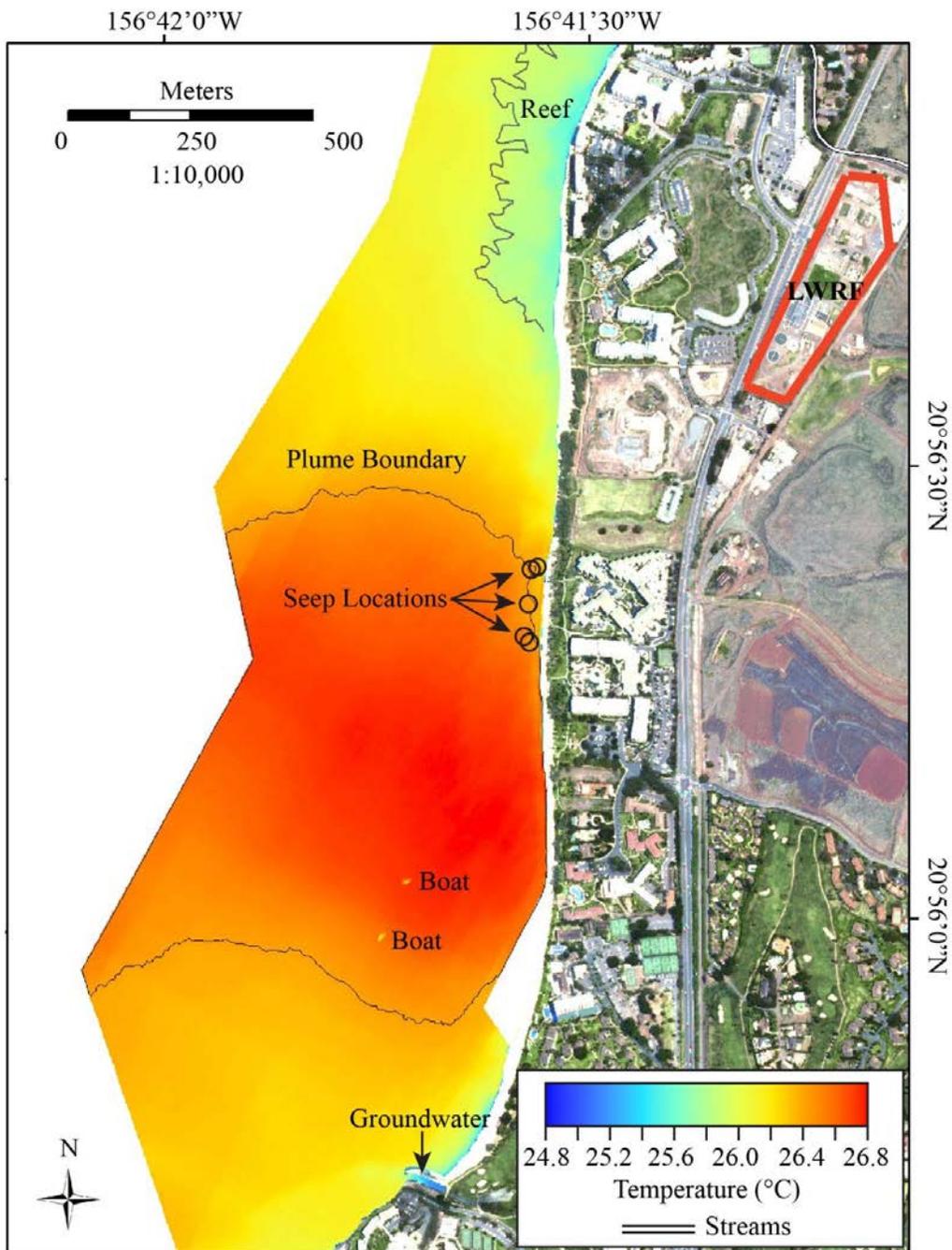
Figure 4-4: Sea-surface temperature map of the thermal anomaly.
The color ramp is exactly the same as Figure 4-3. The plume is greater than 575 m (1886 ft) in width (from the shoreline to the edge of the flight line). There is less than 0.6°C temperature variation within the plume area. The lagoon emptying into the ocean at the southern end of the figure is fed by cold groundwater. Previously identified spring locations are shown on the map and correspond to small-scale and semi-isolated thermal anomalies.
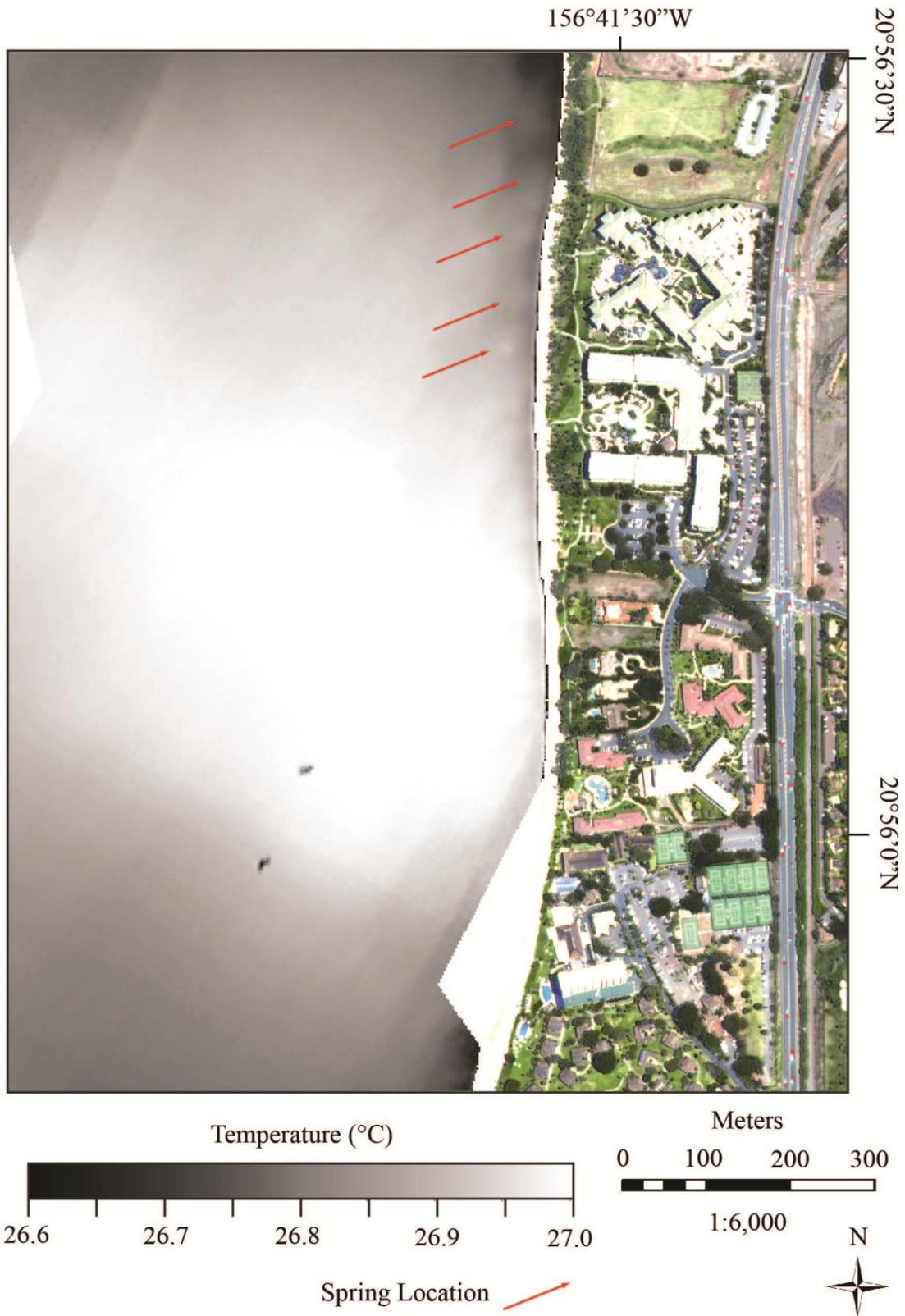
Figure 4-5: Submarine spring locations.
Data are displayed on a gray-scale sea-surface temperature map.
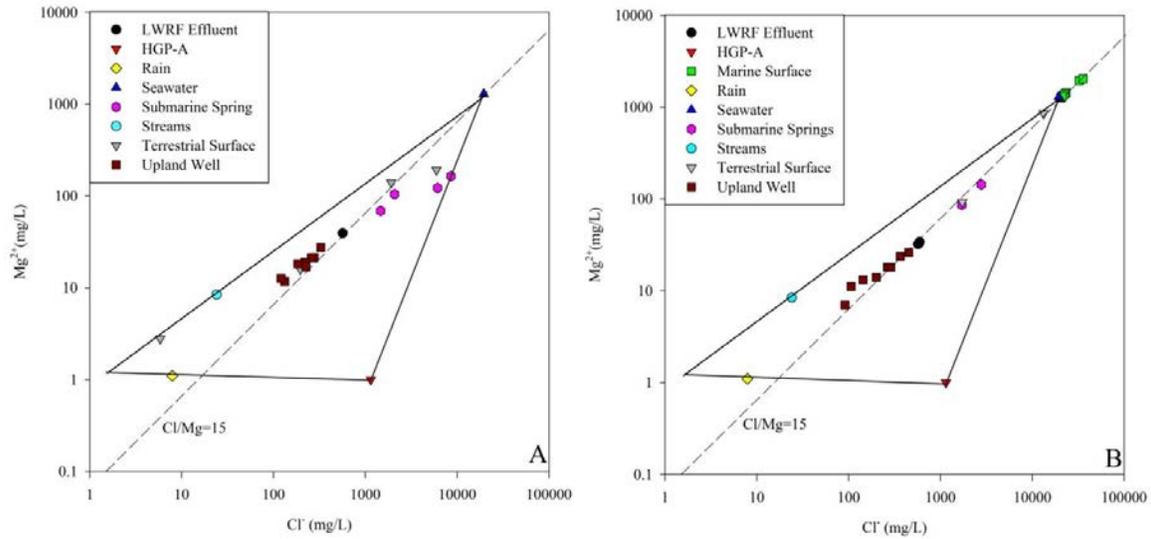
Figure 4-6: Log-Log plot of magnesium versus chloride ion concentrations.
Data from June are plotted in the left panel and data from September are plotted on the right panel. Samples to the right of the Cl:Mg=15 line are significantly anomalous and are indicative of geothermal alteration. All waters from submarine springs plot in the anomalous area of the diagram. The diagram is based on a similar diagram from Cox and Thomas (1979a).
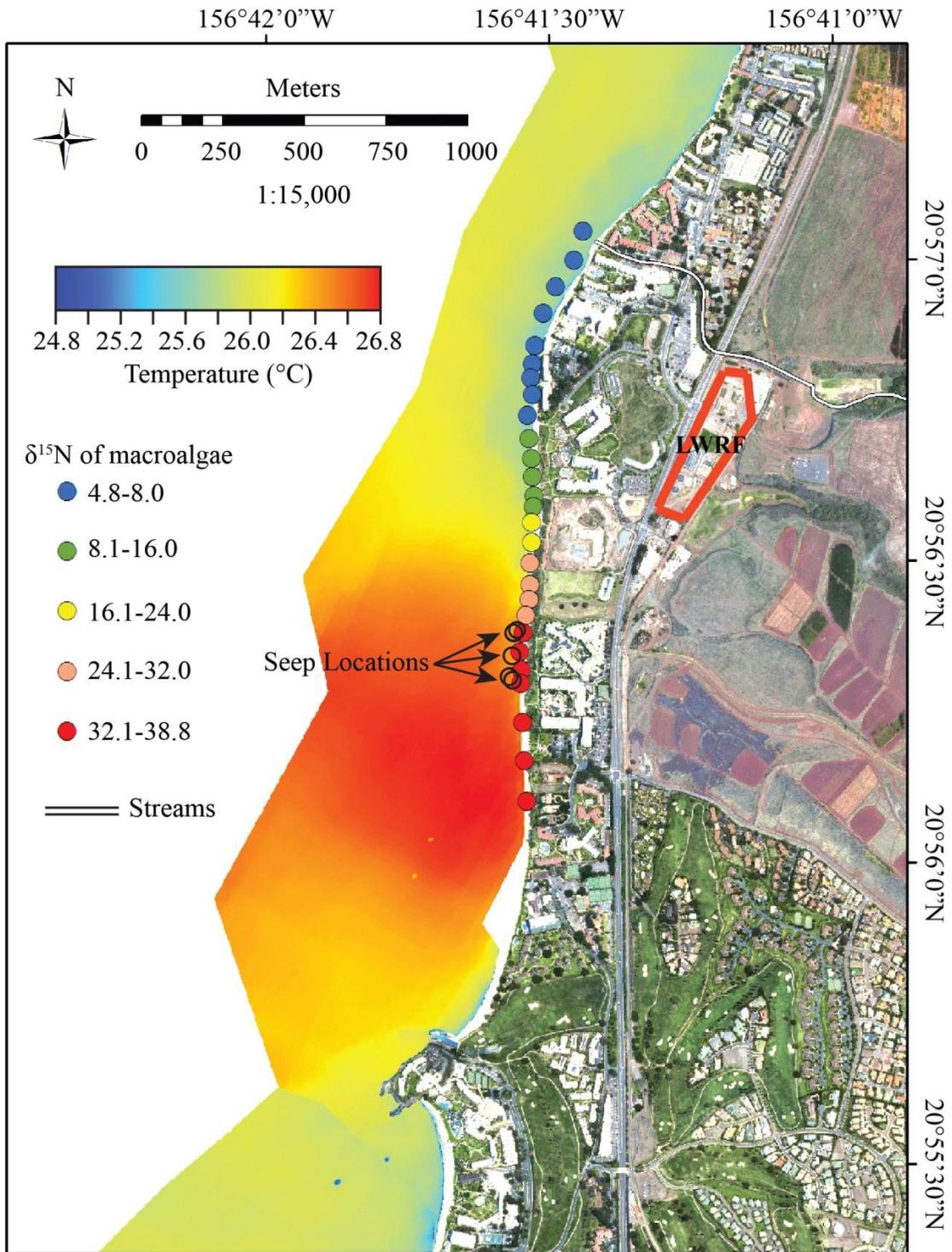
Figure 4-7: δ^{15}N(macroalgae) overlain on the sea-surface temperature map.
Nitrogen isotopic data of macroalgae from Dailer et al. (2010); the highest δ^{15}N values of
macroalgae occur near submarine spring locations and within the thermal anomaly.
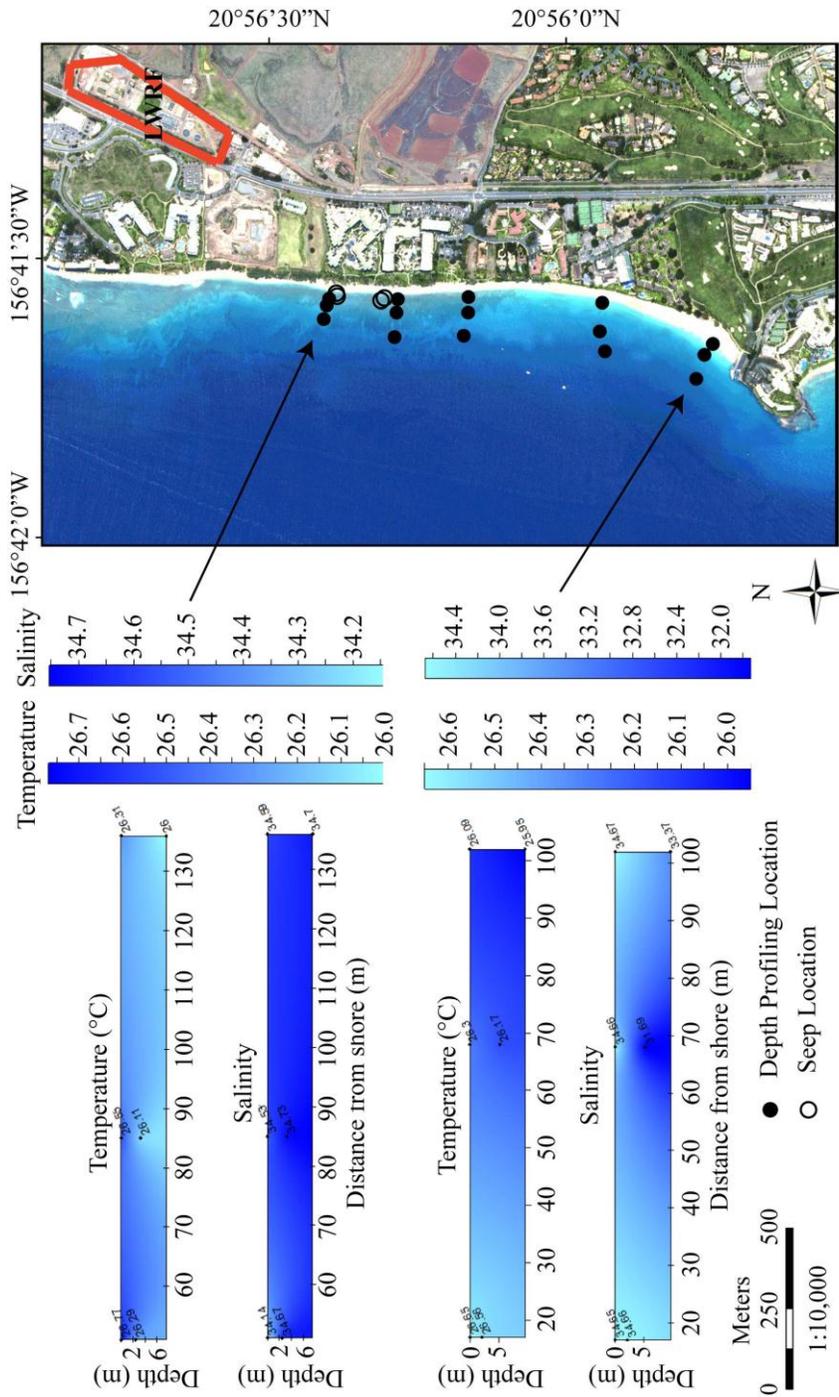
Figure 4-8: Temperature and salinity depth-profile measurements.
Data are reported on horizontal bars for the northernmost and southernmost transects collected in September, 2011. Scales for the temperatures and salinities in the horizontal bars are provided in the adjacent vertical bars. Note that the depth, distance, temperature, and salinity scales are different for the two transects. Data for all transects are given in Table D-1.
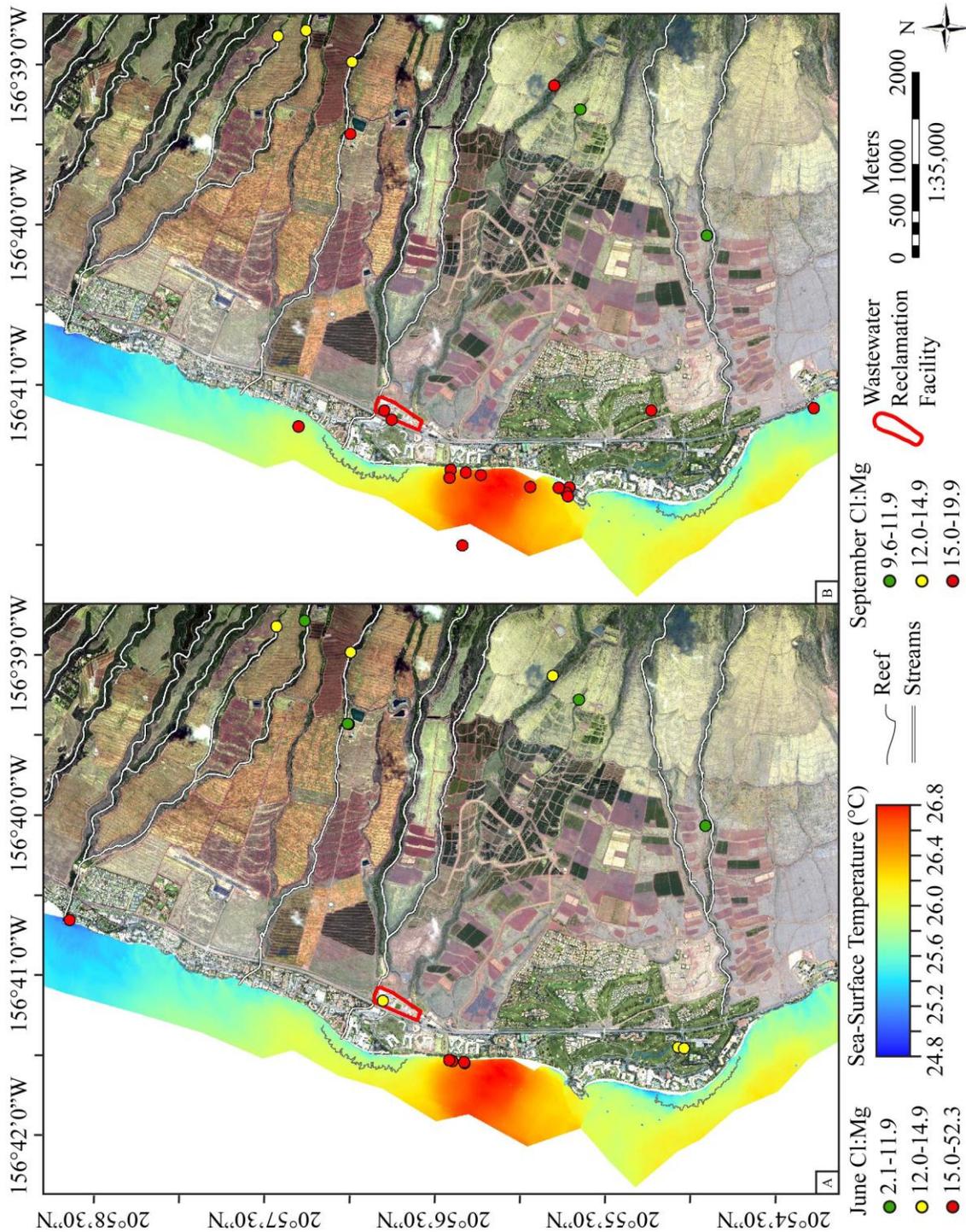
Figure 4-9: Map of the Cl:Mg ratios.
A) June and B) September, 2011. Ratios are plotted for submarine springs, marine waters, effluent, water-supply wells, and one monitoring well. Ratios below 12 are not considered anomalous. Ratios between 12.0 and 14.9 are marginally anomalous and ratios > 15 are significantly anomalous. Ratios >15 can be indicative of geothermal activity.

SECTION 5: SUBMARINE GROUNDWATER DISCHARGE

5.1 INTRODUCTION

5.1.1 Radon and Radium as Geochemical Groundwater Tracers

Radon and radium isotopes are highly enriched in groundwater and depleted in ocean water, and in the absence of other sources, their detection in coastal waters is an indication of submarine groundwater discharge (SGD). A mass balance of these tracers can be used to estimate the amount of groundwater discharge required to supply the observed inventory of these tracers in the coastal zone. Radon can be used to measure groundwater discharge at targeted areas and is therefore applicable for the determination of discharge from targeted submarine spring clusters.

Radon is a naturally occurring radiogenic isotope that enters subterranean groundwater aquifers as a dissolved and chemically inert noble gas after being released in predictable quantities from all rocks, including basalt. Thus, groundwater is accordingly enriched in ^{222}Rn, with activities often 3 to 4 orders of magnitude higher in groundwater than in coastal seawater, making it a superior tracer of coastal SGD (Burnett et al., 2006). Owing to its short half-life (3.8 days) and the fact that ocean water has very low levels of radon, this gas has now almost universally become the routinely measured tracer for SGD flow rates, as the decay rate of ^{222}Rn is comparable to the time scales of many coastal circulation processes (Burnett et al., 2006). The dynamics of groundwater inputs as well as estimates of groundwater discharges may therefore be examined via radon monitoring of coastal waters (Burnett and Dulaiova, 2003). Assessment of possible temporal trends is important because groundwater flow is known to be extremely variable on short (tidal) and long (seasonal change in hydraulic head) time scales. In addition, there is a large spatial variability in SGD that can also be assessed by coastal radon surveys where above background (excess above that produced from its parent ^{226}Ra) radon values in the surface water indicate groundwater inputs.

Radium isotopes are also enriched in groundwater relative to surface waters, especially where saltwater comes in contact with surfaces formerly bathed only in freshwaters. There are four naturally occurring radium isotopes: ^{223}Ra: $T_{1/2}$=11.4 days (d), ^{224}Ra: 3.6 d, ^{226}Ra: 1600 years (y), and ^{228}Ra: 5.8 y. These isotopes are produced in the natural uranium and thorium radioactive decay chains in rocks and sediments. The chemical composition of rocks and the amount of time the water spends underground results in variable radium isotope ratios. The ratio of short-lived ^{223}Ra and ^{224}Ra can be used to identify water that has not spent more than 5 half-lives of ^{223}Ra, or about 60 days in the subsurface as ^{223}Ra will be in disequilibrium with the uranium bearing rocks. This signature can be used to identify groundwater travel time through a substrate as

^{223}Ra/^{224}Ra ratios of newly infiltrated water will be low in comparison to waters that had spent >60 days in contact with the aquifer material.

5.1.2 Acoustic Doppler Current Profiler (ADCP) Measurements

An ADCP measures water velocity profiles in 3 dimensions by transmitting short pulse pairs into the water, and calculating the phase shift between the two acoustic return signals. In a profiler the Doppler effect is used to measure current velocities along three beams, which are sorted into several bins. The High Resolution ADCP allows measurements of small-scale phenomena with a 0.7 cm resolution and high frequency sampling (1 Hz). The High Resolution ADCP has velocity range of 10 m/s and an accuracy of 0.005 m/s. This instrument should be capable of resolving the vertical fluxes from individual submarine springs in the study site (see below), which are <1-20 cm in diameter and discharge water at rates observable with a naked eye. The flux measurements (vertical velocity multiplied by the cross-section of the submarine spring) from individual submarine springs can be summed to estimate groundwater flux from the major submarine springs. The instrument can be deployed for extended time periods to record changes in groundwater flux over time.

Both the radon mass-balance method and ADCP measurements provide groundwater discharge but cannot identify if and what fraction of the groundwater is tertiary treated wastewater. It is however possible to calculate the fraction of fresh groundwater and, in combination with other geochemical information also the fraction of injected tertiary treated wastewater (see Section 6). The relevance of these methods to the overall objectives of the project is to provide groundwater flux from the submarine springs to help determine the dye recovery.

5.1.3 Study Area

The focus area for the radon assessments in this project was along ~5 km of the Kaanapali coastline and is bounded by the intermittent Honokowai Stream in the north and by Hanakao`o Beach Park in the south. Located in the center of the study area are submarine springs that discharge warm, brackish groundwater. Radon surface water surveys were conducted along the 5-km stretch of the coastline while radon and ADCP time series measurements were conducted only at the submarine spring sites (Figure 5-1).

5.2 METHODS

SGD flow rates of the selected study sites were determined via coastal water ^{222}Rn monitoring and mapping surveys. In addition, radon and radium isotopes were measured in piezometers inserted into the submarine springs and groundwater wells located upstream of the discharge site.

5.2.1 Radon Sampling

^{222}Rn was measured continuously in 15-minute intervals for 8-24 hours at the three focus submarine springs and in the surface water, and in 5-minute cycles during two surface water radon/temperature coastline surveys. Time series measurements were established on an inflatable zodiac boat equipped with the following instrumentation: 1) two autonomous radon-in-air detectors (Rad7-Aqua manufactured by Durridge, Inc.; Lane-Smith et al., 2002), one measured submarine spring water and the other surface water radon (Figure 5-2a), 2) a YSI6920 V2-2 multiparameter probe measured temperature and salinity at the surface, and 3) a pressure, temperature and salinity sensor (Schlumberger diver CTD) close to the submarine spring. Water from the submarine springs was pumped using a peristaltic pump and high-density polyethylene (HDPE) tubing attached to each piezometer (Solinst Model 615 6" Drive-point piezometer, Figure 5-2b). Surface water above each submarine spring was pumped using a 12-volt bilge pump. Both pumps transported water to two air-water exchangers, which were attached to the radon-in-air monitors (Figure 5-2a). A radon-in-air monitor measures the radioactive decay rate of ^{218}Po, a daughter of ^{222}Rn by alpha-spectrometry.   The instrument reports the detected ^{218}Po in air, which is then converted to radon in water concentration using factory-calibrated conversion factors (Lane-Smith et al., 2002). The instrument is calibrated yearly against the industry standard at the manufacturer's facility (Durridge, Inc).

^{222}Rn in groundwater was collected from seven groundwater wells within the watershed using 250 ml glass bottles. These were measured the same day as collection in our field laboratory using a Rad-H$_2$O instrument (Durridge, Inc.). The detection limit of this method is significantly higher (20,000 dpm/m^3) than that of the Rad7-Aqua (100 dpm/m^3). Submarine spring water was sampled and analyzed using the RAD7-H$_2$O method repeatedly on February 20, 27 and March 11, 14, 27, 2012. All groundwater well and submarine spring samples were accompanied by salinity measurements.

Radon surveys of coastal surface water were conducted along the length of the Ka`anapali coastline (~5 km) on June 21st 2011, during low tide from 10:00 a.m. to 2:30 p.m. and on September 22nd, 2011 during high tide from 9:00 a.m. to 2:30 p.m. The two surveys were complimentary in order to capture radon activities as close to the coastline as possible. The low-tide survey allowed us to capture higher radon activities but prevented a close approach to the coastline, while in the deeper water at high-tide it was possible to survey closer to the coastline. Radon surveys were conducted using a set-up similar to that used for the submarine spring site monitoring. A RAD7-Aqua was installed on a Boston Whaler, which moved at about 5 km/h speed. A bilge pump towed in the surface water continuously provided water to the air-water exchanger along the surveyed path. Water quality parameters were logged simultaneously with radon measurements during these surveys by a YSI XLM 6000. A Garmin GPSMAP 420s was used to reconstruct the trajectory of the survey and record water depth.

5.2.2 Radon Groundwater Discharge Mass Balance of Submarine Spring Site Time Series Measurements

Groundwater discharge from the time series stationary radon measurements was calculated by a radon mass-balance of surface coastal waters based on Burnett and Dulaiova (2003), where submarine spring radon values were used as radon concentration of the discharging groundwater. Groundwater-derived ^{222}Rn fluxes into the coastal ocean were determined by evaluating the change in inventories between 15-minute measurements of radon in the surface water after correcting for tidal fluctuations, radon losses by atmospheric evasion and mixing with marine waters, which is explained in detail below (Burnett and Dulaiova, 2003):

1. We first performed continuous measurements of ^{222}Rn activities (dpm/m^3) in the coastal water column and in the submarine springs using the RAD7-Aqua instrument as described above, along with continuous measurements of water depth, and water and air temperatures. Wind speed was obtained from a nearby weather station (NOAA station WBAN ID #22552 located at Kapalua, HI) and atmospheric ^{222}Rn concentrations were estimated at 100 dpm/m^3 based on previous radon in air measurements on Maui (Dulaiova, unpublished data).

2. We then calculated excess (unsupported by ^{226}Ra) Ex^{222}Rn inventories for each measurement interval, i.e.,

$$I \ (dpm/m^2) = Ex^{222}Rn \ (dpm/m^3) * \text{water depth} \ (m) \qquad (5\text{-}1)$$

$$Ex^{222}Rn \ (dpm/m^3) = \text{total} \ ^{222}Rn - ^{226}Ra \ (dpm/m^3) \qquad (5\text{-}2)$$

where excess ^{222}Rn activities in the water column were estimated from measurements of ^{226}Ra. We used a ^{226}Ra value of 82 dpm/m^3 measured in offshore ocean water near Hawaii by Street et al. (2008).

3. The calculated inventories were next normalized to mean tidal height to remove the effect of changing inventory due simply to tidal height variations. This normalization was done for each measurement interval by multiplying the unit change in water depth (m) over the measurement interval by the ^{222}Rn activity offshore (dpm/m^3) during the flood tide and by concentrations in nearshore waters for the ebb tide. The flood tide corrections were negative (since the inventory would be increasing due simply to an increase in water depth) and the ebb tide corrections were positive.

4. We next corrected the tide-normalized inventories for atmospheric evasion losses during each measurement interval. The total flux across the air-water interface depends on the molecular diffusion produced by the concentration gradient across this interface and turbulent transfer, which is dependent on physical processes, primarily governed by wind speed. We used the equations presented by Macintyre et al. (1995) that relate gas exchange across the sea-air interface to the gradient in the trace gas concentration,

temperature, and wind speed. After these calculations, the radon water column inventories were corrected for supported ^{222}Rn (from ^{226}Ra), changes in water level, and atmospheric losses. We call these corrected inventories I*(dpm/m^2).

5. "Net" ^{222}Rn fluxes (F_{net}) were then estimated by evaluating the change in corrected inventories (ΔI*dpm/m^2) over each time interval (Δt=15 min.), i.e.,

$$F_{net}(dpm/m^2s) = \Delta I^*(dpm/m^2)/\Delta t(s) \qquad (5\text{-}3)$$

6. These fluxes represented the observed fluxes of ^{222}Rn into the coastal water column with all necessary corrections *except* loss via mixing with lower concentration waters offshore. Minimum mixing losses were estimated from inspection of the F_{net} over time. We based these values on the maximum negative fluxes that were invariably present. Since greater mixing losses could be compensated by higher benthic radon fluxes, our estimates must be conservative. The estimated mixing losses were added to the net fluxes in order to derive "total" Rn fluxes (F_{total}), i.e.,

$$F_{total}(dpm/m^2s) = F_{net}(dpm/m^2s) + F_{mix}(dpm/m^2s) \qquad (5\text{-}4)$$

^{222}Rn fluxes were then converted to water fluxes, specifically advection rates (ω, m/s) by dividing F_{total} by the measured ^{222}Rn concentration in the submarine springs, i.e.,

$$\omega(m/s) = F_{total}(dpm/m^2s)/^{222}Rn_{seep}\ (dpm/m^3) \qquad (5\text{-}5)$$

The calculated advection rates represented water flux per area (m^3/m^2/d) for the area of the water plume in which radon was measured. In order to convert the advection rate to volumetric flux (m^3/d), the advection rate was multiplied by the area of the radon plume originating from the submarine spring site. We determined this area based on the radon survey results, where the area of elevated radon signature above the submarine spring site was used.

5.2.3 Radon Groundwater Discharge Mass Balance of the Coastal Survey

While the time series measurements allows for the creation of a radon mass balance over time, the radon data collected during the coastal surveys provides a 'snapshot' measurements. However, the latter covers a larger length of the coastline. The surface water radon survey can reveal areas with elevated radon levels at which SGD can be

119

evaluated. Radon measurements from the surveys can be converted into SGD fluxes based on the following equation (Dulaiova et al., 2010):

$$Q_{SGD_{tot}} = \frac{A_{Rn\_cw} * V}{\tau * A_{Rn\_gw}},$$
(5-6)

where $Q_{SGD_{tot}}$ is total (fresh and saline) submarine groundwater discharge (m^3/d), A_{Rn_cw} is the radon activity in the coastal water corrected for non-SGD sources and losses, A_{Rn_gw} is the radon activity of the groundwater (dpm/m^3). V is the volume of the coastal water box that the measurement represents (m^3) and τ is the flushing rate of the volume of water considered in the calculation.

Based on equation (5-6), the conversion of surveyed radon activity to groundwater fluxes into the coastal zone may be summarized by the following calculations:

1. Radon activity in the coastal water (A_{Rn_cw}) was the average radon activity along a selected segment of the coastline. We selected several areas for evaluations and averaged the measured radon for each area individually. This activity was corrected for the following non-SGD related sources and sinks of radon in the water column:

a. In situ production from dissolved ^{226}Ra by calculating excess radon as:

$$\text{Excess } ^{222}\text{Rn} = \text{total } ^{222}\text{Rn} - {}^{226}\text{Ra}$$
(5-7)

b. The amount of radon diffusing from the sand and corals was calculated from Tribble et al. (1992) who estimated that in the absence of groundwater advection 10,500 dpm of radon would be deliberated by its production from ^{226}Ra in the coral body per day per 1 m^3 of coral. They also showed that the surface 1 m of coral effectively exchanges water and radon on these time scales, we assume therefore a radon flux of 10,500 dpm/m^3/d, which is distributed within the whole depth of the water column for each m^2.

c. Radon brought to the coast by incoming tides or upstream locations was eliminated from the radon balance by subtracting offshore or upstream radon activities from in situ radon. This influence was minimized or even neglected when the mapping survey occurred at low tide and when the study site was well flushed with low-radon offshore waters at high tide.

d. Radon losses due to radioactive decay were calculated using the coastal water residence time (τ defined below). Due to the short time scale of coastal mixing (here assumed to be tidal), the radioactive decay of radon represented a loss of only 9% over the tidal cycle.

e. Atmospheric losses were calculated from measured wind speeds (NOAA station WBAN ID #22552 located at Kapalua, HI), water temperature and tracer concentration gradients between water and air (Burnett and Dulaiova, 2003):

$$F_{atm} = k(C_w - \alpha C_{atm})$$
(5-8)

where C_w and C_{atm} are the radon activities in water and air, respectively; α is Ostwald's solubility coefficient; and k is the gas transfer velocity, a function of kinematic viscosity, molecular diffusion, and turbulence.

2. For each measurement, the volume of the coastal water box (V) was calculated as LxDxW where L was the length of the coastal segment, D was the average actual water depth for nearshore locations with depths <2m, and it was set as 0.5 m for deeper parts of the transect where the SGD plumes thinned out, and W was the width of the seepage face. The length of the coastal segment was the distance represented by the elevated radon activity. The width of the seepage face was considered the width of the surveyed coastal segment. SGD can also be expressed as discharge per meter of coastline (m^3/m/d), in which case the volume of the coastal box in Eq. (5-6) is divided by the coastline length.

3. The flushing rate (τ) of the coastal box was variable depending on currents and tides. The radon time series measurements indicated that radon concentrations drop to the offshore level at each high tide, which allowed the surface radon to build up by groundwater discharge during low tide. We therefore considered τ as one tidal cycle (12.25 hours). We assumed the same τ for the whole segment of our survey, which was an oversimplified but realistic assumption.

4. Naturally occurring groundwater Radon (A_{Rn_gw}) was represented by the groundwater end-member radon activity that was measured in groundwater wells in West Maui (Table 5-1). These radon concentrations were significantly lower (3,000-47,000 dpm/m^3) than those observed in the submarine springs (30,000-80,000 dpm/m^3).

5.2.4 Radium Sampling

Radium isotopes are typically at such low levels in natural waters, especially in groundwater, that their measurement requires pre-concentration from very large samples. Moore (1976) developed a method where radium can be collected from >100 liters of seawater or fresh water by passing the water through manganese-oxide coated (MnO_2-coated) acrylic fiber. At near neutral pH and under a controlled flow-rate, the fiber quantitatively adsorbs Ra, Pb, Th, Ac and other elements. The MnO_2-coated acrylic fiber is prepared by immersing raw acrylic fiber for about 20 minutes in saturated $KMnO_4$ solution heated to 75°C. When the fiber turns jet black, it is removed from the bath and rinsed thoroughly (Moore, 1976). For applications, approximately 150 cm^3 (~10 grams dry weight) of fiber is packed into a cylindrical cartridge. We used this technique to collect radium isotope samples in 7 groundwater wells and 4 submarine springs. 35-50 L of water was collected for ^{223}Ra and ^{224}Ra analyses into 25 L HDPE "cubitainers." These samples were passed through cartridges with 10 g dry-weight of manganese-coated acrylic fibers to quantitatively remove radium from the water sample (Moore and Reid, 1973). Fibers were triple-rinsed with Ra-free, deionized water in the laboratory and the moisture of the fiber was adjusted to have a water-to-fiber weight ratio in a range from 0.7 to 2.5 (Sun and Torgersen, 1998). The short-lived isotopes ^{223}Ra ($T_{1/2}$ = 11.4 days) and ^{224}Ra ($T_{1/2}$ = 3.6 days) were measured by a delayed coincidence counter system developed by Moore and Arnold (1996). For this measurement, the partially dried fiber

was placed in a helium-circulation system in which the short-lived radon daughters of ^{223}Ra and ^{224}Ra, ^{219}Rn and ^{220}Rn, were swept into a scintillation detector and a delayed coincidence circuit discriminated the alpha decays of the different radium daughters by the timing of the alpha-decay events. The system was calibrated using ^{232}Th and ^{227}Ac standards that are known to have their daughters in radioactive equilibrium and are adsorbed onto a MnO$_2$-coated fiber. Data were processed using procedures described in Garcia-Solsona et al. (2008). Table 5-2 lists the locations of the submarine springs that the samples were collected from as well as the sample names.

5.2.5 Determination of Seep Discharge Velocity via the Acoustic Doppler Current Profiler

We used a High Resolution (HR) Aquadopp profiler (manufactured by Nortek-USA) to measure vertical velocities of the water by orienting the Aquadopp in an upward-looking position so that its beams measured water discharging from one submarine spring at a time. We applied two different settings, for Seep 6 we measured the velocity as an average over a distance of 0.3 m above the seafloor with a blanking distance of 0.2 m, while for Seep 4 we divided the 0.3 m distance into fifteen 2-cm bins, so the vertical velocities were averaged into 15 bins. Additional details of the settings are provided in Table 5-3. At Seep 6, the HR Aquadopp profiler was deployed for 6 hours between 10:40 to 16:40 on September 23, 2011 and at Seep 4 the profiler was deployed for 22 hours between 9:20 am on September 24 until 7:40 am on September 25, 2011.

5.3 RESULTS

5.3.1 Coastal Radon Time Series

Field observations, thermal infrared imaging (TIR) of surface water (see Section 4) and the radon surveys indicated that the submarine springs focus into two clusters to which we refer to as northern and southern clusters. We used Seep NSG-1 and Seep 6 for the two major submarine springs in the northern cluster and Seep 4 in the southern cluster (see Table 2-1). While the submarine springs were benthic point sources, at the surface of the water column they manifested as plumes of warmer, radon-enriched water.

^{222}Rn in Seeps 4. 6, and NSG-a was measured during the June field excursion for a complete tidal cycle (24 hours). Overnight deployment of equipment was impossible for security reasons in September, these time series were deployed for daytime intervals only and covered only one north (Seep 6) and one south (Seep 4) submarine spring. Figure 5-3 shows that for all three submarine springs and during both June and September, ^{222}Rn measured directly from the submarine springs at the seafloor (~20,000-80,000 dpm/m^3) was enriched ten to forty times that which reaches the surface waters (~2,000 dpm/m^3). This suggests intense mixing of groundwater with seawater at a rate of 10-40 times as the submarine springs mix into the coastal zone. Still, the ~2,000 dpm/m^3 measured in surface waters is an order of magnitude above ambient ocean water radon levels (<100 dpm/m^3, Street et al., 2008), so despite the intense mixing, surface waters above the

submarine springs were enriched tenfold the magnitude of background levels. The June time series measurements showed radon activities varying with the tides where higher activities were at low tide, however, this general trend was not distinguishable during September time series measurements. Our findings were in very good agreement with the results of Swarzenski et al. (USGS report, 2012) who measured a range of 15,000-25,000 dpm/m^3 in Seep 4 and 500 -3,500 dpm/m^3 in the surface water in July 2010.

We sampled the submarine springs again in February and March, 2012 and the results showed little variation in radon activities and salinity in the submarine springs. In the south seep group, the average radon from these measurements was $25,000\pm10,000$ dpm/m^3 with an average salinity of 3.1 ± 0.1 (n=5). In the north seep group, radon averaged at $39,000\pm5,000$ dpm/m^3 with an average salinity of 4.6 ± 0.4 (n=4).

5.3.2 Groundwater Fluxes

5.3.2.1 Radon Mass Balance from Time Series Measurements

We used the radon mass balance method described in Burnett and Dulaiova (2003) which uses surface water radon activities/inventories to derive groundwater fluxes. Losses due to radon mixing and atmospheric evasion during the sampling period were lower in June (~1400-1600 dpm/m^2/hour), than in September (~1850-2700 dpm/m^2/hour). Radon fluxes by groundwater discharge ranged from 0 to 10,000 dpm/m^2/hour in June and 0 to 11,500 dpm/m^2/hour in September. Radon fluxes averaged $1,781\pm158$ and $2,533\pm180$ dpm/m^2/hour for June and September, 2011, respectively. Lower radon fluxes occurred at high tide while maximum values were observed at low tide. This indicates that the discharge from the submarine springs is tidally modulated; at high tide the hydraulic gradient between the aquifer and ocean is smaller and more seawater is pushed against the discharging water. At low tide, the hydraulic gradient is larger allowing more groundwater to discharge. Radon fluxes were divided by the seep radon activities to calculate groundwater advection rates. The average ^{222}Rn activity of the submarine springs was $54,900 \pm 2,100$ dpm/m^3 in June and $42,800 \pm 1,950$ dpm/m^3 in September (Table 5-1).

In June 2011, the average advection rates per full tidal cycle were 0.84 m/d from the southern seep group measured above Seep 4, and 0.70 and 0.82 m/d above NSG-a and Seep 6, respectively (Table 5-4). NSG-a and Seep 6 are part of the same northern cluster, so the average advection rate at that site was 0.76 m/d. In September 2011, the average advection rates were 1.32 and 1.06 m/d for the southern and northern submarine spring plumes, respectively.

Advection rates (m/d) can be expressed as a discharge of m^3/m^2/d and can be converted to m^3/d if the area of the groundwater plume is known. Areas for the two submarine spring clusters were derived from the radon surveys, as the area of the plume with surface radon concentrations within 100 dpm/m^3 of the mean radon concentration for each site. Based on the radon survey, the plume area for the southern submarine spring cluster is 70 m x 100 m and northern cluster (Submarine springs 2 and 3) is 60 m x 53 m. Based on

these areas the northern submarine spring cluster had a discharge of 2,400 m^3/d in June and 3,400 m^3/d in September, 2011. The southern submarine spring cluster discharge was 5,900 m^3/d in June and 9,200 m^3/d in September.

5.3.2.2 Radon Mass Balance from Radon Surveys

While the submarine springs were obvious groundwater discharge points, we also surveyed the surrounding coastline to see how significant the submarine springs were for the water balance with respect to other discharge locations. Results from the radon surveys showed several areas of high radon concentrations (at least four to five times ambient marine concentrations) in the surface waters bounding Honokowai Stream, around the north and south submarine springs, around Black Rock, and in the south near Hanakao`o Beach Park (Figure 5-4).

Areas where elevated radon activities were observed in June and September were selected for detailed analysis (Figure 5-5) and are summarized in Table 5-5. At each location, the size of the elevated radon plume was determined as the average distance from the coast where the radon measurements were taken times the length of survey track with surface radon concentrations within 100 dpm/m^3 of the mean radon concentration for each site. We also calculated the average radon activity and evasion and diffusion terms as described in the "Methods" section 5.2.3.

The resulting groundwater discharge rates are total groundwater discharge, i.e. mixtures of fresh terrestrial groundwater and recirculated seawater. For example, in the south cluster, the submarine springs had an average salinity of 3, so not all of 6,300 m^3/d was terrestrial freshwater. The freshwater fraction based on the submarine spring salinity (3) was ~90%, which provides a freshwater discharge of 5,700 m^3/d out of the total of 6,300 m^3/d. We did not have information about the salinity of discharging groundwater at other locations, so only total discharge is reported for those.

5.3.3 Radium Isotope Results

Radium was analyzed in groundwater well and submarine spring waters to determine if disequilibrium between ^{223}Ra to ^{224}Ra and their parents exists in the submarine spring samples. Lower ^{223}Ra to ^{224}Ra activity ratios would indicate waters younger than ~60 days, which is 5 half-lives of ^{223}Ra ($T_{1/2}$=11.4 days). In general, submarine springs had higher radium concentrations than the groundwater wells (Table 5-6).

5.3.4 Determination of Seep Discharge Velocity via the ADCP

During our September 2011 field deployment, we performed two time series measurements, one at Seep 4 in the south submarine spring cluster and one in the northern submarine spring cluster at Seep 6. At Seep 4, the HR Aquadopp profiler was deployed for 6 hours on September 23, 2011 and recorded from high tide to near low tide

(Figure 5-6). Significant wave action produced a turbulent water column resulting in significant upward and downward velocities with an absolute range of 0.03-0.04 m/s. Despite this noise, we believe that the net upward flux is a good approximation for seep discharge velocities. At high tide, the net upward velocity was much smaller (0.01 m/s) than at low tide (0.05 m/s). The average upward velocity for the 6-hour deployment period was 0.02 m/s.

At Seep 6, the HR Aquadopp profiler was deployed for 22 hours on September 24-25, 2011 covering almost a full tidal cycle. At high tide the upward vertical velocities were minimal (0 m/s) and at low tide the observed velocities were 0.025 m/s. The average upward velocity for the 22-hour deployment period was 0.0036 m/s.

5.4 DISCUSSION

5.4.1 Coastal Radon Time Series

Surface water radon activities above the submarine springs were elevated above the natural background levels expected from the decay of dissolved ^{226}Ra as well as that diffusing from the corals and sediments. In the absence of other sources it is safe to assume that the elevated radon originates from the submarine springs. Seep water radon activities exceed those observed in ambient groundwater well waters (average 16,000 ± 14,000 dpm/m^3, n=13), indicating that the water and/or rock chemistry at the submarine springs was different with higher levels of ^{226}Ra on/in the rocks and sediments along the groundwater flow-path, which resulted in higher production of radon. This may be due to differences in the geology along the flow-path of groundwater discharging at the submarine springs (consisting of alluvium) in comparison to higher elevation groundwater wells located in basalt. Another reason may be that redox conditions in the aquifer allowed the precipitation of manganese and iron (oxy)hydroxides that then sorb ^{226}Ra from the groundwater, which released radon. These findings, however, have no influence on the groundwater flux calculations.

5.4.2 Groundwater Fluxes

Radon measured at the surface of the water column above the submarine spring clusters, and therefore the advection rates derived from radon, represented not just one submarine spring, but the whole cluster and also any diffuse seepage that contributed to the radon-enriched buoyant plume. The radon mass-balance method therefore has the advantage that one does not have to quantify the number of discharge points and that all these sources, regardless of their size, are included in the radon mass balance.

The estimated SGD rates based on advection rates derived from the time series radon measurements showed an increase in discharge rates between June and September, 2011 at both locations. The northern seep group had a discharge of 2,400 m^3/d in June vs. 3,400 m^3/d in September, while the southern seep group discharge increased from 5,900 m^3/d to 9,200 m^3/d. Combining the discharges from the northern and southern seep

group, the total flux of water at the study site was 8,300 and 12,600 m^3/d in June and September, respectively (Table 5-4). The largest uncertainty in these estimates is contributed by the errors in the definition of the plume areas. The coastal survey was conducted on a different day than the time series analysis and mixing conditions may have been different between these two time intervals. Other sources of uncertainty are errors on atmospheric evasion and mixing fluxes and resulted in, at most, 60% error on the advection rate estimates (Dulaiova et al., 2010).

Groundwater discharge at the two seep groups is not the only coastal outcrop of groundwater in this area. We surveyed the coastline in the larger vicinity of the submarine springs to look for other possible discharge sites. From the survey, it became obvious that groundwater discharge commonly occurs along this ~5-km stretch of coastline with fluxes at individual locations ranging from ~2,000 to 28,000 m^3/d (Table 5-5). There is significant discharge at locations both south and north of the submarine springs and two of those, Honokowai and Wahikuli Wayside Park which is within the Hanakao`o Beach area defined here (Figure 5-5), were selected as additional tracer dye sampling points (see Section 3).

The discharge determined from the radon survey includes recirculated seawater fluxes and cannot be directly compared to recharge estimates from hydrological models that represent fresh groundwater only (i.e. Gingerich and Engott, 2012). The fraction of recirculated seawater can be calculated if the salinity of the discharging groundwater is known. Except for the submarine springs, we did not identify the individual groundwater sources at each discharge point, so we are not able to calculate freshwater discharges. However, Street et al. (2008) showed that brackish to saline groundwater is the major contributor to total SGD in West Maui. These authors studied Kahana, Mahinahina, Honokowai and Honolua Bay, where 49-77% of SGD occurred as saline discharge.

Another caveat for these fluxes is that they may include stream water. Groundwater fed streams are enriched in radon, and while radon readily escapes from streams by evasion, there may be remaining radon in the water after it discharges to the coastline. There was no observable discharge from any of the streams during our surveys, however, only the drainage canal of the Kaanapali Golf Course was directly connected with the ocean and contributed groundwater and radon to the radon inventory at Black Rock. Fluxes at the other locations represent total groundwater discharge.

Hawaii water quality regulations (Hawaii Department of Health, 2009) governing the discharges to the coastal waters depend on the magnitude of fresh groundwater fraction of SGD per mile of shoreline to set contaminant limits. Although regulatory compliance is beyond the scope of this study, we measured SGD and provide the data.

Two approaches were used to estimate the SGD near the shore in the study area. The first was a water balance approach. For the shoreline of the Honokowai Aquifer System a reasonable estimate of the freshwater component of SGD can made by using the recharge estimate of Engott and Vana (2007) and the rate of groundwater extraction and treated wastewater injection into this groundwater aquifer. The recharge to the

Honokowai Aquifer System estimated by Engott and Varna (2007) varied from 100,100 m^3/d (26.4 mgd) to 101,000 m^3/d (26.7 mgd) with an average recharge estimate of 100,300 m^3/d (26.5 mgd). The estimated recharge varies based on the geology near the coast. The lower range of the estimates excluded areas of coastal sediments or where the top of the Wailuku Basalts was at or below sea level. However, the difference between the high and the low recharge estimates is small, and the average value was used for these calculations. According to the Hawaii Water Plan – Water Resources Protection Plan (Wilson Okomato Corporation, 2008) the pumpage from the Honokowai Aquifer System in 2005 was about 11,500 m^3/d (3.04 mgd). Pumping and SGD represent a significant majority of fresh groundwater losses from the Honokowai Aquifer Sector. The difference between the calculated average rate of recharge and pumpage is about 88,800 m^3/d (23.5 mgd), which, with no other loss terms apparent, should equal the total fresh water fraction of SDG loss to the ocean within the Honokowai Aquifer system. For a shoreline-specific SGD comparison, this value was normalized over the shoreline length of the Honokowai Aquifer Sector. The linear length of the shoreline of the Honokowai Aquifer System is 11,800 m (7.33 mi). Thus, as based on the water balance budget, the shoreline integrated fresh water fraction groundwater SGD for this aquifer is about 7.53 m^3/m/d (3.20 mgd/mi) (Table 5-7).

This recharge is also augmented by injection of treated wastewater at the LWRF. The amount of total recharge plus the annual daily injection rate of injection at the LWRF (ca. 13,200 m^3/d or 3.5 mg/d) is thus 113,500 m^3/d (30.0 mgd). The difference between the calculated average rate of recharge plus injection and the pumpage is therefore about 102,000 m^3/d (27.0 mgd), which, with no other loss terms apparent, should equal the total non-saline water fraction of SDG loss to the ocean within the Honokowai Aquifer system. For a shoreline-specific SGD comparison, this value was normalized over the shoreline length of the Honokowai Aquifer Sector. Thus, as based on a water balance budget that includes the LWRF injection, the shoreline integrated non-saline water fraction of SGD for this groundwater body is about 8.65 m^3/m/d (3.68 mgd/mi) (Table 5-7).

The second approach used the nearshore-marine radon survey to estimate the coastal SGD from North Honokowai to south of Hanakao'o Beach (Figure 5-5). The SGD calculations do not represent the entire shoreline, but rather the areas of the highest discharge rates shown by the boxes in Figure 5-5. Tables 5-4 and 5-5 list these SGD estimates. The summed total SGD for the areas was 54,000 m^3/d (14.3 mgd). The shoreline length from North Honokowai to south of Hanakao'o Beach is 7,250 m (4.50 mi). This gives a total (marine + non-saline) SGD of 7.45 m^3/m/d (3.17 mgd/mi), as integrated over the shoreline (Table 5-7). It is important to note that caution must be exercised in comparing the radon survey calculated total SGD to a fresh groundwater SGD, because: (1) only the areas in the boxes were used in the calculations, which excludes a significant length of shoreline where SGD is also occurring between the boxes in Figure 5-5, and including these areas would increase the total SGD estimate; (2) radon calculated SGD is total SGD and it includes non-saline SGD water (including injected wastewater effluent) and marine SGD. This method cannot discriminate between these sources, and thus fresh groundwater is only a fraction of the total SGD. Stable isotope

mixing analyses (Section 6) indicates that the discharge from the submarine springs that are the focus of this study is primarily (>50%) treated wastewater effluent. Applicable to other areas, Street et al. (2008), estimated that 49 to 77 percent of the SGD may be saline groundwater. Here, however, salinity of the water sampled at the submarine springs is on average about 4.5, indicating it is only moderately brackish. It is interesting to note the close agreement in the water balance and the radon survey specific SGD estimates; but as stated above a direct comparison between the two is not valid due to the limited amount of data available.

5.4.3 Radium Isotopes

There was a large scatter in radium values, which resulted from the variability of the salt content of the sampled water and the geology of the aquifer. Salinity greatly affects dissolved radium concentrations; the higher the salinity the more radium desorbs from particles. This trend was observed in the wells and in the submarine springs, where the submarine springs had significantly higher salinity and radium activities. Because of the difference in geological settings between the upland wells and the submarine springs we expected ^{223}Ra and ^{224}Ra to be produced at a different ratio.

The surficial geology of the coastal area is different (alluvium) than that of the upland groundwater wells (screened in the basalt) and if the alluvium produced a different ^{224}Ra/^{223}Ra activity ratio, all seep ratios should be offset from the groundwater well values. The average ^{224}Ra/^{223}Ra activity ratio in the groundwater wells was ~12 (Figure 5-7). The wells that had ^{223}Ra below the detection limit did not fit the trend because they had measurable ^{224}Ra. The trendline was forced through the origin because the two isotopes behave chemically identically and if zero ^{223}Ra is desorbed, there should also be zero ^{224}Ra activity in the water. There were submarine spring measurements that were significantly different from the groundwater well ratios and plot on the far right: Seep 4 (sample Seep 1 Piez-1), Seep 6 (sample Seep 3 Piez-1) and Seep 3 (sample Seep 4 Piez-1) all had ^{224}Ra/^{223}Ra activity ratios of 5.4 in June, 2011. NSG-a (sample Seep 2 Piez-1), which seems to behave geochemically differently from the other submarine springs (also a salinity of 14.7 indicates the installation of the sampling piezometer was problematic) had a ratio of 26. In September, 2011, however, the submarine spring ratios are much closer to those of the groundwater well ratios, 10 for Seep 4 (sample Seep 1-2 Piez) and 11 for Seep 6 (sample Seep 3-2 Piez). Assuming that the activities of these short-lived isotopes were negligible in the recharging water, the difference between the June and September ratios was due to the change in the groundwater flow regime. Indeed, salinities were much fresher in September when the radon mass balance predicted significantly higher groundwater discharge from the submarine springs. One scenario that could explain this would be the dilution of submarine spring water with groundwater recharged upstream from the injection wells in September. Another consideration is that the June sampling period was unfortunately subject to a large swell event that increased the salinity in the submarine spring samples and likely diluted the actual geochemical properties of the submarine spring water. However, other scenarios are possible and the understanding of the shift in radium ratios in the submarine springs between the June and

September flow regimes requires further investigation which is beyond the scope of this project.

While in other coastal aquifers radium isotopes provided valuable information on water ages, we must conclude that in this setting, the radium data cannot be used to determine ages of the recharged water. This is because it is longer than 60 days and is therefore beyond the sensitivity of the radium method.

5.4.4 Determination of Seep Discharge Velocity via ADCP

The ADCP record (Figure 5-6) indicated that the discharge from individual submarine springs was tidally influenced, probably due to the smaller hydraulic gradient between the aquifer and the ocean at high tide than at low tide. At high tide the velocities were smaller than at low tide. The same trend was also observed from the radon measurements. These submarine springs were the same (Seeps 4 and 6) as the ones later sampled for radon. The ADCP was deployed before the piezometers were inserted into the submarine springs. The average upward vertical velocity of the Seep 4 deployment was 0.02 m/s. Assuming a 0.2 x 0.2 m submarine spring geometry, this velocity corresponds to a groundwater discharge of 70 m^3/d. The average upward vertical velocity for Seep 6 was 0.0036 m/s. Assuming the same 0.2 x 0.2 m submarine spring geometry, the water flux from Seep 6 would be 12 m^3/d. The 0.2 x 0.2 m submarine spring geometry is just an approximation because the exact geometry of the submarine springs is hard to define due to their irregularity. Exact submarine spring geometries including vent dimensions and water cone diameters will be measured and the number of submarine springs will be quantified in the next phase of the project. We will also perform more measurements and improve water velocity measurements by changing the deployment geometry and we will target calmer days with smaller swells.

5.5 SUMMARY

Groundwater discharge from two seep groups described in Table 2-1 were measured directly using a current meter and indirectly via geochemical tracers. As an indirect method we used radon, a naturally occurring radioactive tracer. We constructed a radon mass balance model to estimate discharge from time series radon measurements in the surface water. We found that the groundwater discharge from the submarine springs is tidally modulated with minimal discharge at high tide and increased fluxes at low tide. Due to this variability we expressed discharge in this report as a 24-hour average. The total (fresh + saline) groundwater discharge including the submarine springs and diffuse flow was 8,300 and 12,600 m^3/d in June and September, respectively (Table 5-4). Out of this, fresh groundwater discharge amounted to 6,100 and 10,900 m^3/d in June and September, 2011, respectively. Coastal radon surveys showed that there is significant groundwater discharge along the coastline north and south of the submarine springs. We found several sites with groundwater discharge ranging from 2,000 to 28,000 m^3/d, the highest flux at 28,000 m^3/d was at Hanakao`o Beach Park, the second largest at 15,000 m^3/d was at Honokowai Beach Park. We can also express this flux as volume of water discharged per meter shoreline. For a conservative estimate, we can assume that

groundwater only discharges at the 6 sites indicated in Table 5-4 and on Figure 5-5 along this 5 km coastline. The sum of the fluxes is 54,000 m^3/d, resulting in a groundwater discharge of 10.8 m^3 per m of coastline per day.

Hawaii water quality regulations (Hawaii Department of Health, 2009) governing the discharges to the coastal waters depend on the magnitude of fresh groundwater fraction of SGD per mile of shoreline to set contaminant limits. Two approaches were used to estimate the SGD near the shore in the study area. The first was a water balance approach. For the shoreline of the Honokowai Aquifer System a reasonable estimate of the freshwater component of SGD can made by using the recharge estimate of Engott and Vana (2007) and the rate of groundwater extraction (Wilson Okamoto, 2008). The shoreline integrated fresh water fraction of SGD for this aquifer is about 7.53 m^3/m/d (3.20 mgd/mi) if the LWRF treated wastewater is not considered. If the injection of 13,200 m^3/d (3.5 mgd) of treated wastewater is considered the SGD increases. The shoreline integrated non-saline water fraction of SGD increased to about 8.65 m^3/m/d (3.68 mgd/mi).

The second approach used the nearshore-marine radon survey to estimate the coastal SGD from North Honokowai to south of Hanakao'o Beach (Figure 5-5). The SGD calculations do not represent the entire shoreline, but rather the areas of the highest discharge rates shown by the boxes in Figure 5-5. The summed total SGD for the areas of highest SGD was 54,000 m^3/d (14.3 mgd). This represents a total (marine + non-saline) SGD of 7.45 m^3/m/d (3.17 mgd/mi), as integrated over the shoreline. It is important to note that caution must be exercised in comparing the radon survey calculated total SGD to a fresh groundwater SGD, because: (1) only the areas in the boxes were used in the calculations, which excludes a significant length of shoreline where SGD is also occurring between the boxes in Figure 5-5, and including these areas would increase the total SGD estimate; (2) radon calculated SGD represents total SGD and includes non-saline SGD water (including injected wastewater effluent) and marine SGD. This method cannot discriminate between these sources, and thus fresh groundwater is only a fraction of the total SGD.

An Acoustic Doppler Current Profiler (ADCP) was deployed at a major submarine spring in each seep group. Despite the large swell event that produced noise in the data, the net vertical flux was positive indicating that the instrument recorded the upward flux from the submarine spring. The ADCP record showed that the discharge from the submarine springs was tidally influenced, with lows at high tide and larger fluxes at low tide. At Seep 4 located in the south submarine spring group, the average vertical velocity during the 6-hour deployment was 0.02 m/s. At Seep 6 located in the north submarine spring group the upward vertical velocity averaged at 0.0036 m/s. These water velocities translate to a discharge from the individual submarine springs of approximately 70 and 12 m^3/d from Seep 4 and Seep 6, respectively. Additional ADCP measurements are ongoing, the results of which will be reported in this project's final supplemental report.

Table 5-1: Summary of ^{222}Rn groundwater measurements in the Kaanapali region with average ^{222}Rn from seep time series. Well samples are 250 ml grab samples. Seep samples are the averages of continuously measured activities.

Well Name	Latitude	Longitude	Elevation (m)	^{222}Radon and Error (dpm/m^3) June	September
Kaanapali P1	20.92694	-156.65556	286	7,800 ± 26,000	11,400 ± 31,000
Kaanapali P2	20.92944	-156.65306	280	13,000 ± 29,300	12,900 ± 31,700
Kaanapali P4	20.94917	-156.65028	266	2,600 ± 23,100	2,900 ± 25,200
Kaanapali P5	20.95361	-156.64694	288	na	4,300 ± 26,200
Kaanapali P6	20.95639	-156.64750	290	24,800 ± 35,100	10,000 ± 30,000
Honokowai B	20.93722	-156.64389	266	7,800 ± 26,000	37,100 ± 42,000
Hahakea 2	20.91472	-156.66889	150	29,800 ± 37,200	47,200 ± 45,900
Seep 4 Ave.	20.93860	-156.69321	0	52,100 ± 1,950	30,200 ± 1,680
NSG-a Ave.	20.93980	-156.69298	0	40,300 ± 1,740	na
Seep 6 Ave.	20.94011	-156.69287	0	72,500 ± 2,560	55,400 ± 2,210
Seep Ave.				54,900 ± 2,100	42,800 ± 1,950

na – not available

Table 5-2: Submarine spring locations and the names of samples collected from those locations

Location	Seep Group	Latitude	Longitude	Sample No.	Date	Time
Seep 3	South	20.93864	-156.69312	Seep 4 Piez-1	6/23/2011	17:00
Seep 4	South	20.93860	-156.69321	Seep 1 Piez-1	6/19/2011	15:00
				Seep 1 Piez 2	6/20/2011	15:33
				Seep 1-2 Piez	9/24/2011	16:40
NSG-a	North	20.93980	-156.69298	Seep 2 Piez-1	6/20/2011	16:15
Seep 6	North	20.94011	-156.69287	Seep 3 Piez-1	6/22/2011	12:58
				Seep 3-2 Piez	9/23/2011	16:40

Table 5-3: Settings of the Aquadopp HR profiler applied for submarine spring water vertical velocity measurements. Measurements were done at Seeps 4 and Seep 6.

	Seep 4	Seep 6
Time of first measurement	9/23/2011 10:42:12 AM	9/24/2011 9:20:41 AM
Time of last measurement	9/23/2011 4:38:36 PM	9/25/2011 7:43:07 AM
User setup		
Measurement/Burst interval	1 sec	1 sec
Cell size	300 mm	20 mm
Orientation	UPLOOKING SHALLOW WATER	UPLOOKING SHALLOW WATER
Profile range	0.30 m	0.30 m
Horizontal velocity range	0.61 m/s	1.15 m/s
Vertical velocity range	0.26 m/s	0.48 m/s
Number of cells	1	15
Average interval	1 sec	1 sec
Blanking distance	0.198 m	0.200 m
Number of beams	3	3
Software version	1.08	1.08
Deployment name	NSEEP	Seep3
Deployment time	9/23/2011 10:42:12 AM	9/24/2011 9:20:41 AM
Heading	284.5	342.8
Pitch	1.5	-2.6
Roll	0.3	-0.6
Latitude/Longitude	20.93860N/156.69321W	20.94011N /56.69287W

Table 5-4: Advection rate estimates at the two submarine spring clusters derived from radon time-series measurements.

Location	Plume Area (m^2)	June, 2011				September, 2011			
		Average Advection Rate (m/d)	Discharge (m^3/d)	Salinity	Fresh Discharge (m^3/d)	Average Advection Rate (m/d)	Discharge (m^3/d)	Salinity	Fresh Discharge (m^3/d)
Seep 4	70 x 100	0.84	5,900	7.5	4,600	1.32	9,200	2.9	7,800
NSG-a	60 x 53	0.70	2,200	14.5	1,250	na	na	na	na
Seep 6	60 x 53	0.82	2,600	10.6	1,800	1.06	3,400	4.8	3,100

na – not available

Table 5-5: Groundwater fluxes derived from radon inventory and mass balance at sites with elevated surface radon activities in June and September, 2011.
The surface area was defined as the average distance from coast where the radon measurements were taken times the length of survey track with surface radon concentrations within 100 dpm/m3 of the mean radon concentration for each site.

Site Name	^{222}Rn (dpm/m^3)	Plume Surface Area (m)	Total Groundwater Discharge (m^3/d)	Fresh Groundwater Discharge (m^3/d)	Total Groundwater Discharge per Meter Coastline (m^3/m/d)
Black Rock	800	36 x 370	2,250	na	6
South Cluster	410	70 x 100	6,300	4,900	63
North Cluster	410	60 x 53	2,500	1,800	47
S. Honokowai	1,380	200 x 110	7,100	na	64
N. Honokowai	1,380	150 x 170	7,900	na	46
Hanakao`o Beach	1,200	200 x 1200	28,000	na	23

na – not available

Table 5-6: Radium isotope concentrations and salinities in groundwater wells (June 2011) and submarine springs (June and September 2011).

| Name | Latitude | Longitude | Radium Isotopes (dpm/m^3) | | Salinity |
			^{223}Ra	^{224}Ra	
Kaanapali P1	20.92694	-156.65556	<DL	4.7	0.27
Kaanapali P2	20.92944	-156.65306	<DL	5.3	0.45
Kaanapali P4	20.94917	-156.65028	<DL	7.2	0.51
Kaanapali P5	20.95361	-156.64694	<DL	4.8	0.55
Kaanapali P6	20.95639	-156.64750	0.51	8.1	0.55
Honokowai B	20.93722	-156.64389	1.04	10.8	0.44
Hahakea 2	20.91472	-156.66889	0.30	5.9	0.41
Seep 1 Piez-1 (June)	20.93860	-156.69321	3.06	16.1	7.5
Seep 2 Piez-1 (June)	20.93980	-156.69298	0.58	15.4	14.7
Seep 3 Piez-1 (June)	20.94011	-156.69287	3.24	17.7	10.6
Seep 1-2 Piez (Sept.)	20.93860	-156.69321	1.40	13.6	2.9
Seep 3-2 Piez (Sept.)	20.94011	-156.69287	1.92	21.0	4.8
Seep 4 Piez-1 (June)	20.93860	-156.69310	3.14	16.9	3.5

<DL indicate results below detection limit of 0.1 dpm/m^3
Average 1-sigma measurement uncertainties for ^{223}Ra are 30% while for ^{224}Ra <10%.

Table 5-7: Shoreline SGD Estimations

Water Balance SGD Estimate				
Parameter	Value	Units	Value	Units
Honokowai Shoreline	11,800	m	7.33	mi
Honokowai Recharge	100,300	m^3/d	26.5	mgd
Honokowai Pumpage	11,500	m^3/d	3.04	mgd
Honokowai SGD	88,800	m^3/d	23.5	mgd
Honokowai Spec SGD	7.53	$m^3/m/d$	3.20	mgd/mi
Water Balance Augmented with LWRF Injectate				
Parameter	Value	Units	Value	Units
LWRF Treated Wastewater Injection	13,200	m^3/d	3.50	mgd
Recharge + Injection	113,500	m^3/d	30.0	mgd
Non-saline SGD (Recharge + injection - pumpage)	102,000	m^3/d	27.0	mgd
SGD per Unit of Shoreline	8.65	$m^3/m/d$	3.68	mgd/mi
Radon Survey SGD Estimate				
Parameter	Value	Units	Value	Units
Rn Shoreline	7,250	m	4.50	mi
Sum Rn Discharge	54,000	m^3/d	14.3	mgd
Rn Spec Discharge	7.45	$m^3/m/d$	3.17	mgd/mi
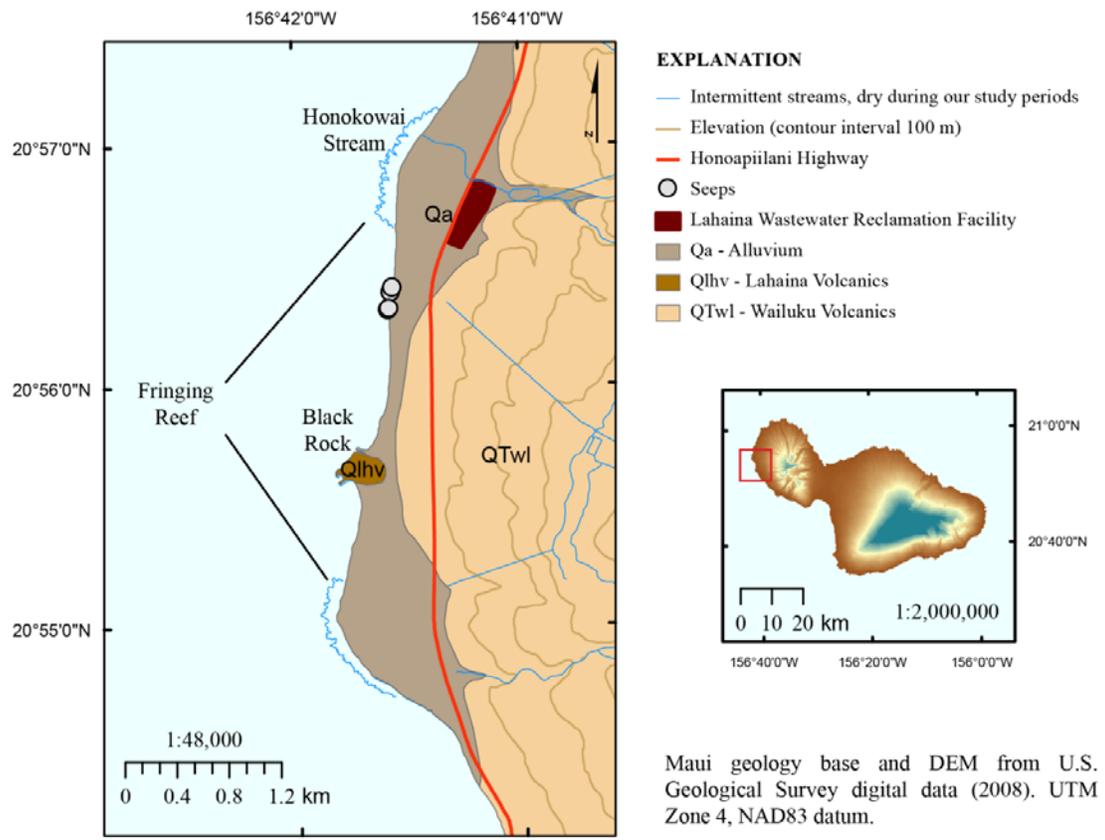
Figure 5-1: Geologic map of the Kaanapali coast with locations of the three focus submarine springs and the LWRF.

Figure 5-2: Photographs of the (a) time series zodiac and (b) piezometer with a hose connector installed in a submarine spring.

Two air-water exchangers on the time series platform are sampling radon from water sampled at the surface (near side with green hose) and from the piezometer directly (far side of zodiac and close-up photograph). Photos by Joseph Kennedy and Meghan Dailer, 2011.
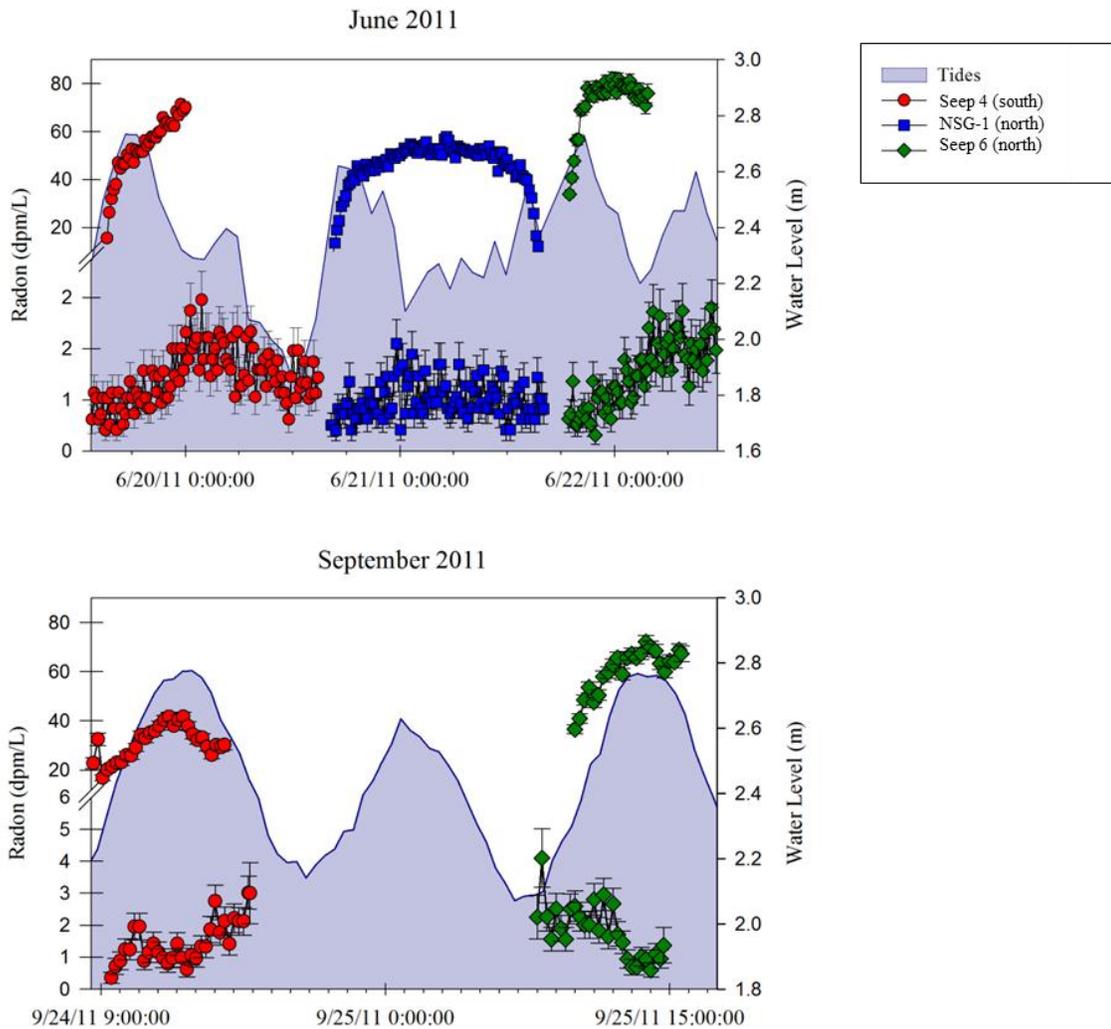
Figure 5-3: ^{222}Rn time series measurements in dpm/L for Seeps 4, NSG-a, and Seep 6, shown with water level.

Data are thirty-second measurements averaged over twenty-five minute intervals to smooth the large scatter due to swell) measured by Diver CTD, during the June and September, 2011 study periods. Error bars show the 1σ error of measured activity over five minute measurement periods.

YSI Temperature (°C)

26.2

24.0

Radon (dpm/L)

- 0.00 - 0.14
- 0.15 - 0.29
- 0.30 - 0.39
- 0.40 - 0.52
- 0.53 - 0.76
- 0.77 - 1.17
- 1.18 - 1.93

Lahaina Wastewater Reclamation Facility

Streams

☆ Seep 1

☆ Seep 2

☆ Seep 3
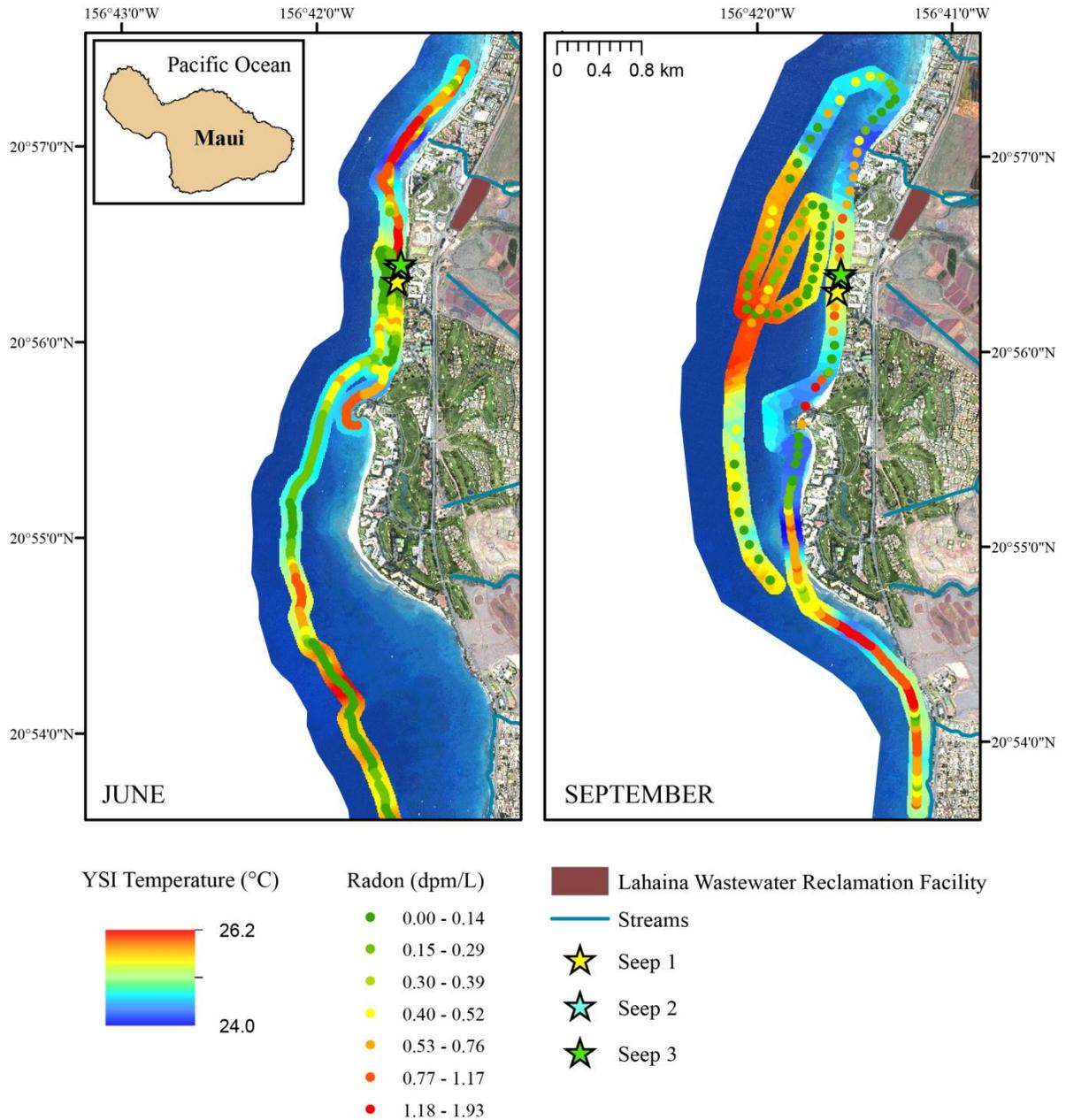
Maui mosaic from NOAA/NOS aerial photography collected from the Pacific Disaster Center, 2000.

Figure 5-4: Results of radon surveys conducted in June and September, 2011.
The maximum activity during both surveys was 1.9 dpm/L. In the absence of other sources of radon, areas of elevated radon indicate groundwater discharge or groundwater-fed stream discharge.
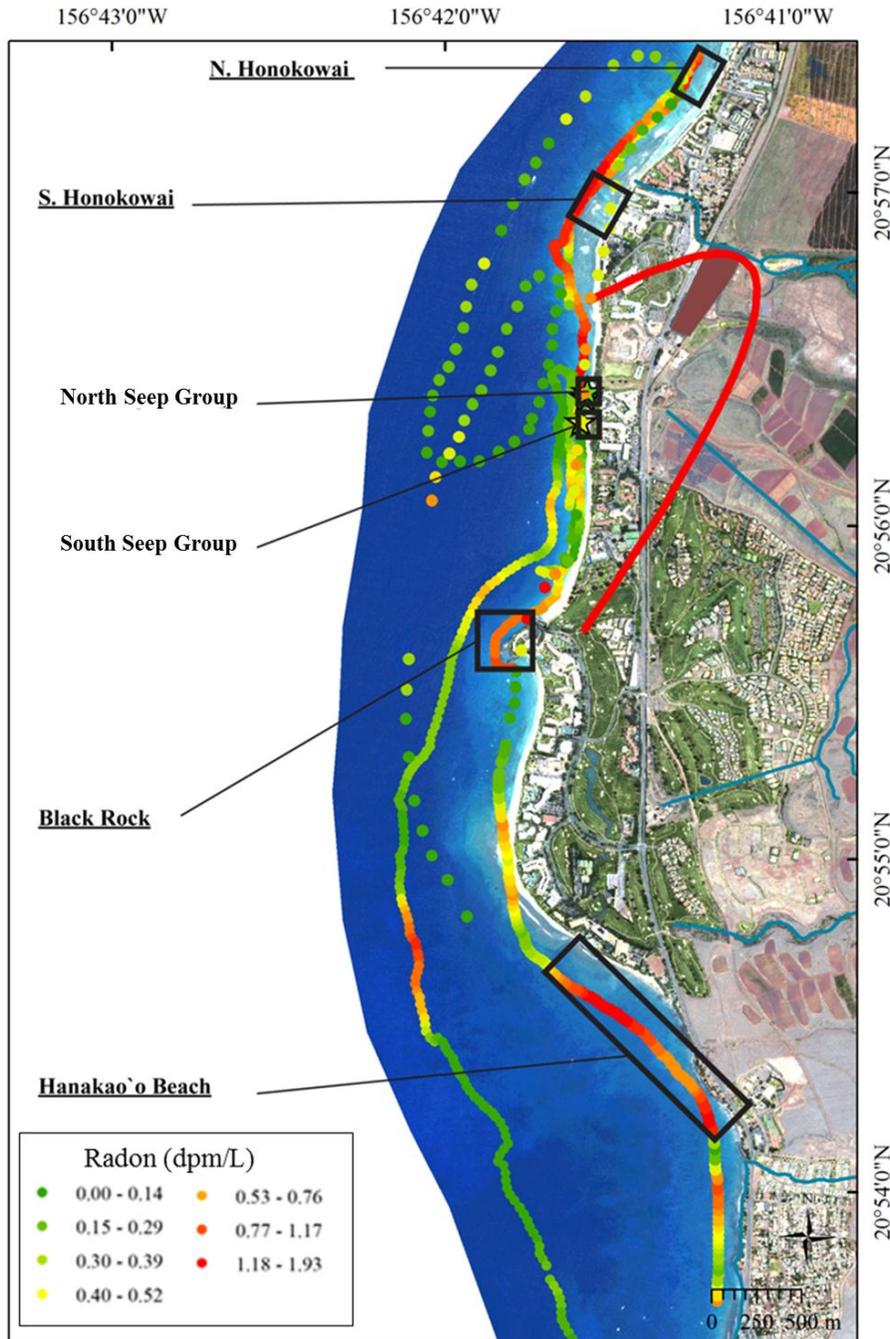
Figure 5-5: Radon activities measured during coastal surveys in June and September, 2011.

The radon color scale is same as for Figure 5-4. Sites with elevated surface radon activities are outlined with a black box. The lengths of the boxes are the approximate lengths of coastline that was within 100 dpm/m^3 of the mean radon concentration for each site and the widths are the distance of the radon survey from the coastline. The latter assumes that groundwater emanates at the coastline. Coastal groundwater fluxes were estimated from these areas.
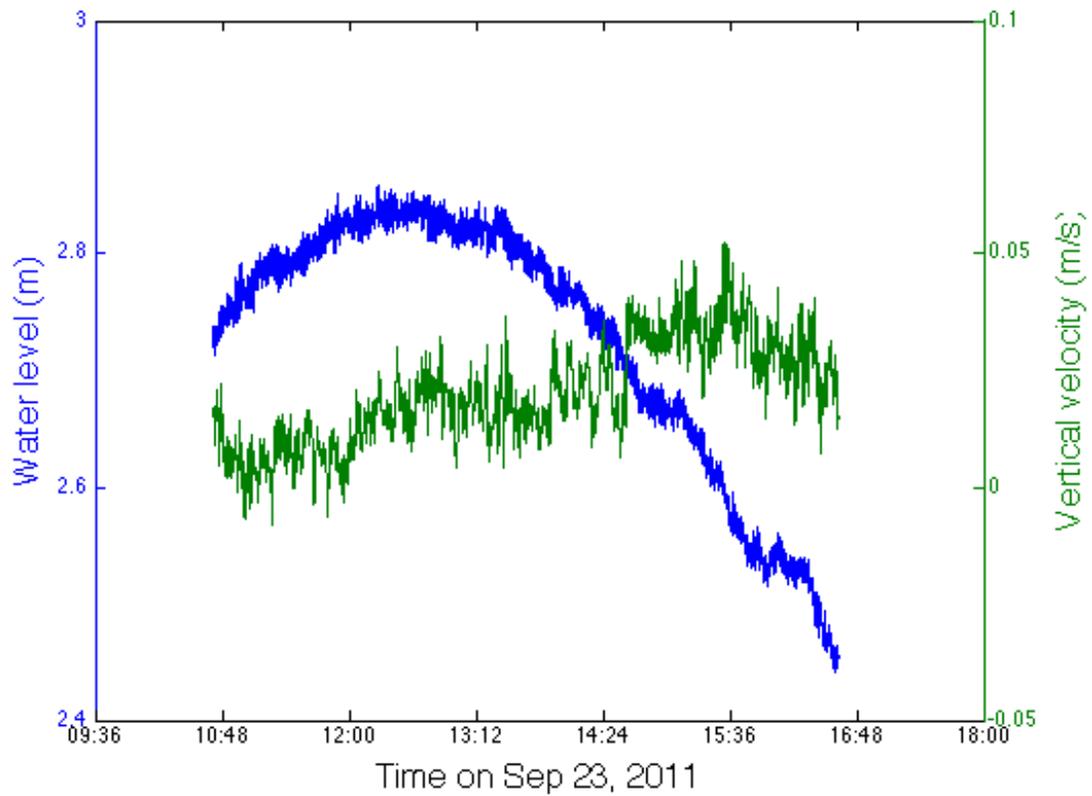
Figure 5-6: HR Aquadopp profiler record from Seep 4 showing water level and vertical water velocity, both recorded at 1 Hz.
The figure shows 1-minute running average of water level (blue) and of vertical water velocity (green).
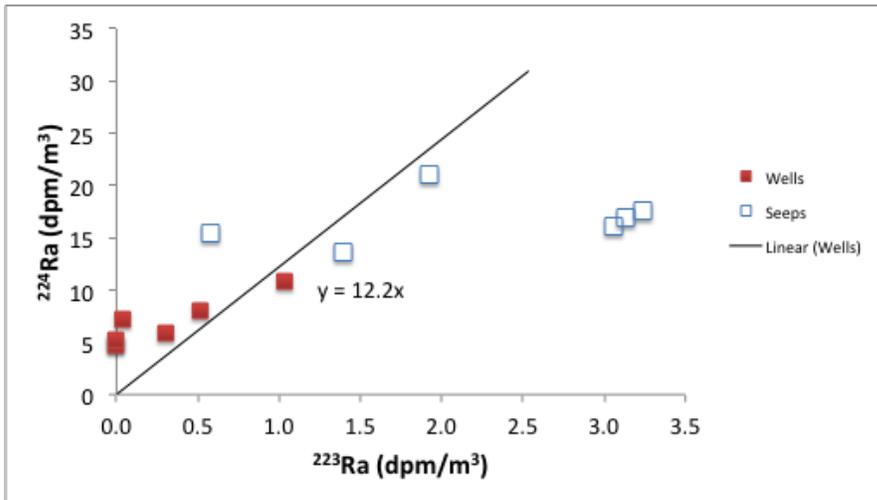
Figure 5-7: ^{224}Ra and ^{223}Ra in dpm/m^3 measured in groundwater wells and submarine springs.
The trendline is forced through the origin to reflect the same chemical behavior of the two isotopes.

SECTION 6: AQUEOUS GEOCHEMISTRY AND STABLE ISOTOPES

6.1 INTRODUCTION

The occurrence of large scale algal blooms in the Kaanapali area (Figure 6-1) during the late 1980s raised concerns regarding the impacts of land use practices on the coastal environment (Tetra Tech, 1993; Dollar and Andrews, 1997). These practices included intensively fertilized and irrigated sugarcane and pineapple agriculture, resort and golf course development, the domestic use of cesspools and septic tanks, and underground treated wastewater effluent injection at the Lahaina Wastewater Reclamation Facility (LWRF), which had been opened in 1975 and newly expanded in 1985. In the following years, several studies, including an inconclusive dye tracer injection test at the LWRF injection wells (Tetra Tech, 1994) were conducted to examine the extent of nutrient loading in the coastal ocean as well as the contribution of various land use practices to this loading. Tetra Tech (1993), Soicher (M.S. Thesis, 1996), and Soicher and Peterson (1997) used various modeling approaches combined with in-situ measurements to assess the contributions of various land use activities to coastal nutrient loading from both ground and surface waters. Dollar and Andrews (1997) and Laws (2004) examined the area's coastal water quality in terms of nutrient loading. Dollar and Andrews (1997) also used stable isotopic tracers in algal tissue to attempt to discern the presence of terrestrially derived N. More recently, Hunt and Rosa (2009), Dailer et al. (2010, 2012), and Swarzenski et al. (USGS report 2012) have used a wide array of approaches to ascertain pathways of nutrient delivery to coastal waters. These approaches include the analysis of wastewater indicator chemicals, nutrient species, and stable isotopes of water and dissolved NO_3^- (Hunt and Rosa, 2009), analysis of stable isotopes of N in algal tissue (Dailer et al., 2010, 2012), and analysis of trace metals, radon, nutrient species, and subsurface electrical resistivity (Swarzenski et al., USGS report 2012).

An understanding of the terrestrial origin and delivery mechanisms of dissolved species (and particularly bio-active nutrient species) to the ocean is vital to establishing a relationship between land-use practices and their impact on the coastal environment. Submarine groundwater discharge (SGD; see Section 5), which is typically enriched in nutrients relative to surface waters, can serve as the primary vehicle for the transport of land-derived nutrients to coastal waters even in areas with significant surface water discharge (Moore, 2006). On large tropical islands like Maui, which are characterized by high rainfall, high relief, and high permeability fractured rock aquifers, SGD comprises a much greater fraction of freshwater coastal discharge than on continents (Zektser, 2000). On the dry leeward sides of these islands, where surface water discharge is nearly non-existent, SGD may comprise nearly all of the land-derived freshwater flux to the coastal ocean (Johnson et al. 2008). Data from hydrogeological budgets and models (Shade, 1996; Engott and Vana, 2007; Gingerich and Engott, 2012) of the Kaanapali area, located on the dry leeward portion of the West Maui Volcano, indicate that SGD contributes

143

significantly more freshwater to the coastal ocean than the area's streams, which discharge to the ocean only intermittently in response to large rainfall events (Tetra Tech, 1993; Soicher and Peterson, 1997). As discussed in Section 5, SGD is the primary delivery mechanism of freshwater to the coastal ocean in the Kaanapali area.

The purpose of our approach has been to (1) determine the origins of nutrients in the area's groundwater, (2) evaluate the down-gradient geochemical evolution of the area's groundwater prior to its discharge to the ocean, and (3) identify the impact of land-derived nutrient fluxes on the geochemistry of coastal marine waters. Special emphasis was placed on determining the geochemical evolution and ultimate fate of the treated LWRF wastewater effluent after its injection (see Section 3), as this source has been identified by several studies (most recently Hunt and Rosa, 2009 and Dailer et al. 2010, 2012) as one of the largest potential contributors to coastal nutrient loading in this area. Field data was for this portion of the study was collected June 19-30, 2011 and September 19-25, 2011. In situ temperature, conductivity, salinity, and pH were collected in the field and Cl^- concentrations, nutrient concentrations, and the stable isotope ratios of H and O in water and N and O in dissolved NO_3^- were measured in the laboratory in order to characterize the geochemistry of the study area's groundwater, surface waters, treated wastewater, and coastal waters. Samples of gas emanating from the submarine springs and the distinctive black mineral coatings and impregnations found on rocks surrounding the submarine springs were also geochemically analyzed. Generally conservative tracers such as the isotopic ratios of H and O in water and Cl^- concentrations were used to evaluate mixing between potential end-members, while N loading was considered together with the isotopic ratios of N and O in dissolved NO_3^- to evaluate origin, evolution, and mixing of N species.

6.2 METHODS

6.2.1 Sample Collection Methods

Groundwater from production wells (PW) was collected using in situ pumps and sampling connections. Groundwater production well pumps were run for a minimum of ten minutes prior to sample collection to purge the well of stagnant water. The ten minute purge time resulted in purging volumes ranging from 21-43 times the calculated well volumes for all wells except for Hahakea 2, for which pump flow rate data was not available. Following well purging, sample collection connections were purged with running sample water for a minimum of two minutes prior to sample collection to ensure adequate flushing of the water delivery line. A reducing adapter with a Tygon tube attached was affixed to the installed sample connections to facilitate sampling.

Grab samples were collected from the Lahaina Deep Monitor Well (a monitor well (MW) with no in-situ pumping apparatus). This well was sampled by lowering bailer bags down the borehole to below the bottom of the solid casing that extended about eight meters below the water table. Once immersed, the bailer bags were opened by pulling up sharply on the retrieval line and filled with water. The bailer bags were then returned to the surface and the water was transferred directly to sample containers. This sampling

method precluded performing an adequate well purge. Submarine spring (SS) water was transferred to sample containers via a battery operated peristaltic pump from piezometers installed in the ocean floor. Each piezometer was attached to 20 to 30 meters of LDPE tubing with a quick-connect fitting. The tubing was purged for a minimum of two minutes prior to sampling to ensure adequate flushing of ocean water. The peristaltic pump flow rate ranged from 0.33 to 0.50 liters per minute. Table 6-1 lists the naming convention used for the geochemical sampling of the submarine springs. Treated wastewater (TW) at LWRF was transferred to sample containers via dipping cup from the effluent stream just prior to injection (see Section 3 for the LWRF plant diagram). R1 (irrigation quality) TW produced by LWRF was sampled directly from an on-site spigot using a reducing adapter with a Tygon tube attached. Accessible marine and terrestrial surface (MS and TS) waters were collected by directly filling sample containers with sample water while stationed on a small boat (for marine waters) or from the water's edge (for terrestrial waters). These samples were collected within 5 cm of the water's surface in all instances.

Temperature, specific conductivity, salinity, and pH were measured via YSI Multi-parameter sonde (600XLM, 6600V2-2, and 6600V2-4 models) using the sonde cap as a continuously overflowing flow-through cell for all PW samples, as well as, the R1 LWRF TW. These parameters were measured for the Lahaina Deep Monitor Well by transferring water collected via bailer bag to the sonde cap for measurement. Temperature, specific conductivity, salinity, and pH of submarine springs waters were measured in conjunction with the dye tracer field monitoring portion of this study (see Section 2). Temperature, specific conductivity, salinity, and pH of MS and TS waters and secondary LWRF TW were measured by immersing the sonde in the water body at the sample location immediately prior to collection.

Nutrient, Cl^-, and NO_3^- isotope samples were collected in acid-cleaned 500 mL HDPE bottles, transferred to a chilled cooler upon collection, and chilled in a refrigerator as soon as practical. PO_4^{3-}, SiO_4^{4-}, NO_3^-, NO_2^-, and NH_4^+ samples were sub-sampled from the collection bottles and filtered through 45 micron surfactant-free cellulose acetate filters into acid-cleaned 60 ml HDPE bottles the evening of collection. Total N (TN) and TP (TP) (150 ml) and NO_3^- isotope (60 ml) samples were sub-sampled unfiltered from the collection bottle. Dissolved NO_3^- isotope samples were subsequently frozen for transport and storage and thawed immediately prior to analysis. All other samples were kept in a chilled cooler or refrigerated during transport and storage, respectively. Discrete salinity samples were collected in acid-cleaned 250 mL HDPE bottles. Water isotope samples were collected with no headspace in 20 ml borosilicate glass vials crimp-sealed with butyl rubber septa.

Samples of gas escaping from the ocean bottom near the submarine springs were collected underwater by inverting open 20 ml borosilicate glass vials over the gas vents, allowing the emanating gas to displace the water in the vial, and finally crimp-sealing the vial with a butyl rubber septa. This sampling method resulted in approximately 4-8 mL of water included with the collected gas. Several coral rubble/rock samples displaying a

distinctive black coating were manually collected from near the submarine spring discharge points and packed in plastic wrap for transport and analysis.

6.2.2 Analytical Methods

All PO_4^{3-}, SiO_4^{4-}, NO_3^-, NO_2^-, and NH_4^+, TN, and TP samples were shipped chilled to the University of Washington School of Oceanography Technical Services (http://www.ocean.washington.edu/services/techservices.html) for analysis. TN and TP concentrations were measured using the methods described in Valderrama (1981). PO_4^{3-}, SiO_4^{4-}, NO_3^-, NO_2^-, and NH_4^+ concentrations were measured using procedures established by UNESCO (1994). Results for these parameters are reported in both micromoles per liter (μM) and in micrograms per liter (μg/L) in the data tables of this Section. When cited in this section's text, values are expressed in both units. Discrete salinity samples were also shipped to this laboratory for analysis, with results reported in dimensionless (UNSECO, 1985) Practical Salinity Units. Seven samples chosen at random were sent to the University of Washington analytical lab as blind duplicates for all nutrient analyses to ensure data quality and consistency. R-squared values for linear regressions performed on plots of the sample-blind duplicate paired results ranged from 0.966 to 0.999 with slopes ranging from 0.85 to 1.00 (Figures 6-4 to 6-10). Total N analyses were the least reproducible, with the lowest R-squared value (0.966) and the slope farthest from 1 (0.85). All other analyses had R-squared values of 0.990 or greater and slopes between 0.964 and 1.00. Reported minimum detection limits (Table 6-2) for all analyses were generally below values measured in this study. However, for several MS samples, reported NO_3^-, NO_2^- and NH_4^+ concentrations were close to and occasionally below detection limits.

Concentrations of the dissolved cation Cl^- were measured at the University of Hawaii Water Resources Research Center Lab using a Dionex DX-120 ion chromatograph. Results for these analyses are reported in milligrams per liter (mg/L). Cl^- check standards were run prior to and after sample analysis. Standard deviation (expressed as a percentage of the check standard accepted values) of the check standard runs (n = 2) was 0.97%.

We measured the isotope ratios of N and O in dissolved NO_3^- were measured by the University of Hawaii Stable Isotope Biogeochemistry Lab using the denitrifier method (Sigman et al., 2001) coupled with the sulfamic acid method of NO_2^- removal during sample preparation (Granger et al., 2006). Samples were analyzed on Thermo Finnigan MAT 252 and 253 Mass Spectrometers using a continuous flow GC-interface. All results are expressed in per mil (‰) notation relative to AIR (primary stable isotope standard for N) or VSMOW (primary stable isotope standard for O). Isotope ratios for N and O were calibrated using the internationally recognized IAEA-N3 NO_3^- standard assigned δ^{15}N of 4.7‰ versus AIR (Bohlke and Coplen, 1995) and a reported δ^{18}O values ranging from 22.7 to 25.6‰ versus VSMOW (Revesz et al., 1997; Bohlke et al, 2003), as well as, an internal lab standard. The IAEA-N3 δ^{18}O value of 22.7‰ versus VSMOW was used for the purposes of this study. All NO_3^- stable isotope samples were analyzed and corrected in batches of twenty runs (including samples, standards, and blanks). Each batch

included at least four standard runs (three runs of NIST-3 and at least one run of an internal lab standard) and two duplicate samples. The average standard deviation of standard and duplicate sample values for each batch were calculated and ranged from 0.23 to 2.26‰ for $\delta^{15}N$ and 0.19 to 4.30‰ for $\delta^{18}O$. Note that samples with the identical standard deviation values were run in the same batch.

Stable isotope ratios of H and O in water were measured by the University of Hawaii Stable Isotope Biogeochemistry Lab using a Picarro Cavity Ringdown Mass Spectrometer. All results are expressed in per mil (‰) notation relative to VSMOW, the internationally recognized stable isotopic benchmark for water. Isotope ratios were calibrated using internal lab standards. Water isotope samples collected in June, 2011 were analyzed coeval with and corrected using four internal lab standards run four times each. The average standard deviation for internal lab standards run with the June, 2011 samples was 0.04‰ for $\delta^{18}O$ and 0.62‰ for δD. Water isotope samples collected in September, 2011 were analyzed coeval with and corrected using the same four internal lab standards, this time with three of the standards run three times each and the remaining standard run twice. The average standard deviation for internal lab standards run with the September, 2011 samples was 0.06‰ for $\delta^{18}O$ and 0.52‰ for δD.

Gas samples were shipped to Isotech Laboratories (http://www.isotechlabs.com) for compositional analysis of $O_2 + Ar$, CO_2, and N_2 via gas chromatography. Rock samples were analyzed for molecular surficial composition at selected points using a JEOL Hyperprobe JXA-8500F ion microprobe at the University of Hawaii SOEST Ion Microprobe facility.

6.3 RESULTS

6.3.1 Sample Locations and Nomenclature

Samples were collected during the periods of June 19-30 and September 19-25, 2011. Sample names, types, times, and locations are listed in Tables 6-3 (June) and 6-4 (September). Individual samples will be referred to in the text by their collection month and sample name (i.e. June sample Kaanapali P-1). In this Section, groups of samples are generally referred to by sample type (i.e. PW). Figures 6-2 (June, 2011) and 6-3 (September, 2011) show sample locations differentiated by sample type. A summary of the water quality and stable isotope results are provided in Table ES-1 through ES-3 and ES-4 through ES-6,

6.3.2 Temperature, Specific Conductivity, Salinity, Cl⁻, and pH

Temperature results (Tables 6-5 and 6-6; Figures E-3 and E-17) indicate distinctions between MW and PW samples (19.13-22.66°C), MS samples (25.08-26.69°C), and the LWRF treated wastewater effluent samples (30.80°C and 29.33°C in June and September, 2011 respectively). It is important to note that the MS and TS samples as well as the June and September, 2011 LWRF treated wastewater effluent samples were

directly exposed to daytime sunlight and consequently may be affected by diurnal temperature variations. PW samples may also be slightly affected by solar heating of the above-ground piping and sampling connections during the day. Temperatures for the submarine spring samples were not measured directly in this portion of the study but were measured during the field monitoring and are reported in Section 2.

Specific conductivity and salinity values (Tables 6-5 and 6-6; Figures E-5 and E-19) show a consistent and coherent positive relationship. This is necessarily the case for the field salinity values, which were calculated from specific conductivity values by the YSI instrument using a standard algorithm. The lab salinity values, which were determined independently of the YSI-determined specific conductivity values, closely match the field salinity values. Salinity results indicate distinctions between monitor well (MW) and production well (PW) samples (0.21 - 0.81), LWRF treated wastewater effluent (TW) samples (1.09 - 1.10), and marine surface water (MS) samples (33.64 - 34.66). Salinities measured in terrestrial (TS) samples in the Black Rock lagoon (June samples Kaanapali 1 and 2; September samples Black Rock 1 and 2) ranged from 1.22 near its landward extent to 23.12 near its mouth. Salinities measured for the submarine spring samples ranged from 7.46 - 14.72 in June, 2011 and 2.92 - 4.80 in September, 2011. All salinities reported for the submarine spring samples represent lab determined values, as physical difficulties in accessing the discharge points combined with rapid mixing of the water column in this area (discussed in Section 4) prevented accurate in situ measurement of these parameters via YSI probe. Additional submarine spring salinity values were measured during the field monitoring portion of this study and are reported in Section 2.

The Cl^- concentrations measured for selected samples to support end member mixing calculations were generally consistent with salinity results. pH values (Tables 6-5 and 6-6; Figures E-7 and E-21) ranged from 7.85-8.07 in the MW and PW samples, 8.03 - 8.16 in the MS samples, and 6.45 and 7.13, respectively, in the June and September LWRF treated wastewater effluent samples. pH values for the submarine spring samples were not measured directly in this portion of the study but were measured during the field monitoring portion of this study and are reported in Section 2.

6.3.3 Nutrients

6.3.3.1 TP and PO_4^{3-}

TP concentrations across the study area ranged from 0.36 to 15.10 μM (11.1 to 467.6 μg/L as P) (Tables 6-7 (6-8) and 6-9 (6-10); Figures E-1 and E-15). MS samples had values ranging from 0.36 to 1.09 μM (11.1 to 33.8 μg/L as P). MW and PW samples had a relatively wide range of values from 1.93 to 9.96 μM (59.8 to 308.5 μg/L as P) . TP concentrations in the LWRF treated wastewater effluent samples ranged from 5.29 μM to 6.66 μM (16 to 206.3 μg/L as P). TP of TS samples collected in the Black Rock lagoon (June samples Kaanapali 1 and 2; September samples Black Rock 1 and 2) ranged from 3.98 to 8.42 μM (123.3 to 260.8 μg/L as P). The submarine spring samples had higher TP concentrations than any other samples collected in the study area, ranging from 11.3 to 15.1 μM (350.0 to 467.6 μg/L as P).

148

PO_4^{3-} concentrations (Tables 6-7 (6-8) and 6-9 (6-10), Figures E-6 and E-20) display trends consistent with to TP concentrations across the study area. MS samples generally had the lowest values measured in the study area, ranging from 0.08 to 0.84 μM (2.5 to 26.0 $\mu g/L$ as P), while the monitor and production well samples displayed a range of values from 1.54 to 8.19 μM (47.7 to 253.6 $\mu g/L$ as P). PO_4^{3-} concentrations in the LWRF treated wastewater effluent samples ranged from 2.27 to 3.43 μM (70.2 to 106.2 $\mu g/L$ as P). TS samples collected in the Black Rock lagoon (June samples Kaanapali 1 and 2; September samples Black Rock 1 and 2) had PO_4^{3-} concentrations that ranged from 1.98 to 5.13 μM (61.3 to 158.9 $\mu g/L$ as P). As was the case with TP, the submarine spring samples had higher PO_4^{3-} concentrations than any other samples collected in the study area, ranging from 9.00 to 13.39 μM (27 to 41 $\mu g/L$ as P).

6.3.3.2 SiO_4^{4-}

SiO_4^{4-} concentrations across the study area covered a wide range from 3.49 to 914.17 μM (98.0 to 25679.0 $\mu g/L$ as Si) (Tables 6-7 (6-8) and 6-9 (6-10); Figures E-4 and E-18). SiO_4^{4-} concentrations of the MW and PW samples ranged from 576.94 to 846.99 μM (16206.2 to 23791.9 $\mu g/L$ as Si) and were consistently over an order of magnitude greater than the marine surface water sample SiO_4^{4-} concentrations, which ranged from 3.49 to 44.47 μM (98.0 to 1249 $\mu g/L$ as Si) (Tables 6-7 (6-8) and 6-9 (6-10)). SiO_4^{4-} concentrations of the LWRF treated wastewater effluent samples ranged from 586.06 to 613.42 μM (16462.4 to 17231.0 $\mu g/L$ as Si). Submarine spring SiO_4^{4-} concentrations ranged from 426.64 to 753.26 μM (11984.3 to 21159.1 $\mu g/L$ as Si). June TS samples Kaanapali 1 and 2, collected near the head of Black Rock lagoon, had the highest SiO_4^{4-} concentrations measured in the study area, with values of 914.17 μM (25679.0 $\mu g/L$ as Si) and 902.45 μM (25350 $\mu g/L$ as Si) respectively.

6.3.3.3 TN, NO_3^-, NO_2^-, and NH_4^+

TN concentrations across the study area ranged from 4.59 to 517.10 μM (64.3 to 7291.1 $\mu g/L$ as N) (Tables 6-7 (6-8) and 6-9 (6-10); Figures E-2 and E-16). MS samples generally had the lowest range of concentrations (4.59 to 21.84 μM (64.3 to 306.0 $\mu g/L$ as N)), while the LWRF treated wastewater effluent samples had the highest range of concentrations (432.63 μM to 517.10 μM (6061.1 to 7291.1 $\mu g/L$ as N)). The TN concentrations of MW and PW samples ranged widely, from 19.75 to 196.92 μM (276.7 to 2758.8 $\mu g/L$ as N), but generally showed little temporal variation between samples collected from the same wells in June and September, 2011. Submarine spring TN concentrations also varied widely, from 23.28 to 115.9 μM (326.2 to 1623.8 $\mu g/L$ as N), while also displaying considerable temporal variation between the June and September, 2011 samples. The September, 2011 submarine spring samples TN concentrations equaled or exceeded 112.24 μM (1572.5 $\mu g/L$ as N) while all of the June, 2011 submarine spring samples Total N concentrations were less than or equal to 46.46 μM (650.9 $\mu g/L$ as N). TS samples from Black Rock lagoon (June samples Kaanapali 1 and 2; September samples Black Rock 1 and 2) had TN concentrations ranging from 153.20 to 339.40 μM (2146.3 to 4755.0 $\mu g/L$ as N).

NO_3^- was the prevalent species of inorganic N found in the study area, with the majority of samples having NO_3^- concentrations greater than combined NO_2^- and NH_4^+ concentrations (Tables 6-7 (6-8) and 6-9 (6-10); Figures E-10 and E-24). MS samples had consistently low (often near and sometimes below the detection limit) levels of NO_3^-, ranging from 0.00 to 10.42 μM (0.0 to 146.0 μg/L as N), but typically near or below 1.00 μM (14.0 μg/L as N). As was the case with TN, the LWRF treated wastewater effluent samples generally had the highest range of NO_3^- concentrations (188.50 to 246.52 μM (2640.9 to 3453.7 μg/L as N)). September TS sample Kaanapali GC-R1 Pond, which contained R1 treated wastewater effluent piped directly from the LWRF, had an NO_3^- concentration of 302.57 μM (4239.0 μg/L as N), the highest measured in the study area. TS samples from Black Rock lagoon (June samples Kaanapali 1 and 2; September samples Black Rock 1 and 2) had a generally high but wide range of NO_3^- concentrations, from 77.28 μM (1082.7 μg/L as N) near the lagoon's mouth to 246.05 μM (3447.2 μg/L as N) near the lagoon's head. MW and PW sample NO_3^- concentrations ranged widely from 11.41 to 177.48 μM (159.9 to 2486.5 μg/L as N). NO_3^- concentrations of submarine spring samples were generally lower than MW, PW, TS, and LWRF treated wastewater effluent concentrations but higher than the MS concentrations, ranging from 6.86 to 26.15 μM (96.1 to 366.4 μg/L as N).

NO_2^- and NH_4^+ were measured in low concentrations (often near detection limits) across most of the study area (Tables 6-7 (6-8) and 6-9 (6-10); Figures E-9, E-14, E-23 and E-28). NO_2^- was found only in trace quantities in MW, PW, and MS samples. The maximum concentration observed in these samples was 0.44 μM (6.2 μg/L as N), with most concentrations less than 0.10 μM (1.4 μg/L as N). The samples with significant concentrations of NO_2^- were the LWRF treated wastewater effluent samples, with concentrations ranging from 30.18 to 37.81 μM (422.8 to 529.7 μg/L as N); the September Kaanapali GC-R1 sample, with a concentration of 16.92 μM (237.0 μg/L as N); the submarine spring samples, with concentrations ranging from 0.70 to 2.20 μM (9.8 to 30.8 μg/L as N); and the TS samples collected in Black Rock lagoon (June samples Kaanapali 1 and 2; September samples Black Rock 1 and 2), with concentrations ranging from 0.43 to 0.68 μM (6.0 to 9.5 μg/L as N). NH_4^+ concentrations displayed a similar distribution to NO_2^- concentrations in samples across the study area, although NH_4^+ occurred in slightly greater concentrations in the MW and PW samples (up to 1.19 μM (16.7 μg/L as N)) than in the MS samples (up to 0.71 μM (9.9 μg/L as N), with most samples near or below detection limits). Like NO_2^-, NH_4^+ was generally found in higher concentrations in the LWRF treated wastewater effluent samples and the September TS sample Kaanapali GC-R1 Pond, with concentrations ranging from 7.35 to 93.26 μM (103.0 to 1306.6 μg/L as N), and the TS samples collected in Black Rock lagoon (June samples Kaanapali 1 and 2; September samples Black Rock 1 and 2), with concentrations ranging from 0.21 to 3.5 μM (2.9 to 49.0 μg/L as N). NH_4^+ concentrations measured for submarine spring samples were generally greater than the majority of the MS sample concentrations and ranged from 0.27 to 0.51 μM (3.8 to 7.1 μg/L as N).

6.3.4 Gas and Coral Rubble/Rock Crust Analyses

Analytical results of the two gas samples collected (Table 6-11) show a composition dominated by N_2 (914,200 to 984,400 ppm), with secondary amounts of O_2 + Ar (15,000 to 84,900 ppm). CO_2 was present in much lesser amounts (500 to 860 ppm). Surficial ion microprobe analyses of coral rubble/rock samples collected directly adjacent to the submarine springs (e.g. Figure 6-13) indicate that the black crust is primarily composed of spherical globules of MnO and perhaps other solid-phase MnO-hydrous species. Other compounds observed on the rock surfaces include biogenic SiO_2, NaCl, and possible $MgCl_2$.

6.3.5 Stable Isotopes

6.3.5.1 $\delta^{18}O$ and δ^2H of Water

$\delta^{18}O$ and δ^2H values measured across the study area ranged from 0.47 to -3.80‰ and 2.82 to -15.70‰, respectively (Tables 6-12 and 6-13; Figures E-11, E-13, E-25, and E-27). No LWRF treated wastewater effluent or MS samples were analyzed from the June, 2011 sampling trip. With the exception of the submarine spring samples, samples of the same type (especially MW and PW, MS, and TW samples) typically displayed similar, tightly grouped values. MW and PW sample $\delta^{18}O$ and δ^2H values ranged from -3.39 to -3.80‰ and -13.85 to -15.70‰, respectively. MS sample $\delta^{18}O$ and δ^2H values ranged from 0.37‰ to 0.47‰ and 2.24‰ to 2.82‰, respectively. $\delta^{18}O$ and δ^2H values measured for the LWRF treated wastewater effluent samples and the September TS sample Kaanapali GC-R1 Pond ranged from-3.06 to -3.12‰ and -11.34 to -11.39‰, respectively. $\delta^{18}O$ and δ^2H values of the submarine spring samples were more variable than those of other sample types, and ranged from to -1.52 to -3.21‰ and -5.19 to -11.44‰, respectively.

6.3.5.2 $\delta^{15}N$ and $\delta^{15}O$ of Dissolved NO_3^-

Dissolved NO_3^- $\delta^{15}N$ and $\delta^{18}O$ values ranged from 0.65 to 93.14‰ and -3.50 to 24.46‰, respectively, across the study area (Tables 6-12 and 6-13); Figures E-12 and E-26). MW and PW sample NO_3^- $\delta^{15}N$ and $\delta^{18}O$ values fell within a tight range from 0.65 to 4.19‰ and -3.50 to 4.30‰, respectively. The LWRF treated wastewater effluent sample NO_3^- $\delta^{15}N$ and $\delta^{18}O$ values were 29.25‰ and 19.82‰, respectively, in June, and 30.85‰ and 15.92‰, respectively, in September. The September LWRF treated wastewater effluent sample LWRF-R1 ($\delta^{15}N$ = 31.5‰, $\delta^{18}O$ = 15.4‰) and September TS sample Kaanapali GC-R1 ($\delta^{15}N$ = 31.5‰, $\delta^{18}O$ = 11.7‰) had NO_3^- $\delta^{15}N$ and $\delta^{18}O$ values similar to those of the June and September LWRF treated wastewater effluent samples. TS samples from Black Rock lagoon (June samples Kaanapali 1 and 2; September samples Black Rock 1 and 2) had NO_3^- $\delta^{15}N$ and $\delta^{18}O$ values ranging from 8.84 to 14.99‰ and -1.82 to 2.84‰, respectively. Submarine spring sample NO_3^- $\delta^{15}N$ and $\delta^{18}O$ values were the highest measured in the study area, ranging from 77.82 to 93.14‰ and 21.56 to 24.46‰, respectively. MS samples showed a wide range of NO_3^- $\delta^{15}N$ and $\delta^{18}O$ values from 11.86 to 57.73‰ and 1.76 to 21.55‰, respectively.

6.4 DISCUSSION

6.4.1 Temperature, Salinity, and pH

6.4.1.1 Temperature

MW and PW sample temperatures (19.13 - 22.66°C) in the study area were consistent with those measured by Thomas (1986) and Soicher (M.S. Thesis, 1996). Though the West Maui region has been assessed as having geothermal potential based on geochemical anomalies and elevated groundwater temperatures in certain areas (Cox and Thomas, 1979; Thomas, 1986), no abnormally elevated groundwater temperatures were measured at any of the wells sampled in this study.

The temperatures of TS samples were in all cases obtained from relatively small, shallow water bodies with direct sun exposure, and were consequently influenced by solar heating. This effect is especially apparent for the June sample Kaanapali GC-2 (32.37 °C), which was sampled from a shallow concrete culvert under the influence of direct afternoon sunlight.

As with the TS water samples, the June and September LWRF treated wastewater effluent samples (30.90 and 29.33 °C, respectively) and the September LWRF-R1 sample (29.64 °C) were undoubtedly warmed by solar radiation during treatment and while passing through open basins prior to injection. As the LWRF wastewater treatment process includes biological nutrient removal (Scott Rollins, County of Maui Wastewater Reclamation Division, personal communication, 2012) exothermic biodegradation of organic compounds (Hellström, 1997, 1999; Gallert and Winter, 2005) may also play an undetermined role in the elevated temperatures found in the June and September LWRF treated wastewater effluent samples and the September LWRF-R1 sample.

MS sample temperatures (25.08-26.69°C) were typical for the area as measured in several previous studies (Tetra Tech, 1994; Dollar and Andrews, 1997; Laws, 2004; Storlazzi et al., 2006). Thermal Infrared Imagery (TIR) collected during nighttime field assessments in May, 2011 (see Section 4) shows a large region of slightly elevated ocean surface temperatures offshore from the submarine springs sampled in this study. This anomaly was not readily discerned in our MS sample temperatures, however, because the MS samples were collected during the day when solar heating was a factor.

Submarine spring sample temperatures were not measured as part of this portion of this study. However, submarine spring discharge temperatures were measured as part of the field monitoring portion of this study (see Section 2). These results show that submarine spring discharge temperature is generally significantly elevated from ambient ocean water, with average monitoring point temperatures reported in Section 2 ranging from 27.4 to 30.1 °C. The presence of similarly elevated temperatures in both the submarine spring samples and LWRF treated wastewater effluent samples provides additional support for a hydrological connection between the LWRF injection wells and the submarine spring discharge confirmed by the dye tracer results (see Section 3).

Continued exothermic biodegradation of organic compounds in the injected LWRF treated wastewater effluent and geothermal heating (see Section 4) are possible mechanisms that could account for the apparent conservation of temperature between the LWRF treated wastewater effluent prior to injection and the submarine spring discharge.

6.4.1.2 Salinity

Salinities for the groundwater monitoring well (MW) and production wells (PW) samples (0.21 - 0.81) in this study were uniformly fresh, with little significant variation throughout the study area. These results are consistent with previous measurements of groundwater salinity in this area by Soicher (M.S. Thesis, 1996).

The widely varying salinities of terrestrial surface water (TS) samples (0.40 – 23.12) appear to be a function of their location and derivation. The salinities of the Black Rock lagoon TS samples (June samples Kaanapali 1 and 2 and September samples Black Rock 1 and 2) were controlled by their distance from the lagoon's ocean connection and decreased from 23.12 near the mouth of the lagoon to 1.22 near the furthest inland extent of the lagoon. The elevated salinities of June TS samples Kahana Stream and Kaanapali GC-1 appear to be primarily a result of evaporative salt enrichment in the relatively stagnant water bodies these samples were collected from, though some saline groundwater influence may be present as well, given the close proximity of these sampling locations to the ocean. The June sample Kaanapali GC-2 consisted of runoff from ongoing golf course irrigation (which itself consists of both municipal supply and LWRF-R1 effluent) and consequently had a low salinity of 0.40.

Salinities measured for LWRF treated wastewater effluent (TW) samples and September TS sample Kaanapali GC-R1 Pond ranged from 1.09 to 1.13 and were similar to the LWRF's treated wastewater effluent salinity of 1.03 reported by Hunt and Rosa (2009). The Kaanapali area's municipal water supply, which is the ultimate source of the bulk of the wastewater received and treated by the LWRF, is derived from roughly 44% groundwater extracted from upland groundwater production wells (PWs) (including several of the wells sampled in this study) and 56% surface water diverted from perennial streams to the north of the study area (Edna Manzano, Maui County Department of Water Supply, personal communication, May 8, 2012). The salinities of the PWs sampled in this study ranged from 0.23 to 0.64 and the salinities of stream water in and near the study area reported by Soicher (M.S. Thesis, 1996) ranged from 0.10 to 0.25. The enrichment in salinity of the TW samples relative to these original sources in likely due to a variety of factors including the concentration of salts in excreta, introduction of salts through normal municipal water use, and evaporative enrichment of wastewater salt content both prior to and during treatment.

Marine surface water (MS) sample salinity measurements had an arithmetic mean of 34.43 and were similar to those measured in several previous studies (Tetra Tech, 1994; Dollar and Andrews, 1997; Laws, 2004; Storlazzi et al., 2006, Hunt and Rosa, 2009). Samples collected well offshore, such as September samples Maui 31 (34.58), 32 (34.58), and 34 (34.56), generally had higher salinities. Samples collected proximal to coastal

fresh submarine groundwater discharge (SGD) points such as the submarine springs and Black Rock lagoon tended to have lower salinities. For example, the September samples Seep 1-2 Surface and Seep 3-2 Surface, which were collected at the ocean's surface directly above submarine springs, had salinities of 33.97 and 34.34 respectively, and the September sample Maui 23, which was collected near the mouth of Black Rock lagoon, had a salinity of 34.14. Samples taken just offshore from Wahikuli Wayside Park, such as September sample Maui 19 (34.25), and Honokowai Beach Park, such as September samples Maui 27 (34.28) and 28 (34.26), also had generally lower salinities, suggesting the influence of fresh SGD in these areas as well. See Section 5 for a quantitative discussion of SGD in the study area.

Submarine spring (SS) salinities measured in this portion of the study (2.92 to 14.72) displayed significant variability between samples but were consistently much lower than values (26.0 to 29.7) reported by Hunt and Rosa (2009). This discrepancy is probably a result of sampling technique, as the piezometers used in this study were better able to limit the inclusion of surrounding ocean water than the inverted funnels used by Hunt and Rosa (2009). The SS salinity values obtained in this study are similar to those obtained by Swarzenski et al. (USGS report 2012), who also used piezometers to obtain their samples. The variability in SS salinity appears to be a function of both piezometer installation and wave action. The higher SS salinities measured in June (7.46 - 14.72) corresponded with a large summer south swell event that was energetic enough to disturb the installation of some of the piezometers. The lower SS salinities measured in September (2.92 - 4.80) corresponded with calm ocean conditions. SS salinities measured daily during the field monitoring portion of this study (see Section 2) confirm the temporal variability of SS salinities in response to tide, wave action, and piezometer installation.

6.4.1.3 pH

MW and PW sample pH values (7.85 to 8.07) were slightly basic, fell within a narrow range and were consistent with those observed in Thomas (1986) for the study area. TS sample pH values, while also tending to be slightly basic, were more variable (7.30 to 8.34), with higher pH values measured in samples with more potential oceanic influence (e.g. June sample Kahana Stream, September sample Black Rock 2) and lower pH values measured in samples with more potential LWRF-R1 irrigation water content (e.g. June samples Kaanapali GC-1 and 2, and September sample Kaanapali GC-R1).

The LWRF treated wastewater effluent samples, though fairly variable, had slightly acidic to slightly basic pH values (6.45 to 7.13) which were generally the lowest of those measured in the study area. This is most likely a result of their high organic matter content promoting the formation of organic acids during the biological degradation process.

Though submarine spring pH values were not measured directly in this portion of the study, average pH values ranging from 7.35 to 7.69 were measured for these locations during the field monitoring portion of this study (see Section 2). These values are

significantly lower than those of upland groundwater and MS samples, suggesting that the submarine spring discharge may contain a significant portion of the injected LWRF treated wastewater effluent, the only known potential contributor of lower pH groundwater in the area.

MS sample pH values fell within a narrow range (8.03 - 8.16) consistent with pH values typically found in bulk ocean water near Hawaii (Fujieki et al., 2011). The pH values obtained for MS samples in this study tended to be higher than those obtained during a shoreline wading survey by Hunt and Rosa (2009) (7.62 - 7.96). This discrepancy is probably due to differences in sample location (though temporal variation may also play a role). MS sample locations in this study ranged from few meters to over one kilometer offshore rather than along the water's edge as in Hunt and Rosa (2009).

6.4.2 $\delta^{18}O$ and δ^2H of Water

6.4.2.1 Background

The relationship between $\delta^{18}O$ and δ^2H values of precipitation around the globe fall along a linear trend ($\delta^2H = 8\ \delta^{18}O+10$) termed the Global Meteoric Water Line (GMWL) (Craig, 1961). The slope of this line is controlled mainly by a temperature-sensitive equilibrium isotope fractionation associated with liquid-vapor phase transitions, whereas the non-zero intercept indicates a small influence by a kinetic isotope effect associated with evaporation into unsaturated air (Craig and Gordon, 1965). Deviations from the GMWL in precipitation are generally indicative of local rather than global meteorological processes. These local variations will produce a Local Meteoric Water Line (LMWL) for any given region, which typically does not deviate greatly from the overall GMWL except in unique environments. A LMWL has never been determined for the West Maui Volcano, but a LMWL for precipitation on the East Maui Volcano ($\delta^2H = 8.2\ \delta^{18}O+14.7$) has been reported by Scholl et al. (2002). Although Scholl et al. (2002) did not collect precipitation on the West Maui Volcano, due to its proximal location in a region of similar climate, their East Maui Volcano LMWL likely provides a better approximation of precipitation in our study area than the GMWL. Since precipitation is the ultimate source of the waters of terrestrial origin sampled in this study, comparison of sample $\delta^{18}O$ and δ^2H values with respect to the best available LMWL, as well as to each other, is a good means to characterize terrestrial water source and evolution.

6.4.2.2 Distribution and Trends

$\delta^{18}O$ and δ^2H results for MW and PW samples form a close grouping of values with arithmetic means of -3.62 and -14.66‰, respectively, and standard deviations of 0.13 and 0.57‰, respectively (n = 16). These values (Figure 6-14) plot closely around the East Maui Volcano LMWL of Scholl et al. (2002). There is also a tendency for the groundwater $\delta^{18}O$ and δ^2H values to decrease from north to south across the study area. This trend can be attributed to both rainout (as the predominant northeasterly trade winds drive the overall flow of moisture from north to south in this region) and amount effect (which results in larger rain events, such as Kona storms, which generally comprise a

greater fraction of precipitation in leeward vs. windward portions of the Hawaiian islands, producing precipitation with lower $\delta^{18}O$ and δ^2H values). See Dansgaard (1964) for a detailed discussion of the physical mechanisms of rainout and the amount effect. The overall homogeneity of upland well $\delta^{18}O$ and δ^2H values across the study area is not unexpected, however, as the area's basal aquifer is recharged primarily from a relatively small area on the higher elevations of the West Maui Volcano where the majority of rainfall occurs (Engott and Vana, 2007). Due to the relative lack of further inputs from precipitation (and from modern agricultural irrigation, which was a significant source of recharge in the past, but has effectively ceased with the demise of sugarcane cultivation in 1999 and pineapple cultivation in 2009) the fresh portion basal aquifer in this area can be assumed to maintain relatively uniform $\delta^{18}O$ and δ^2H values as it flows down-gradient to the ocean.

$\delta^{18}O$ and δ^2H values measured for the September LWRF treated wastewater effluent, LWRF-R1, and Kaanapali GC-R1 samples cluster together tightly with arithmetic mean values of -3.09 and -11.37‰, respectively, and standard deviations of 0.03 and 0.03‰, respectively (n = 3). The single LWRF treated wastewater effluent sample measured Hunt and Rosa (2009) had $\delta^{18}O$ and δ^2H values of -3.21 and -10.90‰, respectively, which, though similar to the values measured in this study, suggests that $\delta^{18}O$ and δ^2H values of LWRF treated wastewater effluent can vary temporally. The LWRF treated wastewater effluent samples are enriched in ^{18}O and ^2H relative to the MW and PW samples. Several possible mechanisms can explain this isotopic enrichment. As discussed above, fresh surface waters diverted from perennial streams to the north of the study area, which would likely be enriched in ^{18}O and ^2H relative to the area's groundwater via partial evaporation, form roughly 56% of the municipal water supply for this area (Edna Manzano, Maui County Department of Water Supply, personal communication, 2012). Partial evaporation during normal municipal and domestic water use could also introduce further evaporative enrichment. The September LWRF treated wastewater effluent, LWRF-R1, and Kaanapali GC-R1 samples all plot slightly below and to the right of the LMWL of Scholl, et al. (2002) (Figure 6-14) an effect consistent with partial evaporation of original precipitation. Finally, organic-rich waters (such as wastewater) may experience a slight enrichment in ^2H via H exchange with organic molecules, which typically have much higher δ^2H values than natural waters (Kendall and Aravena, 2000).

With arithmetic means of 0.42‰ and 2.51‰, and standard deviations of 0.04 and 0.27‰, respectively (n =4), the $\delta^{18}O$ and δ^2H compositions of marine surface (MS) samples form a third set of tightly clustered data that show significant enrichment in ^{18}O and ^2H relative to the MW, PW, and LWRF treated wastewater effluent samples. As would be expected, these values are quite similar to those of the world's ocean (close to 0‰ for both $\delta^{18}O$ and δ^2H). The slight enrichment of ^{18}O and ^2H in these MS samples relative to mean oceanic values is likely a function of the area's leeward location, where lower humidity and higher solar radiation relative to the open ocean would lead to higher evaporation rates, and, consequently, enrichment in ^{18}O and ^2H relative to mean oceanic values.

6.4.2.3 Mixing Analysis

δ^{18}O and δ^2H values measured for the submarine spring samples varied more widely than any other sample type, displaying arithmetic mean values of -2.66 and -9.46‰, respectively, and standard deviations of 0.65 and 2.50‰, respectively (n = 6). Submarine spring samples with higher salinities (such as June samples Seep 2 Piez-1Seep 2 Piez 1 (NSG) and Seep 4 Piez-1) show higher δ^{18}O, δ^2H, and [Cl⁻] values, reflecting a larger fraction of marine contribution. Due to lack of other potentially significant sources in the study area, the submarine spring samples can be assumed to consist of a mixture of upland groundwater, LWRF treated wastewater effluent, and marine waters. The generally conservative nature of ^{18}O and ^{2}H as subsurface tracers (Gat, 1996) combined with the consistent δ^{18}O and δ^2H values of the potential sources allows us to attempt to calculate the fractional contribution of each of these three sources to each submarine spring sample by employing an end-member mixing analysis using the following system of three equations with three unknowns:

$$f_1 + f_2 + f_3 = 1 \qquad \text{(Eq. 6-1)}$$

$$C_1^{18}f_1 + C_2^{18}f_2 + C_3^{18}f_3 = C_t^{18} \qquad \text{(Eq. 6-2)}$$

$$C_1^2 f_1 + C_2^2 f_2 + C_3^2 f_3 = C_t^2 \qquad \text{(Eq. 6-3)}$$

where f represents the fraction of each of the three components (the unknown values), C^{18} represents δ^{18}O and C^2 represents δ^2H. The subscripts 1, 2, and 3 represent the three end-members while the subscript t (for tracer) represents the submarine spring sample under consideration. The arithmetic means of the end-member values were used in the calculations and are listed in Table 6-14. Additional information on the end-member mixing analysis theory and application used here can be found in Christopherson and Hooper (1992), Hooper (2003), Liu et al (2004), and Liu and Koa (2007). In order to more robustly characterize the component fractions of the submarine spring samples, the typically conservative dissolved species Cl⁻ was further substituted for C^1 and C^2 in separate calculations, the results of which are also shown in Table 6-14.

Both September submarine spring samples fit within the three component mixing models (i.e. the data points fell inside of the mixing triangles) shown in Figures 6-14, 6-15, and 6-16 for all three end-member characterizations (δ^{18}O/δ^2H, δ^{18}O/Cl⁻, and δ^2H/Cl⁻). The June submarine spring samples, however, did not all fit the three component mixing models. June sample Seep 1 Piez-1 did not fall within the mixing triangle for the δ^{18}O/δ^2H characterization. June sample Seep 2 Piez-1 fell within the mixing triangle for the δ^{18}O/ δ^2H characterization but not the δ^{18}O/Cl⁻ or δ^2H/Cl⁻ characterizations. June samples Seep 3 Piez-1 and Seep 4 Piez-1 Seep 3 did not fall within the mixing triangles for any of the characterizations. Figures 6-14, 6-15, and 6-16 provide spatial representations of the relationships between the outlying data points and the mixing triangles. We believe that these data points fall outside the three mixing triangles for two reasons: First, the δ^{18}O and δ^2H values of the LWRF treated wastewater effluent end member, approximated in these calculations by the arithmetic mean of LWRF treated wastewater effluent sample values collected in September, 2011, may be temporally

variable. Since the results of the dye tracer portion of the study suggest a 7 to 8 month average travel time for the LWRF treated wastewater effluent from injection to coastal discharge (see Section 3), this temporal variability may result in a different "true" LWRF treated wastewater effluent end member composition for the submarine spring samples analyzed here. In this regard, it is interesting to note that if the LWRF treated wastewater effluent $\delta^{18}O$ and δ^2H values measured by Hunt and Rosa (2009) are substituted for those measured in this study, the resultant $\delta^{18}O/\delta^2H$ mixing triangle would be expanded to accommodate all submarine spring samples collected in this study. Second, the June submarine spring samples were collected during a major south swell event which may have caused the marine component (i.e. increased/decreased salinity) of the submarine spring samples to vary considerably over small time scales (seconds to minutes) during sample collection. Since water analyzed for $\delta^{18}O$ and δ^2H was collected in different containers than water analyzed for [Cl⁻] over the course of several minutes, the $\delta^{18}O$ and δ^2H sample containers may have contained a different fraction of marine water than the [Cl⁻] sample containers filled at the same location. Note that this second confounding factor only applies to the $\delta^{18}O/Cl^-$ and δ^2H/Cl^- characterizations, since $\delta^{18}O$ and δ^2H values were measured from the same sample container.

The results of this end-member mixing analysis, though by no means conclusive due to the relatively small sample sizes and sensitivity of this technique to end-member temporal variation and intra-sample component inconsistency, suggest that the submarine spring samples consist primarily of LWRF treated wastewater effluent, as shown in a ternary plot (Figure 6-17) representing the fractional components of submarine spring samples determined using the three different end-member characterizations ($\delta^{18}O/\delta^2H$, $\delta^{18}O/Cl^-$, and δ^2H/Cl^-). Data points not fitting the mixing models are not shown on Figure 6-17. Note that 8 of 9 submarine spring sample component characterizations that fit the mixing model show LWRF treated wastewater effluent fractions of over 50%. These results lend support to the volumetric model of a similar injected effluent plume in Kihei, Maui, described in Hunt and Rosa, (2009), which predicted large effluent fractions in the center of the plume at the point of discharge.

6.4.3 Nutrients

6.4.3.1 TP and PO₄³⁻

TP and PO_4^{3-} distributions across the study area reflect both current and former land-use practices as well as the geochemical properties of P in subsurface hydrology. P is a highly particle-reactive element (see Berner, 1973; Krom and Berner, 1980; Krom and Berner 1981; Froelich, 1988; Compton et al., 2000; Ruttenberg, 2004; Slomp and Van Cappellan, 2007; and references therein). The tendency of PO_4^{3-} to adsorb to or precipitate as Fe and Al solids with low solubility (Kehew, 2000) can result in low dissolved PO_4^{3-} concentrations in groundwater and retarded subsurface transport, especially at low pH levels. However, in reducing conditions or at moderate pH levels, and especially in aquifers containing carbonate minerals, previously adsorbed PO_4^{3-} can be liberated to solution, resulting in higher dissolved concentrations and enhanced subsurface transport (Robertson et al., 1998). Because of these properties, PO_4^{3-} from

fertilizer application or wastewater injection has the potential for enhanced retention in the subsurface over long periods of time in the absence of mechanisms for remobilization. Though concentrations of organic P were not explicitly determined for this study, they are estimated here by subtracting a sample's measured PO_4^{3-} concentration from its TP concentration (Tables 6-15 and 6-16).

TP and PO_4^{3-} distribution in MW and PW samples indicates a sharp contrast between wells located on former pineapple fields (Lahaina Deep Monitor, Kaanapali P-4, Kaanapali P-5, and Kaanapali P-6) and wells located on former sugarcane fields (Hahakea 2, Kaanapali P-1, and Kaanapali P-2), with the latter having higher TP and PO_4^{3-} concentrations. This dichotomy was also observed in the results of Soicher (M.S. Thesis, 1996), which are compared to the results of this study in Figure 6-18. Though the June, 2011 results showed more variability in the organic and inorganic apportionment of P than the September, 2011 results, MW and PW samples generally contain a majority (70-90%) of TP as PO_4^{3-}. Although application of fertilizer P on pineapple fields in this area has been generally greater than that on sugarcane fields (Tetra Tech, 1993), it is clear that P occurs in greater concentrations in groundwater under former sugarcane fields. Possible explanations for this phenomenon include greater uptake of fertilizer P by pineapple than sugarcane and the lower irrigation rates of pineapple fields relative to sugarcane fields (Tetra Tech, 1993) reducing potential mobilization and transport mechanisms. Honokowai B, a well located up-gradient of all current and former agriculture, contained TP and PO_4^{3-} concentrations similar to those found in the wells located on pineapple fields. This finding suggests that P applied as fertilizer on these fields has not significantly contributed to P loading in groundwater in this portion of the study area. Due to the relative immobility of P in the basal water table, previous studies (Tetra Tech, 1993; Soicher, M.S. Thesis, 1996) have concluded that particulate bearing surface runoff, not groundwater, is the primary delivery mechanism of terrestrial P to the ocean in this region.

The widely varying TP and PO_4^{3-} content of the TS samples reflect their different provenance. June sample Honolua Ditch, which consisted of diverted surface water from perennial streams north of the study area, contained low levels of TP and PO_4^{3-}, consistent with those of previously measured in these streams (Soicher, M.S. Thesis, 1996). June sample Kahana Stream, which was collected from a stagnant water pool in the coastal portion of the stream bed, contained high levels of TP, the majority of which was in organic form. The high concentration of organic P in this sample is most likely the due to the presence of living and decaying organic matter. The TS samples collected in Black Rock lagoon away from the lagoon's mouth (June samples Kaanapali 1 and 2 and September sample Black Rock lagoon 1) contained high levels of TP and PO_4^{3-}. This is potentially indicative of a variety of sources, including high P groundwater (as the lagoon is groundwater-fed and located down-gradient of former sugarcane fields) and LWRF-R1 irrigation water (possibly including fertilizer P) from the surrounding Kaanapali Golf Course. September sample Black Rock 2, collected near the lagoon's mouth, consisted of a substantial portion of seawater (salinity = 23.12) and showed attenuation of the high TP and PO_4^{3-} concentrations found in the fresher portions of the lagoon with low TP and PO_4^{3-} concentration ocean water.

159

TP and PO_4^{3-} concentrations in the LWRF treated wastewater effluent samples and September TS sample Kaanapali GC R-1 were similar to that of the LWRF wastewater effluent sample measured by Hunt and Rosa (2009), but over an order of magnitude less than those reported by Tetra Tech (1993). Figure 6-19 summarizes the results of those previous studies with those of this study. This discrepancy is likely a result of the incorporation of biological nutrient removal to the LWRF wastewater treatment process in 1995 (Scott Rollins, Maui County Wastewater Division, personal communication, 2012). The concentrations of TP and PO_4^{3-} that currently exist in the LWRF treated wastewater effluent samples are surprisingly similar to or even less than that found in PW samples from former sugarcane fields (June and September samples Hahakea 2, Kaanapali P-1, and Kaanapali P-2) and the low-salinity TS samples from Black Rock lagoon (June samples Kaanapali 1 and 2 and September sample Black Rock 1). The June and September LWRF treated wastewater effluent and September LWRF-R1 samples display a sub-equal distribution of organic and inorganic P, while the September Kaanapali GC-R1 sample contained the majority of its P as organic P, likely reflecting biological uptake of PO_4^{3-} in the sun-exposed Kaanapali GC R1 holding pond holding pond.

The submarine spring samples had the highest TP (11.30 to 15.10 μM (350.0 to 467.6 μg/L as P)) and PO_4^{3-} (9.00 to 13.39 μM (278.7 to 414.7 μg/L as P)) concentrations measured in the study area, and were considerably enriched in PO_4^{3-} relative to concentrations measured in the LWRF treated wastewater effluent samples in this study (2.27 to 3.43 μM (70.3 to 106.2 μg/L as P)) and by Hunt and Rosa (2009) (5.0 μM (154.9 μg/L as P)). These high concentrations are consistent with the results of previous P species measurements of submarine spring discharge (Hunt and Rosa, 2009; Swarzenski et al., USGS report 2012) as summarized in Figure 6-21. Note that Figure 6-21 displays un-mixed P species concentrations, which are discussed in greater detail below. The reason for this PO_4^{3-} enrichment at the submarine spring exit portals relative to the injected effluent is not clear. It is possible that a portion of the PO_4^{3-} injected prior to the implementation of biological nutrient removal at LWRF in 1995 remains adsorbed to ferric iron and aluminum oxides and oxy-hydroxide phases in the subsurface and continues to slowly leach into groundwater its prior to coastal discharge as aquifer conditions permit. Release of previously adsorbed PO_4^{3-} is facilitated by the presence of low-oxygen conditions in aquifers. As explained more fully below, there is substantial evidence for the occurrence of bacterially mediated NO_3^- and Mn reduction facilitating the heterotrophic metabolism of organic C in the in the aquifer feeding the submarine spring discharge. These processes can only occur in suboxic conditions (Kehew, 2000), since O_2 is generally the preferred electron acceptor in the metabolism of organic C when it is present. The presence of carbonate marine sediments in the coastal alluvium that forms a portion of the aquifer between the LWRF injection wells and the submarine spring discharge points may also facilitate the liberation of adsorbed PO_4^{3-} to solution along this flow path (Robertson et al., 1998).

MS samples had relatively uniform concentrations of TP and PO_4^{3-} and were consistent with the results of previous studies in this area (Tetra Tech, 1993; Dollar and Andrews,

1997; Laws, 2004; Hunt and Rosa, 2009) (Figure 6-20). We note that for marine surface water (MS) sample comparisons with previous studies, it is important to point out that sampling locations, amount of samples collected, and parameters measured are not consistent among all studies. The results considered in these comparisons were limited to nearshore (within 1 km of the coastline) marine samples collected between Wahikuli Wayside and Honokowai Beach Parks (refer to the works cited for additional information). The majority of P in these samples tended to be organic verses inorganic, reflecting biological uptake of PO_4^{3-} in the marine environment.

6.4.3.2 SiO_4^{4-}

Groundwater in Hawaii tends to show significant enrichment in SiO_4^{4-} relative to surface and marine waters due to input from soil and rock weathering (Mink, 1961). Additionally, SiO_4^{4-} generally displays conservative behavior relative to dissolved N and P species in Hawaiian aquifers, making it a good tracer of SGD in coastal waters (e.g. Johnson et. al., 2008).

SiO_4^{4-} concentrations in MW and PW samples display a contrast between wells located on former pineapple fields (Lahaina Deep Monitor, Kaanapali P-4, Kaanapali P-5, and Kaanapali P-6) and former sugarcane fields (Hahakea 2, Kaanapali P-1, and Kaanapali P-2), with the latter having higher SiO_4^{4-} concentrations. This distinction was also observed in the results of Soicher (M.S. Thesis, 1996) and could be a lingering effect of sugarcane irrigation practices, wherein sugarcane fields received significantly more artificial irrigation than pineapple fields owing to growing requirements (Tetra Tech, 1993). Increased irrigation, especially in dry areas, appears to accelerate soil weathering and leach more SiO_4^{4-} into the underlying groundwater (Mink, 1961). However, since the solubility of SiO_4^{4-} is strongly affected by the presence of organic acids (Bennett et al. 1988) it is also possible that variations in the distribution of these compounds in soils may play a role in the different SiO_4^{4-} concentrations found in the upland portion of study area.

SiO_4^{4-} concentrations in TS samples appear to be a good proxy for their derivation. June samples Honolua Ditch and Kahana Stream both had low SiO_4^{4-} concentrations relative to those of the MW and PW samples collected in this study, reflecting their origins as surface water. The Black Rock lagoon TS samples collected away from the lagoon's mouth (June samples Kaanapali 1 and 2 and September sample Black Rock 1) had the highest SiO_4^{4-} concentrations measured in the study area (860.08 to 914.17 µM (24179.8 to 25679.0 µg/L as Si)). These high concentrations suggest that this water body is principally fed by SiO_4^{4-}-rich groundwater, and likely augmented in SiO_4^{4-} by artificial irrigation of the surrounding Kaanapali Golf Course. The September TS sample Black Rock 2 (SiO_4^{4-} = 293.25 µM (8240 µg/L as Si); Salinity = 23.12), collected near the lagoon's mouth, showed the effects of passive attenuation by low SiO_4^{4-} marine water. Samples collected from water features on the Kaanapali Golf Course itself (June samples Kaanapali GC-1 (723.02 µM (20309.6 µg/L as Si)) and 2 (658.42 µM (18495.0 µg/L as Si) had SiO_4^{4-})) concentrations of similar to those found in groundwater and R1 irrigation

water (576.94 to 846.99 μM (16206.2 to 23766.5 μg/L as Si)), suggesting a combination of these sources.

SiO_4^{4-} concentrations in the LWRF treated wastewater effluent samples and September TS sample Kaanapali GC R-1 (586.06 to 613.42 μM (16462.4 to 17231.0 μg/L as Si)) were generally less than those found in PW samples (Kaanapali P-1, P-2, P-4, P-5 and P-6), which had SiO_4^{4-} concentrations ranging from 638.80 to 846.99 μM (17943.9 to 23791.9 μg/L as Si). The SiO_4^{4-} concentrations of the LWRF treated wastewater effluent samples fit neatly between those of the PW samples and those reported for surface water in the area (18.51 to 248.84 μM (519.9 to 6988.8 μg/L as Si)) by Soicher (M.S. Thesis, 1996). This finding is consistent with the composition of the area's municipal supply water, which, as discussed above, is the primary component of the wastewater treated by LWRF and is derived from a roughly 56:44 mixture of diverted surface water and groundwater extracted from PWs.

Submarine spring sample SiO_4^{4-} concentrations were variable (426.64 to 753.26 μM (11984.3 to 21159.1 μg/L as Si)) and displayed a relationship of decreasing SiO_4^{4-} concentration with increasing sample salinity. Un-mixing of the marine component of the submarine spring samples (Table 6-17, discussed in greater detail below, implies source SiO_4^{4-} concentrations higher than that of the LWRF treated wastewater effluent samples and most of the MW and PW samples. This phenomenon may be another instance of dissolved SiO_4^{4-} augmentation via the aforementioned irrigation effect (Mink, 1961). In this instance, however, LWRF treated wastewater effluent injection, rather than agricultural irrigation, is the source of the unnaturally high aquifer recharge and consequently enhanced rock weathering.

SiO_4^{4-} concentrations in MS samples were typically low, with samples more enriched in SiO_4^{4-} (e.g. June samples Maui 2 (30.23 μM (849.2 μg/L as Si)) and 6 (44.47 μM (1249.2 μg/L as Si)); September samples Maui 19 (15.07 μM (423.3 μg/L as Si)) and 23 (17.28 μM (485.4 μg/L as Si))) also tending to have lower salinities and higher concentrations of dissolved N and P species. This effect is consistent with the previous observations on the utility of SiO_4^{4-} as a SGD tracer in the marine environment. Spatial distribution of SiO_4^{4-} in MS samples suggests SGD in the area is concentrated near Wahikuli Wayside Park, Black Rock Lagoon, and to a lesser extent, in vicinity of the submarine spring discharge points. Enrichment in SiO_4^{4-} near Wahikuli Wayside Park relative to other portions of the study area was also observed by Laws (2004). See Section 5 for additional discussion of SGD in the study area.

6.4.3.3 TN, NO_3^-, NO_2^-, and NH_4^+

The distribution of N species in the study area reflects a variety of processes including point and non-point source loading, biogeochemical transformation, and biological uptake of inorganic N in terrestrial and MS waters. Though organic N concentrations were not explicitly analyzed for this study, they were estimated by subtracting the sum of the measured inorganic N species concentrations (NO_3^-, NO_2^-, and NH_4^+) from measured TN concentrations (Tables 6-15 and 6-16).

NO_3^- and organic N are the dominant N species found in the MW and PW samples owing to the typically well-oxygenated nature of Hawaiian basalt aquifers inhibiting the presence of the reduced inorganic N species NO_2^- and NH_4^+ (Kehew, 2000). Spatial N species distributions also show a marked distinction between wells located on former sugarcane fields (Hahakea 2, Kaanapali P-1, and Kaanapali P-2) and wells located on former pineapple fields (Lahaina Deep Monitor, Kaanapali P-4, Kaanapali P-5, and Kaanapali P-6). Although the former sugarcane field wells were enriched in P and SiO_4^{4-} relative to the former pineapple field wells as discussed above, they were generally depleted in dissolved N relative to the pineapple field wells, and moreover tended to contain a larger fraction of organic N. The mechanism responsible for this disparity is not well understood, but it may be that substantial portion of the N deposited as fertilizer on sugarcane fields has leached down to the water table and moved down-gradient of the sampling locations since the cessation of sugarcane agriculture in 1999. N deposited as fertilizer is typically quickly converted by bacterial nitrification to NO_3^-, which is highly soluble and mobile (Kendall, 1998), and thus would not be expected to remain in an aquifer for long periods of time in the absence of an ongoing source. As pineapple cultivation and associated fertilization has ceased fairly recently, in 2009 (Gingerich and Engott, 2012), it is possible that fertilizer N applied to these fields has not yet had sufficient time to travel down-gradient of the wells sampled in this study. The lack of artificial irrigation required by pineapple crops relative to sugarcane crops may have also played a role in retarding the soil leaching rate and subsequent down-gradient movement of N species in groundwater below pineapple fields. The decrease in current dissolved NO_3^- concentrations in these former sugarcane field wells relative to those measured in previous studies (Souza, 1981; Soicher, M.S. Thesis, 1996) when fertilization of these fields was ongoing, supports the surmised rapid leaching and down-gradient transport of NO_3^- on sugarcane fields and their underlying groundwater (Figure 6-18). Former sugarcane field well samples still contain elevated dissolved N levels relative to those measured at Honokowai B, a well upgradient of any current or former agriculture. This observation suggests that formerly applied fertilizer N is still contributing to N loading in groundwater beneath former sugarcane fields, though to a lesser extent than in the past during ongoing cultivation.

The TS samples collected consisted of stagnant water bodies (June samples Kahana Stream; Kaanapali GC-1 and 2), flowing irrigation water (June sample Honolua Ditch), and the groundwater-fed Black Rock lagoon (June samples Kaanapali 1 and 2; September samples Black Rock 1 and 2). The N species distribution in these samples correlated well with the expected source derivations and presence of biological activity. June samples Kahana Stream and Kaanapali GC-1 and 2 contained substantial fractions of both organic N and the reduced inorganic species NO_2^- and NH_4^+, indicating a depletion of dissolved O_2 caused by heterotrophic consumption of the decaying organic matter visibly present in these water bodies at the time of sampling. June sample Honolua Ditch, which consisted of water diverted from perennial streams to the north of the study area, contained low concentrations of N relative to the other terrestrial samples. The majority of N in this sample was present as NO_3^- (4.40 μM (61.6 μg/L as N)), a concentration similar to those measured by Soicher (M.S. Thesis, 1996) for streams in this region (typically about 0

to10 μM (0.0 to 140.0 μg/L as N)). At the time of sampling, Black Rock lagoon was visibly flowing seaward from its upper reaches. Samples collected away from the lagoon's mouth (June Samples Kaanapali 1 and 2 and September sample Black Rock 1) had higher concentrations of TN (268.08 to 339.4 μM (3755.8 to 4755.0 μg/L as N)) and NO_3^- (222.48 to 246.05 μM (3116.9 to 3447.2 μg/L as N)) than any other non- LWRF treated wastewater effluent samples collected in this study.   These concentrations were similar to those (TN was not measured, NO_3^- + NO_2^- = 254 μM (3558.5 μg/L as N)) found in the Black Rock lagoon sample collected by Hunt and Rosa (2009). The excess of N in the Black Rock lagoon samples relative to the groundwater collected from up-gradient PW samples could be a combined result of continued N leaching from the former sugarcane fields up-gradient of the lagoon (as discussed above) and input from both fertilizer N and N-rich R1 irrigation water applied to the surrounding Kaanapali Golf Course.

Concentrations of N species in the June and September LWRF treated wastewater effluent samples showed considerable variation, with the June sample showing considerable enrichment in TN, NO_2^-, and NH_4^+, relative to the September sample. The LWRF effluent sample collected by Hunt and Rosa (2009) had TN concentrations similar to the September LWRF treated wastewater effluent sample collected in this study, but with higher NH_4^+ concentrations than those measured in here.   This variability in the LWRF treated wastewater effluent composition, generally manifested as high NH_4^+ concentrations, is a function of variability in plant operation including both equipment and personnel factors (Scott Rollins, Maui County Wastewater Division, personal communication, 2012). Even though the LWRF treated wastewater effluent continues to show temporal variability in quality, comparisons of N species concentrations measured since the inception of biological nutrient removal at LWRF in 1995 with those measured prior to this upgrade (e.g. Tetra Tech, 1994) show that this treatment upgrade has been successful in significantly reducing N loading in the LWRF treated wastewater effluent (Figure 6-19). The September LWRF-R1 and Kaanapali GC-R1 samples show similar N species distribution to the September LWRF treated wastewater effluent sample. This is not surprising, since the R1 recycled water is the source of the water for the golf course irrigation. Of note, the September Kaanapali GC-R1 sample, which was collected from an open holding pond on the Kaanapali Golf Course containing R1 effluent supplied directly from LWRF, showed enrichment in NO_3^- and depletion in the reduced species NO_2^- and NH_4^+ relative to the September LWRF treated wastewater effluent samples. This is indicative of bacterially mediated nitrification of these the reduced species in the presence of ample dissolved free O_2.

The June and September, 2011 submarine spring samples also showed considerable variation in N species distribution. Though the September submarine spring samples had lower concentrations of inorganic N than the June samples, they had significantly higher concentrations of TN and organic N. Though TN and organic N was not measured for submarine spring samples by Hunt and Rosa (2009), inorganic N concentrations measured were considerably higher than the concentrations measured in this study and by Swarzenski et al. (USGS report 2012). The difference in inorganic N concentration is even more apparent when the submarine spring samples are adjusted for relative salinities

as discussed below (Table 6-18; Figure 6-21). The mechanisms responsible for this temporal variability are not clear. Since water isotope mixing analysis (discussed above) and dye tracer results (see Section 3) suggest that the submarine spring discharge is primarily LWRF treated wastewater effluent, the aforementioned temporal variability in LWRF treated wastewater effluent N species concentrations may be driving temporal variability in submarine spring N species concentrations. However, the complexity of the transformations undergone by N species in the subsurface environment (e.g. nitrification, denitrification, and annamox (Kendall, 1998)) make temporal correlation of submarine spring N species distribution to injected LWRF treated wastewater effluent N species distribution difficult with currently available data. The correlation between lower NO_3^- concentrations in the submarine spring discharge with higher NO_3^- $\delta^{15}N$ and $\delta^{18}O$ values and the significant reduction of NO_3^- concentrations in the submarine spring discharge relative to the injected LWRF treated wastewater effluent described below are strongly indicative of microbial denitrification during aquifer transport, which is explained more fully below.

The majority of MS samples collected contained low concentrations of N species relative to those measured in other portions of the study area. These results are consistent with past studies, including Hunt and Rosa (2009), Laws (2004), Dollar and Andrews (1997), and Tetra Tech (1993) (Figure 6-20). Elevated MS N species concentrations were generally observed in waters with lower salinities and higher SiO_4^{4-} concentrations. As discussed above and in Section 5, correlation of elevated nutrient levels with lower salinities is indicative SGD influence. MS samples collected in September, 2011 tended to have higher levels of organic N than those collected in June, 2011 though levels of inorganic N were similar, resulting in higher organic N fractions and higher N:P ratios (Figures E-8 and E-22). This phenomenon could be a result of increased biological uptake and incorporation of inorganic N by marine organisms during this time but also may be related to the higher levels of organic N observed in the September submarine spring samples.

6.4.3.4 Salinity Un-mixing of Submarine Spring Sample Nutrient Concentrations

The highly variable salinities of the submarine spring samples measured in this study, previous studies (Hunt and Rosa, 2009; Swarzenski et al., USGS report 2012), and ongoing HDOH sampling can be assumed to be a result of the dilution of the fresh component of the discharge with ambient ocean water. In order to normalize the nutrient concentrations of the fresh component of the submarine spring samples, the following equation was used to un-mix the ambient ocean water component of the samples:

$$C_1 = C_{mix} + (C_{mix} - C_2) \times (S_{mix} - S_1) / (S_2 - S_{mix}) \qquad \text{(Eq. 6-4)}$$

where C_1 is the concentration of component 1, the hypothetical "source;" C_2 is the concentration of component 2, in this case seawater; C_{mix} is the concentration in the mixed sample being evaluated; S_1 is the salinity of component 1, set equal to the suspected parent water; S_2 is the salinity of component 2, in this case seawater; and S_{mix} is the salinity of the mixed sample being evaluated. This technique was also utilized by Hunt and Rosa

(2009). In order to ensure inter-study consistency in the results, the same seawater end member salinity and nutrient concentrations (from Dollar and Andrews, 1997) were utilized for like parameters. End member dissolved oxygen concentrations were taken from the arithmetic mean of the marine samples collected by HDOH in January, 2012. The salinity of the treated wastewater effluent (here, the arithmetic mean salinity of the June and September LWRF treated wastewater effluent samples measured in this study and the single LWRF treated wastewater effluent sample measured by Hunt and Rosa (2009)) was used as the hypothetical source salinity. The parameter values utilized for the calculations are as follows:

$S_1 = 1.07$
$S_2 = 34.93$
$C_2 = 7.19$ mg/L Dissolved Oxygen
$C_2 = 0.12$ μM (3.7 μg/L as P) PO_4^{3-}
$C_2 = 0.33$ μM (10.2 μg/L as P) TP
$C_2 = 11.16$ μM (313.5 μg/L as Si) SiO_4^{4-}
$C_2 = 0.19$ μM (2.7 μg/L as N) NH_4^+
$C_2 = 0.13$ μM (1.8 μg/L as N) $NO_3^- + NO_2^-$
$C_2 = 6.84$ μM (95.8 μg/L as N) TN
$C_2 = 6.53$ μM (91.4 μg/L as N) Organic N

The un-mixing calculation results for Hunt and Rosa (2009), Swarzenski et al. (USGS report 2012), the current study, and samples collected by HDOH in January, 2012 are presented in Tables 6-17 and 6-18. Organic N values were computed by subtracting NO_3^- + NO_2^- and NH_4^+ concentrations from TN concentrations were available. A salinity of 7.46 (the salinity of June sample Seep 1 Piez-1) was used for June sample Seep 1 Piez-2, which was sampled from the same location but not analyzed for salinity. Variations in unmixed N and P species over time are discussed above and shown in Figure 6-21.

6.4.4 Gas and Rock Crust Analyses

6.4.4.1 Submarine Spring Gas Bubbles

Distinctive gas bubbles were observed emanating from the seafloor near the location of June sample Seep 2 Piez-1 (Figure 6-11). The composition of the gas is significantly enriched in N_2, slightly enriched in CO_2, and depleted in O_2 + Ar relative to atmospheric values (Table 6-11). This observation is another indicator of the microbial reduction of NO_3^- to N_2 gas (denitrification) in the aquifer feeding the submarine spring discharge.

6.4.4.2 Rock Crust Composition

The composition of the unusual black crust found coating and impregnating coral rubble and basalt cobbles (Figure 6-12) immediately proximal to the submarine spring discharge points provides additional insight regarding the redox chemistry of the submarine spring discharge. Ion microprobe analyses of these black crusts (e.g. Figure 6-13) indicates a composition dominated by sedimentary MnO, a mineral which commonly precipitates in

the deep sea but is rarely found in typically well-oxygenated nearshore environments. The formation of MnO precipitate requires the oxidation of previously reduced dissolved Mn^{2+}. The presence of this mineral coating suggests that Mn is being reduced as a terminal electron acceptor in the heterotrophic respiration of organic C in the aquifer feeding the submarine springs and subsequently oxidized and precipitated onto nearby rock surfaces immediately following its discharge into well-oxygenated marine water. The use of Mn as a terminal electron acceptor by microorganisms implies that the groundwater feeding the submarine springs is suboxic to anoxic, and that O_2 and NO_3^-, which are preferred as electron acceptors over Mn due to energy yield considerations (Berner, 1980; Kehew, 2000), have already been exhausted. The low un-mixed dissolved oxygen (Table 6-17) and NO_3^- (Table 6-18) concentrations observed in submarine spring samples are consistent with this line of reasoning. Figure ES-4 and 6-25 illustrates the progressive use of different electron acceptor compounds (manifested as their relative concentrations) in the heterotrophic respiration of organic C by microorganisms. The presence of sufficient organic C to fuel the sequential exhaustion of O_2 and NO_3^- in the aquifer feeding the submarine springs is another phenomenon consistent the presence of the injected LWRF treated wastewater effluent, which is typically significantly enriched in organic C relative to ambient groundwater.

6.4.5 $\delta^{15}N$ and $\delta^{18}O$ of Dissolved NO_3^-

6.4.5.1 Background

NO_3^- $\delta^{15}N$ and $\delta^{18}O$ values can be diagnostic of NO_3^- source provenance and various transformative processes in the N cycle (e.g. Kendall, 1998; Sigman et al., 2005). Analysis of these values has been used in groundwater studies (e.g. Aravena and Robertson, 1998) and marine studies (e.g. Casciotti et al., 2002; Lehmann et al., 2004) to trace the sources and evolution of NO_3^-. Especially germane to this study is the use of NO_3^- $\delta^{15}N$ and $\delta^{18}O$ values (coupled with NO_3^- concentration) as an indicator of denitrification, the biologically mediated reduction of NO_3^- to N_2 gas (Kendall, 1998). The microorganisms responsible for denitrification preferentially convert NO_3^- containing the ^{14}N and ^{16}O into N_2, leaving the remaining NO_3^- enriched in ^{15}N and ^{18}O (Kendall, 1998). NO_3^- $\delta^{15}N$ and $\delta^{18}O$ values were measured for several samples collected in this study, including LWRF treated wastewater effluent and submarine spring samples (Figure 6-22). Submarine spring samples collected by HDOH in January, 2012 were also analyzed for these parameters. Additionally, NO_3^- $\delta^{15}N$ and $\delta^{18}O$ values were reported Hunt and Rosa (2009) for several samples in the study area and provide points of comparison to the results of this study.

6.4.5.2 Distribution and Trends

Monitoring Well (MW) and production well (PW) NO_3^- $\delta^{15}N$ and $\delta^{18}O$ values fall in a uniform distribution relative to those measured for other sample types and indicate potential source provenances of fertilizer and naturally occurring NO_3^-. The MW and PW dissolved NO_3^- $\delta^{15}N$ and $\delta^{18}O$ values measured in this study are consistent with the values reported the single PW sampled by Hunt and Rosa (2009). The overlapping range

of $\delta^{15}N$ and $\delta^{18}O$ in potential source values makes the relative contributions of each source impossible to determine definitively, though it is likely that wells with higher NO_3^- concentrations (e.g. June and September samples Kaanapali P-6) have a higher relative contribution of fertilizer-derived NO_3^- than wells with lower NO_3^- concentrations (e.g. June and September samples Honokowai B).

LWRF treated wastewater effluent NO_3^- $\delta^{15}N$ and $\delta^{18}O$ values measured in this study are more enriched in both ^{15}N and ^{18}O than typical sewage values and indicate that the effluent has undergone denitrification from its original state during the biological nitrogen removal treatment process (e.g. Kendall, 1998). The June and September LWRF treated wastewater effluent dissolved NO_3^- $\delta^{15}N$ and $\delta^{18}O$ values measured in this study are higher than those measured by Hunt and Rosa (2009), indicating a greater fraction of NO_3^- removal via denitrification.. This apparent increase in NO_3^- removal at LWRF between 2007 (the year of sampling took place Hunt and Rosa, 2009) and 2011 may be a result of temporal variability in LWRF plant operation and associated effluent composition discussed above. The September sample Kaanapali GC-R1 had a similar dissolved NO_3^- $\delta^{15}N$ value, a lower $\delta^{18}O$ value, a higher NO_3^- concentration, and a lower NH_4^+ concentration than the September LWRF treated wastewater effluent and LWRF-R1 samples. This is likely a result of the nitrification of NH_4^+ to NO_3^- upon exposure to atmospheric oxygen upon transport to the holding pond at Kaanapali Golf Course.

TS samples from Black Rock Lagoon (June samples Kaanapali 1 and 2; September samples Black Rock 1 and 2) tended to have NO_3^- $\delta^{15}N$ values between those of the MW and PW and LWRF treated wastewater effluent samples, and NO_3^- $\delta^{18}O$ values similar to those of upland groundwater. Hunt and Rosa (2009) analyzed a single Black Rock lagoon sample for dissolved NO_3^- $\delta^{15}N$ and $\delta^{18}O$ and reported values similar to those measured in this study. The Black Rock lagoon samples likely contain a mixture of R1 irrigation water NO_3^- (due to their proximal location to the Kaanapali Golf Course), groundwater NO_3^-, and for the higher salinity samples, marine NO_3^-. The relatively high concentrations of NO_3^- in these samples as well as their surficial character (and probable oxic nature) suggests that in-situ denitrification has not played a significant role in their evolution. The wide variety of potential sources and potential confounding transformations, especially nitrification and biological uptake of NO_3^-, make relative contribution of each source difficult to determine for Black Rock lagoon.

The NO_3^- $\delta^{15}N$ and $\delta^{18}O$ values from the submarine springs were the highest of any measured in this study. Dye tracer results (see Section 3) and water isotope mixing analysis indicate that the submarine springs discharge is composed primarily of treated wastewater effluent injected at the LWRF. These submarine spring samples' elevated dissolved NO_3^- $\delta^{15}N$ and $\delta^{18}O$ values, coupled with their low NO_3^- concentrations relative to their injected LWRF treated wastewater effluent source, are indicative of significant denitrification. As discussed in the above, treated wastewater effluent generally contains abundant organic C, which provides sustenance for heterotrophic microorganisms which preferentially use O_2 as an electron acceptor in respiration. When organic C remains in excess as O_2 concentrations decrease, these microorganisms shift to anaerobic respiration using available NO_3^- as an electron acceptor to facilitate their respiration of organic C

(Kehew, 2000). The resultant stepwise conversion of NO_3^- to N_2 constitutes denitrification and, as discussed above, results in elevated $\delta^{15}N$ and $\delta^{18}O$ values in the remaining dissolved NO_3^-. The NO_3^- $\delta^{15}N$ and $\delta^{18}O$ values of submarine spring samples measured in this study are significantly higher than those of the three submarine spring samples analyzed by Hunt and Rosa (2009), although their submarine spring samples had considerable mixing with marine waters due to sample collection technique. Despite sample collection technique, the samples measured in this study had significantly lower NO_3^- concentrations than Hunt and Rosa (2009), indicating a greater degree of NO_3^- attenuation via denitrification, and thus a greater degree of enrichment of ^{15}N in the remaining NO_3^-. The reasons for the increase in NO_3^- attenuation between the LWRF injection wells and the submarine spring discharge between 2007 and 2011 are not well understood, but could include (1) variation in injected LWRF treated wastewater effluent composition, (2) variation in local aquifer conditions affecting the microorganism populations and/or the transit time of the treated wastewater effluent from the LWRF injection wells to the submarine spring discharge points, (3) temporal variation in the fractional contributions of background groundwater and recirculated seawater to the submarine spring discharge. It is interesting to note that the Hawaii Department of Health submarine spring samples collected in January, 2012 had higher dissolved NO_3^- $\delta^{15}N$ and $\delta^{18}O$ values than those measured in this study along with attendant reduced NO_3^- concentrations, indicating biological nitrogen reduction of nearly all the injected LWRF treated wastewater effluent NO_3^- prior to entering the ocean (Table 6-19).

It should be noted that since our dissolved NO_3^- $\delta^{15}N$ and $\delta^{18}O$ analyses were methodologically limited to samples with dissolved NO_3^- concentrations greater than approximately 0.9 μM (12.6 μg/L as N), it is likely that only the marine surface (MS) samples with significant contributions from terrestrial NO_3^- were analyzed. MS sample dissolved NO_3^- $\delta^{15}N$ and $\delta^{18}O$ values varied widely, reflecting different terrestrial sources and different degrees of mixing with oceanic NO_3^-. NO_3^- $\delta^{15}N$ values obtained for MS samples in this study were generally higher than those measured by Hunt and Rosa (2009), while NO_3^- $\delta^{18}O$ values were similar. This disparity is probably a result of the input of the higher $\delta^{15}N$ submarine spring water measured in this study into the marine environment. The higher $\delta^{15}N$ values were found closer to the submarine spring discharge points (near Kahekili Beach Park) and were generally contained within the plume of elevated sea surface temperatures revealed by TIR imagery (see Section 4), while the lower $\delta^{15}N$ values were found near the mouth of Black Rock lagoon and near Wahikuli Wayside Park , a background sampling location south of the submarine spring discharge points. Though not as high as the values found near the submarine spring discharge points, the $\delta^{15}N$ values found in MS samples near Wahikuli Wayside Park are high enough to suggest that denitrification (possibly fueled by input of organic C and NO_3^- from cesspools/septic tanks) is occurring in groundwater entering the ocean as SGD along this stretch of coast as well.

6.4.5.3 Denitrification Analysis

A quantitative analysis of denitrification enrichment factor from the LWRF treated wastewater effluent to the submarine spring discharge points was performed by

considering the denitrification to be a Rayleigh Distillation process with the June and September, 2011 LWRF treated wastewater effluent sample NO_3^- as the original substrate and the submarine spring sample NO_3^- as the remaining substrate. The following equation was used to calculate the enrichment factor of the denitrification reaction (Kendall, 1998):

$$\varepsilon_{p/s} = (\delta_s - \delta_{s,o}) / \ln f \qquad\qquad\qquad (\text{Eq. 6-5})$$

where $\varepsilon_{p/s}$ is the enrichment factor, δ_s is the $\delta^{15}N$ value of the remaining NO_3^-, $\delta_{s,o}$ is the $\delta^{15}N$ value of the original NO_3^-, and f is the ratio of the remaining NO_3^- to the original NO_3^-. The denitrification process appears as a straight line with a slope equal to $\varepsilon_{p/s}$ on a plot of dissolved NO_3^- $\delta^{15}N$ vs. $\ln[NO_3^-]$ (Figure 6-23). The $\varepsilon_{p/s}$ for the data collected in this study was calculated using a linear regression through the submarine spring and LWRF treated wastewater effluent sample $\ln[NO_3^-]$ and NO_3^- $\delta^{15}N$ data pairs and determined to be -18.9‰ (Figure 6-23). This value is within the large range (-30 to -2‰) of denitrification enrichment factors reported in other works (summarized by Granger et al., 2008; Sigman and Casciotti, 2010) and most similar to the -15.9‰ reported by Bottcher et al. (1990) for a groundwater in a gravelly sand aquifer and the -22.9‰ reported by Aravena and Robertson (1998) for groundwater in a septic sand aquifer. Hunt and Rosa (2009) calculated a denitrification enrichment factor of -38‰ for this system. This analysis was based on a comparison of a single submarine spring sample with the LWRF treated wastewater effluent using NO_3^- $\delta^{15}N$ and dissolved inorganic N concentrations and may be inaccurate for these reasons.

$\delta^{15}N$ values of dissolved NO_3^- for three submarine spring samples were reported by Hunt and Rosa (2009). $\delta^{15}N$ values were also measured for six submarine spring samples collected by the Hawaii Department of Health (HDOH) in January 2012. These results, along with unmixed $NO_3^- + NO_2^-$ concentrations and unmixed $NO_3^- + NO_2^-$ fraction relative to the average LWRF treated wastewater effluent $NO_3^- + NO_2^-$ concentration are presented in Table 6-19. Note that $NO_3^- + NO_2^-$ concentrations were used for this analysis due to the lack of uncombined NO_3^- and NO_2^- concentration measurements for the Hunt and Rosa (2009) and HDOH samples. Though $\delta^{15}N$ values vary widely across the studies, there is a strong inverse correlation between $NO_3^- + NO_2^-$ fraction and $\delta^{15}N$ across all samples indicative of the effects of denitrification. A quantitative analysis of denitrification enrichment factor for these samples was performed using equation 6-5 above (although in this case the $NO_3^- + NO_2^-$ fraction was used in place of the NO_3^- fraction as discussed above). Results of this analysis (top plot of Figure 6-24) yielded an enrichment factor of -22.8‰, which is similar to the values obtained for the analysis of the results the current study alone and nearly identical to the -22.9‰ reported by Aravena and Robertson (1998) for groundwater in a septic sand aquifer. The high R^2 value of the correlation (0.934) of $\delta^{15}N$ vs. $\ln[NO_3^- + NO_2^-]$ between samples taken by different studies across a wide time frame is indicative of long term uniformity of the denitrification enrichment factor in this system. The bottom plot of Figure 6-24 provides an alternate graphical representation of the denitrification process occurring within this

system. This representation is based on the following equation describing a Rayleigh Distillation process:

$$R = R_0 f^{(1-\alpha)} \qquad \text{(Eq. 3.6)}$$

where R is the sample NO_3^- $^{15}N/^{14}N$ ratio, R_o is the $^{15}N/^{14}N$ ratio of the source NO_3^- (in this case LWRF treated wastewater effluent), f is the ratio of remaining $NO_3^- + NO_2^-$ to original $NO_3^- + NO_2^-$, and α is the fractionation factor. $^{15}N/^{14}N$ ratios were calculated from $\delta^{15}N$ values using the following equation:

$$(^{15}N/^{14}N)_{sample} = ((^{15}N/^{14}N)_{AIR} (\delta^{15}N_{sample}) / 1000) + (^{15}N/^{14}N)_{AIR} \quad \text{(Eq. 3-7)}$$

where $(^{15}N/^{14}N)_{AIR} = 0.0036765$

The fractionation factor (α) is related to the enrichment factor (ε) by the following relationship:

$$\varepsilon = 1000 (\alpha - 1) \qquad \text{(Eq. 3-8)}$$

Application of this relationship to the data yields an α of 0.98 and a corresponding ε of -20. This enrichment factor is necessarily consistent with that calculated using the previous methods, since the relationships used are nearly identical mathematically.

6.5 SUMMARY

6.5.1 Sources of Nutrients

Though a thorough quantitative evaluation of nutrient sources was not accomplished in this portion of the study, we have identified several potential sources based on the spatial distribution of nutrient species with respect to the current and former land-use practices. These potential sources are as follows:

(1) Fertilizer applied in support of former sugarcane and pineapple agriculture appear to still be contributing to N and P loading of basal groundwater (though to a lesser extent than in the past, when these agricultural practices were ongoing).

(2) Injected LWRF treated wastewater effluent appears to contribute significant amounts of N and P (though much less than prior to treatment upgrades in 1995) to groundwater, though the temporally variable and non-conservative behavior of these species complicates the overall assessment of the magnitude of this source.

(3) LWRF-R1 irrigation water and possibly fertilizer appear to contribute to N and P loading in groundwater supplying Black Rock lagoon.

171

6.5.2 Geochemical Evolution

We have analyzed the fate of the injected LWRF treated wastewater effluent with natural tracers and found evidence for significant down-gradient geochemical evolution nutrient species in the study area. Significant findings are as follows:

(1) Mixing analysis using conservative tracers suggests that discharge from the submarine springs is primarily comprised of injected LWRF treated wastewater effluent, corroborating the results of Section 3.

(2) Though likely subject to temporal variation, the majority of the NO_3^- present in the injected LWRF treated wastewater effluent was attenuated via denitrification prior to discharge at the submarine springs at the time of this study.

(3) The injected LWRF treated wastewater effluent is augmented in PO_4^{3-} prior to its discharge at the submarine springs due to aquifer conditions promoting the dissolution of previously particle-adsorbed PO_4^{3-}.

(4) Groundwater at and down-gradient of locations subjected to significant artificial recharge is augmented in SiO_4^{4-} mobilized via accelerated rock weathering.

6.5.3 Impact on the Marine Environment

By analyzing the spatial distribution of various water parameters in the marine environment, including nutrient concentrations and stable isotope values, we have located several coastal ocean areas of terrestrial nutrient contribution. These are as follows:

(1) The area immediately surrounding the submarine springs, which show a dissolved NO_3^- isotopic signature consistent with the heavily enriched values measured in the submarine springs' discharge.

(2) The area near the mouth of Black Rock lagoon, which shows generally elevated nutrient concentrations relative to nearby waters and a dissolved NO_3^- isotopic signature consistent with values measured in Black Rock lagoon itself.

(3) The area near Wahikuli Wayside Park, which also shows generally elevated nutrient concentrations relative to nearby waters and shows a dissolved NO_3^- isotopic signature suggestive of denitrification from fertilizer or natural sources and/or sewage/manure content.

Table 6-1: Monitoring Point Designations for the Geochemistry Samples.
(see also Section 2, Table 2-1).

Geochemistry Sample Name (This Section)	Tracer Monitoring Point (Sections 2,and 3)	Comments
Seep 1 Piez-1	Seep 4	First sample collected from Seep 4 during the June, 2011 sampling round
Seep 1 Piez-2	Seep 4	Second sample collected from Seep 4 during the June sampling round
Seep 1- 2Piez	Seep 4	Collected during the September sampling round
Seep 2 Piez 1	NSG-a	Collected from the North Seep Group during the June sampling round
Seep 3 Piez 1	Seep 6	Collected during the June sampling round
Seep 3-2 Piez	Seep 6	Collected during the September sampling round
Seep 4 Piez 1	Seep 3	Collected during the June sampling round

Table 6-2: University of Washington Analytical Laboratory Reported Minimum Detection Limits

	TP	TN	PO_4^{3-}	SiO_4^{4-}	NO_3^-	NO_2^-	NH_4^+
	(µM)	(µM)	(µM)	(µM)	(µM)	(µM)	(µM)
Minimum Detection Limit	0.03	0.34	0.03	0.76	0.08	0.01	0.07

	TP	TN	PO_4^{3-}	SiO_4^{4-}	NO_3^-	NO_2^-	NH_4^+
	(µg/L as P	(µg/L as N	(µg/L as P	(µg/L as Si	(µg/L as N	(µg/L as N	(µg/L as N
Minimum Detection Limit	0.9	4.8	0.9	21.3	1.1	0.14	1

Table 6-3: June, 2011 sampling location information

Sample Name	Sample Type	Date	Time[1]	Lattitude[2]	Longitude[2]
Hahakea 2	PW	6/30/2011	13:46	20.91472	-156.66889
Honokowai	MS	6/20/2011	10:40	20.95445	-156.68687
Honokowai B	PW	6/30/2011	10:53	20.93722	-156.64389
Honolua 1	MS	6/20/2011	10:29	21.01397	-156.63771
Honolua 2	MS	6/20/2011	10:34	21.01369	-156.63776
Honolua Ditch	TS	6/29/2011	10:48	20.94957	-156.65773
Kaanapali 1	TS	6/20/2011	13:15	20.92807	-156.69423
Kaanapali 2	TS	6/20/2011	13:30	20.92807	-156.69423
Kaanapali GC-1	TS	6/29/2011	15:06	20.91771	-156.69188
Kaanapali GC-2	TS	6/29/2011	15:23	20.91712	-156.69200
Kaanapali P-1	PW	6/30/2011	11:46	20.92694	-156.65556
Kaanapali P-2	PW	6/30/2011	12:42	20.92944	-156.65306
Kaanapali P-4	PW	6/30/2011	9:29	20.94917	-156.65028
Kaanapali P-5	PW	6/30/2011	8:08	20.95361	-156.64694
Kaanapali P-6	PW	6/30/2011	8:52	20.95639	-156.64750
Kahana Stream	TS	6/30/2011	16:23	20.97703	-156.67772
Lahaina Deep Monitor	MW	6/29/2011	12:35	20.94944	-156.65778
LWRF Treated Effluent	TW	6/30/2011	14:15	20.94652	-156.68660
Maui 1	MS	6/21/2011	8:56	20.90471	-156.68697
Maui 10	MS	6/21/2011	10:54	20.95091	-156.69191
Maui 11	MS	6/21/2011	11:05	20.95507	-156.68829
Maui 12	MS	6/21/2011	12:12	20.93796	-156.69315
Maui 13	MS	6/21/2011	12:46	20.94095	-156.69463
Maui 14	MS	6/21/2011	12:50	20.93915	-156.69409
Maui 15	MS	6/21/2011	12:53	20.93786	-156.69420
Maui 16	MS	6/21/2011	12:55	20.93641	-156.69440
Maui 17	MS	6/21/2011	12:59	20.93449	-156.69470
Maui 18	MS	6/21/2011	13:02	20.93218	-156.69495
Maui 2	MS	6/21/2011	9:07	20.90969	-156.68959

Table 6-3 continued:

Maui 3	MS	6/21/2011	9:18	20.91096	-156.69324
Maui 4	MS	6/21/2011	9:34	20.91979	-156.69766
Maui 5	MS	6/21/2011	9:49	20.92623	-156.69655
Maui 6	MS	6/21/2011	9:59	20.92887	-156.69604
Maui 7	MS	6/21/2011	10:15	20.93187	-156.69368
Maui 8	MS	6/21/2011	10:26	20.93811	-156.69363
Maui 9	MS	6/21/2011	10:39	20.94459	-156.69344
Seep 1 Piez-1	SS	6/19/2011	15:00	20.93860	-156.69321
Seep 1 Piez-2	SS	6/20/2011	15:33	20.93860	-156.69321
Seep 1 Surface	MS	6/19/2011	15:00	20.93860	-156.69321
Seep 2 Piez-1	SS	6/20/2011	16:15	20.93980	-156.69298
Seep 2 Surface	MS	6/20/2011	16:12	20.93980	-156.69298
Seep 3 Piez-1	SS	6/22/2011	12:58	20.94011	-156.69287
Seep 3 Surface	MS	6/22/2011	12:15	20.94011	-156.69287
Seep 4 Piez-1	SS	6/23/2011	17:00	20.93864	-156.69312
Seep 4 Surface	MS	6/23/2011	12:00	20.93864	-156.69312
Wahikuli	MS	6/20/2011	12:43	20.90424	-156.68600

[1]Time is from beginning of sampling.
[2]Datum is WGS-84. Units are decimal degrees.
PW = Production Well
MW = Monitor Well
TS = Terrestrial Surface
TW = Treated Wastewater
SS = Submarine Spring
MS = Marine Surface

Table 6-4: September, 2011 sampling location information

Sample Name	Sample Type	Date	Time[a]	Lattitude[b]	Longitude[b]
Black Rock 1	TS	9/21/2011	15:19	20.92854	-156.69490
Black Rock 2	TS	9/21/2011	15:29	20.92882	-156.69543
Hahakea 2	PW	9/20/2011	12:26	20.91472	-156.66889
Honokowai B	PW	9/20/2011	10:06	20.93722	-156.64389
Kaanapali GC-R1 Pond	TS	9/20/2011	15:04	20.92041	-156.68698
Kaanapali P-1	PW	9/20/2011	11:13	20.92694	-156.65556
Kaanapali P-2	PW	9/20/2011	11:45	20.92944	-156.65306
Kaanapali P-4	PW	9/20/2011	7:30	20.94917	-156.65028
Kaanapali P-5	PW	9/20/2011	8:07	20.95361	-156.64694
Kaanapali P-6	PW	9/20/2011	8:51	20.95639	-156.64750
Lahaina Deep Monitor	MW	9/19/2011	11:05	20.94944	-156.65778
LWRF-R1	TW	9/19/2011	13:42	20.9458	-156.68756
LWRF Treated Effluent	TW	9/19/2011	14:37	20.94652	-156.68660
Maui 19	MS	9/22/2011	9:34	20.90451	-156.68701
Maui 20	MS	9/22/2011	10:02	20.91307	-156.69626
Maui 21	MS	9/22/2011	10:20	20.91965	-156.69722
Maui 22	MS	9/22/2011	10:35	20.92615	-156.69632
Maui 23	MS	9/22/2011	10:45	20.92867	-156.69582
Maui 24	MS	9/22/2011	11:03	20.93207	-156.69362
Maui 25	MS	9/22/2011	11:18	20.93715	-156.69345
Maui 26	MS	9/22/2011	11:36	20.94333	-156.69284
Maui 27	MS	9/22/2011	11:58	20.95129	-156.69130
Maui 28	MS	9/22/2011	12:13	20.95494	-156.68814
Maui 29	MS	9/22/2011	12:25	20.95681	-156.69046
Maui 30	MS	9/22/2011	12:42	20.94946	-156.69643
Maui 31	MS	9/22/2011	12:57	20.94354	-156.69879
Maui 32	MS	9/22/2011	13:06	20.93907	-156.70074
Maui 33	MS	9/22/2011	13:47	20.93892	-156.69548
Maui 34	MS	9/22/2011	13:57	20.93242	-156.70073
Maui 35	MS	9/22/2011	14:21	20.91547	-156.69940

Table 6-4 continued:

Maui 36	MS	9/22/2011	14:35	20.90727	-156.69661
Maui DP 14	MS	9/21/2011	14:29	20.92957	-156.69492
Maui DP 3	MS	9/21/2011	13:14	20.94025	-156.69370
Maui DP 12	MS	9/21/2011	14:15	20.93237	-156.69478
Seep 1 Surface	MS	9/24/2011	16:32	20.93862	-156.69318
Seep 1-2 Piez	SS	9/24/2011	16:40	20.93862	-156.69318
Seep 3 Surface	MS	9/25/2011	15:40	20.94011	-156.69286
Seep 3-2 Piez	SS	9/23/2011	16:40	20.94011	-156.69286

[a]Time is from beginning of sampling.
[b]Datum is WGS-84. Units are decimal degrees.
PW = Production Well
MW = Monitor Well
TS = Terrestrial Surface
TW = Treated Wastewater
SS = Submarine Spring
MS = Marine Surface

Table 6-5: June, 2011 Temperature, Specific Conductivity, Salinity, and pH
(- denotes measurement not available)

Sample Name (Type)	Temperature (°C)	Specific Conductivity (ms/cm)	Field Salinity (PSU)	Lab Salinity (PSU)	pH
Hahakea 2 (PW)	21.43	0.849	0.42	0.41	-
Honokowai (MS)	25.51	-	-	-	8.1
Honokowai B (PW)	21.14	0.875	0.43	0.44	-
Honolua 1 (MS)	25.21	-	-	-	8.13
Honolua 2 (MS)	25.59	-	-	-	8.12
Honolua Ditch (TS)	25.00	0.103	-	-	7.77
Kaanapali 1 (TS)	26.25	2.583	1.33	-	8.24
Kaanapali 2 (TS)	25.42	2.381	1.22	-	7.74
Kaanapali GC-1 (TS)	27.70	6.737	3.68	3.66	7.30
Kaanapali GC-2 (TS)	32.37	0.837	0.40	-	7.68
Kaanapali P-1 (PW)	21.13	0.565	0.27	0.27	-
Kaanapali P-2 (PW)	21.78	0.903	0.44	0.45	-
Kaanapali P-4 (PW)	20.52	1.033	0.51	0.51	-
Kaanapali P-5 (PW)	19.69	0.594	0.29	0.28	-
Kaanapali P-6 (PW)	20.21	1.065	0.53	0.55	-
Kahana Stream (TS)	25.84	18.240	10.77	10.70	8.34
Lahaina Deep Monitor (MW)	21.55	1.012	0.50	0.55	-
LWRF Treated Effluent (TW)	30.90	2.085	-	1.10	6.45
Maui 1 (MS)	25.37	-	-	-	8.12
Maui 10 (MS)	25.08	-	-	-	8.11
Maui 11 (MS)	25.26	-	-	-	8.13
Maui 12 (MS)	25.81	-	-	-	8.16
Maui 13 (MS)	25.37	-	-	-	8.14
Maui 14 (MS)	25.53	-	-	-	8.14
Maui 15 (MS)	25.32	-	-	-	8.14
Maui 16 (MS)	25.30	-	-	-	8.14
Maui 17 (MS)	25.37	-	-	-	8.14
Maui 18 (MS)	25.27	-	-	-	8.14
Maui 2 (MS)	25.31	-	-	-	8.12

Table 6-5 continued:

Maui 3 (MS)	25.22	-	-	-	8.09
Maui 4 (MS)	25.23	-	-	-	8.13
Maui 5 (MS)	25.18	-	-	-	8.13
Maui 6 (MS)	25.11	-	-	-	8.13
Maui 7 (MS)	25.29	-	-	-	8.13
Maui 8 (MS)	25.26	-	-	-	8.13
Maui 9 (MS)	25.26	-	-	-	8.13
Seep 1 Piez-1 (SS)	-	-	-	7.46	-
Seep 1 Piez-2 (SS)	-	-	-	-	-
Seep 1 Surface (MS)	25.86	52.4	34.50	-	-
Seep 2 Surface (MS)	26.04	52.24	34.37	-	-
Seep 2 Piez-1 (SS)	-	-	-	14.72	-
Seep 3 Piez-1 (SS)	-	-	-	10.56	-
Seep 3 Surface (MS)	25.91	51.25	33.64	-	-
Seep 4 Piez-1 (SS)	-	-	-	-	-
Seep 4 Surface (MS)	-	-	-	-	-
Wahikuli (MS)	25.97	-	-	-	8.03

Table 6-6: September, 2011 Temperature, Specific Conductivity, Salinity, and pH (- denotes measurement not available)

Sample Name (Type)	Temperature (°C)	Specific Conductivity (ms/cm)	Field Salinity (PSU)	Lab Salinity (PSU)	pH
Black Rock 1 (TS)	25.75	5.714	3.06	-	7.84
Black Rock 2 (TS)	25.88	36.69	23.12	-	7.97
Hahakea 2 (PW)	20.49	0.695	0.34	0.33	7.97
Honokowai B (PW)	19.74	1.318	0.66	0.64	7.88
Kaanapali GC-R1 Pond (TS)	29.75	2.274	1.16	1.13	7.56
Kaanapali P-1 (PW)	20.70	0.498	0.24	0.23	7.90
Kaanapali P-2 (PW)	19.58	1.084	0.54	0.53	7.85
Kaanapali P-4 (PW)	19.44	1.012	0.50	0.49	8.05
Kaanapali P-5 (PW)	19.13	0.787	0.39	0.38	7.99
Kaanapali P-6 (PW)	19.91	0.431	0.21	0.21	8.07
Lahaina Deep Monitor (MW)	22.66	1.795	0.91	0.81	7.97
LWRF-R1 (TW)	29.64	2.207	1.12	1.10	7.08
LWRF Treated Effluent (TW)	29.33	2.169	1.10	1.10	7.13
Maui 19 (MS)	26.07	52.08	34.25	-	8.10
Maui 20 (MS)	26.12	52.57	34.61	-	8.10
Maui 21 (MS)	25.84	52.53	34.58	-	8.09
Maui 22 (MS)	25.87	52.37	34.46	-	8.09
Maui 23 (MS)	25.74	51.90	34.14	-	8.09
Maui 24 (MS)	25.98	52.38	34.47	-	8.10
Maui 25 (MS)	25.98	52.42	34.5	-	8.10
Maui 26 (MS)	25.83	52.44	34.52	-	8.09
Maui 27 (MS)	25.54	52.11	34.28	-	8.07
Maui 28 (MS)	25.89	52.24	34.26	-	8.11
Maui 29 (MS)	25.93	52.43	34.51	-	8.10
Maui 30 (MS)	26.14	52.54	34.58	-	8.11
Maui 31 (MS)	26.23	52.55	34.58	-	8.11
Maui 32 (MS)	26.29	52.54	34.58	-	8.11
Maui 33 (MS)	26.25	52.48	34.53	-	8.11
Maui 34 (MS)	26.14	52.51	34.56	-	8.11

Table 6-6 continued:

Maui 35 (MS)	26.45	52.52	34.56	-	8.11
Maui 36 (MS)	26.34	52.51	34.55	-	8.11
Maui DP 14 (MS)	26.30	52.65	34.66	-	8.09
Maui DP 3 (MS)	26.31	52.56	34.59	-	8.03
Maui DP12 (MS)	26.26	52.62	34.64	-	8.09
Seep 1 Surface (MS)	26.49	51.72	33.97	-	8.14
Seep 1-2 Piez (SS)	-	-	-	2.92	-
Seep 3 Surface (MS)	26.69	52.23	34.34	-	8.14
Seep 3-2 Piez (SS)	-	-	-	4.80	-

Table 6-7: June, 2011 Nutrient Data in μM

Sample Name (Type)	TP (μM)	TN (μM)	PO_4^{3-} (μM)	SiO_4^{4-} (μM)	NO_3^- (μM)	NO_2^- (μM)	NH_4^+ (μM)
Hahakea 2 (PW)	8.14	149.43	6.18	785.18	101.32	0.05	0.15
Honokowai (MS)	0.41	6.70	0.08	10.34	0.36	0.02	0.01
Honokowai B (PW)	1.97	20.82	1.64	781.69	14.64	0.06	0.07
Honolua 1 (MS)	0.43	6.71	0.14	30.97	0.31	0.02	0.19
Honolua 2 (MS)	0.48	6.85	0.19	20.93	0.29	0.02	0.27
Honolua Ditch (TS)	0.68	6.25	0.57	351.69	4.40	0.06	0.04
Kaanapali 1 (TS)	7.41	288.55	3.51	914.17	225.96	0.68	2.53
Kaanapali 2 (TS)	7.22	268.08	5.13	902.45	222.48	0.56	0.21
Kaanapali GC-1 (TS)	3.06	147.37	1.72	723.02	55.53	2.23	5.94
Kaanapali GC-2 (TS)	4.55	57.10	2.00	658.42	0.74	0.19	9.19
Kaanapali P-1 (PW)	5.95	55.66	3.27	732.53	26.33	0.14	0.06
Kaanapali P-2 (PW)	4.62	74.25	3.38	658.88	32.98	0.06	0.06
Kaanapali P-4 (PW)	2.73	134.04	1.91	648.90	121.85	0.05	0.09
Kaanapali P-5 (PW)	1.93	111.52	1.54	638.80	82.23	0.06	0.10
Kaanapali P-6 (PW)	2.23	173.35	2.21	658.05	136.73	0.09	0.21
Kahana Stream (TS)	8.24	140.98	1.62	172.74	0.09	0.14	4.07
Lahaina Deep Monitor (MW)	2.94	167.13	1.68	576.94	114.75	0.44	0.00
LWRF Treated Effluent (TW)	6.66	517.10	3.30	613.42	188.50	37.81	93.26
Maui 1 (MS)	0.49	6.16	0.23	16.16	1.61	0.02	0.02

Table 6-7 Continued

Maui 10 (MS)	0.39	5.24	0.15	6.14	1.08	0.03	0.12
Maui 11 (MS)	0.38	5.60	0.12	6.42	0.32	0.02	0.00
Maui 12 (MS)	0.41	7.10	0.16	8.71	2.29	0.02	0.00
Maui 13 (MS)	0.44	5.42	0.14	6.10	0.18	0.02	0.00
Maui 14 (MS)	0.42	5.42	0.18	6.96	1.27	0.02	0.09
Maui 15 (MS)	0.41	5.20	0.15	6.08	2.23	0.02	0.04
Maui 16 (MS)	0.39	4.95	0.12	6.50	1.02	0.02	0.00
Maui 17 (MS)	0.38	4.59	0.14	6.92	0.20	0.02	0.00
Maui 18 (MS)	0.40	5.01	0.15	7.49	0.60	0.03	0.00
Maui 2 (MS)	0.59	13.30	0.29	30.23	7.62	0.03	0.07
Maui 3 (MS)	0.36	4.61	0.16	4.79	0.96	0.02	0.03
Maui 4 (MS)	0.40	5.97	0.13	4.77	0.19	0.02	0.00
Maui 5 (MS)	0.42	7.51	0.16	13.10	2.14	0.03	0.00
Maui 6 (MS)	0.64	16.55	0.33	44.47	10.42	0.05	0.16
Maui 7 (MS)	0.41	5.39	0.14	4.88	0.28	0.02	0.00
Maui 8 (MS)	0.39	5.68	0.16	5.59	0.26	0.02	0.09
Maui 9 (MS)	0.38	4.96	0.13	5.00	0.42	0.02	0.00
Seep 1 Surface (MS)	0.47	6.02	0.20	6.73	0.32	0.02	0.13
Seep 1 Piez-1 (SS)	13.58	39.86	11.54	708.57	25.82	2.12	0.44
Seep 1 Piez-2 (SS)	13.25	46.46	11.79	734.20	26.15	2.20	0.48

Table 6-7 Continued

Seep 2 Surface (MS)	0.47	5.69	0.22	8.15	0.27	0.02	0.10
Seep 2 Piez-1 (SS)	13.03	23.28	11.58	426.64	10.13	1.23	0.27
Seep 3 Surface (MS)	0.52	5.33	0.28	17.61	0.54	0.04	0.00
Seep 3 Piez-1 (SS)	11.30	29.10	9.00	543.94	17.16	0.99	0.39
Wahikuli (MS)	1.09	21.84	0.84	31.84	3.55	0.02	0.71

Table 6-8: June, 2011 Nutrient Data in µg/L

Sample Name (Type)	TP (µg/L as P)	TN (µg/L as N)	PO_4^{3-} (µg/L as P)	SiO_4^{4-} (µg/L as Si)	NO_3^- (µg/L as N)	NO_2^- (µg/L as N)	NH_4^+ (µg/L as N)
Hahakea 2 (PW)	252.1	2093.5	191.4	22055.7	1419.5	0.7	2.1
Honokowai (MS)	12.7	93.9	2.5	290.5	5.0	0.3	0.1
Honokowai B (PW)	61.0	291.7	50.8	21957.7	205.1	0.8	1.0
Honolua 1 (MS)	13.3	94.0	4.3	869.9	4.3	0.3	2.7
Honolua 2 (MS)	14.9	96.0	5.9	587.9	4.1	0.3	3.8
Honolua Ditch (TS)	21.1	87.6	17.7	9879.0	61.6	0.8	0.6
Kaanapali 1 (TS)	229.5	4042.6	108.7	25679.0	3165.7	9.5	35.4
Kaanapali 2 (TS)	223.6	3755.8	158.9	25349.8	3116.9	7.8	2.9
Kaanapali GC-1 (TS)	94.8	2064.7	53.3	20309.6	778.0	31.2	83.2
Kaanapali GC-2 (TS)	140.9	800.0	61.9	18495.0	10.4	2.7	128.8
Kaanapali P-1 (PW)	184.3	779.8	101.3	20576.8	368.9	2.0	0.8
Kaanapali P-2 (PW)	143.1	1040.2	104.7	18507.9	462.0	0.8	0.8
Kaanapali P-4 (PW)	84.5	1877.9	59.2	18227.6	1707.1	0.7	1.3
Kaanapali P-5 (PW)	59.8	1562.4	47.7	17943.9	1152.0	0.8	1.4
Kaanapali P-6 (PW)	69.1	2428.6	68.4	18484.6	1915.6	1.3	2.9
Kahana Stream (TS)	255.2	1975.1	50.2	4852.3	1.3	2.0	57.0
Lahaina Deep Monitor (MW)	91.1	2341.5	52.0	16206.2	1607.6	6.2	0.0
LWRF Treated Effluent (TW)	206.3	7244.6	102.2	17231.0	2640.9	529.7	1306.6
Maui 1 (MS)	15.2	86.3	7.1	453.9	22.6	0.3	0.3

Table 6-8 Continued

Maui 10 (MS)	12.1	73.4	4.6	172.5	15.1	0.4	1.7
Maui 11 (MS)	11.8	78.5	3.7	180.3	4.5	0.3	0.0
Maui 12 (MS)	12.7	99.5	5.0	244.7	32.1	0.3	0.0
Maui 13 (MS)	13.6	75.9	4.3	171.3	2.5	0.3	0.0
Maui 14 (MS)	13.0	75.9	5.6	195.5	17.8	0.3	1.3
Maui 15 (MS)	12.7	72.9	4.6	170.8	31.2	0.3	0.6
Maui 16 (MS)	12.1	69.3	3.7	182.6	14.3	0.3	0.0
Maui 17 (MS)	11.8	64.3	4.3	194.4	2.8	0.3	0.0
Maui 18 (MS)	12.4	70.2	4.6	210.4	8.4	0.4	0.0
Maui 2 (MS)	18.3	186.3	9.0	849.2	106.8	0.4	1.0
Maui 3 (MS)	11.1	64.6	5.0	134.6	13.4	0.3	0.4
Maui 4 (MS)	12.4	83.6	4.0	134.0	2.7	0.3	0.0
Maui 5 (MS)	13.0	105.2	5.0	368.0	30.0	0.4	0.0
Maui 6 (MS)	19.8	231.9	10.2	1249.2	146.0	0.7	2.2
Maui 7 (MS)	12.7	75.5	4.3	137.1	3.9	0.3	0.0
Maui 8 (MS)	12.1	79.6	5.0	157.0	3.6	0.3	1.3
Maui 9 (MS)	11.8	69.5	4.0	140.5	5.9	0.3	0.0
Seep 1 Surface (MS)	14.6	84.3	6.2	189.0	4.5	0.3	1.8
Seep 1 Piez-1 (SS)	420.6	558.4	357.4	19903.7	361.7	29.7	6.2
Seep 1 Piez-2 (SS)	410.4	650.9	365.1	20623.7	366.4	30.8	6.7

Table 6-8 Continued

Seep 2 Surface (MS)	14.6	79.7	6.8	228.9	3.8	0.3	1.4
Seep 2 Piez-1 (SS)	403.5	326.2	358.6	11984.3	141.9	17.2	3.8
Seep 3 Surface (MS)	16.1	74.7	8.7	494.7	7.6	0.6	0.0
Seep 3 Piez-1 (SS)	350.0	407.7	278.7	15279.3	240.4	13.9	5.5
Wahikuli (MS)	33.8	306.0	26.0	894.4	49.7	0.3	9.9

Table 6-9: September, 2011 Nutrient Data in μM

Sample Name (Type)	TP (μM)	TN (μM)	PO_4^{3-} (μM)	SiO_4^{4-} (μM)	NO_3^- (μM)	NO_2^- (μM)	NH_4^+ (μM)
Black Rock 1 (TS)	8.42	339.40	4.99	860.08	246.05	0.98	3.50
Black Rock 2 (TS)	3.98	153.20	1.98	293.25	77.28	0.43	1.74
Hahakea 2 (PW)	9.96	182.67	8.19	815.90	109.47	0.11	0.16
Honokowai B (PW)	2.12	19.75	1.61	654.47	16.12	0.05	0.47
Kaanapali GC-R1 Pond (TS)	7.07	481.89	1.34	595.31	302.57	16.92	7.35
Kaanapali P-1 (PW)	6.15	62.49	5.57	846.99	36.66	0.07	0.51
Kaanapali P-2 (PW)	4.51	56.14	3.62	737.37	29.61	0.07	0.44
Kaanapali P-4 (PW)	2.62	127.06	2.03	666.70	119.26	0.07	0.46
Kaanapali P-5 (PW)	2.33	104.26	1.75	638.96	81.77	0.07	0.44
Kaanapali P-6 (PW)	3.00	178.44	2.48	652.28	177.48	0.08	0.47
Lahaina Deep Monitor (MW)	2.36	196.92	1.79	643.81	86.35	0.20	1.19
LWRF-R1 (TW)	6.15	432.63	3.43	586.06	226.41	30.18	19.04
LWRF Treated Effluent (TW)	5.29	457.87	2.27	601.38	246.52	36.33	11.10
Maui 19 (MS)	0.46	13.76	0.22	15.07	0.91	0.06	0.10
Maui 20 (MS)	0.40	11.85	0.12	5.25	0.19	0.04	0.07
Maui 21 (MS)	0.37	10.71	0.12	5.24	0.17	0.03	0.02
Maui 22 (MS)	0.42	13.97	0.16	9.25	0.96	0.03	0.15
Maui 23 (MS)	0.51	16.08	0.20	17.28	2.94	0.06	0.18
Maui 24 (MS)	0.40	12.42	0.14	7.62	0.54	0.03	0.11

Table 6-9 Continued

Maui 25 (MS)	0.42	12.67	0.16	6.41	0.30	0.04	0.18
Maui 26 (MS)	0.39	12.18	0.13	5.32	0.14	0.03	0.20
Maui 27 (MS)	0.39	9.82	0.12	8.65	0.27	0.04	0.18
Maui 28 (MS)	0.41	12.34	0.13	7.84	0.52	0.04	0.13
Maui 29 (MS)	0.39	12.71	0.12	5.56	0.33	0.03	0.07
Maui 30 (MS)	0.38	11.57	0.11	3.81	0.05	0.02	0.05
Maui 31 (MS)	0.38	11.93	0.10	3.80	0.02	0.02	0.02
Maui 32 (MS)	0.39	12.34	0.10	3.66	0.00	0.02	0.02
Maui 33 (MS)	0.36	9.08	0.12	4.05	0.19	0.02	0.06
Maui 34 (MS)	0.40	13.52	0.10	3.64	0.02	0.02	0.01
Maui 35 (MS)	0.41	12.42	0.09	3.63	0.02	0.02	0.04
Maui 36 (MS)	0.38	11.65	0.09	3.49	0.02	0.02	0.05
Maui DP 14 (MS)	0.42	13.36	0.10	3.67	0.54	0.02	0.04
Maui DP 3 (MS)	0.43	12.42	0.16	5.81	0.28	0.03	0.10
Maui DP12 (MS)	0.39	12.71	0.11	3.94	0.06	0.02	0.16
Seep 1 Surface (MS)	0.65	11.57	0.44	21.62	0.52	0.08	0.21
Seep 1-2 Piez (SS)	15.10	115.91	13.39	753.26	10.38	1.92	0.46
Seep 3 Surface (MS)	0.48	13.19	0.21	10.60	0.30	0.04	0.20
Seep 3-2 Piez (SS)	14.56	112.24	12.68	701.07	6.86	0.69	0.51

Table 6-10: September, 2011 Nutrient Data in µg/L

Sample Name (Type)	TP (µg/L as P)	TN (µg/L as N)	PO$_4^{3-}$ (µg/L as P)	SiO$_4^{4-}$ (µg/L as Si)	NO$_3^-$ (µg/L as N)	NO$_2^-$ (µg/L as N)	NH$_4^+$ (µg/L as N)
Black Rock 1 (TS)	260.8	4755.0	154.5	24159.6	3447.2	13.7	49.0
Black Rock 2 (TS)	123.3	2146.3	61.3	8237.4	1082.7	6.0	24.4
Hahakea 2 (PW)	308.5	2559.2	253.6	22918.6	1533.7	1.5	2.2
Honokowai B (PW)	65.7	276.7	49.9	18384.1	225.8	0.7	6.6
Kaanapali GC-R1 Pond (TS)	219.0	6751.3	41.5	16722.3	4239.0	237.0	103.0
Kaanapali P-1 (PW)	190.5	875.5	172.5	23791.9	513.6	1.0	7.1
Kaanapali P-2 (PW)	139.7	786.5	112.1	20712.7	414.8	1.0	6.2
Kaanapali P-4 (PW)	81.1	1780.1	62.9	18727.6	1670.8	1.0	6.4
Kaanapali P-5 (PW)	72.2	1460.7	54.2	17948.4	1145.6	1.0	6.2
Kaanapali P-6 (PW)	92.9	2499.9	76.8	18322.5	2486.5	1.1	6.6
Lahaina Deep Monitor (MW)	73.1	2758.8	55.4	18084.6	1209.8	2.8	16.7
LWRF-R1 (TW)	190.5	6061.1	106.2	16462.4	3172.0	422.8	266.8
LWRF Treated Effluent (TW)	163.8	6414.8	70.3	16892.8	3453.7	509.0	155.5
Maui 19 (MS)	14.2	192.8	6.8	423.3	12.7	0.8	1.4
Maui 20 (MS)	12.4	166.0	3.7	147.5	2.7	0.6	1.0
Maui 21 (MS)	11.5	150.0	3.7	147.2	2.4	0.4	0.3
Maui 22 (MS)	13.0	195.7	5.0	259.8	13.4	0.4	2.1
Maui 23 (MS)	15.8	225.3	6.2	485.4	41.2	0.8	2.5
Maui 24 (MS)	12.4	174.0	4.3	214.0	7.6	0.4	1.5

Table 6-10 Continued

Maui 25 (MS)	13.0	177.5	5.0	180.1	4.2	0.6	2.5
Maui 26 (MS)	12.1	170.6	4.0	149.4	2.0	0.4	2.8
Maui 27 (MS)	12.1	137.6	3.7	243.0	3.8	0.6	2.5
Maui 28 (MS)	12.7	172.9	4.0	220.2	7.3	0.6	1.8
Maui 29 (MS)	12.1	178.1	3.7	156.2	4.6	0.4	1.0
Maui 30 (MS)	11.8	162.1	3.4	107.0	0.7	0.3	0.7
Maui 31 (MS)	11.8	167.1	3.1	106.7	0.3	0.3	0.3
Maui 32 (MS)	12.1	172.9	3.1	102.8	0.0	0.3	0.3
Maui 33 (MS)	11.1	127.2	3.7	113.8	2.7	0.3	0.8
Maui 34 (MS)	12.4	189.4	3.1	102.2	0.3	0.3	0.1
Maui 35 (MS)	12.7	174.0	2.8	102.0	0.3	0.3	0.6
Maui 36 (MS)	11.8	163.2	2.8	98.0	0.3	0.3	0.7
Maui DP 14 (MS)	13.0	187.2	3.1	103.1	7.6	0.3	0.6
Maui DP 3 (MS)	13.3	174.0	5.0	163.2	3.9	0.4	1.4
Maui DP12 (MS)	12.1	178.1	3.4	110.7	0.8	0.3	2.2
Seep 1 Surface (MS)	20.1	162.1	13.6	607.3	7.3	1.1	2.9
Seep 1-2 Piez (SS)	467.6	1623.9	414.7	21159.1	145.4	26.9	6.4
Seep 3 Surface (MS)	14.9	184.8	6.5	297.8	4.2	0.6	2.8
Seep 3-2 Piez (SS)	450.9	1572.5	392.7	19693.1	96.1	9.7	7.1

Table 6-11: Submarine spring gas analysis results.

Values are reported in parts per million by dry volume. Samples were collected coeval with and at the same location as June sample Seep 2 Piez 1 (NSG). Atmosphere values are taken from the NASA Earth Fact Sheet at http://nssdc.gsfc.nasa.gov/planetary/factsheet/earthfact.html.

Sample Name	O_2 + Ar (ppm)	CO_2 (ppm)	N_2 (ppm)
Seep 2 Gas-1	84,900	860	914,200
Seep 2 Gas-2	15,000	500	984,400
Atmosphere	218,800	380	780,840

Table 6-12: June, 2011 stable isotope data
(- denotes measurement not performed)

Sample Name (Type)	$\delta^{18}O$ of H_2O (‰)[1]	δ^2H of H_2O (‰)[1]	$\delta^{15}N$ of NO_3^- (‰)[2]	$\delta^{15}N$ σ (‰)[3]	$\delta^{18}O$ of NO_3^- (‰)[1]	$\delta^{18}O$ σ (‰)[3]
Hahakea 2 (PW)	-3.77	-15.33	0.65	1.15	0.70	1.17
Honokowai B (PW)	-3.79	-15.05	3.15	1.67	-3.50	1.45
Kaanapali 1 (TS)	-	-	12.63	2.26	2.84	4.30
Kaanapali 2 (TS)	-	-	14.99	2.26	-1.82	4.30
Kaanapali GC-1 (TS)	-	-	4.96	1.67	-1.62	1.45
Lahaina Deep Monitor (MW)	-3.55	-13.75	1.80	1.67	-0.22	1.45
LWRF Treated Effluent (TW)	-	-	29.25	0.52	19.82	1.78
Maui 10 (MS)	-	-	52.46	1.00	16.35	0.82
Maui 12 (MS)	-	-	57.73	1.00	21.55	0.82
Maui 14 (MS)	-	-	55.50	1.00	15.52	0.82
Maui 15 (MS)	-	-	54.43	1.00	15.67	0.82
Maui 2 (MS)	-	-	12.71	2.26	6.55	4.30
Maui 5 (MS)	-	-	19.71	1.00	9.24	0.82
Maui 6 (MS)	-	-	18.04	0.56	9.69	0.19
Kaanapali P-1 (PW)	-3.80	-14.94	1.31	1.67	-1.74	1.45
Kaanapali P-2 (PW)	-3.75	-15.30	1.07	1.67	-0.16	1.45
Kaanapali P-4 (PW)	-3.57	-14.51	0.92	0.52	4.30	1.78
Kaanapali P-5 (PW)	-3.45	-14.46	4.19	1.67	3.00	1.45
Kaanapali P-6 (PW)	-3.39	-13.85	3.29	1.67	3.30	1.45
Seep 1 Piez-1 (SS)	-3.21	-11.01	86.47	1.15	21.56	1.17
Seep 1 Piez-2 (SS)	-	-	77.82	0.56	22.86	0.19
Seep 2 Piez-1 (SS)	-1.52	-5.19	-	-	-	-
Seep 3 Piez-1 (SS)	-3.03	-10.91	83.89	0.56	22.07	0.19
Seep 4 Piez-1 (SS)	-2.26	-7.64	-	-	-	-
Wahikuli (MS)	-	-	11.86	0.56	3.53	0.19

[1]Measured relative to VSMOW
[2]Measured relative to AIR
3Average standard deviation of standards and duplicate samples

Table 6-13: September, 2011 stable isotope data
(- denotes measurement not performed)

Sample Name (Type)	$\delta^{18}O$ of H_2O (‰)[1]	δ^2H of H_2O (‰)[1]	$\delta^{15}N$ of NO_3^- (‰)[2]	$\delta^{15}N$ σ (‰)[3]	$\delta^{18}O$ of NO_3^- (‰)[1]	$\delta^{18}O$ σ (‰)[3]
Black Rock 1 (TS)	-	-	10.12	0.23	2.29	0.49
Black Rock 2 (TS)	-	-	8.84	1.00	2.41	0.82
Hahakea 2 (PW)	-3.63	-14.69	0.91	0.23	-0.91	0.49
Honokowai B (PW)	-3.68	-14.69	2.03	0.39	-1.18	1.54
Kaanapali GC-R1 Pond (TS)	-3.09	-11.34	30.78	0.23	11.72	0.49
Lahaina Deep Monitor (PW)	-3.65	-15.70	1.98	0.39	0.79	1.54
LWRF Treated Effluent (TW)	-3.06	-11.37	30.85	0.23	15.92	0.49
LWRF-R1 (TW)	-3.12	-11.39	31.54	0.23	15.03	0.49
Maui 19 (MS)	-	-	22.80	1.00	1.76	0.82
Maui 22 (MS)	-	-	29.22	1.00	8.77	0.82
Maui 23 (MS)	0.37	2.32	17.72	1.00	4.87	0.82
Maui 25 (MS)	0.44	2.82	-	-	-	-
Maui 28 (MS)	0.39	2.24	-	-	-	-
Maui 32 (MS)	0.47	2.64	-	-	-	-
Kaanapali P-1 (PW)	-3.67	-14.64	2.32	0.23	-1.87	0.49
Kaanapali P-2 (PW)	-3.73	-15.11	2.21	0.23	-2.16	0.49
Kaanapali P-4 (PW)	-3.59	-14.65	2.00	0.39	-0.27	1.54
Kaanapali P-5 (PW)	-3.46	-14.03	2.41	0.39	0.50	1.54
Kaanapali P-6 (PW)	-3.42	-13.93	3.49	0.39	0.33	1.54
Seep 1-2 Piez (SS)	-3.10	-11.45	83.03	0.23	24.46	0.49
Seep 3-2 Piez (SS)	-2.85	-10.54	93.14	0.23	22.45	0.49

[1]Measured relative to VSMOW
[2]Measured relative to AIR
[3]Average standard deviation of standards and duplicate samples

Table 6-14: Summary of input parameters for end-member mixing calculations (eq. 6-1 to 6-3) and the ternary component fraction results for all SS samples.

$\delta^{18}O$ / δ^2H End Member Mixing Calculations

Sample Name	$\delta^{18}O$ of H_2O (‰)[1]	δ^2H of H_2O (‰)[1]	Well Fraction	Effluent Faction	Marine Fraction
Well Average	-3.62	-14.66	1.00	0.00	0.00
Effluent Average	-3.09	-11.37	0.00	1.00	0.00
Marine Average	0.42	2.51	0.00	0.00	1.00
Seep 3-2 Piez	-2.85	-10.54	0.10	0.82	0.08
Seep 1-2 Piez	-3.10	-11.45	0.03	0.96	0.00
Seep 1 Piez-1[2]	-3.21	-11.01	-0.70	1.84	-0.14
Seep 2 Piez-1	-1.52	-5.19	0.02	0.53	0.45
Seep 3 Piez-1[2]	-3.03	-10.91	-0.19	1.20	-0.01
Seep 4 Piez-1[2]	-2.26	-7.64	-0.38	1.20	0.18

$\delta^{18}O$ / [Cl⁻] End Member Mixing Calculations

Sample Name	$\delta^{18}O$ of H_2O (‰)[1]	[Cl⁻] mg/L	Well Fraction	Effluent Fraction	Marine Fraction
Well Average	-3.62	229	1.00	0.00	0.00
Effluent Average	-3.09	579	0.00	1.00	0.00
Marine Average	0.42	21355	0.00	0.00	1.00
Seep 3-2 Piez	-2.85	2792	0.28	0.60	0.11
Seep 1-2 Piez	-3.10	1711	0.43	0.51	0.06
Seep 1 Piez-1	-3.21	2085	0.80	0.12	0.09
Seep 2 Piez-1[2]	-1.52	8584	-0.46	1.08	0.38
Seep 3 Piez-1[2]	-3.03	6124	1.86	-1.16	0.30
Seep 4 Piez-1[2]	-2.26	1469	-1.44	2.42	0.02

δ^2H / [Cl⁻] End Member Mixing Calculations

Sample Name	δ^2H of H_2O (‰)[1]	[Cl⁻] mg/L	Well Fraction	Effluent Fraction	Marine Fraction
Well Average	-14.66	229	1.00	0.00	0.00
Effluent Average	-11.37	579	0.00	1.00	0.00
Marine Average	2.51	21355	0.00	0.00	1.00
Seep 3-2 Piez	-10.54	2792	0.21	0.68	0.11
Seep 1-2 Piez	-11.45	1711	0.27	0.67	0.06
Seep 1 Piez-1	-11.01	2085	0.21	0.71	0.08
Seep 2 Piez-1[2]	-5.19	8584	-0.27	0.89	0.38
Seep 3 Piez-1[2]	-10.91	6124	1.06	-0.35	0.28
Seep 4 Piez-1[2]	-7.64	1469	-1.03	2.00	0.03

[1]Measured relative to VSMOW
[2]Does not fit three-component mixing model (negative fractions)

Table 6-15: June, 2011 nutrient species percentages and molar TN:TP ratios

Sample Name (Type)	TP (µM)	Organic P (%)	PO₄³⁻ (%)	TN (µM)	Organic N (%)	NO₃⁻ (%)	NO₂⁻ (%)	NH₄⁺ (%)	N:P Ratio
Hahakea 2 (PW)	8.14	24.08	75.92	149.43	32.06	67.80	0.03	0.10	18.36
Honokowai (MS)	0.41	80.49	19.51	6.70	94.18	5.37	0.30	0.15	16.34
Honokowai B (PW)	1.97	16.75	83.25	20.82	29.06	70.32	0.29	0.34	10.57
Honolua 1 (MS)	0.43	67.44	32.56	6.71	92.25	4.62	0.30	2.83	15.60
Honolua 2 (MS)	0.48	60.42	39.58	6.85	91.53	4.23	0.29	3.94	14.27
Honolua Ditch (TS)	0.68	16.18	83.82	6.25	28.00	70.40	0.96	0.64	9.19
Kaanapali 1 (TS)	7.41	52.63	47.37	288.55	20.58	78.31	0.24	0.88	38.94
Kaanapali 2 (TS)	7.22	28.95	71.05	268.08	16.72	82.99	0.21	0.08	37.13
Kaanapali GC-1 (TS)	3.06	43.79	56.21	147.37	56.78	37.68	1.51	4.03	48.16
Kaanapali GC-2 (TS)	4.55	56.04	43.96	57.10	82.28	1.30	0.33	16.09	12.55
Kaanapali P-1 (PW)	5.95	45.04	54.96	55.66	52.34	47.31	0.25	0.11	9.35
Kaanapali P-2 (PW)	4.62	26.84	73.16	74.25	55.42	44.42	0.08	0.08	16.07
Kaanapali P-4 (PW)	2.73	30.04	69.96	134.04	8.99	90.91	0.04	0.07	49.10
Kaanapali P-5 (PW)	1.93	20.21	79.79	111.52	26.12	73.74	0.05	0.09	57.78
Kaanapali P-6 (PW)	2.23	0.90	99.10	173.35	20.95	78.88	0.05	0.12	77.74
Kahana Stream (TS)	8.24	80.34	19.66	140.98	96.95	0.06	0.10	2.89	17.11
Lahaina Deep Monitor (MW)	2.94	42.86	57.14	167.13	31.08	68.66	0.26	0.00	56.85
LWRF Treated Effluent (TW)	6.66	50.45	49.55	517.10	38.20	36.45	7.31	18.04	77.64
Maui 1 (MS)	0.49	53.06	46.94	6.16	73.21	26.14	0.32	0.32	12.57
Maui 10 (MS)	0.39	61.54	38.46	5.24	76.53	20.61	0.57	2.29	13.44

Table 6-15 Continued

Maui 11 (MS)	0.38	68.42	31.58	5.60	93.93	5.71	0.36	0.00	14.74
Maui 12 (MS)	0.41	60.98	39.02	7.10	67.46	32.25	0.28	0.00	17.32
Maui 13 (MS)	0.44	68.18	31.82	5.42	96.31	3.32	0.37	0.00	12.32
Maui 14 (MS)	0.42	57.14	42.86	5.42	74.54	23.43	0.37	1.66	12.90
Maui 15 (MS)	0.41	63.41	36.59	5.20	55.96	42.88	0.38	0.77	12.68
Maui 16 (MS)	0.39	69.23	30.77	4.95	78.99	20.61	0.40	0.00	12.69
Maui 17 (MS)	0.38	63.16	36.84	4.59	95.21	4.36	0.44	0.00	12.08
Maui 18 (MS)	0.40	62.50	37.50	5.01	87.43	11.98	0.60	0.00	12.53
Maui 2 (MS)	0.59	50.85	49.15	13.30	41.95	57.29	0.23	0.53	22.54
Maui 3 (MS)	0.36	55.56	44.44	4.61	78.09	20.82	0.43	0.65	12.81
Maui 4 (MS)	0.40	67.50	32.50	5.97	96.48	3.18	0.34	0.00	14.93
Maui 5 (MS)	0.42	61.90	38.10	7.51	71.11	28.50	0.40	0.00	17.88
Maui 6 (MS)	0.64	48.44	51.56	16.55	35.77	62.96	0.30	0.97	25.86
Maui 7 (MS)	0.41	65.85	34.15	5.39	94.43	5.19	0.37	0.00	13.15
Maui 8 (MS)	0.39	58.97	41.03	5.68	93.49	4.58	0.35	1.58	14.56
Maui 9 (MS)	0.38	65.79	34.21	4.96	91.13	8.47	0.40	0.00	13.05
Seep 1 Surface (MS)	0.47	57.45	42.55	6.02	92.19	5.32	0.33	2.16	12.81
Seep 1 Piez-1 (SS)	13.58	15.02	84.98	39.86	28.80	64.78	5.32	1.10	2.94
Seep 1 Piez-2 (SS)	13.25	11.02	88.98	46.46	37.95	56.28	4.74	1.03	3.51
Seep 2 Surface (MS)	0.47	53.19	46.81	5.69	93.15	4.75	0.35	1.76	12.11
Seep 2 Piez-1 (SS)	13.03	11.13	88.87	23.28	50.04	43.51	5.28	1.16	1.79
Seep 3 Surface (MS)	0.52	46.15	53.85	5.33	89.12	10.13	0.75	0.00	10.25

Table 6-15 Continued

Seep 3 Piez-1 (SS)	11.30	20.35	79.65	29.10	36.29	58.97	3.40	1.34	2.58
Wahikuli (MS)	1.09	22.94	77.06	21.84	80.40	16.25	0.09	3.25	20.04

Table 6-16: September, 2011 nutrient species percentages and molar TN:TP ratios

Sample Name (Type)	TP (μM)	Organic P (%)	PO$_4^{3-}$ (%)	TN (μM)	Organic N (%)	NO$_3^-$ (%)	NO$_2^-$ (%)	NH$_4^+$ (%)	N:P Ratio
Black Rock 1 (TS)	8.42	40.74	59.26	339.40	26.18	72.50	0.29	1.03	40.31
Black Rock 2 (TS)	3.98	50.25	49.75	153.20	48.14	50.44	0.28	1.14	38.49
Hahakea 2 (PW)	9.96	17.77	82.23	182.67	39.92	59.93	0.06	0.09	18.34
Honokowai B (PW)	2.12	24.06	75.94	19.75	15.75	81.62	0.25	2.38	9.32
Kaanapali GC-R1 Pond (TS)	7.07	81.05	18.95	481.89	32.18	62.79	3.51	1.53	68.16
Kaanapali P-1 (PW)	6.15	9.43	90.57	62.49	40.41	58.67	0.11	0.82	10.16
Kaanapali P-2 (PW)	4.51	19.73	80.27	56.14	46.35	52.74	0.12	0.78	12.45
Kaanapali P-4 (PW)	2.62	22.52	77.48	127.06	5.72	93.86	0.06	0.36	48.50
Kaanapali P-5 (PW)	2.33	24.89	75.11	104.26	21.08	78.43	0.07	0.42	44.75
Kaanapali P-6 (PW)	3.00	17.33	82.67	178.44	0.23	99.46	0.04	0.26	59.48
Lahaina Deep Monitor (MW)	2.36	24.15	75.85	196.92	55.44	43.85	0.10	0.60	83.44
LWRF-R1 (TW)	6.15	44.23	55.77	432.63	36.29	52.33	6.98	4.40	70.35
LWRF Treated Effluent (TW)	5.29	57.09	42.91	457.87	35.80	53.84	7.93	2.42	86.55
Maui 19 (MS)	0.46	52.17	47.83	13.76	92.22	6.61	0.44	0.73	29.91
Maui 20 (MS)	0.40	70.00	30.00	11.85	97.47	1.60	0.34	0.59	29.63
Maui 21 (MS)	0.37	67.57	32.43	10.71	97.95	1.59	0.28	0.19	28.95
Maui 22 (MS)	0.42	61.90	38.10	13.97	91.84	6.87	0.21	1.07	33.26
Maui 23 (MS)	0.51	60.78	39.22	16.08	80.22	18.28	0.37	1.12	31.53
Maui 24 (MS)	0.40	65.00	35.00	12.42	94.52	4.35	0.24	0.89	31.05
Maui 25 (MS)	0.42	61.90	38.10	12.67	95.90	2.37	0.32	1.42	30.17

Table 6-16 Continued

Maui 26 (MS)	0.39	66.67	33.33	12.18	96.96	1.15	0.25	1.64	31.23
Maui 27 (MS)	0.39	69.23	30.77	9.82	95.01	2.75	0.41	1.83	25.18
Maui 28 (MS)	0.41	68.29	31.71	12.34	94.41	4.21	0.32	1.05	30.10
Maui 29 (MS)	0.39	69.23	30.77	12.71	96.62	2.60	0.24	0.55	32.59
Maui 30 (MS)	0.38	71.05	28.95	11.57	98.96	0.43	0.17	0.43	30.45
Maui 31 (MS)	0.38	73.68	26.32	11.93	99.50	0.17	0.17	0.17	31.39
Maui 32 (MS)	0.39	74.36	25.64	12.34	99.68	0.00	0.16	0.16	31.64
Maui 33 (MS)	0.36	66.67	33.33	9.08	97.03	2.09	0.22	0.66	25.22
Maui 34 (MS)	0.40	75.00	25.00	13.52	99.63	0.15	0.15	0.07	33.80
Maui 35 (MS)	0.41	78.05	21.95	12.42	99.36	0.16	0.16	0.32	30.29
Maui 36 (MS)	0.38	76.32	23.68	11.65	99.23	0.17	0.17	0.43	30.66
Maui DP 14 (MS)	0.42	76.19	23.81	13.36	95.51	4.04	0.15	0.30	31.81
Maui DP 3 (MS)	0.43	62.79	37.21	12.42	96.70	2.25	0.24	0.81	28.88
Maui DP12 (MS)	0.39	71.79	28.21	12.71	98.11	0.47	0.16	1.26	32.59
Seep 1 Surface (MS)	0.65	32.31	67.69	11.57	93.00	4.49	0.69	1.82	17.80
Seep 1-2 Piez (SS)	15.10	11.32	88.68	115.91	88.99	8.96	1.66	0.40	7.68
Seep 3 Surface (MS)	0.48	56.25	43.75	13.19	95.91	2.27	0.30	1.52	27.48
Seep 3-2 Piez (SS)	14.56	12.91	87.09	112.24	92.82	6.11	0.61	0.45	7.71

Table 6-17: Un-mixing of Submarine Spring Dissolved Oxygen, TP, PO_4^{3-}, and SiO_4^{4-} values.
(-) indicates parameter not available.

Sample Information				Raw Values				Unmixed Values			
Study	Sample Date	Sample Name	Salinity (PSU)	Dissolved Oxygen (mg/L)	TP (μM)	PO_4^{3-} (μM)	SiO_4^{4-} (μM)	Dissolved Oxygen (mg/L)	TP (μM)	PO_4^{3-} (μM)	SiO_4^{4-} (μM)
Hunt and Rosa, 2009	May-08	L1	26.70	-	-	4.00	-	-	-	16.08	-
		L2	29.70	-	-	2.50	-	-	-	15.53	-
		L5	26.00	-	-	4.20	-	-	-	15.59	-
		Average	**27.47**	**-**	**-**	**3.57**	**-**	**-**	**-**	**15.76**	**-**
Swarzenski et al., USGS report 2012	Jul-10	T1-800-GW	4.42	1.19	-	6.03	104.30	0.53	-	6.68	114.53
		T2-900-GW	1.68	1.88	-	12.78	608.20	1.78	-	13.01	619.15
		T3-1000-GW	2.68	1.28	-	13.52	775.70	0.98	-	14.19	813.87
		T4-1100-GW	1.49	0.70	-	13.20	790.40	0.62	-	13.36	800.19
		T5-1200-GW	2.82	1.11	-	-	581.80	0.78	-	-	612.90
		T6-1300-GW	2.54	0.79	-	13.62	431.90	0.50	-	14.23	451.00
		T7-1400-GW	2.89	1.13	-	13.52	620.00	0.79	-	14.28	654.58
		T8-1500-GW	2.93	1.21	-	13.41	813.90	0.86	-	14.18	860.56
		T9-1600-GW	3.00	1.18	-	13.41	587.60	0.82	-	14.21	622.44
		T10-1700-GW	3.33	1.53	-	13.09	455.40	1.13	-	14.02	487.17
		T11-1800-GW	3.36	1.11	-	8.22	649.30	0.67	-	8.81	695.59
		Average	**2.83**	**1.19**	**-**	**12.08**	**583.50**	**0.86**	**-**	**12.74**	**614.90**
Current Study	Jun-11	Seep 1 Piez 1	7.46	-	13.58	11.54	708.57	-	16.66	14.20	870.80
		Seep 1 Piez 2	7.46[1]	-	13.25	11.79	734.20	-	16.26	14.50	902.39
		Seep 2 Piez 1	14.72	-	13.03	11.58	426.64	-	21.61	19.32	707.26
		Seep 3 Piez 1	10.56	-	11.30	9.00	543.94	-	15.57	12.46	751.41
		Average	**10.05**	**-**	**12.79**	**10.98**	**603.34**	**-**	**17.29**	**14.90**	**817.07**
	Sep-11	Seep 3-2 Piez	4.80	-	14.56	12.68	701.07	-	16.32	14.23	786.48
		Seep 1-2 Piez	2.92	-	15.10	13.39	753.26	-	15.95	14.16	796.15
		Average	**3.86**	**-**	**14.83**	**13.04**	**727.17**	**-**	**16.13**	**14.19**	**791.46**

Table 6-18 Continued

HDOH Sampling Program	Jan-12	North Seep A	3.74	3.77	12.59	-	765.65	3.48	13.64	-	830.24
		North Seep B	4.79	4.14	12.01	-	755.66	3.76	13.45	-	847.55
		North Seep C	4.56	2.78	12.79	-	767.31	2.27	14.22	-	854.20
		South Seep A	2.83	2.77	13.37	-	798.93	2.53	14.08	-	842.12
		South Seep B	4.11	3.00	13.37	-	800.60	2.59	14.66	-	878.47
		South Seep C	17.87	4.16	12.11	-	381.16	1.18	23.71	-	745.52
		Average	**6.32**	**3.44**	**12.71**	**-**	**711.55**	**2.63**	**14.98**	**-**	**839.98**

202

Table 6-18: Un-mixing of Submarine Spring N species values.
(-) indicates parameter not available.

Sample Information				Raw Values				Unmixed Values			
Study	Sample Date	Sample Name	Salinity (PSU)	TN (µM)	NO_3^- $+NO_2^-$ (µM)	NH_4^+ (µM)	Organic N (µM)	TN (µM)	NO_3^- $+NO_2^-$ (µM)	NH_4^+ (µM)	Organic N (µM)
Hunt and Rosa, 2009	May-08	L1	26.70	-	53.30	5.90	-	-	218.88	23.68	-
		L2	29.70	-	35.40	16.30	-	-	228.47	104.49	-
		L5	26.00	-	62.10	-	-	-	235.10	-	-
		Average	**27.47**	**-**	**50.27**	**11.10**	**-**	**-**	**227.59**	**49.69**	**-**
Swarzenski et al., USGS report 2012	Jul-10	T1-800-GW	4.42	11.50	10.50	0.30	0.70	12.01	11.64	0.31	0.06
		T2-900-GW	1.68	48.90	38.40	0.10	10.40	49.67	39.10	0.10	10.47
		T3-1000-GW	2.68	52.80	42.00	0.10	10.70	55.09	44.09	0.10	10.91
		T4-1100-GW	1.49	52.10	42.20	0.10	9.80	52.67	42.73	0.10	9.84
		T5-1200-GW	2.82	-	-	0.10	-	-	-	0.10	-
		T6-1300-GW	2.54	52.50	42.00	0.10	10.40	54.57	43.90	0.10	10.58
		T7-1400-GW	2.89	54.70	41.80	0.10	12.80	57.42	44.17	0.09	13.16
		T8-1500-GW	2.93	52.80	41.60	0.00	11.20	55.47	44.01	-0.01[2]	11.47
		T9-1600-GW	3.00	51.20	41.70	0.20	9.30	53.88	44.21	0.20	9.47
		T10-1700-GW	3.33	50.20	41.40	0.10	8.70	53.30	44.35	0.09	8.86
		T11-1800-GW	3.36	30.90	28.10	2.20	0.60	32.65	30.13	2.35	0.17
		Average	**2.83**	**45.76**	**36.97**	**0.31**	**8.46**	**47.90**	**38.99**	**0.32**	**8.57**
Current Study	Jun-11	Seep 1 Piez 1	7.46	39.86	27.94	0.44	11.48	47.54	34.41	0.50	12.63
		Seep 1 Piez 2	7.46[2]	46.46	28.35	0.48	17.63	55.68	34.91	0.55	20.21
		Seep 2 Piez 1	14.72	23.28	11.36	0.27	11.65	34.38	18.94	0.32	15.11
		Seep 3 Piez 1	10.56	29.10	18.15	0.39	10.56	37.77	25.17	0.47	12.13
		Average	**10.05**	**34.68**	**21.45**	**0.40**	**12.83**	**44.72**	**29.15**	**0.47**	**15.11**
	Sep-11	Seep 3-2 Piez	4.80	112.24	7.55	0.51	104.18	125.29	8.47	0.55	116.27
		Seep 1-2 Piez	2.92	115.91	12.30	0.46	103.15	122.21	13.00	0.48	108.73
		Average	**3.86**	**114.08**	**9.93**	**0.49**	**103.67**	**123.70**	**10.80**	**0.51**	**112.39**

Table 6-18 Continued

		North Seep A	3.74	15.64	13.79	0.14	1.71	16.39	14.96	0.14	1.30
		North Seep B	4.79	6.71	6.71	0.14	-	6.69	7.52	0.13	-
DOH Sampling Program	Jan-12	North Seep C	4.56	4.71	3.29	0.14	1.28	4.47	3.65	0.13	0.68
		South Seep A	2.83	4.93	1.57	0.14	3.22	4.83	1.65	0.14	3.04
		South Seep B	4.11	4.71	3.07	0.14	1.50	4.50	3.36	0.14	1.00
		South Seep C	17.87	3.57	3.21	0.21	0.15	0.35	6.24	0.23	-6.12[2]
		Average	**6.32**	**6.71**	**5.27**	**0.15**	**1.29**	**6.69**	**6.22**	**0.14**	**0.33**

[1]Salinity estimated based on earlier sample from same location.
[2]Calculated value does not conform to mixing model (negative concentration)

Table 6-19: Submarine spring (SS) $\delta^{15}N$ of NO_3^- values, un-mixed $NO_3^- + NO_2^-$ concentrations, and un-mixed $NO_3^- + NO_2^-$ fraction
Fractions are relative to the average $NO_3^- + NO_2^-$ concentration of LWRF treated wastewater effluent samples measured in this study and Hunt and Rosa (2009).

Study	Sample Date	Sample Name	$NO_3^- + NO_2^-$ (μM)	$NO_3^- + NO_2^-$ Fraction	$\delta^{15}N$ of NO_3^- (‰)[2]
Hunt and Rosa, 2009	May-08	L1	218.88	0.96	39.31
		L2	228.47	1.00	39.68
		L5	235.10	1.03	39.75
Current Study	Jun-11	Seep 1 Piez-1	34.41	0.15	86.47
		Seep 1 Piez-2	34.91	0.15	77.82
		Seep 3 Piez-1	25.17	0.11	83.89
	Sep-11	Seep 3-2 Piez	8.47	0.04	93.14
		Seep 1-2 Piez	13.00	0.06	83.03
DOH Sampling Program	Jan-12	North Seep A	14.96	0.07	112.19
		North Seep B	7.52	0.03	123.38
		North Seep C	3.65	0.02	115.53
		South Seep A	1.65	0.01	144.78
		South Seep B	3.36	0.01	130.10
		South Seep C	6.24	0.03	135.85
		LWRF Average[1]	228.39	1.00	27.58

[1] Arithmetic mean of June and September LWRF treated effluent samples measured in this study and the single LWRF effluent sample measured by Hunt and Rosa (2009)
[2] Measured relative to AIR

Figure 6-1: Kaanapali study area aerial view with major land use and location designations.
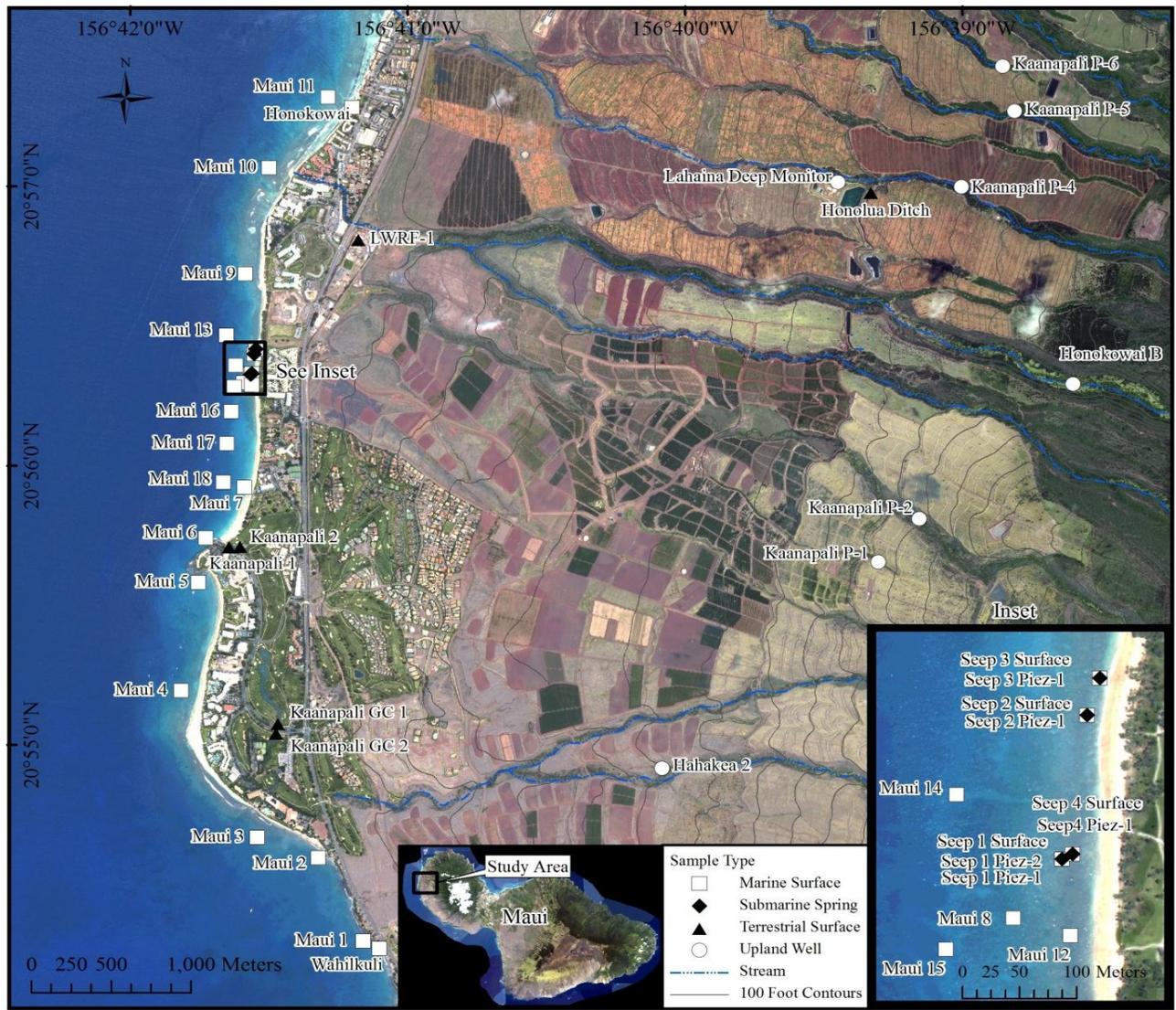
Figure 6-2: June, 2011 Sample Locations.
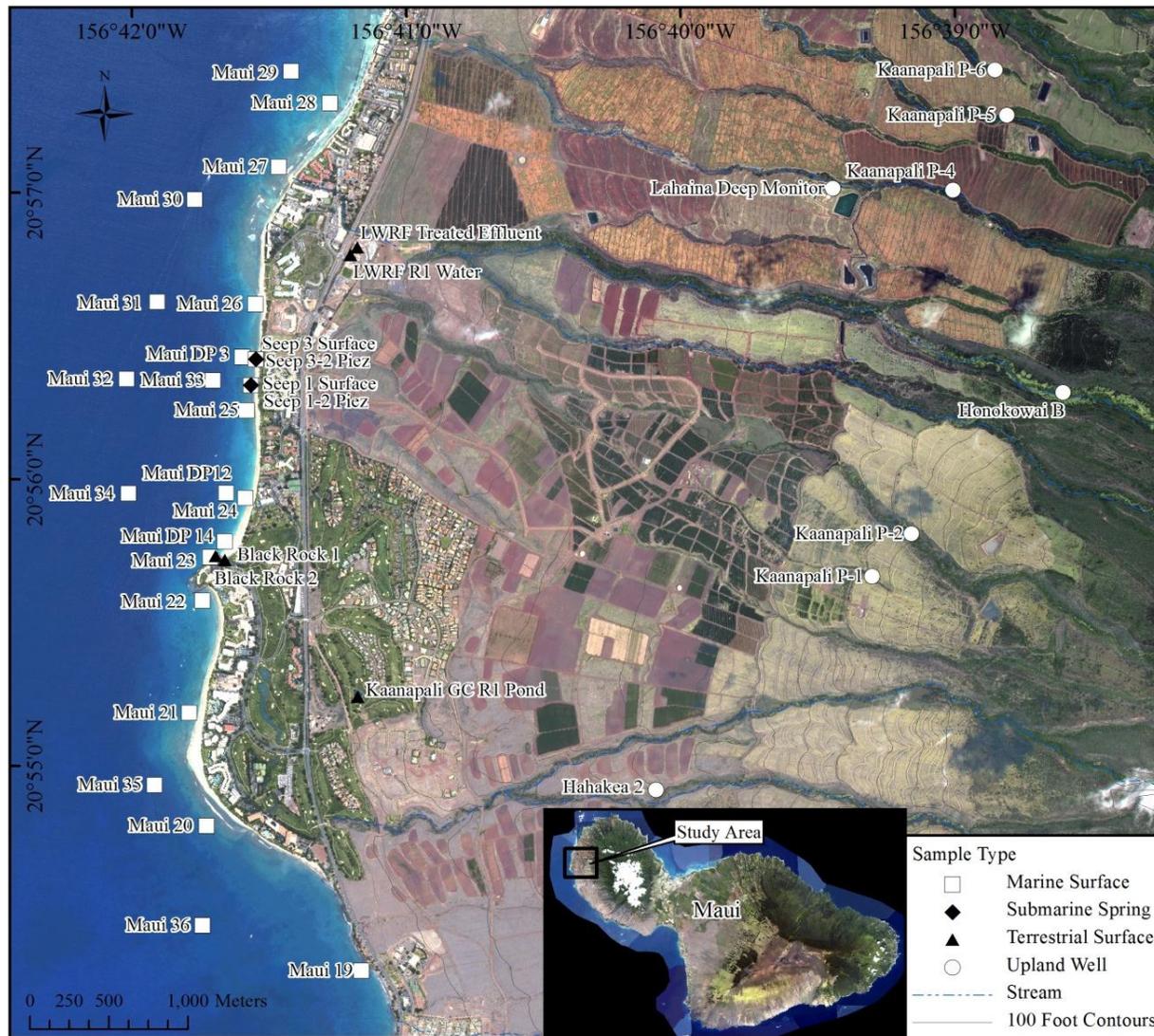
Figure 6-3: September, 2011 Sample Locations
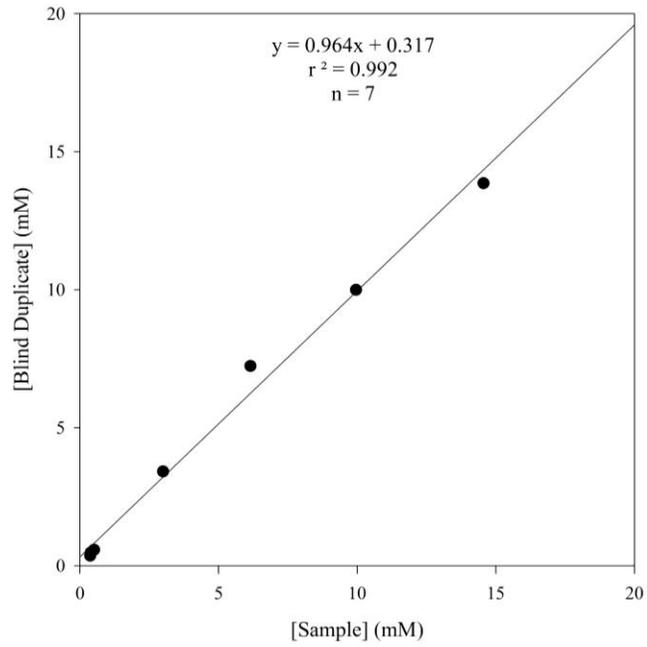
Figure 6-4: TP Blind Duplicate vs. Sample Comparison
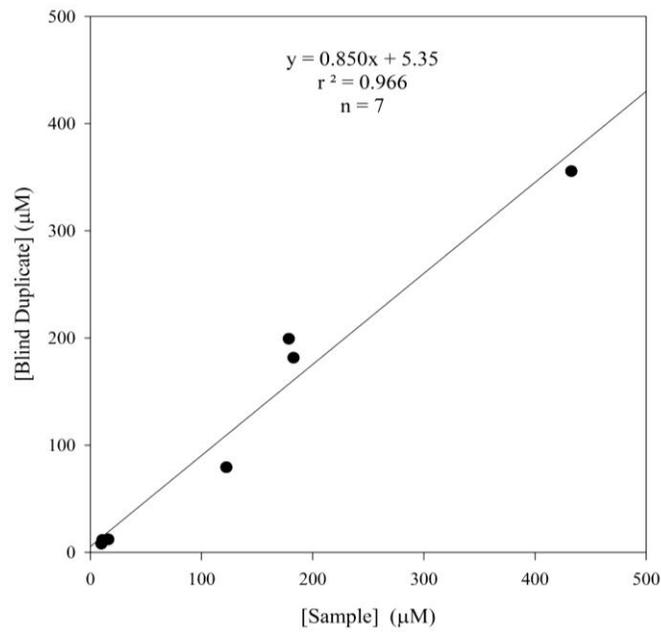
Figure 6-5: TN Blind Duplicate vs. Sample Comparison
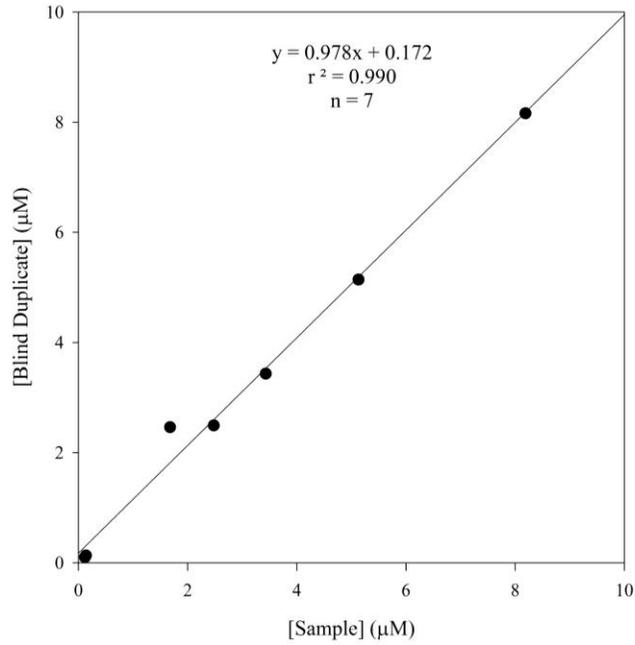
Figure 6-6: PO_4^{3-} Blind Duplicate vs. Sample Comparison
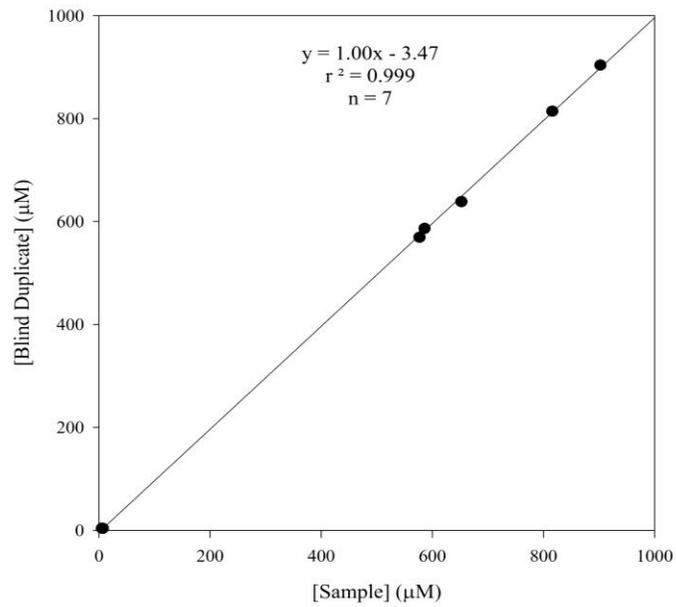
Figure 6-7: SiO_4^{4-} Blind Duplicate vs. Sample Comparison
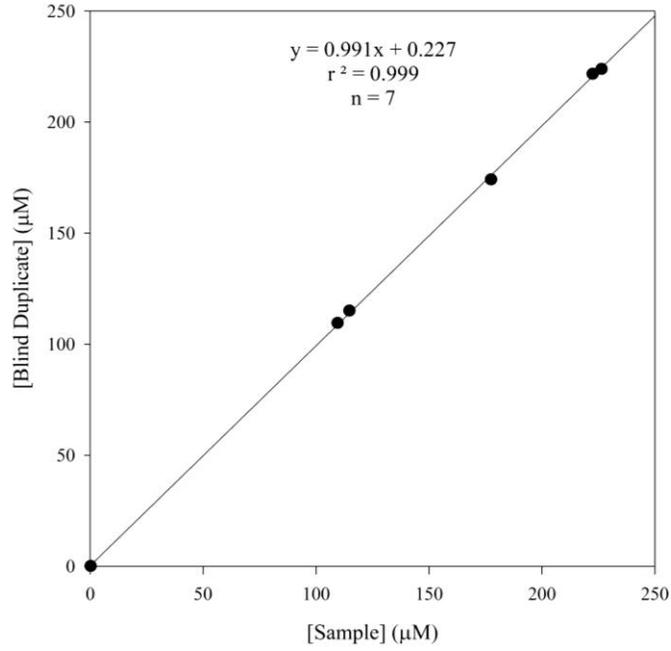
Figure 6-8: NO$_3^-$ Blind Duplicate vs. Sample Comparison
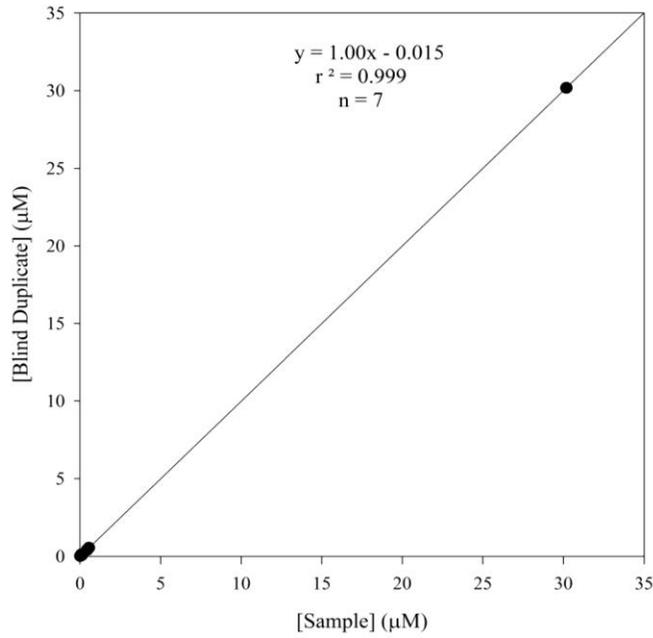
Figure 6-9: NO$_2^-$ Blind Duplicate vs. Sample Comparison
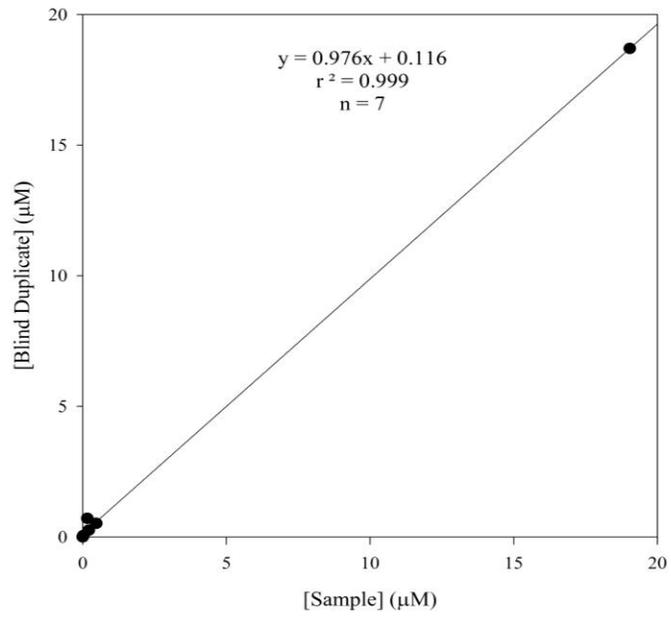
Figure 6-10: NH_4^+ Blind Duplicate vs. Sample Comparison

Figure 6-11: Nitrogen gas bubbles emanating from the seafloor near the submarine springs.
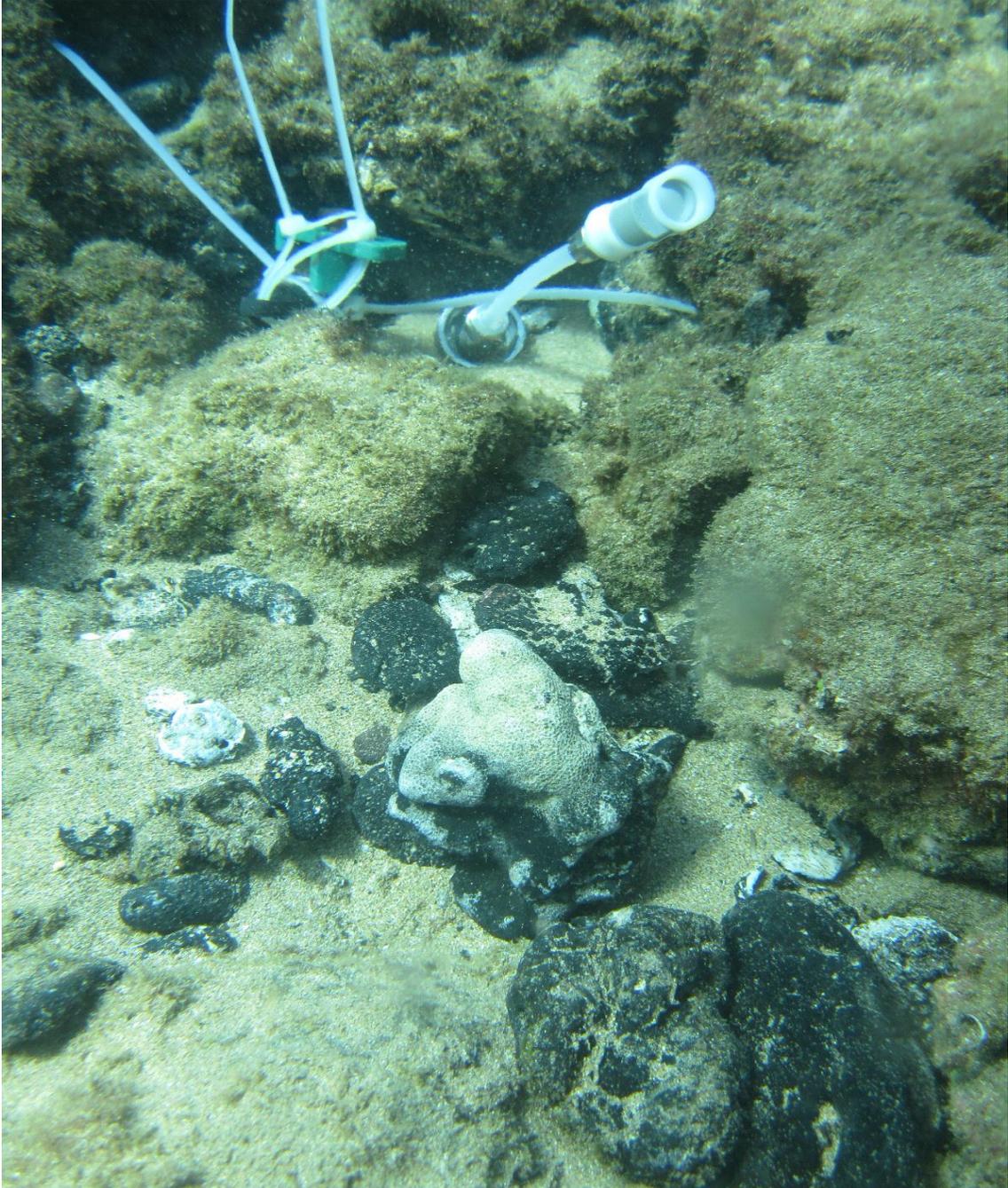
Figure 6-12: Installed piezometer surrounded by black manganese-encrusted rocks and coral rubble at one submarine spring discharge point.
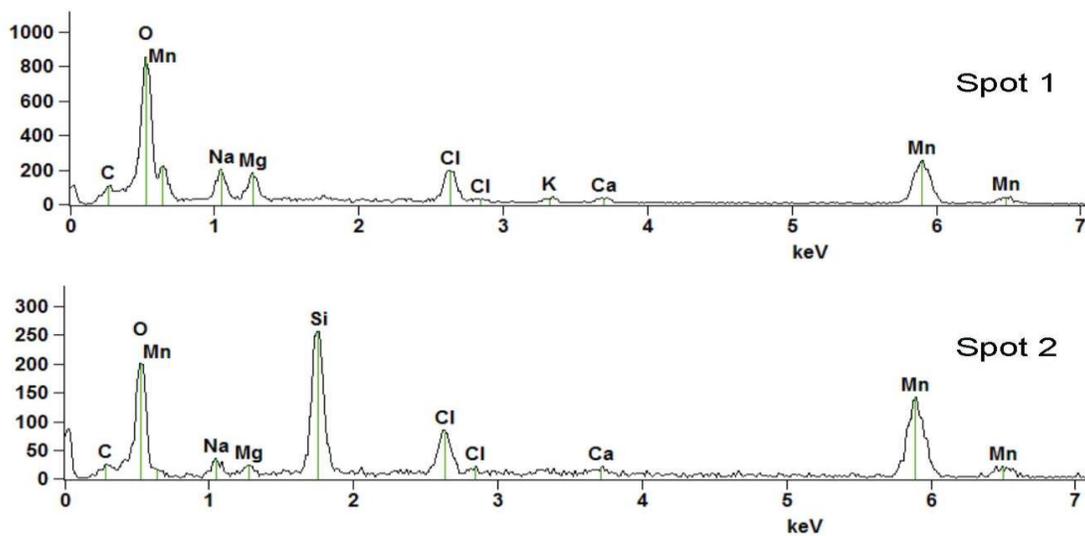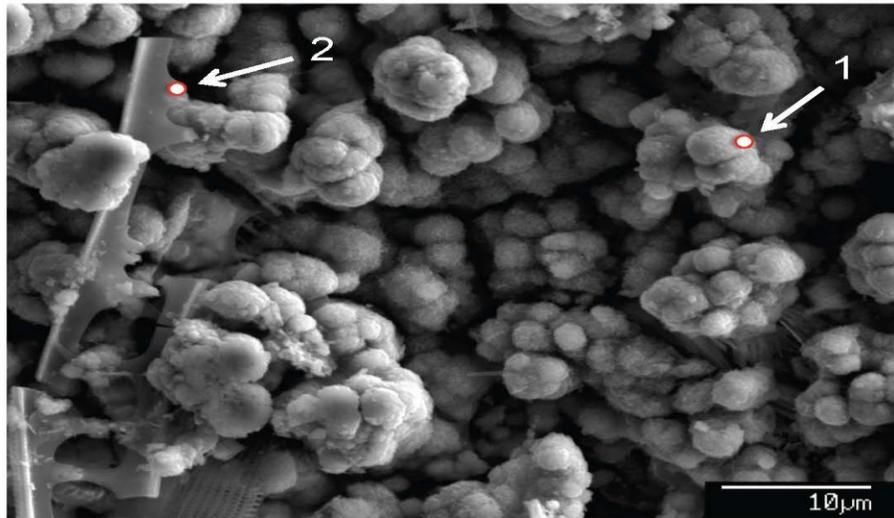
Figure 6-13: Secondary electron imagine of fine-grained manganese precipitates coating rocks/coral rubble near the submarine spring discharge points.

Spots 1 and 2 are labeled on the image above and refer to energy-dispersive X-ray spectra acquired at 15 keV acceleration potential and a beam current of 5 nA. The spherical globules are a form of MnO or perhaps other MnO-hydrous species that have precipitated from the oxidation of reduced aqueous Mn^{2+} in the submarine spring discharge by oxygenated seawater. Spot 2 is from a crushed siliceous marine diatom frustule or other siliceous skeletal grain composed of biogenic opal. Other compounds in the spectra include NaCl and perhaps $MgCl_2$. Microprobe beam diameter was 50 nm.

Figure 6-14: $\delta^{18}O$ and δ^2H values with three-component mixing triangle and LMWL determined by Scholl et al., (2002).

Figure 6-15: $\delta^{18}O$ and [Cl⁻] values with three-component mixing triangle.
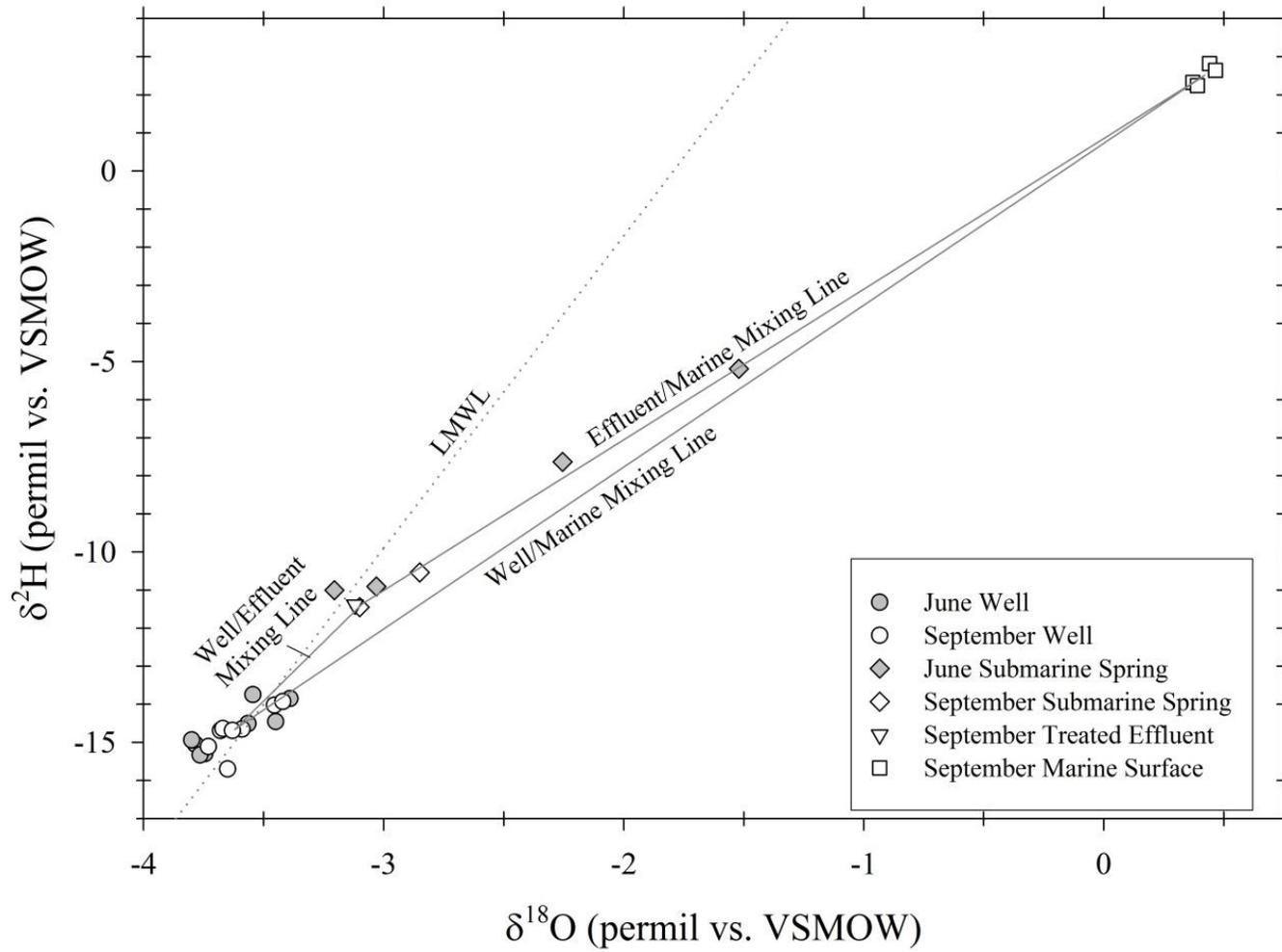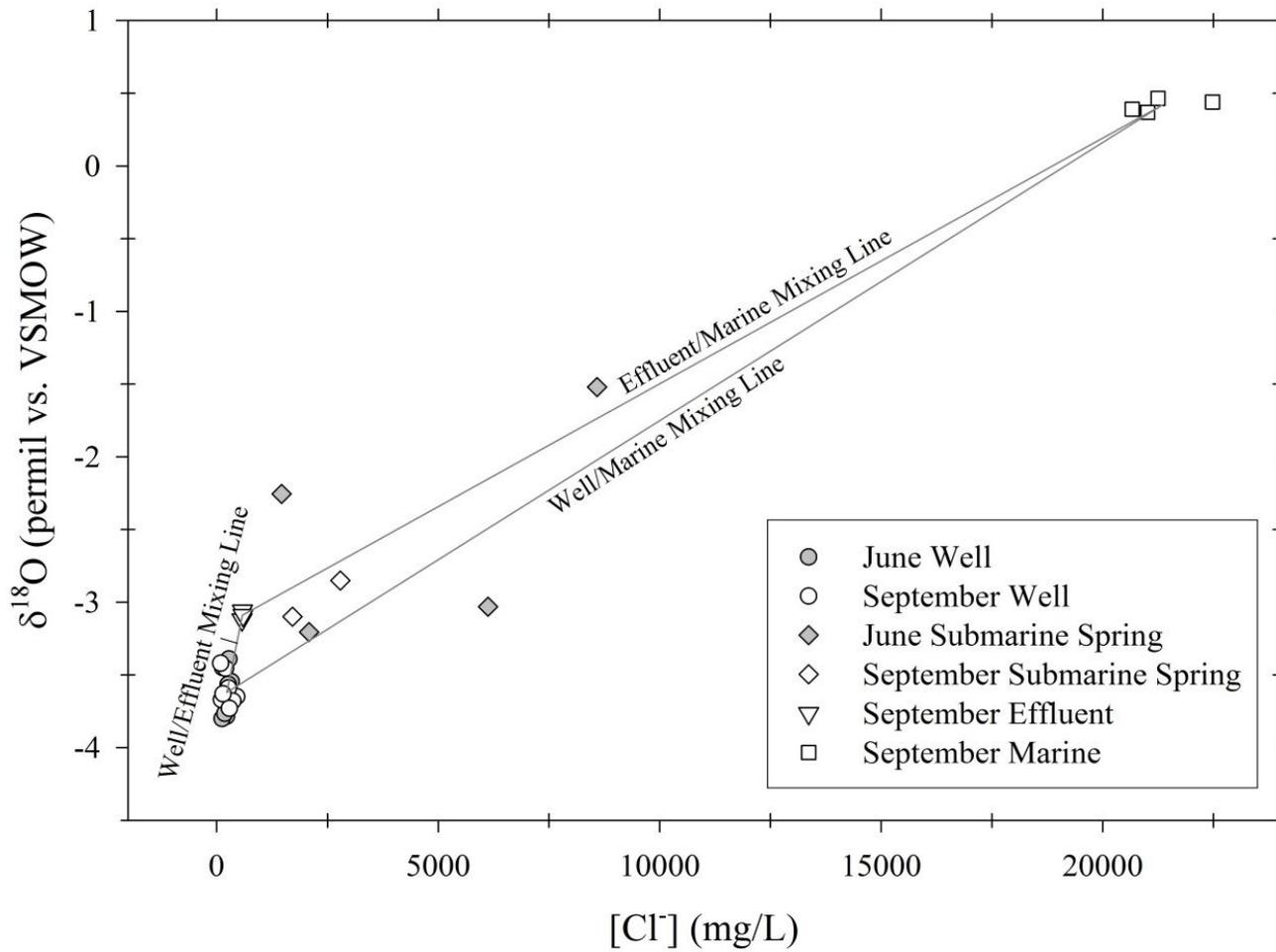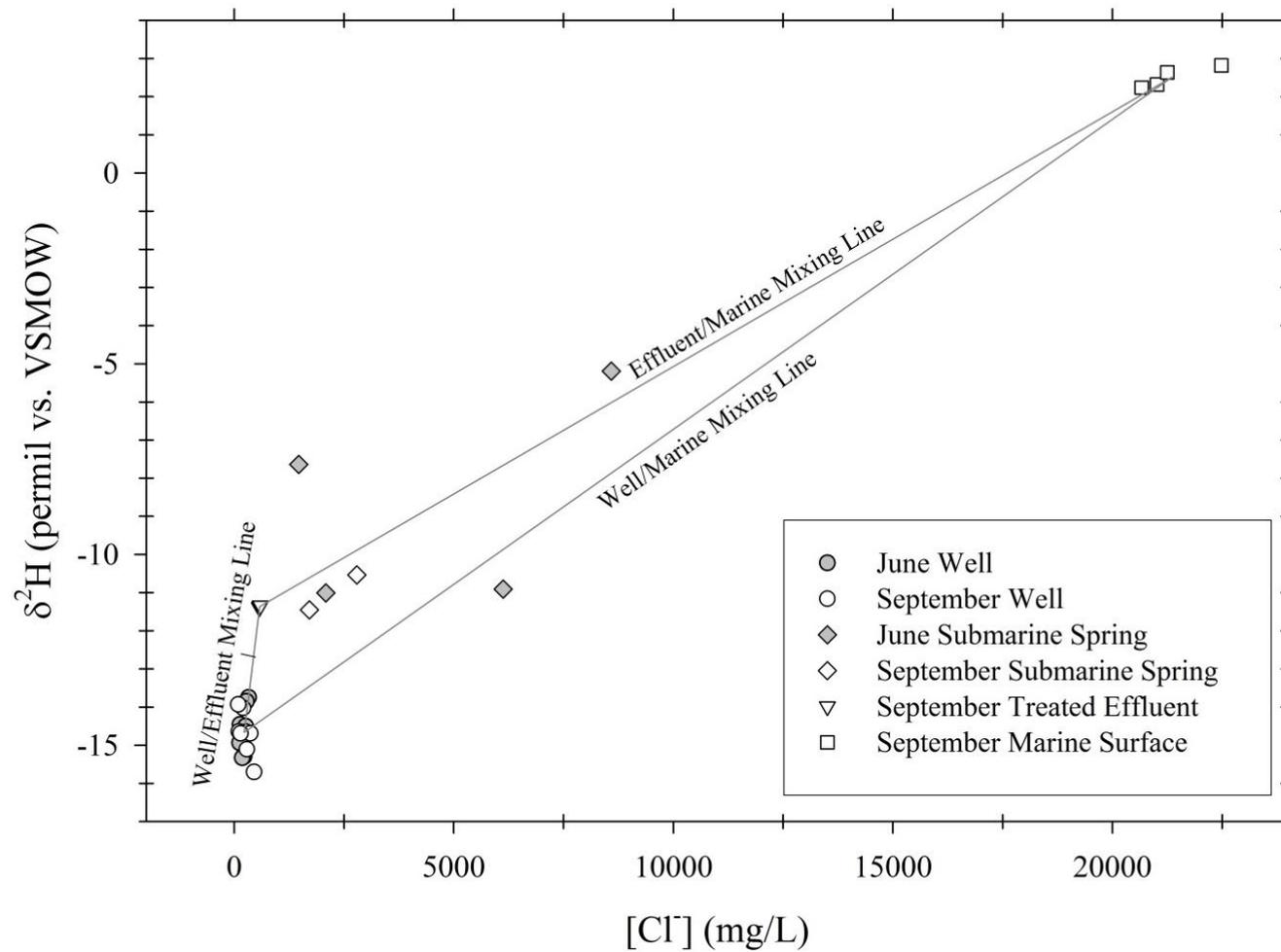
Figure 6-16: δ^2H and [Cl$^-$] values with three-component mixing triangle.
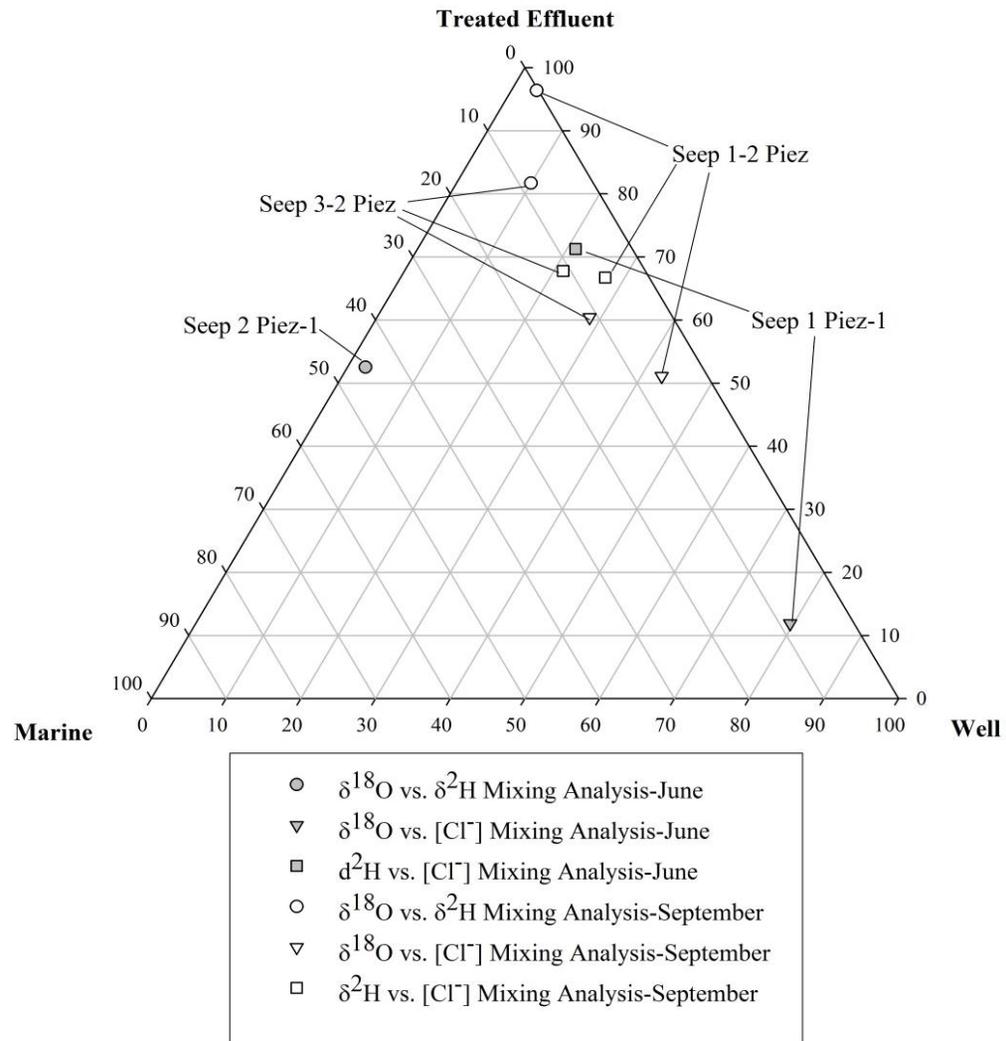
Figure 6-17: Submarine spring component percentages for samples plotting within the mixing triangles shown in Figures 6-14, 6-15, and 6-16.
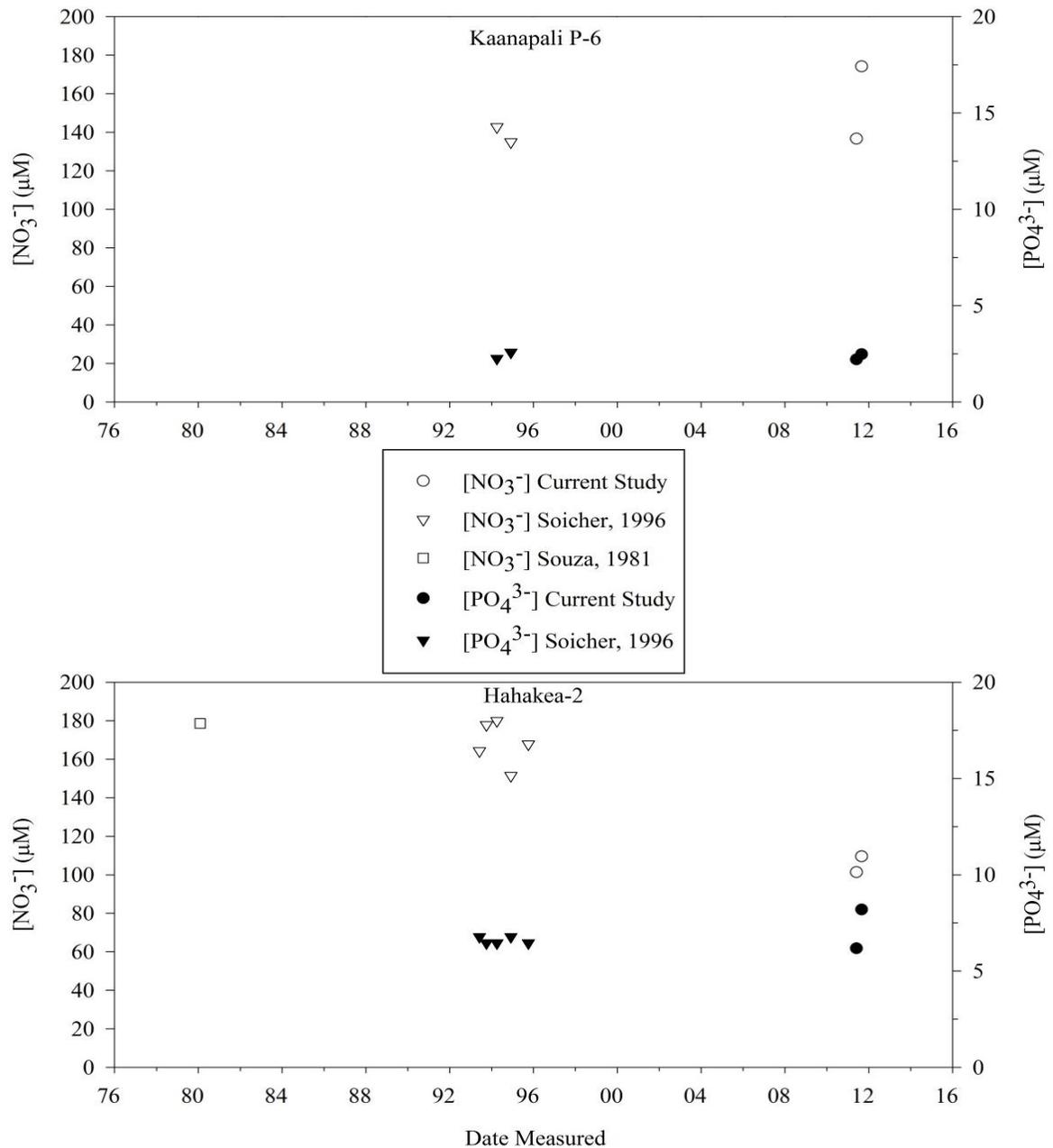
Figure 6-18: Chronology of reported NO_3^- and PO_4^{3-} concentrations for selected groundwater wells.

Wells included are Kaanapali P-6 (located on former pineapple fields) and Hahakea-2 (located on former sugarcane fields). Note the decline in NO_3^- concentration at Hahakea-2 since the cessation of sugarcane cultivation in 1999.
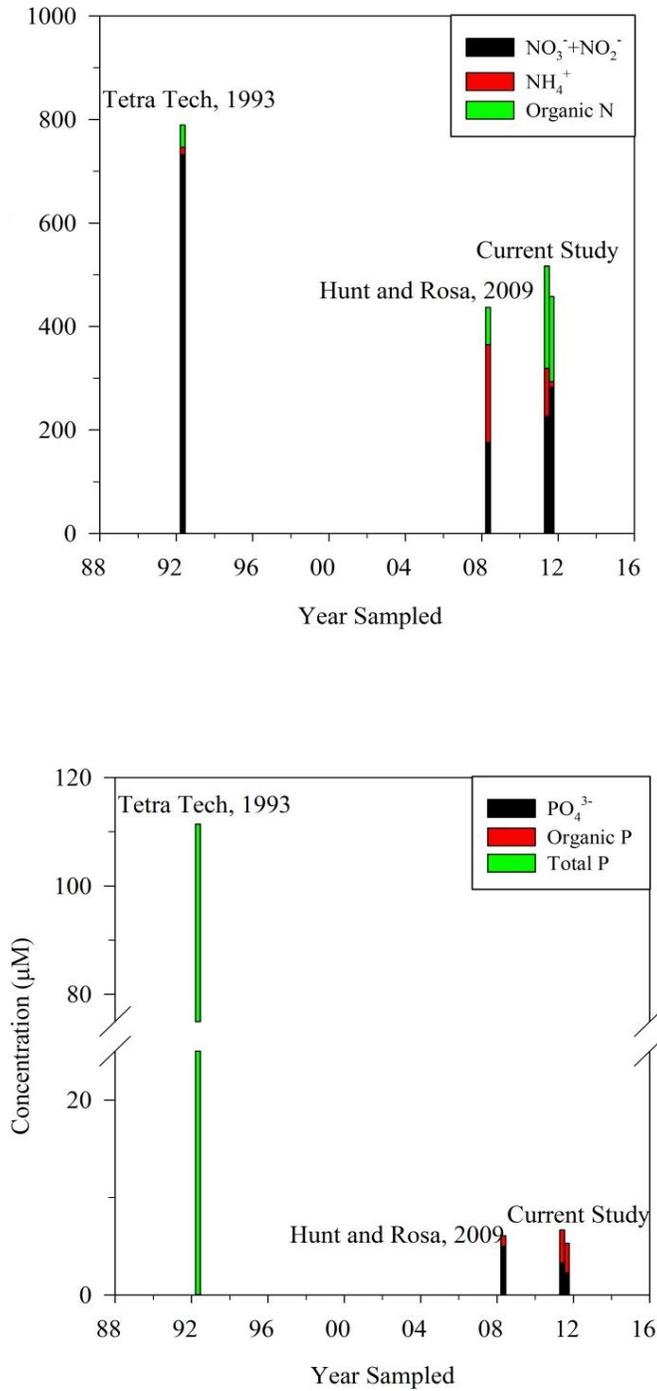
Figure 6-19: Chronology of measured values of N and P species in the LWRF effluent.

The two bars pictured under the "Current Study" label represent June and September, 2011 samples. Though considerable variability exists in the distribution of different species, both N and P concentrations are significantly lower since the inception of biological nutrient removal in 1995.
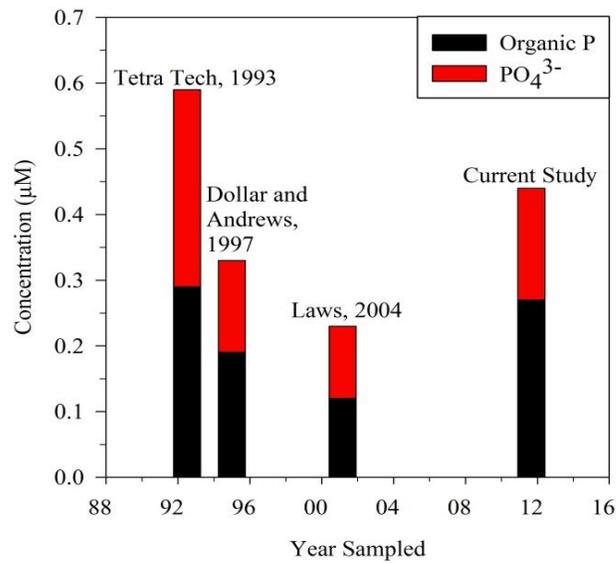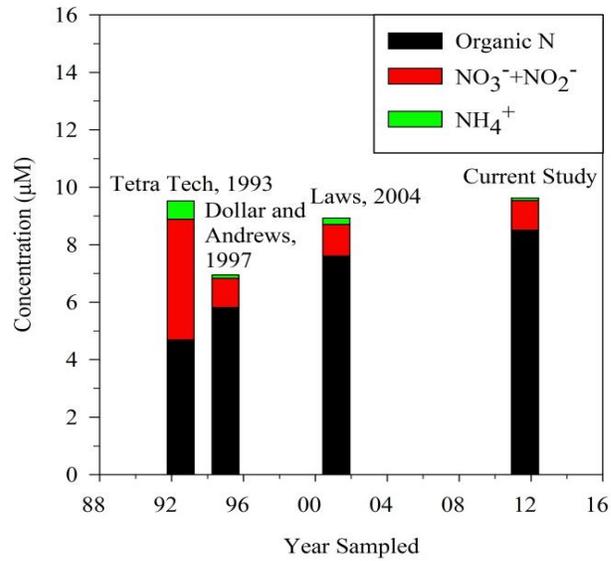
Figure 6-20: Chronology of N (top) and P (bottom) in coastal marine samples in the study area.

The single bar under the heading "Current Study" represents the arithmetic mean of June and September, 2011 samples. Though considerable variability exists, this illustration indicates that there may be to be an overall slight decrease in P species concentration and a decrease in inorganic N species concentration over time.
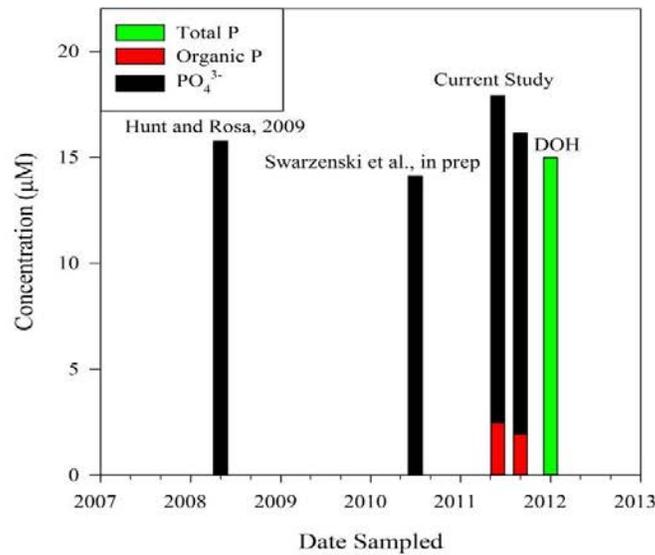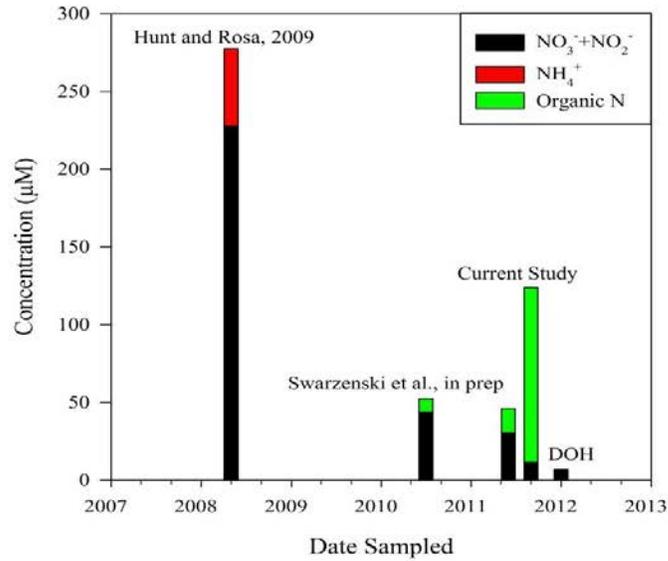
Figure 6-21: Chronology of unmixed N (top) and unmixed P (bottom) distribution in submarine spring (SS) samples.

The two bars pictured under the "Current Study" label represent June and September samples. N concentrations in general and especially inorganic N concentrations show a decrease over time, while P concentrations remain relatively constant.
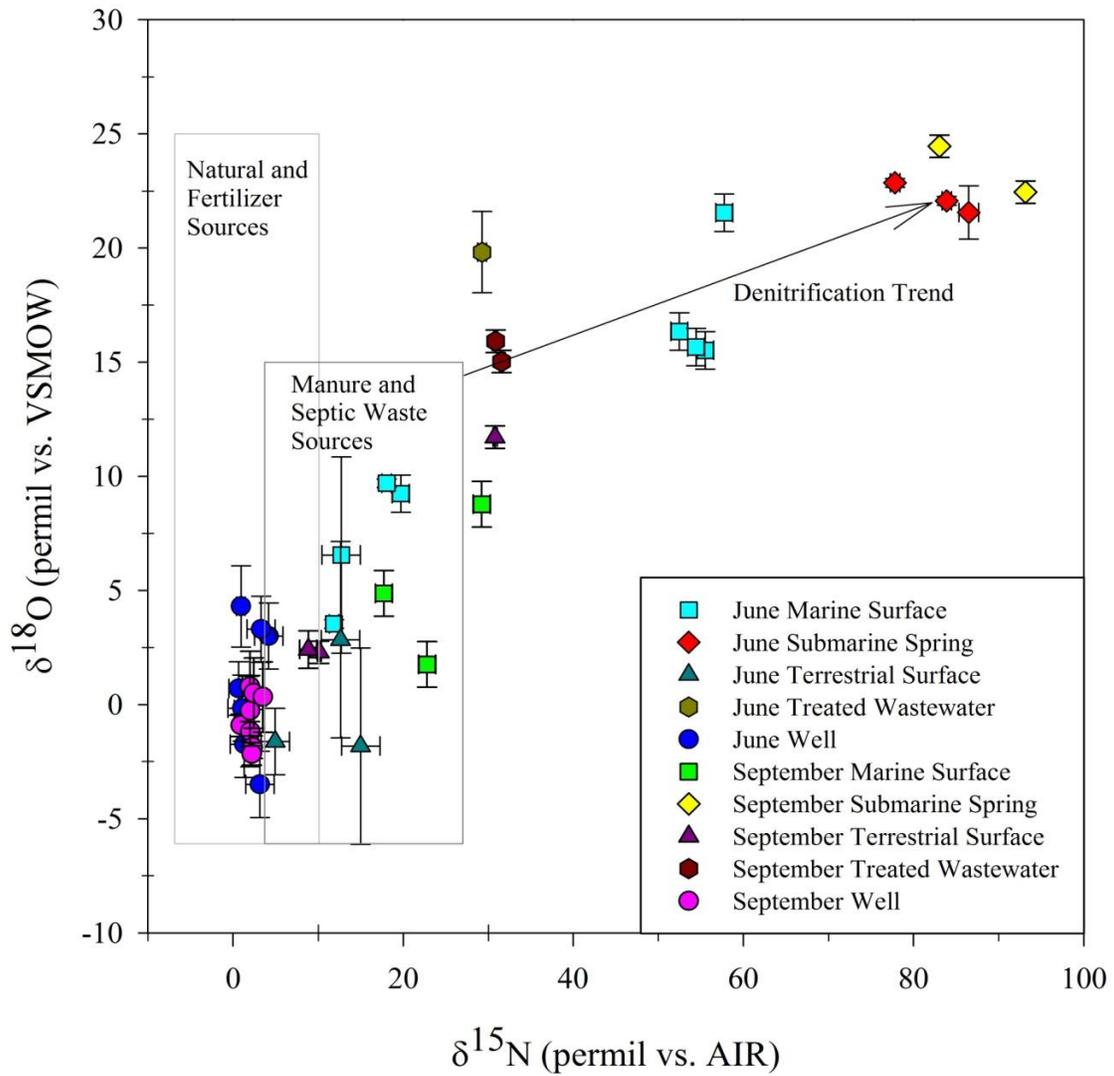
Figure 6-22: Plot of sample $\delta^{15}N$ and $\delta^{18}O$ values including typical source values and denitrification trend.

Error bars represent the one standard deviation (source fields after Kendall, 1998).

Figure 6-23: Plot of sample ln[NO$_3^-$] with δ^{15}N values.

The solid line shown represents a denitrification trend and is a linear regression of the LWRF treated wastewater effluent and submarine spring samples collected in this study. Error bars (δ^{15}N values only) represent one standard deviation.
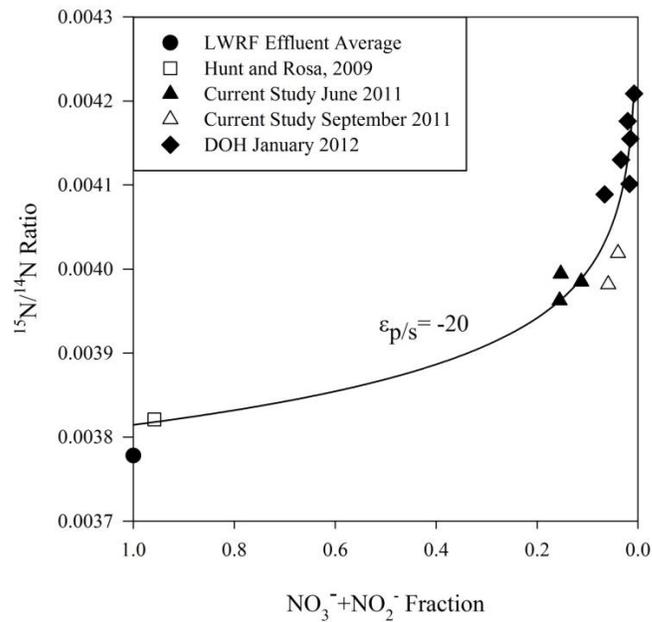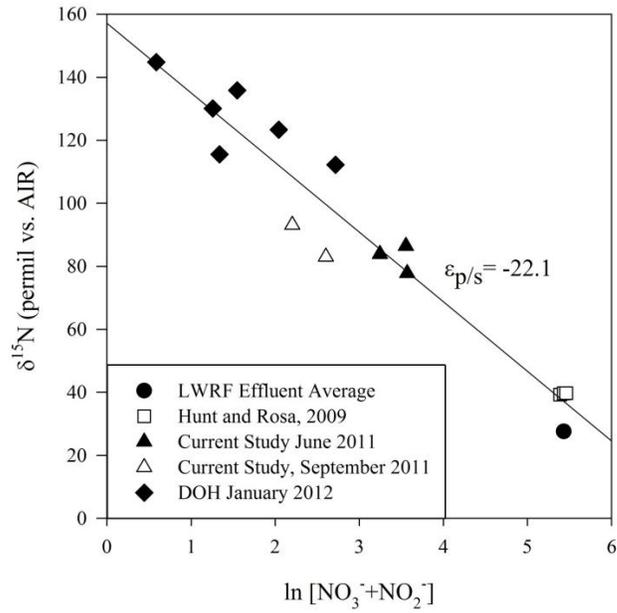
Figure 6-24: Historical data plots of $\ln[NO_3^- + NO_2^-]$ with $\delta^{15}N$ values (top) and $NO_3^- + NO_2^-$ fraction with $^{15}N/^{14}N$ ratio (bottom).

The solid lines represent denitrification relationships shown by linear regression (top) and power function regression (bottom) of the plotted data.
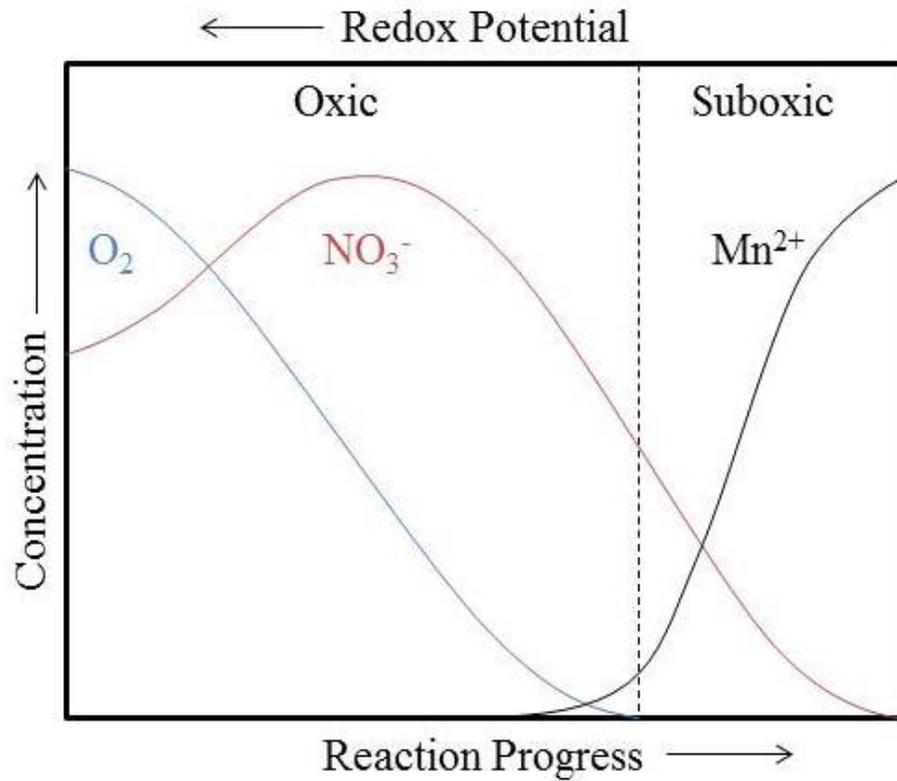
Figure 6-25: Conceptual changes in concentrations of electron acceptors with time or distance along a flowpath with excess organic C present.

The low NO_3^- and dissolved oxygen concentrations in the SS discharge combined with the presence of MnO crusts on rocks near the SS discharge points is suggestive of suboxic aquifer conditions. After Appelo and Potsma, 1993.

This page is intentionally left blank.

SECTION 7: PRELIMINARY GROUNDWATER MODEL

7.1 INTRODUCTION

Groundwater modeling is used by this study to interpret the dye tracer breakthrough curve (BTC), assess processes that affect the fate and transport of the injected LWRF treated wastewater effluent, and evaluate the potential for other deep submarine discharge points. Two modeling approaches have been used to date and are described in the following section: 1) a more geologically complex groundwater flow and transport model that does not consider the interaction between saline and non-saline water; and 2) a geologically simplified model that does consider this interaction. The complexities of groundwater aquifers make direct calculation of the critical tracer test parameters too difficult. This is compounded by the added complexity of study area hydrogeology, where the tracer plume is affected by the density difference between freshwater and salt water, and the fact that the point of monitoring is where this plume enters the marine environment. A numerical model is appropriate for a detailed interpretation of the fate and transport of the dissolved tracer utilized in this study.

7.2 MODELING OBJECTIVES

The objectives are to assess the impacts that aquifer processes, such as sorption, dispersion, and variable density flow, have on the temporal and spatial distribution of the tracer dye concentration at the submarine springs, and to aid in the interpretation of the BTC. In contrast to analytical approaches, numerical solutions rely on more physically based equations that are more realistic if supported by adequate data. Hence, modeling the tracer test results can shed light on the aquifer and hydrologic conditions at the study site. We should realize, however, that there is significant uncertainty regarding aquifer properties and chemical interactions in the aquifer. A major difficulty is related to the potential existence of preferential flow. The adopted modeling approaches are suitable for porous media or if the media can be treated as an equivalent porous media. Models for discrete fractures are not readily available and their data requirements are not easy to satisfy. For this reason, we are limiting the modeling objectives to assessing the influence of a limited number of processes (dispersion, sorption, and varying densities) on the transport of the dye.

This status report describes a number of exploratory models developed for the limited purposes of designing the field tracer test, assessing the preliminary monitoring results, evaluating various site conceptual models and the their limitations, and examining the suitability of equivalent porous media models for the study site. The developed models will be enhanced and calibrated based on data collected over the complete span of the study.

7.3 NUMERICAL MODELING

Three exploratory models were developed in this study, as described below. The first model neglects the density-dependent flow and only considers freshwater movement. This simple model has advantages including the ease of development and use, and the relatively limited data requirements. The saltwater interface used to specify the bottom boundary of the model was based on the density-dependent model developed by Gingerich (2008). This simple model (Planning Model) was aimed at designing the field tracer test and conducting a preliminary assessment of the tracer BTC data. This model was later modified to assist in the interpretation of the BTC (BTC Interpretation Model). The third model (SEAWATs Model) simulates the density-dependent flow in a basic grid-type model. This model was aimed at understanding the spatial distribution of the seawater/freshwater transition zone and the flow path (with an emphasis on the vertical component) of the LWRF treated wastewater effluent from the injection site to the submarine discharge points. At this stage, the only solute simulated in these models was the tracer dye. These models will serve as the basis for developing a more comprehensive model in the next stage of the study.

7.3.1 MODFLOW and MT3DMS Models

The Modular Finite Difference Groundwater Flow Model MODFLOW (Harbaugh et al., 2000), developed by the U.S. Geological Survey, is a widely used program for simulating groundwater systems. In general, the applicability of MODFLOW for this site is limited due to its inability to simulate density-dependent flow. However, the model was used as an initial step, considering the relative ease of using the model in comparison to a variable density model. The center line of the freshwater/seawater mixing zone was taken as a no-flow boundary representing the bottom of the model.

The results of the MODFLOW run were used as an input to the solute transport code Multi-Species Transport Model in Three Dimensions (MT3DMS) (Zheng and Wang, 1999; Zheng, 2006) to simulate the tracer test experiment. MT3DMS is a contaminant transport model that uses the MODFLOW solution to simulate the transport of dissolved multi-species. MT3DMS code simulates the effect of advection (the movement of the dissolved species due to the flow of groundwater), hydrodynamic dispersion (the spreading of the dissolved species due to mechanical dispersion and molecular diffusion), retardation (slowing of the plume transport due to the dissolved species sorbing onto the aquifer matrix), and the first order decay on the dissolved tracer dye.

The primary purpose in developing this Planning Model was to estimate the mass of tracer needed to provide sufficient dye concentrations at the submarine springs to facilitate adequate BTC analysis. The Planning Model was later modified and used as the BTC Interpretation Model to assist in understanding the BTC once the dye was detected.

7.3.2 Conceptual Model

A conceptual model concerns creating a distribution map of hydraulic parameters and features that are critical for the numerical analysis, which are then transferred to a numerical grid to facilitate the groundwater flow and species transport calculations. The modeled area was in the Kaanapali area of West Maui, Hawaii. Figure 7-1 is a map of the modeled area showing the extent of the top layer (layer 1) and the bottom layer (layer 6), as well as the major features such as the Lahaina Wastewater Reclamation Facility (LWRF) injection wells and the submarine springs. The map also illustrates the boundary conditions for layer 1. The model boundaries extend approximately 3,400 meters (m) inland from the shoreline, and 200 to 400 m seaward of the shoreline to about the -15 m bathymetric contour (Figure 7-1). Groundwater flow was modeled using a specified flux and recharge rate as regional inputs, and a specified head at the coastal and submarine boundaries as a regional sink. The northern and southern boundaries of the model were approximately 2,000 and 4,000 m away from the LWRF, respectively. The eastern boundary was a specified flux boundary with 27,400 m^3/d (7.2 million gallons per day [mgd]) of water entering the model. This represents inflow from the recharge areas in the interior highlands of the West Maui Volcano. The northern and southern boundaries were no-flow boundaries that were roughly aligned perpendicular to the groundwater flow direction. The western boundary was a series of specified head arcs at the shoreline and nearshore ocean bottom based on groundwater contours found in Gingerich (2008). The value of the assigned head for the submarine layers was the equivalent to the freshwater head based on the depth of the boundary arc, which was computed as ocean depth multiplied by the difference between the freshwater and saltwater specific gravity (0.025 for this study). The model's bottom boundary was treated as a no-flow boundary. Flux into the top layer was modeled as a groundwater recharge of 0.002 meters per day (m/d) (29 inches per year). Upon reviewing the model, it was found that the proper value of recharge into the modeled area was 0.001 m/d (14 in/yr) (Gingerich, 2008). This oversight will be corrected in future model runs.

Significant features that add water to and extract water from the model were the four LWRF injection wells for water input and the submarine springs (modeled as agricultural drains depicting the submarine springs) for water extraction. For the base simulation, an injection rate of 11,355 m^3/d (3 mgd) at Injection Well 2 was used. The conductance (a composite parameter describing the permeability and thickness of the media surrounding the spring) and bottom elevation of the drains representing the springs were adjusted so that a particle tracking simulation showed the dominant flow from the injection well going to the submarine springs. The hydraulic conductivity of the Wailuku Basalts was adjusted so that the hydraulic head near the LWRF was approximately 1.0 m msl. The MODFLOW simulation was done as a steady state model to provide the groundwater flow regime for MT3DMS, the groundwater transport model.

The area covered by the conceptual model consists of three geologic units (see Section 1 for a more detailed description of the study area). The first unit was the Wailuku Basalts comprised of shield building stage lavas of the West Maui Volcano, which are generally thin-bedded lava flows. The majority of groundwater flow occurs at the interface

between lava flows that commonly consist of clinker zones giving this path a hydraulic conductivity similar to that of clean gravels. The next geologic unit is the sediments, which are comprised of a combination of alluvial material, shoreline deposits, and fossil and modern reef materials. The fine grains of the alluvial sediments and the lithified reef material will give this unit a bulk hydraulic conductivity on the low side. However, preferential flow paths can result in locally high hydraulic conductivity values but were not accounted for in these models. The sediments occur along the coast and extend inland. The third unit was the Lahaina Volcanics, which resulted from post-erosional volcanism and forms localized flows on top of the Wailuku Basalts. In the modeled area, the Lahaina Volcanics were represented by a single cone in the southwest section of the model and have no real impact on groundwater flow between the injection wells and the submarine springs. Table 7-1 lists the hydraulic parameter values assigned to each geologic unit.

The model grid consists of 31,094 cells distributed among six layers. The bottom elevation of the first layer was set at -2 meters in reference to mean sea level (m msl). The bottom elevations of the remaining layers were evenly distributed between -2 m msl and the bottom of the model. The bottom elevation of the bottom layer was set to -12 m msl seaward of the shoreline. The top layer of the model only extended to the shoreline. Layer 2 of the model extended approximately half way between the shoreline and the western extent of the model, where the total thickness of the four layers was 8 m. The grid was refined in the area of the submarine springs. The cell size varies from 10 by 20 m near the submarine springs to 100 by 100 m away from the study area.

The transport model MT3DMS uses the groundwater flow solution from the flow model MODFLOW to simulate the transport of dissolved species in an aquifer. In this preliminary model, only advection and dispersion were simulated. The simulation was run for a total of 1,466 days, with no dye injected for the first 90 days. On day 91, a simulation concentration of 12,000 ppb of Fluorescein (FLT) dye was simulated for a period of 24 hours, which roughly corresponded to the field data. There was no FLT injection for the remaining 1,375 days of the model run. The simulated observation points were located at the North Seep Group (NSG) for the Planning Model and a second was located at the South Seep Group (SSG) for the BTC Interpretation Model.

After the detection of FLT at the submarine springs, the model was modified to more closely reflect the plant conditions and the tracer addition concentration during the actual tracer test. This was done to assist in the interpretation of the BTC and to better understand the potential reasons why the second injected dye, Sulpho-Rhodamine-B (SRB), has not been detected. Table 7-2 shows the well injection rates and dye concentrations used in BTC Interpretation Model. In the final BTC Interpretation Model run, a hydraulic barrier was placed in the model based on the estimated track of the Honokowai ancestral stream (Hunt and Rosa, 2009) in order to redirect groundwater flow, including injected effluent, to the southwest of the LWRF and towards the NSG and SSG.

7.3.3 Exploratory Results

The first runs of this model were used in the design of the tracer field experiment to estimate the mass of dye needed for a successful tracer test. With the exception of adjusting the hydraulic conductivity of the Wailuku Basalts to produce a hydraulic head of about 1 m near the LWRF, no attempt was made to calibrate the model. Figure 7-2 compares the results of the Planning Model run (NSG Planning Model) with the actual dye concentration measured at the NSG (NSG Measured). It successfully estimated a reasonable first arrival and peak time. However, the peak concentration of 7 parts per billion (ppb) was significantly less than the measured peak of about 21 ppb.

The results of the preliminary BTC Interpretation Model simulations indicated that LWRF treated wastewater effluent injection into Wells 3 and 4 redirects the effluent injected into Well 2 to the northwest. However, both the thermal imaging (Section 4, Figure 4-6) and $\delta^{15}N$ values of macroalgae (Hunt and Rosa, 2009; Dailer et al., 2010) indicate that the injectate is not discharging to the nearshore waters northwest of the LWRF and instead it appears to be discharging to the nearshore waters southwest of the LWRF. The use of a simulated barrier along the track of the ancestral Honokowai Stream resulted in FLT flow direction more consistent with the physical evidence.

Figure 7-2 compares the BTC Interpretation Model simulated FLT concentration at the NSG (NSG Modeled w/Barrier), and the SSG (SSG Modeled w/Barrier), with the measured FLT concentrations at each location. With the barrier in place, the simulated FLT arrival time was about a month earlier than the actual first detection. However, the peak concentration of 28 ppb compares more favorably with the measured concentration than that of the Planning Model. The slope of the leading edge of the simulated BTC for the NSG compares favorably with that measured indicating the modeled dispersivity of 50 m is not an unreasonable estimate. The near absence of FLT at the SSG however is problematic. The good agreement between this model and NSG BTC, but the poor agreement with SSG BTC may indicate that the cause of the oblique tracer path is a combination of a subterranean barrier and a preferential flow path. The BTC interpretation model predicted an SRB arrival at the NSG in March, 2012 (Figure 7-3). To date there has been no detection of this dye at either seep group.

7.3.4 SEAWAT Model

The USGS model SEAWAT (Langevin et al., 2007) can be used in simulating groundwater accounting for potential contamination due to seawater/freshwater mixing. SEAWAT combines MODFLOW with MT3DMS in simulating three-dimensional variable density groundwater flow, along with multi-species solute and heat transport. Given the complex hydrogeologic setting of the study site, with anisotropic aquifers and a freshwater/seawater interface, SEAWAT is considered an appropriate modeling code for accurately simulating groundwater flow.

7.3.4.1 Conceptual Model

A three-dimensional grid model was used to simulate the saltwater/freshwater interface. The sub-surface of the study site is not known in sufficient detail to develop a model that accurately reflects the site in three dimensions. Therefore, a simplified model was developed with the objective limited to analyzing the role of multiple densities in the groundwater on the transport of the tracer dye and thus on the effluent (Figure 7-4). The model approximately follows the boundaries of the Honokowai Aquifer Sector (Mink and Lau, 1990) with the submarine portion extending 7,800 m past the generalized shoreline. Layer 1 approximately follows the shoreline. It reflects the general geology of the area, as described above in the MODFLOW model, except that the Lahaina Volcanics were excluded. The submarine surface of the model uses an average bathymetry for the region. The submarine springs, and thus the model monitoring points, were relocated to fall on a direct line from the LWRF injection wells to and extending past the shoreline. No effort was adopted to simulate the exact oblique view of the effluent plume, rather, the flow was assumed to be along a line connecting the injection wells and the monitoring points. The aquifer hydraulic parameters used in this model were those used by Gingerich (2008) and are listed in Table 7-3.

This model grid was made up of 57,000 cells distributed into 12 layers. The top layer extends to 7.5 m below sea level, while the bottom of layer 12 was at -200 m below sea level. The north and south margins of the model were set as no-flow boundaries. The western boundary of the model was set as a specified head based on the depth of mid-point of that layer containing the boundary arc. The eastern margin of layer 1 and layer 2 was a specified flux boundary that adds 20,000 m^3/d (5.3 mgd) of water to the model, simulating inflow from recharge occurring in the interior of the island. A recharge rate of 0.007 m/d (10 in/yr) was assigned to the terrestrial surface of the model, which amounts to 14.4 mgd across the model domain.

The objective of the density-dependent modeling was to study the interaction between waters of three different densities: 1) the very low salinity colder groundwater, 2) the low salinity but warm LWRF treated wastewater effluent, and 3) the saline seawater. The primary objective was to investigate whether the high horizontal to vertical anisotropy is sufficient to keep the warm LWRF treated wastewater effluent in the saline water zone or will buoyancy overcome the low vertical hydraulic conductivity and force the effluent into the shallow groundwater. For additional simplification, heat effects of the warm injected effluent were not explicitly considered and only density variations were simulated.

7.3.5 Exploratory Results

Figure 7-5 illustrates salinity simulation results after 730 days, allowing the interface between freshwater and saltwater to reach a state of approximate equilibrium. The results support the notion that buoyancy forces the non-saline effluent into the shallow

groundwater zone to ultimately exist in the ocean shore, despite the low vertical conductivity of the formation.

7.4 ASSUMPTIONS AND LIMITATIONS

For the planning and BTC interpretation models, the results were based on a MODFLOW model that ignored the effects of density variations. Implicit in the use of this or other models, including those with density effects, is the assumption that the aquifer can be treated as an equivalent porous medium. In such a case, aquifer properties are averaged over a representative elementary volume (REV), preserving the true aquifer's behavior (Bear, 1979). The REV should be large enough to include the effects of solids and fractures (for consolidated material) or solids, fractures, and porous material (for unconsolidated material), but small enough to be treated as a point in mathematical terms. In this case, Darcy's law is valid and the resulting solutions for the hydraulic head or solute concentrations are also averaged over the REV. However, due to preferential flow, BTCs for solute transport can still show multiple peaks, even though Darcy's law is still valid. Multiple peaks can be considered as fluctuations similar to those attributed to heterogeneities. In the case of large fractures, BTCs should display a fast first-arrival and steep ascending and descending legs, which was not manifested in this current study.

It should be stressed that this is a status report presenting preliminary modeling efforts due to the lack of data needed for comprehensive modeling. Factors contributing to modeling uncertainty include an incomplete BTC, which has hampered a complete assessment of the tracer results. In addition, estimating water flux rates for both seeps and diffuse sources are essential for estimating the amount of tracer mass recovered and assessing the overall success of the tracer test. The lack of accurate accounting can imply the existence of discharge points not covered by monitoring activities. The potential presence of other discharge locations is supported by the lack of detection of SRB at the NSG and SSG. The flux rates are also needed for model calibration and validation. However, identifying other discharge points farther from shore and in deeper water are beyond the capabilities of this study. Uncertainty also exists in the models themselves due to the assumptions innate in their mathematical formulation and the lack of accurate supporting data. Results can be non-unique depending on parameter choices.

Accurate estimation of the BTCs was not possible due to the limitations of the model. These limitations include: the absence of variable density flow representation, lack of detailed geological information about the site, including factors related to the apparent oblique nature of the plume path. Although some strong indications exist for such a path, physical features are not well defined.

7.5 CONCLUSIONS

Although the modeling results are only preliminary, a number of initial conclusions can be derived from this effort. The Planning Model, with very minimal calibration, was able

to estimate, reasonably well, the first arrival and peak times. Although submarine springs in the current study are evidence of preferential flow, it seems reasonable enough to treat the aquifer as an equivalent porous media. The calibration values of aquifer parameters in the acceptable ranges, as well as the good match with the first solute arrival, further support this conclusion. The submarine springs act as leakage points and were treated as drains in our simulations with outflow controlled by drain conductance; an option that seems to be an appropriate representation.

The simulated flux of groundwater to the marine environment was within the range independently estimated by other components of this study. Submarine spring water fluxes estimated using radon based methods ranged between 2,200 and 9,200 m^3/d (see Section 5), while the exploratory MODFLOW simulation provided an estimate of 3,300 m^3/d. These preliminary results support the conclusion that the aquifer can be treated as an equivalent porous media. As estimated in Section 5 also, the flux of water at the study site per unit area, including both submarine spring groups and diffuse discharge, ranged between 0.82 and 1.32 m/d. The model estimated a flux of 0.1 m/d near the center of the tracer plume, which is on the lower side, but estimates should improve with further enhancements to the model. We realize, however, that radon-based flux estimates are also highly uncertain, with errors as high as 60%, which add some difficulties regarding model calibration (see Section 5).

7.6 PLANNED MODELING

Future modeling for this project will investigate the processes that affect the transport of the injected LWRF treated wastewater effluent and its eventual discharge into the marine environment. The first process to be investigated will be the effectiveness of the high horizontal to vertical permeability anisotropy on constraining a buoyant plume to the plane of the lava bedding. The lavas in West Maui dip at an angle of 5° to 12° (Stearns and MacDonald, 1942). The low permeability in the vertical direction could result in effluent discharges deeper and farther offshore than those currently observed. The results of the preliminary SEAWATs model seem to indicate the buoyancy of the effluent plume overcomes the low vertical permeability. But this model will be modified so the layering reflects the actual dip of the lava flow and a series of simulations run at different horizontal to vertical permeability anisotropy ratios.

The next process to be investigated is the heat loss from the LWRF treated wastewater effluent that occurs between the point of effluent injection and the discharge at the submarine springs. Section 4 addresses the temperature rise in ocean water where the LWRF treated wastewater effluent is discharging. The LWRF effluent injection sustained for decades, could put the groundwater system in thermal equilibrium allowing the effluent to maintain a higher than ambient temperature during the months that elapse between injection and discharge. Heat transport will be simulated to assess whether it is reasonable for the effluent to remain warm from the point of injection to the point of discharge into the ocean. Otherwise, other processes (as addressed in Section 4), such as geothermal activity or microorganism induced chemical reactions, e.g., those that cause denitrification to remove nitrogen in wastewater, should be considered.

The analytical model QTracer2 (Field, 2002) will be used to analyze tracer data as described in the project's work plan. Tracer tests generally assume that the dyes do not sorb to the aquifer matrix. However, all tracer dyes sorb to some extent (for example see Sabatini, 2000). The transport model MT3DMS will be used to test a reasonable range of sorption values for the tracer dye and compare those to the field measured BTC. Based on this comparison, the probable range of sorption values will be narrowed and that range will be used in the QTracer2 analysis. The MT3DMS model has the advantage over the QTracer2 model in that it can account for the aquifer heterogeneity and anisotropy.

Finally, since the MODFLOW/MT3DMS model has produced reasonable results with minor calibration, various combinations of subterranean barriers and preferential flow paths will be tested to better understand the cause of the oblique travel path between the injection wells and the coastal discharge points. This revised model will also be used in the next phase of research to estimate the amount of tracer mass captured at the seeps, which is important for assessing the potential existence of discharge locations where the tracer is not monitored. The information needed for such calculations are the submarine spring and diffuse fluxes and the tracer dye BTC's. The MT3DMS model has an option to estimate the mass of solute in a time series, which can be integrated numerically by using an excel function to estimate the total mass. For a submarine spring, or a diffuse area, that would be the value of the total mass recovered. The use of the model and field measurements will provide the best accounting estimate of the dye mass discharging into the nearshore waters.

Table 7-1. Hydraulic parameter values for various geologic units used in the MODFLOW model

Geologic Unit	Horiz. Hyd. Conductivity	Vert. Hyd. Conductivity	Long. Dispersivity	Porosity
	(m/d)	(m/d)	(m)	
Wailuku Basalts	900	9	50	0.10
Sediments	3.0	2.0	50	0.20
Lahaina Volcanics	5.0	0.5	50	0.10

Table 7-2. Well Injection and Dye Concentrations for the BTC Evaluation Model

		Well 1	Well 2		Well 3		Well 4	
Start	End	Injection Rate (mgd)	Injection Rate (mgd)	SRB Conc. (ppb)	Injection Rate (mgd)	FLT Conc. (ppb)	Injection Rate (mgd)	FLT Conc. (ppb)
4/29/11	7/28/11	0.2	0.4	0	1.3	0	1.1	0
7/28/11	7/29/11	0.2	0.4	0	1.3	12,800	1.1	12,800
7/29/11	8/11/11	0.2	0.4	2,500	1.3	0	1.1	0
8/11/11	8/12/11	0.0	2.1	0	1.5	0	1.5	0
8/12/11	5/5/15	0.2	0.4	0	1.3	0	1.1	0

Table 7-3. Hydraulic parameter values for various geologic units used in the SEAWATs model

Geologic Unit	Horiz. Hyd. Conductivity	Vert. Hyd. Conductivity	Long. Dispersivity	Porosity
	(m/d)	(m/d)	(m)	
Wailuku Basalts	640	3.2	25	0.1
Sediments	5	0.2	25	0.2

FIGURES
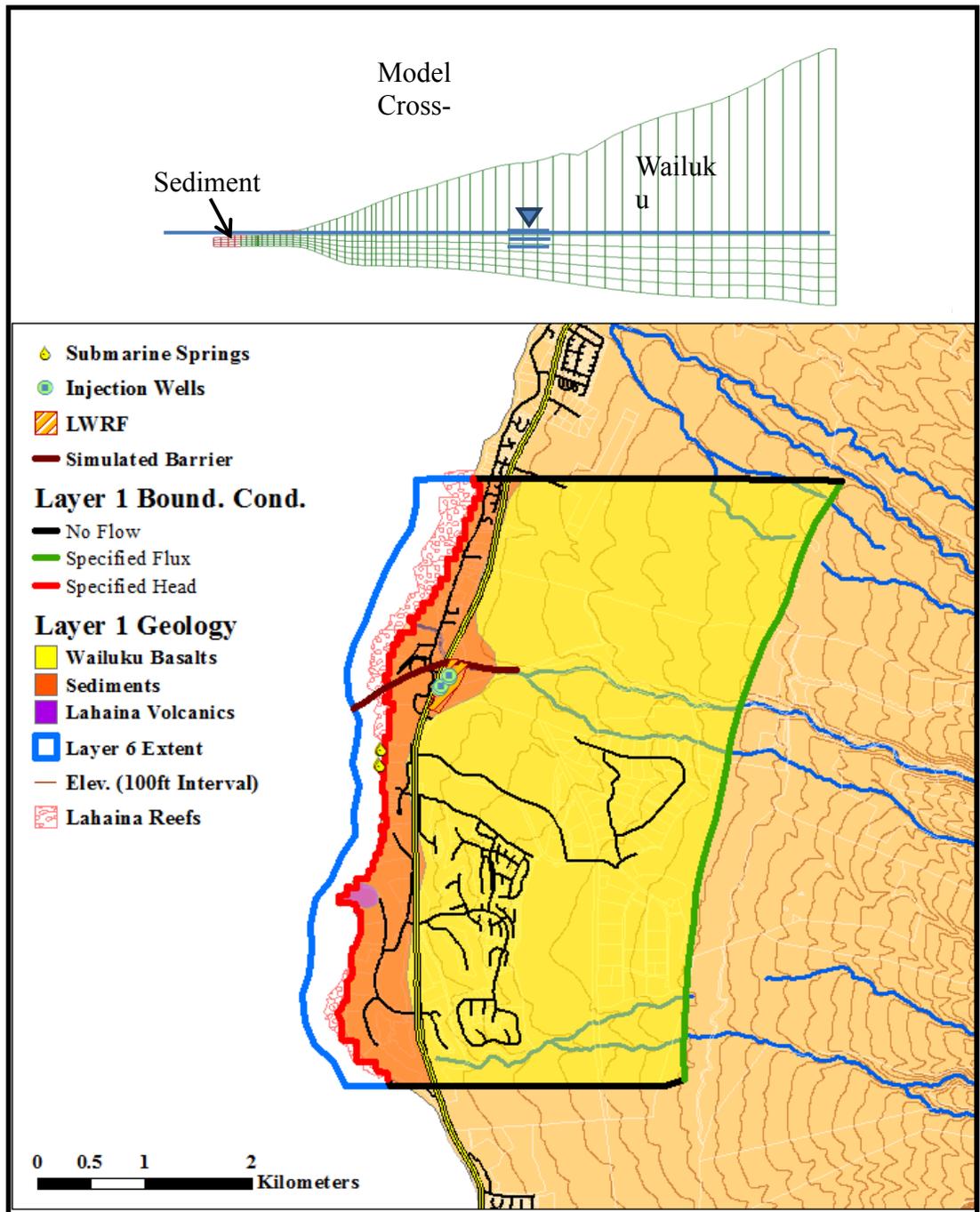
Figure 7-1: Plane view and Cross-section of the MODFLOW modeled area.
The blue in the cross-section view represents the basalt while the violet represents the sediments and the reef formations. In the plane view the green shows the location of the specified flux into the model represent upgradient recharge, while the red arc represent a specified head at the interface with the ocean. The blue arc delineates the furthest seaward extent of the model. This is also a specified head boundary.
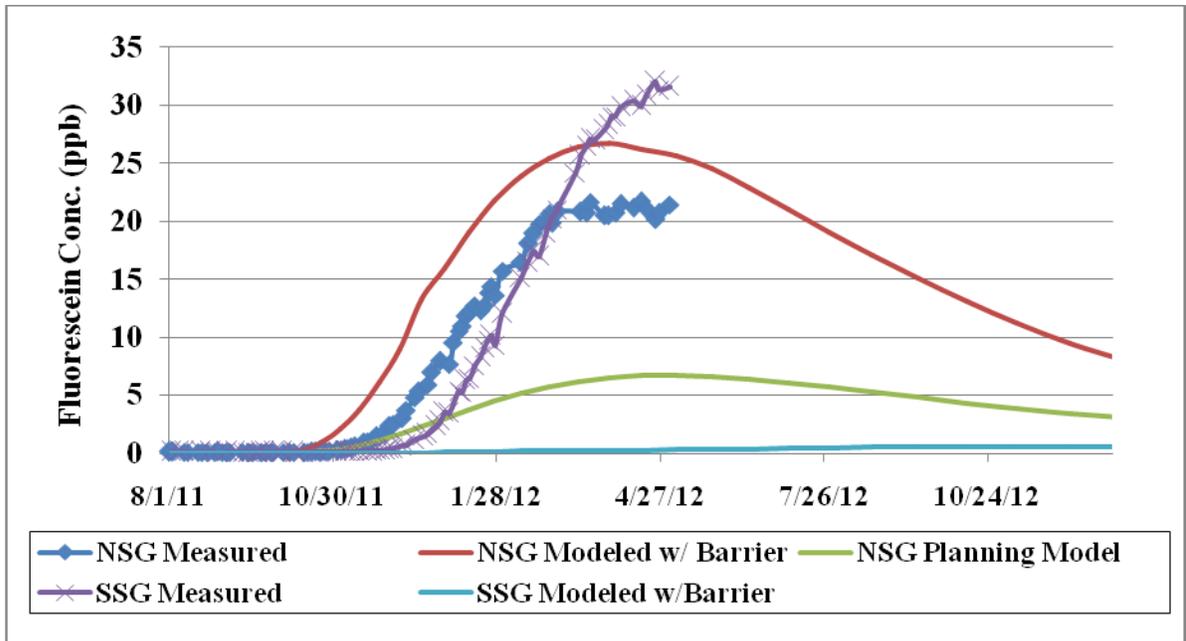
Figure 7-2: Measured and Simulated Fluorescein Concentrations
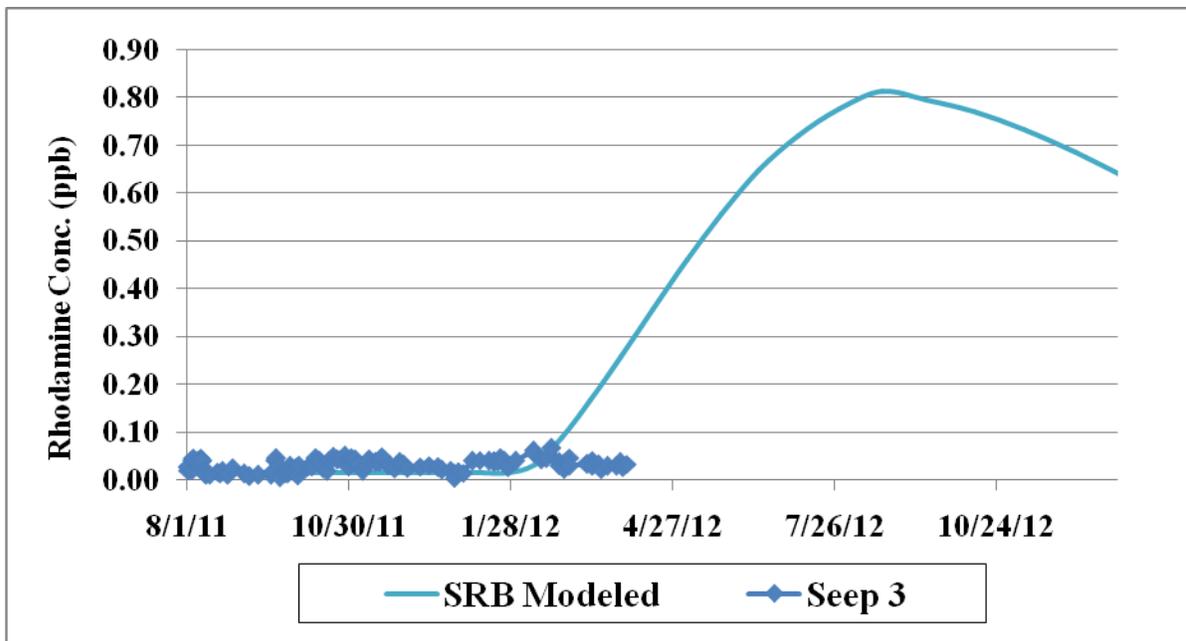
Figure 7-3: Measured and Simulated SRB Concentrations
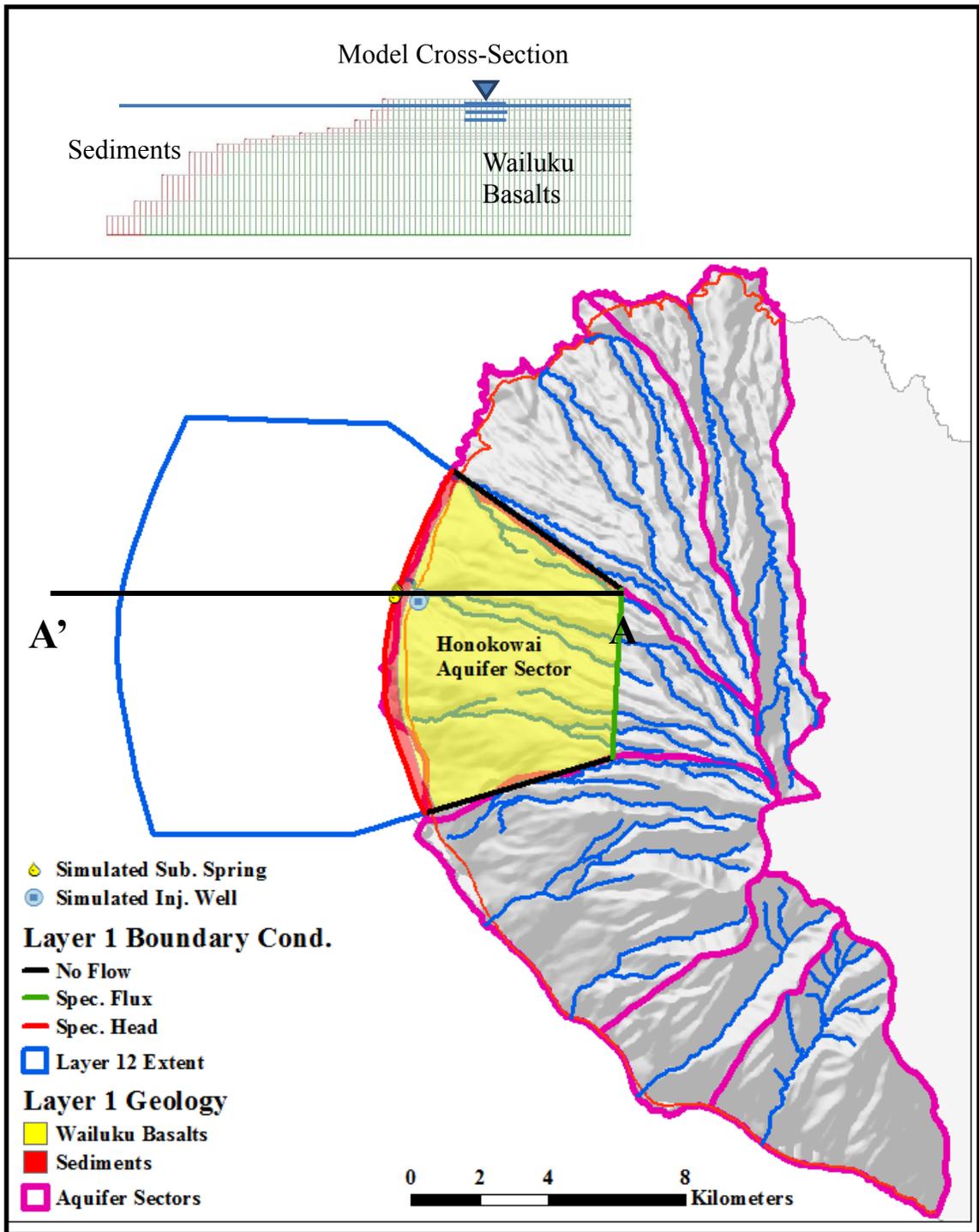
Figure 7-4: Plane view of the SEAWATs modeled area outlining layer 12.
The blue in the cross-section view represents basalt, while the violet represents the sediments and reef formations. In the plane view, the blue arc represents the maximum seaward extent of the model. As with the previous model the green arc delineates a specified flux boundary representing upgradient recharge entering the model. The red represents the specified head boundary for Layer 1.
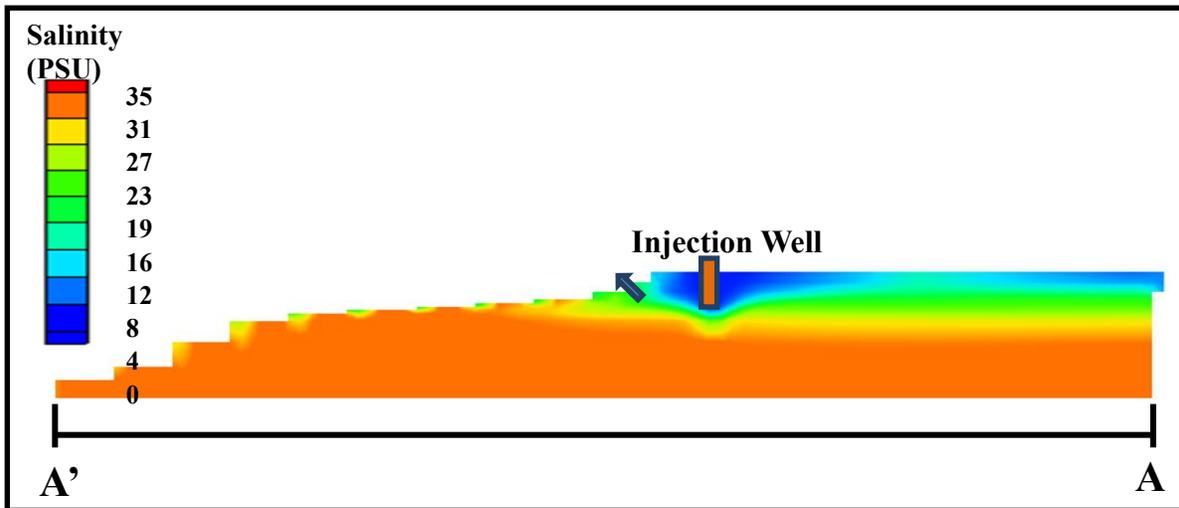
Figure 7-5: SEAWAT hydraulic salinity simulation results at a quasi-area condition. The arrow illustrates the direction of outflow of injected effluent in the nearshore waters.

REFERENCES

Appelo, C.A.J., and Potsma, D., 1993, Geochemistry, groundwater and pollution: Rotterdam, A.A. Balkema, 536 p.

Aley, T., 2002, Groundwater Tracing Handbook − A handbook prepared for the use of clients and collegues of the Ozark Underground Laboratory, Ozark Underground Laboratory, 35 p.

Aravena, R., and Robertson, W. D., 1998, Use of Multiple Isotope Tracers to Evaluate Denitrification in Ground Water: Study of Nitrate from a Large-Flux Septic System Plume: Ground Water, v. 36, no. 6, p. 975-982.

Atkinson, S., Atkinson, M.J., and Tarrant, A.M., 2003, Estrogens from sewage in coastal marine environments: Environmental Health Perspectives, v. 111, p. 531-535.

Baker, A., Inverarity, R, Charlton, M., and Richmond, S., 2003, Detecting river pollution using fluorescence spectrophotometry: case studies from the Ouseburn, NE England. Environmental Pollution, v. 124, p. 57-70.

Banks, W.S.L., Paylor, R.L., and Hughes, W.B., 1996,Using thermal-infrared imagery to delineate ground-water discharge, Ground Water, v. 34, p. 434-443.

Bear, J, 1979, The Hydraulics of Groundwater, McGraw-Hill, London, UK, 567 pgs.

Berner, R.A., 1973, Phosphate removal from sea water by adsorption on volcanic ferric oxides: Earth Planet. Sci. Lett., v. 18, p. 77-86.

Berner, R.A. 1980, Earthy Diagenesis: A Theoretical Approach, Princeton University Press, 241p.

Berner, E. K. and R. A. Brener, 1996, *Global Environment, Water, Air, and Geochemical Cycles,* Prentice-Hall, Upper Saddle, River, NJ, 1996.

Böhlke, J.K., and Coplen, T.B., 1995, Interlaboratory comparison of reference materials for nitrogen-isotope-ratio measurements, in Reference and intercomparison materials for stable isotopes of light elements: Vienna, International Atomic Energy Agency, IAEA-TECDOC-825, p. 51-66.

Böhlke, J.K., Mroczkowski, S, J., and Coplen, T. B., 2003, Oxygen isotopes in nitrate: New reference materials for O-18 : O-17 : O-16 measurements and observations on nitrate-water equilibration: Rapid Communications in Mass Spectrometry, v. 17, p. 1835–1846.

Böttcher, J., Strebel, O., Voerkelius, S., and Schmidt, H. L., 1990, Using isotope fractionation of nitrate nitrogen and nitrate oxygen for evaluation of microbial denitrification in a sandy aquifer: Journal of Hydrology, v. 114, p. 413–424.

Bourke, R., 1996, Maui algae bloom studies-distribution and abundance. Honolulu, Hawaii, Oceanit Laboratories, Inc.

Brown, K., 1995, An injection well effluent transport study, Maui, Hawaii [MS thesis]: San Jose State University, 147 p.

Brown, C.W., Connor, L.N., Lillibridge, J.L, Nalli, N.R., and Legeckis, R.V., 2005, An introduction to satellite sensors, observations and techniques, p. 21-50. *In* R.L. Miller, C.E. Del Castillo and B.A. McKee [eds.], Remote sensing of coastal aquatic environments: Technologies, techniques and applications. Springer.

Brown, T.L., 2009, Fluorescence Characterization of Karst Aquifers in East Tennessee, [M.S. thesis]: Knoxville, University of Tennessee

Burnett, W.C. and Dulaiova, H., 2003. Estimating the dynamics of groundwater input into the coastal zone via continuous radon-222 measurements. Journal of Environmental Radioactivity, v. 69, p. 21-35.

Burnett, W.C., Aggarwal, P.K., Aureli, A., Bokuniewicz, H., Cable, J.E., Charette, M.A., Kontar, E., Krupa, S., Kulkarni, K.M., Loveless, A., Moore, W.S., Oberdorfer, J.A., Oliveira, J., Ozyurt, N., Povinec, P., Privitera, A.M.G., Rajar, R., Ramessur, R.T., Scholten, J., Stieglitz, T., Taniguchi, M. and Turner, J.V., 2006. Quantifying submarine groundwater discharge in the coastal zone via multiple methods. Science of the Total Environment 367, 498p.

Burnham, W.L., Larson, S.Pl, and Cooper, H.H., Jr., 1977, Distribution of injected wastewater in the saline lava aquifer, Wailuku-Kahului Wastewater treatment Facility, Kahului, Maui, Hawaii: U.S. Geological Survey Open-File Report 77-469, 58p.

Casciotti, K. L., Sigman, D. M., Hastings, M. G., Böhlke, J.K., and Hilkert, A., 2002, Measurement of the oxygen isotopic composition of nitrate in seawater and freshwater using the denitrifier method: Analytic Chemistry, v. 74, p. 4905–4912.

Christophersen, N., and Hooper R. P., 1992, Multivariate analysis of stream water chemical data: the use of principal components analysis for the end-member mixing problem: Water Resources Research, v. 28, no. 1, p. 99-107.

Chua, L.H.C., Roberton, A.P., Yee, W.K., Shuy, E.B., Edmond, Y.M., Lo, T.T., and Tan, S.K., 2007, Use of Fluorescein as a Ground Water Tracer in Brackish Water Aquifers, Ground Water, v. 45(1), p. 85-88.

Compton, J., Mallinson, D., Glenn, C.R., Filippelli, G., Föllmi, K., Shields, G. and Zanin, Y., 2000, Variations in the Global Phosphorus Cycle, in Glenn, C.R., Prévôt-Lucas, L., and Lucas J. eds. ,Marine Authigenesis: From Global to Microbial, SEPM Special Publication No. 66, p. 21-33.

County of Maui, 2004, Lahaina Wastewater Reclamation Facility U.I.C. Permit – Permit No. HI596001 – Permit Renewal Application, Dated December 1, 2004.

County of Maui, 2010, Lahaina Wastewater Reclamation Facility Underground Injection Control (UIC) Injection Well Status Report Number 30 - July 2010 – Submitted to: State of Hawaii, Safe Drinking Water Branch

Cox, M.E. and Thomas, D.M., 1979a, Chloride/magnesium ratio of shallow groundwaters as a regional geothermal indicator in Hawaii, Assessment of Geothermal Resources in Hawaii: Number 3, Hawaii Institude of Geophysics, Honolulu, Hawaii, 51 p.

Cox, M.E. and Thomas, D.M., 1979b, Cl/Mg ratio of Hawaiian groundwaters as a regional geothermal indicator, Geothermal Resources Council, Transactions, v. 3, p. 145-148.

Craig, H., 1961, Isotopic variations in meteoric waters: Science, v. 133, p. 1702-1703.

Craig H., and Gordon L., 1965, Deuterium and Oxygen-18 variations in the ocean and the marine atmosphere, In: Tongiori, E., ed., Stable Isotopes in Oceanographic Studies and Paleotemperatures, Spoleto, p. 9-130.

Dailer, M.L., Knox, R.S., Smith, J.E., Napier, M., and Smith, C.M., 2010, Using δ^{15}N values in algal tissue to map locations and potential sources of anthropogenic nutrient inputs on the island of Maui, Hawaii, USA, Marine Pollution Bulletin, v. 60, p. 655-671.

Dailer, M.L., Ramey, H.L., Saephan, S., and Smith, C.M., 2012, Algal $\delta^{15}N$ values detect a wastewater effluent plume in nearshore and offshore surface waters and three-dimensionally model the plume across a coral reef on Maui, Hawai'i, USA, Marine Pollution Bulletin, v. 64, p. 207-213.

Dansgaard, W., 1964, Stable isotopes in precipitation: Tellus, v. 16, p. 436-467.

Davis, S.N., Thompson, G.M., Bently, H.W., and Stiles, G., 1980, Groundwater tracers – A short review, Ground Water, v. 18, pgs. 14-23.

Dever, J.L., 1997, The Geochemistry of Natural Waters: Upper Saddle River, Simon and Schuster, 436 p.

Dollar, S., and Andrews, C., 1997, Algal blooms off west Maui—assessing causal linkages between land and the coast ocean: Final Report for National Oceanic and Atmospheric Administration Coastal Ocean Program Office and University of Hawaii Sea Grant College Program, Honolulu, HI.

Dollar, S.J., Atkinson, M., and Atkinson, S., 1999, Investigation the relationship between cesspool nutrients and abundance of Hypnea musciformis in West Maui, Hawaii: Report State of Hawaii Department of Health, Honolulu, Hawaii.

Donlon, C.J., Keogh,S.K., Baldwin,D.J., Robinson,I.S., Ridley, I., Sheasby, T., Barton,I.J., Bradley,E.F., Nightingale, T.J., and Emery, W., 1998, Solid-state radiometer measurements of sea surface skin temperature, Journal of Atmospheric and Oceanic Technology, v. 15, p. 775-787.

Dulaiova, H., Camilli, R., P. B. Henderson, and M. A. Charette, 2010. Coupled Radon, Methane And Nitrate Sensors For Large-Scale Assessment Of Groundwater Discharge And Non-Point Source Pollution To Coastal Waters, Journal of Environmental Radioactivity, v. 101(7), p. 553-563, doi: 10.1016/j.jenvrad.2009.12.004

Ekern, P.C., and Chang, J.H., 1985, Pan evaporation: State of Hawai'i, 1894-1983: Hawai'i Department of Land and Natural Resources, Division of Water and Land Development, Report R74, Honolulu, HI, 172p.

Ellis, A.J., and Mahon, W.A.J., 1964, Natural hydrothermal systems and experimental hot-water/rock interactions, Geochimica et Cosmochimica Acta, v. 23, p. 1323-1357.

Emery, W.J., Yu, Y., Wick,G.A., Schluessel, P., and Reynolds, R.W., 1994, Correcting infrared satellite estimates of sea surface temperature for atmospheric water vapor attenuation. Journal of Geophysical Research, v. 99(C3), p. 5219-5236.

Emery, W.J., Castro, S., Schluessel, P., and Donlon, C., 2001, Estimating sea surface temperature from infrared satellite and in situ temperature data, Bulletin of the American Meteorological Society, v. 82, p. 2773-2785.

Engott, J.A., and Vana, T.T., 2007, Effects of Agricultural Land-Use Changes and Rainfall on Ground-Water Recharge in Central and West Maui, Hawaii, 1926-2004 – U.S. Geological Survey Scientific Investigations Report 2007-5103, 56p.

Fetter, C.W., 1998, Applied Hydrogeology – Second Edition, Macmillan Publishing Co., 589 pgs.

Field, M.S., Wilhelm, R.G., Quinlan, J.F., and Aley, T.J., 1995, An Assessment of the Potential Adverse Properties of Fluorescent Tracer Dyes Used for Groundwater Tracing, Environmental Monitoring and Assessment, v. 38, p. 75-96.

Field, M.S., 2002, The QTRACER2 Program for Tracer-Breakthrough Curve Analysis for Tracer Tests in Karst and Other Hydrologic Systems: EPA/600/R-02/001, U.S. Environmental Protection Agency

Fisher, J.I., and Mustard,J.F., 2004, High spatial resolution sea surface climatology from Landsat thermal infrared data, Remote Sensing of Environment, v. 90, p. 293-307.

Flury, M., and Wai, N.N. 2003, Dyes as tracers for Vadose Zone Hydrology, Reviews of Geophysics, v. 41(1), p. 2-1 – 2-37.

Froelich P. N., Klinkhammer G. P., Bender M. L., Luedtke N., Heath G. R., Cullen D., Dauphin P., Hammond D., Hartman B., and Maynard V., 1979, Early oxidation of organic matter in pelagic sediments of the eastern equatorial Atlantic: suboxic diagenesis. Geochim. Cosmochim. Acta 43, p. 1075–1090

Froelich, P.N., 1988, Kinetic control of dissolved phosphate in natural rivers and estuaries: A Primary on the phosphate buffer mechanism. Limnology and Oceanography, v. 33, p. 649-668.

Fujieki,L., F. Santiago-Mandujano, P. Lethaby, R. Lukas, D. Karl. 2011, Hawaii Ocean Time-series Program Data Report 20, 2008. School of Ocean and Earth Science and Technology, Univ. of Hawaii, Honolulu, HI, 395 pp.

Fujishima, K., and Fan, P.-F., 1977, Hydrothermal mineralogy of Keolu Hills, Oahu, Hawaii, American Mineralogist, v. 62, p. 574-582.

Galapate, R.P., Baes, A.U., Ito, K., Mukai, T., Shoto, E., and Okada, M., 1998, Technical Note: Detection of Domestic Wastes in Durose River Using Synchronous Fluorescence Spectroscopy, Water Research, v. 32, p. 2232-2239.

Gallert, C., and Winter, J, 2005, Bacterial Metabolism in Wastewater Treatment Systems, In: Winter, J, and Jördening, H. J., eds., Environmental Biotechnology, Concepts and Applications: KGaA, Weinheim, Wiley-VCH Verlag GmbH & Co., p. 1-48.

Garcia-Solsona, E., J. Garcia-Orellana, P. Masqué, and H. Dulaiova, 2008. Uncertainties associated with ^{223}Ra and ^{224}Ra measurements in water via a Delayed Coincidence Counter (RaDeCC), Marine Chemistry, v. 109(3-4), p. 198-219.

Gartner, A., Lavery, P., and Smit, A.J., 2002, Use of ^{15}N signatures of different functional forms of macroalgae and filter feeders to reveal temporal and spatial patterns in sewage dispersal. Marine Ecology Progress Series, v. 235, p. 63-73.

Gat, J.R., 1966, Oxygen and hydrogen isotopes in the hydrologic cycle. Ann. Rev. Earth Sci., v. 25, p. 225-262.

Giambelluca TW, Chen Q, Frazier AG, Price JP, Chen Y-L, Chu P-S, Eischeid J., and Delparte, D., 2011, The Rainfall Atlas of Hawaiʻi. http://rainfall.geography.hawaii.edu.

Gingerich, S.B., and Voss, C.I., 2005, Three-dimensional variable-density flow simulation of a coastal aquifer in southern Oahu, Hawaii, USA: Hydrogeology Journal, v. 13, p. 436-450, 95p.

Gingerich, S.B., 2008, Ground-water availability in the Wailuku area, Maui, Hawaii: U.S. Geological Survey Scientific Investigations Report 2008-5236, 95p.

Gingerich, S. B., and Engott, J.A., 2012, Groundwater Availability in the Lahaina District, West Maui, Hawaii: U.S. Geological Survey Scientific Investigations Report 2012-5010, 90 p.

Granger, J., Sigman, D. M., Prokopenko, M., Lehmann, M. F., and Tortell, P. D., 2006, A method for nitrite removal in nitrate N and O isotope analysis: Limnology and Oceanography: Methods, v. 4, p. 205-212.

Granger, J., Sigman, D. M., Lehmann, M. F., and Torell, P.D., 2008, Nitrogen and oxygen fractionation during dissimilatory nitrate reduction by denitrifying bacteria: Limnology and Oceanography, v. 53, no. 6, p 2533-2545.

Guilbault, G.G. (Ed). 1990. *Practical Fluorescence*, Marcel Dekker, Inc. New York.

Handcock, R.N., Gillespie, A.R., Cherkauer, K.A., Kay, J.E., Burges, S.J., and Kampf, S.K., 2006, Accuracy and uncertainty of thermal-infrared remote sensing of stream temperatures at multiple spatial scales, Remote Sensing of Environment, v. 100, p. 427-440.

Harbaugh, A.W., Banta, E.R., Hill, M.C., McDonald, M.G., 2000, MODFLOW-2000, the U.S. Geological Survey Modular Ground-Water Model – User guide to modularization concepts and the ground-water flow process.

Harvey, R.W., 1997, Microorganisms as tracers in groundwater injection and recovery experiments: A review, FEMS Microbiological Review, v. 20, p. 461-472

Hellström, D., 1997, An exergy analysis for a wastewater treatment plant-an estimation of the consumption of physical resources: Water Environment Research, v. 69, p. 44-51.

Hellström, D., 1999, Exegy Analysis: A Comparison of Source Separation Systems and Conventional Treatment Systems: Water Environment Research, v. 71, no. 7, p. 1354-1363.

Hooper, R. P., 2003, Diagnostic tools for mixing models of stream water chemistry: Water Resources Research, v. 39, no. 3. DOI: 10.1029/2002WR001528.

HSOP, 2010, Hawaii State Office of Planning – Statewide GIS Program, http://hawaii.gov/dbedt/gis/ accessed 9/17/2010.

Hubaux, A., and C. Vos, 1970, Decision and Detection Limits for Linear Calibration Curves, Analytical Chemistry, v. 42(8), p. 849-855

Hunt, C.D., Jr., 1996, Geohydrology of the Island of Oahu, Hawaii: U.S. Geological Survey Professional Paper – 1412-B, 54p.

Hunt, C.D., Jr., 2004, Ground-water quality and its relation to land use on Oahu, Hawaii, 2000-01: U.S. Geological survey Water-Resources Investigations Report 03-4305

Hunt, C.D., Jr., 2007, Ground-water nutrient flux to coastal waters and numerical simulation of wastewater injection at Kihei, Maui, Hawaii: U.S. Geological Survey Scientific Investigations Report 2006-5283, 69 p.

Hunt, C.D., Jr., and Rosa, S.N., 2009, A Multitracer approach to detecting wastewater plumes from municipal injection wells in near shore marine waters at Kihei and Lahaina, Maui, Hawaii: U.S. Geological Survey Scientific Investigations Report 2009-5253, 166p.

Izuka, S.K. and Gingerich, S.B., 1998, Estimation of the depth to the fresh-water/salt-water interface from vertical head gradients in wells in coastal and island aquifers: Hydrogeology Journal, v. 6, p. 365-373.

Izuka, S.K., Oki, D.S., Chen, C., 2005, Effects of irrigation and rainfall reduction on ground-water recharge in the Lihue Basin, Kauai, Hawaii: U.S. Geological Survey Science Investigations Report 2005-5146. 48 p.

Johnson, A.G.,2008, Groundwater discharge from the leeward half of the Big Island, Hawaii [MS. Thesis] Honolulu, University of Hawaii at Manoa, 145 p.

Johnson, A. G., Glenn, C. R., Burnett, W. C., Peterson, R. N., and Lucey, P. G., 2008, Aerial infrared imaging reveals large nutrient-rich groundwater inputs to the ocean: Geophysical Research Letters, v. 35. DOI: 10.1029/2008GL034574.

Käss, W, 1998, Tracing Techniques in Geohydrology. A.A. Balkema Publishers (Taylor and Francis, CRC).

Kehew, A. E., 2000, Applied Chemical Hydrogeology: Upper Saddle River, Prentice Hall, 368 p.

Kelly, J.L., Glenn, C.G., and Lucey, P.G., submitted, High-resolution aerial infrared mapping of groundwater discharge to the coastal zone. Limnology and Oceanography Methods.

Kendall, C., 1988, Tracing nitrogen sources and cycling in catchments. In: Kendall, C., McDonnell, J.J. (Eds.), Catchment Hydrology. Amsterdam, Elsevier Science, p. 519-576.

Kendall, C., and Aravena, R., 2000, Nitrate isotopes in groundwater systems, In: Cook, P., and Herczeg, A. L., eds., Environmental Tracers in Subsurface Hydrology: Boston, Kluwer Academic Publishers, p. 261-297.

Kingscote Chemicals, No Date, Water Tracing Dyes FLT Yellow/Green Products – Technical Data Bulletin, downloaded from http://www.brightdyes.com/technical/FLTGreen.html

Krom, M.D., & Berner, R.A., 1980, Adsorption of phosphate in anoxic marine sediments. Limnology and Oceanography, v. 25, p. 797-806.

Krom, M.D., & Berner, R.A., 1981, The diagenesis of phosphorus in a nearshore marine sediment. Geochimica et Cosmochimica Acta, v. 45, p. 207-216.

Kwon, B.-D., Chung, H.-J., and Lee, H.-S., 1993, Physical properties of volcanic rocks in Chejudo. Journal of Korean Earth Science Society, v. 14(3), p. 348-357 (in Korean).

Lane-Smith, D. R., W. C. Burnett, and H. Dulaiova, 2002. Continuous Radon-222 Measurements in the Coastal Zone, Sea Technology October 2002, p. 37-45.

Langenheim, V.A.M, and Clague, D.A., 1987, The Hawaiian Emperor volcanic chain, part II, stratigraphic framework of volcanic rocks of the Hawaiian Island: Chap. 1 of Decker, R.W., Wright, T.L., Stauffer, P.H., eds. Volcanism in Hawaii: U.S. Geological Survey Professional Paper 1350, v 1, p. 55-84

Langevin, C.D., Shoemaker, W.B., Guo, W., 2003, MODFLOW-2000, the U.S. Geological Survey Modular Ground-Water Model – Documentation of the SEAWAT-2000 Version with the variable-density Flow Process (VDF) and the Integrated MT3DMS Transport Process (IMT) – U.S. Geological Survey Open-File Report 03-426, 54 pgs.

Lau, L.S., and Mink, J.F., 2006, Hydrology of the Hawaiian Islands: Honolulu, University of Hawai'i Press, 274p.

Laws, E.A., Brown, D., and Peace, C., 2004, Coastal water quality in the Kihei and Lahaina districts of the island of Maui, Hawaiian Islands. Impacts from physical habitat and groundwater seepage: implications for water quality standards: International Journal of Environment and Pollution, v. 22, p. 531-547.

Lehman, M. F., Sigman, D. M., and Berelson, W. M., 2004, Coupling the N-15/N-14 and O-18/O-16 of nitrate as a constraint on benthic nitrogen cycling: Marine Chemistry, v. 88, p. 1–20.

Levy, B.S., and Chamber, R.M., 1987, Bromide as a conservative tracer for soil-water studies, Hydrological Processes, v. 1, p. 385-389.

Limtiaco Consulting Group, 2005, Hawaii Water Reuse Survey and Report – Final, Prepared for State of Hawaii, Department of Land and Natural Resources – Commission on Water Resource Management, February 2005.

Liu, F., Williams, M.W., and Caine, N., 2004, Source waters and flow paths in an alpine catchment, Colorado Front Range, United States: Water Resources Research, v. 40, W09401, DOI:10.1029/2004WR003076.

Liu, K.-K., and Kao, S.-J., 2007, A Three End-Member Mixing Model Based on Isotopic Composition and Elemental Ratio: Terr. Atmos. Ocean. Sci., v. 18, no. 5, p. 1067-1075.

MacDonald, G.A., Abbott, A.T., and Peterson, F.L., 1986, Volcanoes in the sea, the geology of Hawaii (2nd ed.): Honolulu, University of Hawaii Press, 517p.

Macintyre, S., Wanninkhof, R., & Chanton, J.P. (1995). Trace gas exchange across the air-sea interface in freshwater and coastal marine environments. In: P.A. Matson, R.C. Harriss (eds.) *Biogenic Trace Gases: Measuring Emissions from Soil and Water, Blackwell Science Ltd.* 52-97.

Malcolm, R.L., Aiken, G.R., Thurman, E.M., and Avery, P.A., 1980, Hydrophilic organic solutes as tracers in groundwater recharge studies, in Contaminants and Sediments, edited by R.A. Baker, p. 71-88, Butterworth-Heinemann

Meus, P., Käss, W., and Schnegg, P.A., 2006, Background and Detection of Fluorescent Tracers in Karst Groundwater, International Congress 'Ground Water in Mediterranean Countries – AQUAinMED, Malaga, Spain, April 24-28, 2006.

Mink, J.F., 1961, Some geochemical aspects of seawater intrusion in an island aqufier, International Association of Scientific Hydrology commission of subterranean waters v. 52, p. 424-429.

Mink, J.F., 1964, Groundwater temperatures in a tropical island environment, Journal of Geophysical Research v. 69, p.5225-5230.

Mink, J.F., and Lau, L.S., 1990, Aquifer identification and Classification for Maui: Groundwater Protection Strategy for Hawaii – Water Resources Research Center Technical Report No. 185, University of Hawaii at Manoa.

Moore, W.S. and Reid, D.F., 1973, Extraction of radium from natural waters using manganese-impregnated acrylic fibers. Journal of Geophysical Research, v. 90, p. 6983-6994.

Moore, W.S., 1976, Sampling Ra-228 in the deep ocean. Deep-Sea Res., v. 23, p. 647-651.

Moore, W.S. and Arnold, R., 1996, Measurement of [223]Ra and [224]Ra in coastal waters using a delayed coincidence counter. Journal of Geophysical Research, v. 101, p. 1321-1329.

Moore, W. S., 2006, The role of submarine groundwater discharge in coastal biogeochemistry: Journal of Geochemical Exploration, v. 88, no. 1-3, p. 389-393.

Nichols, W.D., Shade, P.J., and Hunt, C.D., 1996, Summary of the Oahu, Hawaii, Regional Aquifer-System Analysis: U.S. Geological Survey Professional Paper 1412-A, 61p.

Oberdorfer, J.A., and Peterson, F.L., 1982, Wastewater injection well problems, processes, and standards: Honolulu, University of Hawaii, Water Resources Research Center, Technical Report No. 146. 131p.

Oberdorfer, J.A., 1983, Wastewater Injection: Near-Well Processes and Their relationship to Clogging, [Ph.D. Dissertation] University of Hawaii, Honolulu, HI. 194 p. (with appendices).

Oki, D.S., 2005, Numerical Simulation of the Effects of Low-Permeability Valley-Fill Barriers and the Redistribution of Ground-Water Withdrawals in the Pearl Harbor Area, Oahu, Hawaii: U.S. Geological Survey Scientific Investigations Report 2005-5253, 111p.

Olsen, L.D., and Tenbus, F.J., 2004, Design of a natural-Gradient Ground-Water Tracer Test in Freshwater Tidal Wetland, West Branch Canal Creek, Aberdeen Proving Ground, Maryland, U. S. Geological Survey Scientific Investigations Report 2004-5190

Petty, S., and Peterson, F.L., 1979, Hawaiian waste injection practices and problems: Honolulu, University of Hawaii, Water Resources Research Center, Technical Report No. 123, 104 p.

Poiger, T, J.A. Field, T.M. Field, H. Siegrest, and W. Giger, 1998, Behavior of fluorescent whitening agents during sewage treatment, Water Research, v. 32(6), p. 1939-1947

Révész, K., Böhlke, J.K., and Yoshinari, T., 1997, Determination of δ18O and δ15N in nitrate: Analytical Chemistry, v. 69, no. 21, p. 4375-4380.

Robertson, W. D., Schiff, S. L., and Ptacek, C. J., 1998, Review of phosphate mobility and persistence in 10 septic system plumes: Ground Water, v. 36, p.1000-1010.

Rotzoll, K., and El-Kadi, A.I., 2007. Estimating hydraulic conductivity from specific capacity for Hawaii aquifers, USA: Hydrogeology Journal, v. 16, p. 969-979.

Ruttenberg, K.C., 2004, The global phosphorus cycle, in Holland, H.D. and Turekian , K.K., eds, Treatise on geochemistry, v. 8, Biogeochemistry, p. 585-643.

Sabatini, D.A., 2000, Sorption and Intraparticle Diffusion of Fluorescent Dyes with Consolidated Aquifer Media, Ground Water, v. 38(5), p. 651-656

Schluessel, P., Emery, W.J., Grassl, H., and Mammen,T., 1990,On the bulk-skin temperature difference and its impact on satellite remote sensing of sea surface temperature. Journal of Geophysical Research, v. 95(C8), p. 3341-13,356.

Schofield, J.C., 1956, Methods of distinguishing sea-groundwater from hydrothermal water, New Zealand Journal of Science and Technology, v. 37, p. 597-602.

Scholl, M. A., Gingerich, S. B., and Tribble, G. W., 2002, The influence of microclimates and fog on stable isotope signatures used in interpretation of regional hydrology, East Maui, Hawaii: Journal of Hydrology, v. 264, no. 1-4, p. 170-184.

Scholl, M.A., Gingerich, S.B., Loope, L.L., Giambelluca, T.W., and Nullett, M.A., 2004, Quantifying the importance of fog drip to ecosystem hydrology and water resources in tropical montane cloud forests on East Maui, Hawaii: Venture Capital Project final report, July 2004.

Shade, P.J., 1996, Water budget for the Lahaina district, island of Maui, Hawaii: Water-Resources Investigations Report 96-4238, 27 p.

Shade, P.J., 1997, Water budget for the Iao area, Island of Maui, Hawaii: U.S. Geological Survey Water-Resources Investigations Report 97–4244, 29p.

Shade, P.J., 1999, Water budget of East Maui, Hawaii: U.S. Geological Survey Water Resources Investigations Report 98–4159, 36p.

Sherrod, D.R., Sinton, J.M., Watkins, S.E. and Brunt, K.M., 2007, Geologic map of the state of Hawaii: U.S. Geological Survey Open-File Report 2007-1089, with GIS database.

Sigman, D. M., Casciotti, K. L., 2010, Nitrogen isotopes in the ocean. In: Steel. J.J., Turekian, K.K., and Thorpe, S.A. Encyclopedia of Ocean Sciences. New York, Elsevier, p. 1884-1894.

Sigman, D. M., Casciotti, K. L., Andreani, M., Barford, C., Galanter, M., and Bohlke, J. K., 2001, A Bacterial Method for the Nitrogen Isotopic Analysis of Nitrate in Seawater and Freshwater: Analytical Chemistry, v. 73, no. 17, p. 4145-4153.

Sigman, D. M., Granger, J., DiFiore, P, J., Lehmann, M.M., Ho, R., Cane, G, and van Geen, A., 2005, Coupled nitrogen and oxygen isotope measurements of nitrate along the eastern North Pacific margin: Global Biogeochemistry Cycles, vol. 19, GB4022.

Slomp, C. P., and Van Cappellen, P., 2004, Nutrient inputs to the coastal ocean through submarine groundwater discharge: controls and potential impact: Journal of Hydrology, v. 295, no. 1-4, p. 64-86.

Smart, P.L., and Laidlaw, I.M.S., 1977, An Evaluation of some fluorescent dyes for water tracing, Water Resources Research, v. 13, p. 15-33

Smart, C.C., and Karunaratne, K.C., 2002, Characterization of fluorescence background in dye tracing, Environmental Geology, v. 42, p. 492-498

Smith, C.M., and Smith, J.E., 2007, Algal blooms in north Kihei; an assessment of patterns & processes relating nutrient dynamics to algal abundance: University of Hawaii, Report to City and County of Maui. 65.

Smith, J.E., Runcie, J.W., and Smith, C.M., 2005, Characterization of a large-scale ephemeral bloom of the green alga Cladophora sericea on the coral reefs of West Maui, Hawaii. Marine Ecology Progress Series, v. 302, p. 77-91.

Soicher, A.J., 1996. Assessing Non-Point Pollutant Discharge to the Coastal Waters of West Maui, Hawaii [M.S. thesis]: Honolulu, University of Hawaii, 98 p.

Soicher, A.J., and Peterson, F.L., 1997, Terrestrial nutrient and sediment fluxes to the coastal waters of west Maui, Hawaii, Pacific Science, v. 51, p. 221-232.

Souza, W.R., 1981, Ground-water status report, Lahaina District, Maui, Hawaii, 1980: U.S. Geological Survey Open-File Report 81–549, 2 map sheets.

Souza, W.R., and Voss, C.I., 1987, Analysis of an anisotropic coastal aquifer system using variable-density flow and solute transport simulation. Journal of Hydrology, v. 92, p. 17-41.

Stanley, N.D, Thompson, G.M., Bentley, H.W., and Stiles, G., 1980, Ground-Water Tracers – A Short Review, Ground Water, v. 18(1), p. 14-23

Stearns, H.T., and MacDonald, G.A., 1942, Geology and Groundwater resources of the island of Maui, Hawaii: Hawaii (Territory) Division of Hydrography Bulletin, v. 7, 344p.

Stokes, T.R. and Griffiths, P., 2000, Working Paper 51 – A Preliminary Discussion of Karst Inventory Systems and Principles (KISP) for British Columbia Part, British Columbia Ministry of Forest Research Program, 124 p.

Storlazzi, C.D., Logan, J.B., McManus, M.A., and McLaughlin, B.E., 2003, Coastal circulation and sediment dynamics along West Maui, Hawaii Part II: 2003 Hydrgraphic survey cruises A-3-03-HW and A-4-03-HW report on the spatial structure of currents, temperature, salinity and turbidity along Western Maui: U.S. Geological Survey Open-File Report 03-430, 50 p.

Storlazzi, C. D., McManus, M. A., Logan, J. B., and McLaughlin, B. E., 2006, Cross-shore velocity shear, eddies and heterogeneity in water column properties over fringing coral reefs: West Maui, Hawaii: Continental Shelf Research, v. 26, no. 3, p. 401-421.

Storlazzi, C.D., and Field, M.E., 2008, Winds, waves, tides, and the resulting flow patterns and fluxes of water, sediment, and coral larvae off West Maui, Hawaii: U.S. Geological Survey Open File Report 2008-1215, 13 p.

Street, J.H., Knee, K.L., Grossman, E.E. and Paytan, A., 2008, Submarine groundwater discharge and nutrient addition to the coastal zone and coral reefs of leeward Hawaii: Marine Chemistry, v. 109, p. 355-376.

Stuart, M., Dignan, C., McClary, D., 2008, Evaluation of Marine Response Tools: Subtidal Containment and Treatment System – Prepared for MAF Biosecurity New Zealand, 45 p.

Stumm W. and Morgan J. J. (1996) Aquatic Chemistry. Wiley, New York, 1022p.

Sun, Y., Torgersen, T., 1998. Rapid and precise measurement method for adsorbed ^{224}Ra on sediments. Marine Chemistry, v. 61, p. 163–171.

Sutton, D.J., Kabala, Z.J., Franciso, A., and Vasudevan, D., 2001, limitations and potential of commercially available Rhodamine WT as a groundwater tracer, Water Resources Research, v. 37(6), p. 1641-1656

Swain, L.A., 1973, Chemical quality of ground-water in Hawaii: U.S. Geological Survey Report 48, 54 p.

Swarzenski, P.W., Storlazzi, C.D., Presto, M.K., Gibbs, A.E., Smith, C.G., Dimova, N.T., Dailer, M.L., and Logan, J.B., 2012 (in preparation), Nearshore morphology, benthic structure, hydrodynamics, and coastal groundwater discharge near Kahekili Beach Park, Maui, Hawaii: U.S. Geological Survey Open-File Report 2012-1166, 34 p.

Tetra Tech, Inc., 1993. Preliminary Assessment of Possible Anthropogenic Nutrient Sources in the Lahaina District of Maui – Final: Prepared for USEPA Region 9, the Hawaii Department of Health, and the County of Maui. July 1993, 116p. plus appendixes.

Tetra Tech, Inc., 1994, Effluent fate study, Lahaina wastewater reclamation facility, Maui, Hawaii: Prepared for U.S. Environmental Protection Agency Region 9, 73p. plus appendixes.

Thomas, D. M., 1986, Geothermal resources assessment in Hawaii: Geothermics, v. 15, no. 4, p. 435-514.

Tribble, G.W., F.J. Sansone, R.W. Buddemeier, and Y.-H. Li. 1992. Hydraulic exchange between a coral reef and surface seawater. Geol. Soc. Amer. Bull. 104: p. 1280-1291.

Turner Designs, 1999, Model 10-AU-005-CE Fluorometer User's Manual

U.S.A, 2011, 40 CFR Appendix B to Part 136 – Definition and Procedure for the Determination of the Method Detection Limit – Revision 1.11. http://ecfr.gpoaccess.gov/cgi/t/text/text-idx?c=ecfr&sid=8136cdb6d5784c413366cd1386e6a005&rgn=div9&view=text&node=40:22.0.1.1.1.0.1.7.2&idno=40. Downloaded 5/10/2011.

UNESCO, 1985, The international system of units (SI) in oceanography. UNESCO Technical Papers in Marine Science 45, 124p.

UNESCO, 1994, Protocols for the Joint Ocean Global Flux Study (JGOFS) Core Measurements, IOC Manual and Guides no. 29.

USCB, 2000. Census Tract 316, Maui County. In: Bureau, U.S.C. (Ed.), Washington DC.

USDA, 1972, Soil Survey of Islands of Kauai, Oahu, Maui, Molokai, and Lanai, State of Hawaii, United States Department of Agriculture Soil Conservation Service.

USEPA. 2011. 40 CFR Parts 144 through 147 – UIC Regulations. http://ecfr.gpoaccess.gov/cgi/t/text/text-idx?c=ecfr&sid=a96a3a46e4fc893355a2f89e7d5c7a57&rgn=div5&view=text&node=40:22.0.1.1.6&idno=40 . Downloaded 4/11/2011.

Valderrama, J. C. 1981. The simultaneous analysis of total nitrogen and phosphorus in natural waters: Marine Chemistry v. 10, p. 109–122.

Voss, C.I., and Provost, A.M., 2002, SUTRA, a model for saturated-unsaturated variable density ground-water flow with energy or solute transport: U.S. Geological Survey Open-File Report 02-4231.

West Maui Watershed Management Advisory Committee, 1977, West Maui Watershed Owner's Manual, 18p.

Wheatcraft, S.W., 1976, Waste Injection into the Hawaiian Ghyben-Herzberg Aquifer – a laboratory study using a sand-packed hydraulic model: Honolulu, University of Hawaii, Water Resources Research Center, Technical Report, No. 96. 69 p. (plus appendixes).

Wilson Okamoto Corporation, 2008, Hawaii Water Plan, Water Resource ProtectionPlan, Prepared for the State of Hawaii, Department of Land and Natural Resources, Commission on Water Resource Management

Wilson, R.D., and McKay, D.M., 1996, SF6 as a conservative tracer in saturated media with high intragranual porosity of high organic carbon content, Ground Water, v. 34, p. 241-249

Wisconsin Dept. of Natural Resources, 1996, Analytical Detection Limit Guidance & Laboratory Guide for Determining Method Detection Limits – PUBL-TS-056-96

Wood, P.J., and Dykes, A.P., 2002, The use of salt dilution gauging techniques: ecological considerations and insights, Water Research, v. 36(7), p. 3054-3062

WRCC, 2011, Western Regional Climate Center (http://www.wrcc.dri.edu/CLIMATEDATA.html)

Zektser, I. S., 2000, Groundwater and the Environment: Applications for the global community: Boca Raton, Florida, CRC Press LLC, 192 p.

Zheng, C., Wang, P., MT3DMS: A Modular Three-DimensionalMultispecies Transport Model for Simulation of Advection,Dispersion, and Chemical Reactions of Contaminants in Groundwater Systems; Documentation and User's Guide, U.S. Army Corps of Engineers, Engineer Research and Development Center, 220 pgs.

Zheng, C., 2006, MT3DMS v5.2 – Supplemental User's Guide, Dept. of Geological Sciences, University of Alabama, 46 pgs.

APPENDICES

APPENDIX A: FIELD WATER QUALITY AND FLUORESCENCE MEASUREMENTS OF SUBMARINE SPRINGS AND CONTROL LOCATIONS

APPENDIX FOR SECTION 2:

SUBMARINE SPRING AND MARINE CONTROL LOCATION SAMPLING, WATER QUALITY, AND FLUORESCENCE

This page is intentionally left blank.

Table A-1. Calibration of the handheld YSI for pH and specific conductivity

Model   YSI Model 63   **Serial Number**   07A1999 AA

Date	Time	Parameter (Spec. Cond. or pH)	Units	Exp. Date	Conc. or Stand.	Initial Reading	Corrected Reading	Operator's initials and remarks
7/7/2011	8:00 AM	7.00	pH	5/1/2012	pH 7.00	7.03	7.00	Temperature at 27.3°C
7/7/2011	8:00 AM	10.00	pH	3/1/2012	pH 10.00	9.99	9.99	
7/7/2011	8:00 AM	1000 μS/cm	μS/cm	5/3/2012	1000 μS/cm	1034.00	1043.00	
7/7/2011	8:00 AM	58,700 μS/cm	μS/cm	3/27/2012	58,700 μS/cm	60100.00	61500.00	
7/15/2011	8:00 AM	7.00	pH	5/1/2012	pH 7.00	7.16	7.00	Temperature at 28.3°C
7/15/2011	8:00 AM	10.00	pH	3/1/2012	pH 10.00	10.07	10.00	
7/15/2011	8:00 AM	1000 μS/cm	μS/cm	5/3/2012	1000 μS/cm	1024.00	NA	
7/15/2011	8:00 AM	58,700 μS/cm	μS/cm	3/27/2012	58,700 μS/cm	59000.00	NA	
7/31/2011	12:00 PM	7.00	pH	5/1/2012	pH 7.00	7.04	NA	
7/31/2011	12:00 PM	10.00	pH	3/1/2012	pH 10.00	10.02	NA	
8/8/2011	12:00 PM	7.00	pH	5/1/2012	pH 7.00	7.03	NA	
8/8/2011	12:00 PM	10.00	pH	3/1/2012	pH 10.00	10.01	NA	
8/18/2011	12:45 PM	7.00	pH	5/1/2012	pH 7.00	7.05	6.99	Temperature at 28.9°C
8/18/2011	12:45 PM	10.00	pH	3/1/2012	pH 10.00	9.96	10.02	
8/18/2011	12:45 PM	1000 μS/cm	μS/cm	5/3/2012	1000 μS/cm	1087.00	1086.00	
8/18/2011	12:45 PM	58,700 μS/cm	μS/cm	3/27/2012	58,700 μS/cm	63000.00	62700.00	
8/25/2011	8:15 AM	7.00	pH	5/1/2012	pH 7.00	7.14	6.99	Temperature at 25.7°C
8/25/2011	8:15 AM	10.00	pH	3/1/2012	pH 10.00	9.99	10.03	

Table A-1 Continued Date	Time	Parameter (Spec. Cond. or pH)	Units	Exp. Date	Conc. or Stand.	Initial Reading	Corrected Reading	Operator's initials and remarks
9/1/2011	8:00 AM	7.00	pH	5/1/2012	pH 7.00	7.03	NA	Temperature at 25.5°C
9/1/2011	8:00 AM	10.00	pH	3/1/2012	pH 10.00	10.01	NA	
9/8/2011	8:00 AM	7.00	pH	5/1/2012	pH 7.00	7.06	7.01	Temperature at 25.7°C
9/8/2011	8:00 AM	10.00	pH	3/1/2012	pH 10.00	9.95	9.99	
9/15/2011	8:00 AM	7.00	pH	5/1/2012	pH 7.00	7.02	NA	Temperature at 25.4°C
9/15/2011	8:00 AM	10.00	pH	3/1/2012	pH 10.00	10.03	NA	
9/15/2011	8:00 AM	1000 µS/cm	µS/cm	5/3/2012	1000 µS/cm	1091.00	NA	
9/15/2011	8:00 AM	58,700 µS/cm	µS/cm	3/27/2012	58,700 µS/cm	59300.00	NA	
9/22/2011	8:00 AM	7.00	pH	5/1/2012	pH 7.00	7.10	6.99	
9/22/2011	8:00 AM	10.00	pH	3/1/2012	pH 10.00	10.05	10.01	
9/29/2011	8:00 AM	7.00	pH	5/1/2012	pH 7.00	7.02	NA	
9/29/2011	8:00 AM	10.00	pH	3/1/2012	pH 10.00	10.01	NA	
10/6/2011	8:00 AM	7.00	pH	5/1/2012	pH 7.00	7.04	7.01	
10/6/2011	8:00 AM	10.00	pH	3/1/2012	pH 10.00	10.05	10.00	
10/13/2011	8:00 AM	7.00	pH	5/1/2012	pH 7.00	7.02	NA	
10/13/2011	8:00 AM	10.00	pH	3/1/2012	pH 10.00	10.01	NA	
10/20/2011	8:00 AM	7.00	pH	5/1/2012	pH 7.00	1.01	NA	Temperature at 25.6°C
10/20/2011	8:00 AM	10.00	pH	3/1/2012	pH 10.00	10.03	NA	
10/20/2011	8:00 AM	1000 µS/cm	µS/cm	5/3/2012	1000 µS/cm	1078.00	NA	
10/20/2011	8:00 AM	58,700 µS/cm	µS/cm	3/27/2012	58,700 µS/cm	58900.00	NA	
10/27/2011	8:00 AM	7.00	pH	5/1/2012	pH 7.00	7.05	7.01	
10/27/2011	8:00 AM	10.00	pH	3/1/2012	pH 10.00	10.06	10.02	
11/3/2011	8:00 AM	7.00	pH	5/1/2012	pH 7.00	7.03	NA	

Table A-1 Continued Date	Time	Parameter (Spec. Cond. or pH)	Units	Exp. Date	Conc. or Stand.	Initial Reading	Corrected Reading	Operator's initials and remarks
11/3/2011	8:00 AM	10.00	pH	3/1/2012	pH 10.00	10.04	NA	
11/10/2011	8:00 AM	7.00	pH	5/1/2012	pH 7.00	7.09	7.01	
11/10/2011	8:00 AM	10.00	pH	3/1/2012	pH 10.00	10.02	10.02	
11/17/2011	8:00 AM	7.00	pH	5/1/2012	pH 7.00	7.02	NA	
11/17/2011	8:00 AM	10.00	pH	3/1/2012	pH 10.00	10.01	NA	
11/28/2011	1:00 PM	7.00	pH	5/1/2012	pH 7.00	6.97	6.95	Temperature at 26.1°C
11/28/2011	1:00 PM	10.00	pH	3/1/2012	pH 10.00	10.03	10.03	
11/28/2011	1:00 PM	1000 µS/cm	µS/cm	5/3/2012	1000 µS/cm	1026.00	NA	
11/28/2011	1:00 PM	58,700 µS/cm	µS/cm	3/27/2012	58,700 µS/cm	59600.00	NA	
12/6/2011	8:00 AM	7.00	pH	5/1/2012	pH 7.00	7.02	NA	
12/6/2011	8:00 AM	10.00	pH	3/1/2012	pH 10.00	10.02	NA	
12/13/2011	8:00 AM	7.00	pH	5/1/2012	pH 7.00	7.01	NA	
12/13/2011	8:00 AM	10.00	pH	3/1/2012	pH 10.00	10.03	NA	
12/20/2011	8:00 PM	7.00	pH	5/1/2012	pH 7.00	6.99	7.01	
12/20/2011	8:00 PM	10.00	pH	3/1/2012	pH 10.00	10.04	10.02	
1/3/2012	8:00 PM	7.00	pH	5/1/2012	pH 7.00	7.02	NA	
1/3/2012	8:00 PM	10.00	pH	3/1/2012	pH 10.00	10.02	NA	
1/3/2012	8:00 PM	1000 µS/cm	µS/cm	5/3/2012	1000 µS/cm	1015	NA	Temperature at 27.6°C
1/3/2012	8:00 PM	58,700 µS/cm	µS/cm	3/27/2012	58,700 µS/cm	59800	NA	
1/10/2012	9:00 AM	7.00	pH	5/1/2012	pH 7.00	6.98	7.01	
1/10/2012	9:00 AM	10.00	pH	3/1/2012	pH 10.00	10.04	10.02	
1/17/2012	9:00 AM	7.00	pH	5/1/2012	pH 7.00	6.99	NA	
1/17/2012	9:00 AM	10.00	pH	3/1/2012	pH 10.00	10.00	NA	

Table A-1 Continued		Parameter (Spec. Cond. or pH)	Units	Exp. Date	Conc. or Stand.	Initial Reading	Corrected Reading	Operator's initials and remarks
Date	Time							
1/24/2012	8:00 PM	7.00	pH	5/1/2012	pH 7.00	7.02	7.04	Temperature at 24.4°C
1/24/2012	8:00 PM	10.00	pH	3/1/2012	pH 10.00	10.04	10.11	
1/30/2012	8:00 PM	7.00	pH	5/1/2012	pH 7.00	7.13	7.03	Temperature at 26.3°C
1/30/2012	8:00 PM	10.00	pH	3/1/2012	pH 10.00	10.15	10.06	
1/30/2012	8:00 PM	1000 μS/cm	μS/cm	5/3/2012	1000 μS/cm	1066	NA	
1/30/2012	8:00 PM	58,700 μS/cm	μS/cm	3/27/2012	58,700 μS/cm	59400	NA	
2/8/2012	8:00 PM	7.00	pH	5/1/2012	pH 7.00	7.02	NA	Temperature at 26.1°C
2/8/2012	8:00 PM	10.00	pH	3/1/2012	pH 10.00	10.01	NA	
2/14/2012	8:00 AM	7.00	pH	5/1/2012	pH 7.00	7.03	NA	Temperature at 26.1°C
2/14/2012	8:00 AM	10.00	pH	3/1/2012	pH 10.00	10.02	NA	
2/21/2012	9:00 AM	7.00	pH	5/1/2012	pH 7.00	7.02	NA	Temperature at 26.2°C
2/21/2012	9:00 AM	10.00	pH	3/1/2012	pH 10.00	10.03	NA	
2/28/2012	9:00 AM	7.00	pH	5/1/2012	pH 7.00	7.00	NA	Temperature at 25.9°C
2/28/2012	9:00 AM	10.00	pH	3/1/2012	pH 10.00	10.01	NA	
3/16/2012	9:00 AM	7.00	pH	7/6/2013	pH 7.00	7.09	6.99	Temperature at 25.8°C
3/16/2012	9:00 AM	10.00	pH	7/12/2013	pH 10.00	10.05	10.01	
3/29/2012	8:00 AM	7.00	pH	7/6/2013	pH 7.00	7.05	7.02	Temperature at 25.1°C
3/29/2012	8:00 AM	10.00	pH	7/12/2013	pH 10.00	10.09	10.00	
4/3/2012	7:30 PM	7.00	pH	7/6/2013	pH 7.00	6.37	6.89	Temperature at 28.9°C
4/3/2012	7:30 PM	10.00	pH	7/12/2013	pH 10.00	10.02	9.96	
4/15/2012	7:30 PM	7.00	pH	7/6/2013	pH 7.00	6.97	NA	Temperature at 28.3°C
4/15/2012	7:30 PM	10.00	pH	7/12/2013	pH 10.00	10.03	NA	
5/1/2012	8:00 PM	7.00	pH	7/6/2013	pH 7.00	7.03	NA	Temperature at 26.1°C

Table A-1 Continued Date	Time	Parameter (Spec. Cond. or pH)	Units	Exp. Date	Conc. or Stand.	Initial Reading	Corrected Reading	Operator's initials and remarks
5/1/2012	8:00 PM	10.00	pH	7/12/2013	pH 10.00	10.05	NA	

Table A-2. Calibration of the handheld field fluorometer with 100 ppb standards of
Fluorescein and Rhodamine.
NA = Not Applicable

Model: Aquafluor   Serial Number: 801398

Date	Time	Conc. of Stand. (ppb)	Initial Reading (ppb)	Corrected Reading (ppb)	Fluorescein or Rhodamine
8/2/2011	9:30 PM	100	97.44	99.84	Fluorescein
8/2/2011	9:30 PM	100	86.13	100.1	Rhodamine
8/4/2011	2:15 PM	100	100.70	NA	Fluorescein
8/4/2011	2:15 PM	100	103.30	99.8	Rhodamine
8/8/2011	1:00 PM	100	101.20	NA	Fluorescein
8/8/2011	1:00 PM	100	103.70	99.91	Rhodamine
8/10/2011	9:05 PM	100	99.48	NA	Fluorescein
8/10/2011	9:05 PM	100	96.31	100.1	Rhodamine
8/14/2011	11:00 AM	100	101.90	99.66	Fluorescein
8/14/2011	11:00 AM	100	107.30	99.99	Rhodamine
8/15/2011	9:00 PM	100	98.58	99.72	Fluorescein
8/15/2011	9:00 PM	100	96.46	100.1	Rhodamine
8/16/2011	10:32 PM	100	100.60	NA	Fluorescein
8/16/2011	10:32 PM	100	99.45	NA	Rhodamine
8/22/2011	9:30 AM	100	101.40	99.95	Fluorescein
8/22/2011	9:30 AM	100	102.40	100	Rhodamine
8/27/2011	12:30 PM	100	98.74	99.97	Fluorescein
8/27/2011	12:30 PM	100	97.56	99.84	Rhodamine
8/28/2011	12:00 PM	100	99.77	NA	Fluorescein
8/28/2011	12:00 PM	100	99.51	NA	Rhodamine
8/29/2011	1:30 PM	100	100.20	NA	Fluorescein
8/29/2011	1:30 PM	100	100.10	NA	Rhodamine
8/29/2011	9:30 AM	100	101.60	99.93	Fluorescein
8/29/2011	9:30 AM	100	103.40	99.87	Rhodamine
9/13/2011	8:00 PM	100	98.88	99.97	Fluorescein
9/13/2011	8:00 PM	100	97.57	99.95	Rhodamine

Table A-2 Continued Date	Time	Conc. of Stand. (ppb)	Initial Reading (ppb)	Corrected Reading (ppb)	Fluorescein or Rhodamine
9/19/2011	8:00 PM	100	99.69	NA	Fluorescein
9/19/2011	8:00 PM	100	99.10	NA	Rhodamine
10/3/2011	1:30 PM	100	99.66	NA	Fluorescein
10/3/2011	1:30 PM	100	99.42	NA	Rhodamine
10/7/2011	10:00 AM	100	101.50	99.91	Fluorescein
10/7/2011	10:00 AM	100	105.50	99.7	Rhodamine
10/12/2011	8:00 PM	100	98.71	99.65	Fluorescein
10/12/2011	8:00 PM	100	96.62	99.99	Rhodamine
10/20/2011	8:00 PM	100	101.90	99.85	Fluorescein
10/20/2011	8:00 PM	100	102.70	99.88	Rhodamine
10/28/2011	1:00 PM	100	101.90	99.67	Fluorescein
10/28/2011	1:00 PM	100	105.60	100	Rhodamine
11/4/2011	10:00 AM	100	101.10	99.81	Fluorescein
11/4/2011	10:00 AM	100	104.50	99.97	Rhodamine
11/14/2011	1:00 PM	100	99.05	NA	Fluorescein
11/14/2011	1:00 PM	100	96.31	99.9	Rhodamine
11/18/2011	1:00 PM	100	99.26	NA	Fluorescein
11/18/2011	1:00 PM	100	101.50	100	Rhodamine
11/21/2011	7:00 PM	100	97.66	99.61	Fluorescein
11/21/2011	7:00 PM	100	92.77	99.99	Rhodamine
11/24/2011	12:00 PM	100	103.70	99.65	Fluorescein
11/24/2011	12:00 PM	100	118.10	99.82	Rhodamine
11/26/2011	12:00 PM	100	99.05	NA	Fluorescein
11/26/2011	12:00 PM	100	97.43	99.9	Rhodamine
12/2/2011	1:00 PM	100	98.82	99.81	Fluorescein
12/2/2011	1:00 PM	100	98.35	99.81	Rhodamine
12/11/2011	6:00 PM	100	100.30	NA	Fluorescein
12/11/2011	6:00 PM	100	103.50	99.95	Rhodamine
12/16/2011	8:00 PM	100	100.40	NA	Fluorescein

Table A-2 Continued Date	Time	Conc. of Stand. (ppb)	Initial Reading (ppb)	Corrected Reading (ppb)	Fluorescein or Rhodamine
12/16/2011	8:00 PM	100	102.30	99.94	Rhodamine
1/13/2011	8:00 PM	100	86.09	99.69	Fluorescein
1/13/2011	8:00 PM	100	94.45	99.92	Rhodamine
1/26/2012	8:00 PM	100	98.05	99.75	Fluorescein
1/26/2012	8:00 PM	100	99.29	NA	Rhodamine
1/27/2012	7:30 PM	100	99.79	NA	Fluorescein
1/27/2012	7:30 PM	100	100.60	NA	Rhodamine
2/10/2012	8:00 PM	100	97.48	99.9	Fluorescein
2/10/2012	8:00 PM	100	99.93	99.93	Rhodamine
2/17/2012	5:00 PM	100	100.10	NA	Fluorescein
2/17/2012	5:00 PM	100	103.40	99.8	Rhodamine
2/21/2012	9:00 AM	100	101.70	99.82	Fluorescein
2/21/2012	9:00 AM	100	102.80	99.78	Rhodamine
3/2/2012	1:00 PM	100	97.49	99.79	Fluorescein
3/2/2012	1:00 PM	100	94.69	99.85	Rhodamine
3/13/2012	8:00 PM	100	101.00	99.73	Fluorescein
3/13/2012	8:00 PM	100	103.40	99.97	Rhodamine
3/22/2012	7:00 PM	100	97.47	100.3	Fluorescein
3/22/2012	7:00 PM	100	98.12	99.83	Rhodamine
3/29/2012	7:00 PM	100	101.20	99.62	Fluorescein
3/29/2012	7:00 PM	100	103.50	99.85	Rhodamine
4/2/2012	5:30 PM	100	95.76	99.82	Fluorescein
4/2/2012	5:30 PM	100	88.10	99.8	Rhodamine
4/14/2012	11:00 AM	100	104.30	100.1	Fluorescein
4/14/2012	11:00 AM	100	117.60	100.3	Rhodamine
4/20/2012	5:00 PM	100	102.50	100.6	Fluorescein
4/20/2012	5:00 PM	100	108.80	99.59	Rhodamine
5/3/2012	5:00 PM	100	96.02	99.92	Fluorescein
5/3/2012	5:00 PM	100	95.79	100.1	Rhodamine

Table A-3. South Seep Group water quality parameters
Water quality parameters collected from submarine spring samples in the South Seep
Group (Seeps 3, 4, 5, and 11) with a handheld YSI Model 63 and field fluorescence
measurements of S-Rhodamine-B (SRB) and Fluorescein (FLT) with a handheld
Aquafluor fluorometer model 8000-10 from 7/19/2011 to 5/2/2012.   Missing
fluorescence values are due to shipment of samples prior to analysis.

Location	Date	Time	Temp. (°C)	pH	Spec. Cond. (mS/cm)	Salinity	SRB (ppb)	FLT (ppb)
Seep 3	7/19/2011	10:15 AM	27.2	7.41	5.51	2.8	-0.174	-0.174
	7/20/2011	10:38 AM	27.1	7.36	5.45	2.8	0.725	0.109
	7/21/2011	9:05 AM	25.9	7.36	5.32	2.8	-0.235	0.321
	7/22/2011	10:42 AM	28.3	7.42	5.60	2.8	0.185	0.321
	7/23/2011	10:26 AM	27.8	7.50	6.48	3.3	0.115	0.105
	7/24/2011	10:10 AM	26.4	7.54	6.65	3.5	-0.111	0.012
	7/25/2011	10:47 AM	27.5	7.51	5.64	2.9	0.451	0.269
	7/26/2011	10:12 AM	26.4	7.44	5.45	2.8	0.717	0.077
	7/27/2011	10:55 AM	27.1	7.35	5.31	3.0	0.333	0.050
	7/28/2011	10:16 AM	27.6	7.38	5.50	2.8	-0.099	-0.154
	7/28/2011	4:34 PM	27.0	7.37	5.54	2.9	-0.015	-0.059
	7/29/2011	10:25 AM	26.6	7.40	5.31	2.8	0.302	0.107
	7/29/2011	4:29 PM	28.3	7.45	6.88	3.6	-0.044	0.056
	7/30/2011	11:38 AM	27.8	7.43	5.75	2.9	0.617	0.031
	7/30/2011	5:15 PM	26.8	7.44	5.63	2.9	0.565	-0.002
	7/31/2011	10:51 AM	27.5	7.46	5.49	2.8	0.545	0.031
	7/31/2011	4:52 PM	26.8	7.48	14.91	8.3	1.176	0.022
	8/1/2011	10:49 AM	27.8	7.46	5.51	2.8	0.863	0.224
	8/1/2011	4:21 PM	27.8	7.51	20.73	11.6	0.682	-0.056
	8/2/2011	9:04 AM	25.6	7.49	5.20	2.8	-0.223	-0.174
	8/2/2011	4:12 PM	26.8	7.42	5.41	2.8	0.649	-0.013
	8/3/2011	10:28 AM	30.7	7.30	5.56	2.7	0.414	-0.100
	8/3/2011	4:38 PM	28.6	7.35	5.53	2.8	0.138	0.000
	8/4/2011	11:17 AM	29.9	7.42	5.55	2.8	-0.400	-0.189
	8/4/2011	4:48 PM	27.5	7.47	5.40	2.8	-0.116	-0.097
	8/5/2011	11:07 AM	27.9	7.50	5.50	2.8	0.480	0.096
	8/5/2011	5:17 PM	26.7	7.49	5.41	2.8	-0.527	-0.132
	8/6/2011	9:37 AM	27.1	7.31	5.46	2.8	-0.327	0.052
	8/6/2011	4:01 PM	30.0	7.36	5.70	2.8	-0.303	0.016
	8/7/2011	10:03 AM	26.7	7.44	5.38	2.8	-0.269	-0.040
	8/7/2011	4:18 PM	28.1	7.40	5.52	2.8	-0.062	-0.048
	8/8/2011	10:15 AM	27.8	7.47	6.09	3.1	-0.204	-0.194
	8/8/2011	4:12 PM	29.4	7.44	5.66	2.8	0.512	-0.081
	8/9/2011	10:05 AM	28.2	7.52	5.58	2.8	0.868	-0.030
	8/9/2011	4:02 PM	28.8	7.45	5.63	2.8	0.271	0.121
	8/10/2011	12:29 PM	29.2	7.56	6.47	3.2	-0.040	-0.084
	8/10/2011	4:38 PM	28.3	7.60	5.60	2.8	0.076	-0.078
	8/11/2011	10:04 AM	27.9	7.76	5.53	2.8	-0.490	0.284

Table A-3 Cont. Location	Date	Time	Temp. (°C)	pH	Spec. Cond. (mS/cm)	Salinity	SRB (ppb)	FLT (ppb)
Seep 3 Cont.	8/11/2011	4:27 PM	28.9	7.64	6.75	3.4	-0.834	0.088
	8/12/2011	10:02 AM	26.6	7.64	5.31	2.8	0.359	0.227
	8/12/2011	4:21 PM	29.5	7.61	6.75	3.3	-0.300	0.183
	8/13/2011	9:55 AM	27.0	7.55	5.43	2.8	-0.311	0.351
	8/13/2011	4:02 PM	29.9	7.50	6.43	3.1	0.545	0.346
	8/14/2011	10:26 AM	27.6	7.58	5.50	2.8	0.571	0.296
	8/14/2011	4:23 PM	25.9	7.59	6.34	3.4	0.176	0.402
	8/15/2011	9:56 AM	25.9	7.55	5.29	2.8	0.250	0.201
	8/15/2011	4:08 PM	27.9	7.58	6.68	3.4	0.086	0.294
	8/16/2011	10:22 AM	27.8	7.59	5.52	2.8	-0.014	0.193
	8/16/2011	3:55 PM	28.3	7.55	5.85	2.5	1.065	0.211
	8/17/2011	11:15 AM	29.1	7.61	5.67	2.8	0.822	0.210
	8/17/2011	4:39 PM	28.4	7.58	6.76	3.4	-0.285	0.365
	8/18/2011	10:35 AM	29.9	7.53	5.73	2.8	0.074	0.177
	8/18/2011	4:41 PM	26.7	7.46	5.93	3.1	0.200	0.294
	8/19/2011	10:33 AM	30.1	7.54	6.02	3.0	0.209	0.282
	8/19/2011	4:43 PM	29.2	7.49	5.74	2.8	0.695	0.087
	8/20/2011	10:31 AM	29.5	7.56	6.14	3.0	0.155	0.034
	8/20/2011	4:32 PM	26.6	7.59	5.41	2.8	-0.236	0.228
	8/21/2011	10:34 AM	27.7	7.55	6.07	3.1	-0.151	0.118
	8/21/2011	4:41 PM	28.0	7.54	5.55	2.8	0.812	0.134
	8/22/2011	4:39 PM	29.1	7.53	8.17	4.2	0.636	0.314
	8/22/2011	10:01 AM	28.1	7.57	12.25	6.6	0.172	0.246
	8/23/2011	10:07 AM	30.0	7.54	13.31	6.9	-0.285	0.184
	8/23/2011	4:02 PM	28.2	7.44	7.99	4.1	0.203	0.086
	8/24/2011	11:20 AM	28.4	7.71	28.18	16.1	0.440	0.141
	8/24/2011	5:46 PM	28.0	7.56	5.56	2.9	0.188	0.067
	8/25/2011	10:55 AM	29.8	7.62	5.88	2.9	0.497	0.091
	8/25/2011	5:23 PM	27.6	7.71	5.59	2.9	0.230	0.093
	8/26/2011	10:15 AM	29.0	7.80	5.83	2.9	0.329	-0.035
	8/26/2011	4:24 PM	28.2	7.71	5.82	3.0	0.328	0.338
	8/27/2011	10:51 AM	28.8	7.49	5.72	2.9	0.349	0.092
	8/27/2011	5:29 PM	27.7	7.49	5.70	2.9	0.147	0.375
	8/28/2011	10:17 AM	28.6	7.57	5.65	2.8	0.155	0.033
	8/28/2011	4:36 PM	28.2	7.79	6.00	3.0	0.239	0.269
	8/29/2011	10:32 AM	28.0	7.32	5.64	2.9	0.230	0.326
	8/29/2011	4:37 PM	28.8	7.36	8.47	4.4	0.420	0.082
	8/30/2011	10:10 AM	28.4	7.45	6.19	3.1	0.791	0.185
	9/2/2011	12:17 PM	32.2	7.64	5.86	2.7	-0.345	0.480
	9/2/2011	5:00 PM	28.8	7.61	5.57	2.8	-0.606	0.160
	9/3/2011	10:35 AM	27.4	7.79	5.49	2.8	-0.424	0.501
	9/3/2011	4:47 PM	27.7	7.90	5.51	2.8	-0.320	0.302
	9/4/2011	4:48 PM	30.2	7.39	5.73	2.8	-0.175	0.364

Table A-3 Cont. Location	Date	Time	Temp. (°C)	pH	Spec. Cond. (mS/cm)	Salinity	SRB (ppb)	FLT (ppb)
Seep 3 Cont.	9/5/2011	10:18 AM	29.9	7.46	5.77	2.8	-0.248	0.303
	9/5/2011	4:41 PM	26.8	7.49	5.39	2.8	-0.340	0.387
	9/6/2011	10:04 AM	27.1	7.27	5.49	2.8	-0.415	0.182
	9/6/2011	4:30 PM	30.8	7.48	5.73	2.7	-0.471	0.310
	9/7/2011	10:02 AM	29.3	7.49	6.09	3.0	-0.383	0.264
	9/8/2011	10:09 AM	29.1	7.40	5.63	2.8	-0.741	0.339
	9/9/2011	11:23 AM	30.6	7.45	5.79	2.8	-0.694	0.184
	9/10/2011	11:36 AM	30.4	7.41	5.59	3.0	-0.666	0.219
	9/12/2011	12:39 PM	32.3	7.44	5.83	2.7	0.316	0.462
	9/13/2011	11:52 AM	33.3	7.55	6.05	2.8	-0.130	0.241
	9/14/2011	10:49 AM	32.1	7.53	7.02	3.3	-0.466	0.282
	9/15/2011	10:27 AM	33.2	7.77	6.19	2.8	0.289	0.253
	9/16/2011	12:20 PM	34.9	7.63	6.49	2.9	-0.291	0.147
	9/17/2011	3:37 PM	31.5	7.41	6.92	3.3	-0.384	0.345
	9/18/2011	12:19 PM	31.3	7.39	6.09	2.9	-0.836	0.223
	9/19/2011	11:20 AM	32.6	7.39	17.08	8.5	-0.584	0.199
	9/20/2011	10:30 AM	28.9	7.43	9.83	5.1	0.026	0.235
	9/21/2011	10:08 AM	30.6	7.37	7.49	3.6	-0.302	0.412
	9/22/2011	10:19 AM	29.4	7.94	6.54	3.3	-0.219	0.365
	9/23/2011	10:23 AM	31.1	7.49	6.81	3.2	-0.079	0.391
	9/24/2011	9:55 AM	30.3	7.56	6.58	3.2	0.624	0.324
	9/25/2011	11:24 AM	31.3	7.48	6.70	3.2	-0.308	0.395
	9/26/2011	11:39 AM	32.6	7.57	15.18	7.5	0.331	0.411
	9/27/2011	10:14 AM	30.8	7.46	5.71	2.7	-0.117	0.153
	9/28/2011	10:07 AM	29.2	7.40	5.56	2.8	-0.971	0.283
	9/29/2011	10:14 AM	29.0	7.41	5.56	2.8	-0.589	0.092
	9/30/2011	10:25 AM	30.3	7.43	5.64	2.7	-0.404	0.251
	10/1/2011	10:38 AM	32.9	7.75	5.95	2.7	0.272	0.116
	10/2/2011	1:13 PM	33.8	7.50	6.56	3.0	0.193	0.100
	10/3/2011	10:16 AM	28.4	7.48	5.66	2.9	0.072	0.131
	10/8/2011	5:12 PM	27.8	7.64	5.49	2.8	0.610	0.356
	10/10/2011	12:28 PM	33.6	7.59	6.84	2.8	-0.430	0.403
	10/12/2011	10:07 AM	29.5	7.56	5.53	2.7	-0.243	0.489
	10/14/2011	10:15 AM	30.5	7.55	5.56	2.7	0.338	0.297
	10/16/2011	10:06 AM	31.1	7.55	5.72	2.7	1.344	0.243
	10/18/2011	12:47 PM	31.9	7.60	5.98	2.8	0.547	0.202
	10/20/2011	10:33 AM	29.9	7.63	5.71	2.8	1.019	0.207
	10/22/2011	10:39 AM	30.9	7.67	5.72	2.7	0.176	0.167
	10/24/2011	10:18 AM	32.7	7.49	5.90	2.7	0.435	0.317
	10/26/2011	10:28 AM	31.0	7.50	5.82	2.8	-0.353	0.046
	10/28/2011	10:19 AM	27.7	7.62	5.56	2.8	0.658	0.101
	10/30/2011	12:27 PM	32.7	7.65	6.16	2.9	-0.460	0.271
	11/1/2011	12:26 PM	33.3	7.61	6.14	2.8	-0.150	0.283

Table A-3 Cont. Location	Date	Time	Temp. (°C)	pH	Spec. Cond. (mS/cm)	Salinity	SRB (ppb)	FLT (ppb)
Seep 3 Cont.	11/3/2011	10:21 AM	29.9	7.57	5.79	2.8	-0.257	0.413
	11/5/2011	2:29 PM	33.4	7.56	6.16	2.8	-0.334	0.239
	11/7/2011	10:10 AM	31.0	7.60	5.85	2.8	-0.177	0.523
	11/9/2011	10:54 AM	29.2	7.52	5.68	2.8	0.120	0.307
	11/11/2011	10:44 AM	27.2	7.62	5.51	2.8	-0.180	0.234
	11/14/2011	9:47 AM	29.2	7.22	5.59	2.8	0.418	0.581
	11/16/2011	10:39 AM	28.7	7.27	5.67	2.8	0.725	0.218
	11/18/2011	10:59 AM	28.1	7.36	5.68	2.9	0.723	0.426
	11/21/2011	10:42 AM	30.3	7.44	5.87	2.8	0.223	-0.102
	11/23/2011	10:25 AM	29.3	7.54	5.66	2.8	-0.117	0.127
	11/25/2011	10:47 AM	27.9	7.40	5.60	2.8	-0.170	0.200
	11/28/2011	10:35 AM	29.1	7.60	5.65	2.8	0.443	0.237
	11/30/2011	10:18 AM	27.6	7.45	5.48	2.8	0.285	0.351
	12/2/2011	10:21 AM	27.8	7.45	5.52	2.8	-0.038	0.392
	12/5/2011	10:35 AM	27.7	7.50	5.54	2.9	0.222	0.730
	12/7/2011	10:34 AM	29.0	7.50	5.59	2.8	0.579	0.653
	12/9/2011	10:15 AM	25.4	7.63	5.34	2.8	0.307	0.756
	12/12/2011	10:16 AM	24.6	7.65	5.59	3.0	0.137	1.010
	12/14/2011	10:10 AM	25.7	7.41	5.72	2.9	-0.173	1.237
	12/16/2011	10:16 AM	27.7	7.52	5.62	2.9	0.105	1.468
	12/19/2011	10:26 AM	26.7	7.47	5.65	2.9		
	12/21/2011	11:23 AM	28.3	7.43	5.88	3.0		
	12/23/2011	10:56 AM	24.2	7.63	5.42	3.0		
	12/26/2011	10:57 AM	27.3	7.39	5.66	2.9		
	12/28/2011	10:34 AM	27.7	7.52	6.03	3.1		
	12/30/2011	11:13 AM	28.9	7.65	7.33	3.7		
	1/2/2012	11:37 AM	29.1	7.68	14.89	8.0		
	1/7/2012	3:51 PM	28.5	7.55	5.88	3.0	1.145	18.31
	1/9/2012	12:34 PM	27.8	7.40	5.84	3.0	1.041	20.46
	1/11/2012	11:35 AM	24.9	7.44	5.38	2.9	0.997	22.39
	1/16/2012	2:04 PM	28.4	7.67	5.67	2.8		
	1/19/2012	10:52 AM	28.1	7.52	5.60	2.8	0.896	30.27
	1/21/2012	2:37 PM	28.7	7.52	6.58	3.3	1.080	32.86
	1/23/2012	12:15 PM	26.5	7.49	5.49	2.9	1.556	35.19
	1/25/2012	12:38 PM	28.3	7.51	5.75	2.9	1.069	37.55
	1/27/2012	1:26 PM	29.0	7.74	5.81	2.9	1.140	37.02
	1/31/2012	12:25 PM	27.4	7.60	5.66	2.9	1.332	44.34
	2/10/2012	12:56 PM	27.4	7.64	6.08	3.1	1.453	55.09
	2/14/2012	2:22 PM	28.7	7.58	5.97	3.0	1.771	62.18
	2/17/2012	12:32 PM	26.2	7.65	6.04	3.2	2.455	63.00
	2/20/2012	2:40 PM	29.6	7.59	6.83	3.4	1.759	65.55
	2/24/2012	12:05 PM	27.7	7.64	8.18	4.3	1.336	66.50
	2/27/2012	11:33 PM	28.2	7.66	7.29	3.8	1.677	71.96

Table A-3 Cont. Location	Date	Time	Temp. (°C)	pH	Spec. Cond. (mS/cm)	Salinity	SRB (ppb)	FLT (ppb)
Seep 3 Cont.	3/1/2012	12:34 PM	29.4	7.56	5.94	2.9	2.197	78.06
	3/11/2012	11:59 AM	29.9	7.65	6.26	3.0	2.551	87.31
	3/14/2012	11:05 AM	24.5	7.66	5.56	3.0		
	3/17/2012	10:24 AM	26.0	7.60	5.65	3.0	3.340	99.37
	3/19/2012	10:40 AM	27.4	7.61	5.87	3.0	3.074	101.4
	3/22/2012	10:50 AM	27.5	7.49	6.24	3.2	3.131	98.94
	3/27/2012	10:30 AM	25.5	7.55	5.73	3.1	2.571	104.3
	3/29/2012	11:19 AM	25.6	7.43	5.84	3.1	3.255	106.7
	3/31/2012	4:39 PM	27.4		5.96	3.1	3.897	108.7
	4/2/2012	11:14 AM	26.8		6.11	3.2	3.562	108.5
	4/5/2012	9:25 AM	25.1	7.35	5.72	3.1	2.788	110.9
	4/12/2012	9:34 AM	28.2	7.46	6.03	3.1	3.218	112.6
	4/16/2012	10:42 AM	29.7	7.51	6.14	3.0	2.620	106.0
	4/19/2012	12:18 PM	27.6	7.58	6.15	3.2	2.803	109.7
	4/24/2012	4:08 PM	26.9	7.65	8.27	4.4	3.369	114.9
	4/26/2012	11:40 AM	28.4	7.66	6.34	3.2	3.816	113.5
	5/2/2012	11:44 AM	28.7	7.52	6.61	3.3	4.525	114.7

Location	Date	Time	Temp. (°C)	pH	Spec. Cond. (mS/cm)	Salinity	SRB (ppb)	FLT (ppb)
Seep 4	7/19/2011	10:25 AM	27.8	7.47	6.09	3.1	0.983	0.110
	7/20/2011	10:53 AM	27.9	7.50	6.16	3.1	0.709	0.375
	7/21/2011	9:15 AM	25.9	7.20	5.97	3.2	0.328	0.170
	7/22/2011	10:52 AM	27.6	7.35	6.27	3.2	-0.121	0.185
	7/23/2011	10:31 AM	27.1	7.47	6.10	3.2	0.022	0.232
	7/24/2011	10:20 AM	26.3	7.53	6.61	3.6	1.025	0.151
	7/25/2011	10:48 AM	26.5	7.54	8.45	4.5	-0.056	-0.171
	7/26/2011	10:26 AM	26.4	7.47	6.26	3.4	0.024	0.033
	7/27/2011	11:04 AM	26.7	7.48	6.05	3.2	-0.256	0.077
	7/28/2011	10:25 AM	27.0	7.47	6.16	3.2	0.330	0.100
	7/28/2011	5:01 PM	26.8	7.33	6.43	3.4	0.221	-0.193
	7/29/2011	10:34 AM	26.6	7.38	6.00	3.1	1.056	-0.054
	7/29/2011	4:36 PM	28.0	7.46	9.26	4.8	0.549	-0.052
	7/30/2011	11:44 AM	28.0	7.42	6.27	3.2	-0.291	-0.113
	7/30/2011	6:26 PM	27.0	7.43	7.42	3.9	-0.115	-0.107
	7/31/2011	11:01 AM	27.7	7.43	6.25	3.2	1.021	-0.060
	7/31/2011	5:08 PM	27.4	7.57	22.25	12.7	-0.114	0.091
	8/1/2011	10:49 AM	28.5	7.44	6.82	3.5	0.584	0.086
	8/1/2011	4:32 PM	27.8	7.49	8.24	4.3	0.914	-0.055
	8/2/2011	9:13 AM	26.3	7.48	5.80	3.1	0.474	0.064
	8/2/2011	4:20 PM	27.0	7.38	5.94	3.1	-0.007	0.022
	8/3/2011	10:38 AM	27.4	7.36	6.03	3.1	0.600	-0.126

Table A-3 Cont. Location	Date	Time	Temp. (°C)	pH	Spec. Cond. (mS/cm)	Salinity	SRB (ppb)	FLT (ppb)
Seep 4 Cont.	8/3/2011	4:48 PM	27.0	7.36	6.29	3.3	0.035	-0.190
	8/4/2011	11:23 AM	27.3	7.43	5.97	3.1	-0.102	0.199
	8/4/2011	4:55 PM	27.1	7.42	6.20	3.2	0.799	-0.073
	8/5/2011	11:15 AM	27.6	7.46	6.11	3.1	0.482	0.173
	8/5/2011	5:25 PM	26.4	7.55	5.94	3.1	-0.137	-0.092
	8/6/2011	9:49 AM	26.4	7.42	5.96	3.1	0.740	-0.012
	8/6/2011	4:10 PM	29.1	7.41	6.21	3.1	0.151	-0.031
	8/7/2011	10:13 AM	26.3	7.36	6.03	3.1	-0.384	-0.187
	8/7/2011	4:25 PM	27.4	7.41	6.07	3.1	-0.058	-0.144
	8/8/2011	10:25 AM	28.4	7.44	6.32	2.8	0.152	-0.043
	8/8/2011	4:22 PM	29.0	7.36	6.29	3.1	0.561	-0.129
	8/9/2011	10:18 AM	27.5	7.47	6.17	3.2	0.260	-0.095
	8/9/2011	4:10 PM	28.1	7.42	6.40	3.2	-0.034	-0.056
	8/10/2011	12:40 PM	28.3	7.58	7.77	4.0	-0.027	-0.156
	8/10/2011	4:48 PM	27.9	7.52	6.18	3.2	-0.459	-0.232
	8/11/2011	10:08 AM	27.4	7.67	6.06	3.1	0.733	0.104
	8/11/2011	4:33 PM	28.7	7.66	6.25	3.2	-0.212	0.402
	8/12/2011	10:09 AM	26.7	7.63	5.95	3.1	0.080	0.105
	8/12/2011	4:29 PM	28.9	7.51	8.62	4.4	0.094	0.155
	8/13/2011	10:07 AM	27.5	7.51	6.06	3.1	0.410	0.328
	8/13/2011	4:08 PM	28.2	7.47	9.36	4.9	-0.523	0.004
	8/14/2011	10:37 AM	27.2	7.46	6.02	3.1	0.576	0.358
	8/14/2011	4:30 PM	26.2	7.40	6.96	3.7	0.611	0.311
	8/15/2011	10:04 AM	25.9	7.46	5.88	3.1	0.334	0.185
	8/15/2011	4:16 PM	27.3	7.47	7.12	3.7	0.289	1.335
	8/16/2011	10:30 AM	28.0	7.51	6.07	3.1	0.612	0.330
	8/16/2011	4:03 PM	27.8	7.55	6.20	3.2	0.098	0.182
	8/17/2011	11:27 AM	29.5	7.47	6.18	3.1	-0.049	0.317
	8/17/2011	4:47 PM	28.5	7.45	6.56	3.3	0.861	0.201
	8/18/2011	11:02 AM	29.1	7.50	6.23	3.1	-0.185	0.144
	8/18/2011	4:51 PM	27.5	7.37	6.06	3.1	-0.080	0.821
	8/19/2011	10:45 AM	29.0	7.52	6.19	3.1	-0.288	0.200
	8/19/2011	4:51 PM	28.9	7.52	6.16	3.1		
	8/20/2011	10:40 AM	28.9	7.57	6.20	3.1	0.628	0.322
	8/20/2011	4:39 PM	26.6	7.55	5.92	3.1	0.110	0.165
	8/21/2011	10:44 AM	27.7	7.48	6.05	3.1	0.232	0.191
	8/21/2011	4:55 PM	27.9	7.51	6.10	3.1	0.370	0.582
	8/22/2011	10:12 AM	27.7	7.51	9.62	5.4	0.020	0.304
	8/22/2011	4:48 PM	28.6	7.57	6.51	3.5	0.824	0.345
	8/23/2011	10:25 AM	28.0	7.66	8.49	4.4	-0.332	-0.019
	8/23/2011	4:08 PM	28.3	7.48	7.05	3.9	0.009	0.103
	8/24/2011	11:38 AM	27.5	7.58	9.25	4.9	-0.070	0.081
	8/24/2011	5:58 PM	27.6	7.50	6.06	3.1	-0.130	0.052

Table A-3 Cont. Location	Date	Time	Temp. (°C)	pH	Spec. Cond. (mS/cm)	Salinity	SRB (ppb)	FLT (ppb)
Seep 4 Cont.	8/25/2011	11:05 AM	27.7	7.63	6.99	3.6	0.477	0.100
	8/25/2011	5:35 PM	27.1	7.57	6.02	3.1	0.571	0.541
	8/26/2011	10:24 AM	27.6	7.55	6.93	3.6	0.330	0.162
	8/26/2011	4:33 PM	27.9	7.57	7.10	3.7	0.361	0.372
	8/27/2011	11:02 AM	28.5	7.65	6.33	3.2	0.773	0.029
	8/27/2011	5:41 PM	27.5	7.58	6.06	3.1	0.233	0.371
	8/28/2011	10:22 AM	28.1	7.57	6.13	3.1	0.030	0.038
	8/28/2011	4:44 PM	29.9	7.56	6.11	3.0	0.283	0.119
	8/29/2011	10:42 AM	28.4	7.59	6.21	3.1	0.045	0.095
	8/29/2011	4:41 PM	27.7	7.51	10.40	5.6	0.623	0.388
	9/2/2011	11:53 AM	32.4	7.60	7.63	3.6	0.401	0.151
	9/2/2011	5:14 PM	28.1	7.55	6.94	3.6	0.160	0.335
	9/3/2011	10:44 AM	26.9	7.74	6.25	3.3	-0.168	0.404
	9/4/2011	5:00 PM	29.7	7.47	6.30	3.1	-0.176	0.600
	9/5/2011	10:28 AM	31.0	7.46	7.71	3.8	-0.201	0.247
	9/5/2011	4:50 PM	26.8	7.48	5.99	3.1	-0.536	0.604
	9/6/2011	10:13 AM	28.1	7.35	6.55	3.0	-0.306	0.567
	9/6/2011	4:40 PM	31.0	7.50	6.25	3.0	-0.472	0.253
	9/7/2011	10:10 AM	29.9	7.49	6.83	3.4	-0.464	0.485
	9/8/2011	10:18 AM	29.1	7.47	7.38	3.7	-0.348	0.404
	9/9/2011	11:36 AM	29.4	7.47	9.28	4.7	-0.718	0.337
	9/10/2011	11:52 AM	30.9	7.50	10.99	5.5	-0.880	0.161
	9/12/2011	12:55 PM	29.2	7.48	8.41	4.3	-0.397	0.575
	9/13/2011	12:07 PM	32.9	7.55	10.55	5.0	-0.295	0.262
	9/14/2011	11:03 AM	31.9	7.51	6.91	3.3	0.312	0.122
	9/15/2011	10:45 AM	33.5	7.85	7.08	3.4	-0.590	0.091
	9/16/2011	12:31 PM	34.6	7.55	9.05	4.1	-0.273	0.388
	9/17/2011	3:50 PM	31.5	7.49	10.30	5.1	0.288	0.358
	9/18/2011	12:35 PM	33.9	7.48	7.17	3.3	0.209	0.163
	9/19/2011	11:36 AM	32.3	7.55	13.17	6.5	-0.590	0.070
	9/20/2011	10:41 AM	29.0	7.47	9.92	5.1	-0.414	0.167
	9/21/2011	10:18 AM	31.1	7.51	9.87	4.9	-0.724	0.188
	9/23/2011	10:34 AM	30.1	7.47	9.23	4.6	-0.129	0.297
	9/24/2011	10:05 AM	30.5	7.48	7.61	3.7	-0.326	0.262
	9/25/2011	11:40 AM	31.2	7.41	12.99	6.4	-0.496	0.227
	9/26/2011	11:53 AM	31.6	7.45	9.54	4.7	-0.027	0.445
	9/27/2011	10:25 AM	29.7	7.42	6.21	3.1	-0.183	0.076
	9/28/2011	10:18 AM	29.8	7.43	6.07	3.0		
	9/29/2011	10:31 AM	30.8	7.47	6.18	3.0	-0.842	0.251
	9/30/2011	10:36 AM	30.9	7.44	6.21	3.0	-0.505	0.135
	10/1/2011	10:51 AM	32.5	7.69	6.48	3.0	-0.164	-0.026
	10/2/2011	1:27 PM	32.1	7.40	6.44	3.0	0.645	-0.003
	10/3/2011	10:28 AM	31.4	7.43	6.74	3.2	-0.033	0.003

Table A-3 Cont. Location	Date	Time	Temp. (°C)	pH	Spec. Cond. (mS/cm)	Salinity	SRB (ppb)	FLT (ppb)
Seep 4 Cont.	10/8/2011	5:27 PM	27.2	7.40	5.71	3.1	-0.040	0.540
	10/10/2011	12:37 PM	32.7	7.47	6.51	3.0	-0.047	0.273
	10/12/2011	10:20 AM	30.4	7.46	6.05	2.9	-0.356	0.500
	10/14/2011	10:26 AM	31.0	7.43	6.36	3.0	0.576	0.190
	10/16/2011	10:19 AM	30.9	7.52	7.06	3.4	0.443	0.189
	10/18/2011	12:59 PM	32.2	7.47	6.56	3.1	0.460	0.328
	10/20/2011	10:44 AM	30.5	7.41	9.23	4.6	0.466	0.219
	10/22/2011	10:16 AM	31.9	7.57	6.89	3.3	0.174	0.236
	10/24/2011	10:29 AM	31.3	7.51	6.60	3.2	-0.334	0.130
	10/26/2011	10:39 AM	30.7	7.42	6.34	3.0	-0.106	0.307
	10/28/2011	10:30 AM	29.7	7.48	6.33	3.1	-0.059	0.169
	10/30/2011	12:55 PM	34.3	7.47	6.95	3.2	-0.245	0.285
	11/1/2011	12:37 PM	32.4	7.46	8.52	3.3	-0.598	0.225
	11/3/2011	10:35 AM	31.0	7.45	9.98	5.0	-0.115	0.298
	11/5/2011	2:58 PM	33.2	7.45	6.85	3.2	0.506	0.317
	11/7/2011	10:20 AM	31.9	7.49	6.37	3.0	-0.457	0.347
	11/9/2011	11:19 AM	30.7	7.43	6.32	3.0	0.008	0.319
	11/11/2011	10:55 AM	27.8	7.46	6.81	3.5	-0.339	0.271
	11/14/2011	9:58 AM	29.0	7.26	6.16	3.1	-0.064	0.517
	11/16/2011	10:57 AM	28.9	7.36	6.25	3.1	0.365	0.375
	11/18/2011	11:16 AM	27.5	7.32	6.14	3.2	0.313	0.443
	11/21/2011	10:53 AM	30.0	7.43	6.74	3.3	0.351	0.095
	11/23/2011	10:36 AM	29.0	7.45	6.75	3.4	0.028	0.197
	11/25/2011	10:57 AM	28.2	7.35	6.10	3.1	0.376	0.240
	11/28/2011	10:48 AM	28.7	7.37	7.38	3.7	0.836	0.082
	11/30/2011	10:29 AM	27.3	7.33	6.14	3.2	-0.043	0.044
	12/2/2011	10:34 AM	27.9	7.33	6.78	3.5	0.847	0.260
	12/5/2011	10:46 AM	27.7	7.33	6.11	3.1	0.255	0.476
	12/7/2011	10:45 AM	29.1	7.34	6.38	3.2	0.379	0.362
	12/9/2011	10:25 AM	26.8	7.42	5.95	3.1	0.353	0.485
	12/12/2011	10:29 AM	25.8	7.53	8.02	4.4	-0.282	0.897
	12/14/2011	10:22 AM	27.5	7.33	6.24	3.2	-0.011	0.877
	12/16/2011	10:25 AM	28.0	7.33	6.73	3.4	-0.048	1.143
	12/19/2011	10:37 AM	27.4	7.42	6.10	3.1		
	12/21/2011	11:38 AM	28.2	7.26	6.26	3.2		
	12/23/2011	11:06 AM	24.5	7.43	5.82	3.2		
	12/26/2011	11:17 AM	28.3	7.38	6.35	3.2		
	12/28/2011	10:53 AM	25.8	7.42	6.63	3.6		
	12/30/2011	11:33 AM	30.6	7.54	8.17	4.0		
	1/2/2012	11:50 AM	29.0	7.60	19.18	10.5		
	1/7/2012	4:05 PM	28.3	7.48	6.17	3.1	0.760	15.24
	1/9/2012	12:02 PM	28.3	7.32	6.72	3.5	1.058	16.73
	1/11/2012	11:48 AM	24.9	7.30	5.63	3.1	1.140	19.43

Table A-3 Cont. Location	Date	Time	Temp. (°C)	pH	Spec. Cond. (mS/cm)	Salinity	SRB (ppb)	FLT (ppb)
Seep 4 Cont.	1/13/2012	12:23 PM	25.8	7.45	6.07	3.2	1.297	20.84
	1/16/2012	2:16 PM	27.5	7.40	5.90	3.0		
	1/19/2012	11:18 AM	28.1	7.35	6.04	3.1	1.064	25.69
	1/21/2012	2:51 PM	28.5	7.34	5.99	3.0	1.216	29.20
	1/23/2012	1:26 PM	25.9	7.60	5.81	3.1	1.202	30.96
	1/25/2012	1:39 PM	28.6	7.39	6.14	3.1	1.643	32.35
	1/27/2012	1:49 PM	30.5	7.90	6.42	3.1	0.767	20.16
	1/31/2012	12:39 PM	27.9	7.48	6.11	3.1	1.122	37.17
	2/10/2012	1:16 PM	27.2	7.81	10.46	5.7	1.074	42.32
	2/14/2012	2:38 PM	27.5	7.67	12.30	6.7	1.423	43.47
	2/17/2012	12:47 PM	25.9	7.67	15.82	9.0	2.097	45.24
	2/20/2012	3:00 PM	28.6	7.67	24.16	13.6	0.540	34.78
	2/24/2012	12:20 PM	28.0	7.80	34.57	20.2	0.160	26.45
	2/27/2012	12:13 PM	29.6	7.88	37.70	21.6	0.138	24.57
	3/1/2012	12:50 PM	29.5	7.58	8.16	4.2	1.513	61.65
	3/11/2012	12:23 PM	29.5	7.74	15.40	8.2	2.371	61.15
	3/14/2012	11:17 AM	24.7	7.69	16.57	9.8		
	3/17/2012	10:47 AM	25.9	7.70	26.18	15.8	1.170	48.96
	3/19/2012	10:55 AM	26.9	7.86	36.94	22.5	1.072	32.50
	3/22/2012	11:08 AM	26.4	7.75	30.78	18.6	1.017	42.85
	3/27/2012	11:03 AM	26.5	7.75	28.87	17.3	0.400	46.86
	3/29/2012	11:36 AM	26.6	7.70	28.91	17.4	0.447	43.77
	3/31/2012	4:53 PM	26.3		28.67	17.3	2.033	48.11
	4/2/2012	11:33 AM	27.4		36.30	21.8	1.175	37.00
	4/5/2012	9:40 AM	25.7	7.70	28.56	17.3	1.565	49.81
	4/12/2012	9:50 AM	26.5	7.51	24.15	14.1	2.119	59.14
	4/16/2012	11:12 AM	28.2	7.67	29.52	17.1	1.021	49.91
Location	Date	Time	Temp. (°C)	pH	Spec. Cond. (mS/cm)	Salinity	SRB (ppb)	FLT (ppb)
Seep 5	7/19/2011	10:35 AM	26.7	7.54	5.29	3.1	0.667	0.159
	7/20/2011	11:03 AM	27.8	7.57	6.02	3.0	0.108	0.086
	7/21/2011	9:25 AM	25.5	7.35	5.78	3.1	0.227	0.312
	7/22/2011	11:03 AM	27.2	7.67	5.66	3.1	0.099	0.215
	7/23/2011	10:44 AM	27.1	7.52	5.88	3.0	-0.168	0.006
	7/24/2011	10:30 AM	26.2	7.55	5.79	3.1	-0.346	0.217
	7/25/2011	10:51 AM	27.2	7.56	5.91	3.1	0.423	0.165
	7/26/2011	10:22 AM	26.2	7.52	5.77	3.0	-0.044	-0.002
	7/27/2011	11:12 AM	26.6	7.53	5.81	3.0	0.055	-0.006
	7/28/2011	10:36 AM	27.6	7.47	5.97	3.1	-0.252	0.078
	7/28/2011	4:59 PM	26.4	7.33	5.78	3.0	-0.067	-0.062
	7/29/2011	10:40 AM	27.2	7.33	5.84	3.0	0.084	0.040

Table A-3 Cont. Location	Date	Time	Temp. (°C)	pH	Spec. Cond. (mS/cm)	Salinity	SRB (ppb)	FLT (ppb)
Seep 5 Cont.	7/29/2011	4:51 PM	27.8	7.46	5.98	3.1	0.779	0.102
	7/30/2011	11:53 AM	27.0	7.43	5.90	3.1	0.240	-0.021
	7/30/2011	5:33 PM	27.1	7.44	5.93	3.1	0.682	-0.039
	7/31/2011	11:09 AM	27.4	7.42	5.95	3.1	0.374	0.029
	7/31/2011	5:19 PM	26.6	7.46	6.52	3.4	0.856	0.068
	8/1/2011	4:40 PM	26.6	7.40	6.17	3.3	-0.110	-0.124
	8/2/2011	9:20 AM	26.0	7.49	5.71	3.0	0.113	-0.077
	8/2/2011	4:27 PM	27.3	7.40	5.90	3.0	-0.201	0.015
	8/3/2011	10:44 AM	28.0	7.41	5.94	3.0	-0.345	0.105
	8/3/2011	4:55 PM	26.5	7.32	5.85	3.1	0.546	-0.110
	8/4/2011	11:30 AM	27.5	7.44	5.62	3.0	0.077	-0.122
	8/4/2011	5:02 PM	28.1	7.46	5.64	3.0	0.453	0.062
	8/5/2011	11:21 AM	27.5	7.49	5.91	3.0	-0.415	-0.023
	8/5/2011	5:31 PM	26.4	7.48	5.76	3.0	0.567	-0.110
	8/6/2011	9:44 AM	26.4	7.42	5.83	3.1	0.269	-0.060
	8/6/2011	4:15 PM	28.8	7.41	6.09	3.0	0.076	0.003
	8/7/2011	10:25 AM	26.9	7.42	5.91	3.1	0.140	-0.123
	8/7/2011	4:33 PM	27.0	7.40	5.88	3.1	-0.121	0.062
	8/8/2011	10:32 AM	28.2	7.43	6.09	3.1	0.353	0.008
	8/8/2011	4:33 PM	28.9	7.40	6.10	3.1	-0.238	-0.213
	8/9/2011	10:25 AM	27.2	7.51	5.98	3.1	0.673	0.005
	8/9/2011	4:17 PM	27.9	7.46	6.03	3.1	0.729	0.164
	8/10/2011	1:00 PM	27.7	7.60	6.05	3.1	0.024	0.329
	8/10/2011	4:54 PM	27.5	7.53	6.00	3.1	-0.084	-0.095
	8/11/2011	10:13 AM	27.6	7.68	6.00	3.1	0.067	0.338
	8/11/2011	4:40 PM	28.4	7.74	6.07	3.1	-0.405	0.201
	8/12/2011	10:16 AM	27.1	7.65	5.90	3.1	-0.196	0.185
	8/12/2011	4:36 PM	28.4	7.62	6.09	3.1	-0.360	0.244
	8/13/2011	10:15 AM	27.2	7.54	5.93	3.1	0.555	0.438
	8/13/2011	4:16 PM	27.9	7.55	5.74	3.1	-0.180	0.315
	8/14/2011	10:45 AM	27.0	7.52	5.91	3.1	0.475	0.649
	8/14/2011	4:36 PM	26.1	7.40	5.86	3.1	0.194	0.404
	8/15/2011	10:11 AM	25.6	7.44	5.74	3.1	0.936	0.258
	8/15/2011	4:24 PM	27.1	7.48	5.96	3.1	0.284	0.275
	8/16/2011	10:37 AM	27.9	7.57	5.97	3.0	0.432	0.380
	8/16/2011	4:10 PM	27.3	7.57	5.96	3.1	-0.167	0.239
	8/17/2011	11:21 AM	28.8	7.48	6.07	3.0	0.064	0.202
	8/17/2011	4:54 PM	28.4	7.45	6.05	3.1	-0.132	0.152
	8/18/2011	10:54 AM	28.6	7.50	6.05	3.0	-0.175	0.226
	8/18/2011	5:01 PM	27.7	7.43	5.97	3.1	0.357	0.266
	8/19/2011	10:53 AM	28.4	7.56	6.03	3.1	0.634	0.178
	8/19/2011	4:59 PM	28.5	7.53	6.06	3.1	-0.026	0.058
	8/20/2011	10:46 AM	29.3	7.56	6.12	3.0	-0.102	0.608

Table A-3 Cont. Location	Date	Time	Temp. (°C)	pH	Spec. Cond. (mS/cm)	Salinity	SRB (ppb)	FLT (ppb)
Seep 5 Cont.	8/20/2011	4:46 PM	26.6	7.53	5.84	3.1	-0.007	0.439
	8/21/2011	10:51 AM	27.9	7.48	5.97	3.0	0.130	0.259
	8/21/2011	5:03 PM	27.4	7.53	5.93	3.1	0.402	0.306
	8/22/2011	10:21 AM	27.6	7.57	6.00	3.1	0.156	0.072
	8/22/2011	4:54 PM	28.6	7.63	6.07	3.1	0.015	0.352
	8/23/2011	10:32 AM	28.1	7.63	6.03	3.1	-0.031	0.024
	8/23/2011	4:14 PM	28.8	7.51	6.09	3.1	-0.223	0.399
	8/24/2011	11:46 AM	27.2	7.63	5.91	3.0	0.036	0.399
	8/24/2011	6:06 PM	27.4	7.53	5.94	3.1	0.737	0.186
	8/25/2011	11:15 AM	27.2	7.61	5.95	3.1	0.528	0.119
	8/25/2011	5:45 PM	26.8	7.58	5.90	3.1	1.180	0.155
	8/26/2011	10:32 AM	27.6	7.55	6.01	3.1	0.776	0.124
	8/26/2011	4:41 PM	27.6	7.58	6.04	3.1	1.173	0.048
	8/27/2011	11:11 AM	29.2	7.66	6.10	3.0	0.662	0.541
	8/27/2011	5:51 PM	27.0	7.58	5.90	3.0	0.365	0.141
	8/28/2011	10:30 AM	27.7	7.59	5.99	3.1	0.357	0.403
	8/28/2011	4:54 PM	27.8	7.63	6.01	3.1	0.200	0.090
	8/29/2011	10:51 AM	27.3	7.63	5.90	3.0	0.487	0.106
	8/29/2011	4:49 PM	28.0	7.53	6.09	3.1	0.231	0.195
	9/2/2011	12:07 PM	31.9	7.55	6.34	3.0	-0.412	0.148
	9/2/2011	5:27 PM	28.0	7.54	5.98	3.0	0.106	0.225
	9/3/2011	10:52 AM	27.0	7.70	5.85	3.0	-0.511	0.176
	9/4/2011	5:12 PM	29.6	7.48	6.19	3.1	0.189	0.393
	9/5/2011	10:37 AM	28.2	7.55	6.05	3.1	0.258	0.623
	9/5/2011	4:58 PM	26.6	7.47	5.81	3.0	-0.125	0.306
	9/6/2011	10:21 AM	28.5	7.48	6.08	3.1	0.053	0.536
	9/6/2011	4:49 PM	30.2	7.51	6.19	3.0	0.112	0.572
	9/7/2011	10:18 AM	29.7	7.48	6.18	3.0	-0.390	0.221
	9/8/2011	10:26 AM	29.4	7.49	6.16	3.1	-0.345	0.678
	9/9/2011	11:47 AM	29.8	7.50	6.22	3.0	-0.239	0.155
	9/10/2011	12:00 PM	30.8	7.51	6.40	3.1	-0.550	0.444
	9/12/2011	1:05 PM	30.8	7.46	6.31	3.0	-0.240	0.175
	9/13/2011	12:18 PM	33.5	7.56	10.43	5.0	-0.366	0.198
	9/14/2011	11:13 AM	31.9	7.49	6.91	3.3	-0.266	0.174
	9/15/2011	11:00 AM	33.4	7.85	6.99	3.2	-0.348	0.313
	9/16/2011	12:41 PM	34.9	7.50	9.01	4.1	-0.501	0.288
	9/17/2011	4:03 PM	31.2	7.49	11.04	5.5	-0.070	0.422
	9/18/2011	12:49 PM	34.1	7.50	7.06	3.2	-0.086	0.127
	9/19/2011	11:49 AM	32.2	7.53	12.59	6.2	-0.435	0.252
	9/20/2011	10:50 AM	29.2	7.50	7.00	3.5	0.061	0.283
	9/21/2011	10:27 AM	30.0	7.52	6.84	3.4	-0.652	0.384
	9/23/2011	10:43 AM	28.2	7.49	6.76	3.5	-0.383	0.214
	9/24/2011	9:45 AM	28.3	7.64	6.40	3.2	0.040	0.233

Table A-3 Cont. Location	Date	Time	Temp. (°C)	pH	Spec. Cond. (mS/cm)	Salinity	SRB (ppb)	FLT (ppb)
Seep 5 Cont.	9/25/2011	11:54 AM	31.9	7.43	9.64	4.7	-0.227	0.407
	9/26/2011	12:00 PM	32.1	7.51	7.43	3.6	-0.408	0.247
	9/27/2011	10:36 AM	31.0	7.44	6.19	3.0		
	9/28/2011	10:26 AM	30.8	7.42	6.23	3.0	-0.478	0.057
	9/29/2011	10:46 AM	30.8	7.43	6.18	3.0	-0.672	0.189
	9/30/2011	10:45 AM	29.7	7.44	6.08	3.0	-0.705	0.287
	10/1/2011	11:02 AM	33.4	7.64	6.59	3.0	-0.130	0.283
	10/2/2011	1:48 PM	32.9	7.42	6.52	3.0	0.274	0.052
	10/3/2011	10:38 AM	30.4	7.51	6.35	3.1	0.157	0.117
	10/10/2011	12:47 PM	33.1	7.49	6.53	3.0	-0.506	0.377
	10/12/2011	10:31 AM	30.5	7.51	6.08	2.9	0.330	0.269
	10/14/2011	10:36 AM	30.1	7.51	6.46	3.1	1.103	0.244
	10/16/2011	10:29 AM	31.4	7.49	6.85	3.0	0.647	0.213
	10/18/2011	1:11 PM	31.3	7.45	6.27	3.0	0.913	0.265
	10/20/2011	10:52 AM	31.4	7.49	6.26	3.0	0.693	0.191
	10/22/2011	10:26 AM	30.9	7.54	6.25	3.0	0.099	0.219
	10/24/2011	10:40 AM	29.8	7.49	6.19	3.0	-0.140	0.143
	10/26/2011	10:51 AM	30.8	7.44	6.33	3.1	-0.419	0.153
	10/28/2011	10:44 AM	27.9	7.47	6.02	3.1	-0.110	0.077
	10/30/2011	12:41 PM	34.0	7.47	6.79	3.1	0.430	0.429
	11/1/2011	12:49 PM	29.1	7.45	6.25	3.1	-0.208	0.349
	11/3/2011	10:49 AM	31.3	7.45	6.48	3.1	0.355	0.241
	11/5/2011	2:44 PM	32.8	7.49	6.66	3.1	-0.045	0.228
	11/7/2011	10:33 AM	32.0	7.50	6.43	3.0	-0.023	0.227
	11/9/2011	11:33 AM	30.4	7.47	6.33	3.1	-0.124	0.374
	11/11/2011	11:04 AM	28.1	7.52	6.12	3.1	0.413	0.375
	11/14/2011	10:08 AM	29.1	7.34	6.12	3.0	-0.334	0.206
	11/16/2011	11:09 AM	30.0	7.37	6.28	3.1	0.466	0.595
	11/16/2011	11:09 AM	30.0	7.37	6.28	3.1	0.932	0.363
	11/18/2011	11:29 AM	28.2	7.33	6.17	3.1	0.932	0.363
	11/21/2011	11:05 AM	30.8	7.46	6.39	3.1	0.370	-0.161
	11/23/2011	10:47 AM	29.8	7.45	6.25	3.1	-0.264	0.018
	11/25/2011	11:27 AM	28.2	7.36	6.11	3.1	-0.159	0.138
	11/28/2011	10:58 AM	29.8	7.39	6.23	3.1	0.043	0.180
	11/30/2011	10:40 AM	27.3	7.36	6.15	3.2	0.288	0.069
	12/2/2011	10:43 AM	27.1	7.33	6.50	3.4	1.048	0.345
	12/5/2011	11:03 AM	27.7	7.42	6.79	3.5	0.232	0.331
	12/7/2011	10:56 AM	29.2	7.36	8.28	4.2	-0.054	0.343
	12/9/2011	10:35 AM	27.8	7.41	7.02	3.7	-0.004	0.482
	12/12/2011	10:41 AM	25.8	7.49	6.80	3.7	0.678	0.675
	12/14/2011	10:32 AM	26.1	7.34	8.09	4.4	0.247	1.027
	12/16/2011	10:34 AM	28.3	7.33	7.42	3.8	0.473	0.852
	12/19/2011	10:46 AM	27.3	7.44	7.77	4.1		

Table A-3 Cont. Location	Date	Time	Temp. (°C)	pH	Spec. Cond. (mS/cm)	Salinity	SRB (ppb)	FLT (ppb)
Seep 5 Cont.	12/21/2011	11:48 AM	28.3	7.39	8.15	4.2		
	12/26/2011	11:08 AM	27.6	7.41	9.14	4.8		
	12/28/2011	10:45 AM	26.9	7.41	13.80	7.6		
	12/30/2011	11:24 AM	29.5	7.69	17.01	9.1		
	1/2/2012	12:05 PM	28.9	7.49	27.82	15.6		
	1/7/2012	4:15 PM	27.9	7.33	28.12	16.4	0.686	10.62
	1/9/2012	12:20 PM	29.1	7.65	32.31	18.4	0.898	7.321
	1/11/2012	12:00 PM	24.9	7.54	34.75	21.8	1.456	8.052
	1/13/2012	12:33 PM	28.0	7.50	31.39	18.3	0.907	10.69
	1/16/2012	2:28 PM	27.9	7.46	32.51	19.1		
	1/19/2012	11:31 AM	28.5	7.54	19.09	10.4	0.620	20.93
	1/21/2012	3:03 PM	27.8	7.53	23.17	13.2	0.672	20.38
	1/23/2012	1:36 PM	26.2	7.51	32.25	19.7	0.882	16.32
	1/25/2012	2:16 PM	28.1	7.35	29.88	17.3	0.970	17.71
	1/27/2012	2:24 PM	26.5	7.57	24.80	14.6	1.110	23.32
	1/31/2012	12:51 PM	27.4	7.90	30.70	18.1	0.660	18.69
	2/10/2012	1:30 PM	26.6	7.82	13.03	7.2	0.822	42.04
	2/14/2012	3:13 PM	28.7	7.62	13.88	7.4	1.631	44.08
	2/17/2012	1:00 PM	26.6	7.65	13.57	7.6	1.614	46.94
	2/20/2012	3:14 PM	28.6	7.72	10.52	5.5	0.896	42.94
	2/24/2012	12:36 PM	27.0	7.81	14.24	8.0	1.215	50.06
	2/27/2012	12:24 PM	27.6	7.68	15.12	8.3	0.922	54.02
	3/1/2012	1:04 PM	29.0	7.58	19.08	10.3	1.260	50.53
	3/11/2012	12:38 PM	29.3	7.72	11.47	6.0	2.576	72.06
	3/14/2012	11:30 AM	26.8	7.67	13.25	7.4		
	3/17/2012	10:57 AM	25.0	7.80	15.36	8.9	1.984	72.19
	3/19/2012	11:05 AM	26.7	7.74	19.75	11.4	2.247	65.39
	3/22/2012	11:20 AM	26.6	7.80	25.48	15.0	1.573	57.96
	3/27/2012	11:17 AM	26.7	7.51	18.34	10.4	1.149	72.22
	3/29/2012	11:49 AM	26.7	7.65	21.90	12.2	1.487	70.61
	4/2/2012	11:44 AM	27.0		21.49	12.4	2.276	71.70
	4/5/2012	9:52 AM	25.0	7.63	16.73	9.8	2.606	83.52
	4/12/2012	10:22 AM	26.2	7.45	15.05	8.5	2.375	84.52
	4/16/2012	11:25 AM	28.8	7.51	13.72	7.3	2.028	88.53
	4/19/2012	12:34 PM	27.5	7.63	16.07	8.9	1.941	80.31
	4/24/2012	4:21 PM	26.5	7.80	20.18	11.7	2.223	77.17
	4/26/2012	11:54 AM	28.9	7.59	16.22	8.8	2.420	87.12
	5/2/2012	12:01 PM	28.0	7.59	19.72	11.0	2.575	80.46

Table A-3 Cont. Location	Date	Time	Temp. (°C)	pH	Spec. Cond. (mS/cm)	Salinity	SRB (ppb)	FLT (ppb)
Seep 11 Cont.	1/21/2012	3:14 PM	28.9	7.37	5.00	3.2	1.186	27.72
	1/23/2012	1:46 PM	26.3	7.44	5.93	3.1	1.511	30.38
	1/27/2012	2:13 PM	26.3	7.54	5.96	3.1	1.443	32.72
	2/14/2012	2:58 PM	28.1	7.67	6.37	3.3	1.832	53.16
	2/17/2012	1:14 PM	28.4	7.61	6.60	3.3	2.300	52.41
	2/20/2012	3:27 PM	25.9	7.67	7.03	3.8	2.163	58.40
	2/24/2012	12:53 PM	26.6	7.64	7.83	4.2	1.368	60.77
	2/27/2012	12:52 PM	28.4	7.66	6.39	3.2	1.000	63.39
	3/1/2012	1:17 PM	29.0	7.56	6.54	3.2	1.712	66.71
	3/11/2012	12:52 PM	28.8	7.60	6.36	3.2	1.987	77.12
	3/14/2012	11:42 AM	25.2	7.68	6.03	3.2		
	3/17/2012	10:36 AM	26.6	7.59	6.02	3.2	2.483	82.66
	3/19/2012	11:16 AM	26.6	7.62	6.35	3.3	2.460	86.24
	3/22/2012	11:30 AM	26.3	7.58	8.32	4.5	2.954	84.19
	3/27/2012	11:46 AM	26.6	7.58	6.30	3.3	2.374	87.66
	3/29/2012	12:03 PM	26.8	7.57	6.27	3.3	1.803	89.89
	3/31/2012	5:04 PM	26.1		6.84	3.4	3.062	93.60
	4/2/2012	11:55 AM	26.7		6.27	3.3	3.193	94.86
	4/5/2012	10:04 AM	25.6	7.48	6.08	3.3	3.025	96.61
	4/12/2012	10:37 AM	26.5	7.46	6.28	3.3	2.877	98.57
	4/16/2012	11:55 AM	28.9	7.50	6.56	3.3	2.402	100.8
	4/19/2012	12:46 PM	28.5	7.59	6.65	3.4	1.929	95.58
	4/24/2012	4:31 PM	27.1	7.48	6.48	3.4	2.976	104.5
	4/26/2012	12:14 PM	28.3	7.55	6.68	3.4	3.419	102.9
	5/2/2012	12:14 PM	28.0	7.53	6.74	3.5	3.714	102.8

Table A-4. North Seep Group water quality parameters
Water quality parameters collected from the North Seep Group (Seeps 1, 2, 6, 7, 8, 9, 10, 12, 13, 14, 15, and 16) with a handheld YSI Model 63 and field fluorescence measurements of S-Rhodamine-B (SRB) and Fluorescein (FLT) with a handheld Aquafluor fluorometer model 8000-10 from 7/19/2011 to 5/2/2012 .   Missing fluorescence values are due to shipment of samples prior to analysis in the field.

Location	Date	Time	Temp. (°C)	pH	Spec. Cond. (mS/cm)	Salinity	SRB (ppb)	FLT (ppb)
Seep 1	7/19/2011	9:34 AM	28.3	7.48	7.83	4.0	-0.252	0.187
	7/20/2011	10:11 AM	26.4	7.46	7.69	4.1	0.592	0.308
	7/21/2011	8:42 AM	25.9	7.47	7.52	4.1	0.173	0.425
	7/22/2011	10:14 AM	28.2	7.37	7.80	4.0	0.569	0.206
	7/23/2011	9:37 AM	26.7	7.47	7.68	4.1	0.566	0.036
	7/24/2011	9:33 AM	29.9	7.41	8.15	4.1	-0.078	-0.094
	7/25/2011	10:00 AM	28.4	7.45	8.06	4.2	0.277	0.179
	7/26/2011	9:37 AM	28.1	7.35	8.06	4.2	0.228	0.052
	7/27/2011	10:23 AM	26.7	7.53	8.02	4.3	0.018	-0.252
	7/28/2011	9:44 AM	28.8	7.37	8.40	4.3	0.843	0.188
	7/28/2011	4:16 PM	28.3	7.33	7.68	3.9	0.752	-0.053
	7/29/2011	9:51 AM	26.8	7.27	8.13	4.3	0.062	-0.040
	7/29/2011	4:02 PM	27.9	7.41	7.69	4.0	-0.213	0.000
	7/30/2011	10:55 AM	27.1	7.38	8.14	4.3	0.188	0.023
	7/30/2011	4:37 PM	26.7	7.38	7.34	4.0	0.194	-0.073
	7/31/2011	10:08 AM	29.7	7.39	8.65	4.4	-0.219	-0.122
	7/31/2011	4:27 PM	28.1	7.38	8.15	4.2	0.077	0.145
	8/1/2011	10:10 AM	27.4	7.39	8.05	4.2	0.607	-0.004
	8/1/2011	3:53 PM	27.5	7.37	7.77	4.1	0.263	-0.009
	8/2/2011	8:39 AM	25.3	7.42	7.37	4.0	0.179	-0.102
	8/2/2011	3:43 PM	27.5	7.30	7.79	4.1	0.580	0.158
	8/3/2011	9:52 AM	28.1	7.31	7.82	4.1	-0.200	-0.207
	8/3/2011	4:04 PM	29.2	7.35	8.07	4.1	-0.023	-0.115
	8/4/2011	10:52 AM	29.2	7.38	7.90	4.0	0.212	-0.035
	8/4/2011	4:19 PM	29.3	7.35	7.41	4.1	0.463	-0.049
	8/5/2011	10:30 AM	27.3	7.41	7.51	4.0	-0.097	-0.089
	8/5/2011	4:48 PM	29.9	7.59	8.12	4.1	0.237	-0.097
	8/6/2011	9:10 AM	26.8	7.36	7.82	4.2	-0.022	-0.154
	8/6/2011	3:38 PM	31.3	7.36	8.25	4.0	-0.636	-0.129
	8/7/2011	9:30 AM	26.0	7.51	7.78	4.2	0.334	-0.039
	8/7/2011	3:52 PM	28.5	7.31	7.84	4.0	0.012	0.037
	8/8/2011	9:35 AM	27.6	7.39	8.14	4.3	-0.100	-0.044

Table A-4 Cont. Location	Date	Time	Temp. (°C)	pH	Spec. Cond. (mS/cm)	Salinity	SRB (ppb)	FLT (ppb)
Seep 1 Cont.	8/8/2011	3:43 PM	30.2	7.39	8.05	4.0	-0.127	-0.015
	8/9/2011	9:38 AM	27.0	7.45	8.10	4.3	0.354	-0.097
	8/9/2011	3:35 PM	29.4	7.45	7.97	4.0	-0.020	-0.030
	8/10/2011	11:27 AM	29.1	7.70	8.25	4.3	0.763	0.047
	8/10/2011	4:15 PM	31.8	7.60	8.25	4.0	-0.080	-0.087
	8/11/2011	9:34 AM	28.8	7.60	8.38	4.3	0.432	0.261
	8/11/2011	4:02 PM	31.2	7.71	8.16	4.0	0.503	0.432
	8/12/2011	9:34 AM	28.1	7.65	7.79	4.3	-0.374	0.149
	8/12/2011	3:54 PM	32.0	7.63	8.50	4.1	-0.676	0.065
	8/13/2011	9:32 AM	28.4	7.49	8.36	4.3	0.077	0.141
	8/13/2011	3:35 PM	29.6	7.51	8.26	4.2	0.324	0.282
	8/14/2011	9:56 AM	27.2	7.46	8.13	4.3	0.901	0.440
	8/14/2011	3:49 PM	28.9	7.49	8.12	4.1	0.386	0.360
	8/15/2011	12:39 AM	25.2	7.62	7.64	4.2	0.500	0.307
	8/15/2011	9:20 AM	27.1	7.54	7.98	4.2	0.254	0.278
	8/15/2011	3:33 PM	30.7	7.42	8.47	4.2	0.157	0.313
	8/16/2011	9:55 AM	28.5	7.46	8.12	4.2	0.783	0.328
	8/16/2011	3:25 PM	30.1	7.50	8.37	4.2	0.479	0.308
	8/17/2011	10:23 AM	28.2	7.50	8.06	4.2	0.511	0.281
	8/17/2011	4:11 PM	30.9	7.41	8.39	4.1	0.024	0.510
	8/18/2011	12:50 AM	24.8	7.54	7.57	4.2	0.297	0.271
	8/18/2011	9:23 AM	29.2	7.54	8.03	4.1	0.161	0.237
	8/18/2011	3:51 PM	31.9	7.44	8.47	4.1	0.007	0.210
	8/19/2011	9:51 AM	30.3	7.56	8.19	4.1	-0.045	0.169
	8/19/2011	4:11 PM	29.8	7.46	8.13	4.1	0.018	0.692
	8/20/2011	10:07 AM	27.8	7.48	7.79	4.1	0.130	0.133
	8/20/2011	4:12 PM	27.1	7.46	7.71	4.1	0.095	0.523
	8/21/2011	10:03 AM	27.5	7.44	8.17	4.3	0.120	0.017
	8/21/2011	4:09 PM	28.6	7.48	7.95	4.1	0.273	0.825
	8/22/2011	9:38 AM	27.3	7.48	7.96	4.2	0.801	0.085
	8/22/2011	4:18 PM	31.1	7.54	8.24	4.0	0.804	0.004
	8/23/2011	9:43 AM	27.1	7.45	7.90	4.2	-0.667	0.111
	8/23/2011	3:43 PM	28.1	7.41	7.72	4.0	0.024	0.213
	8/24/2011	10:38 AM	27.2	7.49	8.01	4.2	-0.227	0.063
	8/24/2011	5:01 PM	29.4	7.51	7.32	4.0	-0.120	0.308

Table A-4 Cont. Location	Date	Time	Temp. (°C)	pH	Spec. Cond. (mS/cm)	Salinity	SRB (ppb)	FLT (ppb)
Seep 1 Cont.	8/25/2011	10:08 AM	29.3	7.54	8.39	4.3	0.413	0.552
	8/25/2011	4:44 PM	28.0	7.50	7.74	4.0	0.339	0.271
	8/26/2011	9:45 AM	27.7	7.52	8.29	4.3	0.523	0.119
	8/26/2011	3:54 PM	29.7	7.53	7.94	4.0	1.171	0.116
	8/27/2011	9:38 AM	29.8	7.52	8.46	4.3	0.353	0.285
	8/27/2011	4:12 PM	30.8	7.44	8.10	4.0	0.786	0.090
	8/28/2011	9:36 AM	28.7	7.41	8.37	4.3	0.894	0.084
	8/28/2011	3:54 PM	31.2	7.76	8.31	4.1	0.013	0.065
	8/29/2011	9:57 AM	27.5	7.56	8.05	4.2	0.175	0.069
	8/29/2011	4:12 PM	29.1	7.47	7.97	4.0	0.490	0.137
	8/30/2011	9:39 AM	29.1	7.49	7.52	4.1	0.049	0.210
	9/1/2011	10:31 AM	30.2	7.50	8.19	4.1	-0.399	0.286
	9/1/2011	4:23 PM	29.9	7.45	8.12	4.1	-0.227	0.186
	9/2/2011	10:35 AM	29.2	7.46	7.92	4.0	-0.662	0.159
	9/2/2011	4:06 PM	31.8	7.57	8.47	4.2	-0.473	0.416
	9/3/2011	10:04 AM	27.4	7.60	7.72	4.0	-0.481	0.421
	9/3/2011	4:18 PM	29.0	7.56	8.04	4.1	-0.490	0.361
	9/4/2011	3:52 PM	32.8	7.42	8.53	4.0	-0.741	0.257
	9/5/2011	9:55 AM	29.8	7.45	8.28	4.2	-0.241	0.318
	9/5/2011	4:14 PM	28.0	7.43	7.75	4.0	-0.554	0.249
	9/6/2011	9:39 AM	27.0	7.47	7.95	4.2	-0.201	0.221
	9/6/2011	3:50 PM	30.8	7.27	8.18	4.0	-0.608	0.225
	9/7/2011	9:19 AM	29.0	7.28	8.26	4.2	0.180	0.337
	9/8/2011	9:29 AM	29.5	7.31	8.29	4.2	0.300	0.359
	9/9/2011	10:19 AM	31.2	7.33	8.66	4.2	-0.334	0.286
	9/10/2011	10:20 AM	28.5	7.20	8.84	4.6	-0.478	0.312
	9/11/2011	10:35 AM	31.3	7.46	8.96	4.4	-0.145	0.282
	9/12/2011	11:38 AM	30.8	7.42	10.16	5.1	-0.473	0.444
	9/13/2011	10:36 AM	33.1	7.34	8.98	4.2	0.102	0.316
	9/14/2011	9:42 AM	29.8	7.39	8.50	4.3	-0.259	0.178
	9/15/2011	9:22 AM	30.8	7.41	8.54	4.2	-0.388	0.393
	9/16/2011	11:16 AM	33.4	7.41	9.80	4.6	-0.463	0.212
	9/17/2011	2:23 PM	33.7	7.30	12.39	5.9	0.073	0.208
	9/18/2011	10:58 AM	34.3	7.26	14.80	6.7	-0.596	0.216
	9/19/2011	10:02 AM	30.5	7.40	14.29	7.3	-0.476	0.240

Table A-4 Cont. Location	Date	Time	Temp. (°C)	pH	Spec. Cond. (mS/cm)	Salinity	SRB (ppb)	FLT (ppb)
Seep 1 Cont.	9/20/2011	9:58 AM	31.5	7.51	10.49	5.2	-0.721	0.184
	9/21/2011	9:39 AM	29.5	7.48	10.22	5.2	-0.529	0.299
	9/22/2011	9:27 AM	25.0	7.18	9.54	5.3	-0.100	0.275
	9/23/2011	9:58 AM	30.0	7.43	9.48	4.8	-0.180	0.494
	9/24/2011	9:18 AM	30.3	7.45	11.35	5.8	-0.054	0.223
	9/25/2011	10:20 AM	32.4	7.44	7.64	4.1	-0.195	0.232
	9/26/2011	10:05 AM	30.8	7.45	10.27	5.1	0.303	0.476
	9/27/2011	9:44 AM	29.6	7.44	8.19	4.1	-0.793	0.152
	9/28/2011	9:44 AM	29.5	7.42	8.11	4.1	-0.861	0.026
	9/29/2011	9:46 AM	27.5	7.41	7.73	4.0	-0.034	0.143
	9/30/2011	9:49 AM	29.5	7.46	8.21	4.1	-0.663	0.154
	10/1/2011	10:04 AM	30.9	7.48	8.28	4.1	-0.041	-0.086
	10/2/2011	12:15 PM	34.4	7.41	8.65	4.0	0.044	-0.093
	10/3/2011	9:50 AM	27.3	7.43	7.77	4.1	0.243	0.017
	10/4/2011	9:22 AM	27.8	7.50	8.04	4.2	0.299	0.018
	10/8/2011	4:20 PM	28.9	7.40	8.02	4.1	-0.080	0.360
	10/10/2011	12:05 PM	33.3	7.44	8.62	4.0	-0.416	0.376
	10/12/2011	9:29 AM	29.4	7.43	7.94	4.0	0.715	0.361
	10/14/2011	9:27 AM	29.1	7.37	7.99	4.1	0.335	0.253
	10/16/2011	9:27 AM	28.0	7.41	8.28	4.3	0.514	0.244
	10/18/2011	11:43 AM	33.1	7.47	8.83	4.1	0.388	0.067
	10/20/2011	9:29 AM	28.2	7.38	8.02	4.2	0.426	0.325
	10/22/2011	9:34 AM	29.6	7.43	8.04	4.0	-0.037	0.158
	10/24/2011	9:31 AM	29.6	7.46	8.23	4.1	-0.100	0.212
	10/26/2011	9:30 AM	28.4	7.55	8.00	4.1	0.304	0.284
	10/28/2011	9:35 AM	27.1	7.43	7.62	4.0	0.571	0.251
	10/30/11	11:32 AM	33.0	7.43	8.48	4.0	-0.053	0.552
	11/1/2011	11:29 AM	32.3	7.53	8.42	4.1	-0.238	0.248
	11/3/2011	9:46 AM	29.6	7.41	8.22	4.1	-0.087	0.455
	11/5/2011	1:34 PM	29.2	7.46	8.09	4.1	0.109	0.465
	11/9/2011	10:11 AM	28.6	7.48	8.11	4.2	-0.316	0.764
	11/11/2011	10:05 AM	27.1	7.48	8.09	4.3	-0.050	0.620

Table A-4 Cont. Location	Date	Time	Temp. (°C)	pH	Spec. Cond. (mS/cm)	Salinity	SRB (ppb)	FLT (ppb)
Seep 2	7/20/2011	12:16 PM	29.1	7.35	7.91	4.0	-0.038	-0.279
	7/21/2011	8:38 AM	25.1	7.43	7.41	4.1	-0.099	-0.280
	7/22/2011	10:20 AM	28.6	7.39	8.01	4.1	0.580	0.145
	7/23/2011	9:45 AM	26.5	7.46	7.66	4.1	-0.152	0.135
	7/25/2011	10:08 AM	27.6	7.50	7.97	4.0	0.529	-0.095
	7/26/2011	9:45 AM	27.6	7.44	8.09	4.2	0.788	0.094
	7/27/2011	10:33 AM	26.6	7.47	8.01	4.3	0.147	0.045
	7/28/2011	9:53 AM	28.6	7.39	8.25	4.3	1.049	-0.110
	7/28/2011	4:25 PM	27.5	7.13	7.45	3.9	0.172	0.052
	7/29/2011	10:00 AM	26.8	7.35	8.06	4.3	0.877	0.081
	7/29/2011	4:09 PM	27.5	7.38	7.46	3.9	0.173	0.119
	7/30/2011	11:04 AM	26.9	7.39	8.11	4.3	-0.242	-0.007
	7/30/2011	4:44 PM	27.9	7.33	7.49	3.8	0.252	0.070
	7/31/2011	10:14 AM	30.0	7.41	8.53	4.3	0.165	0.016
	7/31/2011	4:20 PM	28.3	7.34	7.04	4.0	0.839	0.121
	8/1/2011	3:59 AM	28.5	7.39	8.13	4.2	0.114	0.149
	8/1/2011	9:56 AM	26.9	7.31	7.60	4.0	0.702	0.079
	8/2/2011	8:46 AM	25.6	7.42	7.48	4.1	0.159	-0.027
	8/2/2011	3:49 PM	27.8	7.35	7.89	4.1	-0.293	-0.137
	8/3/2011	12:13 AM	24.3	7.23	7.38	4.1	0.179	-0.016
	8/3/2011	9:45 AM	28.3	7.13	8.36	4.4	-0.049	0.017
	8/3/2011	4:11 PM	29.2	7.37	8.13	4.1	-0.315	-0.211
	8/4/2011	10:41 AM	31.4	7.28	7.92	3.9	0.411	-0.128
	8/4/2011	4:12 PM	29.3	7.25	7.91	4.1	-0.164	-0.053
	8/5/2011	12:37 AM	24.9	7.37	7.49	4.1	0.392	-0.030
	8/5/2011	10:46 AM	27.3	7.41	7.62	4.0	-0.380	-0.205
	8/5/2011	4:58 PM	29.8	7.64	8.32	4.2	-0.221	-0.035
	8/6/2011	12:58 AM	24.0	7.23	7.53	4.2	-0.253	-0.074
	8/6/2011	9:00 AM	27.0	7.30	7.95	4.2	-0.437	-0.059
	8/6/2011	3:46 PM	30.8	7.27	8.28	4.1	0.173	-0.044
	8/7/2011	3:15 AM	24.9	7.34	7.68	4.3	-0.293	-0.276
	8/7/2011	9:20 AM	26.0	7.32	7.79	4.3	-0.590	-0.132
	8/7/2011	4:01 PM	28.2	7.33	7.94	4.1	0.552	-0.101

Table A-4 Cont. Location	Date	Time	Temp. (°C)	pH	Spec. Cond. (mS/cm)	Salinity	SRB (ppb)	FLT (ppb)
Seep 2 Cont.	8/7/2011	11:25 PM	25.2	7.28	7.59	4.2	-0.339	-0.217
	8/8/2011	9:27 AM	26.7	7.36	8.10	4.3	0.282	-0.151
	8/8/2011	3:48 PM	30.2	7.41	7.41	4.0	0.138	0.085
	8/9/2011	12:08 AM	26.5	7.42	7.64	4.1	0.368	0.024
	8/9/2011	9:30 AM	27.1	7.44	8.24	4.4	0.377	0.119
	8/9/2011	3:45 PM	29.4	7.45	7.92	4.0	-0.334	0.121
	8/10/2011	12:00 AM	25.2	7.75	7.58	4.2	0.455	-0.026
	8/10/2011	11:18 AM	30.5	7.65	8.64	4.3	0.265	0.102
	8/10/2011	4:19 PM	30.5	7.59	8.07	4.0	0.094	0.115
	8/11/2011	12:26 AM	25.6	7.67	7.58	4.2	0.468	-0.004
	8/11/2011	9:26 AM	29.2	7.56	7.87	4.3	0.031	0.238
	8/11/2011	4:09 PM	30.6	7.67	7.95	3.9	-0.264	0.094
	8/12/2011	12:25 AM	24.5	7.68	7.59	4.2	-0.208	0.047
	8/12/2011	9:27 AM	27.8	7.65	7.72	4.3	0.169	0.005
	8/13/2011	12:28 AM	25.2	7.58	7.67	4.2	0.067	0.267
	8/13/2011	9:25 AM	28.4	7.54	8.31	4.3	0.060	0.293
	8/13/2011	3:45 PM	29.7	7.37	8.22	4.1	-0.261	0.082
	8/14/2011	12:23 AM	24.7	7.56	7.64	4.2	0.867	0.457
	8/14/2011	9:40 AM	28.1	7.43	8.03	4.2	0.790	0.406
	8/14/2011	3:54 PM	28.1	7.43	8.03	4.2	0.147	0.296
	8/15/2011	9:27 AM	26.9	7.53	7.95	4.2	0.439	0.329
	8/15/2011	3:39 PM	29.5	7.49	8.31	4.2	-0.129	0.310
	8/16/2011	10:08 AM	28.0	7.50	8.08	4.2	0.065	0.233
	8/16/2011	3:16 PM	30.1	7.48	8.42	4.2	0.194	0.210
	8/17/2011	10:32 AM	28.9	7.54	8.24	4.2	-0.075	0.135
	8/17/2011	4:03 PM	31.3	7.47	8.53	4.2	-0.320	0.210
	8/18/2011	9:38 AM	29.3	7.49	8.07	4.1	0.097	0.163
	8/18/2011	3:41 PM	32.1	7.54	8.63	4.1	-0.027	0.265
	8/19/2011	9:34 AM	29.3	7.65	8.00	4.1	0.154	0.325
	8/19/2011	4:03 PM	29.8	7.49	8.14	4.1	0.098	0.128
	8/20/2011	10:02 AM	28.8	7.46	7.97	4.1	0.181	0.100
	8/20/2011	4:05 PM	27.4	7.47	7.80	4.1	0.214	0.628
	8/21/2011	9:53 AM	26.5	7.44	7.70	4.1	-0.296	0.055
	8/21/2011	4:03 PM	28.5	7.47	7.98	4.1	0.213	0.471
	8/22/2011	9:31 AM	28.5	7.48	8.11	4.2	0.064	0.394

Table A-4 Cont. Location	Date	Time	Temp. (°C)	pH	Spec. Cond. (mS/cm)	Salinity	SRB (ppb)	FLT (ppb)
Seep 2 Cont.	8/22/2011	4:11 PM	31.1	7.57	8.32	4.1	-0.241	0.197
	8/24/2011	5:10 PM	29.3	7.55	7.96	4.0	0.268	0.108
	8/25/2011	9:58 AM	29.6	7.47	8.49	4.3	-0.120	0.538
	8/25/2011	4:34 PM	28.5	7.51	7.78	4.0	0.496	0.219
	8/26/2011	9:38 AM	27.7	7.50	8.29	4.3	0.446	-0.005
	8/26/2011	3:47 PM	30.6	7.49	7.94	3.9	0.213	0.181
	8/27/2011	9:48 AM	29.1	7.49	8.40	4.3	0.309	0.033
	8/27/2011	4:23 PM	29.4	7.59	7.83	3.9	0.452	0.175
	8/28/2011	9:45 AM	28.3	7.52	8.20	4.2	-0.231	0.106
	8/28/2011	4:02 PM	30.9	7.58	8.12	4.0	0.182	0.178
	8/29/2011	9:49 AM	27.3	7.47	7.97	4.2	0.068	0.094
	8/29/2011	4:05 PM	28.6	7.46	7.76	4.0	0.085	0.063
	8/30/2011	9:33 AM	28.7	7.49	7.95	4.1	0.116	0.489
	9/1/2011	10:49 AM	29.6	7.59	8.11	4.1	-0.355	0.369
	9/1/2011	4:13 PM	30.3	7.51	8.33	4.2	-0.315	0.194
	9/2/2011	10:23 AM	28.9	7.44	8.00	4.1	-0.435	0.156
	9/2/2011	3:55 PM	31.2	7.75	8.74	4.3	-0.311	0.388
	9/3/2011	9:56 AM	27.9	7.65	7.98	4.2	0.155	0.579
	9/3/2011	4:09 PM	29.5	7.56	8.18	4.1	-0.608	0.335
	9/4/2011	3:40 PM	33.8	7.55	8.79	4.1	-0.538	0.282
	9/5/2011	9:46 AM	29.6	7.48	8.41	4.2	-0.318	0.145
	9/5/2011	4:05 PM	28.3	7.46	7.91	4.1	-0.235	0.207
	9/6/2011	9:32 AM	27.0	7.47	8.25	4.4	-0.283	0.599
	9/6/2011	3:59 PM	31.5	7.48	8.46	4.1	-0.046	0.575
	9/7/2011	9:27 AM	29.0	7.47	8.39	4.3	-0.337	0.595
	9/8/2011	9:38 AM	29.6	7.48	8.38	4.2	-0.689	0.137
	9/9/2011	10:30 AM	32.1	7.54	9.26	4.4	-0.193	0.488
	9/10/2011	10:32 AM	27.4	7.48	9.28	4.9	-0.374	0.286
	9/11/2011	10:20 AM	29.0	7.35	11.94	6.2	-0.342	0.491
	9/12/2011	11:26 AM	31.4	7.31	10.85	5.4	-0.184	0.458
	9/13/2011	10:50 AM	33.7	7.49	9.20	4.3	-0.052	0.303
	9/14/2011	9:55 AM	30.2	7.52	9.17	4.6	-0.269	0.211
	9/15/2011	9:34 AM	31.2	7.49	8.73	4.3	-0.068	0.394
	9/16/2011	11:27 AM	33.6	7.48	9.00	4.2	-0.224	0.243
	9/17/2011	2:38 PM	33.9	7.52	12.72	6.1	-0.341	0.342

Table A-4 Cont. Location	Date	Time	Temp. (°C)	pH	Spec. Cond. (mS/cm)	Salinity	SRB (ppb)	FLT (ppb)
Seep 2 Cont.	9/18/2011	11:13 AM	34.5	7.51	14.58	7.0	-0.399	0.112
	9/19/2011	10:18 AM	29.9	7.51	13.06	6.8	-0.548	0.185
	9/20/2011	9:49 AM	31.2	7.45	13.24	6.7	-0.433	0.291
	9/21/2011	9:30 AM	27.7	7.44	11.27	6.0	0.318	0.254
	9/22/2011	9:36 AM	26.2	7.51	17.36	9.9	-0.261	0.202
	9/23/2011	9:39 AM	29.3	7.19	10.98	5.7	0.603	0.138
	9/24/2011	9:09 AM	29.7	7.46	12.23	6.3	0.226	0.184
	9/25/2011	10:02 AM	33.6	7.39	9.59	4.5	-0.307	0.284
	9/26/2011	10:18 AM	31.4	7.52	10.48	5.2	0.160	0.124
	9/27/2011	9:35 AM	28.7	7.47	8.23	4.2	-1.185	0.127
	9/28/2011	9:35 AM	29.5	7.44	8.08	4.1	-0.684	0.227
	9/29/2011	9:34 AM	27.4	7.45	7.88	4.1	-0.039	0.419
	9/30/2011	9:39 AM	29.0	7.47	8.22	4.2	-0.566	0.258
	10/1/2011	9:55 AM	30.0	7.51	8.58	4.3	0.231	-0.012
	10/2/2011	12:27 PM	34.9	7.48	8.88	4.1	0.197	0.182
	10/3/2011	9:40 AM	28.1	7.46	8.74	4.6	0.632	0.300
	10/4/2011	9:34 AM	28.6	7.49	8.60	4.4	0.630	-0.029
	10/8/2011	4:30 PM	28.7	7.46	7.90	4.0	-0.164	0.419
	10/10/2011	11:57 AM	33.9	7.46	8.72	4.0	-0.203	0.359
	10/12/2011	9:38 AM	30.2	7.49	8.00	4.0	-0.131	0.419
	10/14/2011	9:34 AM	29.9	7.48	8.09	4.1	0.178	0.148
	10/16/2011	9:36 AM	27.9	7.50	8.39	4.4	0.558	0.223
	10/18/2011	11:58 AM	34.3	7.52	9.44	4.4	0.483	0.174
	10/20/2011	9:40 AM	28.2	7.51	8.04	4.2	1.172	0.173
	10/22/2011	9:41 AM	30.2	7.50	8.09	4.0	-0.107	0.046
	10/24/2011	9:41 AM	30.2	7.51	8.13	4.1	-0.211	0.264
	10/26/2011	9:40 AM	28.4	7.50	7.92	4.1	-0.233	0.209
	10/28/2011	9:45 AM	27.3	7.47	7.68	4.0	0.508	0.181
	10/30/11	11:44 AM	34.1	7.50	8.66	4.0	-0.302	0.346
	11/1/11	11:42 AM	33.5	7.51	8.52	4.0	-0.341	0.500
	11/3/11	9:39 AM	29.4	7.50	7.99	4.0	-0.121	0.447
	11/5/2011	1:22 PM	30.1	7.49	8.13	4.1	0.109	0.543
	11/7/2011	9:41 AM	26.5	7.43	7.53	4.1	0.649	0.558
	11/9/2011	9:58 AM	28.3	7.51	8.12	4.2	0.537	0.583

Table A-4 Cont. Location	Date	Time	Temp. (°C)	pH	Spec. Cond. (mS/cm)	Salinity	SRB (ppb)	FLT (ppb)
Seep 6	7/19/2011	9:25 AM	27.8	7.36	7.91	4.1	-0.322	0.041
	7/20/2011	9:59 AM	27.0	7.21	7.78	4.1	0.046	-0.116
	7/21/2011	8:25 AM	25.0	7.20	7.00	3.8	0.730	0.044
	7/22/2011	10:03 AM	27.9	7.31	7.71	4.0	0.224	-0.053
	7/23/2011	9:57 AM	27.1	7.40	7.72	4.1	0.070	-0.161
	7/24/2011	9:48 AM	27.8	7.43	7.99	4.2	0.939	-0.062
	7/25/2011	10:16 AM	26.0	7.46	7.72	4.2	0.018	-0.165
	7/26/2011	9:55 AM	27.3	7.40	8.02	4.2	0.152	-0.227
	7/28/2011	9:32 AM	27.9	7.29	7.67	4.2	0.237	0.113
	7/28/2011	4:07 PM	29.5	7.23	7.78	3.9	0.670	0.045
	7/29/2011	1:27 AM	23.8	7.25	7.20	4.1	-0.203	0.073
	7/29/2011	9:43 AM	27.1	7.22	7.97	4.2	0.002	0.020
	7/29/2011	3:55 PM	28.6	7.29	7.76	4.0	0.344	-0.120
	7/30/2011	12:35 AM	24.5	7.28	7.35	4.1	-0.080	-0.020
	7/30/2011	4:24 PM	27.0	7.34	8.10	4.3	0.760	-0.080
	7/31/2011	10:00 AM	27.6	7.38	7.73	4.0	0.140	-0.025
	7/30/2011	11:09 AM	23.9	7.37	7.34	4.1	0.716	-0.021
	7/31/2011	4:10 PM	29.5	7.37	8.52	4.3	-0.243	-0.042
	7/31/2011	12:42 AM	29.0	7.30	8.09	4.1	0.811	-0.021
	8/1/2011	10:04 AM	27.3	7.34	7.97	4.2	0.141	-0.072
	8/1/2011	3:47 PM	29.4	7.32	8.10	4.1	-0.139	-0.234
	8/2/2011	8:29 AM	25.5	7.35	7.43	4.1	-0.341	-0.039
	8/2/2011	3:35 PM	29.4	7.30	8.14	4.1	0.015	-0.113
	8/3/2011	9:58 AM	28.3	7.33	7.96	4.1	0.424	-0.019
	8/3/2011	3:55 PM	30.4	7.21	8.26	4.1	-0.109	-0.123
	8/4/2011	10:56 AM	29.5	7.32	8.12	4.1	-0.174	-0.030
	8/4/2011	4:25 PM	28.3	7.40	8.13	4.0	-0.434	-0.137
	8/5/2011	10:31 AM	27.5	7.27	7.71	4.1	0.653	-0.023
	8/5/2011	4:37 PM	30.6	7.59	7.43	4.1	-0.214	-0.071
	8/6/2011	9:20 AM	27.0	7.36	7.87	4.2	-0.343	-0.225
	8/6/2011	3:30 PM	32.1	7.23	8.47	4.1	0.309	0.115
	8/7/2011	9:40 AM	26.1	7.31	7.85	4.2	0.316	-0.065
	8/7/2011	3:43 PM	29.1	7.30	7.91	4.0	-0.353	-0.020
	8/8/2011	9:42 AM	27.6	7.35	8.22	4.3	-0.021	-0.146
	8/8/2011	3:34 PM	31.6	7.33	8.31	4.0	-0.137	-0.086

Table A-4 Cont. Location	Date	Time	Temp. (°C)	pH	Spec. Cond. (mS/cm)	Salinity	SRB (ppb)	FLT (ppb)
Seep 6 Cont.	8/9/2011	9:48 AM	27.3	7.38	8.21	4.3	0.691	0.017
	8/9/2011	3:30 PM	29.8	7.42	8.10	4.1	0.650	-0.068
	8/10/2011	11:30 AM	29.3	7.69	8.47	4.3	0.480	-0.043
	8/10/2011	4:05 PM	31.9	7.60	8.29	4.0	0.634	-0.229
	8/11/2011	9:37 AM	29.3	7.58	8.49	4.3	-0.055	0.302
	8/11/2011	3:55 PM	31.4	7.63	8.12	3.9	-0.647	0.119
	8/12/2011	9:41 AM	28.1	7.71	8.26	4.3	-0.360	0.270
	8/12/2011	3:37 PM	33.0	7.70	8.53	4.0	0.273	0.126
	8/13/2011	9:40 AM	27.3	7.49	8.15	4.3	-0.405	0.181
	8/13/2011	3:23 PM	30.6	7.47	8.51	4.2	-0.795	0.084
	8/14/2011	4:01 PM	28.0	7.34	8.03	4.2	1.301	0.306
	8/15/2011	9:34 AM	27.0	7.54	7.98	4.2	0.776	0.371
	8/15/2011	3:47 PM	29.5	7.43	8.32	4.2	-0.026	0.398
	8/16/2011	2:39 AM	24.3	7.45	7.59	4.2	0.441	0.386
	8/16/2011	9:47 AM	28.6	7.47	8.18	4.2	-0.063	0.301
	8/16/2011	3:33 PM	30.0	7.55	8.32	4.2	0.056	0.217
	8/17/2011	12:25 AM	24.7	7.54	7.60	4.2	0.824	0.239
	8/17/2011	10:08 AM	28.9	7.51	8.04	4.1	-0.090	0.094
	8/18/2011	9:55 AM	30.0	7.46	8.13	4.1	0.148	0.339
	8/18/2011	4:00 PM	31.6	7.41	8.51	4.1	0.286	0.197
	8/19/2011	9:43 AM	29.2	7.44	8.01	4.1	0.400	0.286
	8/19/2011	3:56 PM	30.7	7.34	8.23	4.0	-0.408	0.012
	8/20/2011	9:54 AM	29.4	7.41	8.04	4.0	0.062	0.506
	8/20/2011	3:57 PM	28.1	7.61	7.87	4.1	-0.063	0.405
	8/21/2011	9:49 AM	26.5	7.47	7.80	4.2	0.704	0.225
	8/21/2011	4:16 PM	28.3	7.94	7.48	4.1	0.604	0.145
	8/22/2011	9:25 AM	29.0	7.40	8.20	4.2	0.138	0.160
	8/22/2011	4:04 PM	31.0	7.73	8.32	4.1	-0.137	0.116
	8/23/2011	9:35 AM	28.2	7.21	8.19	4.2	-0.005	0.174
	8/23/2011	3:36 PM	28.8	7.38	7.82	4.0	0.513	0.068
	8/24/2011	10:26 AM	27.6	7.23	8.22	4.3	0.060	0.217
	8/24/2011	4:50 PM	29.5	7.45	7.94	4.0	-0.134	0.443
	8/25/2011	10:18 AM	28.9	7.51	8.34	4.3	0.141	0.007
	8/25/2011	4:25 PM	28.8	7.53	7.89	4.0	0.420	0.243
	8/26/2011	9:30 AM	29.0	7.50	8.73	4.4	0.806	0.169

Table A-4 Cont. Location	Date	Time	Temp. (°C)	pH	Spec. Cond. (mS/cm)	Salinity	SRB (ppb)	FLT (ppb)
Seep 6 Cont.	8/26/2011	3:38 PM	30.4	7.72	8.01	4.0	0.339	0.109
	8/27/2011	9:57 AM	29.1	7.65	8.40	4.3	0.648	0.108
	8/27/2011	4:32 PM	29.9	7.57	7.95	4.0	0.669	0.280
	8/28/2011	9:52 AM	28.5	7.51	8.26	4.3	0.331	0.191
	8/28/2011	4:08 PM	30.7	7.56	8.19	4.0	0.179	0.514
	8/29/2011	9:39 AM	28.2	7.28	8.02	4.1	0.089	0.021
	8/29/2011	3:55 PM	29.4	7.22	7.97	4.0	0.351	0.197
	8/30/2011	9:24 AM	29.4	7.18	7.77	3.9	0.552	0.482
	9/1/2011	11:00 AM	30.9	7.70	9.67	4.8	-0.162	0.372
	9/1/2011	4:33 PM	31.9	7.50	8.69	4.2	0.082	0.280
	9/2/2011	10:46 AM	30.5	7.55	8.26	4.1	-0.268	0.147
	9/2/2011	4:16 PM	32.5	7.57	10.67	5.1	-0.191	0.182
	9/3/2011	9:45 AM	27.4	7.67	7.86	4.1	0.048	0.149
	9/3/2011	3:59 PM	30.0	7.55	8.27	4.1	0.081	0.399
	9/4/2011	4:05 PM	34.2	7.42	9.88	4.6	0.189	0.436
	9/5/2011	9:32 AM	31.1	7.42	8.54	4.2	-0.476	0.284
	9/5/2011	3:57 PM	29.1	7.33	7.96	4.0	0.376	0.145
	9/6/2011	9:24 AM	26.8	7.33	7.97	4.2	-0.275	0.232
	9/6/2011	4:07 PM	32.0	7.43	8.40	4.0	0.107	0.351
	9/7/2011	9:36 AM	29.0	7.42	8.26	4.2	-0.294	0.360
	9/8/2011	9:46 AM	29.5	7.43	8.29	4.2	-0.742	0.816
	9/9/2011	10:40 AM	34.8	7.43	9.18	4.2	-0.011	0.463
	9/10/2011	10:42 AM	30.1	7.40	7.79	4.3	-0.739	0.167
	9/11/2011	10:48 AM	32.5	7.37	8.98	4.3	0.217	0.209
	9/12/2011	12:00 PM	30.9	7.36	8.66	4.3	0.576	0.389
	9/13/2011	11:02 AM	33.3	7.40	8.99	4.2	-0.482	0.341
	9/14/2011	10:05 AM	31.3	7.39	8.16	4.2	-0.217	0.347
	9/15/2011	9:46 AM	32.0	7.41	8.69	4.2	-0.323	0.254
	9/16/2011	11:37 AM	33.7	7.42	8.92	4.2	-0.548	0.379
	9/17/2011	2:48 PM	32.2	7.46	11.58	5.7	-0.429	0.588
	9/18/2011	11:25 AM	35.9	7.50	10.23	5.7	0.006	0.251
	9/19/2011	10:32 AM	30.2	7.50	13.54	7.0	-0.418	0.499
	9/20/2011	9:40 AM	30.3	7.06	8.68	4.3	-0.415	0.510
	9/21/2011	9:21 AM	28.2	7.34	9.49	5.0	-0.600	0.224
	9/22/2011	9:48 AM	28.7	7.52	12.31	6.5	-0.150	0.396

Table A-4 Cont. Location	Date	Time	Temp. (°C)	pH	Spec. Cond. (mS/cm)	Salinity	SRB (ppb)	FLT (ppb)
Seep 6 Cont.	9/23/2011	9:50 AM	29.9	7.42	9.18	4.6	0.115	0.487
	9/24/2011	8:57 AM	30.0	7.31	9.65	4.8	0.154	0.232
	9/25/2011	10:33 AM	33.3	7.41	9.71	5.4	-0.152	0.126
	9/26/2011	10:36 AM	31.9	7.47	12.01	5.9	-0.576	0.221
	9/27/2011	9:25 AM	29.7	6.90	9.15	4.6	-1.226	0.141
	9/28/2011	9:26 AM	29.9	7.20	8.06	4.0	-0.546	0.163
	9/29/2011	9:21 AM	27.4	7.21	7.72	4.0	-0.729	0.340
	9/30/2011	9:28 AM	28.9	7.23	8.07	4.1	0.092	0.174
	10/1/2011	9:45 AM	29.8	7.44	8.47	4.2	0.265	0.041
	10/2/2011	12:03 PM	33.5	7.27	8.53	4.0	0.194	0.057
	10/3/2011	9:30 AM	27.6	7.25	7.71	4.0	0.486	-0.041
	10/4/2011	9:47 AM	29.1	7.47	8.10	4.1	0.586	-0.024
	10/6/2011	12:18 PM	30.5	7.32	8.39	4.1	0.626	0.472
	10/8/2011	4:09 PM	29.5	7.35	8.02	4.0	-0.366	0.473
	10/10/2011	11:49 AM	34.2	7.30	8.69	4.0	0.295	0.328
	10/12/2011	9:20 AM	28.7	7.46	7.95	4.1	0.011	0.559
	10/14/2011	9:47 AM	28.0	7.44	7.96	4.1	0.376	0.338
	10/16/2011	9:46 AM	28.1	7.43	8.27	4.3	0.489	0.161
	10/18/2011	11:32 AM	32.6	7.30	9.00	4.3	0.146	0.157
	10/20/2011	9:53 AM	28.8	7.42	8.11	4.1	0.222	0.236
	10/22/2011	9:51 AM	30.8	7.46	8.12	4.0	0.232	0.234
	10/24/2011	9:51 AM	29.2	7.43	8.08	4.1	0.418	0.217
	10/26/2011	9:58 AM	28.4	7.42	7.93	4.1	-0.114	0.264
	10/28/2011	9:25 AM	27.0	7.41	7.58	4.0	-0.165	0.293
	10/30/2011	11:18 AM	32.2	7.35	8.29	4.0	-0.085	0.506
	11/1/2011	11:52 AM	31.9	7.42	8.49	4.1	0.137	0.383
	11/3/2011	9:53 AM	29.7	7.39	8.20	4.1	0.228	0.456
	11/5/2011	1:07 PM	30.4	7.35	8.26	4.1	-0.225	0.626
	11/7/2011	9:31 AM	26.1	7.64	7.60	4.1	0.000	0.559
	11/9/2011	9:39 AM	29.3	7.30	8.18	4.1	-0.108	0.670
	11/11/2011	9:54 AM	25.4	7.32	7.92	4.3	-0.405	0.634
	11/16/2011	9:49 AM	27.7	7.42	7.59	3.9	0.167	0.974
	11/18/2011	10:02 AM	29.8	7.70	9.43	4.8	0.596	0.718
	11/21/2011	9:37 AM	28.3	7.24	8.03	4.2	0.909	1.007
	11/23/2011	9:34 AM	27.4	7.27	7.60	4.0	0.533	1.183

Table A-4 Cont. Location	Date	Time	Temp. (°C)	pH	Spec. Cond. (mm/cm)	Salinity	SRB (ppb)	FLT (ppb)
Seep 7	11/16/2011	9:10 AM	27.9	7.29	7.83	4.1	0.116	0.988
	11/18/2011	9:45 AM	27.4	7.28	7.76	4.1	0.951	1.387
	11/21/2011	9:49 AM	28.5	7.34	7.71	4.0	0.171	0.991
	11/23/2011	9:57 AM	27.2	7.45	7.61	4.0	-0.164	1.160
	11/25/2011	10:08 AM	28.0	7.40	8.01	4.2	0.499	1.389
	11/28/2011	9:41 AM	24.9	7.42	11.46	6.5	0.302	1.583
	11/30/2011	10:39 AM	26.0	7.46	7.50	4.0	0.391	1.920
	12/2/2011	9:44 AM	26.1	7.45	7.72	4.2	0.595	2.175
	12/5/2011	10:03 AM	29.6	7.43	7.98	4.0	1.429	2.727
	12/9/2011	9:39 AM	23.9	7.47	7.24	4.1	0.352	3.355
	12/12/2011	9:32 AM	25.1	7.43	7.29	3.9	0.319	3.969
	12/14/2011	9:25 AM	27.7	7.26	7.67	4.0	0.067	4.663
	12/19/2011	9:58 AM	27.3	7.35	7.60	4.0		
	12/21/2011	10:18 AM	26.4	7.44	7.64	4.1		
	12/23/2011	10:10 AM	22.4	7.80	7.83	4.6		
	12/26/2011	10:14 AM	27.0	7.57	7.76	4.1		
	12/28/2011	10:06 AM	29.5	7.42	8.19	4.1		
	12/30/2011	10:21 AM	27.7	7.57	8.44	4.4		
	1/2/2012	10:18 AM	28.4	7.54	15.08	8.2		
	1/4/2012	2:48 PM	29.3	7.59	8.35	4.2	0.91	29.51
	1/7/2012	2:46 PM	29.1	7.46	8.26	4.2	1.28	32.98
	1/9/2012	11:11 AM	28.1	7.32	7.80	4.0	1.26	20.46
	1/11/2012	10:55 AM	25.6	7.48	7.46	4.0	1.22	37.02
	1/13/2012	11:25 AM	27.7	7.44	7.95	4.1	1.43	37.59
	1/16/2012	1:04 PM	29.0	7.44	8.05	4.1		
	1/19/2012	10:12 AM	26.0	7.52	7.97	4.3	1.110	40.56
	1/21/2012	4:00 PM	29.9	7.55	8.38	4.2	1.892	42.59
	1/23/2012	11:30 AM	28.9	7.50	8.09	4.1	2.179	44.31
	1/25/2012	9:43 AM	25.9	7.58	7.55	4.1	1.672	47.59
	1/27/2012	12:20 PM	29.8	7.81	8.32	4.1	2.339	45.29
	1/31/2012	11:13 AM	28.5	7.47	8.00	4.1	1.481	47.98
	2/10/2012	12:06 AM	27.7	7.54	8.15	4.3	1.352	53.22
	2/14/2012	1:17 PM	30.3	7.45	8.48	4.2	1.583	58.23
	2/17/2012	11:20 AM	26.9	7.56	7.97	4.2	2.219	61.30
	2/20/2012	1:46 PM	28.4	7.66	8.15	4.3	1.812	63.28

Table A-4 Cont. Location	Date	Time	Temp. (°C)	pH	Spec. Cond. (mm/cm)	Salinity	SRB (ppb)	FLT (ppb)
Seep 7 Cont.	2/24/2012	11:03 AM	28.7	7.50	8.21	4.2	1.524	60.78
	2/27/2012	10:05 AM	26.3	7.62	7.83	4.2	1.667	65.82
	3/1/2012	11:29 AM	26.4	7.67	7.99	4.3	1.222	66.93

Location	Date	Time	Temp. (°C)	pH	Spec. Cond. (mm/cm)	Salinity	SRB (ppb)	FLT (ppb)
Seep 8	11/16/2011	9:35 AM	27.4	7.45	9.43	5.0	0.267	1.029
	11/23/2011	9:45 AM	26.4	7.26	7.79	4.2	-0.197	1.372
	11/25/2011	10:18 AM	28.3	7.20	8.39	4.3	0.060	1.448
	11/28/2011	9:53 AM	26.2	7.90	10.66	5.9	0.745	1.235
	11/30/2011	10:49 AM	26.9	7.29	7.61	4.0	0.395	2.147
	12/2/2011	9:54 AM	26.5	7.29	7.74	4.1	0.392	2.519
	12/5/2011	9:51 AM	29.3	7.26	8.04	4.1	0.318	2.885
	12/7/2011	9:54 AM	26.3	7.30	7.76	4.2	0.638	2.548
	12/9/2011	9:49 AM	24.8	7.34	7.47	4.1	0.421	3.738
	12/12/2011	9:52 AM	25.2	7.39	7.53	4.1	-0.046	4.244
	12/14/2011	9:44 AM	26.1	7.24	7.67	4.1	-0.022	4.769
	12/16/2011	9:50 AM	28.8	7.28	7.91	4.0	0.211	4.993
	12/19/2011	9:47 AM	26.9	7.32	7.76	4.1		
	12/21/2011	10:43 AM	26.3	7.09	7.85	4.2		
	12/23/2011	10:34 AM	25.6	7.30	7.81	4.2		
	12/26/2011	10:35 AM	28.0	7.29	8.24	4.3		
	12/28/2011	10:15 AM	30.0	7.30	8.61	4.3		
	12/30/2011	10:45 AM	28.9	7.33	8.99	4.6		
	1/2/2012	10:50 AM	28.8	7.85	37.88	22.0		
	1/4/2012	3:17 PM	28.6	7.42	8.51	4.4	1.01	32.79
	1/7/2012	3:08 PM	28.5	7.39	8.36	4.3	1.26	34.99
	1/9/2012	10:36 AM	29.0	7.37	8.15	4.2	1.85	37.18
	1/11/2012	10:33 AM	24.7	7.49	7.67	4.2	1.66	40.60
	1/13/2012	11:02 AM	26.5	7.16	7.85	4.2	1.69	40.83
	1/16/2012	12:47 PM	31.0	7.33	8.41	4.1		

Table A-4 Cont. Location	Date	Time	Temp. (°C)	pH	Spec. Cond. (mm/cm)	Salinity	SRB (ppb)	FLT (ppb)
Seep 9	11/30/2011	9:27 AM	26.5	7.36	7.52	4.0	0.653	1.868
	12/2/2011	9:30 AM	25.8	7.31	7.67	4.2	0.818	2.063
	12/5/2011	9:39 AM	28.6	7.34	7.93	4.0	0.132	2.635
	12/7/2011	9:44 AM	27.4	7.39	7.52	3.9	0.431	2.750
	12/9/2011	9:28 AM	26.7	7.36	7.36	3.9	1.123	3.239
	12/12/2011	9:41 AM	24.8	7.47	7.21	4.0	-0.194	3.909
	12/14/2011	9:35 AM	27.7	7.30	7.66	4.0	0.371	4.623
	12/16/2011	9:37 AM	29.3	7.38	7.69	3.9	0.261	4.693
	12/19/2011	10:06 AM	26.8	7.35	7.64	4.1		
	12/21/2011	10:31 AM	26.2	6.75	7.59	4.0		
	12/23/2011	10:21 AM	23.3	7.32	7.26	4.1		
	12/26/2011	10:24 AM	27.4	7.37	7.75	4.0		
	12/28/2011	9:57 AM	28.1	7.31	7.90	4.1		
	12/30/2011	10:36 AM	28.0	7.42	8.22	4.2		
	1/2/2012	10:36 AM	28.5	7.67	24.95	14.0		
	1/4/2012	3:03 PM	29.5	7.63	10.12	5.2	0.98	28.17
	1/7/2012	2:58 PM	28.7	7.49	14.62	7.9	1.60	28.28
	1/9/2012	10:56 AM	28.8	7.31	8.14	4.2	0.99	32.87
	1/11/2012	10:45 AM	24.7	7.45	7.91	4.4	1.32	35.40
	1/13/2012	11:15 AM	26.2	7.52	28.10	16.8	0.87	22.68
	1/16/2012	1:16 PM	29.4	7.80	31.57	17.9		
	1/19/2012	9:58 AM	26.0	7.65	9.59	5.3	1.319	38.15
	1/21/2012	4:13 PM	30.5	7.75	42.91	24.6	1.131	27.66
	1/23/2012	11:19 AM	28.6	7.65	42.77	25.3	0.487	16.16
Location	Date	Time	Temp. (°C)	pH	Spec. Cond. (mm/cm)	Salinity	SRB (ppb)	FLT (ppb)
Seep 10	1/21/2012	4:26 PM	29.0	7.75	9.73	5.0	1.450	39.94
	1/23/2012	11:03 AM	29.5	7.56	9.73	5.0	1.297	43.14
	1/25/2012	10:30 AM	27.7	7.38	8.25	4.3	2.073	45.76
	1/27/2012	12:34 PM	29.2	7.66	11.85	6.2	1.407	42.12
	1/31/2012	11:29 AM	27.6	7.52	8.53	4.4	1.493	50.41

Table A-4 Cont. Location	Date	Time	Temp. (°C)	pH	Spec. Cond. (mm/cm)	Salinity	SRB (ppb)	FLT (ppb)
Seep 10 Cont.	2/10/2012	11:30 AM	28.5	7.76	9.80	5.1	1.293	53.45
	2/14/2012	12:47 PM	29.5	7.26	8.37	4.2	1.723	57.87
	2/17/2012	11:05 AM	27.2	7.63	8.00	4.3	2.075	62.01
	2/20/2012	1:12 PM	28.4	7.66	8.31	4.3	1.473	64.09
	2/24/2012	10:51 AM	28.4	7.62	7.99	4.1	1.244	61.56
	2/27/2012	9:37 AM	26.7	7.67	9.65	5.2	1.088	58.61
	3/1/2012	11:18 AM	26.5	7.68	7.97	4.3	1.474	65.05

Location	Date	Time	Temp. (°C)	pH	Spec. Cond. (mm/cm)	Salinity	SRB (ppb)	FLT (ppb)
Seep 12	1/25/2012	11:24 AM	29.1	7.36	8.49	4.3	1.667	47.30
	1/27/2012	12:05 PM	29.6	7.78	8.44	4.3	1.219	46.43
	1/31/2012	11:41 AM	29.4	7.62	8.26	4.2	1.188	50.96
	2/10/2012	11:47 AM	27.5	7.63	8.23	4.4	0.833	54.77
	2/14/2012	1:02 PM	29.5	7.43	8.41	4.3	1.956	58.90
	2/17/2012	11:31 AM	27.4	7.61	8.03	4.2	1.983	60.72
	2/20/2012	1:25 PM	28.7	7.68	9.55	4.9	1.506	62.92
	2/24/2012	11:16 AM	27.5	7.56	8.07	4.2	1.356	64.68
	2/27/2012	10:32 AM	26.9	7.56	8.20	4.4	1.178	65.82
	3/1/2012	11:40 AM	28.6	7.60	9.28	4.8	1.166	65.98
	3/14/2012	10:21 AM	26.7	7.73	7.88	4.2		
	3/17/2012	9:36 AM	26.6	7.61	7.90	4.2	2.032	67.00
	3/19/2012	10:12 AM	29.0	7.67	8.13	4.1	2.017	69.70

Location	Date	Time	Temp. (°C)	pH	Spec. Cond. (mm/cm)	Salinity	SRB (ppb)	FLT (ppb)
Seep 13	3/14/2012	9:53 AM	26.0	7.71	7.69	4.2		
	3/17/2012	9:12 AM	29.7	7.69	8.74	4.4	2.320	67.65
	3/19/2012	9:46 AM	28.2	7.67	8.10	4.2	2.113	70.78

Location	Date	Time	Temp. (°C)	pH	Spec. Cond. (mm/cm)	Salinity	SRB (ppb)	FLT (ppb)
Seep 14	3/14/2012	10:11 AM	24.7	7.72	7.67	4.2		
	3/17/2012	9:23 AM	27.8	7.62	8.05	4.2	1.753	66.69
	3/19/2012	9:57 AM	28.7	7.66	8.02	4.1	2.036	70.66

Table A-4 Cont. Location	Date	Time	Temp. (°C)	pH	Spec. Cond. (mm/cm)	Salinity	SRB (ppb)	FLT (ppb)
Seep 15	3/27/2012	9:09 AM	25.6	7.63	8.68	4.8	0.982	66.63
	3/29/2012	10:28 AM	28.1	7.53	8.17	4.2	1.526	66.63
	4/2/2012	10:19 AM	27.1		16.54	9.3	2.393	58.06
	4/5/2012	8:27 AM	24.6	7.47	15.83	9.3	2.148	58.80
	4/12/2012	11:30 AM	31.1	7.48	8.45	4.2	1.769	69.06
	4/16/2012	9:09 AM	26.5	7.45	7.86	4.2	1.895	71.19
	4/19/2012	11:32 AM	31.6	7.61	8.79	4.3	1.524	67.95
	4/24/2012	3:25 PM	29.9	7.71	8.57	4.3	1.988	67.01
	4/26/2012	10:40 AM	30.3	7.72	8.46	4.2	1.959	68.05
	5/2/2012	9:42 AM	29.5	7.58	8.59	4.3	2.378	71.50

Location	Date	Time	Temp. (°C)	pH	Spec. Cond. (mm/cm)	Salinity	SRB (ppb)	FLT (ppb)
Seep 16	4/24/2012	3:11 PM	30.6	7.69	8.95	4.5	2.279	66.07
	4/26/2012	10:53 AM	30.4	7.71	8.79	4.4	2.108	69.64
	5/2/2012	9:32 AM	29.4	7.50	8.81	4.5	2.694	71.13

Table A-5. Water quality parameters collected from control locations
Collected at Honokowai Beach Park, Wahikuli Wayside Park, and Olowalu with a handheld YSI Model 63 and field fluorescence measurements of S-Rhodamine-B (SRB) and Fluorescein (FLT) with a handheld Aquafluor fluorometer model 8000-10 from 8/5/2011 to 5/2/2012.

Location	Date	Time	Temp. (°C)	pH	Spec. Cond. (mS/cm)	Salinity	SRB (ppb)	FLT (ppb)
Honoko-wai Beach Park	8/5/2011	5:54 PM	26.4	8.13	54.60	35.1	-0.021	-0.192
	8/12/2011	5:26 PM	27.3	8.15	56.10	35.4	-0.064	0.046
	8/22/2011	3:25 PM	27.8	8.25	56.10	35.0	-0.227	0.145
	9/2/2011	2:00 PM	28.2	8.27	57.00	35.5	-0.606	0.068
	9/15/2011	12:00 PM	29.3	8.06	55.50	33.2	-0.731	-0.112
	9/26/2011	1:30 PM	28.8	8.00	56.80	34.7	-0.172	0.105
	10/14/2011	1:47 PM	28.3	8.10	56.40	34.4	0.118	0.048
	10/22/2011	1:00 PM	29.2	8.13	58.00	35.7	-0.238	-0.021
	11/14/2011	11:15 AM	27.1	7.90	52.10	32.7	-0.131	0.360
	11/25/2011	12:07 PM	27.2	8.06	51.40	32.3	-0.047	-0.227
	12/9/2011	12:05 PM	28.6	7.96	50.70	30.6	0.186	-0.127
	1/13/2012	3:15 PM	27.1	8.00	55.70	35.4	0.45	-0.02
	1/27/2012	4:34 PM	26.9	8.05	55.50	35.5	0.257	0.323
	2/10/2012	3:34 PM	27.4	8.15	55.60	35.0	-0.501	0.130
	2/17/2012	3:04 PM	27.2	8.06	51.30	32.1	0.271	-0.139
	2/24/2012	3:02 PM	27.6	8.10	56.80	35.7	0.263	-0.058
	3/1/2012	3:05 PM	30.3	7.98	51.00	29.9	-0.634	-0.107
	3/11/2012	2:30 PM	26.1	8.12	53.40	34.5	0.420	1.426
	3/22/2012	3:00 PM	25.1	7.99	47.30	31.3	0.242	0.115
	3/27/2012	2:30 PM	26.5	8.03	53.60	34.4	-0.708	0.112
	4/5/2012	11:55 AM	25.4	7.95	52.80	34.5	-0.183	-0.560
	4/12/2012	2:18 PM	28.8	8.01	56.20	34.4	-0.231	-0.174
	4/19/2012	2:53 PM	26.3	8.02	52.90	33.9	-0.112	-0.450
	5/2/2012	2:28 PM	26.8	7.99	54.00	34.1	0.339	-0.667
Location	Date	Time	Temp. (°C)	pH	Spec. Cond. (mS/cm)	Salinity	SRB (ppb)	FLT (ppb)
Wahikuli Wayside Park	8/5/2011	6:20 PM	25.9	8.16	55.10	35.8	-0.635	-0.635
	8/12/2011	5:50 PM	27.2	8.16	57.40	36.4	0.273	0.134
	8/22/2011	5:45 PM	27.8	8.00	56.40	34.8	-0.292	-0.047
	9/2/2011	1:30 PM	29.7	8.02	56.60	33.6	-0.339	0.247
	9/15/2011	12:00 PM	27.8	8.00	56.20	35.1	-0.747	0.106
	9/26/2011	2:00 PM	27.4	7.99	57.70	36.2	-0.190	0.221
	10/14/2011	2:13 PM	28.2	8.13	56.80	35.2	0.951	0.122
	10/22/2011	1:10 PM	27.9	8.15	57.40	36.1	0.071	-0.125
	11/14/2011	11:34 AM	26	7.89	54.40	35.2	0.548	0.000
	11/25/2011	12:26 PM	25.6	8.05	53.10	34.5	0.046	-0.161

Table A-5 Continued Location	Date	Time	Temp. (°C)	pH	Spec. Cond. (mS/cm)	Salinity	SRB (ppb)	FLT (ppb)
Wahikuli Wayside Park Continued	12/9/2011	12:20 PM	25.3	8.03	52.30	34.5	-0.107	-0.270
	1/13/2012	3:30 PM	26.0	8.01	54.00	35.2	0.74	-0.15
	1/27/2012	4:51 PM	26.0	8.04	53.60	34.7	0.569	0.498
	2/10/2012	3:50 PM	25.8	8.13	52.60	34.0	-0.894	0.067
	2/17/2012	3:20 PM	24.9	8.10	54.00	35.4	0.005	0.021
	2/24/2012	3:36 PM	27.5	8.08	55.00	34.4	-0.367	1.403
	3/1/2012	3:28 PM	26.2	8.10	53.20	33.8	-0.466	0.479
	3/11/2012	3:00 PM	26.0	8.10	53.50	34.1	-0.095	0.452
	3/22/2012	3:30 PM	24.9	8.06	50.40	33.8	0.565	-0.586
	3/27/2012	2:48 PM	26.5	8.10	53.30	34.0	-1.244	-0.516
	4/5/2012	12:13 PM	25.2	8.04	52.80	34.4	-0.026	-0.610
	4/12/2012	2:37 PM	27.2	7.97	52.20	32.7	0.039	-0.369
	4/19/2012	3:13 PM	25.6	7.99	55.40	36.4	-0.820	-0.784
	5/2/2012	2:51 PM	25.7	7.98	55.00	35.7	0.192	-0.781

Location	Date	Time	Temp. (°C)	pH	Spec. Cond. (mS/cm)	Salinity	SRB (ppb)	FLT (ppb)
Olowalu	12/2/2011	8:00 AM	28.8	7.92	56.60	34.7	-0.173	-0.093
	12/9/2011	1:00 PM	24.8	8.03	54.70	36.3	0.252	-0.182
	1/13/2012	4:00 PM	27.6	7.99	48.14	29.5	0.48	0.49
	1/27/2012	5:24 PM	28.4	8.03	54.50	33.5	0.648	0.293
	2/10/2012	4:30 PM	25.3	8.11	53.00	34.6	-0.221	0.198
	2/17/2012	4:00 PM	25.4	8.09	54.00	35.0	0.393	1.154
	2/24/2012	4:19 PM	28.9	8.08	57.60	35.3	-0.784	-0.052
	3/1/2012	4:20 PM	30.0	8.12	55.90	33.4	-0.159	-0.720
	3/11/2012	3:35 PM	29.6	8.08	57.90	35.2	-0.057	1.014
	3/22/2012	4:15 PM	26.0	8.05	58.30	36.3	0.138	-0.336
	3/27/2012	4:00 PM	29.9	8.13	57.10	34.1	-0.976	-0.263
	4/5/2012	1:06 PM	28.8	7.99	56.50	34.6	0.465	0.653
	4/12/2012	3:51 PM	31.5	7.95	57.30	33.3	0.141	-0.392
	4/20/2012	12:02 PM	29.5	7.98	55.00	33.1	-0.535	-0.572
	5/2/2012	3:42 PM	26.4	7.95	55.80	35.8	0.892	0.252

This page is intentionally left blank.

APPENDIX B: FLUOROMETRY PROCEDUES AND DATA

APPENDIX B-1: PROCEDURES FOR ESTABLISHING THE METHOD DETECTION LIMIT

APPENDIX FOR SECTION 3:

FLUORESCENT DYE GROUNDWATER TRACER STUDY

This page is intentionally left blank.

e-CFR Data is current as of June 1, 2011

Title 40: Protection of Environment
PART 136—GUIDELINES ESTABLISHING TEST PROCEDURES FOR THE ANALYSIS OF POLLUTANTS

Browse Previous | Browse Next

Appendix B to Part 136—Definition and Procedure for the Determination of the Method Detection Limit—Revision 1.11

Definition

The method detection limit (MDL) is defined as the minimum concentration of a substance that can be measured and reported with 99% confidence that the analyte concentration is greater than zero and is determined from analysis of a sample in a given matrix containing the analyte.

Scope and Application

This procedure is designed for applicability to a wide variety of sample types ranging from reagent (blank) water containing analyte to wastewater containing analyte. The MDL for an analytical procedure may vary as a function of sample type. The procedure requires a complete, specific, and well defined analytical method. It is essential that all sample processing steps of the analytical method be included in the determination of the method detection limit.

The MDL obtained by this procedure is used to judge the significance of a single measurement of a future sample.

The MDL procedure was designed for applicability to a broad variety of physical and chemical methods. To accomplish this, the procedure was made device- or instrument-independent.

Procedure

1. Make an estimate of the detection limit using one of the following:

(a) The concentration value that corresponds to an instrument signal/noise in the range of 2.5 to 5.

(b) The concentration equivalent of three times the standard deviation of replicate instrumental measurements of the analyte in reagent water.

(c) That region of the standard curve where there is a significant change in sensitivity, *i.e.* , a break in the slope of the standard curve.

(d) Instrumental limitations.

It is recognized that the experience of the analyst is important to this process. However, the analyst must include the above considerations in the initial estimate of the detection limit.

2. Prepare reagent (blank) water that is as free of analyte as possible. Reagent or interference free

301

water is defined as a water sample in which analyte and interferent concentrations are not detected at the method detection limit of each analyte of interest. Interferences are defined as systematic errors in the measured analytical signal of an established procedure caused by the presence of interfering species (interferent). The interferent concentration is presupposed to be normally distributed in representative samples of a given matrix.

3. (a) If the MDL is to be determined in reagent (blank) water, prepare a laboratory standard (analyte in reagent water) at a concentration which is at least equal to or in the same concentration range as the estimated method detection limit. (Recommend between 1 and 5 times the estimated method detection limit.) Proceed to Step 4.

(b) If the MDL is to be determined in another sample matrix, analyze the sample. If the measured level of the analyte is in the recommended range of one to five times the estimated detection limit, proceed to Step 4.

If the measured level of analyte is less than the estimated detection limit, add a known amount of analyte to bring the level of analyte between one and five times the estimated detection limit.

If the measured level of analyte is greater than five times the estimated detection limit, there are two options.

(1) Obtain another sample with a lower level of analyte in the same matrix if possible.

(2) The sample may be used as is for determining the method detection limit if the analyte level does not exceed 10 times the MDL of the analyte in reagent water. The variance of the analytical method changes as the analyte concentration increases from the MDL, hence the MDL determined under these circumstances may not truly reflect method variance at lower analyte concentrations.

4. (a) Take a minimum of seven aliquots of the sample to be used to calculate the method detection limit and process each through the entire analytical method. Make all computations according to the defined method with final results in the method reporting units. If a blank measurement is required to calculate the measured level of analyte, obtain a separate blank measurement for each sample aliquot analyzed. The average blank measurement is subtracted from the respective sample measurements.

(b) It may be economically and technically desirable to evaluate the estimated method detection limit before proceeding with 4a. This will: (1) Prevent repeating this entire procedure when the costs of analyses are high and (2) insure that the procedure is being conducted at the correct concentration. It is quite possible that an inflated MDL will be calculated from data obtained at many times the real MDL even though the level of analyte is less than five times the calculated method detection limit. To insure that the estimate of the method detection limit is a good estimate, it is necessary to determine that a lower concentration of analyte will not result in a significantly lower method detection limit. Take two aliquots of the sample to be used to calculate the method detection limit and process each through the entire method, including blank measurements as described above in 4a. Evaluate these data:

(1) If these measurements indicate the sample is in desirable range for determination of the MDL, take five additional aliquots and proceed. Use all seven measurements for calculation of the MDL.

(2) If these measurements indicate the sample is not in correct range, reestimate the MDL, obtain new sample as in 3 and repeat either 4a or 4b.

5. Calculate the variance (S^2) and standard deviation (S) of the replicate measurements, as follows:

$$S^2 = \frac{1}{n-1}\left[\sum_{i=1}^{n} x_i^2 - \frac{\left(\sum_{i=1}^{n} X_i\right)^2}{n}\right] \quad S = \left(S^2\right)^{\frac{1}{2}}$$

where:

X_I; i=1 to n, are the analytical results in the final method reporting units obtained from the n sample

302

aliquots and Σ refers to the sum of the X values from i=l to n.

6. (a) Compute the MDL as follows:

MDL = t(n-1,1-α=0.99) (S)

where:

MDL = the method detection limit

t(n-1,1-α=.99)= the students' t value appropriate for a 99% confidence level and a standard deviation estimate with n-1 degrees of freedom. See Table.

S = standard deviation of the replicate analyses.

(b) The 95% confidence interval estimates for the MDL derived in 6a are computed according to the following equations derived from percentiles of the chi square over degrees of freedom distribution (χ^2/df).

LCL = 0.64 MDL

UCL = 2.20 MDL

where: LCL and UCL are the lower and upper 95% confidence limits respectively based on seven aliquots.

7. Optional iterative procedure to verify the reasonableness of the estimate of the MDL and subsequent MDL determinations.

(a) If this is the initial attempt to compute MDL based on the estimate of MDL formulated in Step 1, take the MDL as calculated in Step 6, spike the matrix at this calculated MDL and proceed through the procedure starting with Step 4.

(b) If this is the second or later iteration of the MDL calculation, use S^2 from the current MDL calculation and S^2 from the previous MDL calculation to compute the F-ratio. The F-ratio is calculated by substituting the larger S^2 into the numerator S^2_A and the other into the denominator S^2_B. The computed F-ratio is then compared with the F-ratio found in the table which is 3.05 as follows: if S^2_A/S^2_B<3.05, then compute the pooled standard deviation by the following equation:

$$S_{pooled} = \left[\frac{6S_A^2 + 6S_B^2}{12} \right]^{\frac{1}{2}}$$

if S^2_A/S^2_B>3.05, respike at the most recent calculated MDL and process the samples through the procedure starting with Step 4. If the most recent calculated MDL does not permit qualitative identification when samples are spiked at that level, report the MDL as a concentration between the current and previous MDL which permits qualitative identification.

(c) Use the S_{pooled} as calculated in 7b to compute The final MDL according to the following equation:

MDL=2.681 (S_{pooled})

where 2.681 is equal to t(12,1−α=.99).

(d) The 95% confidence limits for MDL derived in 7c are computed according to the following equations derived from precentiles of the chi squared over degrees of freedom distribution.

LCL=0.72 MDL

UCL=1.65 MDL

where LCL and UCL are the lower and upper 95% confidence limits respectively based on 14 aliquots.

Tables of Students' t Values at the 99 Percent Confidence Level

Number of replicates	Degrees of freedom (n-1)	$t_{cn-1,.99})$
7	6	3.143
8	7	2.998
9	8	2.896
10	9	2.821
11	10	2.764
16	15	2.602
21	20	2.528
26	25	2.485
31	30	2.457
61	60	2.390
00	00	2.326

Reporting

The analytical method used must be specifically identified by number or title ald the MDL for each analyte expressed in the appropriate method reporting units. If the analytical method permits options which affect the method detection limit, these conditions must be specified with the MDL value. The sample matrix used to determine the MDL must also be identified with MDL value. Report the mean analyte level with the MDL and indicate if the MDL procedure was iterated. If a laboratory standard or a sample that contained a known amount analyte was used for this determination, also report the mean recovery.

If the level of analyte in the sample was below the determined MDL or exceeds 10 times the MDL of the analyte in reagent water, do not report a value for the MDL.

[49 FR 43430, Oct. 26, 1984; 50 FR 694, 696, Jan. 4, 1985, as amended at 51 FR 23703, June 30, 1986]

Browse Previous | Browse Next

For questions or comments regarding e-CFR editorial content, features, or design, email ecfr@nara.gov.

For questions concerning e-CFR programming and delivery issues, email webteam@gpo.gov.

Section 508 / Accessibility

Decision and Detection Limits for Linear Calibration Curves

André Hubaux[1] and Gilbert Vos[2]

C.C.R. Euratom, 21020 Ispra (Va), Italy

For linear calibration curves, two kinds of lower limits may be connected to the notion of confidence limits— a decision limit, the lowest signal that can be distinguished from the background and a detection limit, the content under which, *a priori*, any sample may erroneously be taken for the blank. From a few algebraical and computational developments, several practical rules are deduced to lower these limits. The influence of the precision of the analytical method, the number of standards, the range of their contents, the various modes of their repartition, and the replication of measurements on the unknown sample are studied from a statistical point of view.

EXTERNAL STANDARDS are of very common use in analytical practice. In many methods, *e.g.*, as in X-ray spectrochemical analysis, the analyst used a linear calibration curve obtained from measurements made on these standards, to estimate the concentration of the unknown. Obviously the sensitivity of his method may be enhanced by a judicious choice of standards, but the quantitative estimate of this enhancement is not straightforward. The various definitions of the detection limits found in the literature, although having different advantages do not explicitly include this influence.

Linning and Mandel (*1*) have presented a very interesting discussion on the determination of the precision of an analytical method involving a calibration curve. They emphasize that, because there is always some scatter in the calibration data, the precision of analysis for an unknown will be poorer than indicated from several repeat determinations on the same sample. Various authors have proposed an objective way to calculate the detection limit of an analytical determination. They suggest that a signal higher than the standard deviation of the background multiplied by a conventionally chosen factor (usually 3), should be considered as characteristic of a detectable amount of the element to be analyzed. Kaiser, in several papers (*2–4*) develops this concept at length and proposes to work at the confidence level of 99.86%, which corresponds to a value of 3 for the factor.

B. Altshuler and B. Pasternak (*5*) have connected the notion of detection limits with the statistical concepts of the errors of the first and second kind; these concepts will be also used in the present text. A review of the published definitions of the limits for qualitative detection and quantitative determination has been done by L. A. Currie (*6*), who proposes to introduce three specific levels: *A decision limit* to which corresponds a critical level L_c, the net signal level (instrument response) above which an observed signal may be recognized reliably enough to be detected; at this limit, one may decide whether or not the result of an analysis indicates presence; *A detection limit*, L_D, the "true" net signal level which may be *a priori* expected to lead to detection; this is the limit at which a given analytical procedure may be relied upon to lead to detection; and *A determination limit*, L_Q, the level at which the measurement precision will be satisfactory for quantitative determination.

We will show how estimates of the decision and detection limits may be introduced by considering the confidence limits of the linear calibration curve. The dependence of these limits upon the standards will thereby be made explicit.

DECISION AND DETECTION LIMITS—A NEW APPROACH

In the analytical methods of interest here, the response signals of a certain number of standards are measured and a straight line (the regression line) is passed through the representative points. This line is an estimate of the true calibration line. It may be predicted that any new standard will give a signal falling in the neighborhood of this obtained line. At this point two questions may arise:

Above which level are the signals significantly different from the background?

Above which concentration is a confusion with the nul concentration unlikely?

To seek an answer, let us scrutinize what the expression "in the neighborhood of" really implies. The representative point of a measured signal does not fall exactly on the line for two independent reasons: the drawn calibration line does not exactly coincide with the true calibration line but is only an estimate (this estimate is based on a limited number of standards); and for a given content, the corresponding response signal does not assume a fixed value but is randomly distributed around a mean value, and this distribution is not exactly known. In order to make precise the combined effects of these two uncertainties, one due to the insufficiency of our information, and the other to a lack of perfect reproductivity inherent to the method, four basic hypotheses are necessary.

First, the standards are supposed to be independent. Practically, this means that they should be prepared separately, *i.e.*, in such a way that they will differ in their preparation, as much from each other as from the samples to be analyzed. This condition is not so easily met as seems at first sight.

Second, the variance of the error distribution of the signals around their expectation is supposed to remain constant. Practically, this means that the scatter of the signals does not depend on the contents, in the studied range of these contents.

Third, the contents of the standards are supposed to be accurately known.

Fourth, it is assumed that the observed signals have a gaussian distribution around their expectation. Although this hypothesis is very widely accepted, it is not certain that it is always correct. On the contrary, K. Behrends (*7*) has shown that the error distribution definitely is not gaussian in a number of cases. But, although another type of distribution would yield somewhat different numerical results than those presented here, it would probably not significantly modify the main conclusions.

[1] C.E.T.I.S.

[2] Analytical Chemistry Section.

(1) F. J. Linning and J. Mandel, ANAL. CHEM., **36** (13), 25A (1964).
(2) H. Kaiser, *Z. Anal. Chem.*, **149**, 46 (1956).
(3) *Ibid.*, **209**, 1 (1965).
(4) *Ibid.*, **216**, 80 (1966).
(5) B. Altshuler and B. Pasternak, *Health Phys.*, **9**, 293 (1963).
(6) L. A. Currie, ANAL. CHEM., **40**, 586 (1968).

(7) K. Behrends, *Z. Anal. Chem.*, **235**, 391 (1967).
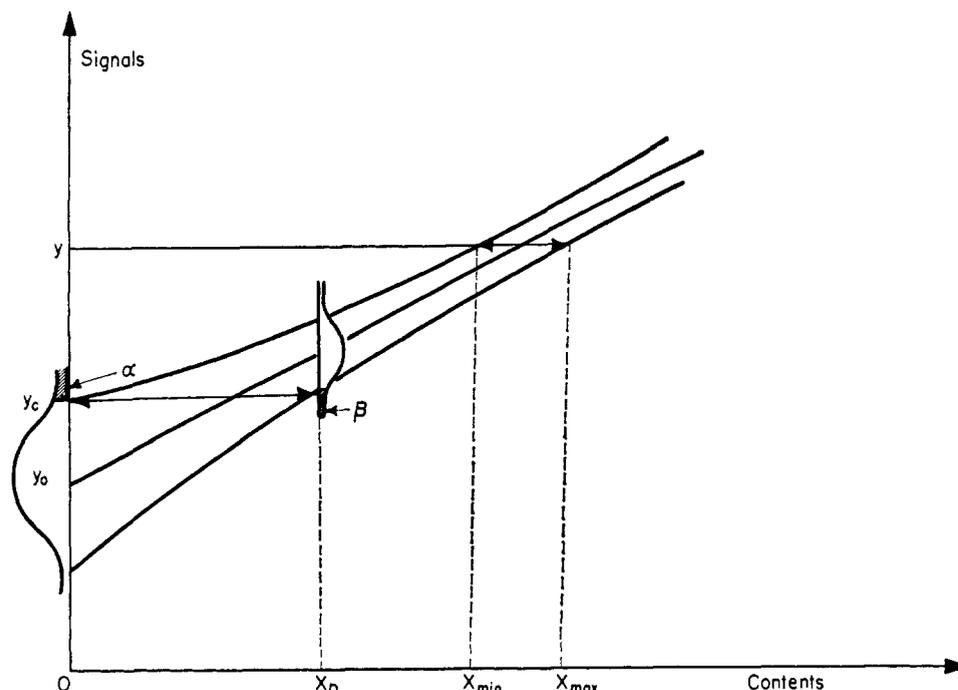
Figure 1. The linear calibration line, with its upper and lower confidence limits. y_c is the decision limit and x_D the detection limit, as explained in text

Starting from these hypotheses, formulas can be established from which several conclusions may be deduced, as will be shown in the next paragraphs. The considerations upon which the reasoning will be based are as follows:

On either side of the regression line, two confidence limits may be drawn, with an *a priori* chosen level of confidence, which we will note as $1-\alpha-\beta$, α and β having prefixed small values, of the order of a few percent (see Figure 1). The regression line and its two confidence limits represent a graphic synthesis of our knowledge about the relationship between content and signal. With it we may predict that an as yet unexplored content will yield a signal falling inside the confidence band. We will do this prediction with $1-\alpha-\beta$ probability; if we did a series of such predictions and then made the measurements, we would observe that, in the long run, we would be right $1-\alpha-\beta$ of the time; α % of the points would fall above the higher limit, and β % under the lower limit. The width of the confidence band depends on: the dispersion of signals for a given content, the knowledge we have of that dispersion and the degree of uncertainty about the true position of the calibration line.

The confidence limits, then, do not represent the dispersion of signals but our capacity to predict likely values for signals, taking into account the actual knowledge we possess of the case.

The confidence band may also be used in reverse; for a measured value y of the signal on a sample of unknown content (see Figure 1) we may predict the range of this content. The intersection of a horizontal line through y with the two confidence limits will define this range $x_{max}-x_{min}$, again with $1-\alpha-\beta$ probability. This, incidentally, is a valid method to estimate confidence limits of contents corresponding to a given signal. In particular, for a measured signal equal to y_c (see Figure 1), the lower limit of content is zero. Signals equal to or lower than y_c have a non-negligible probability to be due to a sample with a nul concentration, and hence we cannot distinguish, with such signals, whether or not the sought element is really present or not.

y_c is then the lowest measurable signal: if we are not ready to take a risk greater than α % to state that the element is present when it is absent (*i.e.*, to take a wrong decision more than α % of the time) we must decide that any signal under y_c must be disregarded. It is then clear that y_c corresponds to L_C as defined by L. A. Currie. More exactly, y_c is the *estimate* of L_c which may be obtained with the knowledge at hand. y_c could also be called the reading threshold, an expression proposed by H. Kaiser in an article published while the present paper was in press [H. Kaiser, ANAL. CHEM., **42** (4), 26A (1970)].

Hence, a measurement being made, we decide whether the sample may be a blank or not. (The blank being a sample which is identical, in principle, to the samples of interest, except that the substance sought is absent, or in such minute quantity that it will give signals not higher than the background). Before making any measurement, on the other hand, we can state that the lowest content we may distinguish from zero is x_D, the abscissa corresponding to y_c on the lower confidence limit. Indeed, with the knowledge in our possession, when we measure an unknown with a content lower than x_D, we run a risk higher than β to obtain a signal lower than y_c, and hence to state that it is a blank. x_D is then our estimate of the "limit of guarantee for purity," as defined by Kaiser (*3*) which in turn is equivalent to the "minimum detectable true activity" of Altshuler and Pasternak (*5*) and to the "detection limit" of Currie (*6*).

It is perhaps not useless to remark that y_c and x_D have not a fixed value. For a given method and a given number of standards they will vary because, first α and β may be chosen at will, according to the acceptable levels of risk one is ready to run to derive false conclusions, and second, by making a second series of standards, identical to the actual series, we would obtain signals differing at random from the actual signals. The regression line and the confidence limits we would then draw would not exactly coincide with the actual lines, and y_c and x_D would be somewhat different. In other words, y_c and x_D are random variables and estimates only.

306

But this is the normal situation whenever randomness is an integral part of the phenomenon.

By way of summary, two sensitivity limits are proposed here: a signal level y_C and a content x_D. These notions are very similar to the lower limits of detection for radioactivity counters proposed by B. Altshuler and B. Pasternak (5). The first limit concerns signals and will lead to an *a posteriori* decision, *i.e.*, a decision taken after the signal is measured; the second limit is relative to contents and is inherent to the method; it specifies *a priori* the content which will be safely detected without confusion with blanks. It will be seen that y_C and x_D are directly connected with the statistical notions of the "errors of the first and the second kind," respectively. [A good introduction to these classical notions will be found in (5)]. As the direct relationship between these limits and the confidence limits is now established, it is clear that the problem is equivalent to the study of the influence of the standards on the confidence limits: to lower y_C and x_D, the confidence limits must be brought nearer to the regression line.

MATHEMATICAL DEVELOPMENTS

Notations. The following notations have already been introduced: α, β, y_C, x_D. We will also use:

Y_o = estimate of the expectation of the response signal for a blank ($x = 0$) (y_o is the intersection of the calibration line with the axis of ordinates)

y_D = signal corresponding to x_D on the calibration line

x_C = abscissa corresponding to y_C on the calibration line

N = number of standards

x_i = concentration of the element of interest in the ith standard ($i = 1, N$)

Σ = the summation sign; stands for $\sum_{i=1}^{N}$

$\bar{x}$ = mean; $\bar{x} = \Sigma x_i / N$

x_1 = lowest concentration within the series of standards

x_N = highest concentration within the series of standards

K = number of standards equal to x_1 in the "three values" repartition of the contents of the standards

$$\lambda_i = \text{dimensionless factor}; \lambda_i = \frac{x_i - x_1}{x_N - x_1} \tag{1}$$

$$\lambda_D = \text{value of } \lambda_i \text{ corresponding to } x_D; \lambda_D = \frac{x_D - x_1}{x_N - x_1} \tag{2}$$

γ = exponent of the parabolic repartition (Eq 24)

y_i = the observed intensity of a characteristic line of the element of interest measured for the ith standard

$\bar{y}$ = mean; $\bar{y} = \Sigma y_i / N$

b = angular coefficient of the regression line, whose equation is:

$$Y = \bar{y} + b(x - \bar{x}) \tag{3}$$

with

$$b = \frac{\Sigma(x_i - \bar{x})(y_i - \bar{y})}{\Sigma(x_i - \bar{x})^2} \tag{4}$$

by the least squares method

Y_i = calculated signal corresponding to x_i

$$Y_i = \bar{y} + b(x_i - \bar{x}) \tag{5}$$

s^2 = the estimate of the residual variance

$$s^2 = \Sigma(y_i - Y_i)^2 / (N - 2); \tag{6}$$

s is the estimate of the residual standard deviation

t = Student's t corresponding to $N - 2$ degrees of freedom and $(1 - \alpha)$ or $(1 - \beta)$ confidence level

$$R = \text{range ratio of the standards } R = (x_N - x_1)/x_1 \tag{7}$$

P = factor of s in Equation 16

$$P = t_{1-\alpha} \sqrt{1 + \frac{1}{N} + \frac{\bar{x}^2}{\Sigma(x_i - \bar{x})^2}} \tag{8}$$

P_{III} = third term under the radical in the preceding equation

$$P_{III} = \frac{\bar{x}^2}{\Sigma(x_i - \bar{x})^2} \tag{9}$$

Q = factor of s in Equation 18

$$Q = t_{1-\beta} \sqrt{1 + \frac{1}{N} + \frac{(x_D - \bar{x})^2}{\Sigma(x_i - \bar{x})^2}} \tag{10}$$

Q_{III} = third term under the radical in the preceding equation

$$Q_{III} = \frac{(x_D - \bar{x})^2}{\Sigma(x_i - \bar{x})^2} \tag{11}$$

n = number of replicates on each unknown sample.

Equations of y_C and y_D. The equations of the upper and lower curves of Figure 1 (*i.e.*, the confidence limits) are derived [see (8) for instance] by considering that any value y corresponding to a given value of x has a gaussian distribution around its calculated value Y. The confidence limits at any point x are then expressed by

$$y = \bar{y} + b(x - \bar{x}) \pm t\sqrt{V[y]} \tag{12}$$

t corresponding to a probability of $1 - \alpha$ for the upper limit and $1 - \beta$ for the lower limit. The variance of y, $V[y]$, is the sum of the variance of Y plus the residual variance

$$V(y) = V[\bar{y} + b(x - \bar{x})] + \sigma^2 \tag{13}$$

with

$$V[\bar{y}] = \frac{\sigma^2}{N}, V[b] = \frac{\sigma^2}{\Sigma(x_i - \bar{x})^2} \tag{14}$$

The residual variance σ^2 may be replaced by its estimate s^2 and Equation 12 becomes

$$y = \bar{y} + b(x - \bar{x}) \pm st \sqrt{1 + \frac{1}{N} + \frac{(x - \bar{x})^2}{\Sigma(x_i - \bar{x})^2}} \tag{15}$$

In particular, for $x = 0$, the upper limit will be

$$y_C = \bar{y} - b\bar{x} + st_{1-\alpha} \sqrt{1 + \frac{1}{N} + \frac{\bar{x}^2}{\Sigma(x_i - \bar{x})^2}} \tag{16}$$

y_C may be considered as the sum of two terms:

$$y_C = Y_o + P \cdot s \tag{17}$$

with Y_o and P as defined in the list hereabove. We have no possibility to reduce Y_o, the intersection of the calibration line with the axis of ordinates. But we may reduce P and s and hence enhance the decision limit.

For the detection limit, it will be convenient to consider y_D, the ordinate of x_D on the regression line. Developments as in

(8) K. A. Brownlee, "Statistical Theory and Methodology in Science and Engineering," John Wiley & Sons, Inc., New York, N. Y., 1960.
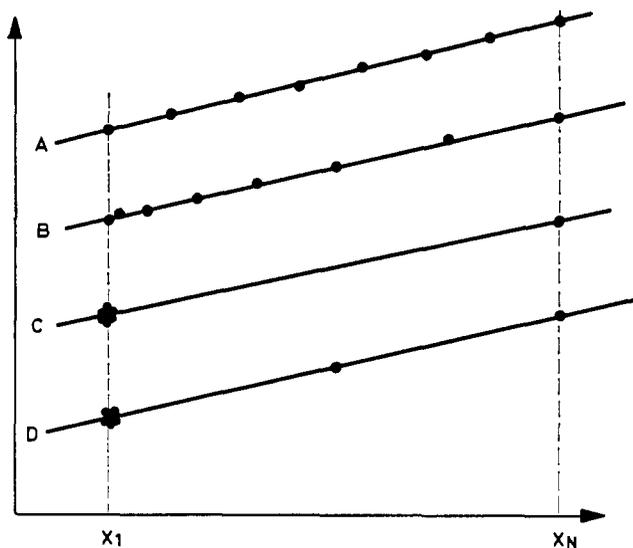
Figure 2. Four types or repartition of the standards

A. Equidistant or linear
B. Parabolic
C. In two values
D. In three values

the preceding paragraph will yield

$$y_D = y_C + st_{1-\beta} \sqrt{1 + \frac{1}{N} + \frac{(x_D - \bar{x})^2}{\Sigma(x_i - \bar{x})^2}} \qquad (18)$$

and a decrease of y_C will generally bring about a decrease of y_D. y_D may be considered as the sum of three terms

$$y_D = Y_o + Ps + Qs \qquad (19)$$

and the problem is thus concerned with the reduction of P and Q.

Computation of P. It will prove useful to express the x's as functions of R, λ_i, and x_1

$$x_i = (1 + \lambda_i R)x_1 \qquad (20)$$

where R represents the "range ratio" of the contents of the standards (Equation 7) and where the λ_i's are dimensionless factors which depend on the repartition of the standards. Let us observe that

$$0 \leqslant \lambda_i \leqslant 1, \lambda_1 = 0, \lambda_N = 1 \qquad (21)$$

It will readily be seen that the third term of P, P_{III}, does not depend on the scale of the x's, but may be expressed as a function of the range ratio and the λ_i's only:

$$\frac{\bar{x}^2}{\Sigma(x_i - \bar{x})^2} = \frac{\left(\bar{\lambda} + \dfrac{1}{R}\right)^2}{\Sigma(\lambda_i - \bar{\lambda})^2} \qquad (22)$$

hence

$$P = t \sqrt{1 + \frac{1}{N} + \frac{\left(\bar{\lambda} + \dfrac{1}{R}\right)^2}{\Sigma(\lambda_i - \bar{\lambda})^2}} \qquad (23)$$

P may thus be expressed as a function of R, for given values of N and several combinations of the λ_i's. When one may prepare the standards at will, he has, theoretically, an infinity of possible ways of distributing the λ's. In practice, however, these modes of repartition are rather limited. We have here selected four types; the first two are of very common use; the
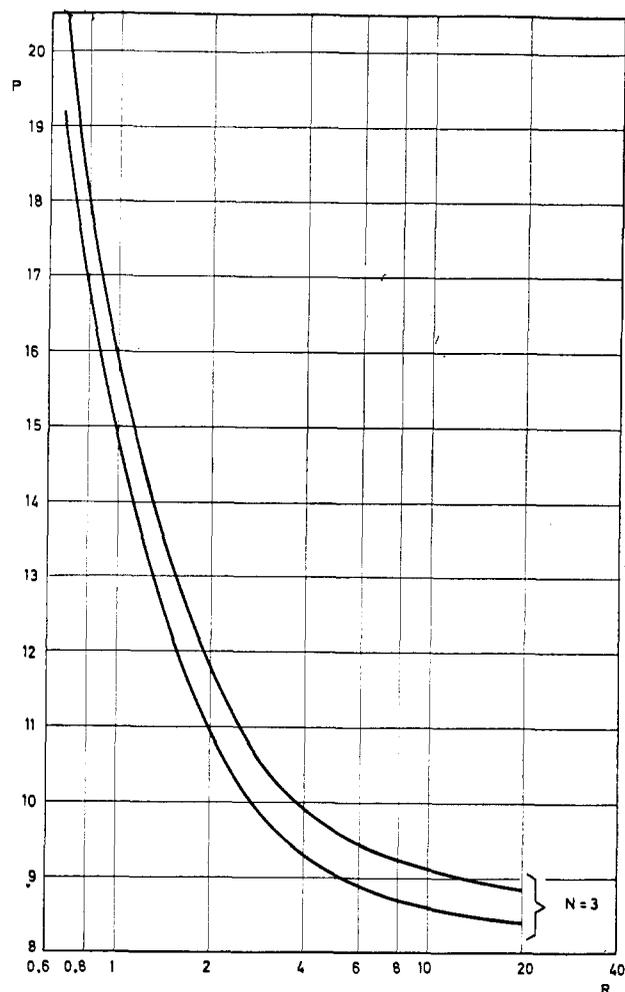
Figure 3. Influence of range (R) on the decision limit, in the case of three standards, with $\alpha = 5\%$; P is in ordinates

Upper curve, linear repartition; lower curve, parabolic repartition with $\gamma = 2$

last two have been introduced for reasons which will be clear later on.

A) the repartition may be linear—*i.e.*, the x's are equidistant (see Figure 2A);

B) the distribution may be parabolic, its general expression being

$$\lambda_i = \left(\frac{i - 1}{N - 1}\right)^\gamma \qquad (24)$$

each λ_i corresponding to one x_i by formula 1. In practice, γ is around 2 or 3. An example would be:

$$10, 12, 18, 29, 43, 61, 85, 110 \text{ ppm};$$

here $\gamma = 2$, $N = 8$, $x_1 = 10$, $x_N = 110$, $R = 10$; this distribution corresponds to line B in Figure 2;

C) a repartition of theoretical importance is one where a certain number of standards all have the smallest permissible content (*i.e.*, equal to x_1) and the others the highest permissible content x_N. This is line C of Figure 2.

D) Finally, we have also studied the disposition

K standards at x_1
1 standard at $(x_1 + x_N)/2$
$N - K - 1$ standards at x_N

This repartition is represented at Figure 2D. We will call it the "three values repartition."

308
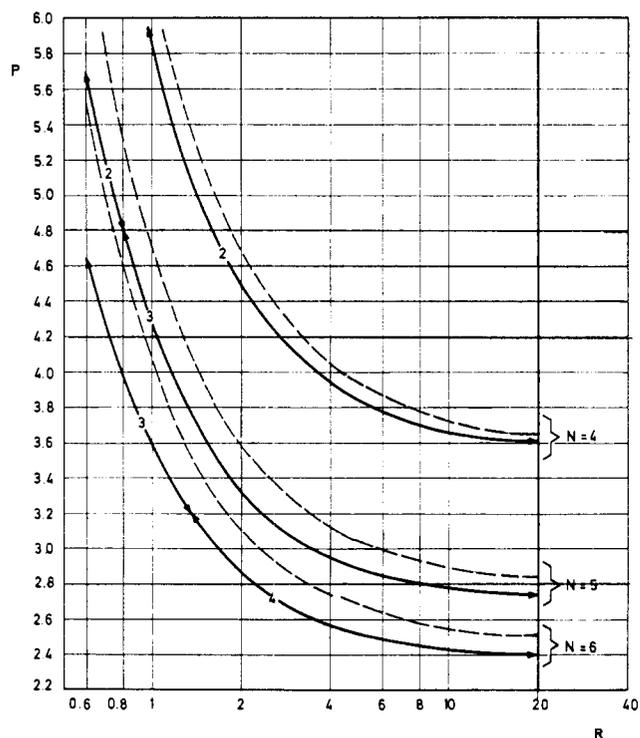
Figure 4. Influence of range R on decision limit, four to six standards, $\alpha = 5\%$. P is in ordinates. For each N, the upper curve corresponds to the parabolic repartition with $\gamma = 2$, and the lower curve to the three values repartition, with the values of K written on the curve

Figure 5. Same as Figure 4, for six to ten standards

Values of P as a function of R have been computed for these four types of repartition and for different values of N. The computations have been done with the program TABFUN (9) on the IBM 360/65 of the CETIS at Ispra (Italy). The principal results are presented in Figure 3 for $N = 3$ and in Figures 4 and 5 for $N=4$ to 10. For the three graphs, R is in abscissae and P in ordinates. In Figure 3, the upper curve corresponds to the linear repartition, and the lower curve to the parabolic repartition with $\gamma = 2$. In Figures 4 and 5, the three values repartition is represented by plain curves. The values of K which give the smallest P are written on these curves, the field of validity being limited by arrows. Thus, for $N = 10, R = 3$, it is seen on Figure 5 that K must be equal to 7. Except for R inferior to 4, an unusual occurrence, K is equal to $N - 2$. The parabolic repartition with $\gamma = 2$ is represented on the same graphs as dotted lines. For the sake of clarity, the curves corresponding to the linear repartition have not been included in graphs 4 and 5. Had they been represented, the parabolic curves would have been roughly at mid-distance between them and the three values curves.

Estimation of Q. Q_{III} contains x_D and hence, unlike P, Q may not be expressed as a function of t, R, N, and the λ's. But, on the other hand, if we could make $\bar{x}$ equal to x_D, Q_{III} would vanish. In practice, as x_D is known only after the standards are measured, it is not possible to realize a complete equality, but a fair approximation will be sufficient. It is thus to be recommended that the contents of the standards be chosen in such a way that $\bar{x}$ will fall in the neighborhood of the region where x_D will most probably be.

Contrary to x_C, which is obtained after few computations, the algebraic expression for x_D is really cumbersome [see (8),

(9) A. Hubaux and M. Lecloux, Tabulation de Fonctions, CEEA Report EUR 2987.f (1966).
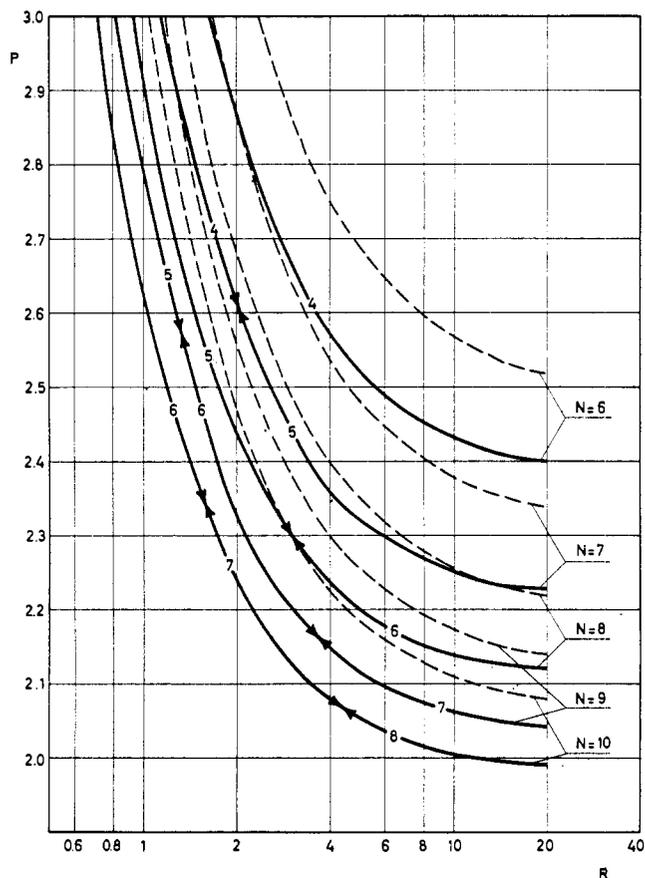
§ 11.5]. A graphical solution will be quicker: compute L_C by Equation 16, possibly using the graphs of Figures 3 to 5, compute three or four points of the lower confidence limit by Equation 15 using the minus sign, and draw the line through the points with a French curve. The intersection of this line with $y = L_C$ has x_D as its abscissa. Let us observe that

$$x_C > x_D - x_C \geqslant \left(st_{1-\beta}\sqrt{1 + \frac{1}{N}} \right)\!\Big/b \qquad (25)$$

the equality on the right being carried out when $x_D = \bar{x}$. When that condition is fulfilled,

$$Q = t_{1-\beta}\sqrt{1 + \frac{1}{N}} \qquad (26)$$

This expression may be used as an estimate of Q in analytical practice.

WAYS TO IMPROVE DECISION AND DETECTION LIMITS

Enhancing the sensitivity of an analytical method can be obtained by improving the precision of the method (s); increasing the number of standards (N); increasing the range of the contents of these standards (R); optimizing the repartition of these standards within this range (the λ_i's and $\bar{x}$); and performing replicate measurements on the unknown sample (n).

Precision. The residual standard deviation s is a good measure of the goodness of fit of the observed signals of the standards, or, in other words, of the precision of the method. It is clear from Equations 17 and 19 that there is a direct relationship between precision and sensitivity: improving the precision will lower the limits y_C and x_D.

Number of Standards. The influence of N is, of course, important, see Figures 3 to 5, especially between 3 and 6. This is due to the fact that t, $1/N$, and $\Sigma(x_i - \bar{x})^2$ all depend on N. Obviously, as results from Equation 18, the influence of N on y_D will be important also. Although the equation cannot be computed in a general way, it may be said, in first approximation, that Q will diminish in the same proportion as P, when N increases.

Range of Contents of Standards. The influence on P of the range ratio R is expressed in Equation 23 and illustrated by Figures 3 to 5. P is very sensitive to small values of the range ratio, say under 10. From 10 to 20, on the other hand, P goes down only a few percent. Above 20, the gain becomes completely negligible. This consideration may be of use in a number of cases: if the lowest possible standard is at 10 ppm, there is no gain in sensitivity by preparing standards with more than 200 ppm. On the other hand, if we have at our disposal only standards between 80 and 120 ppm ($R = 0.5$) we should expect a really poor sensitivity, unless s is very small, that is unless all the observed signals fall neatly on the regression line. Let us note that, when a "blank" is available, x_1 will be very small (it will never be exactly equal to zero) and the range ratio will take a very high value. For all practical purposes, the right extremity of the graphs ($R = 20$) may be used in this case.

The influence of R on Q is not so readily computed. It may be said however, that this influence will be small as long as $\bar{x}$ remains in the neighborhood of x_D, and nil when the two coincide.

Modes of Repartition of Standards. Very often, N is fixed by economical considerations, various conditions determine the value of x_1 and x_N, and s is made as small as practically possible by a careful preparation of the standards and a good checking of the measurements. When N, R, and s are fixed, however, one still has the liberty to distribute the λ_i's in the manner best suited for his purposes. Generally, two aims are pursued: first, to check the linearity of the content/signal relation, and second, to lower the sensitivity limit as much as possible. There is no strategy which optimizes both aims: to obtain a maximum of information on the linearity, the x's should be as far as possible from each other, or, in other words, they should be equidistant (see Figure 2A). On the other hand, the best disposition which we have found after some computations to enhance the sensitivity is to have a certain number of standards with the smallest admissible content (i.e., equal to x_1) and the other standards with the maximum permissible content x_N (see Figure 2C). When the range ratio is greater than 4 or 5, there should be $N - 1$ standards equal to x_1, and only one equal to x_N. The diminution of P, by adopting the second scheme instead of the first, may be as high as 30% when the range ratio is small and remains of the order of 10 to 15% when this ratio tends to infinity. But unfortunately, this disposition is impossible to adopt in practice because there would not be any control on linearity and because any error on the standard at x_N would be impossible to assess.

As an alternative, we have studied what appears to be the best substitute, the three values distribution, as illustrated at Figure 2D, where there is a check on linearity and on the absence of gross errors. The values of P obtained from Equation 23 with this disposition are plotted as plain curves on Figures 4 and 5. As a comparison, the values of P corresponding to the parabolic distribution with $\gamma = 2$ are given as dotted curves. Computations have shown that this parabolic distribution yields a lower P than the equidistant distribution

(2.25 instead of 2.42 with $N = 8$, $R = 10$). But on the other hand, this P is still notably higher than the corresponding P of the three values disposition: 2.13. With the parabolic repartition, this value of 2.13 is not even reached by the use of 9 standards ($P = 2.17$). Thus, with the three values disposition, we may gain the effect on sensitivity of more than one standard. When the range ratio is smaller and N bigger, the gain is still more important: 8 standards with the three values disposition will give a sensitivity as good (for $R = 3$ or less) as 10 standards distributed parabolically: a gain of two standards!

With the three values repartition, $\bar{x}$ is low and, hence, more likely to fall near x_D, thus contributing also to reduce Q. More specifically, it may be shown that, if we take the three values mode with $K = N - 2$, the third term of Q is equal to

$$Q_{III} = \frac{\left(\lambda_D - \dfrac{1.5}{N}\right)^2}{1.25 - \dfrac{2.25}{N}} \tag{27}$$

(the developments are straightforward and too long to be given here). From this equation it will be clear that if λ_D is not too far from $1.5/N$, Q_{III} will be conspicuously smaller than unity; hence, the exact coincidence of $\bar{x}$ and x_D is not required.

Replication on the Unknown. By making n replicates on the unknown sample, the residual variance is divided by n and P must be replaced by P_n, with

$$P_n = t\sqrt{\frac{1}{n} + \frac{1}{N} + \frac{\bar{x}^2}{\Sigma(x_i - \bar{x})^2}} \tag{28}$$

It should be emphasized that this equation applies to replicates which may really be considered as "independent" from each other. It is readily seen that

$$P_n{}^2 = P^2 - \left(1 - \frac{1}{n}\right)t^2 \tag{29}$$

and hence that replication may conspicuously improve the sensitivity. Let us also remark that the influence of replications will have somewhat more effect when P diminishes. For instance, with $N = 4$ and $\alpha = 5\%$, t is 2.92; if P is equal to 3.7, four replications ($n = 4$) will yield $P_4 = 2.7$, a gain of 27%. With $N = 10$, $t_{95\%} = 1.86$; if $P = 2.0$, $n = 4$ will yield $P_{10} = 1.19$, a gain of 40%.

Likewise, Q must be replaced by Q_n, and in symmetry with Equation 29, we have

$$Q_n{}^2 = Q^2 - \left(1 - \frac{1}{n}\right)t^2 \tag{30}$$

Hence, the effect of replication on y_D will be about the same as the effect on y_C.

A further advantage of replication is that it will yield estimates of the residual variance. It will then be possible to test whether this variance remains constant, as supposed in the present developments; if it does, a better estimate of this variance may be obtained and thus a t with more degrees of freedom may be used, and this smaller t will also contribute to diminish y_C and x_D.

CONCLUSIONS

The definition of the decision and detection limits is here attached to the concept of confidence limits. This presents the advantage that the influence of the standards on the sensi-

tivity may be quantitatively estimated. The most important conclusions are:

A direct relationship exists between the precision of the method and its sensitivity.

There is, as expected, an important gain in sensitivity when increasing the number of standards from 3 to 6. Above 10 standards, the gain is of the order of 2 to 1 % on P and Q for one additional standard.

The range ratio should be higher than 10, a condition which is easily met in most cases. But there is no need that it be higher than 20.

When blanks may be added to the series of standards, Figures 3 to 5 may also be used, the results for $R = \infty$ being practically equal to those of $R = 20$.

Where it is important to have a limit of detection as low as possible, it may be of advantage to distribute the standards into three groups of contents only: K standards with the lowest possible content, $N - K - 1$ standards with the highest possible content and one at midway between. The value of K may be read on Figures 4 and 5, where it is seen that when R is greater than 4, $K = N - 2$. This distribution in three values will allow a gain which may be of one or even two standards, when used instead of the more common equidistant or parabolic distributions.

The mean content of the standards, $\bar{x}$, should fall in the neighborhood of the presupposed value of x_D, a requirement which will be easier to meet with the three values repartition.

Replicate measurements on the unknown samples conspicuously improve the decision and detection limits; this improvement may be computed by Equations 29 and 30.

ILLUSTRATIONS

Case 1. In order to be accepted, an organic material should have a chlorine content inferior to 3.5 ppm. The material is to be analyzed by X-ray fluorescence and the lowest possible content for reliable standards (x_1) is 1 ppm Cl. As has been shown, the range of the standards, R, should be around 20, hence $x_N = 21$ ppm. α and β are both chosen as 5%. Six standards are prepared and measured, with contents distributed in the three-values mode, yielding as equation of the regression line $y = 2286 + 54.4 \, x$ (x in ppm, y in counts, for a counting time of 100 seconds) with a standard deviation of 40.0 counts. From Figure 5, $P = 2.39$, hence $y_C = 2382$ and $x_C = 1.77$ ppm. Graphical estimate of x_D yields 3.2 ppm. This value is too high, but duplicates on the unknown will give $P_2 = 1.89$, $Q_2 = 2.08$, and hence $x_D = 2.51$ ppm.

Case 2. Only three standards of a particular impurity in an alloy are available. The contents are 89, 91, and 144 ppm. Hence $\bar{x} = 108$ and $R = 0.62$, a low value indeed! Careful analysis of the three standards gives a regression line with equation: $y = 64690 + 45.2 \, x$ counts (100 sec counting time) and residual standard deviation of 400 counts. $t_{95\%}$ for 1 degree of freedom $= 6.314$. Hence $P = 17.1$ by Equation 8, from which $x_C = 151$ ppm! It may only be concluded that this poor series of standards is really inappropriate. The addition of one standard at 400 ppm (supposing linearity remains) would yield $R = 3.5$, hence $P = 4.0$ and $x_C = 35$ ppm. The decision limit may be lowered by adding to the series a standard with a higher content.

Computer Evaluation of Continuously Scanned Mass Spectra of Gas Chromatographic Effluents

Ronald A. Hites[1] and K. Biemann

Department of Chemistry, Massachusetts Institute of Technology, Cambridge, Mass. 02139

Efficient utilization of the vast amount of data produced by a continuously scanning mass spectrometer coupled to a gas chromatograph required the development of novel data processing techniques. One of the most useful is the display of the change in abundance of certain ions during the gas chromatogram (called "mass chromatogram"). This technique permits detection of the presence or absence of homologous series of compounds as well as specific substances of known or predictable mass spectra. The selection of the m/e values to be plotted can be based on a knowledge of the chemical system under investigation or can be supported by an evaluation of the data itself. Applications of these approaches to geochemical and biomedical problems are discussed.

THE DESIRABILITY of obtaining mass spectral information on practically all components of a complex mixture led to the design of a gas chromatograph–mass spectrometer system which uses a computer to continuously and automatically record mass spectra of the gas chromatographic effluent (1).

[1] NIH predoctoral fellow 1966–68.

(1) R. A. Hites and K. Biemann, ANAL. CHEM., 40, 1217 (1968).

The need to efficiently utilize the resulting data at a speed comparable to that at which they are acquired made it necessary to develop entirely new approaches to this problem. One approach was the computerized searching of reference mass spectra files (2–4). These techniques relieve the chemist from a great deal of routine work but, because of the limited number of spectra in the reference file (ca. 7500 are now available), search results sometimes do not indicate a definite compound. Frequently, the suggestions of such a library search, even though not conclusive, aid in the manual identification of the spectra (2–4). In the course of using these library search techniques for an extended time, several other approaches were developed for certain problems presented by

(2) R. A. Hites and K. Biemann in "Advances in Mass Spectrometry," Vol. 4, E. Kendrick, Ed., The Institute of Petroleum, London, 1968, p 37; presented at the International Mass Spectrometry Conference, Berlin, September 1967.
(3) R. A. Hites, Ph.D. Thesis, Massachusetts Institute of Technology, Cambridge, Mass., 1968.
(4) R. A. Hites, H. S. Hertz, and K. Biemann, Massachusetts Institute of Technology, Cambridge, Mass., unpublished work, 1969.

311

This page is intentionally left blank.

APPENDIX B-2: DYE CONCENTRATIONS: LABORATORY RESULTS

APPENDIX FOR SECTION 3:

FLUORESCENT DYE GROUNDWATER TRACER STUDY

This page is intentionally left blank.

Table B-2.1. Fluorescein Concentrations Measured at the North Seep Group

DATE	No. of Samples	Fluorescein - As Measured (ppb)				Fluorescein -Corrected for Salinity (ppb)*			
		Minimum	Average	Maximum	Std. Dev.	Minimum	Average	Maximum	Std. Dev.
7/5/11	2	0.10	0.11	0.11	0.01	0.10	0.11	0.11	0.01
7/10/11	1	0.10	0.10	0.10		0.10	0.10	0.10	
7/11/11	1	0.09	0.09	0.09		0.09	0.09	0.09	
7/13/11	1	0.10	0.10	0.10		0.10	0.10	0.10	
7/17/11	2	0.08	0.09	0.09	0.01	0.08	0.09	0.09	0.01
7/20/11	1	0.11	0.11	0.11		0.11	0.11	0.11	
7/21/11	1	0.11	0.11	0.11		0.11	0.11	0.11	
7/25/11	1	0.11	0.11	0.11		0.11	0.11	0.11	
7/28/11	2	0.11	0.11	0.11	0.00	0.11	0.11	0.11	0.00
7/29/11	1	0.11	0.11	0.11		0.11	0.11	0.11	
8/1/11	1	0.13	0.13	0.13		0.13	0.13	0.13	
8/2/11	1	0.12	0.12	0.12		0.12	0.12	0.12	
8/3/11	1	0.12	0.12	0.12		0.12	0.12	0.12	
8/9/11	1	0.11	0.11	0.11		0.11	0.11	0.11	
8/11/11	2	0.11	0.11	0.12	0.00	0.11	0.11	0.12	0.00
8/17/11	1	0.11	0.11	0.11		0.11	0.11	0.11	
8/19/11	1	0.09	0.09	0.09		0.09	0.09	0.09	
8/22/11	2	0.11	0.11	0.12	0.01	0.11	0.11	0.12	0.01
8/26/11	1	0.11	0.11	0.11		0.11	0.11	0.11	
8/27/11	1	0.11	0.11	0.11		0.11	0.11	0.11	

*Fluorescein concentration corrected for salinity at Seep 9

Table B-2.1. Fluorescein Concentrations Measured at the North Seep Group (Continued)

		Fluorescein - As Measured (ppb)				Fluorescein -Corrected for Salinity (ppb)			
DATE	No. of Samples	Minimum	Average	Maximum	Std. Dev.	Minimum	Average	Maximum	Std. Dev.
7/5/11	2	0.10	0.11	0.11	0.01	0.10	0.11	0.11	0.01
7/10/11	1	0.10	0.10	0.10		0.10	0.10	0.10	
7/11/11	1	0.09	0.09	0.09		0.09	0.09	0.09	
7/13/11	1	0.10	0.10	0.10		0.10	0.10	0.10	
7/17/11	2	0.08	0.09	0.09	0.01	0.08	0.09	0.09	0.01
7/20/11	1	0.11	0.11	0.11		0.11	0.11	0.11	
7/21/11	1	0.11	0.11	0.11		0.11	0.11	0.11	
7/25/11	1	0.11	0.11	0.11		0.11	0.11	0.11	
7/28/11	2	0.11	0.11	0.11	0.00	0.11	0.11	0.11	0.00
7/29/11	1	0.11	0.11	0.11		0.11	0.11	0.11	
8/1/11	1	0.13	0.13	0.13		0.13	0.13	0.13	
8/2/11	1	0.12	0.12	0.12		0.12	0.12	0.12	
8/3/11	1	0.12	0.12	0.12		0.12	0.12	0.12	
8/9/11	1	0.11	0.11	0.11		0.11	0.11	0.11	
8/11/11	2	0.11	0.11	0.12	0.00	0.11	0.11	0.12	0.00
8/17/11	1	0.11	0.11	0.11		0.11	0.11	0.11	
8/19/11	1	0.09	0.09	0.09		0.09	0.09	0.09	
8/22/11	2	0.11	0.11	0.12	0.01	0.11	0.11	0.12	0.01
8/26/11	1	0.11	0.11	0.11		0.11	0.11	0.11	
8/27/11	1	0.11	0.11	0.11		0.11	0.11	0.11	
8/30/11	1	0.11	0.11	0.11		0.11	0.11	0.11	
9/1/11	1	0.11	0.11	0.11		0.11	0.11	0.11	

*Fluorescein concentration corrected for salinity at Seep 9

Table B-2.1. Fluorescein Concentrations Measured at the North Seep Group (Continued)

| DATE | No. of Samples | Fluorescein - As Measured (ppb) | | | | Fluorescein -Corrected for Salinity (ppb) | | | |
		Minimum	Average	Maximum	Std. Dev.	Minimum	Average	Maximum	Std. Dev.
9/2/11	1	0.11	0.11	0.11		0.11	0.11	0.11	
9/3/11	1	0.11	0.11	0.11		0.11	0.11	0.11	
9/10/11	2	0.11	0.11	0.11	0.00	0.11	0.11	0.11	0.00
9/13/11	1	0.11	0.11	0.11		0.11	0.11	0.11	
9/14/11	2	0.11	0.11	0.11	0.00	0.11	0.11	0.11	0.00
9/16/11	1	0.11	0.11	0.11		0.11	0.11	0.11	
9/20/11	1	0.10	0.10	0.10		0.10	0.10	0.10	
9/21/11	2	0.11	0.11	0.11	0.00	0.11	0.11	0.11	0.00
9/23/11	1	0.11	0.11	0.11		0.11	0.11	0.11	
9/26/11	1	0.10	0.10	0.10		0.10	0.10	0.10	
9/27/11	1	0.11	0.11	0.11		0.11	0.11	0.11	
10/3/11	1	0.11	0.11	0.11		0.11	0.11	0.11	
10/6/11	1	0.11	0.11	0.11		0.11	0.11	0.11	
10/8/11	1	0.10	0.10	0.10		0.10	0.10	0.10	
10/14/11	3	0.10	0.11	0.11	0.01	0.10	0.11	0.11	0.01
10/16/11	1	0.11	0.11	0.11		0.11	0.11	0.11	
10/18/11	3	0.11	0.11	0.12	0.00	0.11	0.11	0.12	0.00
10/20/11	3	0.13	0.13	0.13	0.00	0.13	0.13	0.13	0.00
10/22/11	3	0.13	0.14	0.14	0.00	0.13	0.14	0.14	0.00
10/24/11	3	0.15	0.15	0.16	0.00	0.15	0.15	0.16	0.00
10/26/11	2	0.17	0.17	0.17	0.00	0.17	0.17	0.17	0.00
10/28/11	3	0.19	0.20	0.21	0.01	0.19	0.20	0.21	0.01

*Fluorescein concentration corrected for salinity at Seep 9

Table B-2.1. Fluorescein Concentrations Measured at the North Seep Group (Continued)

DATE	No. of Samples	Fluorescein - As Measured (ppb)				Fluorescein -Corrected for Salinity (ppb)			
		Minimum	Average	Maximum	Std. Dev.	Minimum	Average	Maximum	Std. Dev.
11/1/11	1	0.24	0.24	0.24		0.24	0.24	0.24	
11/3/11	2	0.29	0.29	0.30	0.01	0.29	0.29	0.30	0.01
11/5/11	2	0.35	0.35	0.35	0.00	0.35	0.35	0.35	0.00
11/7/11	2	0.40	0.41	0.42	0.01	0.40	0.41	0.42	0.01
11/9/11	3	0.48	0.50	0.53	0.03	0.48	0.50	0.53	0.03
11/11/11	1	0.58	0.58	0.58		0.58	0.58	0.58	
11/16/11	1	0.89	0.89	0.89		0.89	0.89	0.89	
11/18/11	1	0.94	0.94	0.94		0.94	0.94	0.94	
11/21/11	1	1.18	1.18	1.18		1.18	1.18	1.18	
11/23/11	3	1.37	1.47	1.60	0.12	1.37	1.47	1.60	0.12
11/25/11	1	1.54	1.54	1.54		1.54	1.54	1.54	
11/28/11	2	1.65	1.71	1.77	0.09	1.65	1.71	1.77	0.09
11/30/11	3	2.17	2.32	2.53	0.19	2.14	2.31	2.53	0.20
12/2/11	3	2.39	2.51	2.74	0.20	2.39	2.50	2.74	0.20
12/7/11	3	2.78	2.99	3.12	0.19	2.78	2.98	3.12	0.18
12/9/11	3	3.54	3.72	3.91	0.19	3.48	3.70	3.91	0.22
12/14/11	2	4.82	4.84	4.85	0.02	4.76	4.80	4.85	0.07
12/16/11	1	5.32	5.32	5.32		5.32	5.32	5.32	
12/21/11	1	5.98	5.98	5.98		5.90	5.90	5.90	
12/23/11	2	6.82	6.97	7.13	0.22	6.82	6.97	7.13	0.22
12/28/11	3	7.80	8.00	8.39	0.34	7.75	7.98	8.39	0.36
1/2/12	1	5.25	5.25	5.25		7.66	7.66	7.66	

*Fluorescein concentration corrected for salinity at Seep 9

Table B-2.1. Fluorescein Concentrations Measured at the North Seep Group (Continued)

DATE	No. of Samples	Fluorescein - As Measured (ppb)				Fluorescein -Corrected for Salinity (ppb)			
		Minimum	Average	Maximum	Std. Dev.	Minimum	Average	Maximum	Std. Dev.
1/4/12	3	8.68	9.44	10.40	0.88	8.91	9.52	10.40	0.78
1/7/12	3	9.00	10.14	11.35	1.18	10.08	10.53	11.35	0.71
1/9/12	3	10.59	10.99	11.80	0.70	10.52	10.97	11.80	0.72
1/11/12	3	11.00	11.77	12.82	0.94	11.00	11.77	12.82	0.94
1/13/12	3	6.95	10.56	12.92	3.17	11.69	12.14	12.92	0.68
1/16/12	3	6.99	10.91	13.63	3.48	12.11	12.75	13.63	0.79
1/19/12	2	11.71	12.11	12.51	0.57	12.06	12.29	12.51	0.32
1/21/12	3	8.31	11.22	13.31	2.60	12.02	12.67	13.31	0.91
1/23/12	3	4.56	10.56	13.92	5.21	13.21	13.84	14.38	0.59
1/25/12	3	13.94	14.37	14.66	0.38	13.94	14.37	14.66	0.38
1/27/12	3	12.81	13.62	14.22	0.72	12.81	13.62	14.22	0.72
1/31/12	3	15.02	15.69	16.13	0.59	15.02	15.69	16.13	0.59
2/10/12	3	16.14	16.45	16.76	0.31	16.14	16.45	16.76	0.31
2/14/12	3	17.78	18.09	18.40	0.31	17.78	18.09	18.40	0.31
2/17/12	3	18.60	18.94	19.22	0.31	18.60	18.94	19.22	0.31
2/20/12	3	19.63	19.76	19.93	0.16	19.63	19.76	19.93	0.16
2/24/12	3	19.65	19.96	20.47	0.45	19.65	19.96	20.47	0.45
2/26/12	1	20.57	20.57	20.57		20.57	20.57	20.57	
2/27/12	2	18.63	19.81	20.98	1.66	18.63	19.81	20.98	1.66
3/1/12	3	20.27	20.82	21.50	0.62	20.27	20.82	21.50	0.62
3/14/12	2	20.68	20.79	20.89	0.14	20.68	20.79	20.89	0.14
3/17/12	3	20.41	20.68	21.01	0.31	20.41	20.68	21.01	0.31

*Fluorescein concentration corrected for salinity at Seep 9

Table B-2.1. Fluorescein Concentrations Measured at the North Seep Group (Continued)

DATE	No. of Samples	Fluorescein - As Measured (ppb)				Fluorescein -Corrected for Salinity (ppb)			
		Minimum	Average	Maximum	Std. Dev.	Minimum	Average	Maximum	Std. Dev.
3/19/12	3	21.51	21.61	21.81	0.17	21.51	21.61	21.81	0.17
3/27/12	1	20.21	20.21	20.21		20.48	20.48	20.48	
3/29/12	1	20.61	20.61	20.61		20.48	20.48	20.48	
4/2/12	1	17.40	17.40	17.40		20.72	20.72	20.72	
4/5/12	1	18.03	18.03	18.03		21.46	21.46	21.46	
4/12/12	1	21.30	21.30	21.30		21.16	21.16	21.16	
4/16/12	1	21.81	21.81	21.81		21.67	21.67	21.67	
4/19/12	1	21.09	21.09	21.09		21.02	21.02	21.02	
4/24/12	2	20.17	20.17	20.17	0.00	20.11	20.14	20.17	0.05
4/26/12	2	20.38	20.79	21.19	0.58	20.24	20.72	21.19	0.67
5/2/12	2	21.40	21.45	21.50	0.07	21.33	21.41	21.50	0.12

*Fluorescein concentration corrected for salinity at Seep 9

Table B-2.2. Fluorescein Concentrations Measured at the South Seep Group

DATE	No. of Samples	Fluorescein - As Measured (ppb)				Fluorescein -Corrected for Salinity (ppb)*			
		Minimum	Average	Maximum	Std. Dev.	Minimum	Average	Maximum	Std. Dev.
7/9/11	1	0.10	0.10	0.10		0.10	0.10	0.10	
7/23/11	1	0.12	0.12	0.12		0.12	0.12	0.12	
7/25/11	1	0.11	0.11	0.11		0.11	0.11	0.11	
7/28/11	1	0.13	0.13	0.13		0.13	0.13	0.13	
8/2/11	1	0.12	0.12	0.12		0.12	0.12	0.12	
8/6/11	1	0.14	0.14	0.14		0.14	0.14	0.14	
8/9/11	1	0.12	0.12	0.12		0.12	0.12	0.12	
8/18/11	1	0.11	0.11	0.11		0.11	0.11	0.11	
8/24/11	1	0.12	0.12	0.12		0.12	0.12	0.12	
8/28/11	1	0.01	0.01	0.01		0.01	0.01	0.01	
9/2/11	1	0.12	0.12	0.12		0.12	0.12	0.12	
9/6/11	1	0.12	0.12	0.12		0.11	0.11	0.11	
9/10/11	1	0.07	0.07	0.07		0.07	0.07	0.07	
9/14/11	2	0.11	0.11	0.11	0.00	0.10	0.11	0.11	0.00
9/18/11	1	0.11	0.11	0.11		0.11	0.11	0.11	
9/19/11	2	0.09	0.10	0.10	0.01	0.09	0.10	0.11	0.01
9/20/11	1	0.11	0.11	0.11		0.12	0.12	0.12	
9/22/11	1	0.12	0.12	0.12		0.12	0.12	0.12	
9/28/11	2	0.12	0.12	0.12	0.00	0.12	0.12	0.12	0.00
10/1/11	2	0.11	0.11	0.11	0.00	0.11	0.11	0.11	0.00

Fluorescein concentrations corrected for salinity at Seep 4 and Seep 5

Table B2-2. Fluorescein Concentrations Measured at the South Seep Group (Continued)

DATE	No. of Samples	Fluorescein - As Measured (ppb)				Fluorescein -Corrected for Salinity (ppb)			
		Minimum	Average	Maximum	Std. Dev.	Minimum	Average	Maximum	Std. Dev.
10/2/11	1	0.11	0.11	0.11		0.11	0.11	0.11	
10/8/11	2	0.12	0.12	0.12	0.00	0.12	0.12	0.12	0.00
10/10/11	1	0.11	0.11	0.11		0.11	0.11	0.11	
10/14/11	2	0.11	0.11	0.12	0.00	0.11	0.11	0.11	0.00
10/18/11	2	0.11	0.11	0.11	0.00	0.11	0.11	0.11	0.00
10/22/11	2	0.11	0.12	0.12	0.00	0.11	0.11	0.12	0.01
10/28/11	3	0.11	0.12	0.12	0.00	0.11	0.12	0.12	0.00
11/1/11	1	0.12	0.12	0.12		0.12	0.12	0.12	
11/5/11	3	0.12	0.12	0.13	0.00	0.12	0.12	0.13	0.01
11/7/11	3	0.12	0.13	0.13	0.01	0.12	0.13	0.13	0.01
11/9/11	3	0.12	0.13	0.13	0.01	0.12	0.13	0.13	0.01
11/11/11	2	0.13	0.13	0.13	0.01	0.13	0.13	0.13	0.01
11/14/11	3	0.14	0.15	0.15	0.01	0.14	0.14	0.15	0.01
11/18/11	2	0.17	0.18	0.19	0.01	0.17	0.18	0.19	0.01
11/21/11	2	0.19	0.20	0.21	0.02	0.19	0.20	0.21	0.02
11/23/11	2	0.22	0.23	0.25	0.03	0.21	0.23	0.25	0.03
11/25/11	2	0.25	0.28	0.30	0.03	0.25	0.28	0.30	0.03
11/28/11	3	0.29	0.31	0.37	0.04	0.27	0.31	0.37	0.05
11/30/11	3	0.33	0.37	0.44	0.06	0.33	0.37	0.44	0.06
12/2/11	2	0.38	0.40	0.42	0.03	0.38	0.39	0.40	0.01
12/7/11	3	0.58	0.64	0.76	0.10	0.57	0.64	0.76	0.10
12/9/11	1	0.70	0.70	0.70		0.70	0.70	0.70	
12/14/11	2	1.00	1.17	1.34	0.24	1.00	1.17	1.34	0.24

Fluorescein concentrations corrected for salinity at Seep 4 and Seep 5

Table B2-2. Fluorescein Concentrations Measured at the South Seep Group (Continued)

DATE	No. of Samples	Fluorescein - As Measured (ppb)				Fluorescein -Corrected for Salinity (ppb)			
		Minimum	Average	Maximum	Std. Dev.	Minimum	Average	Maximum	Std. Dev.
12/19/11	2	1.41	1.47	1.53	0.09	1.40	1.46	1.53	0.10
12/21/11	1	1.66	1.66	1.66		1.67	1.67	1.67	
12/26/11	2	2.03	2.33	2.63	0.43	2.05	2.34	2.63	0.41
12/28/11	1	2.71	2.71	2.71		2.76	2.76	2.76	
12/30/11	1	3.55	3.55	3.55		3.55	3.55	3.55	
1/2/12	2	2.11	2.86	3.62	1.07	3.32	3.47	3.62	0.21
1/7/12	3	3.33	4.66	5.87	1.27	4.78	5.37	5.87	0.55
1/9/12	3	2.29	4.61	6.34	2.09	4.22	5.27	6.34	1.06
1/11/12	3	2.47	5.22	7.16	2.45	5.73	6.31	7.16	0.76
1/13/12	2	3.32	5.06	6.80	2.46	6.09	6.45	6.82	0.52
1/16/12	3	3.51	6.49	8.48	2.63	6.75	7.57	8.48	0.87
1/19/12	3	6.19	7.75	9.13	1.48	7.70	8.25	9.13	0.77
1/21/12	4	6.14	8.44	10.30	1.72	8.50	9.05	10.30	0.84
1/23/12	4	4.62	8.61	10.80	2.73	9.24	9.76	10.80	0.72
1/25/12	4	5.09	9.20	11.41	2.80	8.80	10.13	11.41	1.07
1/27/12	3	6.20	8.17	11.30	2.74	6.20	9.34	11.30	2.75
1/31/12	3	5.68	10.47	13.92	4.28	10.29	12.01	13.92	1.82
2/10/12	3	12.66	14.26	17.37	2.69	13.78	15.06	17.37	2.00
2/14/12	4	13.17	15.63	19.52	3.00	14.83	16.41	19.52	2.21
2/17/12	4	13.99	16.17	19.63	2.59	16.08	17.38	19.63	1.56
2/20/12	4	10.81	15.53	19.73	4.23	13.66	16.98	19.73	2.67
2/24/12	4	8.27	16.07	20.57	5.56	17.82	18.99	20.57	1.27
2/27/12	4	7.65	16.93	22.92	6.64	18.22	20.20	22.92	1.99

Fluorescein concentrations corrected for salinity at Seep 4 and Seep 5

Table B2-2. Fluorescein Concentrations Measured at the South Seep Group (Continued)

DATE	No. of Samples	Fluorescein - As Measured (ppb)				Fluorescein -Corrected for Salinity (ppb)			
		Minimum	Average	Maximum	Std. Dev.	Minimum	Average	Maximum	Std. Dev.
3/1/12	4	16.08	19.87	24.98	4.02	17.93	20.98	24.98	2.97
3/11/12	4	18.63	22.97	27.21	3.55	22.18	24.17	27.21	2.14
3/14/12	4	18.33	23.80	29.37	4.70	23.21	25.62	29.37	2.66
3/17/12	4	14.59	23.04	29.94	6.50	24.24	26.41	29.94	2.46
3/19/12	4	9.98	21.69	30.24	8.88	25.46	27.04	30.24	2.18
3/22/12	4	12.89	21.64	30.04	7.88	25.07	26.99	30.04	2.14
3/27/12	4	14.09	23.67	31.65	7.50	25.39	27.84	31.65	2.68
3/29/12	4	13.19	23.77	32.35	8.32	23.90	28.30	32.35	3.48
3/31/12	3	14.19	25.19	32.55	9.71	25.57	28.99	32.55	3.49
4/2/12	4	10.88	23.27	32.55	9.50	26.29	29.00	32.55	2.60
4/5/12	4	15.06	25.43	31.51	7.40	27.15	29.81	31.51	1.90
4/12/12	4	18.13	26.99	34.27	6.85	27.67	30.38	34.27	2.78
4/16/12	3	15.17	25.96	32.02	9.37	27.03	29.92	32.02	2.59
4/19/12	2	28.35	30.80	33.25	3.47	28.35	30.80	33.25	3.47
4/24/12	3	23.65	29.57	34.07	5.36	31.00	32.04	34.07	1.75
4/26/12	3	26.30	29.84	33.25	3.48	29.98	31.32	33.25	1.71
5/2/12	3	24.36	29.33	33.25	4.54	30.39	31.57	33.25	1.50

Fluorescein concentrations corrected for salinity at Seep 4 and Seep 5

Table B-2.3. Sulpho-Rhodamine-B Range Fluorescence

| | North Seep Group (ppb) | | | | | South Seep Group (ppb) | | | | |
DATE	No. of Samples	Minimum	Average	Maximum	Std. Dev.	No. of Samples	Minimum	Average	Maximum	Std. Dev.
7/5/11	2	0.03	0.04	0.04	0.008	2	0.03	0.04	0.05	0.011
7/6/11	2	0.02	0.02	0.02	0.004	3	0.03	0.04	0.05	0.009
7/7/11	2	0.02	0.03	0.03	0.001	3	0.04	0.05	0.05	0.004
7/8/11	1	0.03	0.03	0.03		3	0.04	0.04	0.05	0.005
7/9/11	2	0.03	0.04	0.04	0.002	2	0.04	0.04	0.05	0.010
7/10/11	2	0.04	0.06	0.06	0.002	3	0.02	0.24	0.61	0.324
7/11/11	2	0.03	0.04	0.04	0.010	3	0.04	0.07	0.11	0.036
7/12/11	2	0.03	0.04	0.05	0.006	2	0.02	0.06	0.10	0.056
7/13/11	2	0.04	0.04	0.04	0.006	3	0.05	0.05	0.05	0.003
7/14/11	2	0.02	0.05	0.07	0.037	3	0.04	0.05	0.05	0.002
7/15/11	2	0.02	0.03	0.04	0.003	2	0.03	0.04	0.04	0.013
7/16/11	2	0.03	0.04	0.04	0.011	3	0.02	0.03	0.04	0.010
7/17/11	2	0.03	0.03	0.03	0.003	2	0.05	0.06	0.07	0.013
7/18/11	1	0.03	0.15	0.15		3	0.02	0.05	0.11	0.051
7/19/11	2	0.02	0.04	0.05	0.025	2	0.01	0.02	0.03	0.011
7/20/11	2	0.00	0.01	0.03	0.015	1	0.03	0.03	0.03	
7/21/11	2	0.00	0.01	0.02	0.006					
7/22/11	1	0.01	0.01	0.01						
7/23/11	1	0.01	0.01	0.01		2	0.03	0.03	0.04	0.004
7/24/11						3	0.03	0.03	0.03	0.003
7/25/11	3	0.01	0.01	0.02	0.004	1	0.51	0.51	0.51	
7/26/11	1	0.00	0.00	0.00		1	0.01	0.01	0.01	
7/27/11	2	0.00	0.03	0.04	0.023	1	0.03	0.03	0.03	
7/28/11	3	0.01	0.02	0.03	0.011	2	0.02	0.03	0.03	0.008

Table B-2.3. Sulpho-Rhodamine-B Range Fluorescence (Continued)

| | North Seep Group (ppb) | | | | | South Seep Group (ppb) | | | |
DATE	No. of Samples	Minimum	Average	Maximum	Std. Dev.	No. of Samples	Minimum	Average	Maximum	Std. Dev.
7/29/11	3	0.01	0.02	0.03	0.002	3	0.02	0.03	0.04	0.009
7/30/11	3	0.02	0.02	0.03	0.010	3	0.04	0.04	0.05	0.005
7/31/11	3	0.01	0.02	0.03	0.010	3	0.02	0.10	0.25	0.126
8/1/11	3	0.01	0.03	0.05	0.021	2	0.02	0.04	0.05	0.019
8/2/11	3	0.01	0.03	0.04	0.006	3	0.03	0.03	0.04	0.006
8/3/11	3	0.02	0.02	0.03	0.004	1	0.03	0.03	0.03	
8/4/11	3	0.02	0.03	0.05	0.015	3	0.03	0.07	0.16	0.071
8/5/11	3	0.01	0.03	0.04	0.017	2	0.03	0.04	0.05	0.011
8/6/11	2	0.01	0.02	0.02	0.005	2	0.04	0.05	0.05	0.004
8/7/11	2	0.02	0.03	0.05	0.021	2	0.03	0.03	0.04	0.008
8/8/11	3	0.01	0.02	0.04	0.012	3	0.02	0.04	0.05	0.011
8/9/11	3	0.01	0.03	0.04	0.010	3	0.04	0.04	0.04	0.002
8/10/11	3	0.02	0.08	0.18	0.084	3	0.03	0.04	0.04	0.008
8/11/11	3	0.01	0.02	0.02	0.004	1	0.02	0.02	0.02	
8/12/11	2	0.01	0.02	0.03	0.005	2	0.01	0.06	0.11	0.069
8/13/11	2	0.01	0.01	0.01	0.001					
8/14/11	3	0.01	0.02	0.03	0.004	3	0.01	0.02	0.03	0.008
8/15/11	3	0.02	0.02	0.03	0.004	1	0.03	0.03	0.03	
8/16/11	2	0.02	0.02	0.03	0.006	1	0.01	0.01	0.01	
8/17/11	2	0.02	0.03	0.03	0.012	1	0.03	0.03	0.03	
8/18/11	3	0.02	0.02	0.03	0.005	1	0.02	0.02	0.02	
8/19/11	2	0.01	0.02	0.02	0.007	1	0.03	0.03	0.03	

Table B-2.3. Sulpho-Rhodamine-B Range Fluorescence (Continued)

DATE	North Seep Group (ppb)					South Seep Group (ppb)				
	No. of Samples	Minimum	Average	Maximum	Std. Dev.	No. of Samples	Minimum	Average	Maximum	Std. Dev.
8/20/11	3	0.01	0.02	0.03	0.009	2	0.01	0.02	0.02	0.001
8/21/11	3	0.01	0.02	0.02	0.000	3	0.01	0.02	0.03	0.007
8/22/11	3	0.02	0.02	0.02	0.002	2	0.01	0.02	0.03	0.013
8/23/11	1	0.02	0.02	0.02		1	0.02	0.02	0.02	
8/24/11	2	0.00	0.01	0.01	0.008	2	0.01	0.02	0.04	0.017
8/25/11	1	0.00	0.01	0.01		2	0.02	0.02	0.02	0.005
8/26/11	2	0.01	0.02	0.02	0.001	2	0.02	0.02	0.03	0.002
8/27/11	2	0.02	0.02	0.03	0.006	1	0.02	0.02	0.02	
8/28/11	2	0.00	0.02	0.04	0.024	2	0.01	0.02	0.03	0.016
8/29/11	2	0.00	0.01	0.01	0.003					
8/30/11	1	0.00	0.01	0.01						
9/1/11	3	0.01	0.02	0.03	0.012					
9/2/11	3	0.01	0.02	0.03	0.008	2	0.01	0.02	0.03	0.012
9/3/11	1	0.01	0.02	0.02		2	0.02	0.02	0.03	0.006
9/4/11	3	0.01	0.01	0.02	0.009	1	0.03	0.03	0.03	
9/5/11	1	0.01	0.03	0.03		3	0.01	0.02	0.03	0.013
9/6/11	2	0.01	0.02	0.03	0.013	2	0.02	0.03	0.03	0.004
9/7/11	2	0.01	0.02	0.03	0.013					
9/8/11	1	0.01	0.01	0.01		1	0.03	0.03	0.03	
9/9/11	1	0.01	0.03	0.03						
9/10/11	2	0.01	0.02	0.03	0.017	3	0.01	0.07	0.18	0.094
9/11/11	3	0.01	0.01	0.03	0.010					
9/12/11	1	0.01	0.01	0.01		1	0.03	0.03	0.03	
9/13/11	2	0.01	0.05	0.06	0.011	1	0.03	0.03	0.03	

Table B-2.3. Sulpho-Rhodamine-B Range Fluorescence (Continued)

DATE	North Seep Group (ppb)					South Seep Group (ppb)				
	No. of Samples	Minimum	Average	Maximum	Std. Dev.	No. of Samples	Minimum	Average	Maximum	Std. Dev.
9/14/11	3	0.00	0.02	0.03	0.016	2	0.01	0.03	0.05	0.023
9/15/11	2	0.00	0.01	0.02	0.008					
9/16/11	2	0.01	0.02	0.02	0.002	1	0.02	0.02	0.02	
9/17/11	1	0.02	0.04	0.04		3	0.01	0.02	0.03	0.007
9/18/11	2	0.01	0.01	0.01	0.004	2	0.02	0.03	0.05	0.020
9/19/11	2	0.01	0.02	0.03	0.008	3	0.03	0.03	0.04	0.007
9/20/11	2	0.02	0.04	0.04	0.009	3	0.02	0.03	0.05	0.013
9/21/11	3	0.03	0.03	0.04	0.005	2	0.03	0.03	0.04	0.006
9/22/11	3	0.03	0.04	0.05	0.010	1	0.01	0.01	0.01	
9/23/11	3	0.03	0.03	0.04	0.003	2	0.02	0.02	0.03	0.012
9/24/11	3	0.03	0.04	0.04	0.001	3	0.02	0.03	0.05	0.015
9/25/11	2	0.01	0.01	0.01	0.001	3	0.01	0.02	0.03	0.009
9/26/11	3	0.01	0.02	0.03	0.010	3	0.01	0.03	0.04	0.014
9/27/11	3	0.01	0.02	0.02	0.006	3	0.01	0.01	0.02	0.004
9/28/11	3	0.01	0.01	0.03	0.010	3	0.02	0.03	0.03	0.005
9/29/11	3	0.01	0.02	0.04	0.016	3	0.03	0.03	0.04	0.009
9/30/11	3	0.01	0.01	0.02	0.004	3	-0.01	0.01	0.02	0.018
10/1/11	3	0.00	0.01	0.02	0.012	3	0.03	0.04	0.05	0.013
10/2/11	2	0.00	0.01	0.01	0.000	3	0.01	0.02	0.03	0.013
10/3/11	3	0.01	0.02	0.03	0.012	3	0.01	0.02	0.03	0.009
10/4/11	3	0.01	0.02	0.03	0.010					
10/6/11	1	0.01	0.03	0.03						
10/8/11	3	0.00	0.08	0.21	0.120	2	0.03	0.04	0.05	0.017
10/10/11	1	0.00	0.01	0.01		3	0.02	0.02	0.03	0.007

Table B-2.3. Sulpho-Rhodamine-B Range Fluorescence (Continued)

DATE	North Seep Group (ppb)					South Seep Group (ppb)				
	No. of Samples	Minimum	Average	Maximum	Std. Dev.	No. of Samples	Minimum	Average	Maximum	Std. Dev.
10/11/11	2	0.01	0.02	0.02	0.002					
10/12/11	2	0.01	0.02	0.02	0.008	3	0.01	0.03	0.05	0.020
10/14/11	3	0.01	0.02	0.03	0.008	3	0.03	0.03	0.04	0.008
10/16/11	3	0.01	0.03	0.04	0.011	3	0.02	0.02	0.04	0.010
10/18/11	3	0.02	0.03	0.05	0.013	3	-0.05	0.00	0.03	0.046
10/20/11	3	0.02	0.04	0.04	0.001	3	0.02	0.04	0.06	0.017
10/22/11	3	0.04	0.04	0.05	0.003	3	0.03	0.04	0.05	0.009
10/24/11	2	0.04	0.04	0.04	0.001	3	0.04	0.04	0.04	0.003
10/26/11	3	0.04	0.04	0.05	0.005	3	0.04	0.05	0.05	0.005
10/28/11	3	0.03	0.04	0.05	0.008	3	0.03	0.04	0.05	0.009
10/30/11	1	0.02	0.02	0.02		3	0.02	0.03	0.03	0.004
11/1/11	2	0.02	0.03	0.03	0.000	3	0.04	0.04	0.05	0.003
11/3/11	3	0.03	0.03	0.04	0.005	3	0.04	0.04	0.04	0.002
11/5/11						3	0.02	0.03	0.04	0.010
11/7/11	2	0.03	0.03	0.03	0.003	3	0.02	0.03	0.05	0.017
11/9/11	3	0.02	0.03	0.04	0.008	3	0.03	0.05	0.09	0.035
11/11/11	2	0.02	0.04	0.04	0.003	3	0.04	0.04	0.05	0.003
11/14/11						3	0.04	0.04	0.04	0.002
11/16/11	3	0.03	0.04	0.04	0.004	3	0.04	0.04	0.05	0.005
11/18/11	2	0.02	0.03	0.04	0.011	3	0.04	0.05	0.05	0.007
11/21/11	2	0.02	0.03	0.04	0.008	3	0.03	0.03	0.04	0.005
11/23/11	3	0.02	0.03	0.03	0.006	3	0.02	0.03	0.04	0.010
11/24/11	1	0.02	0.40	0.40						
11/25/11	2	0.02	0.02	0.03	0.003	3	0.02	0.03	0.04	0.012

Table B-2.3. Sulpho-Rhodamine-B Range Fluorescence (Continued)

DATE	North Seep Group (ppb)					South Seep Group (ppb)				
	No. of Samples	Minimum	Average	Maximum	Std. Dev.	No. of Samples	Minimum	Average	Maximum	Std. Dev.
11/28/11	2	0.02	0.03	0.03	0.001	3	0.03	0.03	0.04	0.003
11/30/11	3	0.02	0.03	0.03	0.002	3	0.03	0.03	0.04	0.003
12/2/11	3	0.02	0.02	0.03	0.002	3	0.03	0.03	0.03	0.002
12/5/11	2	0.02	0.03	0.03	0.007	1	0.03	0.03	0.03	
12/7/11	3	0.02	0.03	0.03	0.004	2	0.03	0.03	0.04	0.006
12/9/11	3	0.02	0.03	0.03	0.004	3	0.02	0.03	0.03	0.005
12/14/11	3	0.02	0.03	0.03	0.004	3	0.03	0.03	0.03	0.003
12/19/11	3	0.02	0.03	0.03	0.001	3	0.03	0.03	0.03	0.003
12/21/11	3	0.01	0.01	0.02	0.005	3	0.02	0.02	0.02	0.002
12/23/11	3	0.01	0.01	0.01	0.002	2	0.01	0.02	0.02	0.006
12/26/11	3	0.01	0.01	0.01	0.001	3	0.01	0.02	0.02	0.003
12/28/11	2	0.01	0.05	0.07	0.033	3	0.01	0.02	0.02	0.007
12/30/11	3	0.01	0.02	0.03	0.007	3	0.01	0.02	0.02	0.004
1/2/12	3	0.00	0.01	0.01	0.007	3	0.01	0.02	0.03	0.009
1/4/12	3	0.00	0.04	0.04	0.003					
1/7/12	3	0.03	0.04	0.04	0.008	3	0.03	0.04	0.04	0.007
1/9/12	3	0.03	0.04	0.04	0.004	2	0.03	0.03	0.04	0.013
1/11/12	3	0.03	0.05	0.09	0.028	3	0.02	0.03	0.04	0.012
1/13/12	3	0.02	0.03	0.04	0.007	2	0.03	0.03	0.04	0.006
1/16/12	3	0.02	0.04	0.05	0.008	3	0.03	0.04	0.04	0.008
1/19/12	2	0.03	0.03	0.04	0.008	3	0.03	0.04	0.04	0.005
1/21/12	3	0.03	0.03	0.03	0.003	4	0.03	0.04	0.04	0.003
1/23/12	3	0.02	0.03	0.05	0.016	4	0.03	0.04	0.05	0.010
1/25/12	3	0.02	0.06	0.11	0.045	3	0.03	0.03	0.04	0.008

Table B-2.3. Sulpho-Rhodamine-B Range Fluorescence (Continued)

DATE	North Seep Group (ppb)					South Seep Group (ppb)				
	No. of Samples	Minimum	Average	Maximum	Std. Dev.	No. of Samples	Minimum	Average	Maximum	Std. Dev.
1/27/12	3	0.03	0.04	0.04	0.008	4	0.02	0.03	0.04	0.009
1/28/12	1	0.02	0.02	0.02						
1/31/12	3	0.02	0.04	0.05	0.006	3	0.02	0.03	0.04	0.010
2/10/12	3	0.04	0.04	0.04	0.004	3	0.04	0.05	0.06	0.010
2/14/12	3	0.03	0.04	0.04	0.004	4	0.04	0.04	0.06	0.009
2/17/12	3	0.03	0.04	0.04	0.005	4	0.04	0.04	0.05	0.002
2/20/12	3	0.03	0.04	0.05	0.007	4	0.04	0.05	0.07	0.013
2/24/12	3	0.02	0.02	0.02	0.000	4	0.01	0.02	0.03	0.010
2/27/12	3	0.02	0.02	0.03	0.009	4	0.01	0.02	0.03	0.008
3/1/12	3	0.02	0.02	0.03	0.005	4	0.02	0.03	0.04	0.007
						4	0.02	0.03	0.04	0.007
3/14/12	2	0.02	0.03	0.05	0.017	4	0.02	0.03	0.05	0.015
3/17/12	4	0.02	0.02	0.02	0.001	4	0.02	0.03	0.03	0.006
3/19/12	4	0.02	0.02	0.02	0.003	4	0.01	0.03	0.04	0.015
3/22/12						4	0.01	0.02	0.03	0.010
3/27/12	1	0.02	0.02	0.02		4	0.02	0.03	0.03	0.006
3/29/12	1	0.02	0.02	0.02		4	0.02	0.05	0.11	0.040
3/31/12						3	0.01	0.02	0.03	0.012
4/2/12	1	0.02	0.02	0.02		4	0.02	0.03	0.03	0.008
4/5/12						4	0.03	0.04	0.05	0.011
4/12/12	1	0.02	0.03	0.03		4	0.04	0.04	0.05	0.006
4/16/12	1	0.03	0.04	0.04		3	0.04	0.04	0.05	0.008
						3	0.04	0.05	0.05	0.003
4/24/12	2	0.02	0.03	0.03	0.007	3	0.03	0.04	0.05	0.009

Table B-2.3. Sulpho-Rhodamine-B Range Fluorescence (Continued)

| DATE | North Seep Group (ppb) | | | | | South Seep Group (ppb) | | | | |
	No. of Samples	Minimum	Average	Maximum	Std. Dev.	No. of Samples	Minimum	Average	Maximum	Std. Dev.
4/26/12	2	0.02	0.03	0.03	0.001	3	0.04	0.05	0.05	0.007
5/2/12	2	0.03	0.03	0.04	0.005	3	0.04	0.06	0.09	0.028

APPENDIX C: WATER COLUMN PROFILES

APPENDIX FOR SECTION 4:

**AERIAL INFRARED SEA-SURFACE TEMPERATURE
MAPPING AND POTENTIAL HEAT SOURCES**

This page is intentionally left blank.

Table C-1. Water column temperature and salinity measurements.
Data were collected using a multiparameter sonde (YSI 6600 V2-4; YSI Inc., Yellow Springs, OH) during high-tide conditions from 09:00 a.m. to 02:00 p.m. on 21 September 2011.

Transect	Latitude °N	Longitude °W	Distance from coast (m)	Depth from surface (m)	Temp. (°C)[a]	Salinity
1	20.94009	-156.69308	51	0.00	26.77	34.14
				*2.43	26.29	34.67
	20.94016	-156.69328	85	0.00	26.55	34.53
				*3.24	26.11	34.73
	20.94025	-156.69369	136	0.00	26.31	34.59
				*7.60	26.00	34.70
2	20.93816	-156.69312	34	0.00	26.57	34.29
				*1.21	26.44	34.62
	20.93821	-156.69352	102	0.00	26.41	34.65
				*3.51	26.11	34.73
	20.93827	-156.69425	221	0.00	26.15	34.68
				*10.11	25.98	34.69
3	20.93618	-156.69309	34	0.00	26.28	34.64
				*2.10	26.23	34.67
	20.93620	-156.69355	102	0.00	26.22	34.66
				*6.25	26.06	34.68
	20.93633	-156.69424	221	0.00	26.16	34.67
				*9.78	26.14	34.66
4	20.93243	-156.69332	17	0.00	26.60	34.51
				*2.13	26.29	34.64
	20.93251	-156.69417	153	0.00	26.33	34.61
				*7.40	26.12	34.58
	20.93237	-156.69477	255	0.00	26.26	34.64
				*10.00	25.92	34.67
5	20.92934	-156.69459	17	0.00	26.65	34.65
				*2.10	26.56	34.66
	20.92958	-156.69492	68	0.00	26.30	34.66
				*5.22	26.17	31.69
	20.92982	-156.69563	102	0.00	26.09	34.67
				*9.61	25.95	33.37

[a] Temp. is Temperature
* Denotes measurement taken at the seafloor

This page is intentionally left blank.

APPENDIX D: COASTAL SURFACE WATER RADON ACTIVITIES

APPENDIX FOR SECTION 5:

SUBMARINE GROUNDWATER DISCHARGE

This page is intentionally left blank.

Table D-1. Stationary radon time-series data at submarine springs, June 2011.
Radon activities (dpm/m3) measured in the surface 0.5 m during time-series radon measurement on June 19-22, 2011. Water depth and radon fluxes that were using during the coastal mass balance are indicated as radon flux (dpm/m2/15 min). The advection rates derived from the radon mass balance represent the magnitude groundwater discharge per seep group over time.

Seep 3

Date/time of measurement	Water depth (m)	Total Radon in Water (dpm/m3)	1-sig-error	5: Atm. Flux (dpm/m2/15 min)	1-sig-error	Mixing losses (dpm/m2/15 min)	Total radon flux (dpm/m2/15 min)	1-sig-error	Advection rate (cm/d)	1-sig-error
6/19/11 13:48	2.34	909	274	24	24	0	1008	605	186	111
6/19/11 14:03	2.34	825	261	21	21	176	0	0	0	0
6/19/11 14:18	2.41	494	202	13	13	734	0	0	0	0
6/19/11 14:33	2.40	576	218	15	15	0	213	128	39	24
6/19/11 14:48	2.50	828	262	21	21	0	690	414	127	76
6/19/11 15:03	2.47	328	164	8	8	1241	0	0	0	0
6/19/11 15:18	2.53	827	261	21	21	0	1293	776	238	143
6/19/11 15:33	2.59	413	185	10	10	1023	0	0	0	0
6/19/11 15:48	2.60	912	275	23	23	0	1328	797	245	147
6/19/11 16:03	2.63	664	235	13	13	621	0	0	0	0
6/19/11 16:18	2.65	329	165	6	6	872	0	0	0	0
6/19/11 16:33	2.70	914	276	18	18	0	1605	963	296	177
6/19/11 16:48	2.69	666	235	13	13	657	0	0	0	0
6/19/11 17:03	2.74	415	186	10	10	655	0	0	0	0
6/19/11 17:18	2.73	578	219	17	17	0	464	278	85	51
6/19/11 17:33	2.72	833	264	30	30	0	726	436	134	80
6/19/11 17:48	2.77	1085	301	46	46	0	771	462	142	85
6/19/11 18:03	2.74	835	264	32	32	660	0	0	0	0
6/19/11 18:18	2.78	585	221	21	21	646	0	0	0	0

Seep 3 cont.

Date/time of measurement	Water depth (m)	Total Radon in Water (dpm/m3)	1-sig-error	5: Atm. Flux (dpm/m2/15 min)	1-sig-error	Mixing losses (dpm/m2/15 min)	Total radon flux (dpm/m2/15 min)	1-sig-error	Advection rate (cm/d)	1-sig-error
6/19/11 18:34	2.73	919	277	30	30	0	957	574	176	106
6/19/11 18:49	2.75	836	264	25	25	190	0	0	0	0
6/19/11 19:04	2.73	752	251	23	23	206	0	0	0	0
6/19/11 19:19	2.70	1255	324	38	38	0	1409	846	260	156
6/19/11 19:34	2.70	837	265	26	26	1102	0	0	0	0
6/19/11 19:49	2.68	669	236	20	20	433	0	0	0	0
6/19/11 20:04	2.63	669	236	25	25	0	25	15	5	3
6/19/11 20:19	2.64	1256	324	56	56	0	1617	970	298	179
6/19/11 20:34	2.62	1170	313	62	62	165	0	0	0	0
6/19/11 20:49	2.60	922	278	57	57	594	0	0	0	0
6/19/11 21:04	2.50	1173	313	69	69	0	721	433	133	80
6/19/11 21:19	2.50	753	251	43	43	1010	0	0	0	0
6/19/11 21:34	2.50	1248	322	68	68	0	1307	784	241	145
6/19/11 21:49	2.43	840	265	44	44	977	0	0	0	0
6/19/11 22:04	2.49	839	265	44	44	0	81	49	15	9
6/19/11 22:19	2.41	1008	291	53	53	0	472	283	87	52
6/19/11 22:34	2.41	1602	367	87	87	0	1519	911	280	168
6/19/11 22:49	2.36	1182	316	64	64	947	0	0	0	0
6/19/11 23:04	2.38	1599	367	80	80	0	1102	661	203	122
6/19/11 23:19	2.35	1087	302	51	51	1169	0	0	0	0
6/19/11 23:34	2.32	1602	367	70	70	0	1278	767	235	141
6/19/11 23:49	2.31	1265	327	51	51	729	0	0	0	0

Seep 3 cont.

Date/time of measurement	Water depth (m)	Total Radon in Water (dpm/m3)	1-sig-error	5: Atm. Flux (dpm/m2/15 min)	1-sig-error	Mixing losses (dpm/m2/15 min)	Total radon flux (dpm/m2/15 min)	1-sig-error	Advection rate (cm/d)	1-sig-error
6/20/11 0:04	2.30	1856	396	75	75	0	1441	865	266	159
6/20/11 0:19	2.31	1434	348	58	58	904	0	0	0	0
6/20/11 0:34	2.27	2195	430	89	89	0	1843	1106	340	204
6/20/11 0:49	2.29	1603	368	65	65	1249	0	0	0	0
6/20/11 1:04	2.23	1690	378	65	65	0	264	158	49	29
6/20/11 1:19	2.27	1771	387	65	65	0	302	181	56	33
6/20/11 1:34	2.25	1264	326	43	43	1105	0	0	0	0
6/20/11 1:49	2.27	2365	447	77	77	0	2594	1556	478	287
6/20/11 2:04	2.29	1436	348	57	57	2031	0	0	0	0
6/20/11 2:19	2.27	1774	387	85	85	0	857	514	158	95
6/20/11 2:34	2.31	1775	387	100	100	0	166	100	31	18
6/20/11 2:49	2.31	1172	313	75	75	1318	0	0	0	0
6/20/11 3:04	2.34	1434	348	81	81	0	729	438	134	81
6/20/11 3:19	2.35	1602	368	80	80	0	479	287	88	53
6/20/11 3:34	2.35	1265	327	54	54	732	0	0	0	0
6/20/11 3:49	2.39	1857	396	68	68	0	1525	915	281	169
6/20/11 4:04	2.36	1772	387	64	64	139	0	0	0	0
6/20/11 4:19	2.37	1690	378	60	60	110	0	0	0	0
6/20/11 4:34	2.40	1437	349	51	51	517	0	0	0	0
6/20/11 4:49	2.38	1356	339	47	47	148	0	0	0	0
6/20/11 5:04	2.43	1272	328	44	44	104	0	0	0	0
6/20/11 5:19	2.38	1782	389	62	62	0	1302	781	240	144

Seep 3 cont.

Date/time of measurement	Water depth (m)	Total Radon in Water (dpm/m3)	1-sig-error	5: Atm. Flux (dpm/m2/15 min)	1-sig-error	Mixing losses (dpm/m2/15 min)	Total radon flux (dpm/m2/15 min)	1-sig-error	Advection rate (cm/d)	1-sig-error
6/20/11 5:34	2.42	849	268	28	28	2161	0	0	0	0
6/20/11 5:49	2.37	1867	398	62	62	0	2528	1517	442	265
6/20/11 6:04	2.09	1019	294	33	33	1974	0	0	0	0
6/20/11 6:19	2.11	1017	294	32	32	0	45	27	8	5
6/20/11 6:34	2.02	1188	317	38	38	0	397	238	69	42
6/20/11 6:49	2.21	1781	389	55	55	0	1560	936	273	164
6/20/11 7:04	2.07	1102	306	33	33	1468	0	0	0	0
6/20/11 7:19	1.85	1868	398	57	57	0	1642	985	287	172
6/20/11 7:34	2.33	1613	370	52	52	0	279	167	49	29
6/20/11 7:49	2.13	847	268	24	24	1760	0	0	0	0
6/20/11 8:04	2.16	1271	328	44	44	0	980	588	171	103
6/20/11 8:19	2.06	1270	328	35	35	0	32	19	6	3
6/20/11 8:34	2.22	1267	327	34	34	0	206	124	36	22
6/20/11 8:49	2.07	1435	348	37	37	0	410	246	72	43
6/20/11 9:04	2.30	1011	292	26	26	656	0	0	0	0
6/20/11 9:19	1.88	1514	357	37	37	0	1192	715	208	125
6/20/11 9:34	2.00	1343	336	32	32	147	0	0	0	0
6/20/11 9:49	1.88	1254	324	29	29	147	0	0	0	0
6/20/11 10:04	1.89	1085	301	25	25	284	0	0	0	0
6/20/11 10:19	1.92	1417	344	32	32	0	697	418	122	73
6/20/11 10:34	1.99	915	276	21	21	891	0	0	0	0
6/20/11 10:49	1.96	1162	311	26	26	0	518	311	90	54

Seep 3 cont.

Date/time of measurement	Water depth (m)	Total Radon in Water (dpm/m3)	1-sig-error	5: Atm. Flux (dpm/m2/15 min)	1-sig-error	Mixing losses (dpm/m2/15 min)	Total radon flux (dpm/m2/15 min)	1-sig-error	Advection rate (cm/d)	1-sig-error
6/20/11 11:04	2.03	910	274	20	20	422	0	0	0	0
6/20/11 11:19	1.80	747	249	16	16	315	0	0	0	0
6/20/11 11:34	2.02	496	203	11	11	367	0	0	0	0
6/20/11 11:50	1.87	1161	310	26	26	0	1369	821	239	144
6/20/11 12:05	1.85	1569	360	34	34	0	797	478	139	84
6/20/11 12:20	2.15	829	262	18	18	1151	0	0	0	0
6/20/11 12:35	2.09	1573	361	34	34	0	1635	981	286	171
6/20/11 12:50	2.06	991	286	21	21	1195	0	0	0	0
6/20/11 13:05	2.05	1073	298	23	23	0	192	115	34	20
6/20/11 13:20	1.93	1397	339	31	31	0	694	417	121	73
6/20/11 13:35	2.19	1065	295	23	23	382	0	0	0	0
6/20/11 13:50	2.06	820	259	18	18	519	0	0	0	0
6/20/11 14:05	1.93	899	271	19	19	0	181	109	32	19
6/20/11 14:20	2.04	1394	338	30	30	0	1121	672	196	117
6/20/11 14:35	2.07	903	272	20	20	959	0	0	0	0
6/20/11 14:50	2.15	1150	307	25	25	0	617	370	108	65

Seep 2 Piez-1

Date/time of measurement	Water depth (m)	Total Radon in Water (dpm/m3)	1-sig-error	5: Atm. Flux (dpm/m2/15 min)	1-sig-error	Mixing losses (dpm/m2/15 min)	Total radon flux (dpm/m2/15 min)	1-sig-error	Advection rate (cm/d)	1-sig-error
6/20/11 16:35	2.40	408	182	9	9	0	4	2	1	0
6/20/11 16:50	2.62	327	163	7	7	152	0	0	0	0
6/20/11 17:05	2.62	659	233	16	16	0	887	532	155	93
6/20/11 17:20	2.50	580	219	17	17	192	0	0	0	0

Seep 2 Piez-1 cont.

Date/time of measurement	Water depth (m)	Total Radon in Water (dpm/m3)	1-sig-error	5: Atm. Flux (dpm/m2/15 min)	1-sig-error	Mixing losses (dpm/m2/15 min)	Total radon flux (dpm/m2/15 min)	1-sig-error	Advection rate (cm/d)	1-sig-error
6/20/11 17:35	2.50	658	233	21	21	0	216	130	38	23
6/20/11 17:50	2.54	581	220	21	21	152	0	0	0	0
6/20/11 18:05	2.67	748	249	30	30	0	530	318	93	56
6/20/11 18:20	2.61	1082	300	47	47	0	940	564	164	99
6/20/11 18:35	2.57	330	165	15	15	1948	0	0	0	0
6/20/11 18:50	2.64	581	219	30	30	0	702	421	123	74
6/20/11 19:05	2.61	498	203	27	27	190	0	0	0	0
6/20/11 19:20	2.69	671	237	38	38	0	529	317	92	55
6/20/11 19:35	2.58	666	235	39	39	0	25	15	4	3
6/20/11 19:50	2.52	749	250	46	46	0	262	157	46	28
6/20/11 20:05	2.60	665	235	42	42	130	0	0	0	0
6/20/11 20:20	2.49	502	205	32	32	391	0	0	0	0
6/20/11 20:35	2.45	923	278	61	61	0	1107	664	193	116
6/20/11 20:50	2.45	749	250	50	50	375	0	0	0	0
6/20/11 21:05	2.44	748	250	52	52	0	50	30	9	5
6/20/11 21:20	2.50	582	220	42	42	338	0	0	0	0
6/20/11 21:35	2.52	587	222	44	44	0	63	38	11	7
6/20/11 21:50	2.54	1082	300	84	84	0	1352	811	236	142
6/20/11 22:05	2.53	499	204	35	35	1446	0	0	0	0
6/20/11 22:20	2.45	916	276	59	59	0	1115	669	195	117
6/20/11 22:35	2.34	1167	312	68	68	0	683	410	119	72
6/20/11 22:50	2.32	587	222	31	31	1327	0	0	0	0

Seep 2 Piez-1cont.

Date/time of measurement	Water depth (m)	Total Radon in Water (dpm/m3)	1-sig-error	5: Atm. Flux (dpm/m2/15 min)	1-sig-error	Mixing losses (dpm/m2/15 min)	Total radon flux (dpm/m2/15 min)	1-sig-error	Advection rate (cm/d)	1-sig-error
6/20/11 23:05	2.25	667	236	38	38	0	222	133	39	23
6/20/11 23:20	2.40	1168	312	70	70	0	1349	810	236	141
6/20/11 23:35	2.20	1680	376	108	108	0	1336	802	233	140
6/20/11 23:50	2.26	1260	325	85	85	772	0	0	0	0
6/21/11 0:05	2.27	334	167	22	22	2070	0	0	0	0
6/21/11 0:20	2.34	1347	336	88	88	0	2470	1482	432	259
6/21/11 0:35	2.10	587	222	37	37	1740	0	0	0	0
6/21/11 0:50	2.09	1008	291	63	63	0	948	569	166	99
6/21/11 1:05	2.22	1178	315	70	70	0	556	334	97	58
6/21/11 1:20	2.13	1515	357	84	84	0	833	500	146	87
6/21/11 1:35	2.26	583	221	30	30	1900	0	0	0	0
6/21/11 1:50	2.17	758	252	37	37	0	432	259	75	45
6/21/11 2:05	2.09	1177	315	57	57	0	968	581	169	101
6/21/11 2:20	2.04	668	236	32	32	1032	0	0	0	0
6/21/11 2:35	2.16	585	221	28	28	91	0	0	0	0
6/21/11 2:50	2.10	1253	324	61	61	0	1506	903	263	158
6/21/11 3:05	2.24	837	264	39	39	741	0	0	0	0
6/21/11 3:20	2.21	835	264	37	37	0	33	20	6	3
6/21/11 3:35	2.10	753	251	32	32	150	0	0	0	0
6/21/11 3:50	2.27	928	280	38	38	0	538	323	94	56
6/21/11 4:05	2.32	760	254	31	31	320	0	0	0	0
6/21/11 4:20	2.27	1355	339	56	56	0	1435	861	251	150

Seep 2 Piez-1 cont.

Date/time of measurement	Water depth (m)	Total Radon in Water (dpm/m3)	1-sig-error	5: Atm. Flux (dpm/m2/15 min)	1-sig-error	Mixing losses (dpm/m2/15 min)	Total radon flux (dpm/m2/15 min)	1-sig-error	Advection rate (cm/d)	1-sig-error
6/21/11 4:35	2.13	1354	339	56	56	0	56	33	10	6
6/21/11 4:51	2.26	925	279	38	38	776	0	0	0	0
6/21/11 5:06	2.23	1019	294	43	43	0	254	152	44	27
6/21/11 5:21	2.28	673	238	28	28	717	0	0	0	0
6/21/11 5:36	2.18	589	223	25	25	168	0	0	0	0
6/21/11 5:51	2.17	679	240	28	28	0	226	135	39	24
6/21/11 6:06	2.19	764	255	32	32	0	228	137	40	24
6/21/11 6:21	2.38	850	269	35	35	0	354	212	62	37
6/21/11 6:36	2.27	1359	340	57	57	0	1269	761	222	133
6/21/11 6:51	2.29	759	253	31	31	1320	0	0	0	0
6/21/11 7:06	2.28	594	224	24	24	352	0	0	0	0
6/21/11 7:21	2.31	1018	294	42	42	0	1035	621	181	109
6/21/11 7:36	2.26	507	207	20	20	1161	0	0	0	0
6/21/11 7:51	2.47	1015	293	41	41	0	1368	821	239	143
6/21/11 8:06	2.24	676	239	27	27	810	0	0	0	0
6/21/11 8:21	2.36	930	280	37	37	0	698	419	122	73
6/21/11 8:36	2.34	1182	316	46	46	0	642	385	112	67
6/21/11 8:51	2.42	675	239	26	26	1119	0	0	0	0
6/21/11 9:06	2.27	758	253	29	29	0	230	138	40	24
6/21/11 9:21	2.22	1264	326	48	48	0	1196	718	209	125
6/21/11 9:36	2.17	673	238	25	25	1286	0	0	0	0
6/21/11 9:51	2.41	670	237	25	25	0	142	85	25	15

Seep 2 Piez-1 cont.

Date/time of measurement	Water depth (m)	Total Radon in Water (dpm/m3)	1-sig-error	5: Atm. Flux (dpm/m2/15 min)	1-sig-error	Mixing losses (dpm/m2/15 min)	Total radon flux (dpm/m2/15 min)	1-sig-error	Advection rate (cm/d)	1-sig-error
6/21/11 10:06	2.32	838	265	31	31	0	435	261	76	46
6/21/11 10:21	2.21	1006	290	37	37	0	425	255	74	45
6/21/11 10:36	2.35	920	277	33	33	50	0	0	0	0
6/21/11 10:51	2.30	834	264	29	29	173	0	0	0	0
6/21/11 11:06	2.61	584	220	20	20	424	0	0	0	0
6/21/11 11:21	2.09	1249	323	44	44	0	1781	1068	311	187
6/21/11 11:36	2.16	1165	311	40	40	65	0	0	0	0
6/21/11 11:51	2.23	331	166	11	11	1780	0	0	0	0
6/21/11 12:06	2.14	665	235	23	23	0	768	461	134	81
6/21/11 12:21	2.14	331	166	11	11	703	0	0	0	0
6/21/11 12:36	2.30	745	248	25	25	0	1003	602	175	105
6/21/11 12:51	2.14	829	262	28	28	0	221	132	39	23
6/21/11 13:06	2.40	744	248	24	24	6	0	0	0	0
6/21/11 13:21	2.31	993	286	32	32	0	630	378	110	66
6/21/11 13:36	2.29	497	203	16	16	1129	0	0	0	0
6/21/11 13:51	2.27	1079	299	36	36	0	1369	821	239	144
6/21/11 14:06	2.30	575	217	19	19	1111	0	0	0	0
6/21/11 14:21	2.56	660	233	22	22	0	348	209	61	36
6/21/11 14:36	2.34	493	201	16	16	412	0	0	0	0
6/21/11 14:51	2.29	659	233	22	22	0	410	246	72	43
6/21/11 15:06	2.49	493	201	16	16	297	0	0	0	0
6/21/11 15:21	2.32	1150	307	37	37	0	1673	1004	292	175

Seep 2 Piez-1 cont.

Date/time of measurement	Water depth (m)	Total Radon in Water (dpm/m3)	1-sig-error	5: Atm. Flux (dpm/m2/15 min)	1-sig-error	Mixing losses (dpm/m2/15 min)	Total radon flux (dpm/m2/15 min)	1-sig-error	Advection rate (cm/d)	1-sig-error
6/21/11 15:36	2.37	825	261	27	27	693	0	0	0	0
6/21/11 15:51	2.52	822	260	27	27	0	117	70	21	12
6/21/11 16:06	2.48	659	233	22	22	388	0	0	0	0

Seep 1

6/21/11 19:06	2.58	585	221	20	20	0	250	150	44	26
6/21/11 19:21	2.65	1088	302	37	37	0	1400	840	245	147
6/21/11 19:36	2.61	415	185	14	14	1769	0	0	0	0
6/21/11 19:51	2.65	416	186	14	14	0	28	17	5	3
6/21/11 20:06	2.59	499	204	17	17	0	239	144	42	25
6/21/11 20:21	2.60	583	220	20	20	0	242	145	42	25
6/21/11 20:36	2.73	667	236	23	23	0	306	183	53	32
6/21/11 20:51	2.67	504	206	18	18	426	0	0	0	0
6/21/11 21:06	2.59	672	237	26	26	0	474	284	83	50
6/21/11 21:21	2.49	420	188	17	17	634	0	0	0	0
6/21/11 21:36	2.62	1093	303	49	49	0	1846	1107	322	193
6/21/11 21:51	2.58	250	144	12	12	2197	0	0	0	0
6/21/11 22:07	2.66	835	264	38	38	0	1602	961	280	168
6/21/11 22:22	2.62	924	279	39	39	0	276	166	48	29
6/21/11 22:37	2.52	926	279	36	36	0	40	24	7	4
6/21/11 22:52	2.46	588	222	21	21	829	0	0	0	0
6/21/11 23:07	2.48	842	266	36	36	0	673	404	118	71

Seep 1 cont.

Date/time of measurement	Water depth (m)	Total Radon in Water (dpm/m3)	1-sig-error	5: Atm. Flux (dpm/m2/15 min)	1-sig-error	Mixing losses (dpm/m2/15 min)	Total radon flux (dpm/m2/15 min)	1-sig-error	Advection rate (cm/d)	1-sig-error
6/21/11 23:22	2.64	668	236	32	32	319	0	0	0	0
6/21/11 23:37	2.33	501	205	28	28	411	0	0	0	0
6/21/11 23:52	2.40	1009	291	64	64	0	1307	784	228	137
6/22/11 0:07	2.25	1011	292	57	57	0	60	36	11	6
6/22/11 0:22	2.45	926	279	46	46	0	8	5	1	1
6/22/11 0:37	2.37	758	253	32	32	379	0	0	0	0
6/22/11 0:52	2.50	758	253	27	27	0	103	62	18	11
6/22/11 1:07	2.47	1432	347	56	56	0	1742	1045	304	183
6/22/11 1:22	2.17	1266	327	54	54	354	0	0	0	0
6/22/11 1:37	2.29	1090	302	50	50	222	0	0	0	0
6/22/11 1:52	2.33	758	253	37	37	698	0	0	0	0
6/22/11 2:07	2.23	845	267	43	43	0	245	147	43	26
6/22/11 2:22	2.28	1182	316	62	62	0	864	519	151	91
6/22/11 2:37	2.26	1172	313	62	62	0	40	24	7	4
6/22/11 2:52	2.20	1434	348	78	78	0	669	402	117	70
6/22/11 3:07	2.28	1432	347	76	76	0	174	104	30	18
6/22/11 3:22	2.22	1013	292	52	52	904	0	0	0	0
6/22/11 3:37	2.34	1256	324	64	64	0	736	442	129	77
6/22/11 3:52	2.33	1927	402	96	96	0	1665	999	291	175
6/22/11 4:07	2.25	1435	348	70	70	1075	0	0	0	0
6/22/11 4:22	2.34	2178	427	105	105	0	1957	1174	342	205
6/22/11 4:37	2.38	1350	337	65	65	1825	0	0	0	0

Seep 1 cont.

Date/time of measurement	Water depth (m)	Total Radon in Water (dpm/m3)	1-sig-error	5: Atm. Flux (dpm/m2/15 min)	1-sig-error	Mixing losses (dpm/m2/15 min)	Total radon flux (dpm/m2/15 min)	1-sig-error	Advection rate (cm/d)	1-sig-error
6/22/11 4:52	2.28	1687	377	79	79	0	881	529	154	92
6/22/11 5:07	2.31	2111	422	99	99	0	1125	675	197	118
6/22/11 5:22	2.37	1266	327	59	59	1827	0	0	0	0
6/22/11 5:37	2.41	1519	358	70	70	0	723	434	126	76
6/22/11 5:52	2.45	1689	378	77	77	0	549	329	96	58
6/22/11 6:07	2.30	1772	387	80	80	0	284	170	50	30
6/22/11 6:22	2.48	1266	327	57	57	909	0	0	0	0
6/22/11 6:37	2.46	1606	368	71	71	0	915	549	160	96
6/22/11 6:52	2.35	1942	405	85	85	0	912	547	159	96
6/22/11 7:07	2.58	1944	405	84	84	0	499	299	87	52
6/22/11 7:22	2.43	1774	387	75	75	365	0	0	0	0
6/22/11 7:37	2.68	2192	430	91	91	0	1617	970	282	169
6/22/11 7:52	2.46	1516	357	62	62	1752	0	0	0	0
6/22/11 8:07	2.57	1433	347	58	58	5	0	0	0	0
6/22/11 8:22	2.45	1009	291	40	40	1050	0	0	0	0
6/22/11 8:37	2.41	1681	376	65	65	0	1712	1027	299	179
6/22/11 8:52	2.65	1427	346	54	54	255	0	0	0	0
6/22/11 9:07	2.60	1596	366	59	59	0	506	303	88	53
6/22/11 9:22	2.61	1342	335	49	49	600	0	0	0	0
6/22/11 9:37	2.46	1673	374	59	59	0	924	554	161	97
6/22/11 9:52	2.46	1253	324	43	43	989	0	0	0	0
6/22/11 10:07	2.52	1839	392	62	62	0	1605	963	280	168

Seep 1 cont.

Date/time of measurement	Water depth (m)	Total Radon in Water (dpm/m3)	1-sig-error	5: Atm. Flux (dpm/m2/15 min)	1-sig-error	Mixing losses (dpm/m2/15 min)	Total radon flux (dpm/m2/15 min)	1-sig-error	Advection rate (cm/d)	1-sig-error
6/22/11 10:22	2.45	1417	344	48	48	1016	0	0	0	0
6/22/11 10:37	2.60	1915	399	63	63	0	1547	928	270	162
6/22/11 10:52	2.39	2246	432	73	73	0	933	560	163	98
6/22/11 11:07	2.43	1908	398	60	60	680	0	0	0	0
6/22/11 11:22	2.35	1578	362	49	49	751	0	0	0	0
6/22/11 11:37	2.34	1825	389	55	55	0	635	381	111	67
6/22/11 11:52	2.35	1492	352	44	44	722	0	0	0	0
6/22/11 11:57	2.61	1373	614	40	40	0	77	46	13	8

Table D-2. Radon surface-water coastal survey data, June 2011.
Radon activities (dpm/m3) measured in the surface 0.5 m during a coastal survey on June 21, 2011.

Latitude	Longitude	Date/time of measurement	Water depth (m)	Total Radon in Water (dpm/m3)	1-sig-error
20.8871	-156.6902	6/21/11 8:19	34.1	833	481
20.8899	-156.6904	6/21/11 8:24	29.0	275	275
20.8917	-156.6912	6/21/11 8:29	37.5	275	275
20.8956	-156.6887	6/21/11 8:39	32.6	275	275
20.8975	-156.6861	6/21/11 8:44	29.6	274	274
20.9003	-156.6859	6/21/11 8:49	29.3	1374	614
20.9028	-156.6863	6/21/11 8:54	30.8	1375	615
20.9050	-156.6872	6/21/11 8:59	27.1	826	477
20.9075	-156.6884	6/21/11 9:04	29.6	1378	616
20.9099	-156.6899	6/21/11 9:09	31.7	0	0
20.9109	-156.6931	6/21/11 9:14	36.3	1928	729
20.9129	-156.6957	6/21/11 9:19	34.7	0	0
20.9148	-156.6974	6/21/11 9:24	27.7	1660	678
20.9172	-156.6983	6/21/11 9:29	25.9	828	478
20.9191	-156.6979	6/21/11 9:34	32.6	827	477
20.9211	-156.6973	6/21/11 9:39	20.4	829	478
20.9231	-156.6966	6/21/11 9:44	21.6	827	477
20.9255	-156.6961	6/21/11 9:49	31.4	1106	553
20.9275	-156.6975	6/21/11 9:54	22.6	829	478
20.9287	-156.6964	6/21/11 9:59	14.0	830	479
20.9299	-156.6945	6/21/11 10:04	21.9	551	389
20.9311	-156.6949	6/21/11 10:09	15.5	275	275
20.9318	-156.6937	6/21/11 10:14	28.7	548	388
20.9340	-156.6934	6/21/11 10:19	27.4	0	0
20.9366	-156.6938	6/21/11 10:24	30.8	0	0
20.9390	-156.6935	6/21/11 10:29	28.3	274	274
20.9415	-156.6931	6/21/11 10:34	29.9	1928	729
20.9441	-156.6933	6/21/11 10:39	30.5	826	477
20.9467	-156.6938	6/21/11 10:44	29.0	278	278
20.9487	-156.6937	6/21/11 10:49	25.0	833	481
20.9504	-156.6924	6/21/11 10:54	20.4	1109	554
20.9522	-156.6910	6/21/11 10:59	25.6	275	275
20.9540	-156.6892	6/21/11 11:04	31.4	550	389
20.9562	-156.6877	6/21/11 11:09	31.4	1377	615
20.9551	-156.6886	6/21/11 11:14	39.0	276	275

Latitude	Longitude	Date/time of measurement	Water depth (m)	Total Radon in Water (dpm/m3)	1-sig-error
20.9530	-156.6907	6/21/11 11:19	27.4	828	478
20.9506	-156.6926	6/21/11 11:24	36.0	1662	679
20.9477	-156.6940	6/21/11 11:29	32.3	1104	552
20.9464	-156.6941	6/21/11 11:34	21.0	1096	548
20.9444	-156.6938	6/21/11 11:39	32.0	289	289
20.9395	-156.6932	6/21/11 11:49	9.1	544	385
20.9394	-156.6932	6/21/11 11:54	10.4	283	283
20.9396	-156.6930	6/21/11 11:59	6.7	543	384
20.9399	-156.6936	6/21/11 12:04	6.7	544	385
20.9396	-156.6933	6/21/11 12:09	13.4	271	271
20.9375	-156.6932	6/21/11 12:14	29.0	0	0
20.9348	-156.6932	6/21/11 12:19	31.7	547	387
20.9318	-156.6936	6/21/11 12:24	36.0	0	0
20.9357	-156.6937	6/21/11 12:35	24.4	514	373
20.9381	-156.6939	6/21/11 12:40	25.0	274	274
20.9404	-156.6937	6/21/11 12:45	27.1	239	239
20.9390	-156.6941	6/21/11 12:52	34.4	0	0
20.9367	-156.6944	6/21/11 12:56	34.4	69	34
20.9339	-156.6947	6/21/11 13:01	29.6	516	289
20.9317	-156.6958	6/21/11 13:06	36.9	309	375
20.9296	-156.6984	6/21/11 13:11	37.5	516	275
20.9265	-156.6997	6/21/11 13:16	37.2	275	274
20.9230	-156.7006	6/21/11 13:21	39.9	274	239
20.9205	-156.7020	6/21/11 13:26	36.6	239	34
20.9177	-156.7020	6/21/11 13:31	35.1	34	307
20.9147	-156.7022	6/21/11 13:36	32.9	375	527
20.9120	-156.7014	6/21/11 13:41	30.8	1026	335
20.9088	-156.7010	6/21/11 13:46	39.0	473	142
20.9067	-156.6996	6/21/11 13:51	36.6	0	0
20.9042	-156.6979	6/21/11 13:56	29.3	0	0
20.9014	-156.6971	6/21/11 14:01	34.7	0	0
20.8983	-156.6958	6/21/11 14:05	37.8	0	0
20.8950	-156.6944	6/21/11 14:10	40.5	271	271
20.8916	-156.6935	6/21/11 14:15	40.8	0	0
20.8883	-156.6918	6/21/11 14:20	38.7	271	271
20.8874	-156.6890	6/21/11 14:25	38.4	544	384

Table D-3. Stationary radon time-series data at submarine spring sites, September 2011.
Radon activities (dpm/m3) measured in the surface 0.5 m during time-series radon measurement on September 24-25, 2011. Water depth and radon fluxes that were using during the coastal mass balance are indicated as radon flux (dpm/m2/15 min). The advection rates derived from the radon mass balance represent the magnitude groundwater discharge per seep group over time.

Seep 3

Date/time of measurement	Water depth (m)	Total Radon in Water (dpm/m3)	1-sig-error	5: Atm. Flux (dpm/m2/15 min)	1-sig-error	Mixing losses (dpm/m2/15 min)	Total radon flux (dpm/m2/15 min)	1-sig-error	Advection rate (cm/d)	1-sig-error
9/24/11 11:01	2.58	708	416	13	13	0	933	560	209	126
9/24/11 11:16	2.60	884	280	16	16	0	483	290	108	65
9/24/11 11:31	2.68	1239	318	22	22	0	1027	616	230	138
9/24/11 11:46	2.67	1237	355	22	22	0	18	11	4	2
9/24/11 12:01	2.72	1951	319	34	34	0	2028	1217	455	273
9/24/11 12:16	2.72	1950	292	33	33	0	33	20	7	4
9/24/11 12:31	2.71	885	265	15	15	2884	0	0	0	0
9/24/11 12:46	2.79	1148	293	20	20	0	813	488	182	109
9/24/11 13:01	2.76	1420	354	25	25	0	783	470	176	105
9/24/11 13:16	2.79	1150	294	20	20	692	0	0	0	0
9/24/11 13:31	2.76	969	234	17	17	489	0	0	0	0
9/24/11 13:46	2.78	795	307	14	14	458	0	0	0	0
9/24/11 14:01	2.75	971	294	17	17	0	506	304	114	68
9/24/11 14:16	2.75	1415	343	25	25	0	1248	749	280	168
9/24/11 14:31	2.74	976	344	17	17	1191	0	0	0	0
9/24/11 14:46	2.70	618	406	11	11	969	0	0	0	0
9/24/11 15:01	2.70	1064	494	19	19	0	1222	733	274	164
9/24/11 15:16	2.65	975	396	17	17	223	0	0	0	0
9/24/11 15:31	2.64	1331	434	23	23	0	967	580	217	130
9/24/11 15:46	2.58	1331	353	23	23	0	24	15	5	3

Seep 3 cont. Date/time of measurement	Water depth (m)	Total Radon in Water (dpm/m3)	1-sig-error	5: Atm. Flux (dpm/m2/15 min)	1-sig-error	Mixing losses (dpm/m2/15 min)	Total radon flux (dpm/m2/15 min)	1-sig-error	Advection rate (cm/d)	1-sig-error
9/24/11 16:01	2.57	1862	442	32	32	0	1403	842	315	189
9/24/11 16:16	2.51	2751	433	23	23	0	2304	1382	517	310
9/24/11 16:31	2.46	1773	433	15	15	2436	0	0	0	0
9/24/11 16:46	2.42	2126	516	4	4	0	873	524	196	118
9/24/11 16:51	2.44	1413	949	21	21	1679	0	0	0	0

Seep 1										
9/25/11 9:15	2.00	1904	406	53	53	1245	0	0	0	0
9/25/11 9:30	2.10	1558	367	43	43	509	0	0	0	0
9/25/11 9:45	2.08	2509	466	69	69	0	2066	1240	358	215
9/25/11 10:00	2.20	2594	474	71	71	0	539	323	93	56
9/25/11 10:15	2.30	2266	444	63	63	449	0	0	0	0
9/25/11 10:30	2.31	2007	418	56	56	521	0	0	0	0
9/25/11 10:45	2.31	2011	419	56	56	0	67	40	12	7
9/25/11 11:00	2.43	2797	494	78	78	0	2209	1325	383	230
9/25/11 11:15	2.45	1834	400	51	51	2256	0	0	0	0
9/25/11 11:30	2.47	2953	507	80	80	0	2878	1727	499	299
9/25/11 11:45	2.42	1645	377	43	43	3188	0	0	0	0
9/25/11 12:00	2.50	2670	480	69	69	0	2752	1651	477	286
9/25/11 12:15	2.59	1719	384	44	44	2195	0	0	0	0
9/25/11 12:30	2.65	1461	354	37	37	554	0	0	0	0
9/25/11 12:45	2.60	942	284	24	24	1352	0	0	0	0
9/25/11 13:00	2.56	686	243	17	17	647	0	0	0	0
9/25/11 13:15	2.59	681	241	16	16	0	20	12	3	2
9/25/11 13:30	2.70	1021	295	25	25	0	1000	600	173	104

Seep 1 cont. Date/time of measurement	Water depth (m)	Total Radon in Water (dpm/m3)	1-sig-error	5: Atm. Flux (dpm/m2/15 min)	1-sig-error	Mixing losses (dpm/m2/15 min)	Total radon flux (dpm/m2/15 min)	1-sig-error	Advection rate (cm/d)	1-sig-error
9/25/11 13:45	2.62	939	283	23	23	199	0	0	0	0
9/25/11 14:00	2.62	597	226	15	15	882	0	0	0	0
9/25/11 14:15	2.65	1110	308	27	27	0	1399	839	242	145
9/25/11 14:30	2.71	941	284	23	23	377	0	0	0	0
9/25/11 14:41	2.63	1371	560	34	34	0	1197	718	208	125

Table D-4. Radon surface-water coastal survey data, September 2011.
Radon activities(dpm/m3) measured in the surface 0.5 m during a coastal survey on September 22, 2011.

Latitude	Longitude	Date/time of measurement	Total Radon in Water (dpm/m3)	1-sig-error
20.8946	-156.6864	9/22/11 9:01	810	468
20.8961	-156.6863	9/22/11 9:06	264	264
20.8975	-156.6863	9/22/11 9:11	530	375
20.8991	-156.6863	9/22/11 9:16	809	467
20.9004	-156.6864	9/22/11 9:21	1081	540
20.9022	-156.6865	9/22/11 9:27	0	0
20.9035	-156.6868	9/22/11 9:32	1622	662
20.9053	-156.6876	9/22/11 9:37	811	468
20.9069	-156.6891	9/22/11 9:42	813	469
20.9086	-156.6909	9/22/11 9:47	1358	607
20.9099	-156.6929	9/22/11 9:52	1348	603
20.9114	-156.6949	9/22/11 9:57	539	381
20.9130	-156.6962	9/22/11 10:02	269	269
20.9149	-156.6966	9/22/11 10:07	813	470
20.9166	-156.6969	9/22/11 10:12	544	385
20.9185	-156.6971	9/22/11 10:17	813	469
20.9202	-156.6973	9/22/11 10:22	264	264
20.9218	-156.6971	9/22/11 10:27	270	270
20.9245	-156.6965	9/22/11 10:32	0	0
20.9261	-156.6964	9/22/11 10:34	0	0
20.9271	-156.6962	9/22/11 10:39	531	376
20.9287	-156.6959	9/22/11 10:45	1902	719
20.9309	-156.6945	9/22/11 10:54	795	459
20.9315	-156.6939	9/22/11 10:58	0	0
20.9316	-156.6939	9/22/11 11:03	264	264
20.9339	-156.6934	9/22/11 11:08	0	0
20.9351	-156.6935	9/22/11 11:13	529	374
20.9364	-156.6934	9/22/11 11:18	793	458
20.9386	-156.6932	9/22/11 11:22	528	374
20.9400	-156.6930	9/22/11 11:27	793	458
20.9414	-156.6930	9/22/11 11:31	532	376
20.9433	-156.6929	9/22/11 11:36	1059	530
20.9459	-156.6923	9/22/11 11:43	529	374
20.9471	-156.6921	9/22/11 11:46	534	378
20.9493	-156.6917	9/22/11 11:53	546	386
20.9504	-156.6915	9/22/11 11:57	541	382
20.9522	-156.6907	9/22/11 12:00	264	264

Latitude	Longitude	Date/time of measurement	Total Radon in Water (dpm/m3)	1-sig-error
20.9538	-156.6894	9/22/11 12:08	0	0
20.9545	-156.6887	9/22/11 12:12	541	382
20.9558	-156.6883	9/22/11 12:16	264	264
20.9563	-156.6887	9/22/11 12:20	270	270
20.9537	-156.6939	9/22/11 12:33	541	382
20.9525	-156.6948	9/22/11 12:36	0	0
20.9507	-156.6960	9/22/11 12:42	269	269
20.9481	-156.6972	9/22/11 12:46	0	0
20.9465	-156.6981	9/22/11 12:50	537	380
20.9433	-156.6991	9/22/11 12:57	267	267
20.9407	-156.7003	9/22/11 13:03	262	262
20.9391	-156.7008	9/22/11 13:05	0	0
20.9381	-156.7008	9/22/11 13:10	267	267
20.9370	-156.7009	9/22/11 13:15	0	0
20.9365	-156.7001	9/22/11 13:20	0	0
20.9366	-156.6993	9/22/11 13:25	0	0
20.9366	-156.6983	9/22/11 13:30	0	0
20.9371	-156.6973	9/22/11 13:35	0	0
20.9376	-156.6965	9/22/11 13:40	0	0
20.9395	-156.6953	9/22/11 13:47	0	0
20.9441	-156.6944	9/22/11 13:52	0	0
20.9443	-156.6964	9/22/11 13:57	268	268
20.9394	-156.6986	9/22/11 14:02	267	267
20.9346	-156.7007	9/22/11 14:07	804	464
20.9237	-156.7020	9/22/11 14:12	0	0
20.9181	-156.7011	9/22/11 14:18	0	0
20.9138	-156.6989	9/22/11 14:22	0	0

APPENDIX E: SPATIAL DISTRIBUTION OF GEOCHEMICAL PARAMETERS

APPENDIX FOR SECTION 6:

AQUEOUS GEOCHEMISTRY AND STABLE ISOTOPES

This page is intentionally left blank.
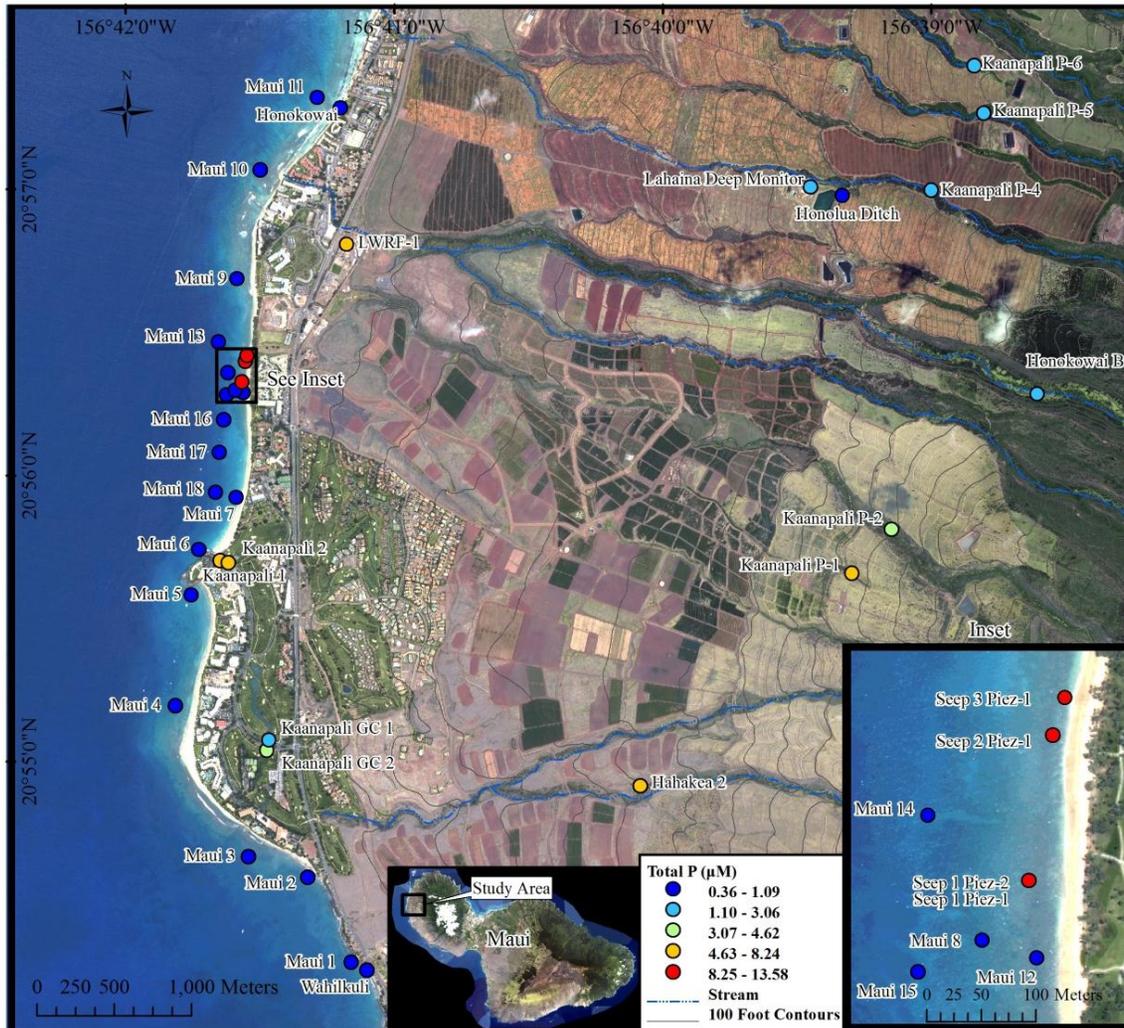
Figure E-1: June, 2011 TP distribution.
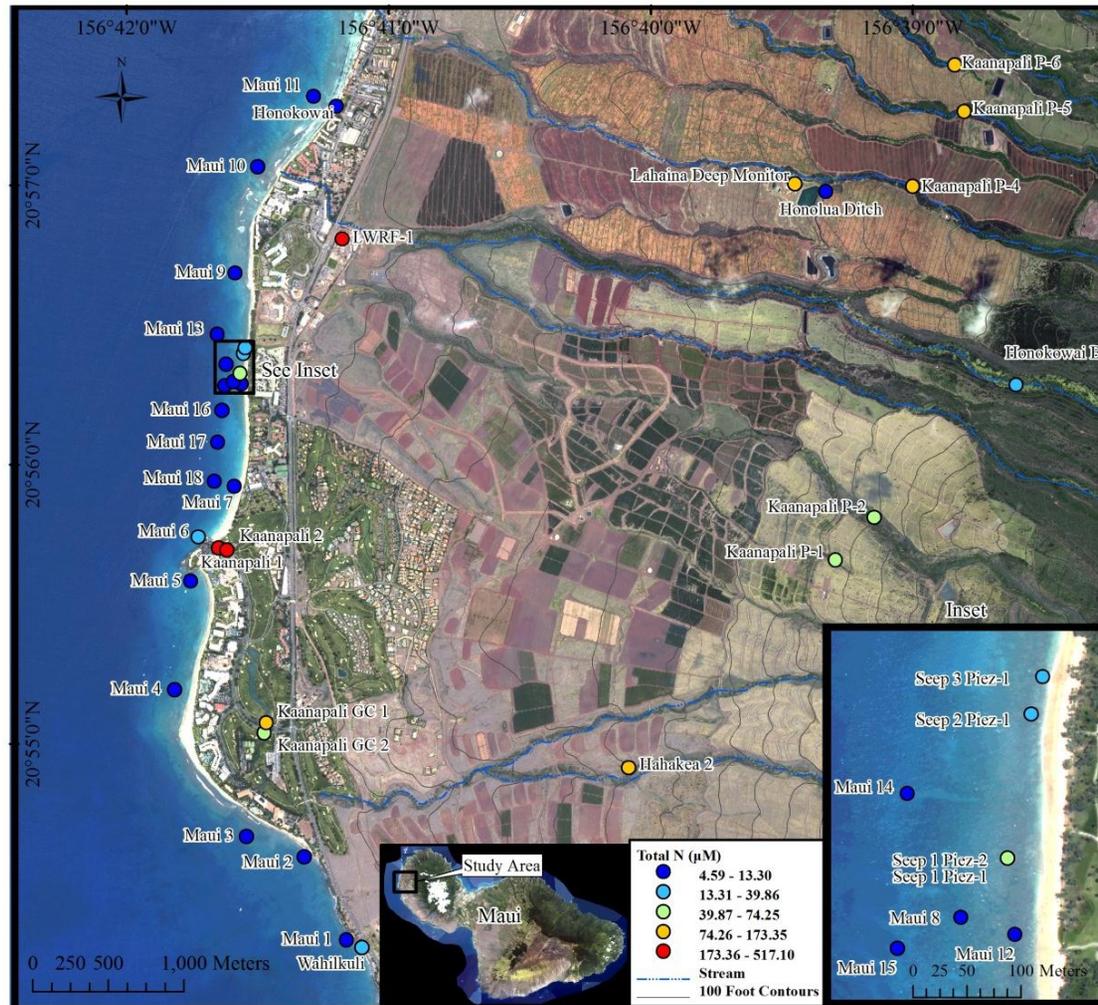
Figure E-2: June, 2011 TN distribution.

Figure E-3: June, 2011 Temperature Distribution.
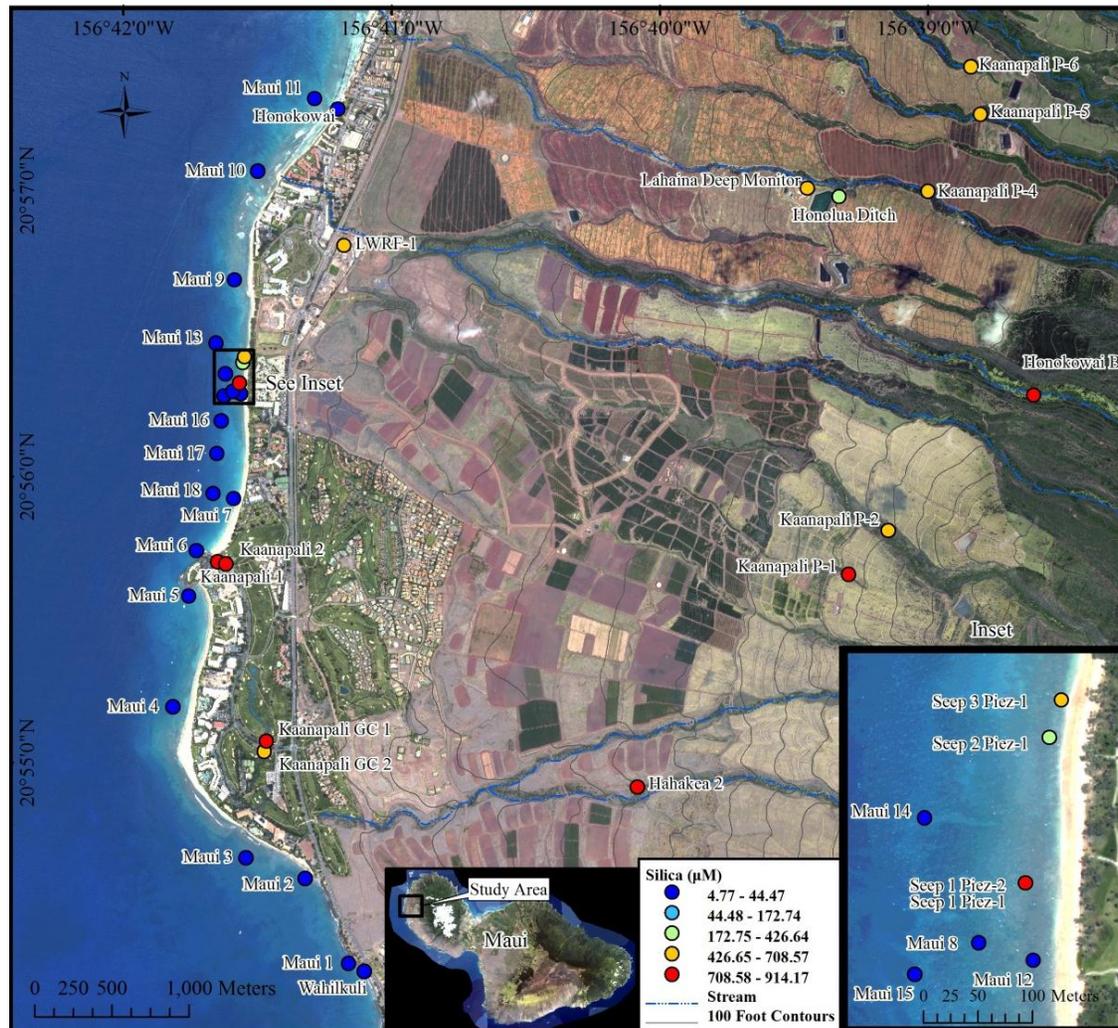
Figure E-4: June, 2011 SiO_4^{4-} distribution.
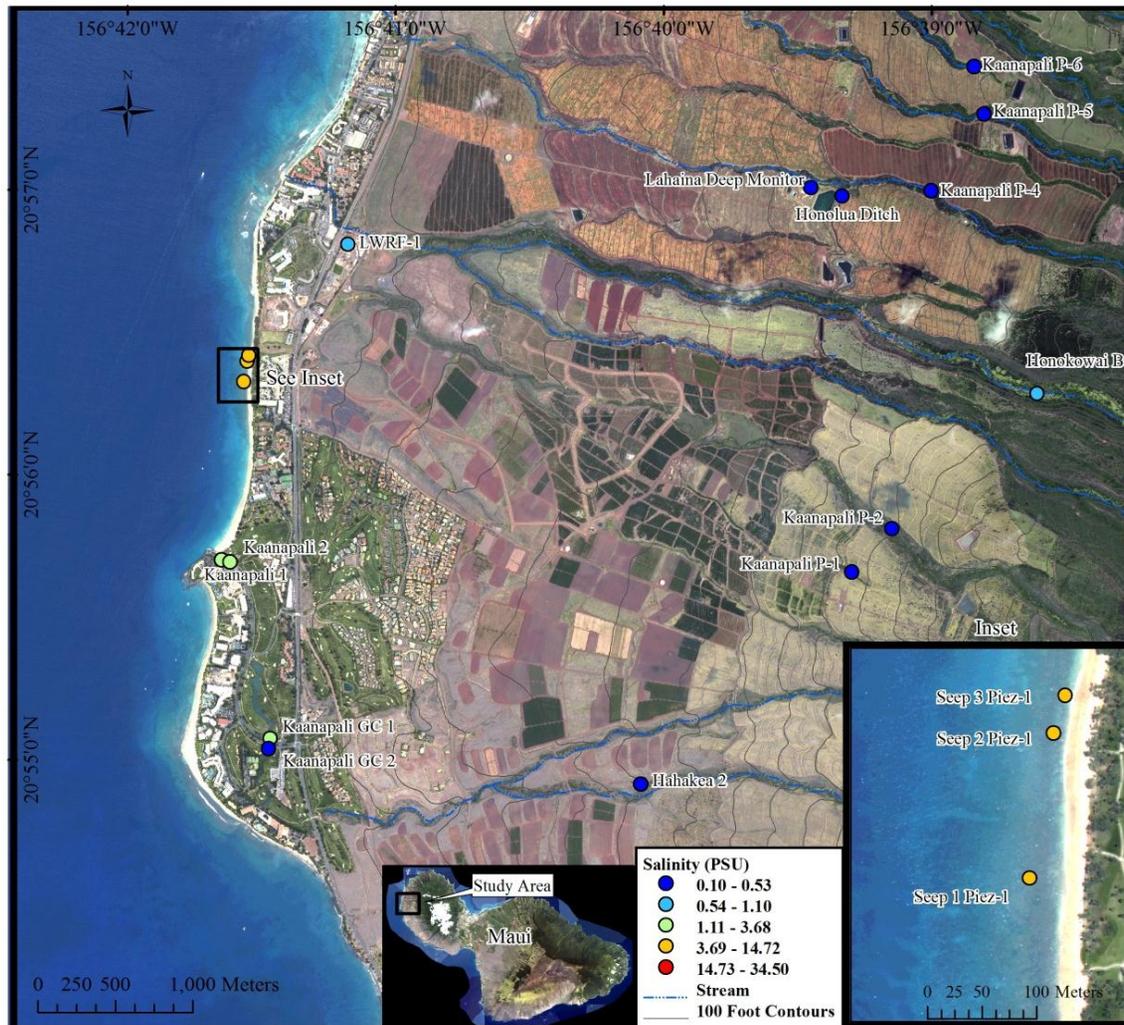
Figure E-5: June, 2011 Salinity distribution.
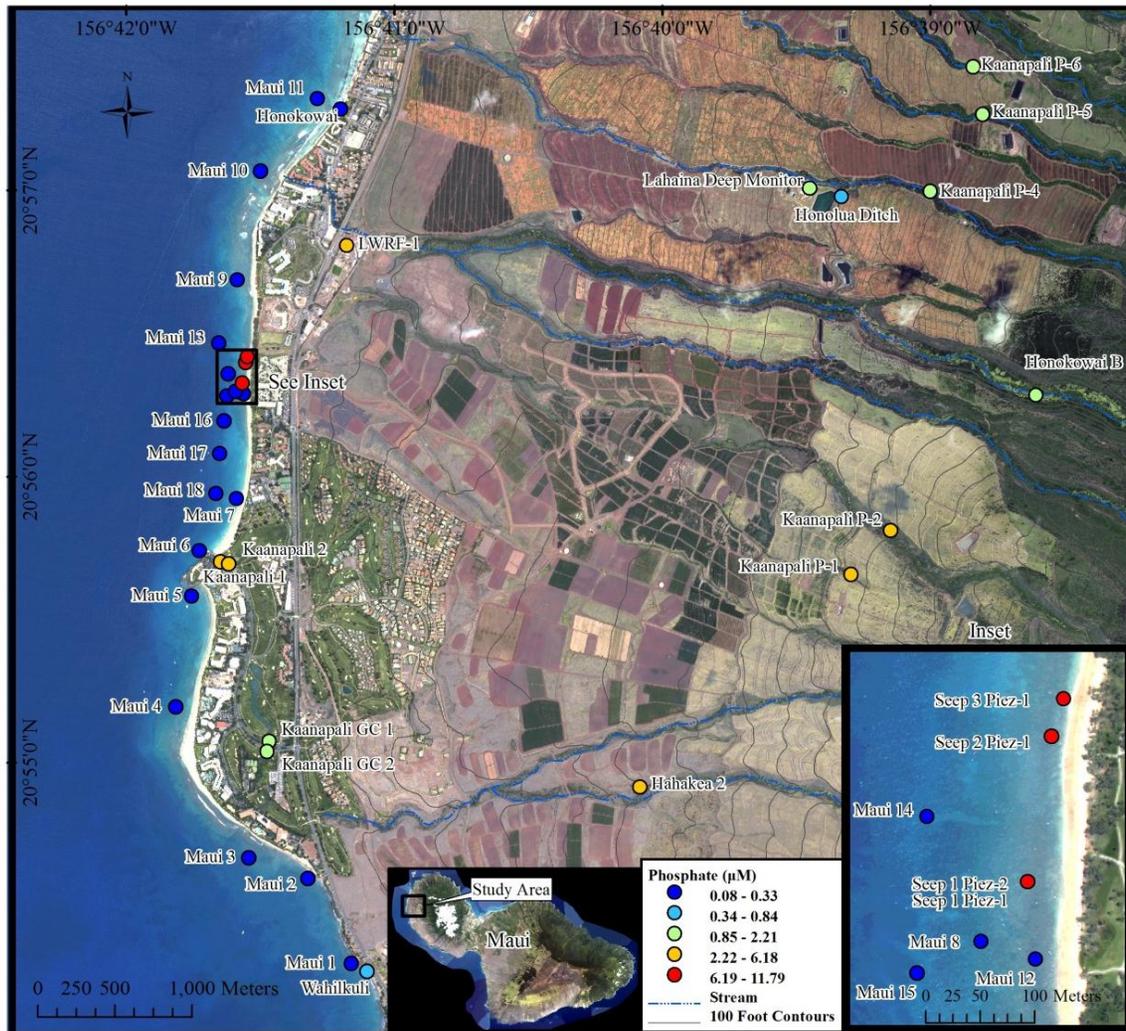
Figure E-6: June, 2011 PO$_4^{3-}$ distribution.
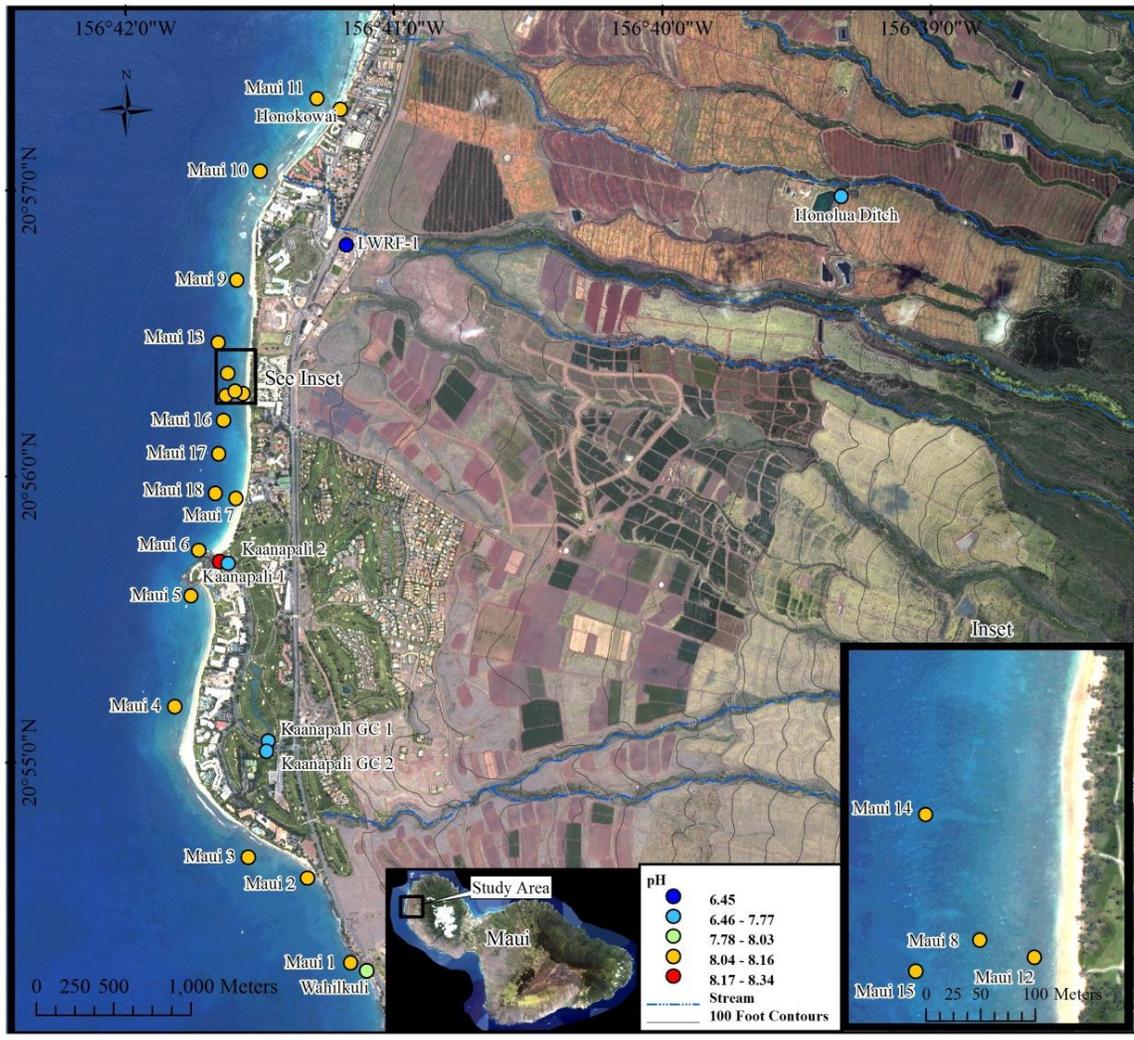
Figure E-7: June, 2011 pH distribution.
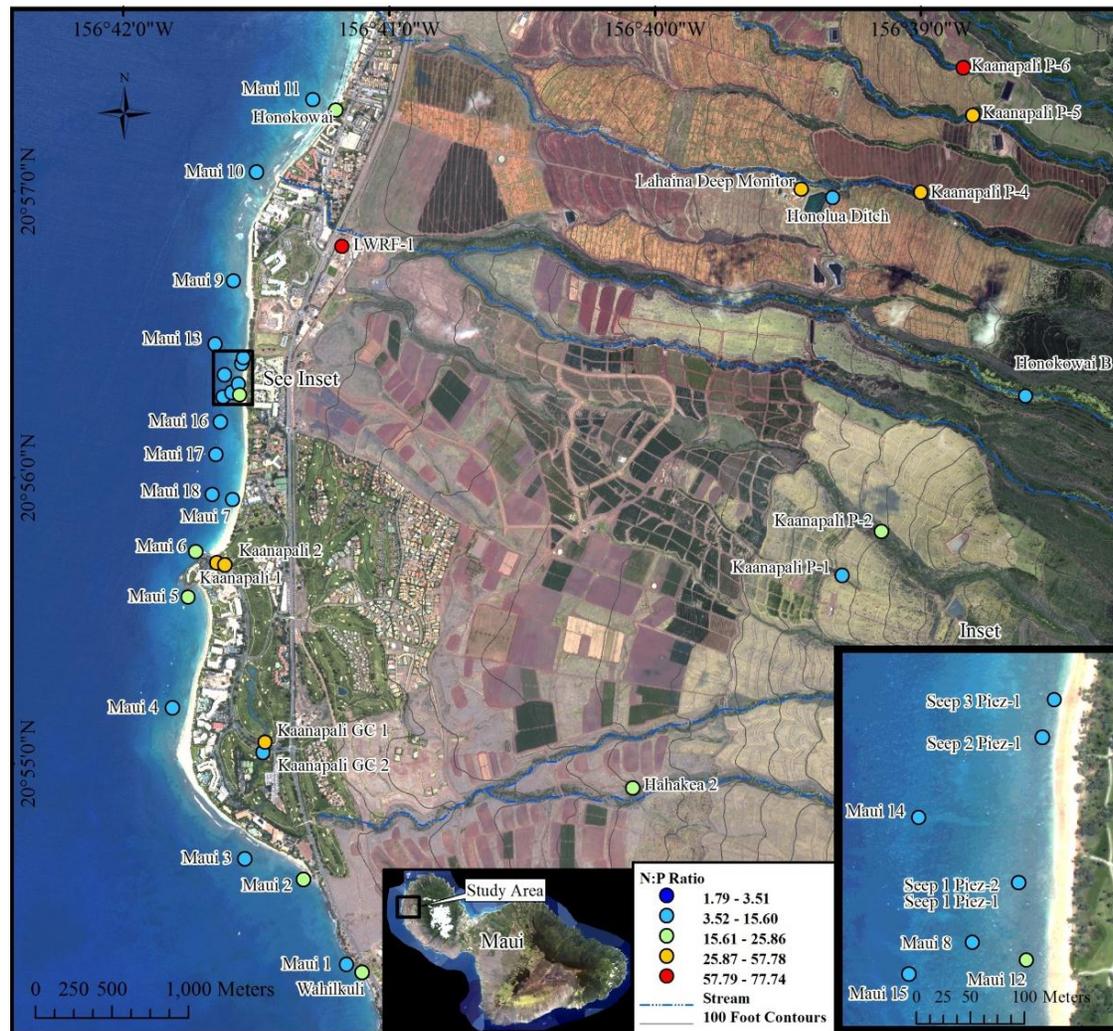
Figure E-8: June, 2011 N:P ratio distribution.
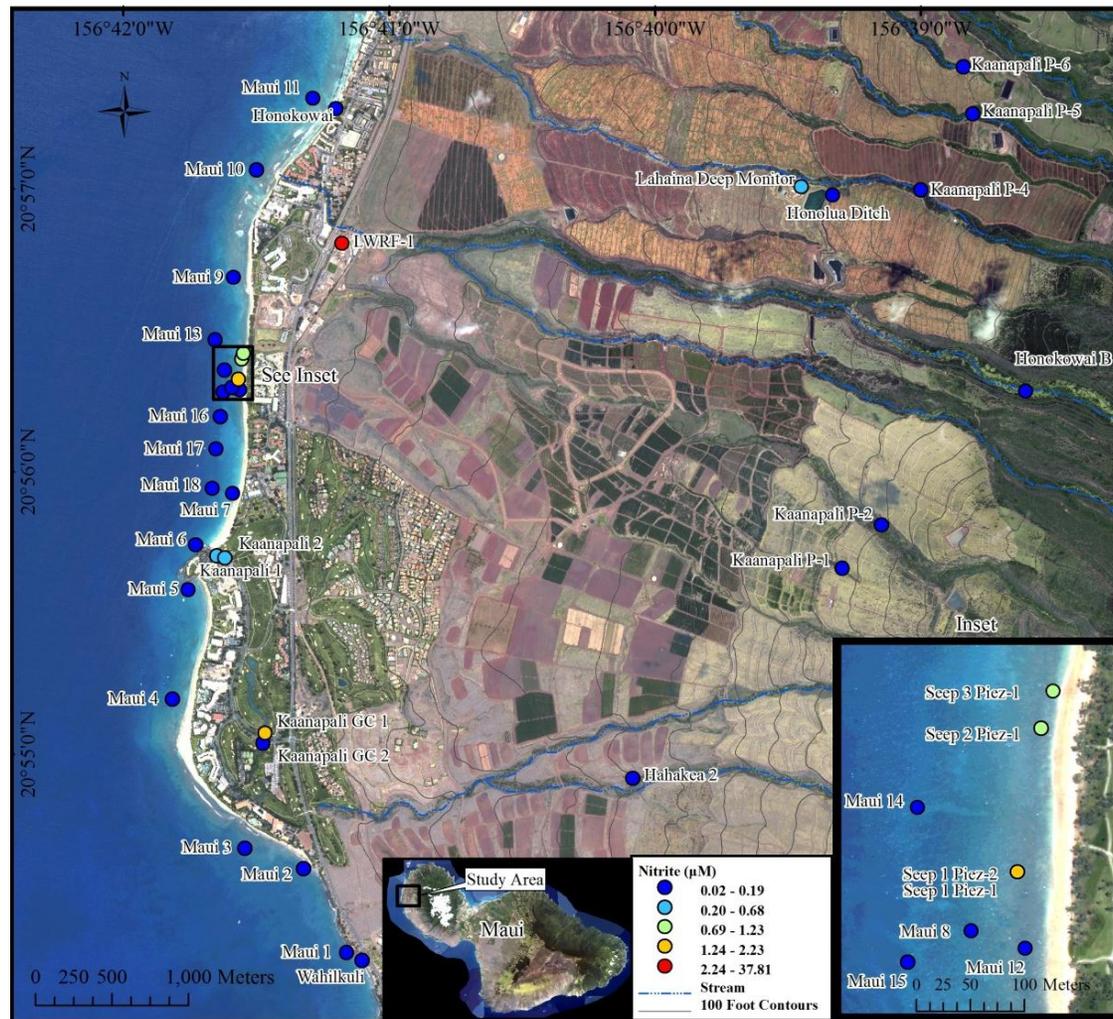
Figure E-9: June, 2011 NO$_2^-$ distribution.
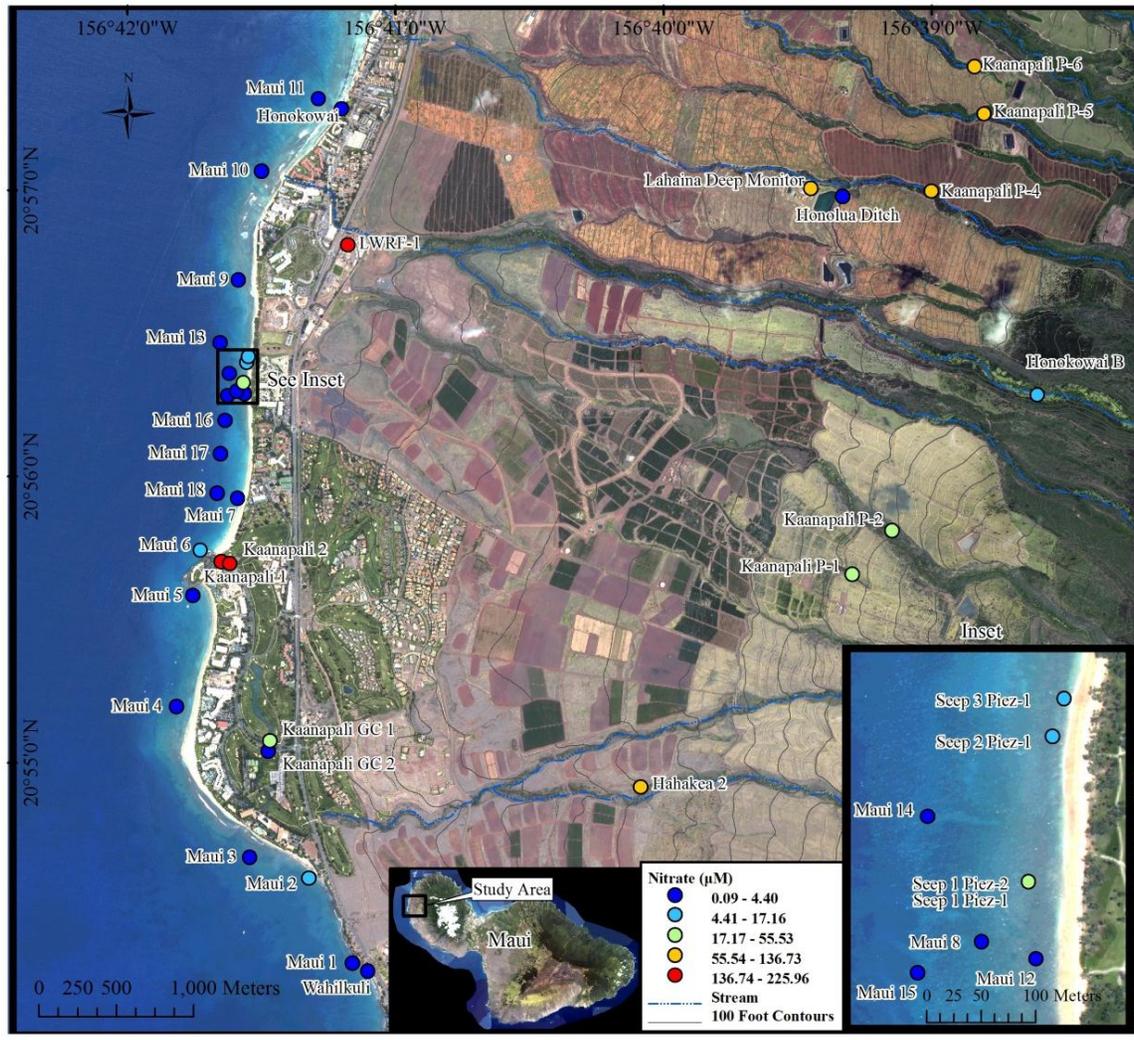
Figure E-10: June, 2011 NO$_3^-$ distribution.
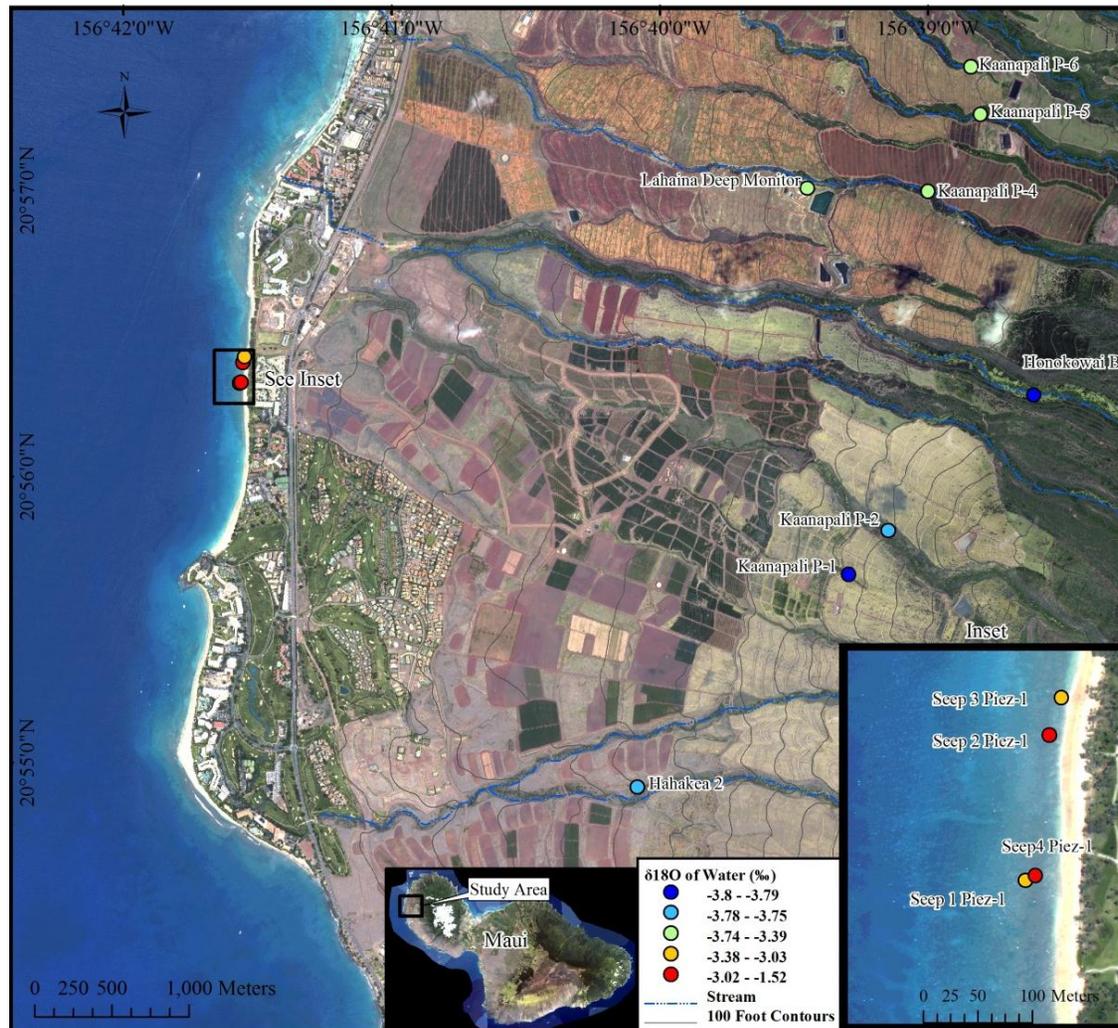
Figure E-11: June, 2011 $\delta^{18}O$ of H_2O distribution.
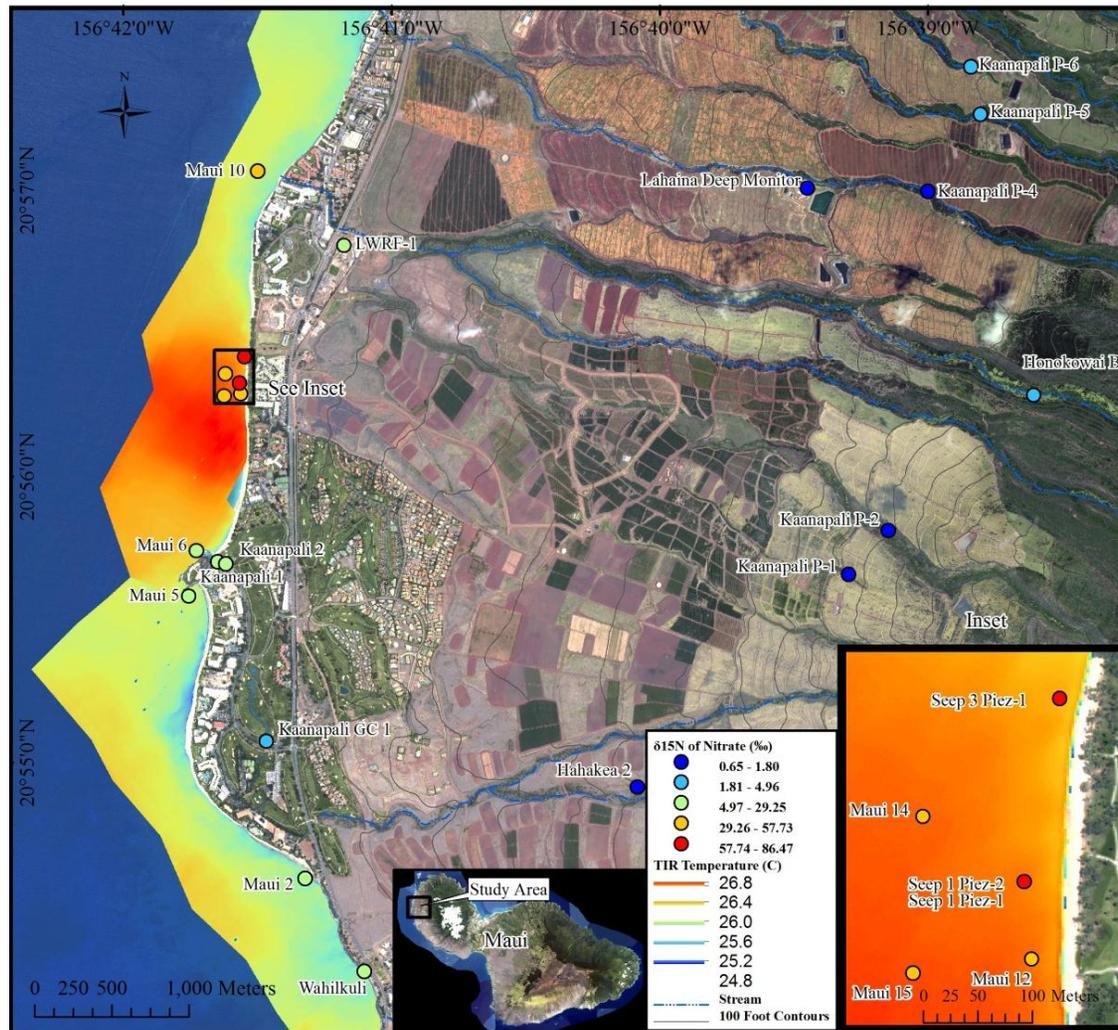
Figure E-12: June, 2011 $\delta^{15}N$ of NO_3^- distribution with TIR temperature overlay.
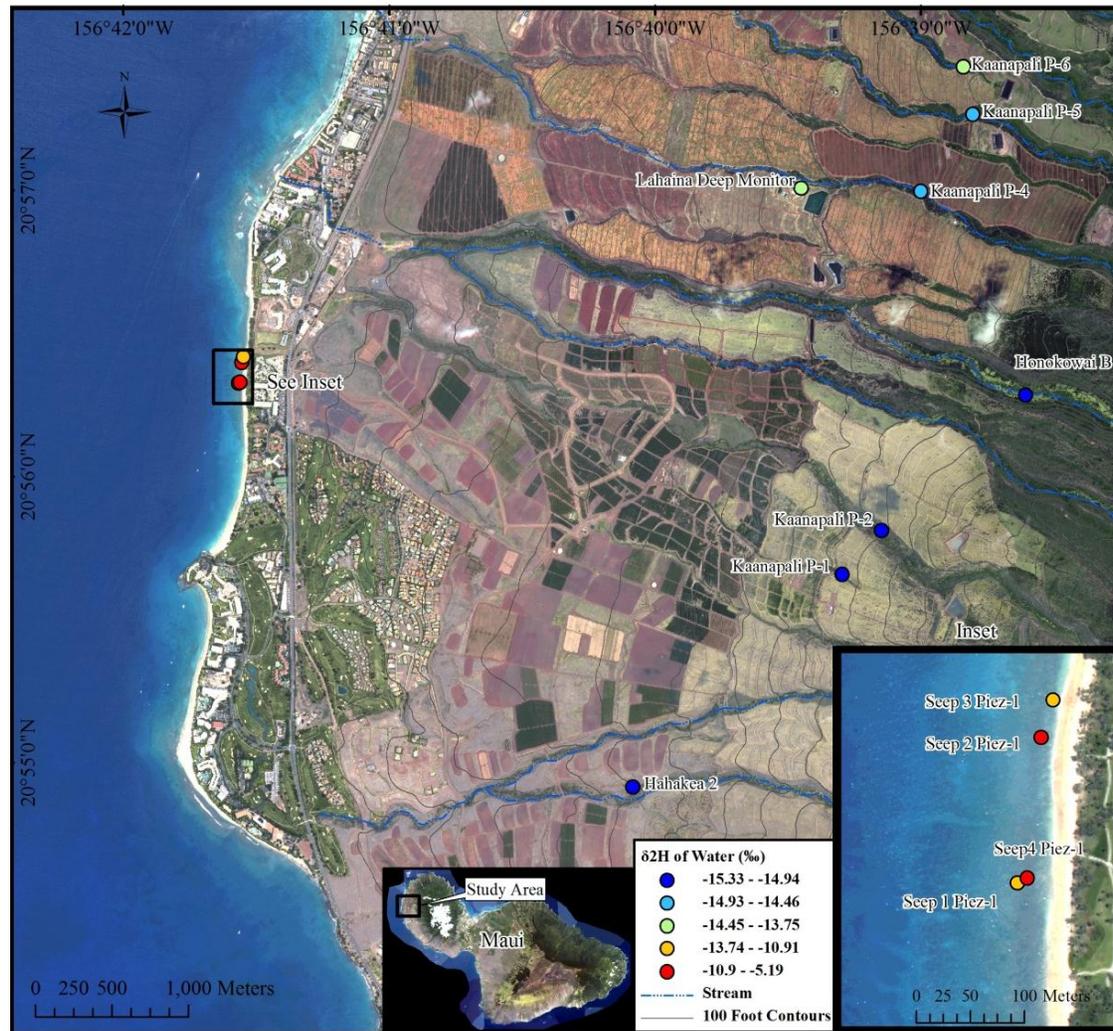
Figure E-13: June, 2011 δ^2H of H$_2$O distribution.
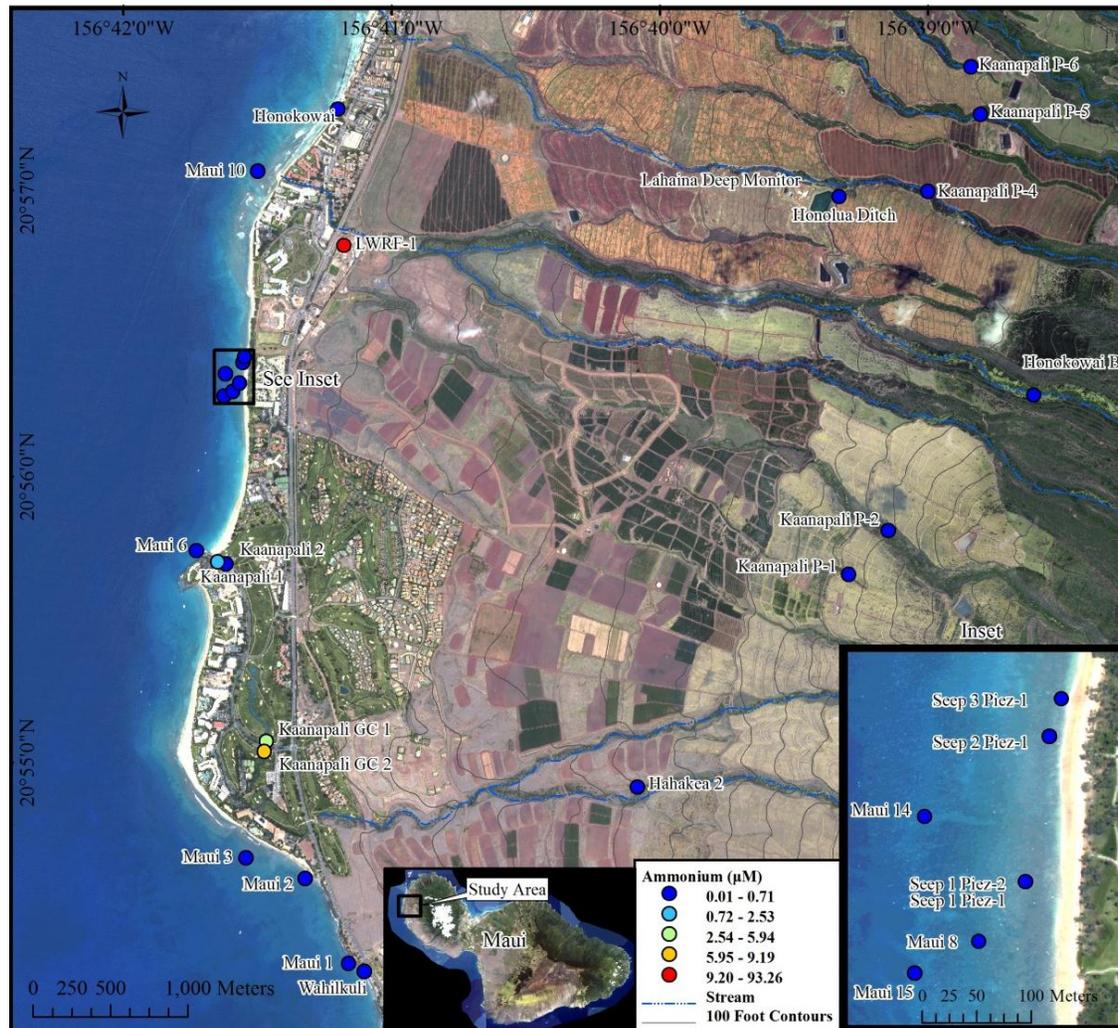
Figure E-14: June, 2011 NH_4^+ distribution.
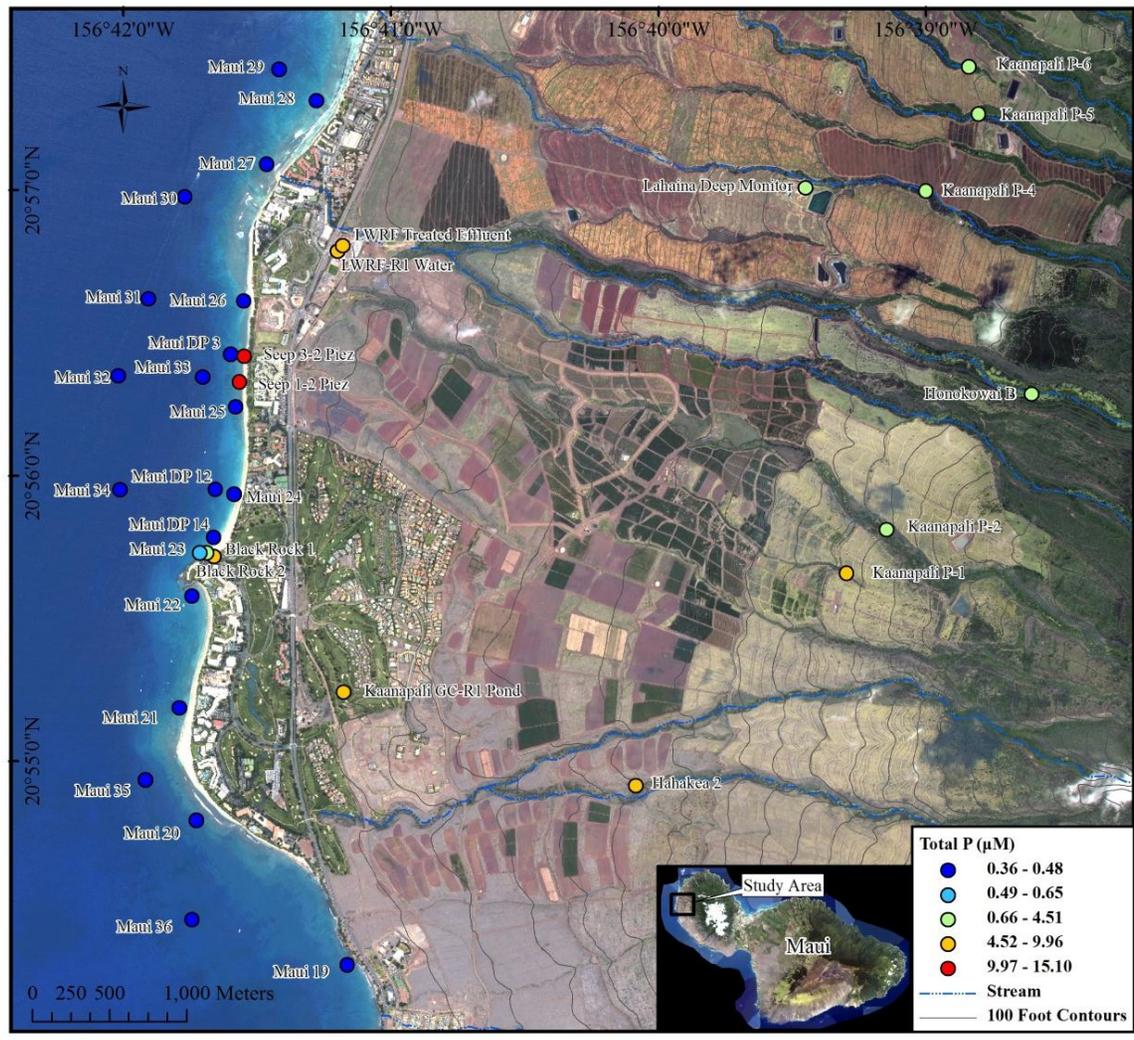
Figure E-15: September, 2011 TP distribution.
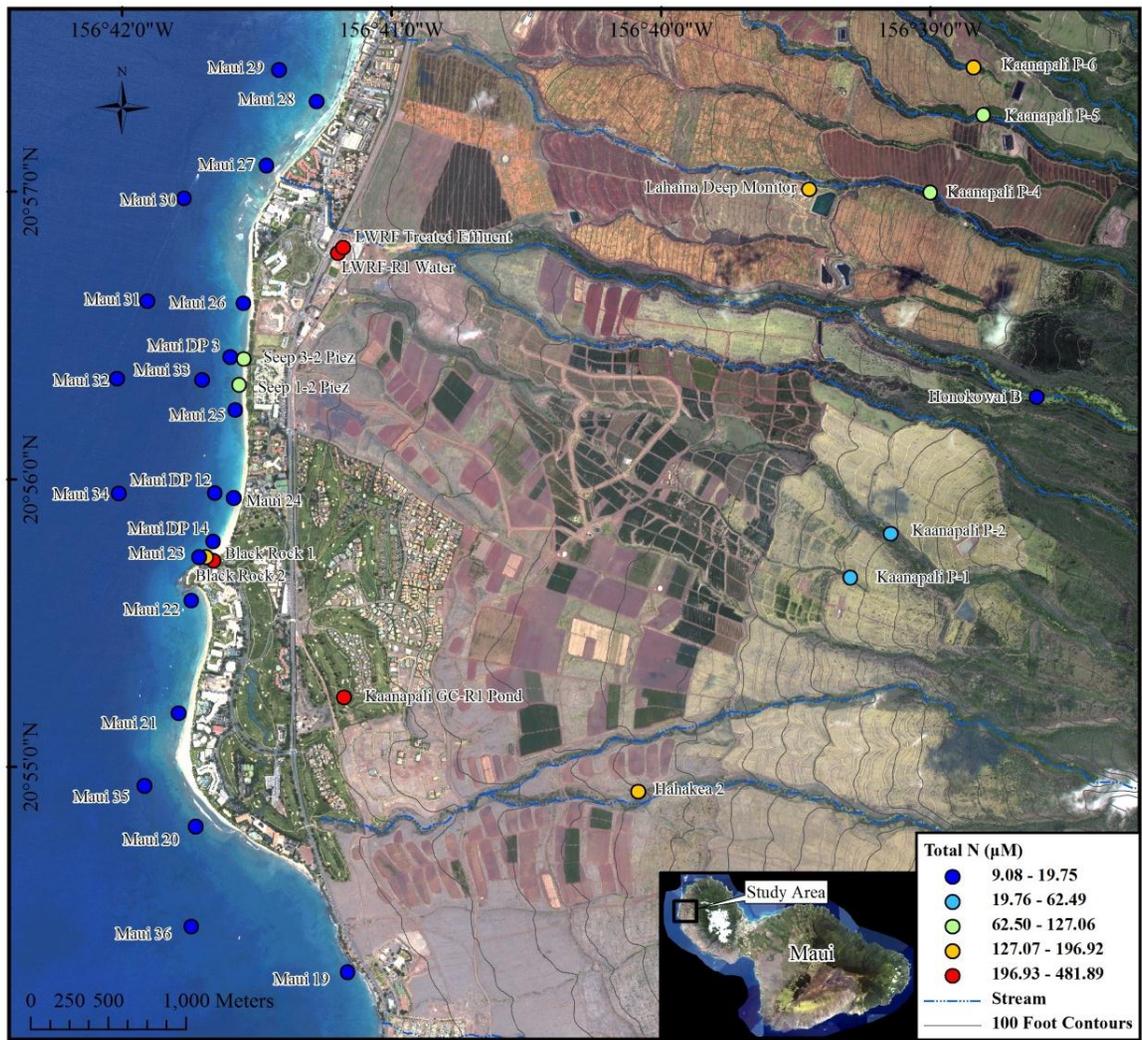
Figure E-16: September, 2011 TN distribution.
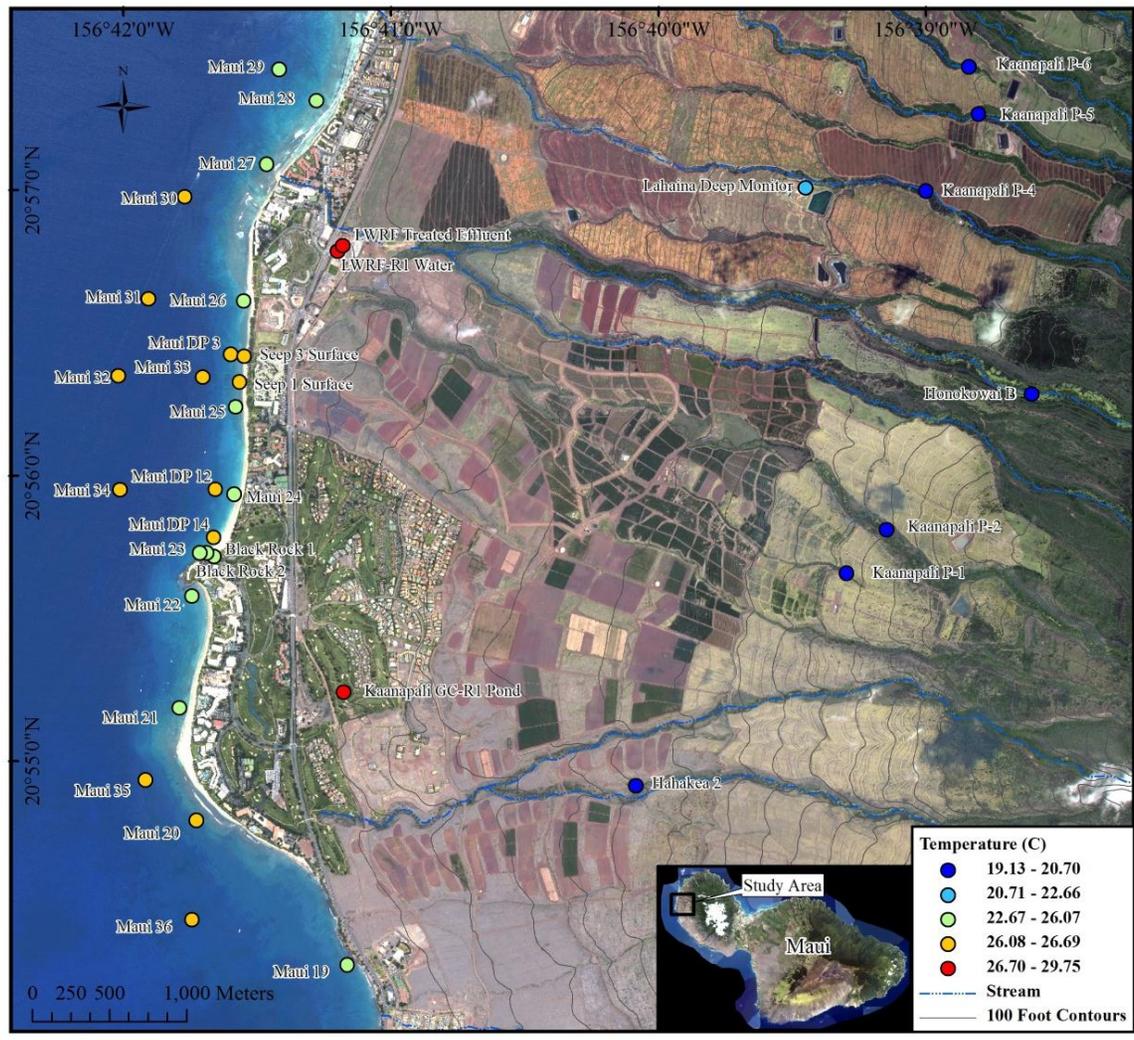
Figure E-17: September, 2011 Temperature distribution.
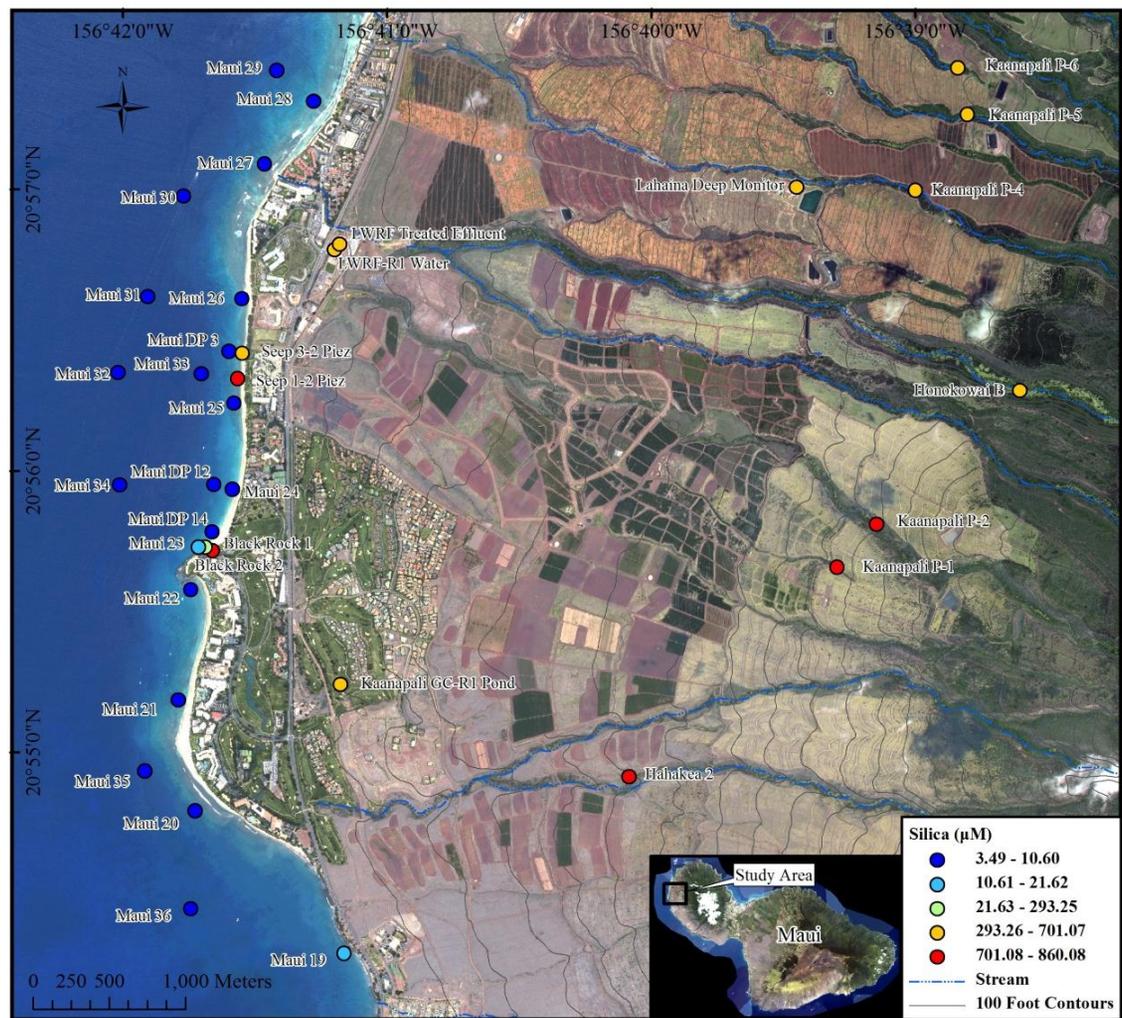
Figure E-18: September, 2011 SiO_4^{4-} distribution.
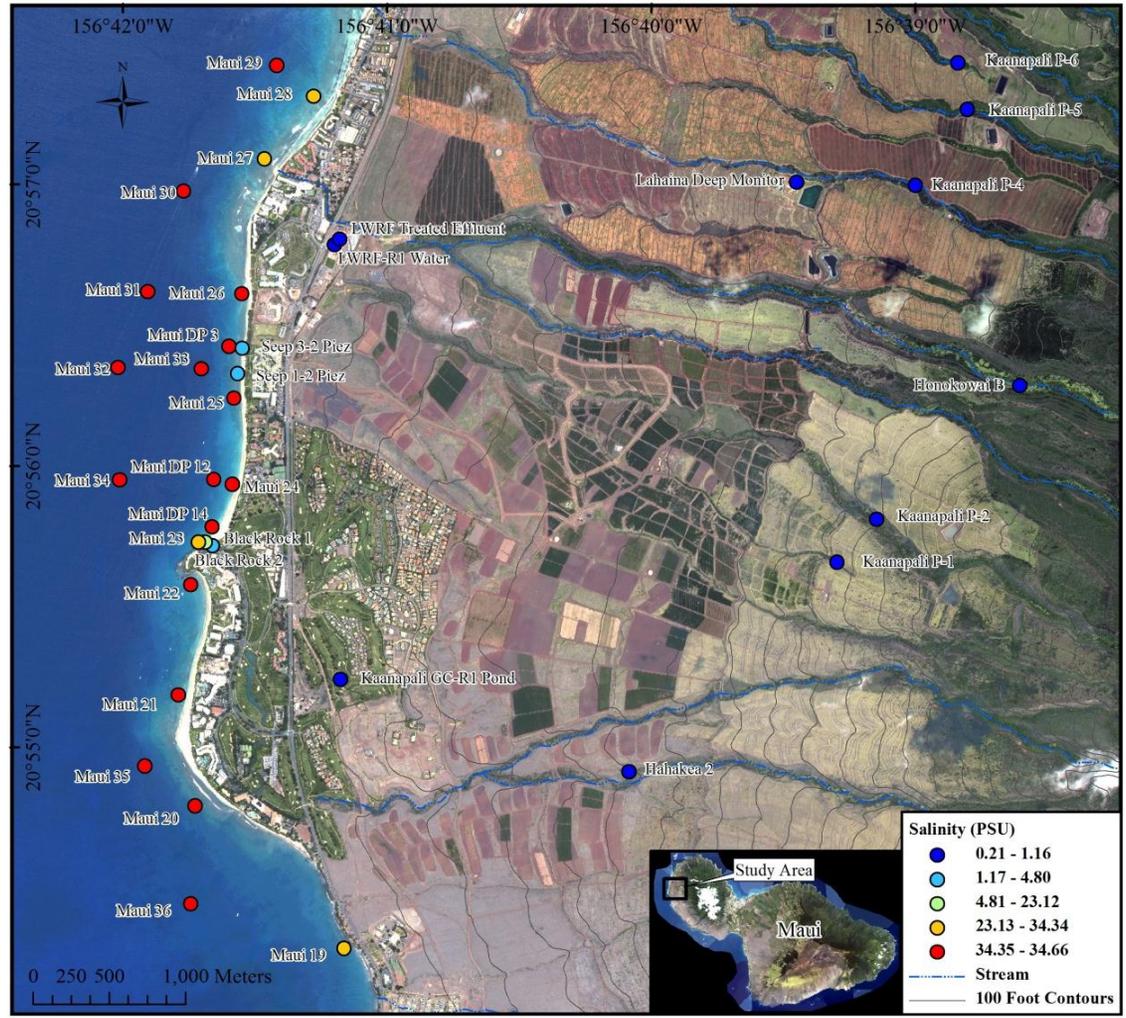
Figure E-19: September, 2011 Salinity distribution.
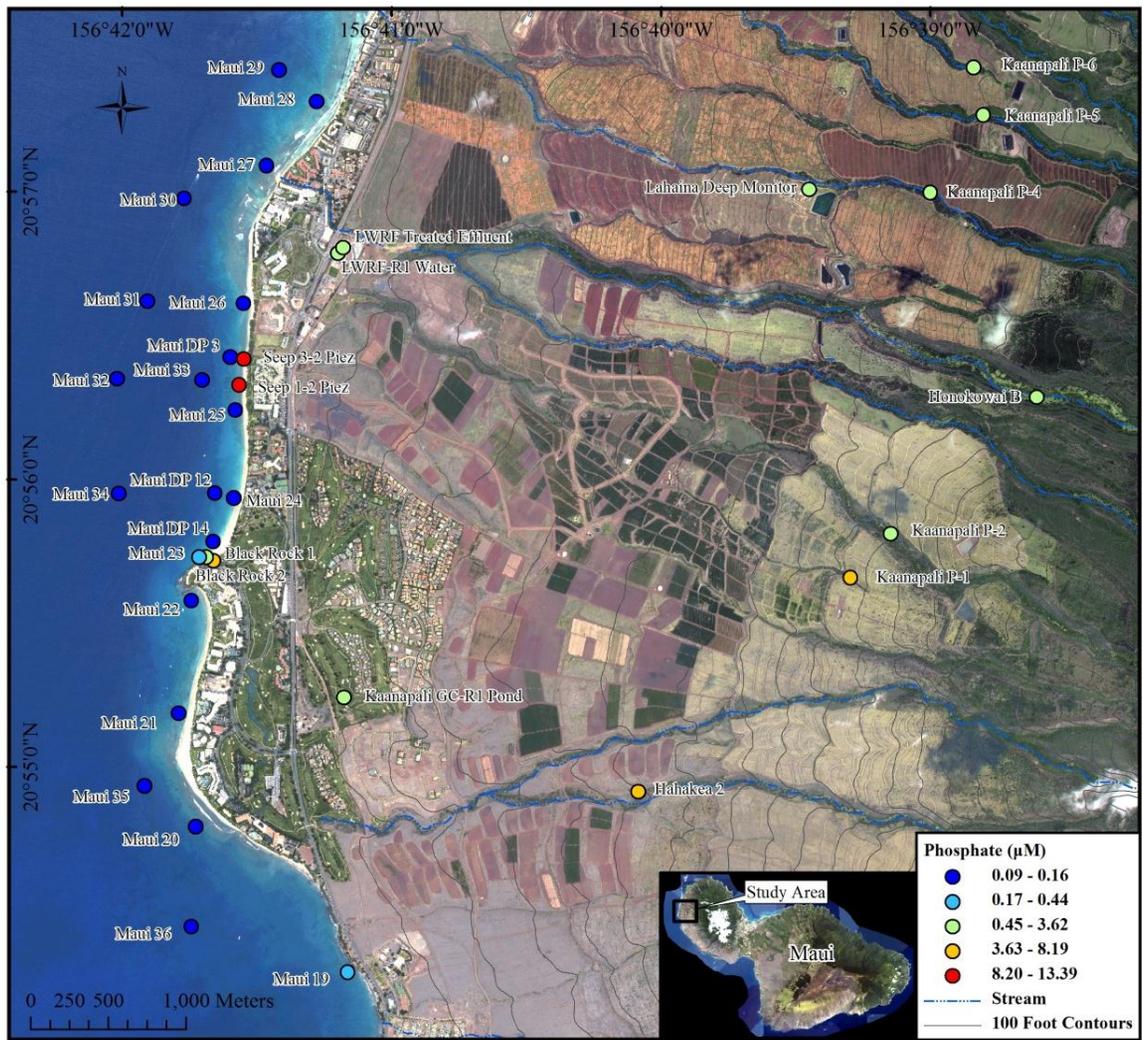
Figure E-20: September, 2011 PO_4^{3-} distribution.
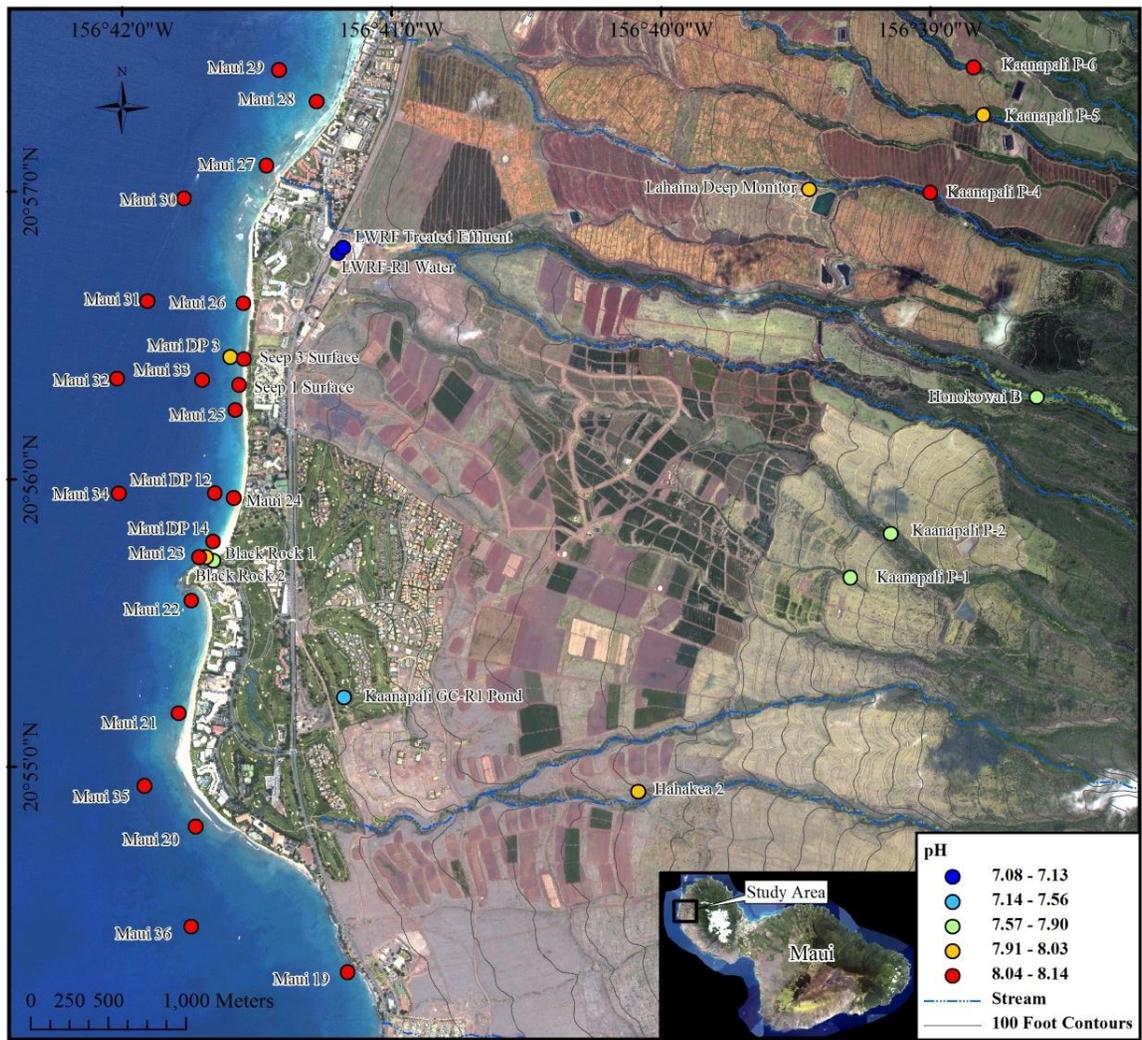
Figure E-21: September, 2011 pH distribution.
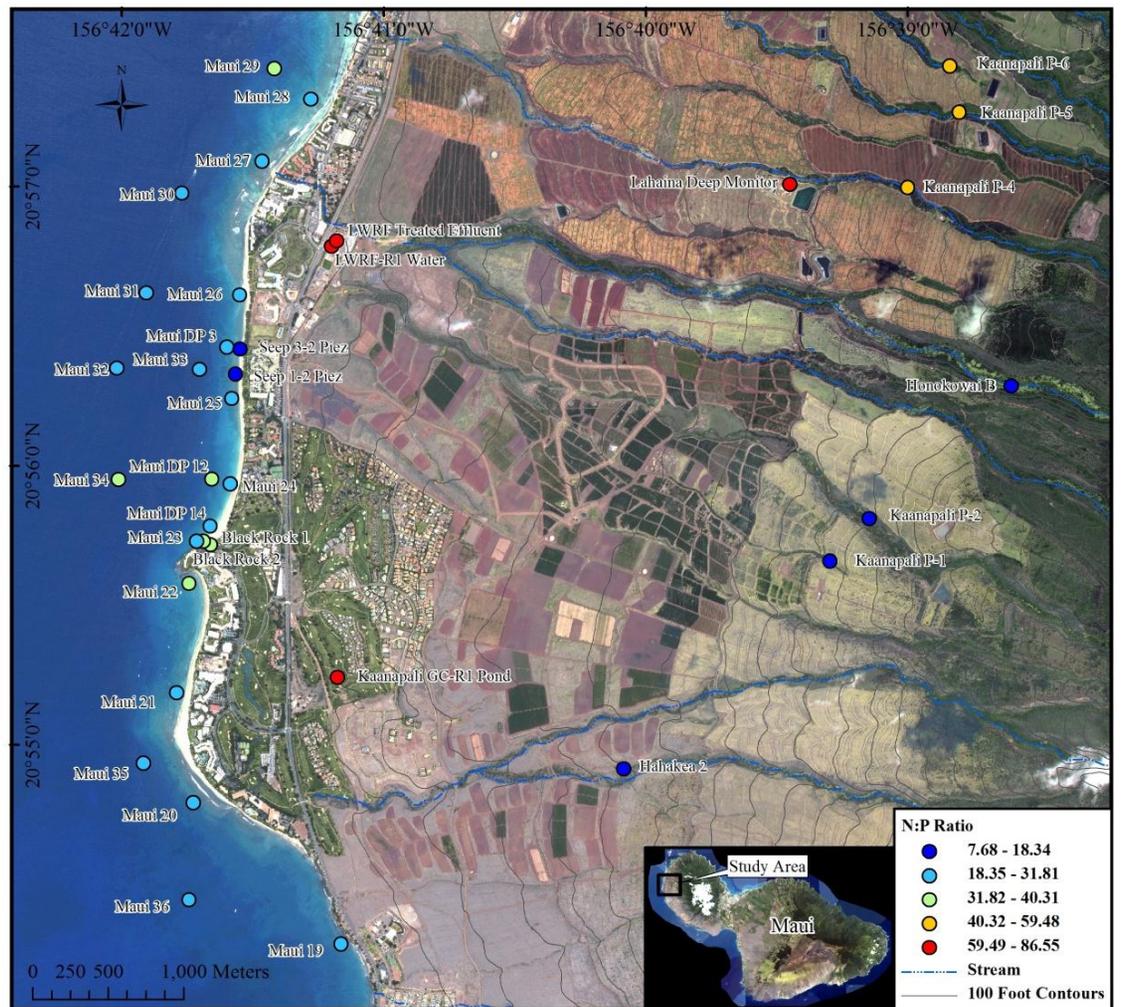
Figure E-22: September, 2011 N:P ratio distribution
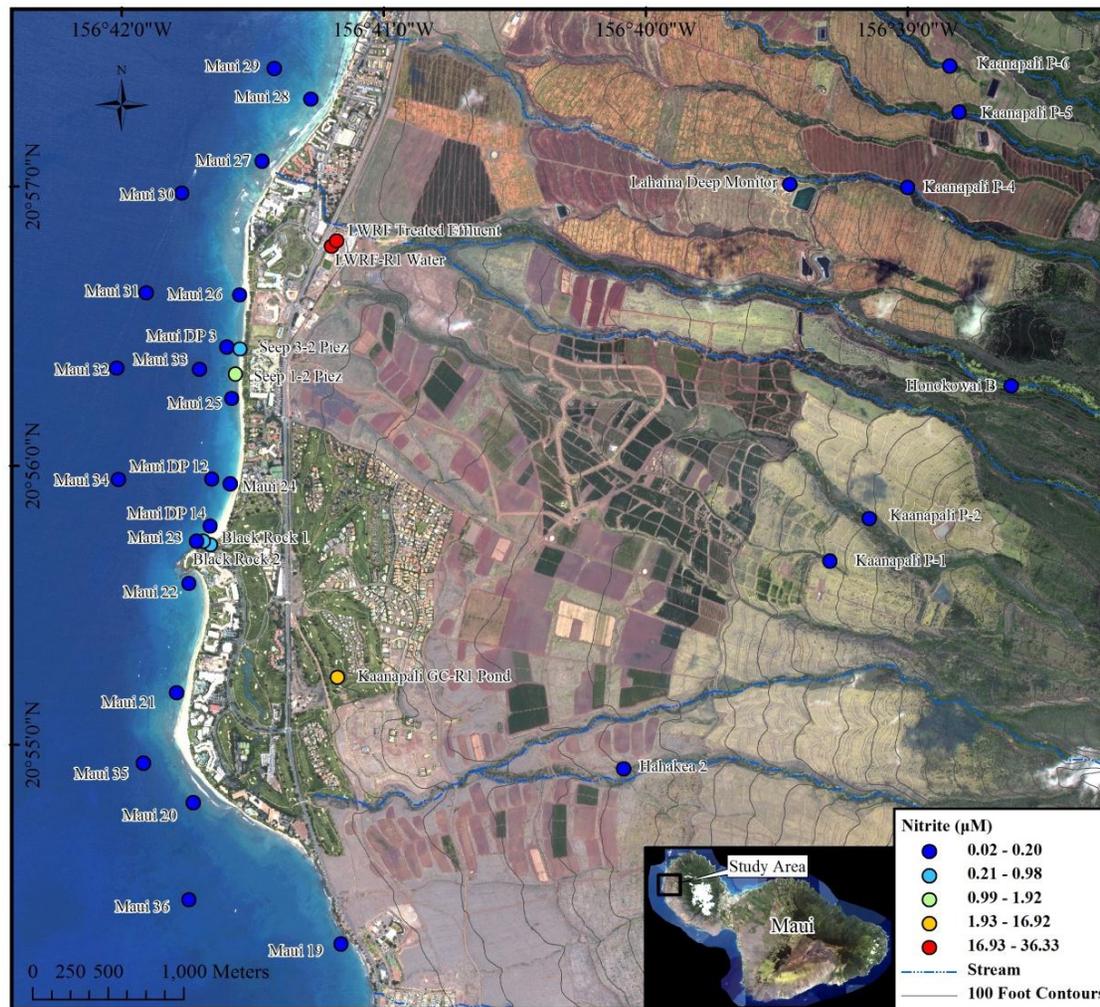
Figure E-23: September, 2011 NO$_2^-$ distribution.
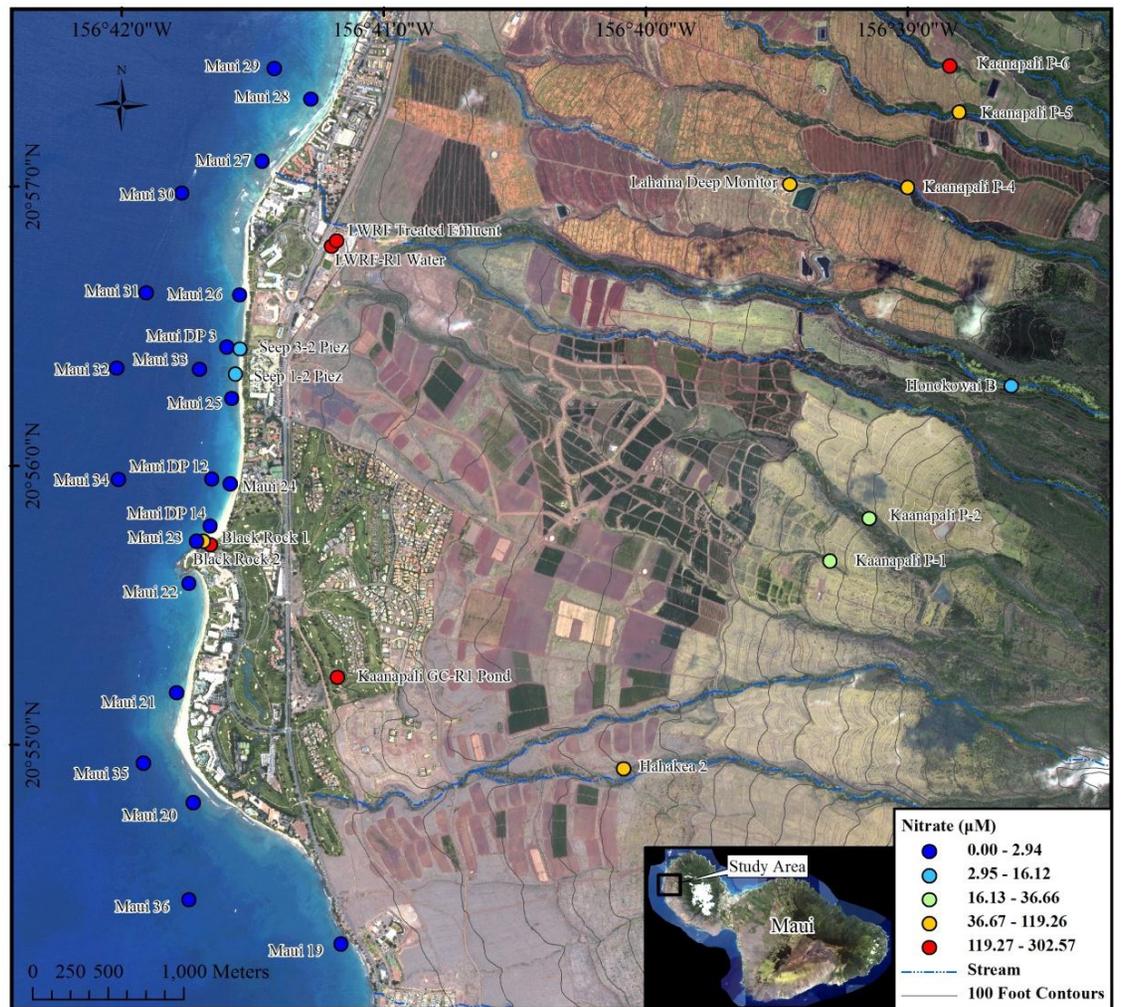
Figure E-24: September, 2011 NO$_3^-$ distribution.
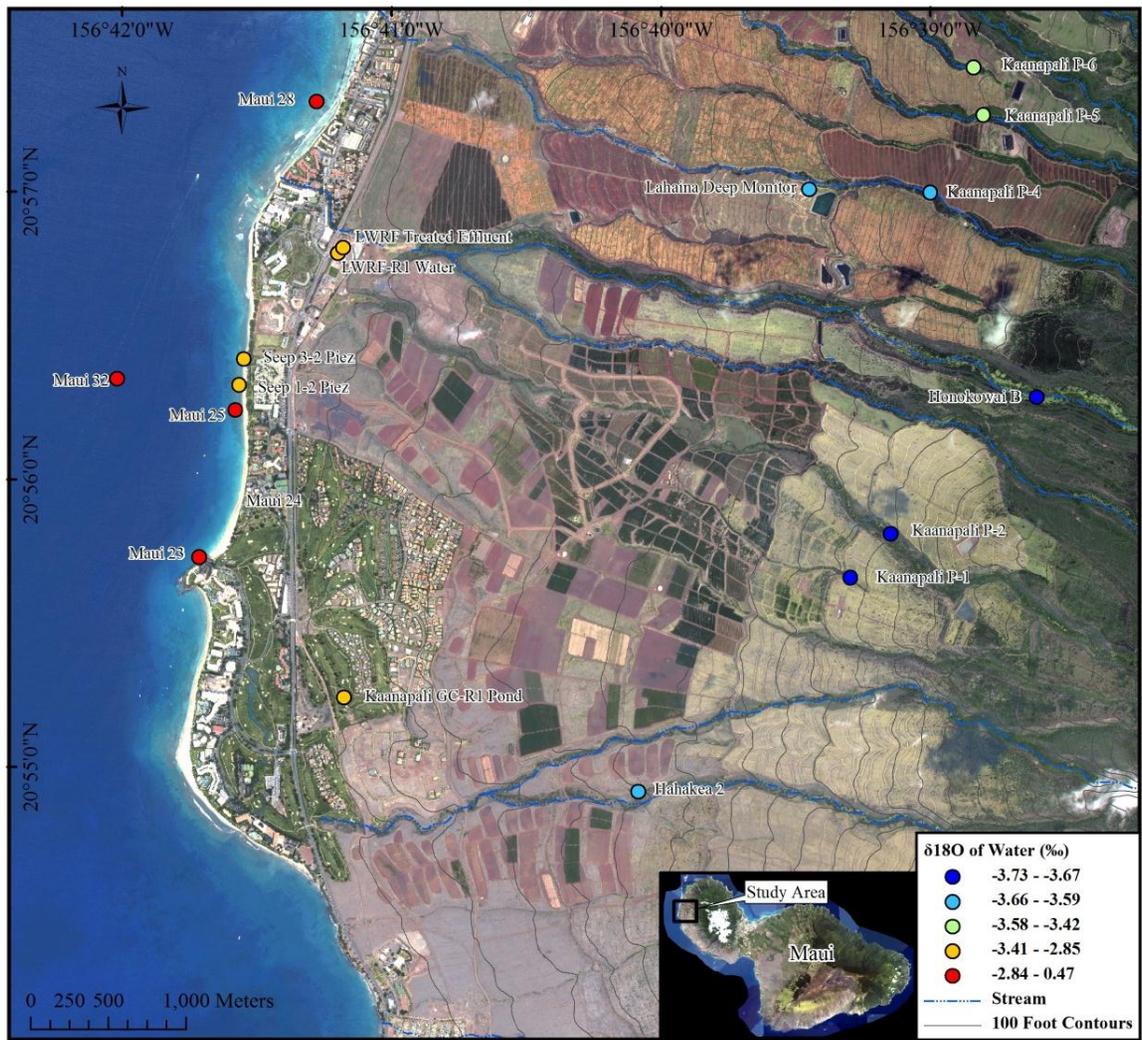
Figure E-25: September, 2011 δ^{18}O of H$_2$O distribution.
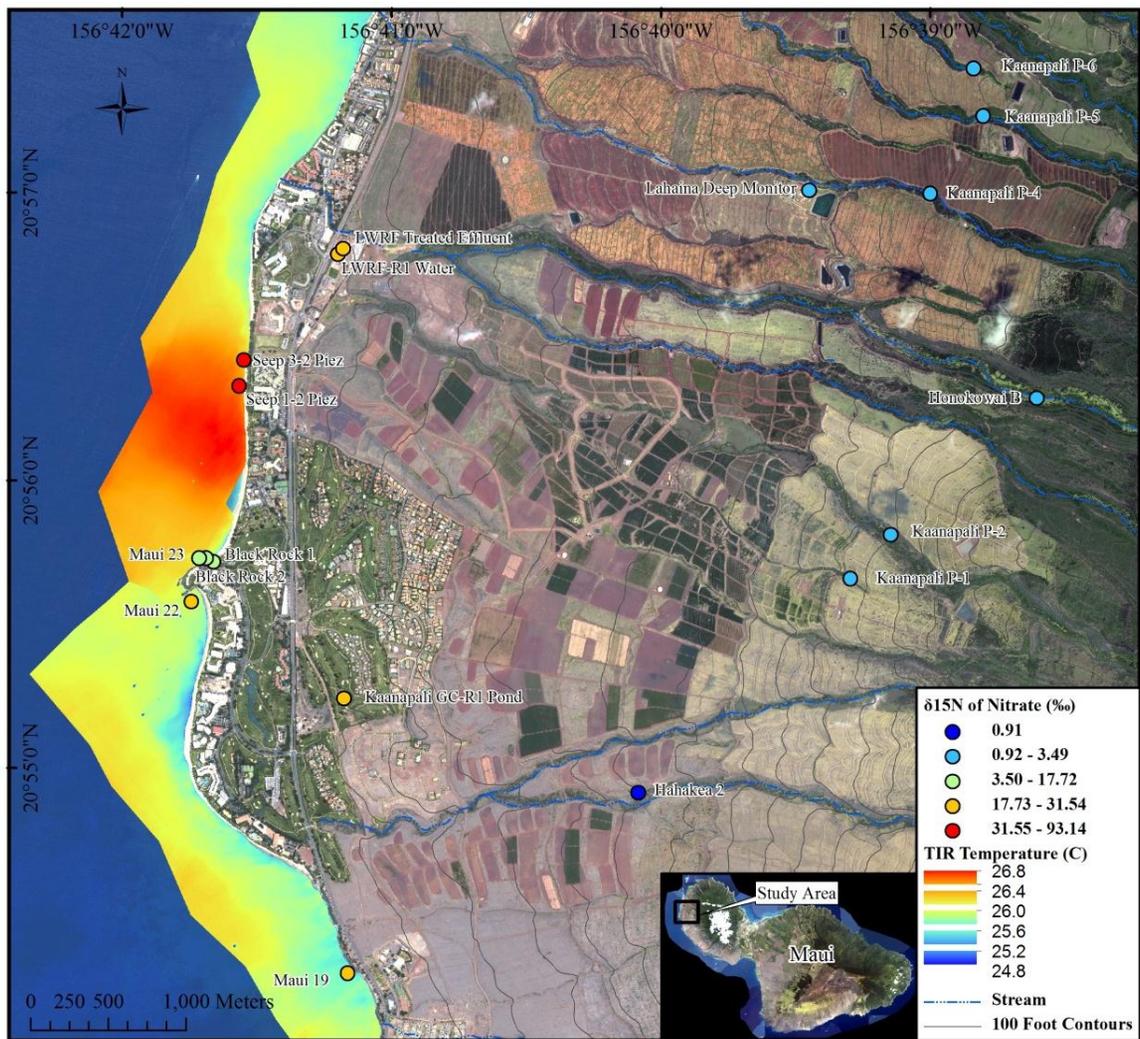
Figure E-26: September, 2011 $\delta^{15}N$ of NO_3^- distribution with TIR temperature overlay.
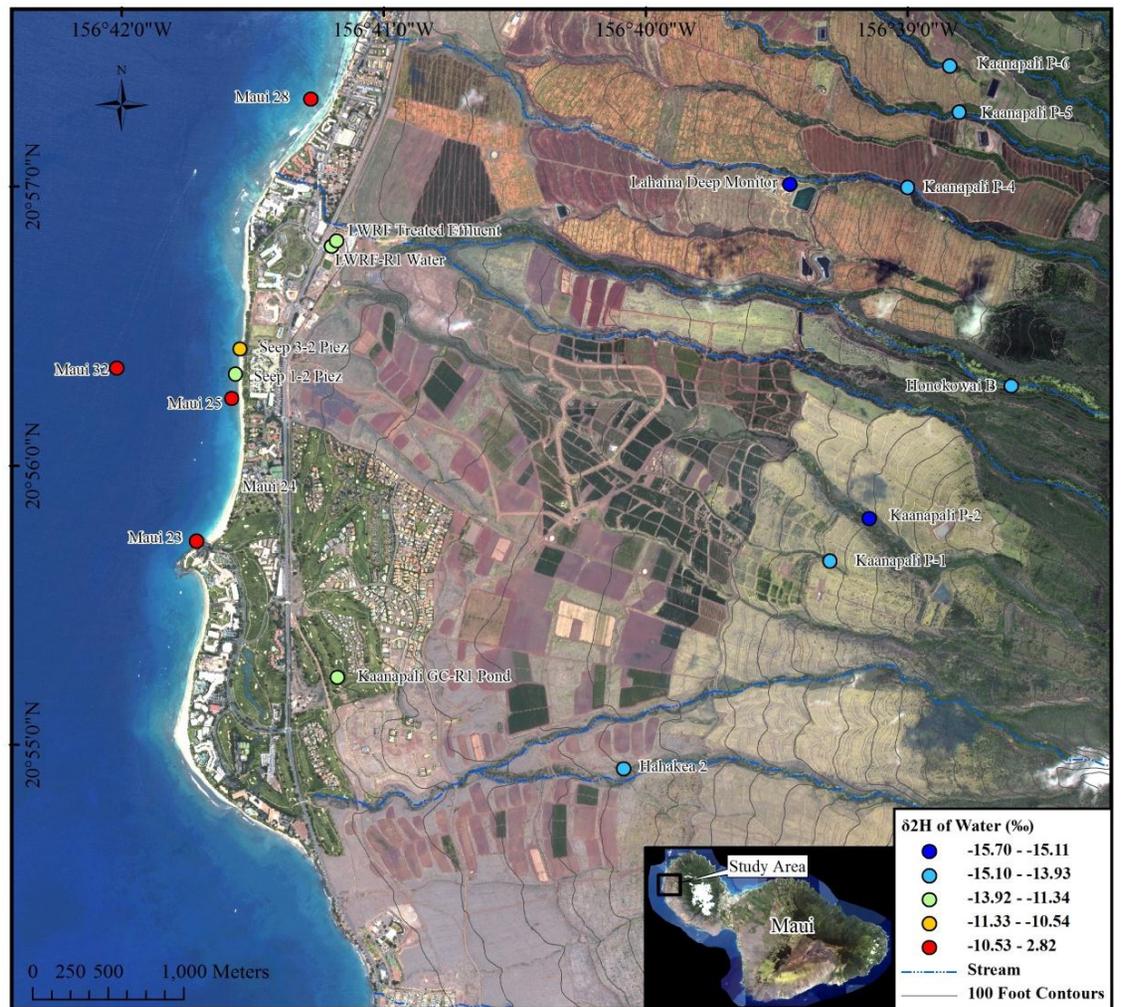
Figure E-27: September, 2011 δ^2H of H$_2$O distribution.
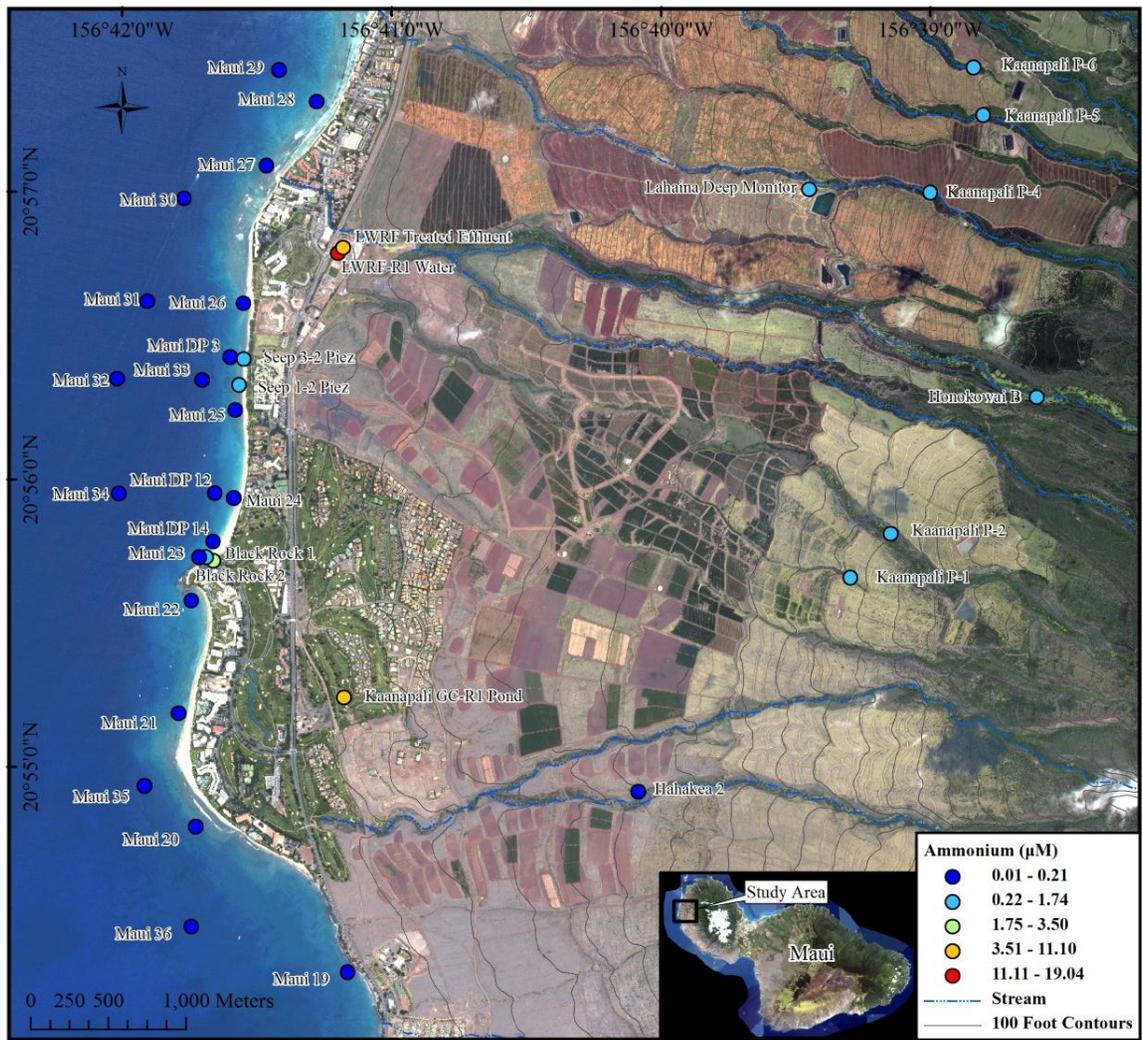
Figure E-28: September, 2011 NH$_4^+$ distribution.

APPENDIX F: GEOCHEMICAL FIELD SAMPLING METHODS AND PROTOCOLS

This page is intentionally left blank

UHM SGD Group Sample Guidebook

Contributors:

Jacque Kelly
Kayla Holleman
Henrieta Dulaiova
Christine Waters
Craig Glenn

July 18, 2011

Contents

Sample Sheets

All of the sample sheets that we use are attached to the end of this guide.

1. "Everything" Log Sheet (for all of the samples found in this guidebook)
2. Rn Platform Log Sheet
3. Depth Profiling Log Sheet
4. Cruise Log Sheet
5. RaDeCC Log Sheet
6. YSI Calibration Sheet (From YSI)

Sample Guidebook

This sample guidebook is only meant to be a guide to ensure that the sample and laboratory procedures undertaken by all scientists in our lab are internally consistent. The contents of this guidebook are meant to provide each scientist with enough direction so that the scientist can better understand and appreciate the minutia of the sample and laboratory procedures, and where applicable, adapt the procedures to better fit the needs of the scientist.

Sample Duplicates

It is imperative to have duplicate samples analyzed. How many, exactly is at the will of the scientist, the $ allowance available, as well as the number of times that that scientist resamples a particular water body and consistently uses the same reliable lab procedures.

A good general rule is to use 10% as a guiding number to gauge how many duplicates are needed. The best number of duplicates actually depends on how different your water masses are; in our coastal work, the salinities (and water chemistries) are very different. So, for us, we have to make sure that different salinities/very different general water chemistries are being checked as well. This pertains to both nutrients as well as stable isotopes, but for stable isotopes, although they are the most expensive, a 15-20% duplicate sampling scheme may be more appropriate due to the many variables that can enter into the final number coming out of the mass spec.

Also understand that there is natural duplication that can occur in other settings that can reduce the number of duplicates needed. For example, if you are running a vertical profile through the water column with a lot of samples spanning an gentle general change in chemistry (an oxygen minimum profile or its nutrient mirror, for example), then one could lax off on the number of duplicates because of the small, progressive natural variation in the profile being measured.

Nutrients Sampling Method (TOTALS)

************************************ (Total N&P) ************************************

You do not need to wear sample gloves, but please do not touch the inside of the caps or bottles or the lips of the bottles with your hands.

---You will need the following---

- 250 ml HDPE Nutrient-Clean (Acid-Clean) Bottle
- YSI (multiparameter meter)
- GPS
- Sample Log Sheet
- Sample Tape

- Sharpie
- Peristaltic Pump (optional)
- Nutrient-Clean (Acid-Clean) Peristaltic Pump Hose (MUST have if using peristaltic pump)

---You must collect the following ---

- Sampling Time
- ALL YSI Parameters
- Sample Depth
- Latitude/Longitude
- Person(s) Collecting Sample

---General Instructions---

Bottles and caps need to be thoroughly rinsed with sample water (rinse each bottle and cap three times with sample water). The bottles are then filled, sealed, and labeled. If you are using the peristaltic pump, use Nutrient-Clean (Acid-Clean) sample hose ONLY. Keep sample chilled and in a dark place while in the field.

---Sampling Procedure---

1. Thoroughly rinse the sample bottle three times with sample water
2. Fill the sample bottle with sample water
3. Label the sample
4. Chill the sample in a dark place (cooler with blue ice) until returning to the lab/condo
5. At the lab/condo Either (1) Freeze the sample for long-term storage OR (2) Chill the sample for short-term storage and immediate sample analysis

---Additional Notes---

- ✓ It is best to store the chilled samples in a dark place. If you are storing the sample in a refrigerator that will be opened frequently, like one at a condo, it is be best to put the samples in a box to keep light away from them so that the microbes in the sample are as inactive as possible and will be less likely to eat the nutrients in your sample.

Nutrients Sampling Method (SPECIFIC NUTRIENTS)

********************** (PO_4^{3-}, $Si(OH)_4$, NO_3^-, NO_2^-, NH_3) ***********************

You NEED to wear gloves.
---You will need the following---

- 60 ml HDPE Nutrient-Clean (Acid-Clean) Bottle
- Nutrient-clean (Acid-Clean) Syringe
- De-ionized Water
- 0.45 µm GF/C Filter
- YSI (multiparameter meter)
- GPS
- Sample Log Sheet

- Sample Tape
- Sharpie
- Nitrile Gloves
- Peristaltic Pump (optional)
- Nutrient-Clean (Acid-Clean) Peristaltic Pump Hose (MUST have if using peristaltic pump)

---You must collect the following---

- Sampling Time
- ALL YSI Parameters
- Sample Depth
- Latitude/Longitude
- Person(s) Collecting Sample

---General Instructions---

The bottles and caps need to be thoroughly rinsed with filtered sample water (rinse each bottle and cap three times with filtered sample water). The bottles are then filled, sealed, and labeled. If you are using the peristaltic pump to collect the sample into the syringe, please use Nutrient-Clean (Acid-Clean) sample hose ONLY. Keep sample chilled while in the field.

---Sampling Procedure---

1. Put gloves on
2. Rinse a nutrient-clean (acid-clean) syringe three times with sample water
3. Fill this syringe with sample water
4. Rinse a second nutrient-clean (acid-clean) syringe with de-ionized water three times [THIS STEP IS ONLY NECESSARY FOR FIRST USE OF EACH FILTER – see additional notes below]
5. Fill this syringe with de-ionized water
6. Attach a 0.45µm GF/C filter to the de-ionized water rinsed syringe and squirt at least 10 ml of de-ionized water through the filter (to get rid of any nutrient signature from the filter)
7. Transfer the de-ionized rinsed filter to the first, sample-rinsed syringe filled with sample water and filter ~15 ml of sample water into the 60 ml bottle. Put the lid on the bottle and shake the sample bottle. Decant (pour out) the water and repeat two more times to rinse the bottle with filtered sample water
8. Squirt EXACTLY 55 ml of sample water into the sample-rinsed 60 ml HDPE bottle
9. Label the sample (SEE LABELING CONVENTION BELOW)
10. Either (1) Freeze the 60 ml sample for long-term storage OR (2) Chill the sample for short-term storage and immediate analysis

We use the 60 ml bottles for two different types of samples. To avoid confusion, please use: Sample Name and NUTS

       Example: Our Spring NUTS

--Additional Notes--

✓ The filter can be used for the next sample if you purge it with at least 15 ml of new sample water

✓ Store the used filter in the filter packaging between sample use to prevent contamination from your working space

✓ The syringe can also be used for the next sample if you thoroughly rinse it with the new sample three times

✓ It is best to store the chilled samples in a dark place. If you are storing the sample in a refrigerator that will be opened frequently, like one at a condo, it is be best to put the samples in a box to keep light away from them so that the microbes in the sample are as inactive as possible and will be less likely to eat the nutrients in your sample.

δ¹⁵N & δ¹⁸O (nitrate) Sampling Method

You do not need to wear gloves, but please do not touch the inside of the caps or bottles or the lips of the bottles with your hands.

--You will need the following--

- 60 ml HDPE Acid-Cleaned Bottle
- YSI (multiparameter meter)
- GPS
- Sample Log Sheet
- Sample Tape

- Sharpie
- Peristaltic Pump (optional)
- Nutrient-Clean (Acid-Clean) Peristaltic Pump Hose (MUST have if using peristaltic pump)

--You must collect the following --

- Sampling Time
- ALL YSI Parameters
- Sample Depth
- Latitude/Longitude
- Person(s) Collecting Sample

--General Instructions--
The bottles and caps need to be thoroughly rinsed with sample water (rinse each bottle and cap three times with sample water). The bottles are then filled, sealed, labeled, chilled, and then frozen.
--Sampling Procedure--
1. Thoroughly rinse the sample bottle three times with sample water
2. Fill the sample bottle with approximately 55 ml of sample water (leave head space for water expansion during freezing)
3. Label the sample
4. Chill the sample while in the field
5. Freeze the sample immediately upon returning from the field

We use the 60 ml bottles for two different types of samples. To avoid confusion, please use the following labeling convention: Sample Name and δ¹⁵N(NO₃⁻)
Example: Our Spring δ¹⁵N(NO₃⁻)

--Sample Splitting Materials--
If you are splitting the nitrate isotope sample from the nutrient sample, you will also need:
- Nutrient-Clean (Acid-Clean) Syringe
--Sample Splitting-General Instructions--
Samples will be split from the 500 ml Total N&P sample back in the lab/condo. Sample splits are best taken ASAP. The bottles and caps should be thoroughly rinsed with sample water (rinse each bottle and cap three times with sample water). The bottles are then filled, sealed, labeled, and frozen (as above).
--Sample Splitting Additional Notes--
- ✓ The syringe can be used for the next sample if you thoroughly rinse it with the new sample three times
- ✓ Nitrite will be removed from the sample in the lab using established laboratory procedures

---Additional Notes---

✓ Nitrite will be removed from the sample in the lab using established laboratory procedures - please see: Granger and Sigman (2009) Removal of nitrite with sulfamic acid for nitrate N and O isotope analysis with the denitrifier method; Rapid Communications in Mass Spectrometry, v 23, 3753-3762.

δ¹⁸O & δD (water) Sampling Method

You do NOT need to wear gloves, but please do not touch the inside of the vials and keep contact with the septa at a minimum.

---You will need the following---

- 20 ml Glass Vial
- Acid-Cleaned Septa
- Aluminum Seal
- E-Z Crimper
- 2 Liter Beaker
- Peristaltic Pump

- Peristaltic Pump Hose
- YSI (multiparameter meter)
- GPS
- Sample Log Sheet
- Sample Tape
- Sharpie

---You must collect the following ---

- Sampling Time
- ALL YSI Parameters
- Sample Depth
- Latitude/Longitude
- Person(s) Collecting Sample

---General Instructions---

Bottles and septa should be thoroughly rinsed with sample water (rinse each bottle and septa three times with sample water). The bottles are then filled under water, septa sealed under water, checked for bubbles, crimp sealed above water, and labeled.

---Sampling Procedure---

1. Rinse the vial and septa with sample water three times
2. Rinse the beaker with sample water three times
3. Put the septa and vial into the beaker
4. Place the peristaltic pump tubing at the very bottom of the vial and fill the vial from the bottom up, allowing the vial to overflow with sample water (overflow water volume should be at least 60 ml)
5. Once enough water is present to cover the vial in the beaker and at least three volumes of water have passed through the sample bottle, tap out air bubbles from the septa
6. Slowly remove the hose from the sample vial and seal the vial underwater with the septa
7. Firmly holding the septa in place, remove the vial+septa from the beaker and invert to check for bubbles. If no bubbles are present, place the aluminum seal over the septa and vial and crimp seal it. If bubbles are present, pour out the water from the vial and beaker and repeat the procedure from step 3 above
8. Dry the vial, label it, and store it in a safe place at room temperature

Radon Grab Sample Sampling Method

You do NOT need to wear gloves.

---You will need the following---

- 250 ml bottle (preferably for salinity 15+)
- 40 ml bottle (use if 250 ml bottle is NOT available, but ONLY for salinity 0 to 15)
- YSI (multiparameter meter)
- GPS

- Sample Log Sheet
- Sample Tape
- Sharpie
- Filling container (optional)
- Peristaltic Pump and Hose (optional)

---You must collect the following ---

- Sampling Time
- ALL YSI Parameters
- Sample Depth
- Latitude/Longitude
- Person(s) Collecting Sample

---General Instructions---

The bottles and caps need to be thoroughly rinsed with the sample water (rinse each bottle and cap three times with sample water). The bottles are then filled (typically under water), sealed (typically under water), checked for bubbles, and labeled. The samples HAVE to be analyzed ASAP because the half life of radon is 3.8 days.

---Sampling Procedure---

There are three different procedures for filling radon sample bottles. Pick the procedure that is appropriate for your sampling set-up.

IF USING PUMP/HOSE AND A FILLING CONTAINER

1. Rinse the sample bottle and lid with sample water three times
2. Rinse the beaker/filling container with sample water three times
3. Put the bottle and lid into the beaker/filling container
4. Run the peristaltic pump at a very low speed so that the Rn does not degas
5. Put the peristaltic pump tubing ALL the way to the bottom of the sample bottle and fill the bottle from the bottom up, allowing it to overflow with at least three volumes of sample water
6. Once at least three volumes of water have flushed the bottle and enough water is present to cover the bottle in the beaker/filling container, tap out air bubbles from the cap
7. Slowly remove the hose from the sample bottle, and run the hose over the cap wile under water to put fresh sample water in the cap and then seal the bottle underwater
8. Remove the sealed bottle from the beaker/filling container and invert it to check for bubbles
9. If no bubbles are present, dry the bottle, label it, and store it in a safe place. If bubbles are present, empty the sample bottle and beaker/filling container and repeat the procedure from step 5 above
10. Store the sample at room temperature
11. Analyze the sample ASAP

IF USING PUMP/HOSE BUT NO FILLING CONTAINER

1. Rinse the sample bottle and lid with sample water three times
2. Run the peristaltic pump at a very low speed

3. Put the peristaltic pump tubing ALL the way to the bottom of the sample bottle and fill the bottle from the bottom up, allowing it to overflow with at least three volumes of sample water
4. Slowly remove the hose from the sample bottle, immediately put sample water into the cap, and carefully flip the cap over to seal the bottle
5. Invert the bottle to check for bubbles
6. If no bubbles are present, dry the bottle, label it, and store it in a safe place. If bubbles are present, empty the sample bottle and repeat the procedure from step 14 above
7. Store the sample at room temperature
8. Analyze the sample ASAP

<p style="text-align:center; color:red;">IF COLLECTING WITHOUT PUMP/HOSE AND FILLING CONTAINER
(LEAST PREFERRED METHOD – LAST RESORT METHOD)</p>

1. Rinse the sample bottle and lid with sample water three times
2. Fill sample bottle underwater, allowing air inside the bottle to escape and be replaced by sample water
3. Fill the cap with sample water and seal the sample underwater
4. Invert the bottle to check for bubbles
5. If no bubbles are present, dry the bottle, label it, and store it in a safe place. If bubbles are present, empty the sample bottle and repeat the procedure from step 21 above
6. Store the sample at room temperature
7. Analyze the sample ASAP

Radium Sampling Method

You do NOT need to wear gloves, but bring your muscles.

---You will need the following--

- Radium sample container
- Mn Fibers
- Mn Filter Cartridge
- Mn Filter Hose
- Weighing Scale
- YSI (multiparemeter meter)
- GPS

- Sample Log Sheet
- Sharpie
- Peristaltic Pump and Hose (optional)
  - Mesh Screen for the Mn Cartridge
- If Particulates are Present USE EITHER:
  - Raw (white) Mn Fibers
  - 0.45 µm GF/C filter

---You must collect the following --

- Sampling Time (both start and stop)
- ALL YSI Parameters
- Sample Depth
- Latitude/Longitude
- Person(s) Collecting Sample

---General Instructions--

The bottles and caps should be thoroughly rinsed with the sample water (rinse each container and cap three times with sample water). The containers are then filled, sealed, labeled, weighed, connected to the Mn cartridge with Mn fibers inside, and filtered.

---Sampling Procedure--

> The sample container filling procedure is always the same, but there are two different procedures for filtering the sample water through the Mn cartridge. Pick the procedure that is appropriate for your sampling set-up.

FILLING THE SAMPLE CONTAINER

1. Label the sample container with the sample name
2. Rinse the sample container three times with sample water
3. Fill the sample container, recording the sample filling start and stop time
4. If particulates are present and you are using a peristaltic pump to pump water into the sample container, you can insert a 0.45 µm filter in-line with the peristaltic pump hose to prevent the particulates from entering the sample container OR you can filter out the particulates when you filter the sample water through the Mn Cartridge (see below)
5. Put the cap on the sample container and slowly tip the container over to check for leaking water. If water leaks, try resealing the container with the same cap or pick a different cap and rinse it three times with sample water and try sealing the container (some caps just do not work well)
6. Weigh the sample container

FILTERING THE SAMPLE WITHOUT A PERISTALTIC PUMP

1. Put Mn fibers into the Mn cartridge and label the Mn cartridge with the sample name. If particulates are present in the sample, use a small wad of raw (white) fibers in the Mn cartridge where the water enters the cartridge to capture the particulates (discard the wad of raw fibers once you are done with step 5 below)

2. Connect the Mn cartridge to the sample container
3. Slowly tip the sample container over to slowly fill the Mn cartridge with sample water, allowing time for the fibers to become saturated and for air bubbles in the cartridge to escape
4. Once water is near the top of the cartridge, slowly tip the cartridge to the ground and adjust the flow rate of the water so that less than 1 L/min of water is flowing through the cartridge (You may prefer to hang the cartridge for faster flow or let air into the sample container if the flow slows down)
5. Once all water is filtered through the cartridge, remove the Mn fibers from the Mn filter cartridge, squeeze the fibers out, and return the Mn fibers to the sample bag labeled with the sample name. Discard raw white fibers if you used them to filter out particulates
6. If the sample is brackish to saline, once the sample water has flushed through the Mn fibers, thoroughly rinse the Mn fibers with de-ionized water that has drained through a different Mn cartridge filled with Mn fibers
7. Store the Mn fibers at room temperature

FILTERING THE SAMPLE WITH A PERISTALTIC PUMP

1. Put Mn fibers into the Mn cartridge and label the Mn cartridge with the sample name. Put mesh screen at the drain end of the Mn cartridge to prevent the fibers from escaping from the cartridge. If particulates are present in the sample, use a small wad of raw (white) fibers in the Mn cartridge where the water enters the cartridge to capture the particulates (discard the wad of raw fibers once you are done with step 5 below)
2. Connect the Mn cartridge to the sample container
3. Slowly tip the sample container over to slowly fill the Mn cartridge with sample water, allowing time for the fibers to become saturated and for air bubbles in the cartridge to escape
4. Once water is near the top of the cartridge, slowly tip the cartridge to the ground and adjust the flow rate of the water so that less than 1L/min of water is flowing through the cartridge (You may prefer to hang the cartridge for faster flow or let air into the sample container if the flow slows down)
5. Once all water is filtered through the cartridge, remove the Mn fibers from the Mn filter cartridge, squeeze the fibers out, and return the Mn fibers to the sample bag labeled with the sample name. Discard raw fibers if you used them to filter out particulates
6. If the sample is brackish to saline, once the sample water has flushed through the Mn fibers, thoroughly rinse the Mn fibers with de-ionized water that has drained through a different Mn cartridge filled with Mn fibers
7. Store the Mn fibers at room temperature

Chlorophyll-a Sampling Method

---You will need the following---

- 500 mL bottle
- GPS
- YSI (multiparameter meter)
- Gloves
- 2.5 cm Filters
- Aluminum Foil
- Vacuum-Sealed Carboy
- Vacuum-Sealed Pump

- Frits
- Small and Large Funnel
- Filtration Apparatus
- Tweezers
- Sample Log Sheet
- Sample Tape
- Sharpie

---You must collect the following ---

- Sampling Time (bottles placed and removed)
- ALL YSI Parameters
- Sample Depth
- Latitude/Longitude
- Person(s) Collecting Sample

--General Instructions--

Bottles and caps should be thoroughly rinsed with sample water (rinse each bottle and cap three times with sample water). Fill the sample bottle and chill immediately.

--Sampling Procedure--

FIELD PREP PROCEDURE

1. Combust filters at 450°C for four hours.
2. Combust aluminum foil at 450°C for four hours.

FIELD PROCEDURE

1. Rinse the sample bottle and lid with sample water three times
2. Fill the bottle and seal it
3. Place sample bottle in a cooler for storage

LAB PROCEDURE

1. Put on gloves
2. Using cleaned tweezers, securely place the frit on the small funnel and place the filter on the frit
3. Twist the small funnel with frit and filter into the large funnel and then seal it onto the 500 mL sample bottle
4. Place the sample bottle on the filtration apparatus
5. When the bottles are securely placed switch the filtration apparatus to the open position and turn the pump on
6. After the water is drained from the sample bottle, remove the bottle from the filtration apparatus and using tweezers, remove the filter
7. Place the filter in combusted aluminum foil and wrap to close
8. Label the foil and freeze the sample immediately at -20°C. If the samples are to be stored for longer than a week freeze the samples at -80°C.

---Additional Notes--------------------------------

- ✓ Ensure the sample is not exposed to light!
- ✓ Ensure that the water is kept chilled until filtration!
- ✓ Ensure that water does not get into the pump!
- ✓ Record filtration time!

Photosynthetic Production Sampling Method

---You will need the following---

- 500 mL bottle
- GPS
- YSI (multiparameter meter)
- Gloves
- 2.5 cm Filters
- Aluminum Foil
- Vacuum-Sealed Carboy
- Vacuum-Sealed Pump
- 25 ml Combusted Glass Vials
- Pipette

- Bicarbonate spike
- Aluminum Seal
- Frits
- Small and Large Funnel
- Filtration Apparatus
- Tweezers
- Sample Log Sheet
- Sample Tape
- Sharpie

---You must collect the following ---

- Sampling Time (bottles placed and removed)
- ALL YSI Parameters
- Sample Depth
- Latitude/Longitude
- Person(s) Collecting Sample

---General Instructions---

Bottles and caps should be thoroughly rinsed with sample water (rinse each bottle and cap three times with sample water). Fill the sample bottle and chill immediately.

---Sampling Procedure---

FIELD PREP PROCEDURE

1. Combust filters at 450°C for four hours.
2. Combust aluminum foil at 450°C for four hours.
3. Prepare bicarbonate spike

FIELD PROCEDURE

1. Rinse the sample bottle and lid with sample water three times
2. Fill the dark bottle and seal it
3. Place dark bottle in a cooler for storage
4. Fill the light bottle and add 50 μL of spike. Seal bottle and leave for up to 24 hours in the field.

LAB PROCEDURE

1. Put on gloves
2. Using cleaned tweezers, securely place the frit on the small funnel and place the filter on the frit
3. Twist the small funnel with frit and filter into the large funnel and then seal it onto the 500 mL sample bottle
4. Place the sample bottle on the filtration apparatus
5. When the bottles are securely placed switch the filtration apparatus to the open position and turn the pump on
6. After the water is drained from the sample bottle, remove the bottle from the filtration apparatus and using tweezers, remove the filter

---

7. Place the filter in combusted aluminum foil and wrap closed.
8. Label the foil and freeze the sample immediately at -20°C. If the samples are to be stored for longer than a week freeze the samples at -80°C.

LAB ANALYSIS PREP FOR DARK BOTTLE SAMPLES
1. Put on gloves
2. Spike filters with phosphoric acid.
3. Allow filters to dry in a desiccator for at least 24 hours
4. Set out tin boats, weigh paper, tray, and supplies for natural abundance samples.
5. Weigh a tin boat on an analytical scale. Record weight
6. Fold filter in tin boat and reweigh. If the filter has a lot of organic material cut the filter. If the filter is cut weigh the whole filter. Record weights
7. Place weighed filter wrapped in tin boat into tray. Record well number

LAB ANALYSIS PREP FOR DARK BOTTLE SAMPLES
1. Put on gloves
2. Spike filters with phosphoric acid.
3. Allow filters to dry in a desiccator for at least 24 hours
4. Set out tin boats, weigh paper, tray, and supplies for incubated samples.
5. Weigh a tin boat on an analytical scale. Record weight
6. Fold filter in tin boat and reweigh. If the filter has a lot of organic material cut the filter. If the filter is cut weigh the whole filter. Record weights
7. Place weighed filter wrapped in tin boat into tray. Record well number

---Additional Notes----------------------------------

✓ Ensure the sample is not exposed to light!
✓ Ensure that the water is kept chilled until filtration.
✓ Ensure that water does not get into the pump!
✓ Lab analysis prep for the dark bottle samples should be completed before light bottle samples to eliminate   possible contamination.

CFC Sampling Method – Bottles

Filling procedure – FOLLOW EXACTLY

(!) Instruction given below MUST BE followed to the letter to obtain good results with the bottle sampling method for CFCs in ground water.

Make sure you have ABSOLUTELY NO lubricants, oils, greases, sprays, or plastic materials on your hands when you sample (including sun-block or lotion). Do NOT wear gloves to sample.

---You will need the following---

- 125 ml Boston Round Bottles (three per site)
- Plastic Aluminum-Foil-Lined Caps
- 2 Liter Glass Beaker
- Viton MasterFlex Compatible Tubing

- Electrical Tape
- YSI (multiparameter meter)
- GPS
- Sample Log Sheet
- Sample Tape

- Sharpie
- Towel
- Bubble Wrap
- Peristaltic Pump (optional)

---You must collect the following ---

- Exact time of capping of CFC Bottle 1
- Exact time of capping of CFC Bottle 2
- Exact time of capping of CFC Bottle 3
- ALL YSI Parameters
- Collect a $\delta^{18}O$(water) & δD (water) sample
  - NOTE Exact time of sampling
- Latitude/Longitude
- Person(s) Collecting Sample

---General Instructions---

Bottles and caps need to be thoroughly rinsed with the sample water (rinse each bottle and cap three times with sample water). Fill the bottles underwater in a glass beaker and cap them underwater. Collect three bottles per well or spring. After filling one bottle, decant (pour out) all water in the beaker and start over for the next bottle. Fill and label the bottles sequentially starting with bottle #1.


FIGURE EXPLANATION
A. Good example. Very tiny bubble formed.
B. Poorly taped cap, air leak - note the large bubble that formed.
C. Cap taped with masking tape, poor seal and large air bubble formed.

1. After the well has been purged, rinse the sample bottle three times with sample water
2. Rinse the beaker three times with sample water
3. Place the bottle in the beaker and then insert one end of the viton tubing ALL the way to the bottom of the bottle
4. Fill the bottle until the bottle overflows (see figure below – cartoon 1)
5. Continue to overflow the bottle until the beaker overflows, allowing at least 2 liters of water to flow through the bottle and out of the beaker (see figure below – cartoons 2 & 3) ---- Flushing the bottle with more water is far better than with less water
6. Select a cap and tap it under water to dislodge air bubbles
7. Slowly remove the viton tubing from the bottle and tightly cap the bottle underwater without allowing the water in the bottle to come in contact with air (see figure below – cartoon 4)
8. Remove the capped bottle from the beaker, dry the bottle and RE-tighten the cap ---- The tighter the cap the better (see figure below – cartoon 5)
9. Invert the bottle, tap it and check for air bubbles (see figure below – cartoon 6). If there are bubbles, empty the bottle and beaker and repeat the procedure from step 3 above. If it is necessary to refill the bottle, you MUST USE a new cap
10. If there are no bubbles, tape the cap securely to the bottle with electrical tape. Wrap the tape in a clockwise direction looking down from the bottle top. Two rounds of electrical tape are needed (see figure below – cartoon 7)
11. Label each bottle with the well name, date, and time of sampling and the sequence number of each bottle as it was collected, one through three, in the order of collection
12. Bubble-wrap each bottle and store them upside down at room temperature until shipment. It is normal for a bubble to form in most samples after the sample has been stored for a short while.

Glenn/Dulaiova SGD Group
Updated by JLK - 7/19/2011
Page 18
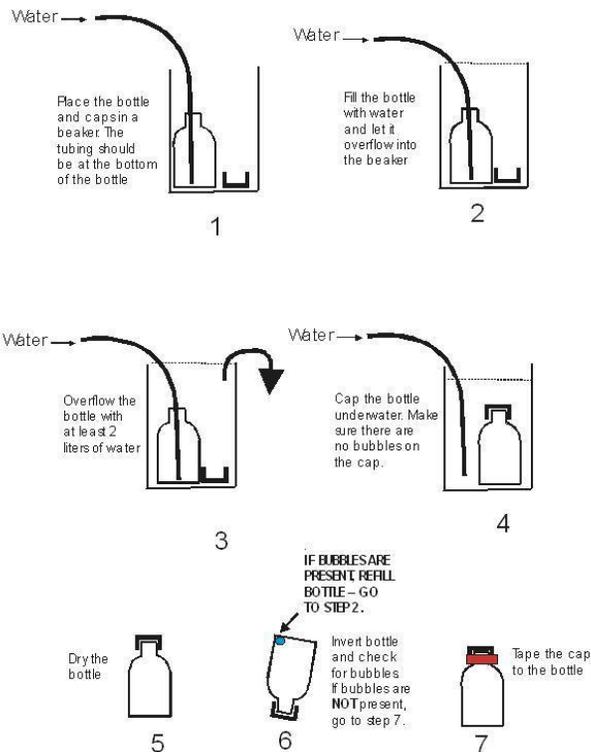
Trace Metals Sampling Method

Please wear gloves and please do not touch the inside of the caps or bottles or the lips of the bottles with your hands.

---You will need the following---

- 100 ml HDPE Trace-Metal Clean (Acid-Clean) Bottle
- Trace-Metal Clean (Acid-clean) Syringe
- 0.45 μm GF/C filter
- YSI (multiparameter meter)

- GPS
- Sample Log Sheet
- Sample Tape
- Sharpie

---You must collect the following --

- Sampling Time
- ALL YSI Parameters
- Sample Depth
- Latitude/Longitude
- Person(s) Collecting Sample

---General Instructions---

If sampling around Oahu, pre-fill bottles with 20 □L of trace metal grade cc. HCl. Do not rinse bottles or caps with water. If shipping bottles to other locations, do NOT pre-fill with acid and the bottles and caps should be thoroughly rinsed with sample water (rinse each bottle and cap three times with sample water). The bottles are then filled, sealed, and labeled. When back in the lab, add 20 □L of trace–metal grade cc. HCl. Store bottles in plastic bags and prevent from soiling.

---Sampling Procedure---

1. Put gloves on
2. Rinse the trace-metal clean syringe three times with sample water
3. Fill the syringe with sample water
4. Flush the filter with one syringe volume of sample water
5. Filter some sample water into the sample bottle to rinse the bottle, decant (pour out) the water from the bottle and repeat two more times.
6. Fill the bottle with filtered sample water
7. Label the sample
8. Put the sample in a plastic bag
9. Store at room temperature

---Additional Notes--

- ✓ It is inappropriate to leave your sample bottles open while prepping other bottles or to reach over your sample, et cetera...
- ✓ Reuse the syringe and filter for the next sample but rinse thoroughly with the new sample water

General Info

Sample Name: _____

Location Description: _____

_____

Date: _____ Sampling Start Time: _____ Sampling Stop Time: _____

Sample Collectors: ☐JLK ☐KDH ☐CAW ☐HD ☐CRG ☐JJK ☐KKM ☐JB ☐Other: _____

GPS

☐ GPS 1 ☐ GPS 2 ☐ GPS 3 ☐ Garmin ☐ Other: _____

Latitude: _____ N Longitude: _____W Waypoint #: _____

Datum: ☐WGS84 ☐NAD83 ☐Other: _____ Uncertainty: ± _____ ft

YSI

☐Craig's ☐V22 ☐V24 ☐Other: _____

Time: _____ Depth: _____ m DO: _____ %

Temp: _____ °C pH: _____ DO: _____ mg

Spec. Cond: _____ mS/Cm°C ORP: _____

Salinity: _____ Chl: _____ µg/L

Nutrients

Total
Collect 125 ml DUPLICATE?: ☐Yes ☐No
Time: _____
☐Refrigerated ☐Frozen [FOR STORAGE]

Specific
Collect 55 ml DUPLICATE?: ☐Yes ☐No
Time: _____
Filtered By: _____ Split By: _____
Split from total nutrients?: ☐Yes ☐No
☐Refrigerated ☐Frozen [FOR STORAGE]

$\delta^{15}N$ & $\delta^{18}O$ (nitrate)
Collect 55 ml DUPLICATE?: ☐Yes ☐No
Time: _____
☐Refrigerated ☐Frozen [FOR STORAGE]
Split from total nutrients?: ☐Yes ☐No
If split, split by: _____
Date Nitrite Removed: _____
Notes: _____
_____

Radon
Time: _____
☐40 ml ☐250 ml
Analyzed By: _____
Date Analyzed: _____
Time Analyzed: _____
RAD7 #: _____

Radium
Start Time: _____
Stop Time: _____
QBs: _____
Volume: _____

$\delta^{18}O$ & δD (water)
DUPLICATE?: ☐Yes ☐No
Time: _____

Primary Productivity

Dark Bottle
Bottle ID: _____
Time: _____
Filtered? ☐Yes ☐No
Frozen? ☐Yes ☐No

Light Bottle
Bottle ID: _____
Deployment Time: _____
Retrieval Time: _____
Filtered? ☐Yes ☐No
Frozen? ☐Yes ☐No

Chlorophyll
Time: _____
Volume: _____
Filtered? ☐Yes ☐No

Salinity
Collect 100 ml in a 125 or 250 ml bottle
Time: _____

Trace Metals
Time: _____
Filtered? ☐Yes ☐No
Acid Spiked? ☐Yes ☐No

CFCs
Bottle 1 Time: _____
Bottle 2 Time: _____
Bottle 3 Time: _____

Notes
_____
_____
_____

General Info

Sample Name: _____

Location Description: _____

_____

Date: _____ Sampling Start Time: _____ Sampling Stop Time: _____

Sample Collectors: ☐JLK ☐JF ☐CAW ☐HD ☐CRG ☐JJK ☐KKM ☐JB ☐Other: _____

GPS

☐ GPS 1 ☐ GPS 2 ☐ GPS 3 ☐Garmin ☐Other: _____

Latitude: _____ N Longitude: _____W Waypoint #: _____

Datum: ☐WGS84 ☐NAD83 ☐Other: _____ Uncertainty: ± _____ ft

YSI

☐Craig's ☐V22 ☐V24 ☐Other: _____

Time: _____ Depth: _____ m DO: _____ %

Temp: _____ °C pH: _____ DO: _____ mg

Spec. Cond: _____ mS/Cm$^{°C}$ ORP: _____

Salinity: _____ Chl: _____ µg/L

Rad 7

☐ 2356 ☐ 2357 ☐ 2540 ☐ Other: _____

Time Deployed: _____ Time Retrieved: _____

Logging Interval: _____ File Name: _____

Battery Life: _____ Free Memory: _____

Diver CTD

Deployment Location (on platform): _____

Time Start: _____ Time Stop: _____

Time Deployed: _____ Time Retrieved: _____

Logging Interval: _____ Baro #: _____

Days Memory: _____ Diver # & File Name: _____

Diver CTD

Deployment Location (on platform): _____

Time Start: _____ Time Stop: _____

Time Deployed: _____ Time Retrieved: _____

Logging Interval: _____ Baro #: _____

Days Memory: _____ Diver # & File Name: _____

Diver CTD

Deployment Location (on platform): _____

Time Start: _____ Time Stop: _____

Time Deployed: _____ Time Retrieved: _____

Logging Interval: _____ Baro #: _____

Days Memory: _____ Diver # & File Name: _____

Notes

_____

_____

_____

_____

Sample: _____ Date: _____ Sample Collectors: _____

YSI: _____ GPS #: _____ Waypoint #: _____ Latitude: _____ Longitude: _____

Depth (m)	Time (24hr)	Temperature (°C)	Specific Conductivity	Salinity	pH	ORP	Chlorophyll	DO (%)	DO mg

NOTES:_____
_____
_____

UHM SGD Research Group Depth Profiling Sheet

<table>
<tr><td rowspan="7">Location Info</td><td>Sample ID: _____</td></tr>
<tr><td>Cruise ID: _____   Station ID:_____</td></tr>
<tr><td>Start Latitude:_____N Longitude:_____W</td></tr>
<tr><td>Stop Latitude:_____N Longitude:_____W</td></tr>
<tr><td>Total Depth:_____</td></tr>
<tr><td>Date: _____</td></tr>
<tr><td>Sampling Time: _____</td></tr>
</table>

Nutrients	Total	*Collect 125 ml* DUPLICATE?:☐Yes ☐No Time: _____ ☐Refrigerated ☐Frozen [FOR STORAGE]
	Specific	*Collect 55 ml* DUPLICATE?: ☐Yes ☐No Time: _____ Filtered By: _____ Split By: _____ Split from total nutrients?:☐Yes ☐No ☐Refrigerated ☐Frozen [FOR STORAGE]

Salinity	*Collect 125 ml in a 250 ml bottle* Time:_____
Notes	_____ _____ _____ _____

Radium Sampling Log				Nuts
Sample ID	CTD ID	Depth	Volume	

System#	Sample ID	Time start	Time stop	Time run	219 cts	220 cts	Tot cts	219 cpm	220 cpm	Tot cpm	Flow	Spike

CALIBRATION WORK SHEET

Date of Calibration: _____   Sonde ID: _____

Technician: _____

RP DO membrane changed?   Y   N   *Note: Wait 3 to 6 hours before calibrating for unattended*
RP DO membrane o-ring changed?   Y   N   *deployments; run in Discrete mode for 10 minutes to accelerate*
                                                              burn in. (Rapid Pulse DO Only)
Turbidity wiper changed?   Y   N   Chlorophyll wiper changed?   Y   N
ROX DO wiper changed?   Y   N   BGA-PE wiper changed?   Y   N
BGA-PC wiper changed?   Y   N   Rhodamine wiper changed?   Y   N

Note: If parking problems occur with optical probes having a serial number 07L (Dec 07) or older, be sure the firmware is 3.06 or later. Parking issues with optical probes having a serial number prior to 07L may be related to a dirty wiper body or pad.

Record sonde battery voltage: _____ (if applicable)

Record Calibration Values
Standard   Pre Cal / Post Cal

Record the following diagnostic numbers <u>after</u> calibration.

6560 Conductivity cell constant _____	Range 5.0 $\pm$ .45	Temperature _____	____Sonde
Integrated conductivity cell constant_____	Range 5.0 $\pm$ .70	Conductivity _____	____/____
pH mv Buffer 7 _____	Range 0 $\pm$ 50 mv	pH 7 _____	____/____
pH mv Buffer 4 _____	Range +180 $\pm$ 50 mv*	pH 4 _____	____/____
pH mv Buffer 10 _____	Range -180 $\pm$ 50 mv *	pH 10 _____	____/___

*Note: Millivolt span between pH 4 and 7 should be $\approx$ 165 to 180 mv   ORP   _____   ____/___

      Millivolt span between pH 7 and 10 should be $\approx$ 165 to 180 mv   Turbidity   _____   ____/____

DO charge (RP only) _____	Range 25 to 75	Turbidity _____	____/____
DO gain _____	Range 0.7 to 1.4	Turbidity 0.5_____	____/____
ODO gain _____	Range 0.85 to 1.15	Chlorophyll _____	____/____
		Chlorophyll _____	____/____

Turbidity standard used in calibration _____   DO RP   _____   ____/____

Manufacturer and part number _____   DO ROX   _____   ____/____

                                                          BGA PE/PC _____   ____/____

Barometric Pressure: _____mmHg   BGA PE/PC _____   ____/____

DO % Calculated – (BARO mmHg divided by 7.6) = % saturation   Rhodamine   _____   ____/____

    Example: 760 $\div$ 7.6 = 100.0%

Depth Calibration - If zero was entered, record barometric pressure at time of calibration _____mmHg

Depth Calibration - If offset depth was entered, record value _____ meters/feet and pressure _____ mmHg

Depth Calibration (Vented) – Acceptable calibration constant: 0.0 psig $\pm$ 0.15 _____

Notes:

APPENDIX G: DRAFT REPORT REVIEW COMMENTS AND UNIVERSITY OF HAWAII RESPONSES AND CORRECTIONS

This page is intentionally left blank.

APPENDIX G-1: Draft report review comments from the County of Maui

This page is intentionally left blank.

Tracer Study Comments (County of Maui)
June 29, 2012

General comments:

-- These comments should not be considered conclusive or exhaustive as the County has not yet had the opportunity to receive input from its consultants. Furthermore, while we appreciate the amount of data that has been shared to date, the County has not received or been privy to the full breadth of the study results nor has had the opportunity to independently review the data, which makes a comprehensive analysis difficult.

-- The draft tracer study has not been peer reviewed and it is premature at this time to use the preliminary findings to make conclusory statements that are not yet supportable.

> *First, Merriam Webster defines "Conclusory" as "consisting of or relating to a conclusion or assertion for which no supporting evidence is offered." The report based on this project was not peer reviewed considering that such a process would greatly delay delivery of the report and add significant costs. However, the report is subjected to a stakeholder review, which is consistent with what is normally done for similar studies. We would like to stress that the County's use of the word Conclusory is inappropriate considering that significant scientific evidence has been provided to support our conclusions. Tools and approaches utilized are not new but have been used by our group and others in previous studies, which <u>have</u> <u>been</u> published in peer-reviewed publications. These include the tracer test procedure, infrared and radon techniques, and geochemical-analysis techniques. Limitations of each technique and the resulting uncertainties are carefully described where needed.*
>
> *More significantly, the tracer test portion of this report has been reviewed by Dr. Malcolm Field, a leading expert on tracer tests. He has been consulted at various stages of the project, including the design of the test and interpretation of results. In fact, we are currently addressing his concerns regarding the interpretation of test results.*
>
> *Manuscripts are currently being prepared to publish various chapters in peer-reviewed journals. Our experience points towards success of that goal. However, we believe subjecting this study to peer review would not satisfy Maui County's concerns considering that the County rejects the findings of the peer-reviewed studies of Dailer et al. (2010) and Hunt and Rosa (2009).*

The tracer study is one of several ongoing studies that together may provide a better overall understanding of the variety of influences on the near shore waters off of the Kaanapali coastline.

> *We agree that our study is one of many addressing the source of nutrients to the near shore waters of West Maui. We have cited most if not all in our report. If*

*we have missed an important study we will certainly include it as appropriate if
the reviewers bring it to our attention.*

-- The results of the Thermal Infrared Survey show "thermal anomaly" -- or, an area of
slightly normal water that extends approximately 2000 feet and 166 acres offshore of the
Kaanapali area. There are several possible theories being explored for the findings,
including geothermal heating of groundwater. No single study currently provides an
adequate basis for making conclusory statements about ultimate fate of the R-1 and R-2
water.

> *First, it is important to point out that our study is the first to document this large
> thermal anomaly, and we made no conclusory statements. Evidence has been
> provided for all conclusions made. As we have already pointed out in the report,
> as based on the current scientific evidence, the heat for sustaining this thermal
> anomaly has not been solely attributed to the warm injected effluent alone.*

-- Rhodamine B, which was placed into Well 2, has not been detected in the freshwater
seeps being monitored by the study's scientists for nearly a year to date, which suggests
that the R-1 and R-2 water placed into Well 2 does not migrate to these nearshore waters.

> *The lack of Sulpho-Rhodamine B (SRB) detection does strongly indicate that with
> the current injection configuration that Well 2's effluent does not discharge at the
> monitored submarine springs. However, the injection rate into Wells 3 and 4 is
> greater than that into Well 2. This creates an upward cone around Wells 3 and 4
> similar to but opposite of the cone of depression that surrounds pumping wells.
> This will displace the discharge from Well 2 and divert it to other marine
> discharge points. These discharge points certainly could be deeper and further
> off-shore. However, if Well 2 was the only injection well in service, it is very
> possible that its effluent could discharge at the submarine springs that are
> currently monitored since there would be no interference from Wells 3 and 4. It
> would take another tracer test with Well 2 as the primary injection well and a
> coastal surveillance program capable of detecting non-saline discharge in water
> deeper and farther away from the shoreline to assess any impact this injection
> configuration would have on the near shore waters.*

-- The County strongly urges the authors to conduct the necessary tests to determine the
source of the visible green haze that appeared in the South Seep testing area. It is the
County's understanding that Fluorescene should not be visible at the levels being noted in
the preliminary lab results, and the County believes it is very important to identify the
nature and source of this substance. The County further believes that the visible detection
of this substance only at the South Seeps and not in the North suggests that it is not
Fluroescene, which preliminary results appear to point to detection at both the North and
South Seeps.

> *We agree that definitively identifying source of the green tint observed at the
> submarine springs is important. We are currently working on understanding the*

cause of the green coloration. However, a preliminary finding is that the generally observed visual limit of 100 ppb for FLT applies to small volumes of water containing this dye. In a laboratory setup, we observed a visible green tint in a 1-liter FLT solution mixed to a concentration of 35 ppb. This concentration is comparable to what is being measured at the South Seep Group. More details on how we are resolving this issue are contained in our response to comments from the EPA. Also, it is important to note that the FLT concentration measured at the South Seep Group is about 1.5 times that measured at the North Seep Group. Thus, it would be expected that any green anomaly due to FLT in the water would be much more likely at the South Seep Group.

This is an interim report for the tracer test interpretation because the tracer breakthrough curve is still developing and a final report providing much more details on the tracer test will be released early next year (2013). However, for this interim report we will include a summary of efforts to date to identify the source of the green tint.

-- The County urges the authors to use the proper terms, being "R-1 and R-2 reclaimed water" rather than "effluent" to promote a better understanding of what exactly is being placed into the injection wells at the Lahaina Wastewater Treatment Plant. This will clarify the distinction between R-1 and R-2 reclaimed water and other liquids or materials entering the groundwater from other potential sources.

According to "Guidelines for the Treatment and Use of Recycled Water, Hawaii Dept. of Health (2002), the term "reclaimed" has been replaced by "recycled". Recycled water is defined as wastewater that by design is intended or used for a beneficial purpose. Since the water that is the focus of this study is disposed of by injection it is not recycled water. A more accurate term that would convey that the water has been subjected to significant treatment would be "tertiary treated wastewater". However, in our revisions we have tried to be as consistent as possible and have opted to use the relatively compact and universally understood terms "treated wastewater" for the main effluent output of the LWRF, and R-1 for the LWRF treated wastewater effluent that has also undergone additional UV treatment. We believe these terms are consistent with HDOH and EPA regulations and understandings. In some cases in our writing we have also used the words "treated wastewater effluent" as well, which we feel is also correct.

-- The County understands that this early draft report has been based on deviating results between field and lab data that may point to errors in collection, analysis, or deviation in calibration methods used in the testing equipment. Further independent analysis should be conducted to identify possible reasons for the significant deviations in the quantities of Fluorescene detected in the field samples and those tested at the UH laboratory.

The difference between the field and laboratory analysis resulted from using deionized (DI) water to make the initial calibration solutions. The fluorescence of FLT starts decreasing with pH when pH reaches 6.5 (Smart and Laidlaw, 1977).

Unfortunately, the pH of DI water is controlled by atmospheric CO_2 dissolving into water driving the water slightly acidic (Dever, 1997, Chapter 3). We recently measured the pH of DI water and submarine spring water. The pH of DI water was about 5.0 while that of Seep 1 water was 7.9. The intent when using DI water was to calibrate the fluorometer with standards that had the minimum natural fluorescence. However, the low pH of DI water was not accounted for when this approach was taken.

The field fluorometer has been used to assess fluorescence trends in between delivery of samples to UH for laboratory analysis. For this reason it was important to maintain an uninterrupted analytical record for the field fluorometry. To maintain this continuity, the DI based calibrations were continued in the field when the problem with these solutions was discovered. A correlation between the field and laboratory fluorescence values showed that the field readings can be corrected to laboratory readings by using a correction factor of 0.33. The raw field values were included in the report for transparency. We realize that the confusion caused by having two fluorescence values for a single sample outweighs the need for continuity in the field measurement history. We have prepared submarine spring based calibration solutions and we now use these to calibrate the field fluorometer.

-- The County submits that it is an overstatement to suggest an absolute "proven hydrologic connection" between Wells 3 and 4 and the near shore seeps, given significant issues presented by the preliminary data, including the unidentified "green haze," as well as the unidentified but presumably oblique assumed pathway of the R-1 and R-2 water. The precise subsurface pathway and the processes taking place during the significant presumed travel time remain to be characterized and tested. Further, the results of the thermal testing suggest that there are significant ecological processes at work in the region, to the extent of a 166 acre mass of warmer water, which might result from several sources, including geothermal activity.

We submit that the hydraulic connection between Wells 3 and 4 and the submarine springs has been proven by the presence of FLT at these locations. The green haze even if from some other source does not weaken the analytical work that has been done to show that FLT is present. The completed comprehensive background fluorescence study showed no interference from any significant sources in the FLT wavelength range. Background fluorescence in the FLT wavelength range was about 0.11 ppb. Thus the contribution to fluorescence in the FLT wavelength from sources other than this dye is insignificant when compared to concentrations being measured.

The tracer portion of this study is still evolving and not all available results have been included in this interim report. However, we did add the results of a synchronous scan showing that, with exception of magnitude since the concentrations are different, the fluorescence spectrum in the FLT range of submarine spring water matches that of a laboratory prepared FLT solution. (A

424

previous response addresses the reason for the mismatch between field and laboratory analyses.)

-- If conclusory statements are made with regard to the positive identification of Fluroescene from Wells 3 and 4, unbiased scientific reporting should support equally conclusory statements with regard to the lack of detection of Rhodamine B from Well 2, i.e., that the preliminary results have show that there is no proven hydrologic connection between Well 2 and the near shore waters at Kaanapali.

Again, our statements cannot be defined as conclusory, since scientific evidence is provided to support our positive detection of FLT at the submarine springs. Also, as previously stated, the lack of SRB detections is insufficient evidence to state that effluent from Well 2 does not discharge into nearshore waters.

Executive summary:

Page ii – "The facility produces secondary ***tertiary*** treated water (***secondary treated with filtration and since October 2012 has been disinfected with chlorine to an R-2 standard),*** which is disposed ….". <u>The definition of tertiary is secondary treatment with advanced filtration and disinfection?</u>

We have changed this sentence accordingly, which now reads:

"The facility produces treated wastewater (tertiary treated with filtration and since October 2011 has been disinfected with chlorine to an R-2 standard), which is disposed of via four on-site injections wells, and tertiary treated wastewater that is disinfected with UV radiation to meet R-1 reuse water standards."

Page ii – "….since the release of the Tetra Tech (1993) study appear to have reduced overall LWRF." <u>Sentence is not complete. (Perhaps "…LWRF **contribution**."?)</u>

Thank you, we have made that correction.

Page iv and v, Page 56: It is too speculative at this time to use the term "preferential flow path" when referencing the hypothetical destination of the Well 2 injected R-1 and R-2 water.

There were no conclusions made as to existence of a preferential flow path so this comment does not seem appropriate.

Page v – (pg 59 also)"….demonstrates a definite hydraulic connection between injection Wells 3 and 4 and the near shore waters at Kaanapali…". As noted, it is an overstatement to suggest an absolute "proven hydrologic connection" between Wells 3 and 4 and the near shore seeps, given significant issues presented by the preliminary data.

As previously stated, the detection of FLT does show such a connection.

The County believes the first sentence of the Introduction at Page v, without the following clarification/addition would be misleading and does not include information critical to an understanding of the larger issue. We recommend adding the following to that paragraph: "The first detection of the initial breakthrough curve occurred 84 days following injection of the dye, and the peak detection occurred in April 2012, 9 months following injection. The significant delay between dye injection and detection suggests that potential environmental or health issues may be mitigated by the attenuated travel time. Further, other studies point to a 90 percent reduction in the nitrogen level of the R-1 and R-2 reclaimed water entering the wells."

We cannot address the issue of mitigation of <u>all</u> constituents and potential environmental and health issues, considering that these are beyond the scope of this research.

Page ix: Add: Wahikuli is an unsewered area with many unconnected cesspools.

We have added that caveat, but Wahikuli is significantly south of the study area and it is highly unlikely the on-site sewage disposal systems there are influencing the chemistry of the water in the study area.

Section 1
1.3 pg. 2 "The facility produces ~~secondary~~ *tertiary* treated wastewater, which is disposed of via four on-site injection wells and tertiary treated wastewater that is disinfected…" Again, it's all tertiary treated water.

We will make that change.

1.3 pg. 3 "The LWRF consists of two *separate* plants *capable of* operating in parallel." <u>This should be revised as the 1975 side is operable but not currently in use due to the flow volumes.</u>

We will make that change.

1.3 pg. 3 "…but per EPA's approval the facility is operating under the expired permit until a renewal is approved" The DOH permit is in a similar state.

We will make that change.

1.4 pg. 5 revise for clarity: "since the LWRF was identified as a ***potential*** contributor…"
Section 2 2.2.3 pg. 27 "Waihikuli Beach Park is south of the ….." Note that Waihikuli is an
unsewered area with many active cesspools, which should be included in any reference.

> *The statement refers to the conclusions of TetraTech's 1993 report and is*
> *accurate as it is written in our draft report.*

Section 2
2.2.3 pg. 27 "Waihikuli Beach Park is south of the ….." <u>Note that Waihikuli is an unsewered</u>
<u>area with many active cesspools, which should be included in any reference.</u>

> *We thank the County for this comment and have addressed it in Section 2.2.3.*

2.2.3 pg. 27 "Olowalu is located ………. has no known land-based pollution impacts…."
This statement is inaccurate as there are residences and commercial buildings in the area on
cesspools and septic, major road construction, and also this area is a popular location for
snorkeling, surfing, and other beach activities. There are no restrooms in the area.

> *We thank the County for this comment and have addressed it in Section 2.2.3.*

2.3.1 pg. 28 "The submarine spring water sampled through piezometers generally had a
low*er* pH, low*er* salinity, and low*er* specific conductivity compared…." "<u>low is misleading</u>
<u>should be "lower" in all three instances.</u>

> *We thank the County for this comment and have addressed it in Section 2.2.3.*

Section 3
3.2.3.3 pg 54 <u>Concentrations are being adjusted because of mixing with seawater under the</u>
<u>seabed, this is part of the underground process. There isn't adjustment for mixing with other</u>
<u>groundwater.</u>

> *We feel there might some misunderstanding here. Seawater being captured by the*
> *piezometers is most likely not from an underground source since their length is*
> *only 6 inches and they are driven into a crevice. This adjustment was done to*
> *estimate the true FLT concentration in the SGD by removing the dilution caused*
> *by the seawater being captured when the sample was drawn. The submarine*
> *spring salinity baseline of 3-4 parts per thousand represents the sub-seafloor*
> *mixing of the treated wastewater, fresh groundwater, and saline groundwater.*
> *The samples for which the FLT concentrations were adjusted had salinities much*
> *higher than 4 parts per thousand. Undoubtedly there is some native groundwater*
> *in the mix. The contribution of the fresh groundwater fraction at the submarine*
> *springs has been estimated by this study using oxygen and hydrogen isotopes.*
> *From a tracer test perspective however, this is not necessary. The percent*
> *recovery of the dye mass injected will be based on total groundwater flux, so*
> *parsing the groundwater out into its individual source end members is not*

necessary. At the conclusion of this study (final supplementary report), percent recovery calculations will be done to estimate the fraction of effluent injected in Wells 3 and 4 that may be accounted for based on our groundwater flux survey and the tracer dye breakthrough curve

3.2.3.3 pg 55 "…with the expectation…" Editorial suggestion: "..exception"..

Thank you, we will make that correction.

3.2.3. pg 56, first paragraph. The County submits that the following should be deleted from the second sentence, as it is premature to make such firm conclusions: "implying it may have a hydraulic connection with a preferential flow path." Such conclusion is not supported by the available data.

We are not making firm conclusions here. Our use of the word "implying" shows that we are not concluding that a preferential path exists. It is a possibility.

3.4, pg 59, last paragraph. The first sentence should be revised by deleting "show a definite" to "suggest a" … hydraulic connection. As noted, it is an overstatement to suggest an absolute "proven hydrologic connection" between Wells 3 and 4 and the near shore seeps, given significant issues presented by the preliminary data.

The weight of the evidence shows that a hydraulic connection does exist. This weight includes not only the detection of FLT at the submarine springs, but an elevated temperature anomaly in study area, elevated nitrogen-15 to nitrogen-14 ratios, and the detection of pharmaceuticals (Hunt and Rosa, 2009). Each line of evidence taken individually indicates a wastewater linkage. Since the artifacts are concurrent in space and time, the linkage between the discharge monitored at the submarine and the effluent injection at the LWRF is difficult to refute.

Page 60, first partial sentence. Delete "proven" as it is not supportable, as identified above.

Again, as stated above the weight of the evidence shows that such a connection does exist.

Section 4
4.4.1 pg 88 "the warmest area of the entire coastline mapped (Figures 4-3 and 4-4) corresponds to the geographic location where the effluent enters the ocean….." The word "effluent" should be replaced with "warmer spring water" since at the time of this portion of the study no connection was established, and the reason for the warm water has not been determined.

> *Again as stated above, the weight of the evidence does show a hydraulic connection does exist between Injection Wells 3 and 4 and the submarine springs being monitored. We listed the other possible heat sources to be on the cautious side. However, correlation with the effluent can be established when temperature rise is combined with other evidence.*

4.4.2 & 4.4.3.1 pg. 89 "Since the water column is well-mixed with respect to temperature, and our infrared camera detected the warm signal from the top skin of the water, potential sources of heat necessary to generate the large thermal anomaly must be considered." "The effluent is naturally warm with injection waters ranging from 26-31°C (79-88°F), the lower end of which is consistent with water temperatures observed in the thermal anomaly." The author is assuming that the temperature measured at the ocean surface is the discharge temperature of the submarine springs. In fact, the submarine spring temperature would need to be significantly warmer to mix with the mass of ocean water and cause a thermal shift in the entire mass. We know from the surface salinities that the mixed water is mostly seawater and that water has a high heat capacity. A calculation could be made based on ocean temperature and assumed water mass to get an estimation of expected temperature. Conversely one could attempt to measure the temperature in the piezometers.

> *We refer you to Figure 2-4 in the draft that shows that when a temperature and electrical conductivity logger is buried in the sand near the north seep group, the temperature increases to 28 °C and the specific electrical conductivity decreases to about 1 millisiemen per centimeter. The low specific conductivity shows that the temperature being measured is that of the non-saline submarine groundwater. The elevated temperature shows that the submarine groundwater will warm the surrounding seawater as it discharges from the seafloor. Since effluent injection has been going on for many decades, the heat from the effluent does not have to "warm the surrounding seawater" since it has reached a state of quasi-equilibrium. The added heat only has to balance the heat losses due to factors such as cool seawater being carried into the plume by currents or heat loss at the sea surface.*

4.4.3.3 Exothermic Reactions Related to Organic Decomposition by Bacteria

We could not find in the literature the portion of Gibbs free energy produced by the denitrification of nitrate that was released as heat, but we did find that 24 -35 KJ/ g (dry weight) of biomass produced is evolved as heat (Samuellson et. al. 1998, Reiling and Zuber, 1983). The heat capacity of water at 27° C is 4.179 J/g K. Therefore raising the temperature of 4 million gallons of water 1 degree would need to result in 1808 g/day of dry biomass production. It seems highly improbable that there is enough nitrate to cause this change and at this rate of deposition, one might expect the aquifer to become clogged. With more research work one should be able to calculate the evolved heat and thus potential maximum temperature change which could be produced from the available nitrate.

As described above it is not necessary to "heat up" the water but rather balance out the heat losses. More importantly, denitrification is only one of many exothermic reactions that occur in the natural attenuation of effluent.

4.5 Summary "….anomaly, no new spring locations were identifiable by infared thermography." Add: This study does not preclude the possibility that other seeps in deeper offshore water contributed to this anomaly."

Yes it is true that other spring locations may exist.

4.5 Summary For accuracy's sake, the summary should note that the Cl:Mg ratios of the seeps indicate a good possibility of geothermal activity causing the temperature differential of the seeps.

It is inaccurate to conclude that because the submarine spring discharge has geochemical indicators consistent with having cycled through a geothermal reservoir that this geothermal influence is the cause of the elevated temperature. In fact Cox and Thomas (1979) state in their paper on using the Cl:Mg ratio as a geothermometer that the temperature of the shallow groundwater was a poor indicator of geothermal influence. They further state that many of the groundwater temperatures measured in the Puna geothermal area of the Big Island are below the 26 °C anomalous threshold. Therefore, we feel that it is not necessary to detail the Cl:Mg chemistry in the summary since it is adequately covered in the body of Section 4 and the various factors that could be the cause of the warm anomaly are already covered in the summary.

Section 5:
Figure 5-7: Are the wells in this figure injection or groundwater wells? It should be more accurately labeled to avoid confusion. If it is only the ratio of the injection wells, why weren't the groundwater wells also plotted?

> *We identified all wells throughout the text, groundwater vs injection well. In this specific case it was groundwater wells and we have clarified this in the figure caption.*

There is the assumption that the Seep Sample is composed entirely of treated wastewater, and results contain anomalies, yet throughout this report the assumption is made that the seep water is mainly wastewater in origin. This has not been quantified or proven and thus should not be reported.

> *We specifically stated in this Section of the Report that radon / radium and the ADCP measurement cannot distinguish between ambient groundwater and treated wastewater. The text includes the following: "Both the radon mass-balance method and ADCP measurements provide groundwater discharge but cannot identify if and what fraction of the groundwater is tertiary treated wastewater."*

Based on the data there seems to be significantly more SGD discharge in Honokao'o and Honokowai. Testing should be done to characterize this water.

> *We agree, but extending this study to additional locations is beyond the scope of the current study.*

Section 6:
6.2.1 & 4.2.2 Well purge times may be insufficient. Well purge time should be calculated based on volume and pump flow rate to replace the entire volume 3 to 5 times. The deep monitor well purge is definitely insufficient.

> *Yes, we agree that the Lahaina Deep Monitoring Well was not purged to 3 to 5 wellbore volumes. Since there is no pump installed in this well, purging this volume of water is not feasible. We have clarified in the final version of this report that the sample collected from this well was a grab sample. For the wells with pumps, a minimum ten-minute purge was more than sufficient. This resulted in 21-37 well volumes being pumped prior sampling.*

6.4.1.1 Was the temperature measured at the site of the piezometers or after traveling through the length of tygon tubing? Depending on the length, surface area, and temperature differential between the SS water and seawater, the sample water may have cooled significantly between the seeps and the sampling point. Also, the temperature range stated here for SS 27.4-30.1 °C differs from data in Table 2-2 which shows temperatures as high as 35.9 °C . Actual SS temperature is most likely above the TW temperature and not an "apparent conservation of temperature" as stated.

These temperatures were measured after travelling through the length of tubing. We acknowledge that this may result in both cooling of the discharge as it flows through the underwater portion of tubing but also subsequent warming of the discharge as it flows through the portion of tubing exposed to sunlight, sand, and ambient air temperatures. As noted in the revision these indirectly measured temperatures are generally slightly warmer than our in-situ measurements of vent discharge temperatures from CTD and temperature logger time series (Figures 2-4 through 2-7, with a range from roughly 25-28 °C), which indicates that significant cooling between the submarine springs and the measurement point does not occur. On the contrary, it appears that the warming effects of the sun and sand on the water flowing through the sample tubing may outweigh the cooling effects of the ocean. The temperature range cited in section 6.4.1.1 is explicitly stated in the text to be the range of average temperatures in Table 2-2 and is correct.

6.4.1.3 "These values are significantly lower than those of upland groundwater and MS samples, suggesting that the SS discharge may contain a significant portion of injected TW, the only known? potential contributor of lower pH groundwater in the area.." Rainwater which is a likely component of the SS, has a pH of 5.6 to 5.8.

The submarine springs are located beneath the ocean's surface and receive no direct contribution from rainwater. Rainwater interacts with the subsurface as it infiltrates to the water table, acquiring the dissolved content that results in the slightly basic pH values typical of groundwater in this area (and in Hawaii as a whole). pH values of groundwater measured in this and previous studies do not appear to show decreasing trends with down-gradient travel.

6.4.2.2 The conclusions drawn from these models are not realistic because the standard deviation for $\delta^{18}O$ is greater than the difference between the various sources. There is limited data for TW and there may be other components mixing in such as rainwater. As stated by the author, the single data point for TW does not account for temporal variability. Most studies using the type of model cited include throughfall and soil water in addition to groundwater (D.A. Burns et al. 2001), this study uses only TW and seawater as the mixing components, while this simplifies calculations and concepts, it is not necessarily an accurate picture of the subterranean processes which are occurring. The data outliers support this hypothesis, yet the author cites the
model as evidence that there is a large component of wastewater in the SS.

> *Standard deviations for $\delta^{18}O$ of water were 0.04‰ for the June samples and 0.06‰ for the September samples as stated in section 6.2.2. These values are significantly less than the differences between the various sources (as stated in Table 6-15, the Well Average $\delta^{18}O$ is -3.62‰, the Effluent Average $\delta^{18}O$ is -3.09‰, and the Marine Average $\delta^{18}O$ is 0.42‰). The paper cited above deals with quantifying end-member composition of surface water, not groundwater. Consideration of throughfall and soil water are not necessary when characterizing the submarine spring discharge because these sources must first infiltrate to the water table and become groundwater before they can discharge beneath the ocean's surface.*

6.4.3.2 High SiO_4^{4-} values of SS are attributed to increased rock weathering by TW. It seems unlikely that TW would have a higher SiO_4^{4-} concentration, since it is directly injected into aquifer and not percolated through the soil. A more plausible explanation is that the water is geothermal. These waters are enriched in silicate. This theory agrees well with the high SS temperatures.

> *Though the possibility of geothermal influence cannot be discounted, the augmentation of silica in the submarine springs and at Black Rock lagoon, where high temperatures are not present, seems more likely to be a result of artificially high recharge rates (golf course irrigation in the case of Black Rock lagoon) enhancing weathering of the subsurface. Cox and Thomas (1979) discuss the issues with using silica concentrations in Hawaiian groundwater as an unambiguous proxy for thermal alteration in the following paragraph:*
>
> *"The effect of temperature on silica concentrations has been well established in laboratory and field surveys in geothermal areas (Ellis and Mahon,1964; Truesdell, 1975; Truesdell and Fournier, 1977). Silica concentrations in the Puna geothermal area on Hawaii island are consistently higher than the local background. This also occurs in other areas which, based on geological data, are considered to have geothermal potential. Nonetheless, other non-thermal phenomena have a significant impact on groundwater silica concentrations. The most important of these are, groundwater residence time, recharge rates, soil/rock type and recharge from irrigation return water. Consequently, it was*

433

often difficult, if not impossible, to differentiate between thermal and non-thermal groundwaters based on silica concentrations alone."

6.4.3.3 pg 148 "Since the R1 effluent is produced by UV disinfection of the secondary treated effluent" <u>Effluent from Lahaina WWRF actually undergoes tertiary treatment (filtration and disinfection).</u>

We have removed the reference to "secondary treated effluent" from the report. Thank you for this clarification.

" Since water isotope mixing analysis and dye tracer results (see Section 2) strongly suggest that the SS discharge is ~~primarily~~ ***includes*** TW injected at the LWRF,…" <u>There is not a value in section 2 that indicates the amount of the contribution of the different constituents to the SS. In fact, it was stated in this section that "the data collected to date are not sufficient to estimate percent of dye mass injected that can be accounted for by the discharge at the submarine springs monitored by this study." The isotope mixing model as discussed earlier, is not compelling evidence for this conclusion.</u>

We made a typographical error. The paragraph cited above should refer to Section 3 (dye tracer results), not Section 2 (field sampling). This has been be corrected in the final draft. It is the reinforcement of the dye tracer results with the water isotope mixing model that we consider to "strongly suggest" that the submarine spring discharge is primarily (over 50%) effluent.

6.4.3.4 There is insufficient data to assume that the submarine springs is primarily treated wastewater. The County submits that such fluid should be properly referred to as "groundwater" rather than "treated wastewater."

The fluid emanating from the ocean floor is generally referred to as "submarine spring discharge." As discussed in the mixing model section, it consists of a mixture of background groundwater, treated wastewater, and ocean water. Mixing model results suggest that the submarine spring discharge is primarily (over 50%) treated wastewater.

6.4.4.1 There is no description of the method for the collection of the gas samples.

This description appears in the final paragraph of section 6.2.1:

"Samples of gas escaping from the ocean bottom near the submarine springs were collected underwater by inverting open 20 ml borosilicate glass vials over the gas vents, allowing the emanating gas to displace the water in the vial, and finally crimp-sealing the vial with a butyl rubber septa. This sampling method resulted in approximately 4-8 mL of water included with the collected gas."

6.4.4.2 Analysis of black deposit on stones was high in MnO. The author explained this as being due to the water being anoxic, **but fails to mention** that this is also a characteristic of geothermal water. This is more probable considering nitrate concentrations have been measured in the SS.

> *We acknowledge that geothermal waters are typically low in dissolved oxygen, but contribution of water from a geothermal source is not in and of itself sufficient to account for the degree of nitrate reduction observed, which requires the presence of excess dissolved organic carbon which could be provided by treated wastewater but not background groundwater or geothermal sources.*

6.4.5.2 & 6.4.5.3 Again the water isotope mixing analysis (Section 6.4.2.2 discussed earlier) is used as evidence that SS is primarily TW. All discussion stem from this assumption that is taken as a fact. Production well (PW) values should be included in the charts and calculations in table 6-16 (pg. 183) and figure 6-24 (pg. 204).

> *Use of production well values is not appropriate in Table 6-16 or Figure 6-24 because they would result in fractions significantly greater than 1 for the Hunt and Rosa, 2009 samples. Additionally, upland groundwater does not contain sufficient dissolved organic carbon to support this extent of denitrification observed in this system. The use of LWRF effluent as the end member for the denitrification yields better data correlation than the use upland groundwater and a similar enrichment factor to that determined for a septic plume by Aravena and Robertson (1998).*

6.5.1 pg. 154 "(2) Injected LWRF effluent appears to contribute ~~introduces~~ significant amounts of N and P…" Existing cesspools/septic systems contribute N and P to the groundwater This should be No. (4).

> *Cesspools and septic tanks MAY likely contribute N and P to groundwater in the southern portion of the study area, but not in the vicinity of LWRF and the submarine springs, which is primarily sewered. Potential contributions of N from cesspools and septic tanks to the ocean near Wahikuli Beach is discussed in the main body of text, but was not considered to be germane enough to the focus of this report to be included in the conclusions of Section 6.*

6.5.2 pg. 155 "(1) Mixing analysis using conservative tracers suggests that the SS discharge is ~~primarily~~ *contains* injected LWRF effluent, corroborating the results of Section 3." No one has determined the percentage breakdown of the contributors to the SS so stating "primarily" is an
unsupported opinion.

> *The word "primarily" was chosen because 8 of the 9 samples that fit the mixing model showed effluent fractions in excess of 50%.*

6.5.2 pg. 155 "(3) Injected LWRF effluent is augmented in PO_4^{3-} prior to its discharge at the SS's due to aquifer conditions promoting the dissolution of previously particle-adsorbed PO_4^{3-}. Phosphate and silicate loading seen in SS may also be a result of fertilizer inputs down gradient of measured PWs.

> *The distribution of phosphate in this study appears to correlate more with aquifer geochemistry than with fertilizer inputs. This is demonstrated by the historical stability of phosphate levels in groundwater despite the cessation of intensive fertilization of sugar cane and pineapple fields as well as the lack of evidence for significant down-gradient augmentation of phosphate concentrations. The large disparity in phosphate concentrations observed at the Black Rock lagoon and at the submarine springs, both of which are located down-gradient of all potential fertilizer inputs, suggest that a mechanism other than fertilizer inputs is responsible for this phenomena. Fertilizers do not generally contain significant amounts of silica.*

Section 7

7.6 pg 213 The County would appreciate information on the "planned modeling" for this project, including the identity of the people, agencies, or firms working on the modeling and its estimated completion time frame.

> *The groundwater modeling will be done at the University of Hawaii, Dept. of Geology and Geophysics. Dr. Aly El-Kadi will be supervising the modeling and Mr. Robert Whittier will be the primary modeler. The modeling is planned to be completed by October of 2012. The report states the modeling scenarios that are to run.*

APPENDIX G-2: Draft report review comments from the USEPA Region IX

This page is intentionally left blank.

Draft Initial Report: Lahaina Groundwater Tracer Study

Comments from Nancy Rumrill

1) The Lahaina Groundwater Tracer Study has been well-planned and conducted as documented in the Draft Initial Report. The draft report does a good job reporting on the status of the work related to the tracer study, including the results to date.

2) One area that needs stronger documentation is the issue of calibration standards for the field and lab samples, where a decision was made that is counter to the original work plan of June, 2011 (i.e., using seep water for lab calibration standard vs. DI water for field standard). In addition, to the extent there are any other instances where the study implementation has diverged from the original plan, it is important to document and explain that in the report.

> *We recognize that the use of seep water based calibration standards is a deviation from the approved work plan (the EPA was briefed on this problem and the correctives actions on 1/31/12). We have added detail needed to document the problem with the DI-based calibration solution. We have also strived to be watchful for any other areas where it became necessary to deviate from what was initially conceptualized as final product.*

3) As recognized in discussion with UH researchers, fluorescence is a temperature-sensitive phenomenon, so the calibration standards/procedures need to be performed at the same temperature at which the dye analyses are performed. On page 25 in the draft report, it is stated that samples are immediately placed in a cooler before and after field fluorescence measurements of FLT and SRB. Please clarify the procedures used for field measurement and describe any variation in temperature from initial measurement when the sample is collected versus when the field measurement for fluorescence is obtained. Is the temperature regulated and checked at the point of field analysis? Please describe how field measurement procedures are conducted to minimize errors resulting from potential temperature differences.

> *In the case the tracer dyes, we use "coolers" as unrefrigerated, yet light-impenetrable travel and storage totes. The tracer dye samples are placed in the cooler to protect them from light, but unlike storage of nutrient samples, there is no ice or other cold medium in the cooler. Thus, the samples remain at ambient temperature until after the laboratory analysis. Fluorescein has a temperature coefficient of -0.36 percent per degree centigrade. Since the samples are analyzed at room temperature both in the field and in the laboratory, the fluorescence difference due to any small temperature difference is not significant. More details were added to report to document both and field and laboratory analyses.*

4) The Aquafluor user's manual states that when you start to see visual color in the sample, it is an indicator that the sample may be above the upper limit of linearity. With the presence of the visible green in the seeps, is it possible that the upper limit of linearity has been reached although the lab results (which appear to be in the "non-visible" range) are considered more accurate? For the Model 10AU Fluorometer used in the lab, Page A9-1 of the user's manual discusses how to improve the Model 10AU (for use with fluorescein) by changing the light source and filters. If this has not already been considered, describe the current selection and how changing these factors may improve sensitivity. If feasible, we recommend running some duplicate samples in the lab with alternate light sources and/or filters to optimize the quality of lab fluorescence results.

> *All laboratory analysis to date, both with the Turner 10AU and the Hitachi F4500, indicate that our recovered and measured concentration of FLT are still well within the linear range for all instruments used. If and when our analyses indicate FLT concentrations approaching or exceeding 100 ppb, dilutions will be done to ensure that the undiluted analyses are maintained withing the linear range of the fluorometer. The Aquafluor User's manual lists the linear range for FLT as 0 – 300 ppb. The field and laboratory results are significantly below this threshold.*

> *Testing we have done in the laboratory indicates that if the volume is large enough (a 2 liter beaker) that FLT can produce a green discoloration in the water at about 35 ppb. This is the concentration being measured at Seep 3 where the green tint is most visible. We are also investigating a sampling rig that can reach further into the seep orifice than is now currently possible with the piezometers. This may help determine whether or not the piezometers are capturing the peak dye concentration.*

> *The Turner 10AU has the optics and filters installed that are those recommended on Page A9-1 of the user's manual. Any other filter/light source would make this instrument insensitive to FLT.*

5) On Page 60 of the draft report, it is not appropriate to state that the present "study indicates the **effluent** from Well 2 is not discharging at the submarine springs that are currently being monitored" because not enough is known about whether/how dye loss may have played a role in causing inconclusive data at this point. The possibility should be recognized that the SRB tracer may be prevented from emerging at detectable levels at the monitored seeps because of adsorption subsurface, destruction from chlorine residual, and/or other factors altering the SRB tracer.

> *We have modified the summary conclusion section regarding the non-detection of SRB to more accurately consider the various reasons this dye has not been detected.*

6) Figure 2-8 and Table A-3 show SRB concentrations increasing. The report seems to only discuss this on page 59 with an explanation that the FLT trace slightly elevates the fluorescence in the SRB wavelength. Because not enough is known about this distortion of the data, this information is important to consider, and UH researchers should note the need to conduct additional analysis of this data in the draft report.

> *Since it is the laboratory analysis that is required to identify the cause the increasing concentrations in the SRB data, this problem has been discussed in more detail in Section 3 and more evidence has been provided to support our conclusion of "bleed over" from the strong FLT fluorescence. The cause of false SRB indications of the field fluorometer is explicied stated in Section 2 and the details supporting the conclusion are given in Section 3.*

7) Please edit for typos as follows:

Page ii, 3rd paragraph, last sentence at "...reduced overall LWRF." is missing a word.

Page iii, 1st paragraph, 3rd line at "the probable extend of effluent plume..." maybe meant extent.

Page iv, last paragraph, 4th line from the bottom at "...InjectionWell 2 on August 11, 2012" change date to 2011.

Page v, 1st paragraph, 2nd line at "...in late October, 2012.." change date to 2011.

Page ix, 3rd paragraph, 2nd to last sentence at "...NSG is March 2012" change "is" to "in."

Page 5, 3rd paragraph, "This injection last for 58 days" should be "lasted."

Page 26, 1st paragraph, last sentence, "2.2.2 Submarine Spring...." should be formatted as a heading.

Page 26, 2nd paragraph, 2nd to the last sentence at "...from 10/8/2011 to 1/31/2011..." change January date to 2012.

Page 27, 1st paragraph, 2nd line at "...lost on 1/24/1012..." change date to 2012.

Page 59, 2nd paragraph, 5th line at "...in late October, 2012..." change date to 2011.

> *All typographical errors listed above have been corrected. Thank you very much for the careful reading.*

Comments from Hudson Slay and Wendy Wiltse

Major Comments:

General: For such a lengthy and detailed technical report, this is quite well written and very readable. We appreciate the factual and neutral tone of the report and the way alternatives are discussed, as for the cause of the thermal anomaly.

Executive Summary: Upon a reread of the executive summary after going through the whole document, the executive summary does not always seem to paint the same picture as the body of the document. It is understandable that the executive summary is more generic than the individual sections but the major take away messages as well as the integration of appropriate information across the different sections of the document could/should be reflected here. As an example, the Aqueous Geochemistry section should paint more of picture of the atypical suboxic/anoxic conditions in the aquifer resulting from the large amount of effluent carbon which leads to significant denitrification as well as the development of manganese precipitates. Also, it would be very helpful to better integrate the groundwater flux information with the nutrient data.

> *We have worked to make the executive summary more detailed and at the same time we have heightened its overview. Major highlights have been added, followed by a still condensed, yet now more elaborated discussion of many aspects of the major findings (including successive stages of microbial nutrient redox cycling, and denitrification processes, etc.). Accurate water fluxes must await completion of our new ADCP deployments, and when obtained more accurate nutrient fluxes from the submarine spring will be possible. In regards to nutrients, please also see our reply that follows under the questions regarding "nutrient units" below.*

Cause of thermal anomaly. (Section 4.4, Page 89-90 and Table 4-2 Page 93-4) With respect to Cl:Mg values being an indicator of geothermal activity, is it possible that the Cl levels and Cl:Mg ratios at the LWRF and seeps are influenced by the chlorine disinfection of effluent prior to injection? The effect of chlorine disinfection on these indicators should be discussed in the report. We need to identify the form of chlorine being used at the LWRF for disinfection and well cleaning and how it might affect chloride ion concentrations. A half reaction of chlorine dioxide (ClO2) does yield the Cl- ion. If the addition of chlorine/chlorine dioxide from the LWRF does affect Cl- then whenever Cl is used as a conservative dissolved species this addition/spike needs to be accounted for.

> *We believe that chlorination should not be a significant contributor to elevated chloride ion concentration (and potentially higher Cl:Mg ratios) in the submarine spring samples. Per EPA 832-F-99-062 (Wastewater Technology Fact Sheet: Chlorine Disinfection), the maximum typical chlorine dose used during wastewater disinfection is 20 mg/L. Assuming all this 20 mg/L of chlorine was converted to Cl- ions (an improbably conservative assumption, given the behavior of chlorine in water), the resultant Cl- concentration would increase by 20 mg/L. The submarine spring Cl- concentrations ranged from 1469 to 8584 mg/L, so chlorination would account for 1.4% at most of the observed chloride in the submarine spring samples, even with these conservative assumptions described above. This 1.4% level of variation is near analytical accuracy for Cl- and does*

442

Nutrient units. We appreciate that uM is a common unit for reporting nutrient concentrations in the scientific literature, but EPA and DOH use micrograms per liter (ug/L) for reporting water quality data and for regulatory purposes. The Hawaii Water Quality Standards are critical threshold concentrations defined in Rule as ug/L. To assist EPA and DOH in interpreting and applying the data from this report, the Section 6.3 results for nutrients should also be reported as ug/L. We suggest that the ug/L be shown in parentheses within the text, and separate data tables (comparable to Tables 6-8,6-9, 6-12) present the ug/L concentrations. The appropriate state water quality standards for coastal waters (dry) should also be included in the ug/L tables, and any measured concentrations in marine waters that exceed the standards should be noted in bold or italics. EPA can advise you in how to present this information. Nutrient fluxes. It would be really useful from a management perspective, to know how the SGD nutrient fluxes at the seeps compare with those at other sites, including sites with similar agricultural history, other wastewater sources, and sites with minimal anthropogenic influence. The report estimates groundwater fluxes (Section 5.3.2), but is silent on nutrient fluxes. Are data available to estimate nutrient fluxes from seeps and other nearby sites; if not, what additional data would be required?

Nutrient concentrations in ug/L have been included in the report as new sets of tables and we have integrated these units into the text where applicable. As units based on weight concentrations are generally useless for geochemical manipulations that compare different elements or compounds (which is but one reason why moles are used in the scientific literature), we have not changed our illustrations or calculations. Regarding water quality standards and issues of compliance, it has been agreed between the UH and the EPA (both prior to and subsequent to the above comments) that UH will not include in its report the applicable water quality standards or make any comparisons, and that instead the EPA will assume that role and will coordinate with HDOH on such tasks.

We have data to make some nutrient fluxes calculations for the submarine springs, though the temporally variable nutrient concentrations of the discharge measured in this study, ongoing DOH sampling, and previous studies will result in a wide (over an order of magnitude) range of estimates. We do not have adequate data to characterize nutrient concentrations of SGD in the Wahikuli and Honokowai portions of the study area. Such data could be possible, but would require new shoreline piezometer samples at these locations. Additionally, it may be possible to characterize the nutrient flux from Black Rock lagoon, but this would require an accurate assessment of the discharge from this body of

water to the ocean. This later data could potentially be obtained in a future project using ADCP current measurements or portable stream gaging device.

Other Comments:

Page ii, para 1: rewrite suggestion: " The Pioneer Mill…, when it ceased sugarcane production **on approximately 6000 acres** and **some** of the land was subsequently converted…".

Thank you. This has been added.

S/W 6 Page ii, paragraph 2: What is the average daily volume of R1 water sold?

This correction has been added and updated according to recent information provided by Scott Rollins with Maui County.

S/W 7 Page ii, paragraph 3, final sentence rewrite suggestion: However, as discussed in Section 6, …. LWRF [add] **nitrogen and phosphorus loadings?** This statement needs to clarify if this is referring to effluent nutrient concentrations or also to loads.

This has been rewritten to explain more clearly.

S/W 8 Page ii, paragraph 4, 3rd sentence rewrite suggestion: '…the most conclusive **tracers in the nearshore marine environment were** pharmaceuticals, ….'

We have updated and made this change.

Page iii, paragraph 4: include salinity units

As noted in the text, salinity is measured and reported in Practical Salinity Units , which by definition are unitless and units are thus not used.

Page iv, 1st full paragraph: Please include the distance of Honokowai Beach Park and Wahikuli Beach Park to the study site as was done for Olowalu

This has been added to Section 2.2.3

Page iv. 3rd full paragraph: Second to last sentence is confusing. FLT fluorescence was detected in October and mid-November but not pronounced until January? What defines "pronounced"?

This has been clarified in the text.

Wouldn't it be clearer to say fluorescence peaked or exceeded a certain amount in January/February?

> *This has been clarified.*

Page v, 1st paragraph, 1st sentence: '…after about 84 days **from time of dye addition to Injection wells 3 and 4**.'

> *This paragraph has been rewritten for additional clarity. Thank you.*

Page v, 3rd paragraph, 3rd sentence: where breakthrough curve used the first time, include (BTC)

> *Corrected.*

Page v, 3rd paragraph, final sentence: '…farther from shore and **in** deeper **water**.'

> *Thank you, we have made this change.*

Page vii, 2nd paragraph, 2nd sentence: With respect to the total groundwater discharge including the seeps and diffuse flow, understand it is a 24 hour average but is this over a particular length of shoreline, area or model grid? Does the 'fresh groundwater flow' include effluent or not?

> *The discharge is for the two submarine spring sites above which we found a pronounced elevated radon signal in the surface water. As explained in the text (and now re-emphasized in the text) radon and salinity cannot identify if the fresh groundwater flow includes effluent or not. The stable isotope analysis can help answering this question and is discussed in Chapter 6.*

Page viii, 3rd paragraph, #2: clarify that N and P reduction is concentration, total load or both. The data do not support the statement in #2 parentheses "though much less than prior to treatment upgrades in 1995" because the report only presents historical concentrations, not loads.

> *We do not currently have the comprehensive historical nutrient concentration data and injection rate data from LWRF that would be required to estimate loading from plant inception to present. LWRF has provided us with the figure below that shows their estimate of historical N discharge in lbs/year, but not the actual data.*
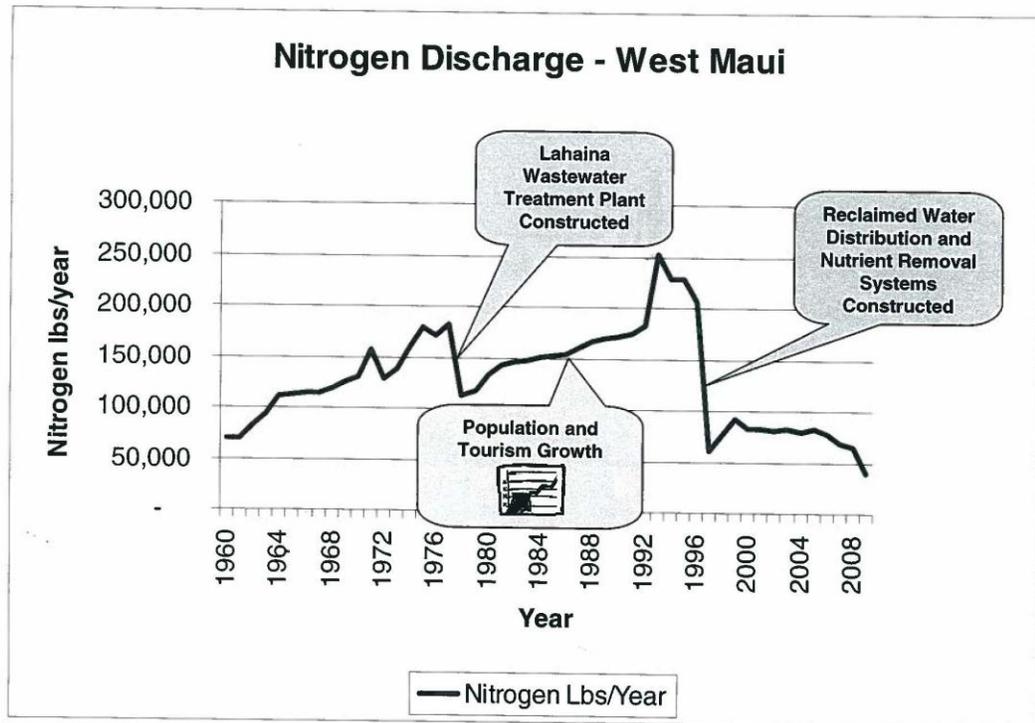
Figure G-1: Nitrogen discharge history for West Maui.

Page viii, third paragraph, #3: There may be other reasons for P concentrations at seeps being higher than in injected effluent. There could be a P supplement from landscape fertilizers (NPK) used in the overlying resort lands, or P concentrations in effluent may be highly variable. Need to do a more convincing job of explaining why you think aquifer conditions promote release of P.

We do not have adequate data to do more than speculate on the nature of this phenomenon. The lack of monitoring points between the injection wells and the coast makes it impossible to directly ascertain the geochemical processes taking place in the injected effluent as it travels down-gradient. The P concentrations seen in the submarine spring discharge is significantly higher than those in nearby Black Rock lagoon, which would be expected to have similar if not greater P input from agricultural and resort fertilization. This suggests that that the augmentation seen in P at the submarine spring discharge points in related to the unusual geochemical phenomena unique to this system in the study area. P concentrations in effluent (since 1995) and submarine spring discharge samples

446

have been relatively temporally stable (See Figures 6-19 and 6-21). In addition, we have clearly described and referenced in detail the affinities for P to sorb or desorb from different compounds in the revised section 6.4.3.1 (Tp and PO4) and there and subsequently discuss its enhancement in the seeps relative to other inputs, including the LWRF.

Page viii, 1st paragraph: please expand the final sentence or explain figure ES-3 and relationship between TIR and N15 differently re covariance?.

This point has been moved to and expanded in the subsection of the Executive Summary that discusses our TIR results. Please note that in the final report that figure number is ES-6

Page ix. Top #3: Explain that Wahikuli watershed had sugarcane ag until 1999 and currently has hundreds of onsite septic and cesspool waste water systems.

This has been done.

Figure ES-2: Hanaka'oo Beach Park is shown in the wrong location. Why is it even labeled here?

This has been corrected.

Figure ES-3: Caption should clarify that circles are N15 in water.

This has been corrected. Please note that in the final report that figure number is ES-6

Page 5 1st paragraph, Second to last sentence: Again, data presented show decreased nutrient concentrations after biological treatment but loads are not evaluated. Please evaluate nutrient loads pre- and post biological treatment/initiation of reuse.

We cannot properly evaluate historical loading (fluxes) without comprehensive nutrient and injection rate data from plant inception to present, and we have not had access to such data.

Page 5 1st paragraph: Last sentence rewrite: "concluded that wastewater injection wells were the largest source of **nitrogen and** phosphorus by at least one order of magnitude."

The EPA is correct that, in addition to P, we failed to also cite that work's estimate of the proportion of N-loading from the WLRF injection wells. This sentence references the "West Maui Watershed Owner's Manual," where in Table 5 on page 18 of that document (which includes the findings of Tetra Tech) it

estimates that, as of 1996, wastewater injection well contribution of P to the ocean were an order of magnitude greater than that from other sources (83 lbs/day from injection wells versus 5.7 lbs/day from other sources); i.e. 94% from injection wells vs. 6% from other sources. However, according to that publication, this "magnitude" of nutrient loading does not seem to be true for N (150 lbs/day from Injection Wells vs. 112 lbs/day from other sources; i.e. 57% N from injection wells vs. 42% from other sources). We have thus re-written this sentence to more accurately report the findings of that publication, stating:

"The West Maui Watershed Owner's Manual (West Maui Watershed Management Advisory Committee, 1997) reevaluated N and P loadings in the watershed and concluded that as of 1996, wastewater injection wells contributed ca. 94% of land-derived phosphorus-loading and ca. 57% of land-derived nitrogen-loading to the ocean, relative to the other sources evaluated (cesspools and inputs from pineapple-, sugar cane- and golf course-developed lands)."

Page 14. Table 1-2: It would be useful to include injection rate data for December to March time because these are peak visitor months and rainy season when reuse is at minimum.

> *These data have now been obtained from from Maui Co. and updated in the revised report.*

Page 19 Figure 1-5: Suggest omitting these figures because they are inaccurate. They do not show Kaanapali golf course which was built in 1960's. Kapalua golf course was built in 1990 but is shown to be existing 1980-84. Pineapple expanded into Honolua about 1990 but is shown back in 1926.

> *At the EPA's above request, the historical land-use reconstruction maps twice published by the USGS as a basis for two West Maui groundwater studies have been removed from the report. We had thought maps useful to help make the report more all encompassing as we feel they are, to our knowledge, the best overall representation of historic West Hawaii land-use available, and we felt that shortfalls in accuracy were outweighed by their larger area coverage and overall benefit for reference. We felt their sources well referenced, especially considering the great difficulty in recreating accurate land-use history, and for the most part well substantiated.*

Page 27. 2.2.3: The report needs to clarify locations of control stations. Here Wahikuli is shown as control for dye studies. Some of the figures and other parts of report refer to Hanakao'o. Which sites were used in what sections?

> *Hanakao'o was a mistake with reference to control sites. This has been corrected.* The locations of other discrete samples should be clear from the lat/long data and sample maps.

Page 31, Control locations: more detail about the control locations and sampling seems to be needed. Actual sample location (e.g., depth?, distance from shore?, surface?, bottom?, seep?), number and frequency of sampling---the current information is not clear.

This has been clarified in Section 2.2.3

Page 27. 2.2.3, Page 31: "Olowalu is located ~13 km south of the main study area and currently has no known land-based pollution impacts due to the lack of development and the termination of sugar cane operations in the late 1990's." Not clear that this statement is completely accurate---the land-based pollution impacts in this area seem to be similar to those in the Honokowai and Wahikuli watershed with respect to legacy agriculture nutrient inputs via groundwater.

This has been corrected in Section 2.2.3

Page 35: Figure 2-2 shows Hanakao'o and Wahikuli Beach Parks to be the same location. The land use histories differ for these two sites so please use the correct place names. Hanakao'o (Chinese cemetery, Canoe Beach) shoreline has heavy sedimentation from agricultural runoff and is downgradient of Kaanapali golf course, as evidenced by the many golf balls in the water there. Wahikuli is shoreline is downgradient of hundreds of septic systems and cesspools and historical sugarcane fields, some are now active corn fields.

This has been corrected in Section 2.2.3

Section 3.4, Page 59, 5th line: should be 'late October **2011'** not 2012.

Thank you, we made that correction.

Page 73. Figure 3-10: Wahikuli Wayside Park is marked at the location of Hanakao'o.

Thank you, we have made that correction.

Page 103. Figure 4-9: Cl-Mg Ratios > 15 can be indicative of geothermal activity, yet this figure shows high ratios in waters off Wahikuli and Honokowai Beach Parks where there is cold SGD. How do these observations affect the likelihood of geothermal activity accounting for the temperature anomaly at the seeps? It appears that ratios in this range are characteristic of SGD.

Cl-Mg ratios > than 15 are indicative of geothermal activity in groundwater. Seawater typically has consistent Cl-Mg ratios near 15. The values measured in

449

seawater in this study are consistent with this observation. The locations cited above are marine samples and are shown by green squares in Figure 4-6. Thus, the ratios in the above samples do not necessarily indicate geothermal activity, but more likely represent marine samples.

Page 106, paragraph 3, and P 115 5.4.3 paragraph 2: Section 5.4.3 says that the difference between June and September ratios was due to change in groundwater flow regimes. Radon surveys on June 21 occurred at low tide, September 22 surveys occurred at high tide. Explain any differences in flux estimates and radon ratios that are attributable to tide stage.

> *The two surveys were complimentary, we filled in areas that we missed in June later in September. In the report we listed discharge from the combination of June/September measurements. For each site we used the measurements that were the closest to the coastline in order to better define SGD. It is impossible to speculate on high vs low-tide difference at each site and doing a time-series measurement at each site was beyond the scope of this study. In the report on the previous p. 106 and in the current Section 5.2.1 we included the following:*
>
> *"The two surveys were complimentary in order to capture radon activities as close to the coastline as possible. The low-tide survey allowed us to capture higher radon activities but prevented a close approach to the coastline, while in the deeper water at high-tide it was possible to cruise closer to the coastline."*

Page 111, 5.3.1. paragraph 2: This section states that "surface waters above the seeps were enriched tenfold the magnitude of background levels". What does this mean for nutrients, pharmaceuticals, and other contaminants that emanate from the seeps? Are they also likely elevated in surface waters?

> *Radon is a radioactive-conservative tracer and does not take part in any chemical reactions in the coastal ocean. Its radioactive decay can be neglected due to the short time scale of mixing but it is a gas and undergoes evasion form the surface of the water column. We estimated that 3-10% of radon is lost by evasion over a tidal cycle. We can use radon as a mixing tracer, i.e. assume that the 10 to 40-fold dilution of radon between the seep water and surface water column also applies to other solutes. Whether a pollutant would be detectable in the surface water will depend on its measurement sensitivity and how conservative its behavior is in the coastal ocean. Our radon detection techniques are very sensitive and this may not be the case for other chemicals that emanate from the seeps.*

P 114. 5.4.2 paragraph 3: Section 3 states that Wahikuli Wayside Park, not Hanakao'o Beach Park was a dye sampling location.

> *The Hanakao`o Beach area identified as a high discharge area during the radon surveys is 1.2 km wide and includes the Wahikuli sampling site. We clarified this in the text as: "There is significant discharge at locations both south and north of the seeps and two of those, Honokowai and Wahikuli Wayside Park which is within the Hanakao`o Beach area defined here (Figure 5-5), were selected as dye concentration sampling points (see Section 3.0)."*

Page 116. 5.4.4: Clarify whether discharge rates refer to the seeps sampled via piezometer, or to the fields of seeps around the piezometers. Also clarify what future work on seep geometries will entail. Will this work focus on the known seep fields or characterize all the warm seeps, or all the wastewater seeps? 5.5. Same question, do the discharge rates in the final sentence refer to individual sampled seeps or to the known fields of seeps.

> *Seep 4 and Seep 6 were the same seeps as sampled later by piezometers from the geochemical tracers. We included the following in the report:*

> *"These seeps were the same (Seep 4 and 6) as the ones later sampled for radon. The ADCP was deployed before the piezometers were inserted into the seeps… Exact seep geometries including vent dimensions and water cone diameters will be measured.*

> *To better estimate the seep velocity, the ADCP has been deployed in ideal conditions two times (for two days each time) since the initial report was submitted and we plan to deploy the ADCP additional times when conditions are ideal in the future.*

> *On-going SCUBA surveys are being conducted from Honokowai Point to Black Rock (from the very shallow nearshore waters to offshore waters of ~25ft depth) to: (1) locate and record with a handheld GPS additional submarine spring (seep) locations, (2) measure the width and length of the seep, (3) photograph the seep, and (4) sample the seep water from the point of discharge in the sea floor with sterile syringes which is then immediately transferred to sterile opaque bottles in the field. The samples are treated the same as those described in Section 2 (stored and shipped in room temperature coolers to Oahu for analysis).*

5.5. Same question, do the discharge rates in the final sentence refer to individual sampled seeps or to the known fields of seeps.

> *We clarified the sentence to: "These water velocities translate to a discharge from individual seeps of approximately 70 and 12 m^3/d water from Seep 4 and Seep 6, respectively."*

P 119. Table 5-4: It would be useful to give the rate of discharge per unit area of seabottom or length of shoreline.

We added a discharge per length of shoreline to the table.

P. 125. Figure 5-5: More confusion…does the arrow for Honokao'o Beach point to Hanakao'o or to Wahikuli? Hanakao'o is misspelled.

As indicated above, the Hanakao`o Beach area identified as a high discharge area during the radon surveys is 1.2 km wide and includes the Wahikuli sampling site.

P. 129, 6.2.1: Clarify at what depth the marine surface samples were taken…at the surface or below the surface? The type of sample should be recorded, particularly because the seep water may form a thin layer at the surface of the water column.

Marine surface samples were taken at the ocean's surface at a depth of no more than 5 cm. The undulating nature of the ocean's surface makes precise depth determinations within this range impossible.

P.133, 6.3.3.1: Second sentence. "Low" is relative. The text should explain that MS samples for TP were low relative to groundwater and seep samples, lower by an order of magnitude. DOH and EPA, consider "low" to be concentrations below the applicable water quality standard, and that comparison was not made. In general, it is useful to point out order of magnitude differences where they exist. For example, most well samples had total nitrogen concentrations an order of magnitude higher than marine samples. Most well samples had nitrate concentrations 1-2 orders of magnitude greater than marine samples. Total phosphorus in seep samples was at least an order of magnitude higher than in wells and marine waters.

We have not made comparisons relative to EPA and HDOH tasks in evaluating conformance to State water quality standards, but we have strived to be very exacting in reporting the measured abundance of elements in the text.

Section 6.4.3. Nutrients: Comparisons are made in this section to marine nutrient concentrations reported in previous studies. It should be noted that not all of the studies sampled in the vicinity of the seeps. Laws (2004) station at "North Beach" was Kahekili Beach Park. Dollar and Andrews (1997) did not sample at Kahekili. They sampled at the mouth of Honokowai Stream which is further north, and directly makai

of the LWRF. Laws (2004) station "Papakea" was also at the mouth of Honokowai Stream.

> *The idiosyncrasies of these individual studies with regard to sampling locations have been noted in the revised version of this report. For previous studies, all marine surface sampling points within the boundaries of the current study area (roughly Honokowai to Wahikuli) were included to provide the best comparison to the data collected by the current study. The intention was not to limit the comparison to the area proximal to the submarine springs.*

Section 6.4.3 and Figure 6-19: This comment relates to the LWRF load reductions since 1995 when biological nutrient removal was initiated. The N and P concentrations are lower than in 1995 but the overall nutrient loading is dependent upon the volume of effluent discharged to the injection wells. A table and discussion of any changes in the volume and nutrient loads of effluent placed into the injection wells should be included. TheWest Maui Watershed Owners Manual (1997) estimated that biological treatment and the initiation of wastewater reuse at Kaanapali golf course resulted in 66% and 70% reduction in N and P loads, respectively, between 1993 and 1996. This estimate was based on concentration and flow data from LWRF. We believe that nutrient concentrations and flows have increased since 1996, but nutrient loads may still be lower than pre-1993 levels. The report should evaluate loads

> *As discussed above, we need comprehensive injection rate and nutrient data to make such calculations.*

This page is intentionally left blank.

**APPENDIX G-3: Draft report review comments from the USEPA
Office of Research and Development**

This page is intentionally left blank

Draft Comments on the Draft Initial Tracer Report
United States Environmental Protection Agency
OFFICE OF RESEARCH AND DEVELOPMENT
National Center for Environmental Assessment (8623P)

Malcolm Field, Ph.D.
Research Hydrogeologist
Quantitative Risk Methods Group

First, if we accept that the de-ionized water was a problem for the fluorescein standards why then are the SRB standards also being treated as though there were a problem. It is a known fact that low pH water reduces the fluorescence signal of fluorescein (by a factor of 5 for pH < 2.5), which is not the case for SRB so UH personnel did not need to alter the SRB standards. However, the draft study clearly shows that the SRB concentrations are rising in the *in situ* field measurements for Seep 3 (see Appendix A, Table A-3, p. 243−244) , indicating SRB-dye recovery. However, Figure 7-3, p. 217 of the study suggests no SRB-dye recovery at Seep 3 based on laboratory measurements (I cannot find any listing of the SRB laboratory results in the draft study). The SRB-dye recoveries reported in Table A-3 are especially important because it suggests that the second dye injection, SRB injection into Well 2, may also be upwelling near shore as well. Now you also have reason to be concerned about Well 2 in addition to concerns regarding Wells 3 and 4 that received fluorescein dye earlier.

Second the creation of the new laboratory standards using seep water may be a problem. It is not stated in the draft report when the seep water was collected for use in making the laboratory standards, but if there was any dye in the seep water from the injection, then the new standards will have been adversely affected. This can be shown by the basic procedure for a serial dilution.

For a standard concentration of 100 ug/L using a fluorescein dye batch requires the following:

$$C_f = C_S S_G \left(\frac{W_d}{V_w + V_d} \right)_1 \times \left(\frac{V_d}{V_w + V_d} \right)_2 \times \left(\frac{V_d}{V_w + V_d} \right)_3$$

$$\begin{array}{ccc} \text{Step 1} & \text{Step 2} & \text{Step 3} \end{array}$$

(1)

where the parameters listed in Equation (1) are defined in table 1.

Table 1. Definiton of variables for Equation (1) and values assigned according to the Lahania fluorescein tracer test.

Parameter	Step	Definition	Value	Explanation
C_f	⋯	Final concentration	100 µg/L	Common Maximum Standard
C_S	⋯	Concentration of dye solution	77 %	As sold by manufacturer
S_G	⋯	Specific gravity	1.0 g/cm³	Assumed for this example
W_d	1	Weight of dye	10 g	Calculated for this example
V_w	1	Volume of added diluent	2476 mL	Calculated for this example
V_d	1	Pipet volume of dye	10 mL	Water for this step
V_w	2	Volume of added diluent	3500 mL	Diluent = water
V_d	2	Pipet volume of dye	20 mL	From Step 1
V_w	3	Volume of added diluent	3500 mL	Diluent = water
V_d	3	Pipet volume of dye	20 mL	From Step 2

Applying the values in Table 1 to the parameters shown in Equation (1) and multiplying by 1.0×10^7 (conversion of 77% to µg/L) results in a C_f = 100 µg/L if the diluent water is dye-free (i.e., de-ionized water). However, if seep water used to make the standards was not dye-free because the seep water was collected sometime after low concentrations of dye were starting to breakthrough at the seeps, then C_f will be reduced accordingly. For example, if the seep water had a background concentration of 0.3 µg/L, then C_f = 30 µg/L and all subsequent measured concentrations based on this standard will also be reduced accordingly (as stated by UH personnel). If the 0.3 µg/L value truly represents background concentrations, then the estimated C_f = 30 µg/L is valid. However, if the estimated C_f = 30 µg/L is a result of the released dye exiting the seep at the time of water collection, then the estimated C_f = 30 µg/L is invalid and measured laboratory concentration are incorrectly low. I am unable to resolve this issue, but UH personnel may be able to do so if they can provide a clear explanation of when and where seep water was collected for creating laboratory standards. (It should be noted that once a tracer is released it is a generally accepted notion that no downgradient water can be considered representative of background any longer because it is unknown when breakthrough has begun).

Third, prior to yesterday's discussion, I was not prepared to believe that the green-tinted water upwelling around the seeps was in fact fluorescein because (1) why would the leakage be occurring around the piezometers and not in them, and (2) the concentration of the green-tinted water had to be much greater than that which was being reported by laboratory measurements of the fluorescein, otherwise the green-tinted water would not be visible to the naked eye. However, given the problems that UH personnel have had with shifting sands burying the piezometers and the probable turbidity of discharge water, it is very likely that the piezometers have become clogged with sediment, which would force seep water to flow around the piezometer. In addition, if the green-tinted water flowing around the piezometer does in fact exhibit excitation and emission peaks matching that of fluorescein, then the *in situ* fluorescein measurements may more

accurately reflect reality (i.e., the greater measured *in situ* fluorescein concentrations approach that which is visible to the naked eye than do the laboratory measurements).

Fourth, it appears that UH personnel are adjusting their laboratory measurements of fluorescein concentrations to match their model predictions. To my thinking, this is backwards. I have never heard of adjusting physically measured parameters to match model predictions. Models are useful tools for design of such experiments, but our lack of knowledge of actual environmental conditions and inability to fully model all environmental aspects renders models poor substitutes for reality at best. Typically, to improve our models we adjust model parameters to match measured parameters.

On a somewhat related note, it was stated yesterday that transport from the injection wells to the seeps must be via a porous medium that can be represented by a representative elementary volume (REV) because transport is slow and because of the gently rising breakthrough curves (BTCs); steep rising and descending limbs in a BTC only result from transport via fractures or conduit, which is just not true.

My initial estimate for transport from Wells 3 and 4 to Seep 3 suggest transport velocities of about 8.6 m/d (28 ft/d) is probably too rapid for transport through porous media. Also, the calculated Peclet number of 105 suggests advective transport greatly exceeds diffusive/dispersive transport.

As for the limbs of a BTC, the steepness of the limbs is unrelated to the medium through which it is migrating. I have measured and modeled several instances in which the descending limb of a BTC measured in a karst conduit exhibited a very long tail (which I attributed to immobile flow regions in the conduit where my tracer dye was held in temporary detention prior to being released back into the mobile flow region). A colleague of mine has conducted tracer tests in the Wakulla Springs system in Florida (gigantic submerged cave system) with a very slowly rising limb to his BTCs.

My general sense of the Lahaina study is that it is comprehensive and well done. My criticisms of the preliminary assessments of the tracer test may or may not be easily resolved.

UH Responses to EPA's Comments

First, if we accept that the de-ionized water was a problem for the fluorescein standards why then are the SRB standards also being treated as though there were a problem. It is a known fact that low pH water reduces the fluorescence signal of fluorescein (by a factor of 5 for pH < 2.5), which is not the case for SRB so UH personnel did not need to alter the SRB standards.

> *We agree that the use of deionized (DI) water did not negatively affect the fluorescence of the SRB calibration standards. The observed difference between the SRB calibration solutions prepared with submarine spring water vs. those prepared with DI water was very small and could have been due to measurement inconsistencies when mixing the two batches. The primary reason for using submarine spring water for the SRB standards was to maintain consistency with the FLT methods.*

The SRB-dye recoveries reported in Table A-3 are especially important because it suggests that the second dye injection, SRB injection into Well 2, may also be upwelling near shore as well. Now you also have reason to be concerned about Well 2 in addition to concerns regarding Wells 3 and 4 that received fluorescein dye earlier.

> *When the samples are measured with the field fluorometer, the strong fluorescence of Fluorescein "bleeds over" and causes a response in the SRB channel. This has been verified by reading samples that only contain Fluorescein with the SRB channel of the field fluorometer (Figure G-2). This test showed that (and the results are included in the final version of the report) the SRB channel of the field fluorometer responds to in a very linear manner to increasing concentrations of fluorescein. Also, neither the laboratory fluorescence measurements nor the synchronous scans show any indication of SRB in the submarine spring samples analyzed with the exception of three samples collected in February 2012. These three samples showed a very small degree of elevated fluorescence in the wavelength range of SRB. However, due to the very low signal these results are only evaluated as possible detections. The tests performed to verify the interference between channels of the handheld fluorometer can be found in Section 2.3.4.*

> *UH does need to clarify that the absence of SRB at the monitored seeps does not preclude the possibility that the effluent could upwell in the same locations where Fluorescein is currently observed if effluent was injected into Well 2 only. It would take a third tracer test with injection into Well 2 only to confirm whether or not this arrangement would result in effluent discharge into the near shore waters. This has been clarified in the in Subsection 3.3.1.2 of the final interim report.*

Second the creation of the new laboratory standards using seep water may be a problem. It is not stated in the draft report when the seep water was collected for use in making the laboratory standards, but if there was any dye in the seep water from the injection, then the new standards will have been adversely affected. This can be shown by the basic procedure for a serial dilution.

Yes, not specifying in the report the collection dates of the seep water used in calibration solutions was an oversight. However, the seep water used to mix the dye standards was from samples collected prior to July 28, 2012, the date of the FLT dye addition. The interim report has been revised to make clear that the seep water used to make the calibration standards was collected prior to dye addition.

Third, prior to yesterday's discussion, I was not prepared to believe that the green-tinted water upwelling around the seeps was in fact fluorescein because (1) why would the leakage be occurring around the piezometers and not in them, and (2) the concentration of the green-tinted water had to be much greater than that which was being reported by laboratory measurements of the fluorescein, otherwise the green-tinted water would not be visible to the naked eye. However, given the problems that UH personnel have had with shifting sands burying the piezometers and the probable turbidity of discharge water, it is very likely that the piezometers have become clogged with sediment, which would force seep water to flow around the piezometer. In addition, if the green-tinted water flowing around the piezometer does in fact exhibit excitation and emission peaks matching that of fluorescein, then the *in situ* fluorescein measurements may more accurately reflect reality (i.e., the greater measured *in situ* fluorescein concentrations approach that which is visible to the naked eye than do the laboratory measurements).

We agree that cause of the green tint is still unresolved. But, we have observed that Fluorescein may be visible at concentrations less than the generally accepted value of 100 ppb if the volume is large enough. A 35 ppb FLT solution mixed in 2 L beaker in the lab did have a green tint (Figure G-3). This solution was mixed with seep water and the photograph was taken within an hour after the solution was mixed. We interpret this to mean that if the water column is long enough, Fluorescein is visible at concentrations less than 100 ppb. This of course is dependent on the solution being accurately mixed, but we believe it was. We also agree that some of the green wisps shown in the video were very vivid. We plan to conduct further investigations to determine whether or not the piezometers are capturing the peak concentration. A summary of efforts to resolve the source of green tint can be found in Section 3.2.4 of the final report.

Fourth, it appears that UH personnel are adjusting their laboratory measurements of fluorescein concentrations to match their model predictions. To my thinking, this is backwards. I have never heard of adjusting physically measured parameters to match model predictions. Models are useful tools for design of such experiments, but our lack of knowledge of actual environmental conditions and inability to fully model all environmental aspects renders models poor substitutes for reality at best. Typically, to improve our models we adjust model parameters to match measured parameters.

This is a misunderstanding resulting from the poor choice to use the word "predicted" during the discussion about the fluorometer calibration. "Predicted" was meant to refer to the instrument response versus that expected based on the FLT solution concentrations used to verify instrument linearity.

The analytical results have not been adjusted to show better agreement with the model. We agree that it is the model that needs to be modified so it agrees more closely with the measured breakthrough curve. To date the modeling is very

preliminary. The MODFLOW/MT3D model has been modified from the initial planning model to more accurately reflect the dye injection concentrations and duration. Also it was further modified to evaluate the effect that imposing a hard barrier to the north of the plant had on the modeled breakthrough curve. But again we have modified the model based on analytical results but we have not modified the analytical results based on the modeling.

We hope that these clarifications help to address the concerns of the EPA regarding the Lahaina Groundwater Tracer Study. We strongly agree that the cause of the green color observed at the seeps remains unresolved. This is an important issue and we will further investigate the source of this anomaly. We appreciate this opportunity to discuss the science associated with this important project.
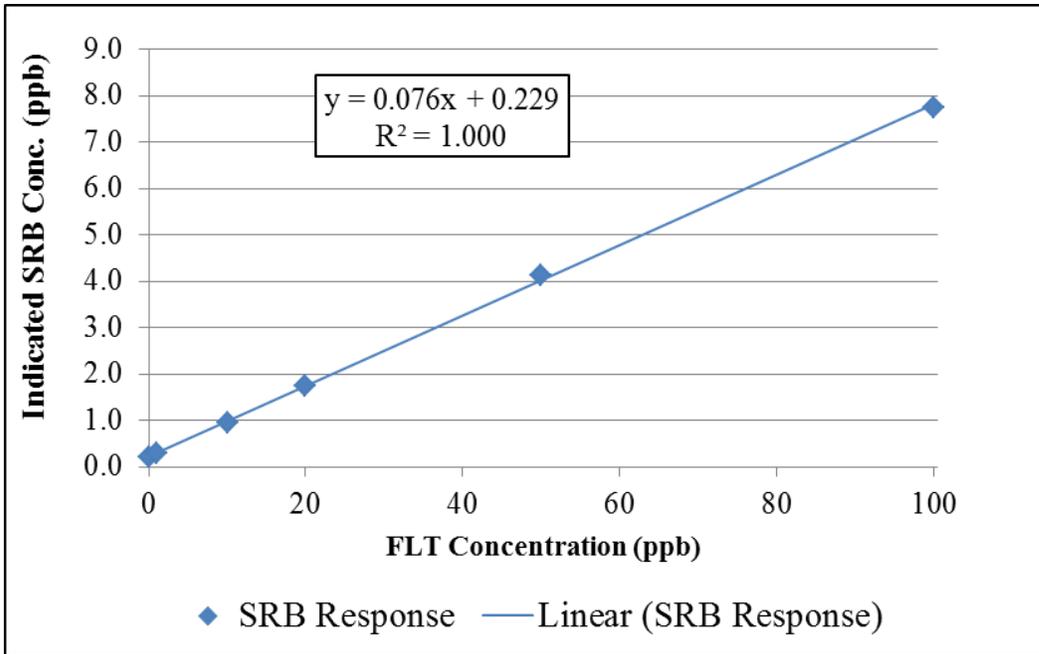
Figure G-2: The handheld fluorometer SRB channel response to FLT (only) calibration solutions.
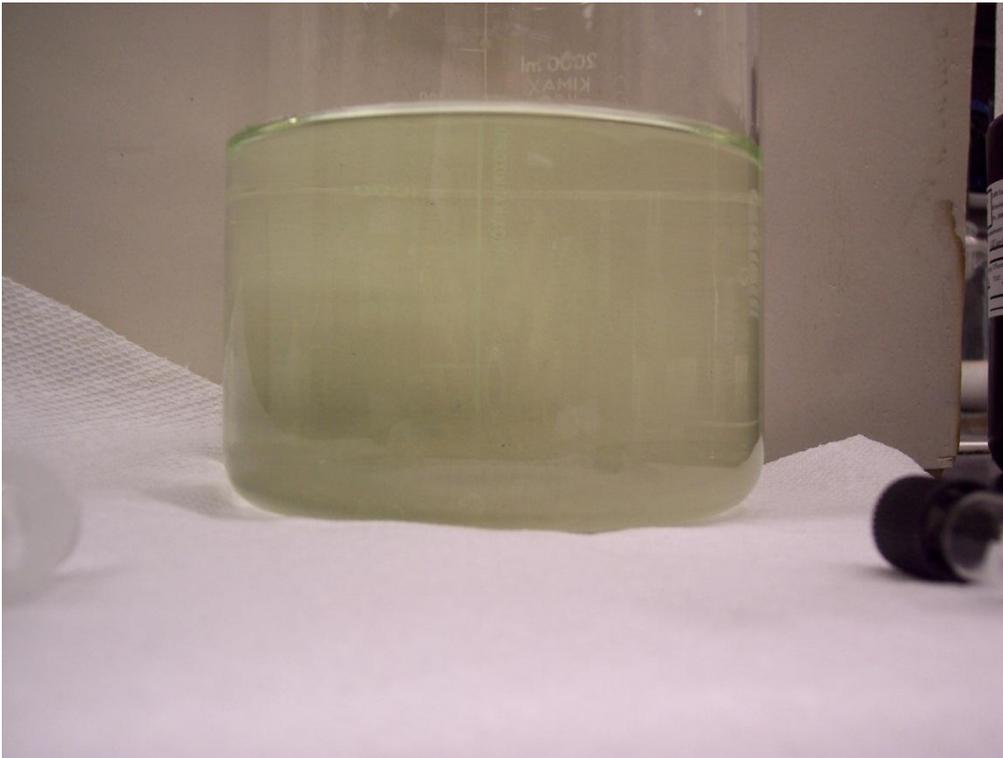
Figure G-3: A visible green tint in a 35 ppb laboratory FLT solution.
The solution was mixed using submarine spring water and the photo was taken within an hour of mixing the solution.